Author:
Mat Noh, Muhamad Alfakri

Title:
Evaluation of the progenitor potential of monocyte/macrophage subsets in cardiovascular disease

Evaluation of the progenitor potential of monocyte/macrophage subsets in cardiovascular disease

Muhamad Alfakri Mat Noh

A dissertation submitted to the University of Bristol in accordance with the requirements for award of the degree of Doctor of Philosophy (Translational Health Sciences) in the Faculty of Health Sciences, Bristol Medical School

Aug 2021

Word count 45,458

Abstract

Current research has suggested that monocyte/macrophages can coexist as different phenotypes which display an array of disparate properties. Monocyte/macrophage subsets may also divergently harbour the ability to acquire characteristics of other vascular cell types, such as vascular smooth muscle cells (VSMC) and endothelial cells. These findings imply that monocytes yield progenitor potential which could be potentially exploited for therapeutic purposes. The aim of this study is to robustly assess the progenitor potential of different *in vitro* monocyte/macrophage subsets into other vascular cells, namely, VSMCs and endothelial cells. Cultured human primary monocytes with subsequent polarisation with macrophage-colony stimulating factor (M-CSF) and termed M-Mac, or granulocyte-macrophage colony stimulating factor (GM-CSF) and termed GM-Mac, can appear like VSMCs based on the expression of genes/proteins considered specific to VSMCs (namely α-SMactin, caldesmon, calmodulin, myosin heavy chain-11, smoothelin, and vimentin). GM-Macs display a greater VSMC-like gene expression pattern compared to their M-Mac counterparts, through up-regulation of α-SMactin, caldesmon, calmodulin, myosin heavy chain-11, smoothelin, and vimentin. Interestingly, gene and protein expression of the endothelial cell (EC)-specific markers PECAM-1 (CD31) and VE-cadherin (CDH5) are also expressed by cultured macrophages. Mirroring the VSMC-like cell experiments, GM-Macs display greater expression of EC markers than M-Macs. These findings infer that pro-inflammatory GM-Macs already harbour the ability to express VSMC-like and EC-like genes/proteins, whereas their anti-inflammatory M-Mac counterparts do not. Accordingly, we propose that GM-Macs may foster the ability to mimic vascular cells (VSMCs and/or ECs) in response to injury or under angiogenic conditions, to provide temporary barrier function for example. Interestingly, the growth factors FGF2 and VEGF-A were shown to upregulate PECAM-1 and VE-cadherin expression in M-Mac but not GM-Mac. We also observed an inverse relation between expression of VE-cadherin mRNA and protein expression in M-Mac after stimulation with FGF2, suggesting the involvement of a post-transcriptional regulatory mechanism. Indeed, M-Mac VE-cadherin protein expression was identified to be dependent upon microRNA (miR)-27a-3p. Moreover, miR-27a-3p levels appear to be regulated through a FGF-receptor type-1 and signal transducer and activator of transcription-3 (Stat3) signalling pathway. Finally, GM-Macs and FGF2-stimulated M-Macs harboured the ability to form angiogenic sprouts, supporting their transition towards an endothelial cell-like phenotype. In conclusion, the novel findings within this thesis demonstrate the divergent progenitor capacity of macrophage subsets, which may be utilised for cardiovascular therapeutic purposes.

Acknowledgements

I want to thank my supervisor Professor Dr Jason Lee Johnson for his unwavering support during this PhD project. Thank you so much for the excellent opportunity to work on this exciting research project. I appreciate your kind support and belief in me. Without Prof Johnson's guidance, enthusiasm and wisdom, I may not have been able to complete this study. And thank you for the understanding when I was not feeling well and unable to be in the office/lab.

To my co-supervisor, Professor Dr Sarah George, thank you for your continuous support. It was an excellent experience to work with you. Your insight throughout this PhD journey is much appreciated. Prof George's dedication, and organised work inspired me to carry on with the project. The meetings with lab members every Wednesday is an experience that I will miss very much. I have learnt a lot from you and the entire lab members. Thank you also for your concern on my health issues.

I would like to express my appreciation to Dr Karina De Gregoli for the advice and assistance throughout my research work. From the first-time meeting with Prof Johnson to sketch my very first lab work, followed by all the questions (I mean all matters including the annoying ones) until to the end of my lab works. I will never forget you as the person who taught me everything about working in the lab, always be organised and careful and source-person during my difficult times. Thank you, Karina, I have learned so much from you.

I thank all Prof Johnson's lab members, especially Dr Najmi M. Anuar, who has helped me during my first few months in the lab. To, Dr Rosaria Bianco, who willingly listened to my concerns, always motivating me when I was down, for the valuable tips and help with lab matters. Not to forget Prof George's lab members especially Dr Kerry Wadey, Dr Cressinda Lyon, Dr Helen William, Dr Bethan Monk, Dr Aleksandra Frankow, Dr Nadiah Sulaiman, Dr Andrew Bond, Dr Alexander Ward, Dr Silvia Boyajian and Dr Lien Mario Reolizo for all your help and support directly or indirectly in the lab and office, as well as for the chit chat during free and busy times. Not to forget Dr Steve J Simmonds, Dr Priyantha Kulatilake and Dr Georgia May Connolly, who helped me with bloodletting procedures. And to all others lab members and technicians in Research Floor Level Seven Queens Building, Bristol Royal Infirmary. Thank you all for being kind and patient with me all the time.

Finally, not to forget my family whose patience and generosity enabled me to take this PhD to completion. I was back on track and excited over my work in the early 2018 when I received the news of my mother's health deterioration and had to fly back to be with her until her last breath. Not long after, about a year later my father passed away. It was sudden news, and I never expected it as my father was in good health. I'm sad, not being able to share this success and happiness with my dear and beloved mother (Kamariah Aman; Apr 2018), my late father (Mat Noh Abd Wahab; Apr 2019), my dear brother (Saiful Nijam; 2009), my sister-in-law (Rafidah Harun; 2019), my dear nephews (Iskandar and Asyraf; 2020), and my dearest beloved sister Kamisah Mat Noh (kak dek; 16 July 2021). May all of you rest in peace.

I owe a debt of gratitude to my alma mater University Malaya for providing me with a fully supported study leave and to the Ministry of Higher Education, Malaysia for the sponsorship.

The experience of travelling to Bristol and living here is a once in a lifetime opportunity which may never happen again.

Author declaration:

I declare that the work in this dissertation was carried out in accordance with the requirements of the University's Regulation and Code of Practice for Research Degree Programmes and that it has not been submitted for any other academic awards. Except where indicated by specific reference in the text, work is the candidate's own work. Work done in collaboration with, or with assistance of, others, is indicated as such. Any views expressed in the dissertation are those of the author.

Signed: Date: 16/08/2021

Published Abstracts

M A Mat Noh, K Di Gregoli, S J George, J L Johnson; P22 PRO- AND ANTI-INFLAMMATORY MACROPHAGES DISPLAY DIVERGENT POLARISATION TOWARDS VASCULAR SMOOTH MUSCLE-LIKE AND ENDOTHELIAL-LIKE PHENOTYPES, Cardiovascular Research, Volume 114, Issue suppl_2, 1 September 2018, Pages S7–S8, https://doi.org/10.1093/cvr/cvy216.025

Unpublished Abstracts

M A Mat Noh, K Di Gregoli, S J George, J L Johnson; P25 MICRORNA-27a* REGULATES VE-CADHERIN EXPRESSION IN *IN VITRO* MACROPHAGE (BAS 2019)

Poster presentations

1. Poster presenter. British Atherosclerosis Society Autumn Meeting, Queens College, Cambridge; 6th – 7th September 2018.
2. Poster presenter. BSCR Autumn Meeting 2018, The Edge, Endcliffe Village, University of Sheffield; 10th – 11th September 2018.
3. Poster presenter. Bristol Heart Institute Specialist Research Institute - 2nd Annual Meeting, Life Sciences Building Atrium, University of Bristol. 20th September 2018.
4. Poster presenter. British Atherosclerosis Society Autumn Meeting, Keble College, Oxford; 26th – 27th September 2019.

Table of Contents

ABSTRACT I

ACKNOWLEDGEMENTS II

PUBLISHED ABSTRACTS IV

LIST OF FIGURES XII

LIST OF ABBREVIATIONS XX

1 INTRODUCTION 1

1.1 ATHEROSCLEROSIS 1

1.2 MONOCYTE SUBSETS 16

1.3 MACROPHAGE CLASSIFICATION 20

1.4 THE ROLE OF MONOCYTES AND MACROPHAGES IN ATHEROSCLEROSIS 22

1.5 MACROPHAGE SUBPOPULATIONS IN ATHEROSCLEROSIS 25

1.6 COLONY STIMULATING FACTORS AS REGULATORS OF MACROPHAGE PHENOTYPES 29

1.7 PROGENITOR POTENTIAL OF MONOCYTES AND MACROPHAGES 32

1.8 HYPOTHESES 35

1.9 PROJECT AIMS AND OBJECTIVES 35

2 MATERIALS AND METHODS 36

2.1 MACROPHAGE CULTURE AND POLARISATION 36

2.1.1 Isolation of Human Peripheral Blood Monocytes 36

2.1.2 Isolation of PBMCs from whole blood by density gradient centrifugation 36

2.1.3 Isolation of monocytes by adhesion 38

2.2 RPMI/FCS MEDIA 38

2.3 MACROPHAGE CULTURE 38

2.4 CELL COLLECTION FOR RNA ANALYSIS 39

2.5 RNA EXTRACTION AND PURIFICATION 39

2.6 RNA QUANTIFICATION 41

2.7 CDNA SYNTHESIS (REVERSE TRANSCRIPTION POLYMERASE CHAIN REACTION, RT-PCR) 42

2.8 96-well Quantitative-Polymerase Chain Reaction (Q-PCR) 44
2.9 Q-PCR data analysis 47
2.10 Western Blotting 47
2.10.1 Cell collection for protein analysis 47
2.10.2 Protein assay (Protein quantification) 47
2.10.3 Polyacrylamide Gel Electrophoresis (PAGE) 48
2.10.4 Stain free gels 48
2.10.5 Blotting & Immunodetection 49
2.11 Immunocytochemistry 52
2.12 Statistical analysis 54
3 *IN VITRO* HUMAN MACROPHAGES DISPLAY DIVERGENT POLARISATION TOWARDS VASCULAR SMOOTH MUSCLE CELL-LIKE PHENOTYPES 55
3.1 Introduction 55
3.1.1 Phenotypic modulation of vascular smooth muscle cells 55
3.1.2 Signalling factors supporting phenotypic modulation of vascular smooth muscle cells. 56
3.1.3 Gene and protein markers commonly associated with a vascular smooth muscle cell phenotype 58
3.2 Aim of this chapter 60
3.3 Materials and Methods 62
3.3.1 Macrophage culture 62
3.3.2 Stimulation of human macrophages with vascular smooth muscle cell (VSMC)-associated growth factors 62
3.3.3 Polarisation of mature human macrophages (M-Mac) to different phenotypes 63
3.3.4 Culture of human vascular smooth muscle cells (VSMCs) 64
3.4 Results 65
3.4.1 In vitro cultured human macrophages exhibit mixed morphology 65
3.4.2 GM-CSF-directed macrophage maturation is associated with increased expression of VSMC-associated markers in comparison to M-CSF matured macrophages 69

3.4.3 PDGF-BB and TGFβ1 co-stimulation divergently affects VSMC-associated marker expression between M-CSF and GM-CSF-matured macrophages *76*

3.4.4 Differing human macrophage phenotypes display distinct changes in their expression of VSMC-associated markers *85*

3.4.5 The expression of VSMC-related markers in M-CSF and GM-CSF matured macrophages relative to human coronary artery VSMCs *105*

3.4.6 In vitro macrophages retain macrophage marker expression after co-stimulation with PDGF-BB and TGFβ1 ..... *112*

3.5 DISCUSSION 115

3.6 CONCLUSION 122

4 *IN VITRO* MACROPHAGES DISPLAY DIVERGENT POLARISATION TOWARDS ENDOTHELIAL CELL-LIKE PHENOTYPES BY PRO-ANGIOGENIC GROWTH FACTOR 123

4.1 INTRODUCTION 123

4.1.1 Endothelial cell phenotypes *123*

4.1.2 Modulators of endothelial cell behaviour and function *125*

4.1.3 Gene and protein expression markers commonly associated with an endothelial cell *126*

4.2 AIM OF THIS CHAPTER 127

4.3 MATERIALS AND METHODS 127

4.3.1 Macrophage culture *127*

4.3.2 Stimulation of human macrophages with endothelial cell-associated growth factors *128*

4.3.3 Culture of human umbilical vein endothelial cells *129*

4.4 RESULTS 130

4.4.1 GM-CSF-directed macrophage maturation is associated with increased expression of EC-associated markers in comparison to M-CSF matured macrophages *130*

4.4.2 The effect of endothelial cell-associated growth factors on macrophage subset expression of endothelial cell-related genes *136*

4.4.3 Upregulation of PECAM-1 and VE-cadherin upon 4-days stimulation with VEGF-A and FGF2 in M-CSF macrophage *141*

4.4.4 The expression of endothelial cell-related markers in M-CSF and GM-CSF matured macrophages relative to human umbilical vascular endothelial cell levels 156

4.5 DISCUSSION 160

4.6 CONCLUSION 165

5 REGULATION OF VE-CADHERIN EXPRESSION IN MACROPHAGE BY MIR-27A-FGFR1-STAT3 PATHWAY 166

5.1 INTRODUCTION 166

5.1.1 The role of macrophage in angiogenesis 166

5.1.2 Non-endothelial vasculature 168

5.1.3 MicroRNA and angiogenesis 169

5.2 AIM OF THIS CHAPTER 173

5.3 MATERIALS AND METHODS 175

5.3.1 Macrophage culture and stimulation with FGF2 growth factor 175

5.3.2 Quantitative-PCR for microRNAs 175

5.3.3 Transfection experiment 176

5.3.4 Neutralising FGFR1-antibody experiment 177

5.3.5 STAT3 inhibitor experiment 177

5.3.6 Matrigel angiogenesis assay 178

5.4 RESULTS 179

5.4.1 FGF2 stimulation downregulates microRNA-27a-3p expression in M-CSF directed macrophages 179

5.4.2 Regulation of VE-cadherin protein expression by miR-27a-3p in M-CSF directed macrophages . 183

5.4.3 FGF2 signalling through FGFR1 regulates M-CSF matured macrophage VE-cadherin expression FGF2/FGFR1 regulates VE-cadherin expression 194

5.4.4 The STAT3 transcription factor regulates VE-cadherin expression in M-CSF matured macrophages 199

5.4.5 FGF2 stimulation of M-CSF matured macrophages increases in vitro angiogenesis 206

5.5 DISCUSSION 209

5.6 CONCLUSIONS 214

6 GENERAL DISCUSSION, CONCLUSION, LIMITATIONS AND FUTURE DIRECTIONS 215

6.1 General Discussion 215

6.2 Concluding remarks 223

6.3 Limitations of the study 224

6.4 Future directions 226

7 REFERENCES 228

8 APPENDIX A – (RESULT, CHAPTER 3) 259

8.1 Expression of VSMC-related markers in baseline M-CSF and GM-CSF macrophage and the effects of PDGF-BB and TGFβ1 259

8.1.1 Representative image for Stain Free Gel for baseline macrophage 259

8.1.2 CT values - caldesmon 260

8.1.3 Full blot image - caldesmon 260

8.1.4 CT values - calmodulin 261

8.1.5 Full blot image - calmodulin 261

8.1.6 CT values - Myh11 262

8.1.7 Full blot image - Myh11 262

8.1.8 CT values - smoothelin 263

8.1.9 Full blot image - smoothelin 263

8.1.10 CT values - vimentin 264

8.1.11 Full blot image - vimentin 264

8.2 Differing human macrophage phenotypes display distinct changes in their expression of VSMC-associated markers 265

8.2.1 Representative image for Stain Free Gel for M-CSF macrophage, IFNγ/LPS, IL-4 and IL-10, co-stimulation with PBGF-BB and TGFβ1 265

8.2.2 Representative image for Stain Free Gel for M-CSF, OxPAPC, PF4 and OxLDL 265

8.2.3 CT values - caldesmon 266

8.2.4 Full blot image – caldesmon 266

8.2.5 CT values – calmodulin 267

8.2.6 Full blot image – calmodulin 267

8.2.7 CT value – smoothelin 268

8.2.8 Full blot image – smoothelin 268

8.2.9 CT value - vimentin 269

8.2.10 Full blot image – vimentin 269

8.2.11 Full blot image - vimentin 270

8.2.12 CT value – Myh11 270

8.2.13 Full blot image – Myh11 271

8.2.14 Full blot image - smoothelin 271

8.2.15 Full blot image - caldesmon 272

8.2.16 Full blot image - calmodulin 272

9 APPENDIX B (RESULT, CHAPTER 4) 273

9.1 REPRESENTATIVE IMAGE FOR STAIN FREE GEL FOR BASELINE MACROPHAGE M-CSF & GM-CSF DAY-8, DAY-11 AND DAY-14 273

9.1.1 CT values - PECAM-1 273

9.1.2 Full blot image – Stain free gel and PECAM-1 274

9.1.3 CT values - VE-cadherin 274

9.1.4 Full blot image – VE-cadherin 275

9.1.5 CT values - PECAM-1 276

9.1.6 CT values – VE-cadherin 277

9.1.7 CT values – PECAM1 278

9.2 REPRESENTATIVE IMAGE FOR STAIN FREE GEL FOR BASELINE MACROPHAGE M-CSF STIMULATED WITH 50 NG/ML ENDOTHELIAL GROWTH FACTOR FOR FOUR-DAY 279

9.2.1 Full blot image – PECAM-1 279

9.2.2 CT values – VE-cadherin 280

9.2.3 Full blot image – VE-cadherin 280

9.2.4 CT values – PECAM1 280

9.3 REPRESENTATIVE IMAGE FOR STAIN FREE GEL FOR BASELINE MACROPHAGE GM-CSF STIMULATED WITH 50 NG/ML ENDOTHELIAL GROWTH FACTOR FOR FOUR-DAY 281

9.3.1 Full blot image – PECAM-1 281

9.3.2 CT values – VE-cadherin 282

9.3.3 Full blot image – VE-cadherin 282

10 APPENDIX C (RESULT, CHAPTER 5) 283

10.1 CT VALUES FOR MICRORNA 283

10.1.1 CT values for microRNA-101-3p 283

10.1.2 CT values for microRNA-101-5p 283

10.1.3 CT values for microRNA-27a-3p 284

10.1.4 CT values for microRNA-27a-5p 284

10.1.5 Full blot image for transfection experiment 285

10.1.6 CT values VE-cadherin mRNA (transfection experiment) 285

10.1.7 CT values microRNA-27a-3p (transfection experiment) 286

10.1.8 CT values FGFR1 mRNA (transfection experiment) 286

10.1.9 CT values VE-cadherin mRNA (FGFR1 neutralising antibody experiment) 286

10.1.10 Full blot (FGFR1 neutralising antibody experiment) 287

10.1.11 CT values microRNA-27a-3p (FGFR1 neutralising antibody experiment) 287

10.1.12 CT values FGFR1 mRNA (neutralising antibody experiment) 287

10.1.13 Full blot (FGFR1 neutralising antibody experiment) 288

10.1.14 Full blot STAT3 (neutralising antibody experiment) 288

10.1.15 Full blot VE-cadherin and STAT3 (niclosamide experiment) 289

10.1.16 CT values VE-cadherin mRNA (niclosamide experiment) 290

LIST OF FIGURES

Figure 1.1.1 Spectrum of clinical conditions due to atherosclerosis 3

Figure 1.1.2 Schematic diagram of a medium sized artery 6

Figure 1.1.3 Low-density lipoprotein (LDL) retention within the arterial wall..... 7

Figure 1.1.4 Different classes of lipoproteins 9

Figure 1.1.5 Lipoprotein structure 10

Figure 1.1.6 Schematic diagram of a stable atherosclerotic plaque 14

Figure 1.4.1 Monocytes and macrophages in atherosclerosis 24

Figure 1.5.1 Specific macrophage subpopulations found within atherosclerosis plaques 26

Figure 1.6.1 Haematopoietic cytokines involved in the differentiation of blood cells and immune cells..... 30

Figure 1.6.2 Colony stimulating factors (CSF) as regulators of macrophage phenotype 31

Figure 2.1.1 Isolation of PBMCs 36

Figure 2.1.2 Isolation of PBMCs using SepMate^{TM} tubes 37

Figure 2.10.1 Schematic diagram layering of an assembled transfer pack (Bio-Rad)..... 49

Figure 3.1.1 Phenotypic switching of vascular smooth muscle cell phenotype. 56

Figure 3.4.1 Effect of M-CSF and GM-CSF maturation on the morphology of human macrophages 65

Figure 3.4.2 Effect of M1 and M2 polarisation on the morphology of M-CSF matured human macrophages . 67

Figure 3.4.3 Photomicrograph of foam cells in culture. 68

Figure 3.4.4 Photomicrograph of primary arterial vascular smooth muscle culture in DMEM full media. 68

Figure 3.4.5 GM-CSF maturation increases human macrophage α-SM-actin protein expression compared to M-CSF matured macrophages. 70

Figure 3.4.6 Caldesmon mRNA and protein expression in macrophage baseline cultures. 71

Figure 3.4.7 GM-CSF maturation increases human macrophage calmodulin mRNA and protein expression compared to M-CSF matured macrophages..... 72

Figure 3.4.8 Myh11 mRNA and protein expression in macrophage baseline cultures. 73

Figure 3.4.9 GM-CSF maturation increases human macrophage smoothelin mRNA and protein expression compared to M-CSF matured macrophages..... 74

Figure 3.4.10 GM-CSF maturation increases human macrophage vimentin mRNA and protein expression compared to M-CSF matured macrophages.....75

Figure 3.4.11 The effects of PDGF-BB and TGFβ1 co-stimulation on calmodulin mRNA and protein expression in M-CSF polarised macrophages. 78

Figure 3.4.12 The effects of PDGF-BB and TGFβ1 co-stimulation on Myh11 mRNA and protein expression in M-CSF polarised macrophages. 79

Figure 3.4.13 The effects of PDGF-BB and TGFβ1 co-stimulation on smoothelin mRNA and protein expression in M-CSF polarised macrophages. 80

Figure 3.4.14 PDGF-BB and TGFβ1 increases human M-CSF polarised macrophage vimentin mRNA and protein expression. 81

Figure 3.4.15 The effect of PDGF-BB and TGFβ1 co-stimulation on caldesmon mRNA and protein expression in GM-CSF polarised macrophages. 82

Figure 3.4.16 The effects of PDGF-BB and TGFβ1 co-stimulation on calmodulin mRNA and protein expression in GM-CSF polarised macrophages. 83

Figure 3.4.17 The effects of PDGF-BB and TGFβ1 co-stimulation on vimentin mRNA and protein expression in GM-CSF polarised macrophages. 84

Figure 3.4.18 The effects of PDGF-BB and TGFβ1 co-stimulation on caldesmon mRNA and protein expression in M-CSF/IFNγ/LPS polarised macrophages. 87

Figure 3.4.19 The effects of PDGF-BB and TGFβ1 co-stimulation on calmodulin mRNA and protein expression in M-CSF/IFNγ/LPS polarised macrophages. 88

Figure 3.4.20 The effects of PDGF-BB and TGFβ1 co-stimulation on smoothelin mRNA and protein expression in M-CSF/IFNγ/LPS polarised macrophages. 89

Figure 3.4.21 The effects of PDGF-BB and TGFβ1 co-stimulation on vimentin mRNA and protein expression in M-CSF/IFNγ/LPS polarised macrophages. 90

Figure 3.4.22 The effects of PDGF-BB and TGFβ1 co-stimulation on caldesmon mRNA and protein expression in M-CSF/IL4 polarised macrophages. 91

Figure 3.4.23 The effects of PDGF-BB and TGFβ1 co-stimulation on calmodulin mRNA and protein expression in M-CSF/IL4 polarised macrophages. 92

Figure 3.4.24 The effects of PDGF-BB and TGFβ1 co-stimulation on calmodulin mRNA and protein expression in M-CSF/IL10 polarised macrophages. 93

Figure 3.4.25 The effects of PDGF-BB and TGFβ1 co-stimulation on smoothelin mRNA and protein expression in M-CSF/IL10 polarised macrophages. 94

Figure 3.4.26 The effects of PDGF-BB and TGFβ1 co-stimulation on vimentin mRNA and protein expression in M-CSF/PF4 polarised macrophages. 95

Figure 3.4.27 The effects of PDGF-BB and TGFβ1 co-stimulation on Myh11 mRNA and protein expression in M-CSF/oxPAPC polarised macrophages. 96

Figure 3.4.28 The effects of PDGF-BB and TGFβ1 co-stimulation on vimentin mRNA and protein expression in M-CSF/oxPAPC polarised macrophages. 97

Figure 3.4.29 The effects of PDGF-BB and TGFβ1 co-stimulation on smoothelin mRNA and protein expression in M-CSF/oxPAPC polarised macrophages. 98

Figure 3.4.30 The effects of PDGF-BB and TGFβ1 co-stimulation on caldesmon mRNA and protein expression in M-CSF/oxLDL polarised macrophages. 99

Figure 3.4.31 The effects of PDGF-BB and TGFβ1 co-stimulation on calmodulin mRNA and protein expression in M-CSF/oxLDL polarised macrophages. 100

Figure 3.4.32 The effects of PDGF-BB and TGFβ1 co-stimulation on Myh11 mRNA and protein expression in M-CSF/oxLDL polarised macrophages. 101

Figure 3.4.33 The effects of PDGF-BB and TGFβ1 co-stimulation on vimentin mRNA and protein expression in M-CSF/oxLDL polarised macrophages. 102

Figure 3.4.34 The effects of PDGF-BB and TGFβ1 co-stimulation on smoothelin mRNA and protein expression in M-CSF/oxLDL polarised macrophages. 103

Figure 3.4.35 Summary result for polarised M-CSF macrophages with PDGF-BB + TGFβ1 co-stimulation 104

Figure 3.4.36 Caldesmon mRNA and protein expression in M-CSF or GM-CSF polarised macrophages relative to human coronary artery VSMC. 106

Figure 3.4.37 Calmodulin mRNA and protein expression in M-CSF or GM-CSF polarised macrophages relative to human coronary artery VSMCs. 107

Figure 3.4.38 Myh11 mRNA and protein expression in M-CSF or GM-CSF polarised macrophages relative to human coronary artery VSMCs.....108

Figure 3.4.39 Smoothelin mRNA and protein expression in M-CSF or GM-CSF polarised macrophages relative to human coronary artery VSMCs. 109

Figure 3.4.40 Vimentin mRNA and protein expression in M-CSF or GM-CSF polarised macrophages relative to human coronary artery VSMCs.....110

Figure 3.4.41 Summary result for VSMC and macrophage 111

Figure 3.4.42 Fluorescent immunocytochemistry for Mac-2 (galectin-3) protein expression in human macrophage subsets with and without PDGF-BB and TGFβ1 co-stimulation. 113

Figure 3.4.43 Effect of M-CSF or GM-CSF macrophage maturation and subsequent co-incubation with PDGF-BB and TGFβ1 on Mac-2 expression. 114

Figure 4.4.1 PECAM-1 mRNA and protein expression in macrophage baseline cultures. 131

Figure 4.4.2 GM-CSF maturation increases human macrophage PECAM-1 protein expression compared to M-CSF matured macrophages.....132

Figure 4.4.3 VE-cadherin mRNA and protein expression in macrophage baseline cultures 134

Figure 4.4.4 GM-CSF maturation increases human macrophage VE-cadherin protein expression compared to M-CSF matured macrophages 135

Figure 4.4.5 PECAM-1 mRNA expression in human macrophages stimulated with endothelial cell related growth factors for 24 hours.....138

Figure 4.4.6 VE-cadherin mRNA expression in human macrophages stimulated with endothelial cell related growth factors for 24 hours.....139

Figure 4.4.7 Summary of results for the effect of 24 hour stimulation with VEGF-A or FGF2 on the mRNA expression of PECAM1 and CDH5 (VE-cadherin) in 7-day differentiated macrophages.....140

Figure 4.4.8 PECAM-1 mRNA and protein expression in M-CSF macrophages stimulated with endothelial cell related growth factors for four-days. 142

Figure 4.4.9 Immunofluorescence localisation of PECAM-1 in M-CSF macrophages stimulated with endothelial cell-related growth factors for four-day.....143

Figure 4.4.10 Quantification of immunofluorescence cell positivity of PECAM-1 in M-CSF macrophages stimulated with endothelial-cell related growth factors for four-days. 144

Figure 4.4.11 VE-cadherin mRNA and protein expression in M-CSF macrophages stimulated with endothelial cell-related growth factors for four-days. 146

Figure 4.4.12 Immunofluorescence localisation of VE-cadherin in M-CSF macrophages stimulated with endothelial cell-related growth factors for four-days. 147

Figure 4.4.13 Quantification of immunofluorescence cell positivity of VE-cadherin in M-CSF macrophages stimulated with endothelial cell-related growth factors for four-days. 148

Figure 4.4.14 PECAM-1 mRNA and protein expression in GM-CSF macrophages stimulated with endothelial cell-related growth factors for four-days. 149

Figure 4.4.15 Immunofluorescence localisation of PECAM-1 in GM-CSF macrophages stimulated with endothelial cell-related growth factors for four-days. 150

Figure 4.4.16 Quantification of immunofluorescence cell positivity of PECAM-1 in GM-CSF macrophages stimulated with endothelial cell-related growth factors for four-days. 151

Figure 4.4.17 CDH5 (VE-cadherin) mRNA and protein expression in GM-CSF macrophages stimulated with endothelial cell-related growth factors for four-days. 152

Figure 4.4.18 Immunofluorescence localisation of VE-cadherin in GM-CSF macrophages stimulated with endothelial cell-related growth factors for four-days. 153

Figure 4.4.19 Quantification of immunofluorescence cell positivity of VE-cadherin in GM-CSF macrophages stimulated with endothelial cell-related growth factors for four-days. 154

Figure 4.4.20 Summary of results for the effects of 4-day stimulation with endothelial cell-related growth factors on the mRNA and protein expression of PECAM-1 and CDH5 (VE-cadherin) in 7-day differentiated macrophages. 155

Figure 4.4.21 PECAM-1 mRNA and protein expression in human macrophage subsets and human umbilical vein endothelial cells. 157

Figure 4.4.22 CDH5 (VE-cadherin) mRNA and protein expression in human macrophages and human umbilical vein endothelial cells. 158

Figure 4.4.23 Summary of results for the relative mRNA and protein expression of PECAM-1 and VE-cadherin in baseline macrophage subsets and HUVECs. 159

Figure 5.1.1 Macrophage role in brain endothelium repair 167

Figure 5.4.1 Expression of miR-27a-3p in human macrophage subsets. 180

Figure 5.4.2 Expression of miR-27a-5p in human macrophage subsets. 180

Figure 5.4.3 Summary of results for the relative VE-cadherin mRNA and protein expression alongside miR-27a-3p levels in M-CSF and GM-CSF matured macrophage subsets with and without FGF2 stimulation 181

Figure 5.4.4 Validation of RVG-9dr-mediated transfection. 185

Figure 5.4.5 VE-cadherin protein expression in M-CSF directed macrophages with or without a miR-27a-3p-mimic or inhibitor. 186

Figure 5.4.6 Immunofluorescence labelling for VE-cadherin in M-CSF directed macrophages with or without a miR-27a-3p-mimic or inhibitor. 187

Figure 5.4.7 Quantification of immunofluorescence cell positivity of VE-cadherin in M-CSF macrophages with or without a miR-27a-3p-mimic or inhibitor. 188

Figure 5.4.8 CDH5 (VE-cadherin) mRNA expression in M-CSF directed macrophage with or without a miR-27a-3p-mimic and -inhibitor. 190

Figure 5.4.9 Effect of miR-27a-3p mimic or inhibitor treatment on M-CSF matured macrophage miR-27a-3p levels. 192

Figure 5.4.10 Summary of results assessing the effect of a miR-27a-3p mimic or inhibitor on mRNA and protein expression of VE-cadherin alongside miR-27a-3p levels in M-CSF directed macrophages with and without FGF2 stimulation. 193

Figure 5.4.11 FGFR1 mRNA expression in M-CSF matured macrophages. 194

Figure 5.4.12 Addition of a FGFR1 neutralising antibody prevents FGF2-induced regulation of VE-cadherin mRNA and protein expression in M-CSF matured macrophages. 196

Figure 5.4.13 Addition of a FGFR1 neutralising antibody prevents FGF2-induced regulation of miR-27a-3p expression in M-CSF matured macrophages. 197

Figure 5.4.14 FGFR1 mRNA and protein expression were unaffected by addition of a FGFR1 neutralising antibody in M-CSF matured macrophages. 198

Figure 5.4.15 FGF2 stimulation increases STAT3 phosphorylation in M-CSF matured macrophages and is dependent on FGFR1. 200

Figure 5.4.16 Niclosamide (STAT3 inhibitor) decreases VE-cadherin protein expression and STAT3 phosphorylation in FGF2 stimulated M-CSF macrophages. 202

Figure 5.4.17 Niclosamide decreases VE-cadherin expression and STAT3 phosphorylation in FGF2 stimulated M-CSF macrophages. 203

Figure 5.4.18 Niclosamide (STAT3 inhibitor) reduces VE-cadherin protein expression and STAT3 phosphorylation in FGF2 stimulated M-CSF macrophages. 204

Figure 5.4.19 Niclosamide (STAT3 inhibitor) increases CDH5 (VE-cadherin) mRNA expression and microRNA-27a-3p levels in FGF2 stimulated M-CSF macrophages. 204

Figure 5.4.20 Summary of results assessing the effect of a FGFR1 neutralising antibody on M-CSF directed macrophages. 205

Figure 5.4.21 Summary of results assessing the effect of STAT3 inhibition on FGF2-stimulated M-CSF directed macrophages. 205

Figure 5.4.22 FGF2 stimulation of M-CSF matured macrophages increases *in vitro* angiogenesis. 207

Figure 5.4.23 Niclosamide (STAT3 inhibitor) reduces *in vitro* angiogenesis in FGF2-stimulated M-CSF matured macrophages. 208

LIST OF TABLES

Table 1.2.1 Classification of human monocytes based upon CD14 and CD16 cell-surface receptor expression, and characterisation of mouse monocytes based on Ly6C cell-surface levels **19**

Table 1.3.1 *In vitro* macrophage phenotypes **20**

Table 2.3.1 Growth factors for macrophages used in this study. **39**

Table 2.7.1 Reverse-transcription reaction components **42**

Table 2.7.2 Reverse Transcription reaction components (miScript) **43**

Table 2.8.1 QuantiTect primer assay used for QPCR **44**

Table 2.8.2 Home designed primers used in the study **45**

Table 2.8.3 Master reaction mixture including LightCycler® 480 SYBR Green I Master reaction mix **46**

Table 2.8.4 QPCR reaction protocol used in the study **46**

Table 2.10.1 Primary antibodies used for immunodetection of VSMC-markers by Western blotting **50**

Table 2.10.2 Primary antibodies used for immunodetection of EC-markers by Western blotting **51**

Table 2.10.3 Secondary antibodies used for immunodetection by Western blotting **51**

Table 2.11.1 Primary antibodies used for immunofluorescence labelling of VSMC-markers **53**

Table 2.11.2 Primary antibodies used for immunofluorescence labelling of EC-markers **53**

Table 3.2.1 Polarisation of macrophages into various phenotypes *in vitro* **61**

Table 3.3.1 Vascular smooth muscle cell-associated growth factors used for macrophage stimulation **62**

Table 3.3.2 Factors used for the polarisation of distinct macrophage phenotypes **63**

Table 4.3.1 Endothelial cell-associated growth factors used for macrophage stimulation **129**

Table 4.4.1 References for endothelial cell-related growth factors concentrations used *in vitro* **137**

Table 5.3.1 Primer assay used for QPCR **175**

Table 5.3.2 Master reaction mixture LightCycler® 480 SYBR Green I Master for microRNA Q-PCR **176**

Table 5.3.3 Reagents used in transfection experiment **177**

LIST OF ABBREVIATIONS

α-SM-actin = α smooth muscle actin
ACS = acute coronary syndrome
ANOVA = Analysis of variance
ANPTL5 = Angiopoietin-like 5
ATF2 = activating transcription factor-2
ATP = adenosine triphosphate
CAD = coronary artery disease
CD = cluster of differentiation
CXCL4 = (C-X-C motif) chemokine ligand 4
DAPI = 4',6-diamidino-2-phenylindole
DMEM = Dulbecco's modified Eagle's Medium
DPBS = Dulbecco's Phosphate Buffered Saline
ECG = electrocardiogram
ECs = endothelial cells
eNOS = endothelial nitric oxide synthase
FCS = Foetal Calf Serum
FGF2 = fibroblast growth factor 2
FGFR1 = fibroblast growth factor-receptor 1
Gal-3 = galectin-3
GM-CSF = granulocyte macrophage colony stimulating factor
GM-Mac = GM-CSF derived macrophage
HBSS = Hank's Balanced Salt Solution
HGF = Hepatocyte growth factor
HSC = Haematopoietic stem cells
HUVECs = Human umbilical vein endothelial cells
ICAM-1 = intercellular adhesion molecule 1
IFNγ = interferon γ
IGF-1 = Insulin-like growth factor 1
IgG = immunoglobulin G
IL = interleukin
LPS = lipopolysaccharide
M-CSF = macrophage colony stimulating factor
M-Mac = M-CSF derived macrophage
M1 = classically activated phenotypes
M2 = alternatively activated phenotypes
MCP-1 = monocyte chemotactic protein-1
MI = myocardial infarction
MMP = matrix metalloproteinases
Myh11 = myosin heavy chain 11
NAb = neutralising antibody
NFκB = nuclear factor-kappa B
NO = nitric oxide
NSTEMI = non-ST segment elevation myocardial infarction
oxLDL = oxidised low-density lipoprotein
oxPAPC = oxidised 1-palmitoyl-2-arachidonoyl-sn-glycero-3-phosphorylcholine
PBMC = peripheral blood mononuclear cells
PDGF-BB = Platelet derived growth factor BB
PECAM-1 = Platelet Endothelial Cell Adhesion Molecule-1

PF4 = platelet factor 4
RPMI = Roswell Park Memorial Institute Medium
STAT3 = Signal Transducer and Activator of Transcription 3
STEMI = ST segment elevation myocardial infarction
TGFβ1 = Transformation growth factor β1
TIMP-3 = Tissue inhibitor of metalloproteinases-3
TNFα = tumour necrosis factor α
VCAM-1 = vascular cell adhesion molecule-1
VEGF-A = vascular endothelial growth factor A
VSMCs = vascular smooth muscle cells
vWF = von Willebrand Factor

1 Introduction

1.1 Atherosclerosis

Coronary artery disease (CAD) due to atherosclerosis is listed as the most common cause of death not only within western countries, but more recently also in less-developed parts of the world (World Health Organisation, 2014). CAD can be defined as a spectrum of clinical manifestations due to underlying atherosclerosis that causes occlusion of an affected coronary artery and associated ischaemia of the related myocardial tissue. Depending on the severity of the arterial occlusion and degree of myocardial ischaemia (Figure 1.1.1), CAD can be categorised based on the clinical manifestations/presentation into stable angina and acute coronary syndrome (ACS) (Sanchis-Gomar *et al.,* 2016). Stable angina is associated with significant occlusion of one or more coronary arteries, and can be triggered by physical exertion or emotional stress that places further oxygen demand from the arterial supply to the myocardial tissue, with symptoms (such as chest pain) typically resolving after administration of glyceryl trinitrate (National Clinical Guidelines Centre, 2011). On the other hand, acute coronary syndrome (ACS) is associated with thrombus formation overlying an unstable atherosclerotic plaque and can be further stratified as unstable angina or myocardial infarction (MI) (Libby and Theroux, 2005). Unstable angina is associated with chest pain at rest (without a triggering factor) and pathologically characterised by ischaemia of the myocardial tissues without necrotic changes. However, if left untreated, MI can ensue.

The diagnosis of ACS requires careful interpretation of clinical signs and symptoms (most commonly chest pain with other non-constitutional signs/symptoms, such as tachycardia, perfuse sweating, and hypertension) together with raised circulating cardiac proteins (for example troponin and creatinine kinase) as well as changes in electrocardiogram (ECG) (Barstow *et al.*, 2017). Elevated levels of cardiac enzymes require at least 3-4 hours before their detection in the serum, thus are not considered as a sensitive early detection tool compared to ECG (Kumar and Cannon, 2009). Therefore, ECG is the easiest and earliest test that is commonly performed in suspected MI patients.

Nevertheless, no changes in ECG does not rule out MI, as in the case of non-ST segment elevation myocardial infarction (NSTEMI) (Barstow *et al.,* 2017). Therefore, through the ECG findings upon presentation of high-risk patient to emergency, MI can be classified as either STEMI (ST segment elevation myocardial infarction) or NSTEMI.

These two spectrums of CAD require different therapeutic interventions (Jneid *et al.,* 2017) even though the underlying pathogenesis of both are relatively similar. Previously, MI used to be classified based on the extent of non-viable (necrotic) myocardial tissue (heart wall), however, this no longer applies, as MI should be treated as soon as possible to prevent further damage to the heart (myocardium).

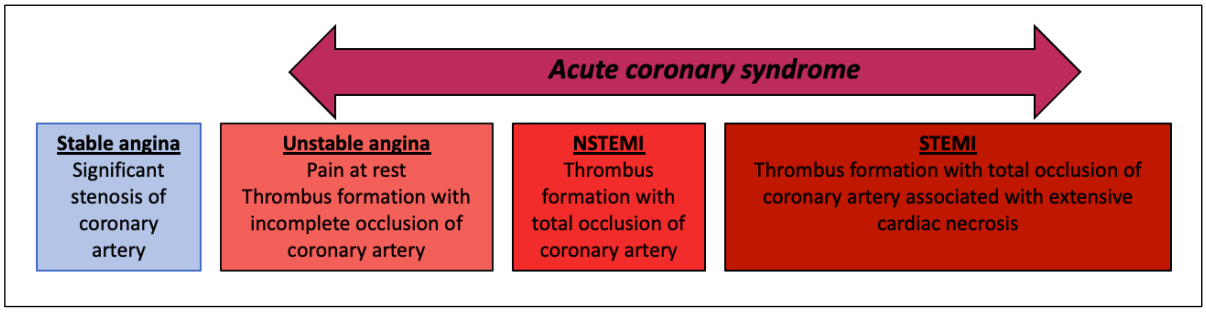

Figure 1.1.1 Spectrum of clinical conditions due to atherosclerosis

Based on clinical presentation, coronary artery disease is classified into stable angina and acute coronary syndrome (ACS). Stable disease is associated with chest pain commonly associated with physical exertion or emotional stress. Significant blockage or stenosis of the arterial lumen by atherosclerotic plaque is the underlying pathology. Chest pain can occur without any triggering factor during rest and is classified as unstable angina and may be relieved upon administration of glyceryl trinitrate (GTN), a vasodilator agent. It is associated with sudden blockage of the coronary artery due to thrombus formation overlying an atherosclerotic plaque, this blockage does not however cause complete obstruction. Persistent chest pain not relieved by vasodilator agents warrants prompt intervention as it indicates MI with almost total to complete lumen occlusion by thrombus formation over an atherosclerotic plaque. Based on ST segment evaluation from an electrocardiogram, MI can be classified into ST-elevation or non-ST elevation MI. STEMI is associated with significant cardiac muscle (myocardium) death (necrosis) compared to less extensive damage to the myocardium in NSTEMI.

Adapted from original source https://www.thrombosisadviser.com/coronary-and-peripheral-artery-disease.

Atherosclerosis is a focal, chronic inflammatory, fibro-proliferative response to injury, which despite the presence of systemic risk factors, occurs at localised susceptible sites within main arteries such as the coronary and carotid arteries.

It is believed that endothelial dysfunction plays a significant role in initiating atherosclerosis before any visible structural changes within the vessel wall (Gimbrone and García-Cardeña, 2016; Stary, 2000). In addition to atherogenesis, endothelial dysfunction persistently contributes to subsequent plaque progression and associated complications such as plaque rupture and thrombus formation (Bonetti *et al.*, 2003). Systemic risk factors continually expose the endothelium to hypertension, excess lipid (hyperlipidaemia), hyperglycaemia as well as tobacco toxins (as in chronic smoking), collectively identified as traditional risk factors of atherosclerosis, and can all induce and contribute to ongoing endothelial injury or dysfunction in part through increased oxidative stress (Singh and

Jialal, 2006). Oxidative stress reduces the bioavailability of nitric oxide (NO), one of the most important substances released by intact functional endothelium for normal vascular homeostasis. Reduced bioavailability of NO is associated with vasospasms, thrombosis, vascular inflammation, and the migration and proliferation of medial vascular smooth muscle cells (VSMCs) into the intima, all actions which collectively promote atherogenesis (Förstermann, 2010; Singh and Jialal, 2006).

As mentioned above, atherosclerosis occurs at selective sites such as the branching points (for example bifurcations) or curvatures within major arteries. At these locations, the pattern of blood flow is disturbed, resulting in haemodynamically-characterised oscillatory low shear stress, that predisposes to endothelial dysfunction (Chiu and Chien, 2011). In the straight segments of artery, where blood flow is unidirectional with haemodynamically normal laminar shear stress, the endothelium is protected from becoming dysfunctional through the maintained expression of Krüppel-Like Factor 2 (KLF2) and nuclear factor (erythroid-derived 2)-like 2 (NRF2) transcription factors (Fledderus *et al.,* 2008). NRF2 regulates expression of downstream genes associated with antioxidant molecules such as catalase, superoxide dismutase (SOD), and glutathione, which collectively protect from oxidative stress (Gupte *et al.,* 2013). Whereas KLF2 is involved with variety of biochemical process that are critical to the regulation of endothelial homeostasis, such as inducers of endothelial nitric oxide synthase (eNOS) and thrombomodulin (TM), enzymes responsible for sustained NO production and anti-coagulant release at the luminal surface of endothelial cells, respectively (SenBanerjee *et al.,* 2004).

Reportedly, KLF2 can also inhibit the activity of the nuclear factor-kappa B (NFκB)- and activating transcription factor-2 (ATF2)-signalling pathways, both key regulators of pro-inflammatory responses (Nayak *et al.,* 2011). KLF2 binds to p300, a critical NFκB co-activator, and hence inhibits the expression of NFκB-mediated down-stream pro-inflammatory genes such as intercellular adhesion molecule 1 (ICAM-1), vascular cell adhesion molecule-1 (VCAM-1), E-selectin, platelet-derived growth factor -BB (PDGF-BB), interleukin-1alpha (IL-1α), bone morphogenic protein-4 (BMP-4),

monocyte chemotactic protein-1 (MCP-1) and the vasoconstrictor gene endothelin-1 (ET-1) (Jha and Das, 2017; Nigro *et al.,* 2011). Whereas by preventing nuclear localisation of phosphorylated ATF2, KLF2 supresses activator protein-1 (AP-1) down-stream gene expression, a prominent pro-inflammatory transcription factor (Fledderus *et al.,* 2007).

On the contrary, disturbed and oscillatory low shear stress areas are associated with reduced KLF2 and NRF2 expression, and concomitant upregulation of the AP-1 and NFκB pro-inflammatory signalling pathways (Nagel *et al.,* 1999). Thus, endothelial cells exposed to disturbed-flow are pre-conditioned with high oxidative stress and pro-inflammatory states and hence predisposed to initiate atherogenesis (Nigro *et al.,* 2011). Besides differential gene expression, the arterial endothelium at disturbed flow regions also undergo rapid and constant turnover, which is associated with increased vascular permeability, favouring lipid insudation within the arterial wall (Chien, 2003; Chiu *et al.,* 1998).

In addition, alterations in blood flow and shear stress also affects the behaviour of medial VSMCs. Reportedly, disturbed oscillatory shear stress is associated with reduced VSMC apoptosis via an (endothelial-derived) NO dependant signalling pathway (Bennett, 1999; Fitzgerald *et al.,* 2008), enhanced VSMC migration via increased matrix metalloproteinase (MMP) expression (such as MMP-2) (Garanich *et al.,* 2005), and heightened VSMC proliferation via PDGF-BB and TGFβ-signalling pathways (Palumbo *et al.,* 2002; Ueba *et al.,* 1997). Collectively, these findings demonstrate that VSMC at athero-prone sites acquire specific characteristics, which are associated with features of a synthetic VSMC phenotype (refer to section 3.1.1 Phenotypic modulation of vascular smooth muscle cells).

Within the normal artery (Figure 1.1.2), VSMCs are not usually present within the tunica intima but are the main cellular component of the underlying tunica media. Nevertheless, in some areas of arterial segments (such as branch points/bifurcations and curvatures), VSMCs accumulate within the tunica intima in early life without any associated lipid accumulation, and are termed as adaptive or

diffuse intimal thickenings (Nakashima *et al.,* 2002; Nakashima *et al.,* 2007). However, these intimal thickenings can progress later in life to involve lipid accumulation and various degrees of monocyte infiltration and subsequent macrophage accumulation (Nakashima *et al.,* 2002). Therefore, there are athero-prone areas within coronary and carotid arteries predisposed to atherosclerotic plaque development.

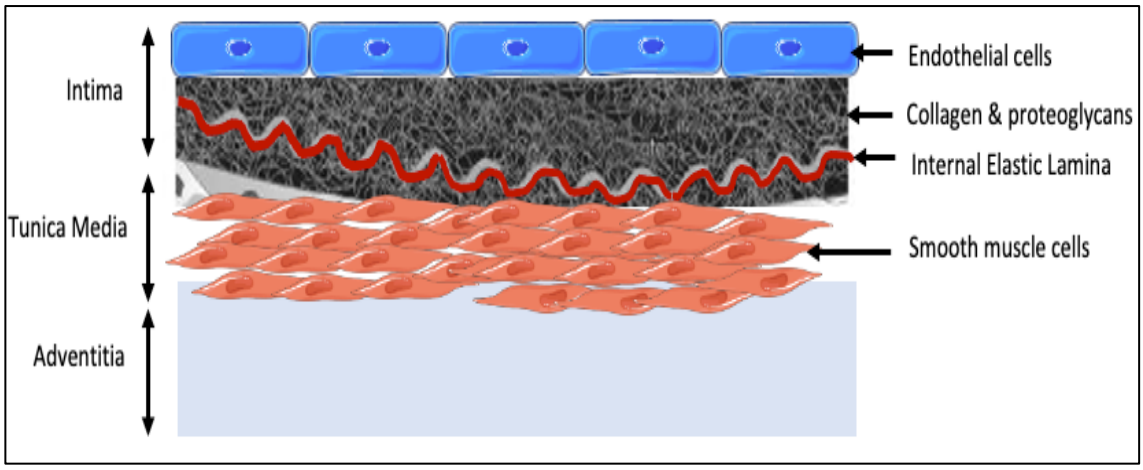

Figure 1.1.2 Schematic diagram of a medium sized artery

The arterial wall of a healthy artery is comprised of a monolayer of endothelial cells resting upon basement membrane. Beneath the endothelial layer is a potential subendothelial space comprised of extracellular matrix proteins such as collagen and proteoglycans. The intima is thin layer (size is exaggerated in this diagram) separated by an internal elastic lamina from the underlying tunica media, which consists of vascular smooth muscle cells and extracellular matrix components. However, in some regions vascular smooth muscle cells may be present within the tunica intima without any lipid deposition, termed as adaptive intimal thickening. Image adapted from original source (Lusis, 2000) and made using elements retrieved from https://smart.servier.com.

Essentially, the transformation of adaptive intimal thickenings into early atherosclerotic lesions involves the perpetual accumulation and retention of lipid within the wall at these sites (Figure 1.1.3). Interestingly, lipid accumulation within the arterial wall has been documented not only in the diseased arterial wall but also within the healthy artery (Rapp, 1989; Smith and Staples, 1982). This suggests that normal lipid metabolism involves its entry into and efflux from the arterial wall. Relatedly, chronic hyperlipidaemia is another important regulator in the pathogenesis of

atherosclerosis besides endothelial dysfunction, even in the absence of other risk factors (Glass and Witztum, 2001).

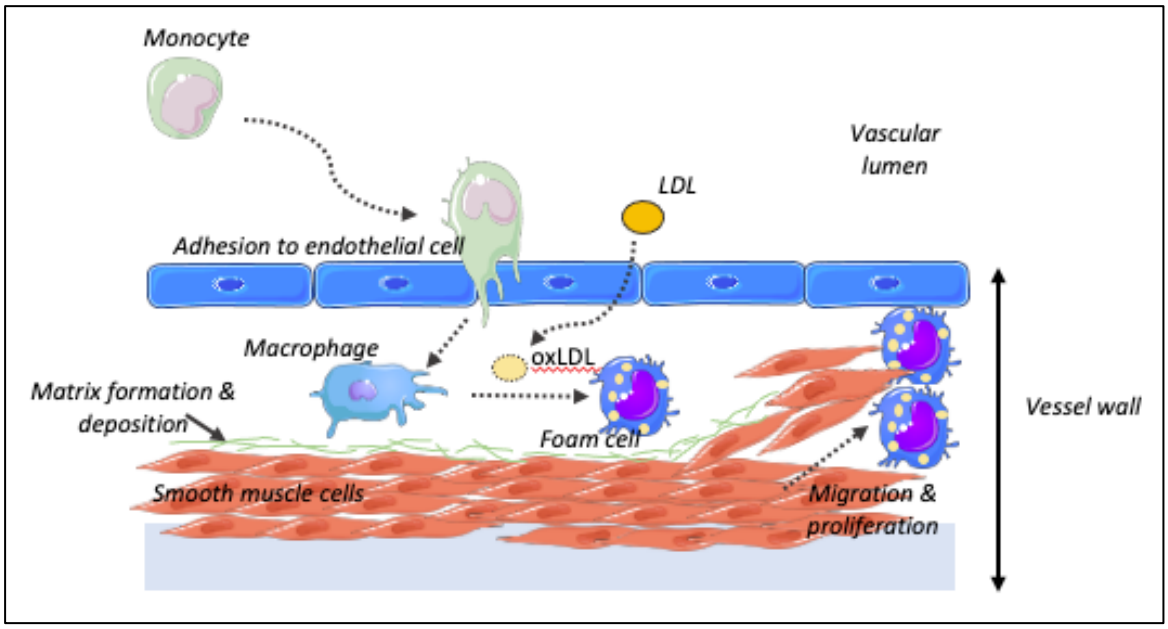

Figure 1.1.3 Low-density lipoprotein (LDL) retention within the arterial wall

In the atheroprone region of an artery, an insult to the integrity of endothelium can be triggered by disturbed/oscillatory low shear stress through elevated oxidative stress and reduced bioavailability of NO. This is associated with conditions that favours atherogenesis such as upregulation of adhesion molecules (i.e. E-selectin and VCAM-1), platelet activation, VSMC migration and proliferation, and heightened permeability associated with lipoprotein insudation and infiltration of inflammatory cells (monocytes). Lipoprotein accumulation within the intimal thickening can interact with proteoglycans and undergo modification (oxidation) that allows internalisation by macrophage and their subsequent transformation into foam cells. This stage is thought to be reversible or can progress into the earliest form of atherosclerotic plaque, a pathological intimal thickening (Kolodgie et al., 2007; Nakashima et al., 2007). There are little or no fibrotic changes at this stage. Such early lesions are often referred to as fatty streaks or intimal xanthomas and are visible en face as a flat or slightly raised yellowish discolouration on the luminal aspect of an artery. Image adapted from original source (Heinecke, 2006) and made using elements retrieved from https://smart.servier.com.

Lipids such as cholesterol are insoluble in water and must be transported throughout the circulating blood by lipoproteins, which exist and are classified dependent on their different particle density (Figure 1.1.4). However not all lipoproteins cause atherosclerosis, with the commonly described low density lipoprotein (LDL) considered the major causal lipoprotein in atherosclerosis, in part due to its abundancy within the circulating blood, especially during fasting states (Linton, 2019). Traditionally, measuring LDL-cholesterol levels have been common practice in assessing cardiovascular risk (Arsenault *et al.,* 2011). However, patients with coronary artery disease may have normal plasma LDL-cholesterol levels (Genest *et al.,* 1992; Lamarche *et al.,* 1997). Possibly, measurement of LDL cholesterol underestimates smaller (dense) LDL particles which are more atherogenic (Mudd *et al.,* 2007). Indeed, small LDL particles are more atherogenic than larger size LDL particles due to its reduced affinity to bind to LDL receptor, therefore less clearance/uptake by peripheral tissues which allows them to be more available in the blood stream (Ivanova *et al.,* 2017).

Recent evidence demonstrates that not only LDL, but other apolipoprotein-B-containing lipoproteins with a diameter of less than 70 nm, such as chylomicron remnants, VLDL, IDL and Lp (a) are capable of promoting atherosclerosis (Borén and Williams, 2016; Williams and Wu, 2016). Apolipoproteins are an integral part of the structure that envelopes the hydrophobic lipid (of lipoprotein structure) (Figure 1.1.5). Several classes of apolipoprotein have been described with apolipoprotein-B commonly associated with atherosclerosis (Shapiro and Fazio, 2017). Compelling evidence has emerged that measurement of plasma levels of apolipoprotein-B may provide better picture of cardiovascular risk alongside LDL-cholesterol (Carr *et al.,* 2019; Martin *et al.,* 2009).

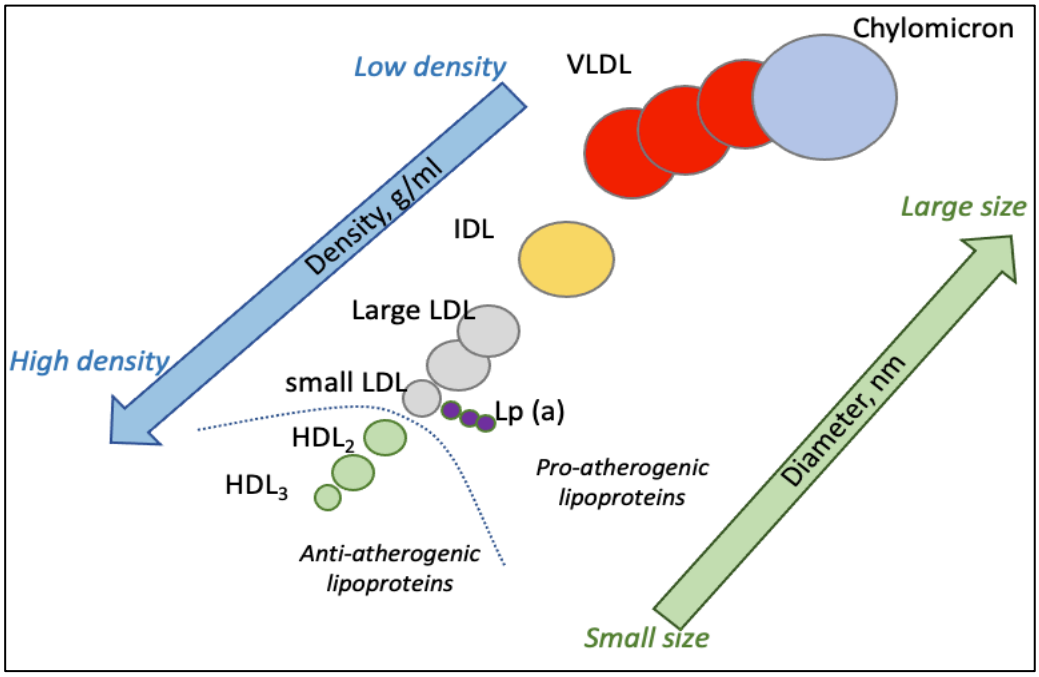

Figure 1.1.4 Different classes of lipoproteins

Based on their size and density, lipoproteins carry lipid (in the forms of triglycerides and cholesterol ester) within the circulatory system and can be classified into chylomicrons, VLDL, IDL, LDL and HDL. Chylomicrons are the largest lipoprotein and function to transport digested triglycerides from the small intestine to peripheral tissues. In the peripheral tissues (such as muscle, adipose and cardiac tissue) chylomicrons are metabolised by the lipoprotein lipase enzyme and then transported to the liver for subsequent metabolism to produce low density lipoproteins (VLDL, IDL and LDL) before distribution back into circulation. On the other hand, HDL transports lipid away from peripheral tissues (including the vessel wall) to the liver. Reportedly, HDL is associated with antioxidant and anti-inflammatory properties, and is therefore considered an anti-atherogenic lipoprotein (Rye et al., 2009). LDL, IDL and VLDL are classed as pro-atherogenic lipoproteins or famously described as 'bad cholesterol'. Chylomicrons, however, are controversial whether they can be considered pro-atherogenic due to their larger size and therefore inability to cross the endothelium. However, a few studies documented evidence that chylomicrons (of size less than 70 nm) may possibly contribute to atherosclerosis (Nakano et al., 2008; Pal et al., 2003). (VLDL = very low density-lipoprotein, IDL = intermediate density lipoprotein, LDL = low density lipoprotein, Lp (a) = lipoprotein a is part of LDL particle, HDL = high density lipoprotein (HDL_2 and HDL_3 are different density of HDL)). Image adapted from original source (Feingold and Grunfeld, 2018).

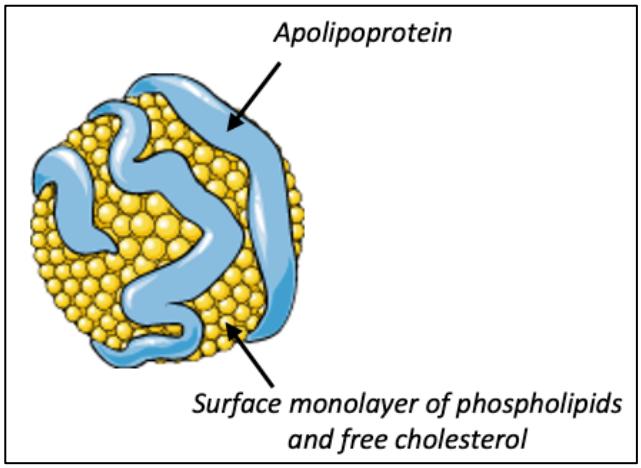

Figure 1.1.5 Lipoprotein structure

Lipoprotein molecules are comprised of an internal hydrophobic core (consists of triglyceride and cholesterol ester) surrounded by a monolayer of phospholipids, free cholesterol, and apolipoprotein. Apolipoproteins serve as a scaffold that secures the entire lipoprotein structure in place and serves as a ligand for lipoprotein receptors (i.e LDL-receptor) expressed by endothelial cells, vascular smooth muscles cells and monocyte/macrophages. Apolipoprotein-B is associated with VLDL remnants, IDL, LDL and Lp (a), whereas apolipoprotein-A is associated with HDL. Reportedly, apolipoprotein-E is associated with reduced atherosclerosis plaque progression (Greenow et al., 2005; Raffai et al., 2005). Image adapted from original source (Feingold and Grunfeld, 2018) and made using elements retrieved from https://smart.servier.com.

Intriguingly, low-density lipoprotein cholesterol (LDL-C) recruitment into the arterial wall of a healthy artery occurs at the same rate between athero-prone and athero-protected areas (Schwenke and Carew, 1989). Therefore, atherosclerosis occurs not merely due to higher lipid influx but most importantly, LDL-C retention within the adaptive intimal thickening. Indeed, an *in vivo* study has shown that through genetic manipulation of perlecan heparan sulphate proteoglycans (a major component of adaptive intimal thickenings) in a mouse model of atherosclerosis, lower subendothelial lipoprotein retention is detected and results in decreased aortic atherosclerotic plaque formation, despite heightened endothelial permeability to LDL-C (Tran-Lundmark *et al.,* 2008).

A study has suggested the possible pathway for circulating LDL uptake by endothelial cells in atherosclerosis is transcytosis mediated through scavenger receptor-B1 (SR-B1), activin receptor-like kinase 1 (ALK1), and caveolin-dependent mechanisms (Zhang *et al.,* 2018). Membrane bound LDL-C

is then transported across endothelium to the basolateral compartment and subsequent release into the subendothelial space.

Reportedly, the ionic binding between positively charged amino acids in apolipoprotein-B100 and negatively charged sulphate and carboxylic acids-glycosaminoglycan (-GAG) chains of proteoglycans leads to structural changes in apolipoprotein-B, hence causing lipid modification and retention within the subendothelial space (Khalil *et al.,* 2004). Modification and oxidation of LDL-C results in the formation of oxidised-LDL (oxLDL), an immunogenic LDL which serves as a potent inducer of circulating monocytes (and other inflammatory cells) towards sites of LDL retention. This is achieved through the enhanced endothelial cell expression of adhesion molecules (i.e ICAM-1, VCAM-1 and specific integrins) (Yamada *et al.,* 2008) alongside release of select chemokines (i.e monocyte chemoattractant protein-1 (MCP-1), RANTES (regulated upon activation, normal T cell expressed and secreted also known as (C-C) motif ligand 5; CCL5), and fractalkine (CX3CL1)) (Hansson, 2009).

Modification and oxidation of LDL is a complex biochemical process which is crucial to the development of atherosclerotic plaques. While native LDL is not taken up by macrophages, several studies have shown a contributory role for LDL oxidation to atherogenesis. An *in vivo* study demonstrated the importance of the lipid oxidation hypothesis by using probucol, an antioxidant that prevents LDL oxidation, which results in the reduction of atherosclerotic plaque formation in hypercholesterolaemic mice (Kita *et al.,* 1987). Another *in vivo* study showed that overexpression of 15-lipoxygenase, an enzyme involved in LDL oxidation within the vascular endothelium, resulted in the enhanced development of atherosclerotic plaques within LDL-receptor deficient mice (Harats *et al.,* 2000). Similarly, deficiency of 12/15-lipoxygenase (a macrophage-derived LDL oxidising enzyme) resulted in reduced atherosclerosis in Apoe deficient mice (Huo *et al.,* 2004).

The increased expression of adhesion molecules by endothelial cells facilitates the rolling and adhesion of circulating monocytes on the endothelium and their ensuing *trans*-endothelial migration towards focal sites oxLDL (Blankenberg *et al.,* 2003). This process is promoted through endothelial

cell secretion of chemokines (MCP-1/CCL2 and CX3CL1) and concomitant monocyte expression of the associated cognate receptors (CCR2 and CX3CR1, respectively), which act as signalling cues to direct monocytes (and other inflammatory cells) towards sites of oxLDL retention within intimal thickenings (Zernecke and Weber, 2014).

Besides its putative role as a chemotactic agent for monocyte/macrophages towards focal sites within intimal thickenings, oxLDL also plays significant role in enhanced expression and release of growth factors by macrophage and endothelial cells, such as platelet derived growth factor (PDGF) and fibroblast growth factor-2 (FGF2), which can induce VSMC migration and proliferation (Lindner *et al.,* 1991; Stiko-Rahm *et al.,* 1992). An additional recent report suggests that oxLDL promotes VSMC migration and proliferation via osteopontin, a chemotactic cytokine-like protein (Liu *et al.,* 2014). Reportedly, oxLDL also enhanced collagen production by VSMCs *in vitro* and *in vivo* (Jimi *et al.,* 1994; Jimi *et al.,* 1995), suggesting oxLDL can also contribute to establishment of the fibrous cap within atherosclerotic lesions (Maiolino *et al.,* 2013). On the contrary, oxLDL also modulates expression, secretion, and activation of matrix metalloproteinase-9 (MMP-9), an enzyme proposed to be associated with degradation of the fibrous cap and therefore predisposing atherosclerotic plaques to rupture (Sanda *et al.,* 2017). It has long been suggested that despite its immunogenic nature, oxLDL is also cytotoxic to vascular cells and may cause cell death (Cathcart *et al.,* 1985; Hsieh *et al.,* 2001), thus supporting a role for oxLDL to the development of the necrotic core within atherosclerotic plaques. In addition, oxLDL is also associated with reduced prostacyclin secretion, a known inhibitor of platelet activation, thus oxLDL may also indirectly promote platelet adhesion (Thorin *et al.,* 1994), and therefore predispose to thrombus formation during atherosclerotic plaque disruption. Indeed, a recent study showed that oxLDL can induce platelet activation via tyrosine kinase and Rho kinase signalling pathways (Wraith *et al.,* 2013).

After their transmigration into intimal thickenings, monocytes interact with the local environment and can either egress back into the circulation (Quintar *et al.,* 2017), or undergo differentiation into

macrophages. Maturation into macrophages is associated with up-regulation of scavenger receptors (such as cluster of differentiation 36 (CD36) (Park, 2014) and lectin-like oxidised LDL receptor-1 (LOX-1) (Xu *et al.,* 2013)), which permits the macrophages to engulf oxLDL, a process which transforms them into foam cell macrophages, the presence of which is a hallmark of atherosclerosis. At this stage, the lesion in humans is termed a pathological intimal thickening (Kolodgie *et al.,* 2007; Nakashima *et al.,* 2007), but also referred to as a fatty streak or intimal xanthoma (particularly in animal models) and is grossly visible *en face*. Such lesions may progress further or can regress.

The progression of a pathological intimal thickening into an advanced atherosclerotic plaque (Figure 1.1.6) involves marked foam-cell macrophage apoptosis, ineffective clearance of dying foam cells, and the consequential formation of a lipid-rich, necrotic core (Kolodgie *et al.,* 2007). The process is somewhat different in mouse models of atherosclerosis, where intimal xanthomas consist mainly of foam-cell macrophages, with proliferation and migration of medial VSMC into the intima alongside collagenous matrix deposition to form the fibrous cap overlying the developing necrotic core. In human and mouse developing plaques, the recruitment and activation of other inflammatory cells is observed including T-cells (Hansson, 2009). Collagenous matrix deposition mainly by VSMC leads to formation and maintenance of the fibrous cap overlying the lesion. Overtime, the plaque may reach its optimal growth, and further progression is thought to involve the repeated rupture and healing of advanced plaques, alongside compensatory adaptation of the arterial wall itself, a process termed outward arterial remodelling. Reportedly, outward (or compensatory) arterial remodelling is an important process that accompanies atherosclerotic plaque development in order to maintain lumen size and therefore preserve normal blood flow (Schoenhagen *et al.,* 2001). This process involves a dynamic interplay between cell proliferation, apoptosis, matrix synthesis and degradation.

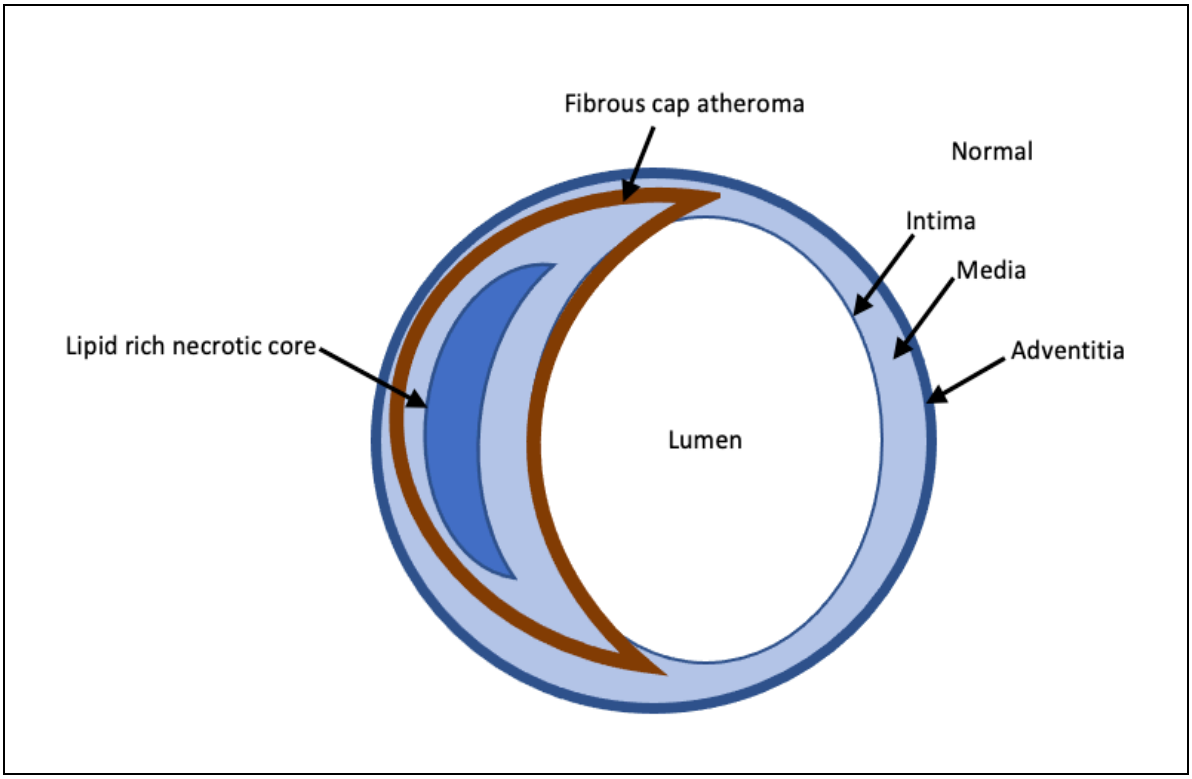

Figure 1.1.6 Schematic diagram of a stable atherosclerotic plaque

Schematic diagram representative of a stable atherosclerotic plaque with a necrotic core and intact thick fibrous cap overlain by endothelial cells. The lesion may result in luminal encroachment, and therefore cause varying degrees of lumen stenosis. Stable plaques are commonly clinically asymptomatic. In the same section of the artery, the wall opposite to the site of the atherosclerotic lesion displays a normal intima. Image adapted from original source (Insull, 2009).

During their progression, atherosclerotic plaques undergo continuous remodelling involving a balance between matrix deposition and degradation. Heightened degradation through the action of proteases such as matrix metalloproteinases (MMP) can weaken the fibrous cap and predispose it to rupture (Johnson, 2017). The formation of intraplaque blood vessels from the adventitial vasa vasorum (termed neovascularisation) are also associated with plaque instability (Kolodgie *et al.,* 2003; Michel *et al.,* 2011), which alongside increased matrix degradation and VSMC death within the fibrous cap, predispose to rupture and subsequent thrombosis formation. Reportedly, some plaques rupture and heal without any clinical manifestation (Arbab-Zadeh and Fuster, 2015; Burke *et al.,* 2001; Mann and Davies, 1999), while ruptured plaques with marked thrombosis can cause sudden luminal blockage and therefore disrupt arterial supply to the affected myocardial tissue (ischaemia), clinically manifest as myocardial infarction (MI).

In the majority of MI cases, the blockage is due to atherosclerotic plaque rupture and ensuing thrombosis formation. However, about one third of MI cases are not associated with plaque rupture, and instead attributed to endothelial erosion, a mechanism involving loss of endothelial cells overlying an otherwise intact plaque (but highly stenotic), triggering thrombosis formation (White *et al.,* 2016).

Most of the therapeutic strategies for clinically-relevant atherosclerosis focus on the management of circulating lipid levels through the administration of lipid-lowering agents (such as statins), or the complications of plaque rupture (thrombosis or marked stenosis) which involves delivery of an anti-coagulant drug (such as Prasugrel), or interventions including reperfusion therapy, stenting, or coronary artery bypass grafting, depending on disease extent. However, in opposition to lipid management, the focus on plaque inflammation as an interventional target has only recently become an area of active research.

Reportedly, AGI-1067 (also known as succinobucol), is a phenolic antioxidant and a derivative of the lipid-lowering agent probucol, and has been shown to inhibit tumour necrosis factor alpha (TNFα) induced VCAM-1, MCP-1 and E-selectin expression in human aortic endothelial cells, alongside reducing LDL levels and preventing the development of atherosclerotic plaques in both Apoe-deficient and Ldlr-knockout mice, without exerting a lipid-lowering effect (Sundell *et al.,* 2003). However, clinical trial of succinobucol did not support its therapeutic use for atherosclerosis (Tardif *et al.,* 2008a; Tardif *et al.,* 2008b). Some *in vivo* studies have proposed an athero-protective role for interleukin-6 (IL-6) (Madan *et al.,* 2008; Schieffer *et al.,* 2004). However, IL-6 has been shown to have a causal association with coronary artery disease based on genetic and biomarker data (Sarwar *et al.,* 2012; Swerdlow *et al.,* 2012).

Interleukin-1β (IL-1β) is a prominent inflammatory cytokine proven to be associated with human atherosclerotic plaque progression (Dewberry *et al.,* 2000). Reportedly, an *in vivo* study showed cholesterol crystal enhanced IL-1β secretion through the nucleotide-binding oligomerisation

domain-like [NOD-like] receptor protein 3 (NLRP3) inflammasome, promoted atherosclerosis (Duewell *et al.,* 2010). Canakinumab is an antibody targeting IL-1β and clinically licensed for treatment of rheumatologic autoimmune diseases such as cryopyrin-associated periodic syndrome and systemic juvenile idiopathic arthritis (Lachmann *et al.,* 2009; Ruperto *et al.,* 2012). Recently, a clinical trial assessing the effectiveness of canakinumab treatment in cardiovascular disease patients with high circulating levels of C-reactive protein (CRP), demonstrated dose-specific IL-1β inhibition proved beneficial through the reduction of cardiovascular events (including nonfatal myocardial infarction, nonfatal stroke, or cardiovascular death) over a five-year follow-up period, in the absence of lowering plasma LDL levels (Ridker *et al.,* 2017). However, canakinumab treatment was associated with a significant increased death rate related to infection (i.e sepsis), associated with low white cell count as canakinumab systemically blocked IL-1β and not specifically within atherosclerotic plaques. These recent clinical findings strongly support a causal role for plaque inflammation in atherosclerosis and associated major adverse cardiovascular event.

Therefore, research on inflammatory cells (especially monocyte/macrophages) and their related signalling pathways offers promising novel therapeutic targets, while also considering the potential adverse effects connected with systemic anti-inflammatory treatments. Indeed, monocyte/macrophages can exist as divergent phenotypes with pro- and anti-inflammatory properties, necessitating the need to fully characterise their behaviour and function before the application of anti-inflammatory treatments for atherosclerosis prevention.

1.2 Monocyte subsets

In humans, monocytes account for 1% - 9% of total leukocyte numbers within the peripheral circulation (Lynch *et al.,* 2018). Monocytes are primarily generated within the bone-marrow (from haematopoietic cells) but can also be released into the circulation from the spleen. Monocytes circulate within the blood before they leave the blood stream to be recruited to tissues to transform into tissue macrophages or dendritic cells (DC) (Auffray *et al.,* 2009; Haskó and Pacher, 2012).

Human monocytes co-exist as different subpopulations which are classified (in humans) based upon their expression of specific cell-surface receptors, mainly cluster of differentiation 14 (CD14) and CD16. CD14 serves as a co-receptor along with Toll Like Receptor-4 (TLR4) and lymphocyte antigen 96 (also known as Myeloid Differentiation factor 2, MD2), for the detection and uptake of bacterial lipopolysaccharide (LPS). On the other hand, CD16 (also known as Fc Fragment of immunoglobulin-gamma (IgG) Receptor IIIa, FCGR3A) participates in antigen-antibody complex clearance from the circulation, alongside additional antibody-dependent responses. Both are therefore surface receptors which play key roles during the early stages of immune responses (Yang *et al.,* 2014). Therefore, monocyte subpopulations are stratified upon their CD14 and CD16 cell-surface expression as classical, intermediate and nonclassical monocyte subsets (Table 1.2.1).

The dominant monocyte subpopulation is the classical type which are considered to display high phagocytosis function. Accordingly, this subset expresses genes associated with phagocytosis, and those related to anti-microbial proteins, angiogenesis, wound healing, and coagulation (Idzkowska *et al.,* 2015; Wong *et al.,* 2011). Classical monocytes also highly co-express other cell-surface receptors such as (C-C) motif chemokine receptor type 2 (CCR2) the receptor for monocyte chemoattractant protein-1 (MCP-1), which plays a key role in monocyte chemotaxis at sites of inflammation including atherosclerotic plaques. CD62 or leukocyte-selectin (L-selectin) is a cell adhesion molecule involved in monocyte adherence and retainment at sites of inflammation and is also highly expressed by $CD14^{++}CD16^{-}$ classical monocytes.

Opposingly, non-classical monocytes ($CD14^{+}16^{++}$) exhibit low cell-surface expression of CCR2 and CD62 but express abundant cell-surface C-X3-C motif chemokine receptor 1 (CX3CR1), which is also known as the fractalkine receptor, and is involved in regulating chemotaxis of this subpopulation (Ancuta *et al.,* 2003). Based upon the spatial and temporal expression of fractalkine, $CD14^{+}CD16^{++}$ non-classical monocytes are proposed to have patrolling properties (Ancuta *et al.,* 2003).

As their name suggests, intermediate monocytes ($CD14^{+}CD16^{+}$) have been proposed as a transition state between the classical to non-classical monocytes, as monocytes are thought to arise from a single common precursor (Idzkowska *et al.,* 2015). Moreover, following induction with macrophage colony-stimulating factors (M-CSF), there is an expansion of intermediate monocytes before progression into the non-classical type (Weiner *et al.,* 1994). As expected, intermediate monocytes display characteristics of the other two subtypes, for example, they express CCR2 (a feature of classical monocytes) and CX3CR1 (a marker of nonclassical monocytes). Nevertheless, intermediate monocytes are now recognised as not just a mere transition state between the two subtypes, but separately associated with antigen presentation and T-cell activation, and therefore proposed to be actively involved in inflammatory mediated processes (Stansfield and Ingram, 2015).

In mice, monocytes are classified based upon the density of lymphocyte antigen 6 complex (Ly6C) surface receptor into high, middle, or low (Table 1.2.1). $Ly6C^{high}$ and $Ly6C^{middle}$ are considered analogous to human classical monocytes, displaying abundant expression of CCR2 and highly inflammatory function, whereas the $Ly6C^{low}$ sub-population exhibit low CCR2 expression and serve as patrolling subset associated with repair function (Yang *et al.,* 2014).

Table 1.2.1 Classification of human monocytes based upon CD14 and CD16 cell-surface receptor expression, and characterisation of mouse monocytes based on Ly6C cell-surface levels

(CD = a cluster of differentiation; CCR = (C-C) motif chemokine receptor; CX3CR1 = (C-X3-C) motif chemokine receptor 1; Ly6C = lymphocyte antigen 6 complex; MNC = Mononuclear cells). Adapted from (Yang et al., 2014)

Species	Subsets	Surface markers	% in MNC	Chemokine receptors	Function(s)
Human	Classical	$CD14^{++}CD16^{-}$	80-95	$CCR2^{high}CX3CR1^{low}$	Phagocytosis
	Intermediate	$CD14^{+}CD16^{+}$	2-11	$CCR2^{mid}CX3CR1^{high}CCR5^{+}$	Highly inflammatory
	Non-classical	$CD14^{+}CD16^{++}$	2-8	$CCR2^{low}CX3CR1^{high}$	Patrolling
Mouse	$Ly6C^{high}$ ($Ly6C^{+}$)	$CD11b^{+}CD115^{+}Ly6C^{high}$	40-45	$CCR2^{high}CX3CR1^{low}$	Phagocytosis & Pro-inflammatory
	$Ly6C^{middle}$ ($Ly6C^{+}$)	$CD11b^{+}CD115^{+}Ly6C^{middle}$	5-32	$CCR2^{high}CX3CR1^{low}$	Highly inflammatory
	$Ly6C^{low}$ ($Ly6C^{-}$)	$CD11b^{+}CD115^{+}Ly6C^{low}$	26-50	$CCR2^{low}CX3CR1^{high}$	Patrolling; tissue repair

1.3 Macrophage classification

Similar to monocytes, the diversity of macrophages (Table 1.3.1) can be appreciated based on their cell-surface receptor expression, alongside their production of key cytokines and growth factors (Colin *et al.*, 2014). The two most commonly described macrophage subsets are the classically activated (M1) and alternatively activated (M2) macrophages.

Table 1.3.1 *In vitro* macrophage phenotypes

Overview of macrophage subsets, principal inducers, and their characteristics. (IFNγ: interferon γ ; LPS: lipopolysaccharide; TNFα: tumour necrosis factor alpha; IL: interleukin; CXCL: C-X-C motif chemokine ligand; MHC: major histocompatibility complex; CD: cluster of differentiation; MARCO: macrophage receptor with collagenous structure; iNOS: inducible nitric oxide synthase; STAT: signal transducer and activator of transcription; NF-κB p: Nuclear factor-kappa B-cell p heterodimer; IRF5: interferon regulatory factor 5; MR: mannose receptor; TGFβ : transforming growth factor beta: IL-Ra: interleukin-1 receptor antagonist; CCL: (C-C) motif chemokine ligand; IRF4: interferon regulatory factor 4; PPARγ: peroxisome proliferator-activated receptor gamma; IC: immune complexes; TLR: toll like receptor; IL-IR: interleukin-1 receptor; A2R: adenosine A_{2A} receptor agonist; VEGF: vascular endothelial growth factor). Adapted from (Colin et al., 2014).

Macrophage phenotype	Inducers	Markers and surface molecules	Cytokine and chemokine production	Regulators	Functions in atherosclerosis
M1	IFNγ, LPS, TNF	IL-1β, IL-6, IL-12, IL-23, TNFα, CXCL9, CXCL10, CXCL11, MHCII, CD86, CD80, MARCO	IL-6, TNFα, IL-23, iNOS	STAT1, NF-kB p65/p50, IRF5	Microbicidal, tumour resistance
M2a	IL-4, IL-13	MR, MHCII,	IL-10, TGFβ, IL-Ra, CCL17, CCL22, CCL18	STAT6, NF-kB p50/p50, IRF4, PPARc	Wound healing macrophages
M2b	IC, TLR, IL-1R ligands	MR, MHCII, CD86	IL-1 β, IL-6, TNFα, IL-10^{high} and IL-12^{low}		Immunoregulation
M2c	IL-10, Glucocorticoids, TGFβ	MR, CD163	IL-10, TGFβ	STAT3	Efferocytosis capacity
M2d	TLR+A2R ligands	TNFα^{low}, IL-12^{low}, VEGF	IL-10^{high}, VEGF, TNFα^{low}, IL-12^{low}	NF-kB	Pro-tumoural, proangiogenic capacity

Classically activated macrophages (M1) are induced by T-helper 1 (Th-1) cytokines (produced by Th-1 lymphocytes) such as IFNγ, alongside inflammatory cytokines including TNFα and microbial products, for example lipopolysaccharides (LPS) (Mosser and Edwards, 2008). M1 macrophages are considered to promote inflammatory responses via secretion of pro-inflammatory cytokines including interleukin-6 (IL-6), IL-1β, TNFα, IL-2, and IL-23 (Colin *et al.,* 2014). They also produce toxic agents such as nitric oxide and reactive oxygen species (ROS) to curb infection (Mosser, 2003). Several chemokines are also expressed and released by M1 macrophages, for instance CXCL9, CXCL10, and CXCL5, which act to promote further recruitment of Th1 lymphocytes and natural killer (NK) cells, and therefore linked with sustained inflammation (Colin *et al.,* 2014). These functions are beneficial during acute infection responses for the resolution of infection, but may impair wound healing if their presence and action is prolonged, resulting in chronic sterile inflammation (Colin *et al.,* 2014). Induced by T-helper 2 (Th-2) lymphocyte cytokines, alternatively activated macrophages (M2) are considered to be principally involved in tissue repair and resolution processes (Mosser, 2003). Accordingly, they display phagocytic, pro-angiogenic and pro-fibrotic properties (Colin *et al.,* 2014). More recently, alternatively activated macrophages (M2) have been further subclassified into M2a, M2b, M2c and M2d subsets, with specific inducers identified alongside particular secretory products (as shown in Table 1.3.1). Functionally, M2a macrophages are involved in wound healing, M2b and M2c macrophages are classified to have immunoregulatory roles (Mosser and Edwards, 2008), whereas M2d macrophages are involved in tumour growth (Haskó and Pacher, 2012; Zhou *et al.,* 2020). The M2 macrophage subsets exhibit high levels of mannose receptor (CD206) expression except for M2d macrophages (Colin *et al.,* 2014). Collectively, M2 macrophages have been shown to have anti-inflammatory properties except for M2b macrophages, which secrete pro-inflammatory factors similar to M1 macrophages alongside high levels of the anti-inflammatory molecule IL-10, but low IL-12 expression (Table 1.3.1).

1.4 The role of monocytes and macrophages in atherosclerosis

As cells of innate immune system, monocytes and macrophages have been demonstrated to play a key role in the development of atherosclerosis, as depletion of monocytes from the circulation was associated with reduced atherosclerotic plaque formation in a rabbit model (Ylitalo *et al.,* 1994). Additionally, increased monocyte number within the blood, termed as monocytosis, strongly correlates with atherosclerotic plaque progression and incidence of MI (Raffort *et al.,* 2017).

Figure 1.4.1 illustrates how classical and non-classical monocyte subsets participate in atherosclerosis (Johnson and Newby, 2009). Modified LDL (chiefly oxLDL) induces vessel wall expression of the CCL2 (MCP-1) chemokine which interacts with its cognate receptor CCR2 on monocytes in order to attract circulating classical monocytes into the developing lesion. Differentiation of monocytes into macrophages ensues with subsequent oxLDL internalisation. Scavenger receptor-mediated oxLDL uptake by macrophages and ongoing oxLDL accumulation results in the formation of lipid-laden macrophages, more commonly termed as foam cells (Kunjathoor *et al.,* 2002). Ingested oxLDL can undergo degradation, or after processing be released (efflux) from the cell via the reverse cholesterol transport mechanism via HDL, which has been associated with plaque regression (Tall *et al.,* 2008).

During this innate immune response, non-classical monocytes can be recruited to the lesion. Reportedly, this process is mediated by the chemokine receptors for CX3CL1 and CCL5 (Johnson and Newby, 2009; Tacke *et al.,* 2007). Macrophages (and other immune cells such as dendritic cells) present antigen on their cell surface to T-lymphocytes. As a result, various cytokines are produced to promote plaque growth such as IFNγ and TNFα. Both cytokines are known to be pro-inflammatory and widely researched as potential therapeutic targets for the treatment of atherosclerosis (Brånén *et al.,* 2004; Gotsman and Lichtman, 2007). On the contrary, some of the cytokines produced are anti-inflammatory such as interleukin-10 (IL-10) which is reported to exert athero-protective effects

(Han and Boisvert, 2015). Another molecule released from macrophages considered to be athero-protective is transforming growth factor-beta (TGFβ) (Toma and McCaffrey, 2012).

Supporting key roles for the monocyte populations to the development of atherosclerosis, genetic deletion of CCL2 and CX3CL1 chemokine or their receptors (CCR2 and CX3CR1 respectively) was associated with reduced atherosclerotic plaque size in murine models through blunting monocyte/macrophage accumulation (Saederup *et al.,* 2008). The differentiation of monocytes into distinct macrophage phenotypes requires different cytokines as depicted in Figure 1.4.1. However, there is scant evidence that specific monocyte subsets give rise to select macrophage subpopulations, and area of research that obviously warrants further investigation.

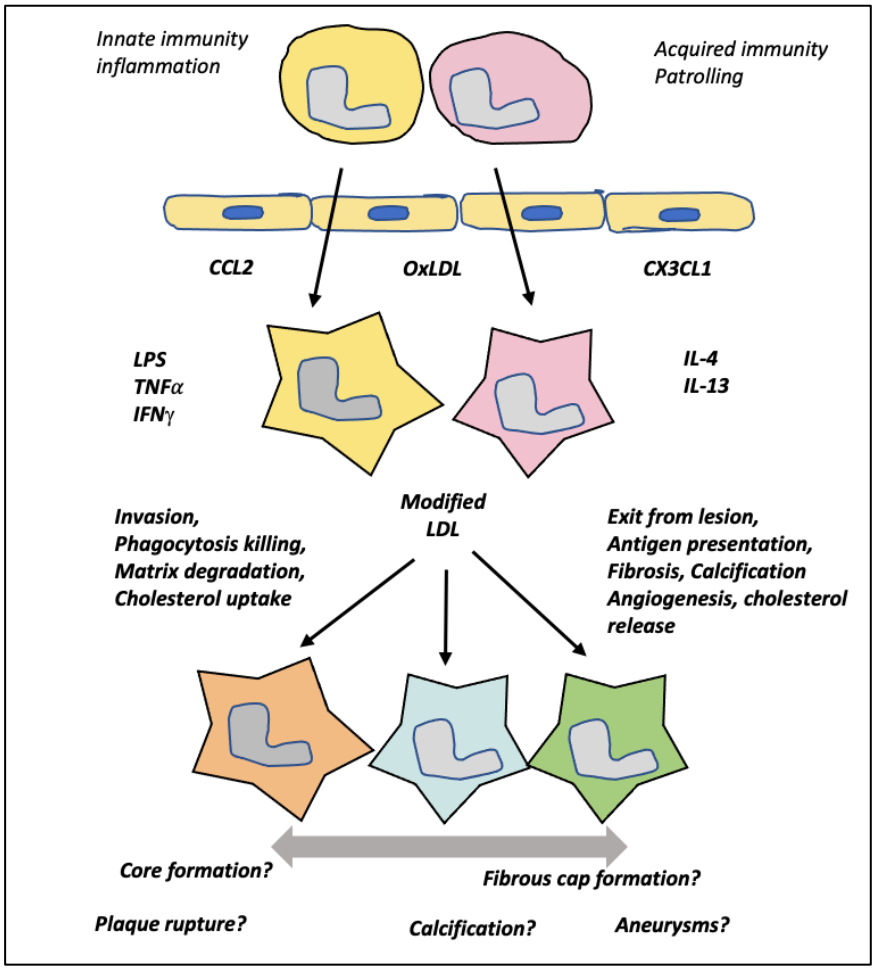

Figure 1.4.1 Monocytes and macrophages in atherosclerosis

Innate immune responses involve mainly CCL2 mediated monocyte (CD14+CD16- or classical monocytes) chemotaxis whereas further immunoinflammatory responses entail the CX3CL1 mediated pathway (CD16+ non-classical monocyte population). Subsequently, macrophage interaction with local cues determines their roles in atherosclerosis progression. For example, pro-inflammatory growth factors/cytokines (LPS, TNFα and IFNγ) are associated with expansion of atherosclerotic plaque (such as necrotic core formation) and weakening of the fibrous cap (causing plaque rupture) which suggests characteristics of M1 macrophages. On the other hand, interaction of intimal macrophages with anti-inflammatory growth factors/cytokines (such as IL-4 and IL-13) is associated with fibrous cap formation, plaque calcification and neovascularisation, characteristics attributed to the diverse alternatively activated macrophage (M2) population. Other M2 macrophage roles in atherosclerosis are described in section 1.5 (Macrophage subpopulations in atherosclerosis) (CCL2 = chemokine (C-C motif) ligand 2, oxLDL = oxidised low-density lipoprotein, CX3CL1 = chemokine (C-X3-C motif) ligand 1, LPS = lipopolysaccharide, TNFα = tumour necrosis factor alpha, IFNγ = interferon gamma, IL-interleukin). Image adapted from original source (Johnson and Newby, 2009).

1.5 Macrophage subpopulations in atherosclerosis

Macrophages are essential in the initiation and progression of atherosclerosis (Johnson and Newby, 2009). During atherosclerosis, macrophages accumulate within developing lesions in part due to reduced emigration (Ludewig and Laman, 2004). There is a specific distribution of macrophage subpopulations within atherosclerotic plaques. At plaque shoulders, where it is prone to rupture, M1 macrophages appear to be the dominant population. Within the fibrous cap, M1 and M2 macrophage distribution is similar, while in the adventitial region of atherosclerotic plaques, M2 macrophages predominate (Stöger *et al*., 2012). Overall, M1 macrophages predominantly populate in unstable plaques in comparison to stable lesions (Cho *et al*., 2013; Lee *et al*., 2013). Figure 1.5.1 summarises the diverse macrophage subpopulations within atherosclerotic plaques, their proposed mediators, and cell-surface receptors (Colin *et al*., 2014).

Classically activated macrophages (M1) which can be induced by IFNγ, LPS, oxLDL, and cholesterol crystals, exert pro-inflammatory properties associated with increased expression of TNFα, CD86 and MHCII, which are associated with atherosclerotic plaque progression. M(hb) is haemoglobin/haptoglobin-stimulated macrophage subset which is located and dominates within sites of intraplaque haemorrhage. This subset is proposed to clear free haemoglobin from within intra—plaque bleeds through the CD163 receptor (Araujo *et al*., 2012). M(hb) macrophages are also associated with elevated expression of IL-10, an anti-inflammatory cytokine. The release heme by M(hb) may primes macrophage into M(heme) with expression of activating transcription factor (ATF)-1 and heme oxygenase-1 (HMOX1), both prevents formation of foam cells and are therefore anti-atherogenic. Thus, both CD163 M(Hb) and M(heme) can be considered as atheroprotective macrophage subset. However, recent finding suggests that CD163 high M(hb) macrophage assists in plaque angiogenesis, heightened vascular permeability, and exerts a pro-inflammatory role via hypoxia inducible factor-1 α (HIF1α)/ vascular endothelial cell growth factor A (VEGF-A) dependant pathway (Guo *et al*., 2018).

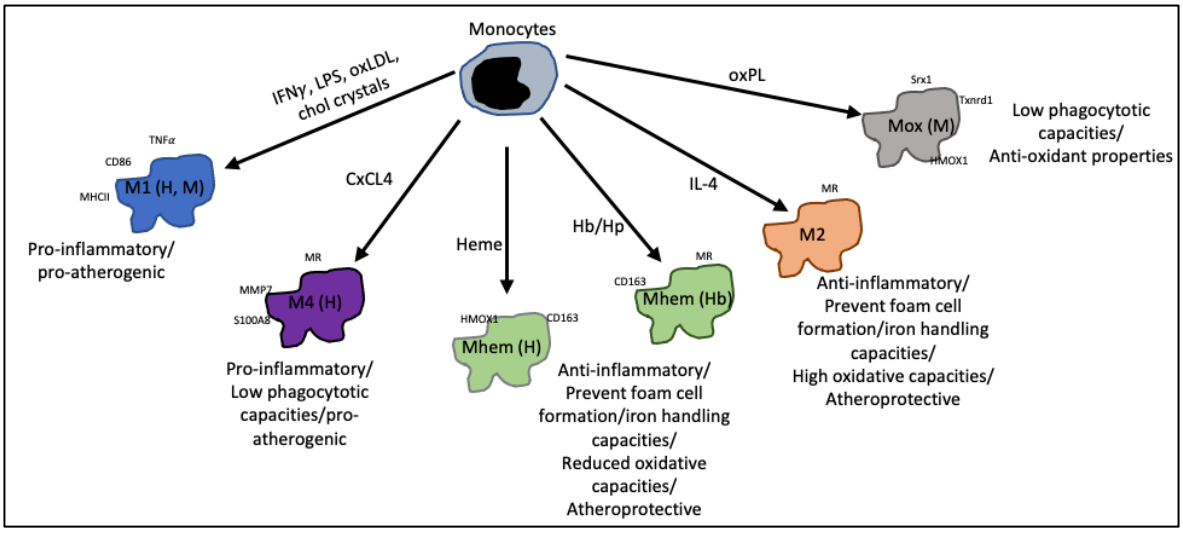

Figure 1.5.1 Specific macrophage subpopulations found within atherosclerosis plaques

Various macrophage subpopulations have been detected within atherosclerotic plaques and specific roles proposed in both human (H) and mouse (M) lesions. M4, M(hem), M(Hb) and M2 macrophage subsets are considered less likely to transform into foam cells. Inducers and associated cell-surface receptors are indicated by arrows and at cell periphery, respectively. Currently, the Mox subset had not been reported in human atherosclerotic lesions. (M1 = classically activated macrophage, M4 = PF4 (CXCL4) activated macrophage, Mhem = heme activated macrophage, M(Hb) = hemoglobin/haptoglobin (Hb/Hp) activated macrophage, M2 = IL-4 activated macrophage, Mox = oxPL (oxidised phospholipid) activated macrophage, IFNγ = interferon γ, LPS = lipopolysaccharide, chol = cholesterol crystal, TNFα = tumour necrosis factor α, CD = cluster of differentiation, MHCII = major histocompatibility complex II, PF4 = platelet factor 4, CXCL4 = (C-X-C motif) chemokine ligand 4, MR = mannose receptor, MMP7 = matrix metalloproteinase 7, S100A8 = S100 calcium binding proteins, HMOX1 = heme oxygenase-1, Srx1 = sulforedoxin-1, Txnrd1 = thioredoxin reductase 1). Image adapted from original source (Colin et al., 2014).

The M4 macrophage subset is considered alternatively activated by platelet factor 4 (PF4) which is also known as (C-X-C motif) chemokine ligand 4 (CXCL4), which does not readily take up lipid owing to reduced expression of scavenger receptors (including CD36 and SCARB1). Reportedly, the M4 subset is associated with reduced expression of CD163 and HMOX1 enzyme, and is associated with high expression of pro-inflammatory cytokines such as IL-6 and TNFα, hence rendering them to be classed as pro-atherogenic (Domschke and Gleissner, 2019). M4 macrophages are found within the intima and adventitia of unstable plaques. The mannose receptor CD206, matrix metalloproteinase 7 (MMP-7) and S100A8 are considered markers for the M4 macrophage subset (Domschke and Gleissner, 2019).

IL-4 activated macrophages (M2a macrophage subset) is associated with anti-inflammatory production of growth factors/cytokines such as fibronectin, insulin-like growth factor (IGF), and transforming growth factor beta (TGFβ). Similar to M4 macrophages, the M2a subset also express high levels of CD206, a carbohydrate receptor with high phagocytosis function for the clearance of dying/dead cells, but not to readily ingest lipids. These lines of evidence suggest the role of M2a macrophages is to stabilise atherosclerotic plaques, supported by their prevalence within the fibrotic cap and lowly detected within the lipid core (Chinetti-Gbaguidi *et al.,* 2011). However, it has been shown that when IL-4 activated M2a macrophages interact with oxLDL, they produce pro-inflammatory cytokines such as IL-8 (Hirose *et al.,* 2011). Relatedly, M-CSF has also been deemed an activator for M2 macrophage polarisation, and induces an increase in IL-6 and MCP-1 expression, both of which are pro-inflammatory mediators (van Tits *et al.,* 2011).

In vivo studies have also postulated a macrophage sub-population that is induced by oxidised phospholipids (oxPL) termed as Mox, and is associated with lower phagocytosis activity and higher antioxidant properties linked to their elevated levels of enzymes such as HMOX-1, thioredoxin reductase 1 (Txnrd1) and sulforedoxin-1 (Srx1) (Kadl *et al.,* 2010). However, more recent *in vivo* findings proposed that the Mox subset served as a pro-inflammatory and pro-atherogenic macrophage population (Que *et al.,* 2018).

Besides their primary role in mediating inflammatory responses during atherosclerosis, monocytes and macrophages can also mediate VSMC responses. Macrophages can facilitate medial VSMC migration through the secretion of proteases (such as MMPs) that degrade the extracellular matrix to permit VSMC motility (Newby, 2005), and additionally by expression of chemokines or growth factors such as macrophage migratory inhibitory factor (MIF) (Schrans-Stassen *et al.,* 2005) and extracellular vesicle release (Niu *et al*., 2016). MIF is a pro-inflammatory cytokine secreted by macrophages, VSMCs, and endothelial cells (van der Vorst *et al.,* 2015), and is reportedly able to promote VSMC differentiation (Fan *et al*., 2017) and migration (Schrans-Stassen *et al*., 2005), and

therefore proposed to contribute to atherosclerotic plaque development (Chen *et al*., 2015). In a recent report, extracellular vesicles released by foam cell macrophages were taken up by VSMC, and able to modulate the actin cytoskeleton and focal adhesions through the extracellular-regulated kinase (ERK) and protein kinase B (Akt) signalling pathways, promoting VSMC adhesion and migration (Niu *et al*., 2016).

Within advanced atherosclerotic plaques, macrophages secrete proteases with the ability to degrade collagen and also induce VSMC apoptosis (through loss of cell-to-matrix and cell-to-cell junctions), both actions which can weaken the integrity of the fibrous cap and render it prone to rupture (Newby, 2007; Skjøt-Arkil *et al*., 2010). The production of reactive oxygen species by macrophages is also thought to cause VSMC death (Li *et al*., 1997). Furthermore, apoptosis of foam cell macrophages and VSMCs contribute to central necrosis of the atherosclerotic plaque and subsequent expansion of the necrotic/lipid core. Macrophages also secrete pro-angiogenic factors and can therefore promote neovascularisation within atherosclerotic plaques, possibly via a CD163/HIF1α/VEGF-A pathway, with the formation of neovascularisation considered to predispose to intraplaque haemorrhage, plaque destabilisation, and subsequent clinical events such as MI (Guo *et al*., 2018).

1.6 Colony stimulating factors as regulators of macrophage phenotypes

Haematopoietic cytokines are a family of glycoprotein molecules which act on haematopoietic progenitor cells and their progeny to stimulate cell proliferation and differentiation into specific blood cell types (Metcalf, 2008). As depicted in Figure 1.6.1, numerous cytokines have been identified to take part in the production of blood cells, including immune cells. Blood cells are constantly produced from common progenitor cells to maintain steady state levels in healthy individuals to replace the matured cells which have a limited life span. Some cytokines show limited lineage specificity such as erythropoietin (EPO), thrombopoietin (TPO), IL-2 and IL-7, while others display a broad range of activity including colony stimulating factors (CSF).

Of interest, there are four colony stimulating factors (CSF) which have been classified based on the cells they primarily stimulate, namely macrophage-colony stimulating factor (M-CSF), granulocyte/macrophage -colony stimulating factor (GM-CSF), granulocyte-colony stimulating factor (G-CSF), and multi-potential colony stimulating factor (multi-CSF) which is more commonly referred to as interleukin-3 (IL-3). CSFs are secreted by various cell types, including immune cells themselves, endothelial cells and VSMCs (Barreda *et al*., 2004). CSFs stimulate cell proliferation and colony formation by promoting clonal cell growth and supressing apoptosis. Their secretion is tightly regulated by positive and negative feedback mechanisms, and increased under certain stimuli such as infection and stress (Barreda *et al*., 2004).

Through the action of CSFs, two distinct macrophage subsets (Figure 1.6.2) have been identified *in vitro*, namely M-Mac and GM-Mac, based on differentiation with M-CSF or GM-CSF, respectively (Waldo *et al*., 2008). When compared to M-Mac, GM-Mac are characterised as highly invasive, have an increased susceptibility to apoptosis, are more proliferative, and accumulate modified LDL more rapidly. They are also associated with increased expression of MMP-12, MMP-14 and the microRNA (miR) miR-181b and reciprocal reduced expression of TIMP-3, and lower levels of miR-24 (which

targets MMP-14), and galectin-3 (Gal-3) (Di Gregoli *et al*., 2014; Di Gregoli *et al*., 2017; Di Gregoli *et al*., 2020; Johnson *et al*., 2014).

Therefore, GM-Mac are considered a pro-inflammatory macrophage subset and associated with the progression of atherosclerotic lesions towards an unstable plaque phenotype. Conversely, M-CSF polarised macrophages (M-Mac) can be regarded as anti-inflammatory and associated with a stable plaque phenotype (Di Gregoli *et al*., 2017; Di Gregoli *et al*., 2020; Johnson *et al*., 2014; Johnson *et al*., 2008).

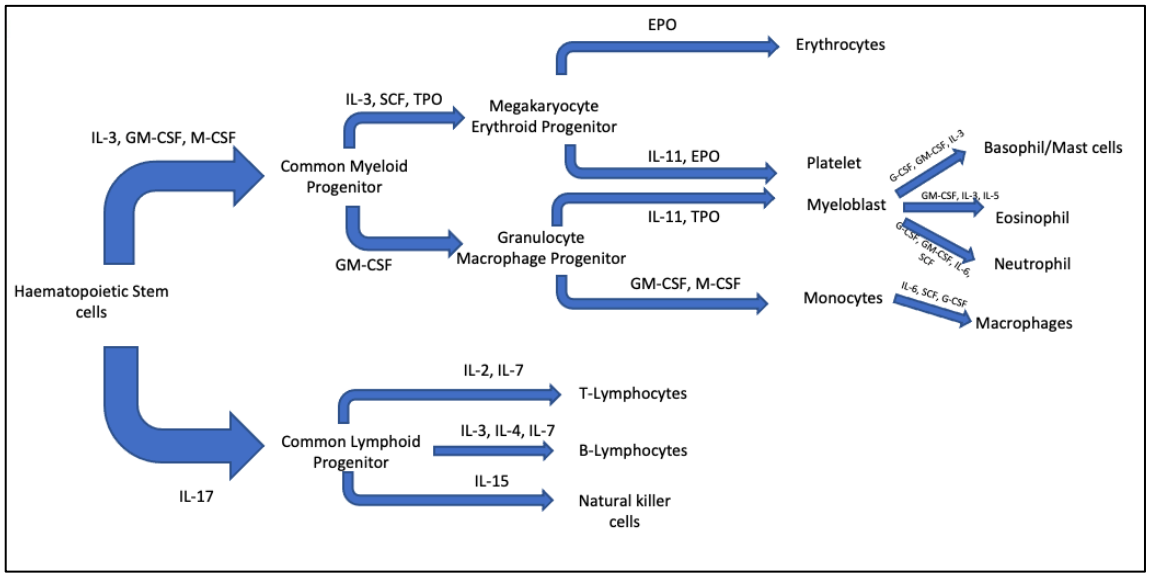

Figure 1.6.1 Haematopoietic cytokines involved in the differentiation of blood cells and immune cells

Haematopoietic stem cells (HSC) give rise to cells of myeloid and lymphoid origin. Myeloid lineage cells eventually give rise to red blood cells, platelets, granulocytes (basophil, eosinophil and neutrophil) and monocyte/macrophages (including dendritic cells, Langerhans cells, and Kupffer cells). Lymphoid lineage cells included all lymphocytes and natural killer cells. (IL = interleukin, M-CSF = macrophage colony stimulating factor, GM-CSF = granulocyte-macrophage colony stimulating factor, G-CSF = granulocyte colony stimulating factor, TPO = thrombopoietin, SCF = stem cell factor, EPO = erythropoietin). Image adapted from original source https://www.sigmaaldrich.com/technical-documents/articles/biofiles/hematopoietic- cytokines.html.

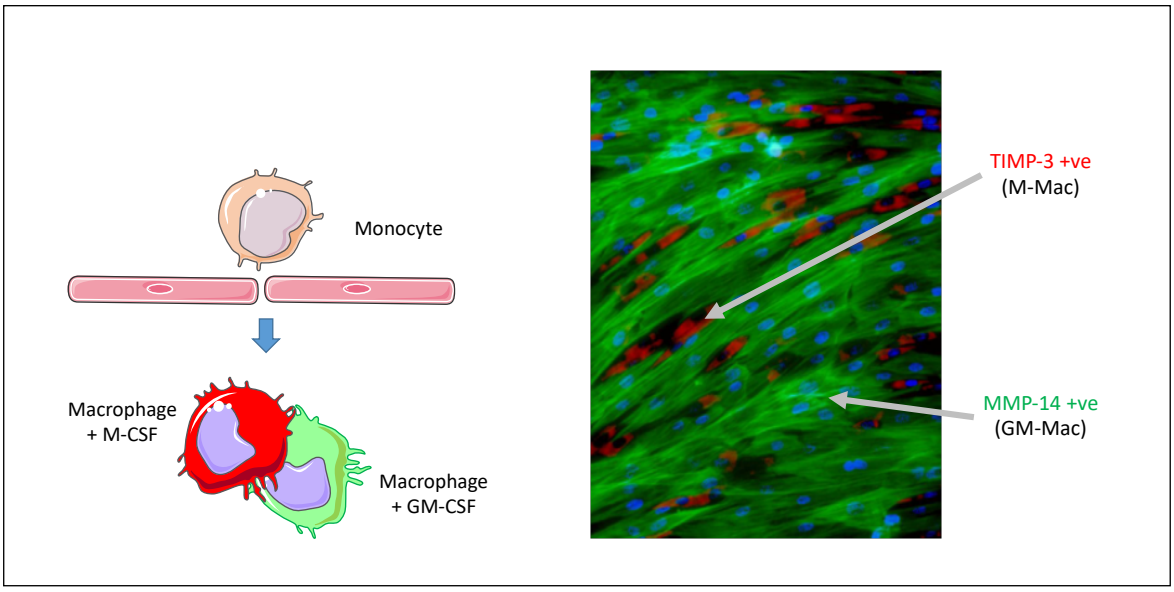

Figure 1.6.2 Colony stimulating factors (CSF) as regulators of macrophage phenotype

M-CSF polarised macrophages (M-Mac) display heightened expression of TIMP-3 (red cells), which has been implicated in the resolution of inflammation and therefore the anti-inflammatory actions of M-Macs (Casagrande et al., 2012). Conversely, GM-CSF polarised macrophages (GM-Mac) have marked MMP-14 levels (green cells), which affords these macrophages with augmented destructive activity and therefore propagate atherosclerotic plaque instability. (TIMP-3 = Tissue inhibitor of metalloproteinases-3, MMP-14 = Matrix metalloproteinases-14) (Di Gregoli et al., 2014; Johnson et al., 2008). Image on the left-hand side made using elements retrieved from https://smart.servier.com. Fluorescence image on the right-hand side courtesy from Dr Johnson.

1.7 Progenitor potential of monocytes and macrophages

Together with dendritic cells, monocytes and macrophages form the mononuclear phagocyte system. They exhibit phagocytic capacity and antigen presenting function (Gordon and Plüddemann, 2019). However, recent evidence has suggested that monocytes harbour the ability to differentiate into cell types with non-phagocytic properties.

Indeed, recent studies have suggested that under *in vitro* conditions, human monocytes have the capacity to differentiate into non-phagocytic pluripotent stem-like cells with a variety of different names including; pluripotent stem cells (PSCs) (Zhao *et al.,* 2003); monocyte-derived multipotential cells (MOMC) (Kuwana *et al.,* 2003; Seta and Kuwana, 2010); a CD14+CD43$_{low}$KDR+ subset (KDR stands for kinase insert domain receptor, which is also known as VEGFR2) (Romagnani *et al.,* 2005); and programmable cells of monocyte origin (PCMO) (Ruhnke *et al.,* 2005a; Ruhnke *et al.,* 2005b; Ungefroren and Fändrich, 2010). A study by Romagnani and colleagues have shown that CD14+CD34$_{low}$ cells are the major source of circulating endothelial progenitors (Romagnani *et al.,* 2005). While Harraz *et al*, reported CD14^{+} monocytes have the potential to be incorporated into the endothelium of blood vessels in ischaemic mouse limbs and transdifferentiate into endothelial cells (Harraz *et al*., 2001).

Additionally, it has been reported in the literature that CD14^{+} monocytes co-express endothelial lineage markers and form cord-like structures *in vitro* in response to pro-angiogenic factors (Fernandez Pujol *et al*., 2000; Schmeisser *et al*., 2001). In addition, peripheral blood mononuclear cells (PBMC) cultured with macrophage-colony stimulating growth factor (M-CSF) for 5 days exhibit fibroblast like morphology with expression of CD14 and CD45, alongside the haematopoietic stem cell (HSC) surface receptor CD34 (Zhao *et al*., 2003). These cells were also induced towards other cell types including macrophages, T-lymphocytes, epithelial cells, neuronal cells, endothelial cells and liver cells, through stimulation with different growth factors, and were therefore considered to exhibit pluripotency (Zhao *et al*., 2003). However, it must be noted, that in most cases the evidence

of differentiation towards a specific cell type was determined through the evaluation of a single cell-type specific marker, for example von Willebrand Factor (vWF) to confirm differentiation into an endothelial cell. Moreover, only approximately 10% of PBMCs are monocytes and it is plausible that a circulating progenitor cell type which can respond to M-CSF, is present within the circulation (and therefore PBMC preparations) and accounts for the pluripotent cell type observed in some of the above studies.

In another study, human PBMCs cultured upon fibronectin produced mesenchymal progenitor cells which expressed CD14, CD45 and CD34 with a mixed morphology and phenotypic features of phagocytes, endothelial cells, and mesenchymal cells (Kuwana *et al.,* 2003). These cells were termed as monocyte-derived multipotential cells (MOMC) or monocyte derived mesenchymal progenitor cells (MOMP) and exhibited decreasing proliferation rates with subsequent passage and stopped growing after the fifth passage (Kuwana *et al.,* 2003; Kuwana *et al.,* 2006; Seta and Kuwana, 2007). Co-culture of MOMC with embryonic rat cardiomyocytes produced cells with electrophysiological characteristics of cardiac muscle tissues after three weeks with the ability to beat spontaneously and produce action potentials (Kodama *et al.,* 2005). Similarly, co-culture of MOMC with neuronal cells resulted in neuronal lineage cells (Kodama *et al*., 2006). Additionally, MOMC treated with pro-angiogenic growth factors led to cells with endothelial cell characteristics (Kuwana *et al*., 2006). However, the efficiency of MOMC differentiation towards an endothelial cell-like phenotype is higher than that towards cardiomyocytes and neuronal cells (Kodama *et al*., 2005; Kodama *et al.,* 2006; Kuwana *et al*., 2003; Kuwana *et al*., 2006).

In a different study, human PBMCs were shown to differentiate into a phenotype which acquired a state of plasticity or programmability, with surface expression of CD14, CD90 (thymocyte differentiation antigen 1; Thy-1) and CD115 (also known as colony stimulating factor 1 receptor; CSF1R and macrophage colony-stimulating factor receptor; M-CSFR) following 6-day treatment with M-CSF and human interleukin-3 (IL-3) (Pufe *et al.,* 2008; Ruhnke *et al.,* 2005b; Ungefroren *et al.,*

2010). These cells were termed as programmable cells of monocyte origin (PCMO) and shown to resume cell division in a CD115-dependent manner (Pufe *et al.,* 2008; Ruhnke *et al.,* 2005b; Ungefroren *et al.,* 2010). Incubation of PCMOs with hepatocyte condition medium and islet-cell condition medium resulted in their transformation into liver cells and pancreatic cells, respectively, with associated secretory function observed *in vitro* and *in vivo* (Ruhnke *et al.,* 2005b). In another study, collagen-producing chondrocytes were successfully yielded from PCMOs upon stimulation with various related growth factors (Pufe *et al.,* 2008).

Collectively, these findings provide insight that under specific conditions and within specific microenvironments, PBMCs and by inference, monocyte/macrophages can be modified to exit from their original state and associated properties and transform towards new cell types, mimicking characteristics under which they are newly 'programmed'. Indeed, human blood monocytes have been extensively studied within regenerative medicine research (such as tissue engineering), as a potential alternative to embryonic stem cells as they can be readily retrieved from venepuncture and are simpler to maintain under tissue culture conditions (King and Perrin, 2014; Ungefroren *et al.,* 2010).

In regard to cardiovascular diseases such as atherosclerosis, a similar approach could be studied, and potentially exploited, in a therapeutic preventative aspect. It would therefore be pertinent to study the capacity of differing macrophage subsets to transform towards vascular cell phenotypes, particularly macrophage subsets associated with cardiovascular diseases, and investigate the mechanisms involved in order to potentially promote or retard phenotypic differentiation for possible therapeutic purposes.

1.8 Hypotheses

Select phenotypes of macrophage harbour the potential to differentiate towards vascular cell types.

1.9 Project Aims and Objectives

I. Evaluate the potential of differing human macrophage subsets to transform towards a VSMC-like phenotype, using growth factors shown to modulate the differentiation of VSMCs, and through assessing the expression of markers purported to be VSMC-specific.
II. Evaluate the potential of differing human macrophage subsets to transform towards an endothelial cell-like phenotype, using growth factors shown to stimulate endothelial cell growth, and through assessing the expression of markers purported to be endothelial cell-specific.
III. Assess the contributory role of microRNA in regulating macrophage subset transformation towards an endothelial cell-like phenotype.

2 Materials and Methods

2.1 Macrophage culture and polarisation

2.1.1 Isolation of Human Peripheral Blood Monocytes

Materials: Ethylenediaminetetraacetic acid (EDTA) tubes, Falcon tubes, Ficoll-Paque™ PLUS (GE Healthcare), SepMate™ tubes (Stem Cell technologies), Dulbecco's Phosphate Buffered Saline (DPBS; 1X; Gibco by Life Technologies™), Hank's Balanced Salt Solution (HBSS; PAA The cell culture company) and RPMI/FCS media (see RPMI/FCS media below).

2.1.2 Isolation of PBMCs from whole blood by density gradient centrifugation

Human blood samples (between 20-25ml) were collected from random healthy subjects, according to ethical governance and guidelines (South West 4 Research Ethics Committee reference 09/H0107/22). The blood was collected in EDTA tubes and processed within two hours of collection. EDTA-treated (anti-coagulant) blood was diluted (1:1) with sterile DPBS and layered carefully over Ficoll-Paque PLUS media (GE Healthcare Life Sciences) at ~45° tilted Falcon tube to avoid intermixing. The tubes were then subjected to centrifugation at 400 g (room temperature with the brake off) for 25 minutes to produce cell layers (Figure 2.1.1).

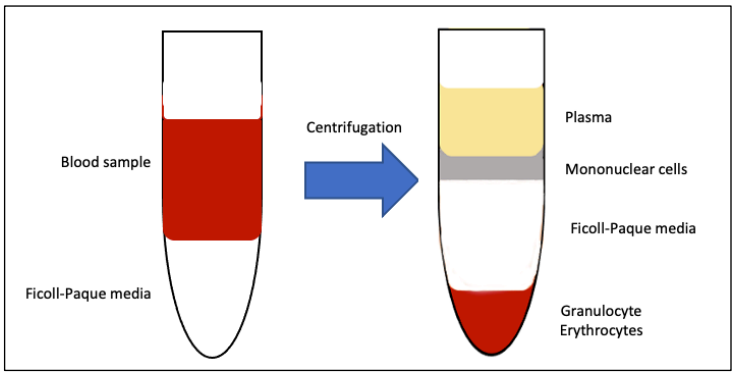

Figure 2.1.1 Isolation of PBMCs
DPBS-diluted blood layered on top of Ficoll-Paque (in 1:1). Differential migration during centrifugation results in the formation of layers containing different cell types: aggregated underneath a clear Ficoll-paque layer are erythrocytes, while mononuclear cells and other sediment particles appear as a cloudy white ring at the interface of plasma (topmost layer) and Ficoll-Paque due to their lower density. Image adapted from original source https://www.gelifesciences.com/.

The cloudy layer containing the PBMCs was collected and washed with sterile HBSS before centrifugation at 400 g (for 15 minutes). After centrifugation, the supernatant was removed to recover the pellet (at the bottom of the tube). New sterile HBSS was added, and the cell pellet resuspended by drawing in and out of pipette gently. The sample was submitted to centrifugation for 10-minutes, and the wash step repeated twice more.

During this PhD, the group changed to using SepMate™ tubes as they save hands-on-time and are more reproducible, giving consistent yields with minimal carry over of toxic Ficoll-Paque. For the isolation of PBMCs using SepMate™ tubes, firstly Ficoll-Paque was added through the central hole inside the tubes. DPBS diluted blood was then added into the tube by pipetting it down the side of the tubes (in a vertical position). The blood is kept separated from the Ficoll-Paque by an insert within the SepMate™ tubes. Subsequently, the sample was subjected to centrifugation for 10 minutes at 1200 g at room temperature with the brake on (Figure 2.1.2). The top liquid layer was collected which contains enriched mononuclear cells and plasma by pouring it off into a Falcon tube swiftly and avoiding placement of the SepMate™ tube in an inverted position for more than two seconds. The collected cells (and plasma) were washed with HBSS by centrifugation at 300 g for 10 minutes. The wash step was repeated for a further two times.

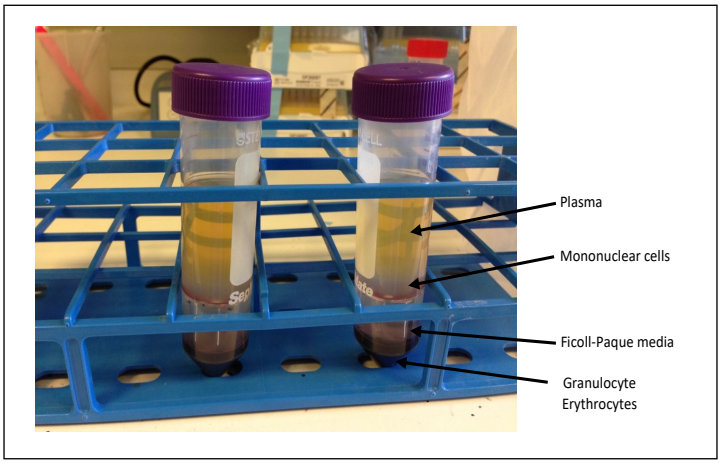

Figure 2.1.2 Isolation of PBMCs using SepMate™ tubes
Isolation of PBMCs using SepMate™ tubes reduces the centrifugation time into 10 minutes as compared to our former method. The density gradient medium used in this study is Ficoll-Paque™.

2.1.3 Isolation of monocytes by adhesion

After a final wash with HBSS, the cell pellet was re-suspended in RPMI/FCS media (see section 2.2 RPMI/FCS media). Cells were suspended at a concentration of 2.5 X 10^6 per ml and were transferred to a plastic 12-well tissue culture plate and incubated for 2 hours at 37°C (5% CO_2). The cells were then washed with sterile DPBS for three times to remove non-adherent cells before being cultured in RPMI/FCS media supplemented with colony stimulating factors (CSF).

2.2 RPMI/FCS media

Materials: DPBS (Dulbecco's Phosphate Buffered Saline; 1X; Gibco by Life Technologies™), RPMI 1640 media (Gibco by Life Technologies™), L-Glutamine (PAA), Penicillin (Invitrogen), Streptomycin (Invitrogen), Gentamicin (PAA), and 10% Foetal Calf Serum (FCS; Life Technologies). The full media used to support differentiation of PBMCs to macrophage and referred to as RPMI/FCS media, consisted of RPMI 1640 (Sigma-Aldrich) supplemented with 1% Penicillin/Streptomycin (100 U/ml Penicillin; 100 µg/ml streptomycin) (Invitrogen), 10% Foetal Calf Serum (Gibco), 200 mM L-Glutamine and 10 mg/ml Gentamicin (PAA). All supplements were filtered through a 0.20 µm sterile filter, and the media stored at 4°C when not in use, and pre-warmed before adding to cells.

2.3 Macrophage culture

Macrophage-colony stimulating factor (M-CSF) which is also known as colony stimulating factor-1 (CSF-1) and granulocyte/macrophage-colony stimulating factor (GM-CSF) which is also known as CSF-2, are important haematopoietic growth factors and potent cytokines for cell survival, proliferation, differentiation, and activation (Fleetwood *et al.,* 2009). Blood monocytes will not survive if cultured in medium alone without CSFs (Akagawa, 2002). Accordingly, blood monocytes were cultured in RPMI/FCS media supplemented with M-CSF (40 ng/ml) or a combination of M-CSF + GM-CSF (20 ng/ml each) for six days to produce fully differentiated macrophages, polarised towards M-Mac or GM-Mac respectively. The media was changed to fresh RPMI/FCS plus the respective CSFs at day 3 or 4 of incubation.

Table 2.3.1 Growth factors for macrophages used in this study.
*(M-*CSF *= macrophage-colony stimulating factor, GM-CSF = granulocyte/macrophage-colony stimulating factor, both are* recombinant *human* proteins*)*

Factors	Stock concentration	Working concentration	Dilution factor	Supplier	Catalogue No.
M-CSF	100 µg/ml	40 ng/ml	1:2500	R&D	130-096-492
GM-CSF	100 µg/ml	20 ng/ml	1:1250	R&D	130-093-865

2.4 Cell collection for RNA analysis

Qiazol lysate

Total RNA, including microRNA, was extracted using Qiazol (miRNeasy mini-kit, Qiagen, cat. No. 217084). Upon the end of planned culture experiments, cells were washed with sterile PBS before 350 µl Qiazol lysis buffer was added. Cell lysates were then scraped using a blue pipette tip to aid lysis, before transferal into a sterile RNase/DNase-free Eppendorf tube and stored at -80^{o}C until the RNA extraction and purification procedure.

Cell lysate in RLT buffer

RLT lysate buffer (RNeasy plus mini-kit, Qiagen, cat. No. 74134) was used to collect mRNA only. β-mercaptoethanol was added to RLT lysis buffer at 1:100 v/v as per manufacturer's instructions. Cells were washed with sterile PBS twice before 350 µl RLT lysis buffer was directly added onto the cells. The lysates were then scraped using a 1ml syringe barrel and the cell lysate transferred into a sterile RNase/DNase-free Eppendorf tube and stored at -80^{o}C until the RNA extraction and purification procedure.

2.5 RNA extraction and purification

Materials used as follows: 1) miRNeasy mini-kit, Qiagen cat. No. 217004 (contains RNeasy mini spin columns, collection tubes (1.5 ml and 2 ml), Qiazol lysis reagent, RNase free buffers (RWT and RPE) and RNase-free water); or 2) RNeasy plus mini-kit, Qiagen, cat. No. 74134 (contains: gDNA eliminator spin column, RNeasy mini spin columns, RPE buffer, RWI buffer, RLT buffer and RNase-free water).

Protocol for RNA extraction and purification: miRNeasy minikit

The cell lysate (in Qiazol) was thawed and briefly centrifuged before the addition of 140 µl chloroform. The mixture was vortexed for 15 seconds and then left at room temperature for 3 minutes before centrifugation at 12000 g speed at 4^{o}C for 15 minutes. The centrifugation results in the generation of a two-layer phase; an upper aqueous clear layer above a bottom pink layer. The top aqueous phase (containing the RNA) was collected and transferred to a RNAse free Eppendorf tube (Ambion) while the pink solution was discarded. Next, 525 µl absolute ethanol was added to the collected clear aqueous phase and mixed thoroughly by pipetting up and down. The mixed solution ~ 700 µl in volume was then transferred to a column tube and centrifuged at 8000 g for 15 seconds at room temperature. The flow-through was discarded and 700 µl RWT buffer added to the column before centrifugation at 8000 g for 15 seconds at room temperature. The flow-through was once again discarded and 500 µl RPE buffer added before centrifugation at 8000 g for 15 seconds at room temperature. This step was repeated with RPE buffer with a 2-minute centrifugation. Again, the flow-through was discarded, and the collection tube changed before centrifugation at 16000 g for 1 minute at room temperature. The column was then placed in a new Eppendorf RNAse free tube. Then, 30 µl RNAse free H_2O was added directly on top of the membrane inside the column before centrifugation at 8000 g for 1 minute to elute the RNA.

Protocol for RNA extraction and purification: RNeasy plus mini kit

The cell lysate (in RLT buffer) was thawed and briefly centrifuged. The sample was then transferred to a genomic (g) DNA eliminator spin (purple) column (RNeasy plus mini kit, Qiagen) and centrifuged for 30 seconds at 8000 g. The flow through was collected and the column discarded. Then, 350 µl 70% alcohol was added to the sample (flow through) and mixed well by pipetting up and down. The mixture was then transferred to a RNeasy spin (pink) column (RNeasy plus mini kit, Qiagen) and centrifuged for 15 seconds at 8000 g. The flow through was discarded and the column kept. Next, 700 µl RW1 buffer was added to the column and centrifuged for 15 seconds at 8000 g. The flow

through was discarded and the column kept before addition of 500 µl RPE buffer to the column and centrifuged (for 15 seconds at 8000 g). This step was repeated with 500 µl RPE buffer and centrifuged for 2 minutes at 8000 g. The flow through was discarded and the column placed in a new collection tube for a 1-minute centrifugation. The collection tube was then changed with a new Eppendorf RNAse free tube (Qiagen), and 30 µl RNAse free H_2O (Qiagen) added directly on top of the column membrane. The column was centrifuged for 1 minute at 8000 g to elute the RNA. The column was discarded, and RNA sample kept at -20^{o}C or -80^{o}C before the RNA quantification procedure.

2.6 RNA Quantification

Initial RNA concentrations were determined using a NanoDrop^{TM} 1000 Spectrophotometer (Thermo Scientific). The absorbance rate at 260/280 was used to assess the purity of RNA. Initial RNA concentrations (ng/µl) were recorded for calculation of mRNA volume for the subsequent RT-PCR reaction. This facilitated the use of the same RNA concentration to generate equal amounts of cDNA. Samples with a 260/280 ratio <1.8 (contamination with ethanol or phenol) or a 260/230 ratio >2.2 (contamination with nucleic acid) were excluded from further analysis.

2.7 cDNA synthesis (Reverse Transcription Polymerase Chain Reaction, RT-PCR)

Materials used: miScript II RT kit (cat. no. 218161), QuantiTect Reverse Transcription Kit (cat. no. 205313), and Thermal Cycler C1000 TouchTM (Bio-Rad).

All reactions were set up on ice to minimise the risk of RNA degradation.

RT-PCR using QuantiTect RT kit (for RLT lysate)

The QuantiTect Reverse Transcription Kit contains: 1) 7x gDNA Wipeout Buffer, 2) RNase-free water, 3) Quantiscript Reverse Transcriptase, 4) 5x Quantiscript RT Buffer and 5) RT Primer Mix.

Firstly, the purified RNA sample (+ RNase-free water) was incubated with 2µl/reaction gDNA wipeout buffer (total volume reaction = 14 µl), at 42°C for 2 minutes to remove contaminating genomic DNA. Following the gDNA elimination process, reverse transcription reaction was performed by adding RT primer mix (volume: 1x), RT Quantiscript buffer (4x) and Quantiscript reverse transcriptase (1x). Total reaction volume was 20µl (Table 2.7.1), and was placed within a Thermal Cycler C1000 Touch™ (Bio-Rad) and incubated at 42°C for 30 minutes followed by 95°C for 3 minutes. The cDNA was stored at -20°C until required for the QPCR reaction procedure.

Table 2.7.1 Reverse-transcription reaction components
RT master mix consisted of Quantiscript Reverse Transcriptase, RT Buffer and RT Primer Mix. RT Primer Mix and RT buffer were premixed (1:4) for routine RT reaction and stored at -20°C.

Component	Volume/reaction (µl)
Quantiscript Reverse Transcriptase	1
Quantiscript RT Buffer, 5x	4
RT Primer Mix	1
gDNA elimination reaction components (H2O + Vol.RNA + gDNA)	14
Total volume/reaction	20

RT-PCR using miScript II RT kit for total RNA (Qiazol lysate)

The miScript II RT kit contains: 1) miScript Reverse Transcriptase mix, 5x miScript HiFlex buffer, 10x Nucleics mix and RNase-free water.

Reverse transcription PCR of purified RNA was performed with miScript II RT kit using the reaction components shown in Table 2.7.2. Firstly, the reaction mix was prepared by adding miScript Reverse Transcriptase mix, Nucleics mix and 5x miScript HiFlex buffer to an RNase/DNase-free Eppendorf tube. The reaction mixes were vortexed briefly before addition of the purified RNA (+ RNase free water) for a total reaction volume of 20 µl for each sample.

The reaction was carried out in a Thermal Cycler C1000 Touch^{TM} (Bio-Rad) at 37^{o}C for 60 minutes followed by 95^{o}C for 5 minutes.

Table 2.7.2 Reverse Transcription reaction components (miScript)

Components	Volume/ reaction (µl)
miScript Reverse Transcriptase mix	2
5x miScript HiFlex buffer	4
10x Nucleics mix	2
Template RNA + RNase free H_2O	12

2.8 96-well Quantitative-Polymerase Chain Reaction (Q-PCR)

96-well Quantitative-PCR (Q-PCR) (or real-time PCR) was performed using LightCycler® 480 SYBR Green I Master (Roche, Germany, cat. No. 04707516001). The primers used for human genes are described in Table 2.8.1 (designed and purchased from Qiagen) or Table 2.8.2 (home designed primers, purchased from Sigma-Aldrich). Qiagen primers were reconstituted in 1.1 ml Tris ethylenediaminetetraacetic acid EDTA (TE) buffer, pH 8.0 and aliquoted in DNAse free tubes. Home designed primers comprised of separate forward and reverse primers which were reconstituted in TE at a volume instructed on the manufacturers sheet and used in 1:2 for each.

Table 2.8.1 QuantiTect primer assay used for QPCR

QuantiTect primers contain a mix of lyophilised forward and reverse primers for a specific target. Each assay is derived from gene sequences contained within the NCBI Reference Sequence database (https://www.ncbi.nlm.nih.gov/refseq/).

Gene name	Gene symbol	Cat. No.	Refseq transcripts
α-SM-actin	ACTA2	QT02407307	NM_001141945, NM_001613
β-actin	ACTB	QT00095431	NM_001101, XM_006715764
Calmodulin-1	CALM1	QT00997906	NM_001166106, NM_006888
Calponin-1	CNN1	QT00067718	NM_001299, XM_005259741
Desmin	DES	QT00071778	NM_001927
Smoothelin	SMTN	QT00026677	NM_001207017, NM_001207018
Transgelin (SM22-alpha)	TAGLN	QT00072247	NM_001001522, NM_003186
Vimentin	VIM	QT00095795	NM_003380, XM_006717500

Table 2.8.2 Home designed primers used in the study

Primers were designed using the primer blast programme on the Sigma-Aldrich website.

Gene name	Forward/Reverse	Primer Sequence (5' – 3')
CDH5 (VE-cadherin)	Forward	CGCAATAGACAAGGACATAAC
	Reverse	TATCGTGATTATCCGTGAGG
Caldesmon	Forward	AAACGCCAGAAGATGCCAGA
	Reverse	ACACCACTGCTTTTCTGCAC
FGFR1	Forward	AGGAACTTTTCAAGCTGC
	Reverse	CATCATGTACAGCTCGTTG
FGFR2	Forward	ATGGAGATATGGAAGAGGAC
	Reverse	CATCTTCTGGCTCTAATGTG
FGFR3	Forward	GAAGATGCTGAAAGACGATG
	Reverse	GCAGGTTGATGATGTTTTTG
FGFR4	Forward	CTGAGGACAATGTGATGAAG
	Reverse	CCGTTGCTGGTTTTCTTATAG
FLT1	Forward	ATGTGAAACCCCAGATTTAC
	Reverse	TGATTGTAGGTTGAGGGATAC
KDR	Forward	GTACATAGTTGTCGTTGTAGG
	Reverse	TCAATCCCCACATTTAGTTC
KLF4	Forward	TCTTGAGGAAGTGCTGAG
	Reverse	ATGAGCTCTTGGTAATGGAG
MYH1	Forward	CCGGGAAAACCGAAAACACC
	Reverse	CCAGCTCTCCGTAGGCAAAA
NANOG	Forward	CCAGAACCAGAGAATGAAATC
	Reverse	TGGTGGTAGGAAGAGTAAAG
PECAM-1	Forward	AGATACTCTAGAACGGAAGG
	Reverse	CAGAGGTCTTGAAATACAGG
SOX2	Forward	ATAATAACAATCATCGGCGG
	Reverse	AAAAAGAGAGAGGCAAACTG
VWF	Forward	TGTATCTAGAAACTGAGGCTG
	Reverse	CCTTCTTGGGTCATAAAGTC
36B4	Forward	GCCAGCGAAGCCACGCTGCTGAAC
	Reverse	CGAACACCTGCTGGATGACCAGCCC

Table 2.8.3 Master reaction mixture including LightCycler® 480 SYBR Green I Master reaction mix

*It is essential the SYBR Green I Master reaction mix is protected from light. *For the PCR primers 1 µl for the QuantiTect primers were used, whereas 0.5 µl for each of the forward and reverse home-designed primers were used.*

Reagent/components	Volume (µl)
Water, PCR grade	3
*PCR Primer(s)	1
SYBR Green I Master	5
Total volume/reaction	9

The reaction mix shown in Table 2.8.3 was mixed thoroughly by pipetting up and down several times (without vortexing). The master reaction mixture was loaded into the respective wells of a 96-well plate followed by 1µl of sample/well (cDNA, at same concentration for each reaction). Total volume for each reaction was 10µl. Each cDNA sample was analysed in duplicate. As negative controls, a blank RT reaction sample was used for each primer. Once mixture loading was completed, the plate was sealed with sticky sealing plastic (Greiner Bio-one, cat. no. 676040). The plate was then centrifuged for 30 seconds at 500 g on an MPS-1000 mini-plate spinner (Labnet) before being loaded into a Roche LightCycler® 480. The PCR programme 'SYBR Green I 96-II' was run with the protocol summarised in Table 2.8.4.

Table 2.8.4 QPCR reaction protocol used in the study

Step	Temperature (°C)	Duration	Number of cycles
Pre-incubation	95°C	5 minutes	1
Amplification	Denaturation: 95°C	10 seconds	45
	Annealing: 60°C	10 seconds	
	Extension: 72°C	10 seconds	
Melting curve	95°C	5 seconds	1
	65°C	60 seconds	
	97°C	Continuous	
Cooling	40°C	10 seconds	1

2.9 Q-PCR data analysis

The expression of a specific gene for each experimental condition was expressed as Cycles to Threshold (C_T), which were obtained from the LightCycler® 480 software after each reaction had completed. This value corresponds to the number of cycles an amplified cDNA template takes to reach a linear threshold of fluorescence detection (otherwise known as amplicon concentration) and was used for calculating fold changes in mRNA expression. As cDNA samples were analysed in duplicate, two C_T values were derived per sample and were therefore averaged to give a mean C_T value for each sample. The 2^- ΔΔCT were calculated for each sample and averaged for the group to reflect average fold change in expression against a control group for each experiment. With regards to mRNA normalisation, the expression of two housekeeping genes was assessed, 36B4 and β-actin.

2.10 Western Blotting

2.10.1 Cell collection for protein analysis

Cells were washed twice with sterile PBS, before 120µl of 5% SDS lysis buffer (50 mM Tris-HCL pH 6.8, 10% Glycerol, 5% SDS) were added. The cells were scraped with the insert of a 1ml syringe and lysates were collected in Eppendorf tubes (0.5ml). Cell lysates were stored at -20°C until use for protein assay and electrophoresis procedure.

2.10.2 Protein assay (Protein quantification)

Materials used as follows: Micro Bicinchoninic Acid (BCA) Protein Assay Kit (Thermo Scientific, cat.no. 23235) contains Micro BCA Reagent A (MA), Micro BCA Reagent B (MB), Micro BCA Reagent C (MC) and Bovine Serum Albumin (BSA) 2 mg/ml; high-performance liquid chromatography (HPLC) water and SDS lysis reagent; plate reader used is a Thermo Scientific Multiskan EX; 96-well plate (flat bottom).

Protocol for protein assay using Micro BCA Protein Assay Kit

First, 140µl of HPLC water were added into the respective wells of a 96-well plate (flat bottom) followed by 5µl of sample (in SDS lysate buffer) in duplicate. A set of protein standards was prepared using BSA at the following concentrations; 0, 0.1, 0.25, 0.5, 1.0, 2.5, 5.0, 10 mg/ml. Next, 150µl of the BCA reaction mix which comprises of Reagent A, Reagent B and Reagent C (in 25:24:1 volume), were added to each well. The reactions were then incubated for 1 hour at 37°C before analysis at 560 nm on ELISA plate reader (Thermo Scientific Multiskan EX). The protein concentration for each sample was obtained using the BSA standard curve.

2.10.3 Polyacrylamide Gel Electrophoresis (PAGE)

Gel electrophoresis to separate different protein sizes was performed using a Bio-Rad system. Cell lysates (in SDS) were diluted in HPLC water (amount determined from the protein assay) in order to obtain equal protein concentrations within a total 20µl volume. Subsequently, 5µl of bromoethanol blue (as electrophoretic colour marker) and 1.5µl of β-mercaptoethanol (a reducing agent to allow protein molecules to undergo electrophoresis consummately by molecular weight) were added to each sample. The mixture was incubated at 95°C for 10 minutes. Then, the mixture was briefly centrifuged before loading into Mini-PROTEAN® TGX Stain Free Gels (Bio-Rad, cat. no. 456-8024 for 7.5% polyacrylamide gels; or cat. no. 456-8084 for 4-15% polyacrylamide gels) and subjected to electrophoresis in a Mini-PROTEAN® Tetra Cell (Bio-Rad, 165-8004) filled with 10% running buffer (Bio-Rad cat. no. 161-0732) for 30 minutes at 200V. A Protein marker (Geneflow Limited, cat. no. S60024) was used as a molecular weight marker.

2.10.4 Stain free gels

Once electrophoresis is completed, the gels are then exposed to ultraviolet (UV) light using a ChemiDoc™ MP System (Bio-Rad, cat. no. 170-8280), to activate a covalent reaction between tryptophan residues in the (protein) samples with the trihalo-compounds in Mini-PROTEAN® TGX Stain Free Gels. This interaction results in a fluorescent signal that can be captured by the

ChemiDoc™ software and subsequently used to evaluate equal protein loading and as a control when calculating relative expression of a target protein.

2.10.5 Blotting & Immunodetection

Materials used for blotting: Trans-Blot® Turbo™ Transfer Instrument and Cassettes (Bio-Rad, cat. no. 170-4155), Midi/Mini Nitrocellulose Transfer (ready to use) pack with two buffer-saturated ion reservoir stacks and pre-wetted nitrocellulose 0.2 µm membrane (Bio-Rad, cat. no. 170-4158) and membrane roller (Bio-Rad, cat. no. 1651279).

The electrophoretically separated protein gel was subsequently transferred to a 0.2µm pore nitrocellulose membrane between two reservoir stacks (Figure 2.10.1) inside a trans-blot cassette. Any bubbles trapped between the two stacks were removed through use of a membrane roller before the top cassette was put in place. The cassettes were then loaded into a trans-blot instrument and transfer carried out for 7 minutes at 40 volts.

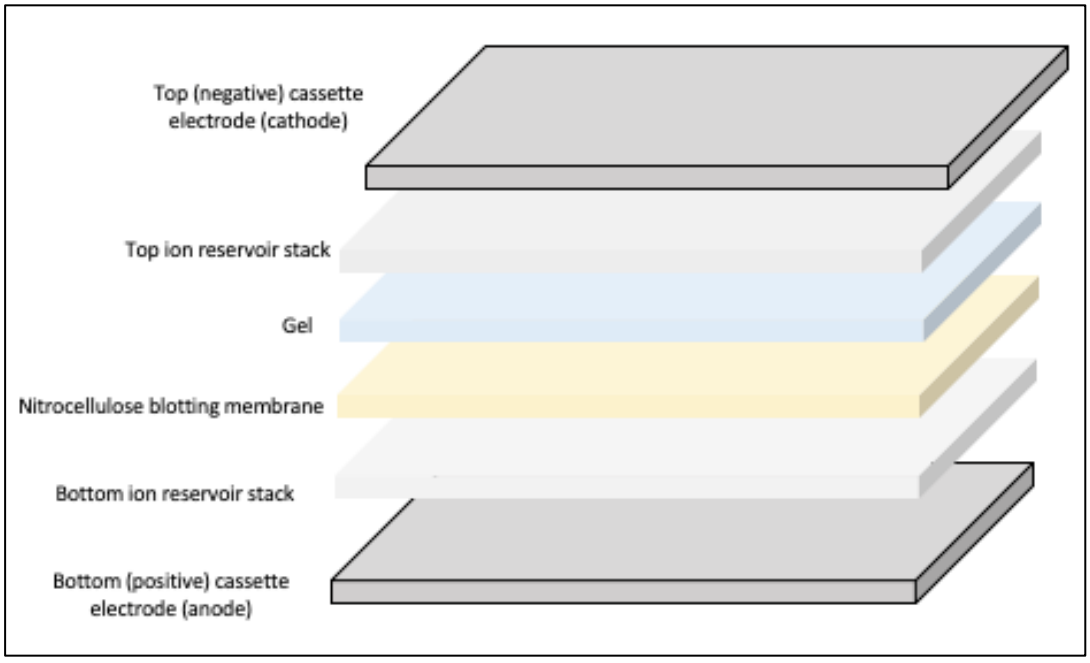

Figure 2.10.1 Schematic diagram layering of an assembled transfer pack (Bio-Rad)
The gel is sandwiched between two buffered-saturated stacks and directly above a blotting membrane, to ensure efficient transfer of proteins from the gel to the membrane. (Image adapted from original source https://www.bio-rad-antibodies.com/western-blot-protocol.html).

Following the trans-blotting, the nitrocellulose membrane was then incubated with 5% milk solution in Tris-Buffered Saline-Tween (TBS-T; 200mM Tris, 2% Tween 20, pH 7.6), for 30 minutes on a roller to block any non-specific antibody binding.

Materials used for immunoblotting: SignalBoost™ Immunoreaction Enhancer Kit (Merck Millipore, cat. no. 407207) contains: Solution 1 for primary antibodies (KP31812) and Solution 2 for secondary antibodies (KP31855).

The membrane was washed with TBS-T buffer and incubated overnight at 4°C with the relevant primary antibody (Table 2.10.1 and Table 2.10.2) diluted to the desired concentration in SignalBoost Solution 1.

Table 2.10.1 Primary antibodies used for immunodetection of VSMC-markers by Western blotting
(CALM1 = calmodulin-1, Myh11 = myosin heavy chain-11, SMTN = smoothelin, CST = Cell Signalling Technology).

Antibody	Species	Molecular Weight (kDa)	Concentration	Supplier	Cat. No.
Caldesmon-1	Rabbit	70-80 (non-muscle) 120-150 (smooth muscle)	1/1000	CST	#12503
Calmodulin-1	Rabbit	15	1/1000	Abcam	Ab45689
Myosin heavy chain 11	Rabbit	227 - 250	1/1000	Abcam	Ab 82541
Smoothelin	Mouse	110 (long isoform) 59 (short isoform)	1/250	Santa Cruz biotech	Sc-376902
Vimentin	Rabbit	57	1/1000	CST	#5741

Table 2.10.2 Primary antibodies used for immunodetection of EC-markers by Western blotting

All antibodies are from Cell Signalling Technology (CST).

Antibody	Species	Molecular Weight (kDa)	Concentration	Cat. No.
FGF Receptor 1	Rabbit	90, 120, 145	1/500	D8E4 XP (#9740)
PECAM-1 (CD31) (89C2)	Mouse	130	1/1000	#3528S
Phospho-Stat3 (Tyr 705)	Rabbit	79, 86	1/1000	D3A7 XP (9145)
Phospho-Stat5 (Tyr694)	Rabbit	90	1/500	(#9351)
Stat3 (total Stat3)	Rabbit	79, 86	1/500	D1B2J #30835
Stat5a (4HI) (total Stat5)	Mouse	90	1/500	#4807
VE-cadherin (D87F2)	Rabbit	130-140	1/1000	#2500S

After overnight incubation with the relevant primary antibody, the membrane was washed in TBS-T twice and incubated in 5% milk (in TBS-T) for 30 minutes at room temperature.

Subsequently, the membrane was incubated with the relevant secondary IgG antibodies (Table 2.10.3) directed against the appropriate species (all Dako) diluted 1:1000 in SignalBoost Solution 2 for 1 hour at room temperature.

Table 2.10.3 Secondary antibodies used for immunodetection by Western blotting

(IgG = Immunoglobulin, HRP = Horseradish Peroxidase. All antibodies are from Dako)

Secondary Antibodies	Cat. No.
Polyclonal Goat Anti-Rabbit IgG/ HRP	P0448
Polyclonal Goat Anti-Mouse IgG/ HRP	P0447
Polyclonal Rabbit Anti-Goat IgG/HRP	P0449

After the incubation, the membrane was washed in three changes of TBS-T, followed by a 30 minute wash and three further 5 minute washes.

Materials used for immunodetection: Luminata™ Forte Western chemiluminescent HRP substrate (Merck Millipore, cat. no.12634645) and ChemiDoc™ MP Imaging System (Bio-Rad).

To detect the HRP-labelled proteins, an Enhanced Chemi-Luminescence (ECL) Luminata Forte Western HRP Substrate detection solution was used. The membrane was incubated for 3 minutes with ECL and luminescence was then detected by ultraviolet light using the ChemiDoc™ MP Imaging System. The relative density of the detected bands was determined using Image Lab™ software version 5.1 (Bio-Rad) by optical densities (mm^2) and normalised to stain-free gels.

2.11 Immunocytochemistry

Fluorescence immunocytochemistry (ICC) was deployed to detect VSMC and EC markers as listed in Table 2.11.1 and Table 2.11.2. Firstly, cells (5 X 10^5 cells in 200 µl) were seeded in 8-well Millicell EZ glass slides (Merck Millipore, cat. no. PEZGS0816) and subjected to the relevant experimental conditions until ready for fixation. Consequently, cells were washed twice with DPBS and fixed in 3% (w/v) paraformaldehyde/PBS for 10 minutes at room temperature. After washing three times with PBS, the cells were permeabilised with 0.2% (v/v) Triton X-100/PBS. The cells were then briefly washed with PBS, and non-specific antibody binding was blocked by Image-iT FX signal enhancer (Invitrogen, cat. no. 136933) for 30 minutes at room temperature. The cells were then incubated with the relevant primary antibodies (Table 2.11.1 and Table 2.11.2) overnight at 4°C. The following day, cells were washed three times with PBS and incubated with a relevant fluorescently-conjugated secondary antibody (either anti-mouse, anti-goat, or anti-rabbit IgG according to the species of the respective primary antibody) diluted 1:100 in PBS for 1 hour at room temperature in the dark (wrapped with aluminium foil). Finally, cells were washed twice with PBS, and the slides mounted with glass coverslips and Prolong Gold containing 4',6-diamidino-2-phenylindole (DAPI) (Invitrogen,

cat. no. P36931) as a nuclear counterstain. The cells were then imaged, and representative fields acquired using an Olympus BX41 microscope and Q-capture pro 6.0 software. Nuclei appeared blue and positive protein expression was green.

Table 2.11.1 Primary antibodies used for immunofluorescence labelling of VSMC-markers
(α–SM-actin = α- smooth muscle actin, Myh11 = myosin heavy chain-11)

Antibody	Dilution	Cat. No.	Supplier	Species	Secondary antibody
α-SM-actin	1/200	A-2547	Sigma	Mouse	Goat anti-mouse
Caldesmon	1/400	Ab45689	Abcam	Rabbit	Goat anti-rabbit
Mac-2 (Galectin-3)	1/200	CL8942AP	Cedar Lane	Goat	Rabbit anti-goat

Table 2.11.2 Primary antibodies used for immunofluorescence labelling of EC-markers
(CD31 = cluster of differentiation 31. All antibodies are from Cell Signalling Technology).

Antibody	Dilution	Cat. No.	Species	Secondary antibody
PECAM-1 (CD31)	1/1600	#3528S	Mouse	Goat anti-mouse
VE-cadherin	1/1600	#2500S	Rabbit	Goat anti-rabbit

2.12 Statistical analysis

Statistical analysis was performed using GraphPad InStat statistical software. For experiments comparing means of more than two groups, a repeated measures analysis of variance (ANOVA) test was used with a Tukey-Kramer Multiple Comparisons post-test. If matching of samples was not effective, a Friedman (non-parametric repeated measures ANOVA) test was used with a Dunn post-test. All data is presented as mean ± standard error of the mean (±SEM). When data were presented as a fold change and compared to 1 or 100, a paired two-tailed t-test was used for normally distributed data. If data failed the normal distribution test and assumed to have different standard deviations, the alternate (Welch) t test was used. If samples still failed to display Gaussian distribution, a Mann-Whitney (non-parametric) test was used. An output of $P<0.05$ was accepted as significantly different in all statistical tests.

3 *In vitro* human macrophages display divergent polarisation towards vascular smooth muscle cell-like phenotypes

3.1 Introduction

3.1.1 Phenotypic modulation of vascular smooth muscle cells

Vascular smooth muscle cells (VSMCs) populate the medial compartment of the vessel wall, within which they regulate physiological blood flow by dynamically controlling vessel luminal diameter, through contraction and relaxation. During vasculogenesis, VSMCs exhibit a highly proliferative and migratory phenotype associated with heightened extracellular matrix synthesis, while at the same time acquiring contractile capabilities before their differentiation towards a contractile phenotype (Owens *et al.,* 2004). Within healthy arteries, VSMCs proliferate at very low rates in order to retain their contractile function, hence the contractile phenotype nomenclature (although they are also sometimes termed quiescent). Contractile VSMCs are characterised by marked expression of contractile proteins such as α-smooth muscle actin (α-SM-actin), caldesmon, and smooth-muscle myosin heavy chain-11 (Myh11) (Dobnikar *et al.,* 2018). VSMCs can also exist as a synthetic phenotype which are present during both developmental processes such as neovascularisation in the embryo (Ball *et al.,* 2010) and vessel formation (Owens *et al.,* 2004), and also during cardiovascular disease states including adverse vascular remodelling and atherosclerosis (Chistiakov *et al.,* 2015). The shift between the two phenotypes can be modulated by various factors such as inflammation, signalling factors including platelet derived growth factor-BB (PDGF-BB) and transforming growth factor-β1 (TGFβ1), mechanical stimulation, extracellular matrix proteins (i.e fibronectin and laminin) and their degradation, and endothelial cells (Figure 3.1.1). Phenotypic modulation of VSMCs from a contractile form to a synthetic proliferative phenotype has been proposed to play a significant role during the pathogenesis of vascular diseases including atherosclerosis (Newby, 2005).

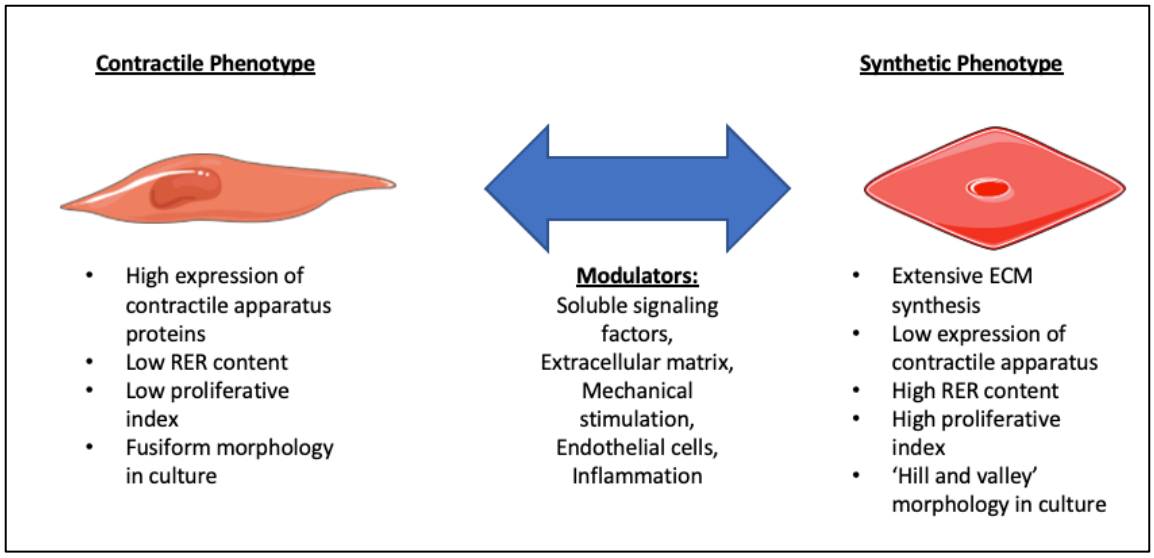

Figure 3.1.1 Phenotypic switching of vascular smooth muscle cell phenotype.
A simplified diagram summarising the triggers and characteristics of vascular smooth muscle cell phenotypic modulation. Example of soluble signalling factors are PDGF-BB, TGFβ1, basic fibroblast growth factor, insulin like growth factor, and endothelin-1. (RER: rough endoplasmic reticulum; ECM: extracellular matrix). Image adapted from original source (Beamish et al., 2010) and made using elements retrieved from https://smart.servier.com.

3.1.2 Signalling factors supporting phenotypic modulation of vascular smooth muscle cells.

Reportedly, PDGF-BB and TGFβ1 act as signalling cues for the proliferation and phenotypic switching of VSMCs from a contractile state towards a synthetic phenotype. PDGF-BB is a known mitogen and chemoattractant for VSMC *in vitro* (Hwang *et al*., 2020; Pukac *et al.,* 1998; Zhao *et al*., 2011), and has been documented to promote VSMC migration and proliferation *in vivo* (Ferns *et al*., 1991; Rutherford *et al*., 1997), and subsequent intimal thickening *in vivo* (Jawien *et al*., 1992). Therefore, PDGF-BB promotes phenotypic switching of VSMCs into synthetic cells. PDGF-BB binds to the PDGF-beta receptor (PDGFR-β) and activates downstream signalling pathways including ERK, p38 mitogen-activated protein kinase (p38 MAPK) pathways and phosphatidylinositol 3-kinase-Akt (PI3K-Akt) to enhance VSMC phenotypic switching (Yamaguchi *et al*., 2001). PDGF can be found within mammalian serum as it is readily released by platelets during thrombosis formation (Ross *et al*.,

1974). Since its discovery, purportedly many cell types have been shown to produce PDGF, including vascular endothelial cells, macrophages, VSMCs and fibroblasts (Bowen-Pope and Raines, 2011).

Phenotypic switching of VSMCs from a contractile to a synthetic state is associated with a reduced synthesis of α-SM-actin, the protein responsible for the contractile function of VSMCs. The phenomenon of the phenotypic switching VSMCs indicates that VSMCs are not terminally differentiated cells, but retain remarkable plasticity and exist as a continuum of the two phenotypes (Casscells, 1991). In addition to effects on VSMCs, PDGF-BB also influences the chemotactic activity of macrophages (Inaba *et al*., 1993), and therefore proposed to be involved in attracting inflammatory cells (such as monocyte/macrophages and neutrophils) to the sites of platelet release (vascular injury) (Deuel *et al*., 1982), and as such considered a major growth factor for macrophages and VSMCs in atherosclerosis (Kozaki *et al*., 2002; Tang *et al*., 2005; Wågsäter *et al*., 2009).

TGFβ1 is a polypeptide member of the TGF superfamily of cytokines and is secreted by many cell types. Its functions include control of cell growth, proliferation, and differentiation, apoptosis, inflammation, tissue repair, and the related expression of extracellular matrix proteins during vascular remodelling (Blobe *et al.,* 2000; Guo and Chen, 2012). TGFβ1 and its downstream signalling factors such as Smad proteins (similar to mothers against decapentaplegic, Sma gene in *Caenorhabditis elegans* and mothers against decapentaplegic gene in *Drosophila*) (Derynck *et al*., 1996) are important regulators of VSMC phenotypic switching (Tang *et al*., 2011). TGFβ1 contributes to the development of SMCs from embryonic stem cells and phenotypic switching during disease states (Sinha *et al*., 2004). Reportedly, an *in vivo* study demonstrated TGFβ1-deficient mice display defective haematopoiesis and vasculogenesis, resulting in inadequate capillary tube formation and unstable vessels with reduced cellular adhesiveness (Dickson *et al.,* 1995). TGFβ1 has also been shown to play a major role in promoting alternative activation of macrophages (Gong *et al.,* 2012). Co-operative actions of PDGF-BB and TGFβ1 have been proposed to promote wound healing, supporting their utility for therapeutic purposes (Pierce *et al.,* 1989).

In addition, a number of other modulators have been shown to direct VSMC phenotypic modulation, including FGF2, insulin-like growth factors (IGFs), epidermal growth factor (EGF), α-thrombin, factor Xa, angiotensin II (Ang II), endothelin-1, and unsaturated lysophosphatidic acids (Beamish *et al.,* 2010). However, in order to successfully induce VSMC-like cells from progenitor cell populations, researchers have previously cultured human embryonic stem cells (Gerecht-Nir *et al.,* 2003; Vo *et al.,* 2010) and human pluripotent stem cells (Wanjare *et al.,* 2013) with a combination of PDGF-BB and TGFβ1. Therefore, in this study both growth factors were used in combination to determine if primary macrophage subpopulations harboured the progenitor potential to differentiate towards a VSMC-like phenotype.

3.1.3 Gene and protein markers commonly associated with a vascular smooth muscle cell phenotype

The diverse function of VSMCs is in part attributable to the variety of gene and protein products they express. However, no single marker (at the gene or protein level) has been shown to be exclusive to VSMCs (Owens *et al.,* 2004). However, due to their abundance a few selected VSMC-associated markers are commonly used to define a VSMC phenotype, including vimentin, calmodulin, smoothelin, caldesmon, smooth muscle myosin heavy chain-11, and α-SM-actin (Owens *et al.,* 2004).

Vimentin is an intermediate filament, a major cytoskeletal structure that supports organelles within the cytoplasm and thus is important for cellular mechanical integrity (Katsumoto *et al.,* 1990). Vimentin is found in almost all eukaryotic cells, including fibroblasts, endothelial cells, and commonly used as a marker for epithelial-mesenchymal transition (EMT) (Satelli and Li, 2011) and endothelial to mesenchymal transition (EndMT) (Hong *et al.,* 2018). However, vimentin is highly expressed by VSMCs within large-sized arteries such as the aorta and carotid arteries (van Engeland *et al.,* 2019). It is involved in regulating force transmission and contraction in VSMCs (Wang *et al.,* 2006). Interestingly, human bone marrow mesenchymal stem cells have low vimentin expression

which is increased upon their differentiation towards a macrophage-like phenotype (Beneš *et al.,* 2006).

Calmodulin is a calcium binding protein, found in many cells including VSMCs and monocytes. It mediates the effect of calcium as part of calcium signal transduction pathway and activates many enzymes related to cell metabolism, inflammation, apoptosis, immune response, and smooth muscle contraction. For smooth muscle cell contraction, activation of calmodulin-dependent myosin light-chain kinase (MLCK) by calcium catalyses myosin phosphorylation which then triggers cross-bridging and the development of force contraction of VSMCs (Walsh, 1994). In macrophages, calmodulin-inducible nitric oxide synthase (iNOS)-complexes are responsible for coordinating pathways involving inflammatory cytokines such as TNFα, and in response to bacterial infection (Smallwood *et al.,* 2006; Weber *et al.,* 2006).

Smoothelin is a specific marker for contractile VSMCs (van der Loop *et al.,* 1997; van der Loop *et al.,* 1996). There are two smoothelin isoforms, A and B with molecular weights of 59 kDa and 110 kDa respectively. Smoothelin A is expressed by visceral smooth muscle cells while smoothelin-B is expressed by VSMCs. It has been demonstrated that smoothelin is encoded by a single gene on chromosome 22 but is transcribed by two different promoters to generate the two isoforms (Krämer *et al.,* 2001; van Eys *et al.,* 2007). Little is known about smoothelin function. However interruption of the smoothelin gene in mice resulted in reduced contraction force of peristalsis that leads to starvation (Niessen *et al.,* 2005) and reduced arterial contractility (Rensen *et al.,* 2008), therefore smoothelin is an integral part of the contractile machinery within smooth muscle cells.

Caldesmon is widely expressed not only in VSMCs but also in various non-muscle cells. Two isoforms of caldesmon delineate its distribution, the high molecular weight form is found in smooth muscle cells whereas, the low molecular weight isoform is expressed by non-smooth muscle cells. Caldesmon and tropomyosin are described as regulatory actomyosin-binding proteins that create cross bridge formation to produce contraction in smooth muscle cells (Somara *et al.,* 2009).

Myosin is a major contractile protein described as an actin-associated motor protein which generates forces via hydrolysis of adenosine triphosphate (ATP). Up to 35 classes of myosin have been described (Odronitz and Kollmar, 2007) with various functions demonstrated which not only affect contractility but involve processes such as cell migration, cell division, phagocytosis, cytokinesis and cell polarity, particularly in non-muscle cells (Leal *et al.,* 2003). Smooth muscle myosin heavy chain-11 (SMMHC11), which also known as myosin-11 (Myh11), can give rise to a number of isoforms including SM1, SM2 and SMemb (non-muscle isoform) in smooth muscle cells (Aikawa *et al.,* 1993). Myh11 is considered a robust marker that demarcates contractile VSMCs from their synthetic counterparts (Beamish *et al.,* 2010).

Lastly, α-SM-actin is a ~43 kDa protein expressed by contractile VSMCs and commonly used as a marker of smooth muscle lineage. Its expression is reduced upon arterial injury (Hao *et al.,* 2003), and its expression is therefore associated with reduced VSMC proliferation and migration (Chen *et al.,* 2016), and subsequently utilised as a marker of the contractile VSMC phenotype. The main function of α-SM-actin is force generation (Kim *et al.,* 2008) and thus related with regulation of arterial contractility and blood pressure homeostasis (Schildmeyer *et al.,* 2000). Reportedly, α-SM-actin is also expressed by myofibroblasts (Gan *et al.,* 2007), endothelial cells treated with TGFβ1 (Arciniegas *et al.,* 1992) and monocyte/macrophages under certain conditions *in vitro* (Ludin *et al.,* 2012).

3.2 Aim of this chapter

The aim of this chapter was to evaluate the expression of genes and proteins commonly associated with VSMCs, in distinct human *in vitro* macrophage subsets, namely M-CSF directed, and GM-CSF directed macrophages. Subsequently, the effects of PDGF-BB and TGFβ1 on VSMC-linked mRNA and protein expression was determined during *in vitro* culture of human macrophage subsets.

In addition, the expression of various VSMC specific markers in other differing macrophage phenotypes was evaluated in culture (as summarised in Table 3.2.1). Lastly, a comparison of the

expression patterns of *in vitro* primary macrophages with primary VSMCs was conducted alongside assessing the expression of a macrophage marker (Mac-2).

Table 3.2.1 Polarisation of macrophages into various phenotypes *in vitro*

(M1 = classically activated macrophage; IFNγ = interferon γ; LPS = lipopolysaccharide; M2a = interleukin-4 (IL-4) activated macrophage; M2c = interleukin-10 (IL-10) activated macrophage; M4 = platelet factor 4 (PF4) activated macrophage; Mox = oxidised 1-palmitoyl-2-arachidonoyl-sn-glycero-3-phosphorylcholine (oxPAPC) activated macrophage; foam cell = oxLDL activated macrophage; CXCL4 = (C-X-C motif) chemokine ligand 4); oxLDL = oxidised low-density lipoprotein)

Macrophage phenotype	Cytokines/factors	Key Reference(s)
M1	IFNγ and LPS	(Martinez *et al.,* 2006),
M2a	IL-4	(Stein *et al.,* 1992),
M2c	IL-10	(Lang *et al.,* 2002),
M4	PF4 (CXCL4)	(Gleissner *et al.,* 2010),
Mox	oxPAPC	(Kadl *et al.,* 2010) and
Foam cell	oxLDL	(Kruth *et al.,* 2002)

3.3 Materials and Methods

3.3.1 Macrophage culture

Human monocyte-derived macrophages were isolated and generated as outlined in the methods sections 2.1 and 2.2.

3.3.2 Stimulation of human macrophages with vascular smooth muscle cell (VSMC)-associated growth factors

Following 7 days differentiation and maturation in culture, human macrophages were co-stimulated with 10 ng/ml PDGF-BB and 1 ng/ml TGFβ1 for three days to assess their capacity to differentiate towards VSMC-like cells. The details of the growth factors are detailed in Table 3.3.1. The media and growth factors were changed one day before cell collection.

Table 3.3.1 Vascular smooth muscle cell-associated growth factors used for macrophage stimulation
(PDGF-BB = platelet derived growth factor BB; TGFβ1 = transforming growth factorβ1)

Growth Factors	Stock concentration	Dilution	Working concentration	Brand/Company	Catalogue No.
Human PDGF-BB	100 μg/ml	1/1000	100 ng/ml	Miltenyi Biotec	130-108-164
Human TGFβ1	20 μg/ml	1/2000	10 ng/ml	R&D Systems	240-B

Human recombinant PDGF-BB (received at a concentration of 25 μg) was reconstituted in sterile PBS at a concentration of 100 μg/ml and aliquoted. The recombinant human TGFβ1 (received at a concentration of 20 μg) was reconstituted in 900 μl 4 mM HCl and 100 μl 10 mg/ml bovine serum albumin (BSA) to make a 20 μg/ml TGFβ1 stock.

3.3.3 Polarisation of mature human macrophages (M-Mac) to different phenotypes

Mature M-CSF directed human macrophages (which we term M-Mac) were polarised with the designated inducers to generate different macrophage phenotypes as summarised in Table 3.3.2. The polarisation factors were added to RPMI/FCS + M-CSF. The macrophages were cultured for two days to induce polarisation before stimulation with the VSMC-associated growth factors PDGF-BB and TGFβ1 for three days (with a media and growth factor change after day two).

Table 3.3.2 Factors used for the polarisation of distinct macrophage phenotypes
(LPS = Lipopolysaccharide; IFNγ = Interferon γ; IL-4 = Interleukin-4; IL-10 = Interleukin-10; PF4 = platelet factor 4; CXCL4 = (C-X-C motif) chemokine ligand 4; oxPAPC = oxidised 1-palmitoyl-2-arachidonoyl-sn-glycero-3-phosphorylcholine; oxLDL = oxidised low-density lipoprotein).

Macrophage phenotypes	Stimulating Factors	Supplier	Catalogue No.	Stock concentration	Working concentration	Dilution factor
M1	LPS	(Sigma Aldrich)	L8274	1 mg/ml	100 n g/ml	1/10000
	IFNγ	(R&D systems)	285-IF	200 µg/ml	20 ng/ml	1/10000
M2a	IL-4	R&D systems	204-IL	100 µg/ml	20 ng/ml	1/5000
M2c	IL-10	Miltenyi Biotec	130-093-948	100 µg/ml	20 ng/ml	1/5000
M4	PF4/ CXCL4	R&D Systems	795-P4	250 µg/ml	10 ng/ml	1/25000
Mox	oxPAPC	Hycult Biotech	HC4035	25 µg/ml	25 µg/ml	1/1
Foam cells	oxLDL	Alfa Aesar	J65261	1 mg/ml	10 ng/ml	1/100000

3.3.4 Culture of human vascular smooth muscle cells (VSMCs)

Primary VSMCs isolated from human coronary artery (purchased from PromoCell; cat. no. C-12511) were used as a positive control for this study. VSMCs were maintained under culture conditions within Dulbecco's modified Eagle's Medium (DMEM) (Sigma; PAA, E15-005) supplemented with Penicillin/Streptomycin (100 U/ml Penicillin; 100 µg/ml streptomycin) (Invitrogen), 10% Foetal Calf Serum (Gibco), 200 mM L-Glutamine and 10 mg/ml Gentamicin (PAA). All supplements were added using a syringe filter to prevent infection, mixed well, and stored at 4°C. VSMCs were cultured for three days (with a media and growth factor change after day two) in 100 ng/ml PDGF-BB and 10 ng/ml TGFβ1 prior to collection for mRNA and western blotting analysis.

3.4 Results

3.4.1 *In vitro* cultured human macrophages exhibit mixed morphology

Under phase contrast microscopy, human blood-derived monocytes differentiated in the presence of M-CSF (M-Mac) for seven days displayed an elongated morphology interspersed with occasional circular macrophages, whereas GM-CSF directed macrophages (GM-Mac) exhibited a spherical appearance (Figure 3.4.1 a and b respectively). This is in line with the findings of Waldo *et al* (2008) which also described monocyte-derived macrophages showing a rounded morphology when differentiated in the presence of GM-CSF, while under M-CSF maturation, the majority of macrophages are elongated with the presence of many vacuoles (Waldo *et al.,* 2008). Stimulation for three days with PDGF-BB and TGFβ1 had no effects on cell morphology in either macrophage phenotype, when observed by phase contrast microscopy.

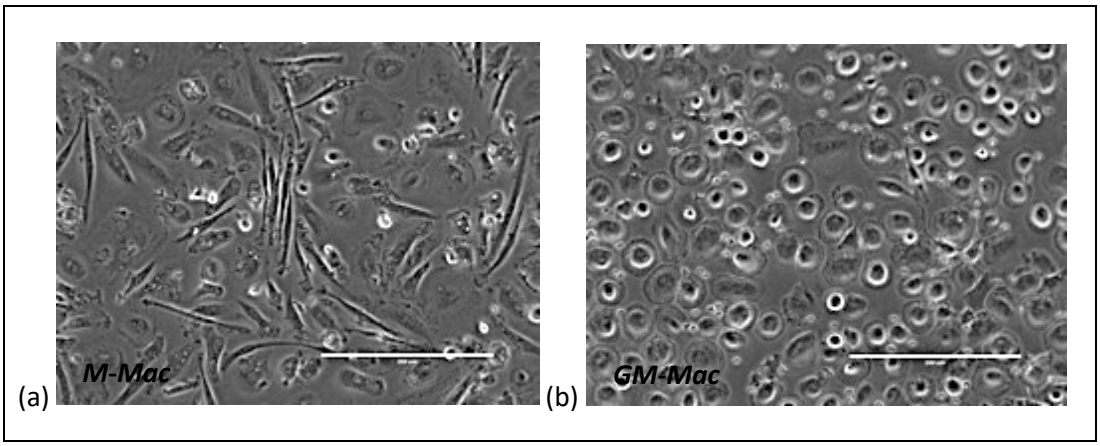

Figure 3.4.1 Effect of M-CSF and GM-CSF maturation on the morphology of human macrophages

Representative phase contrast microscopy images of (a) seven-day M-CSF (40 ng/ml) directed human macrophages (M-Mac), and (b) seven-day GM-CSF (20 ng/ml) directed macrophages (GM-Mac). Scale bars represent 200 μm.

In order to determine if the morphology of M-CSF-matured human macrophages (M-Mac) is affected by polarisation towards classically (M1) or alternatively (M2) activated phenotypes, M-Macs were stimulated for two days with polarising factors then observed under phase contrast microscopy. M1 polarisation with LPS and IFNγ resulted in M-Macs exhibiting clumps, analogous to colony formation

(Figure 3.4.2 b). Opposingly, M2a macrophage polarisation with IL-4 resulted in no marked difference in morphology when compared to control non-polarised M-CSF-matured macrophages (Figure 3.4.2 c). However, M2c polarisation with IL-10 appeared to increase the proportion of elongated macrophages relative to the rounded cells, in comparison to non-polarised M-Macs (Figure 3.4.2 d).

Exposure of M-Macs to oxLDL and subsequent intracellular accumulation (also referred to as foam cell formation and analogous to lipid-laden macrophages within atherosclerotic plaques) induced cells to acquire a more rounded morphology alongside the formation of occasional colonies/clumps (Figure 3.4.3 a). Oil red O staining to detect neutral lipids, demonstrated macrophage foam cell formation as observed by intracellular lipid accumulation (Figure 3.4.3 b).

For comparison, cultured primary human coronary artery VSMCs displayed an elongated appearance (Figure 3.4.4) not too dissimilar to the elongated morphology observed within a population of the M-CSF matured macrophages.

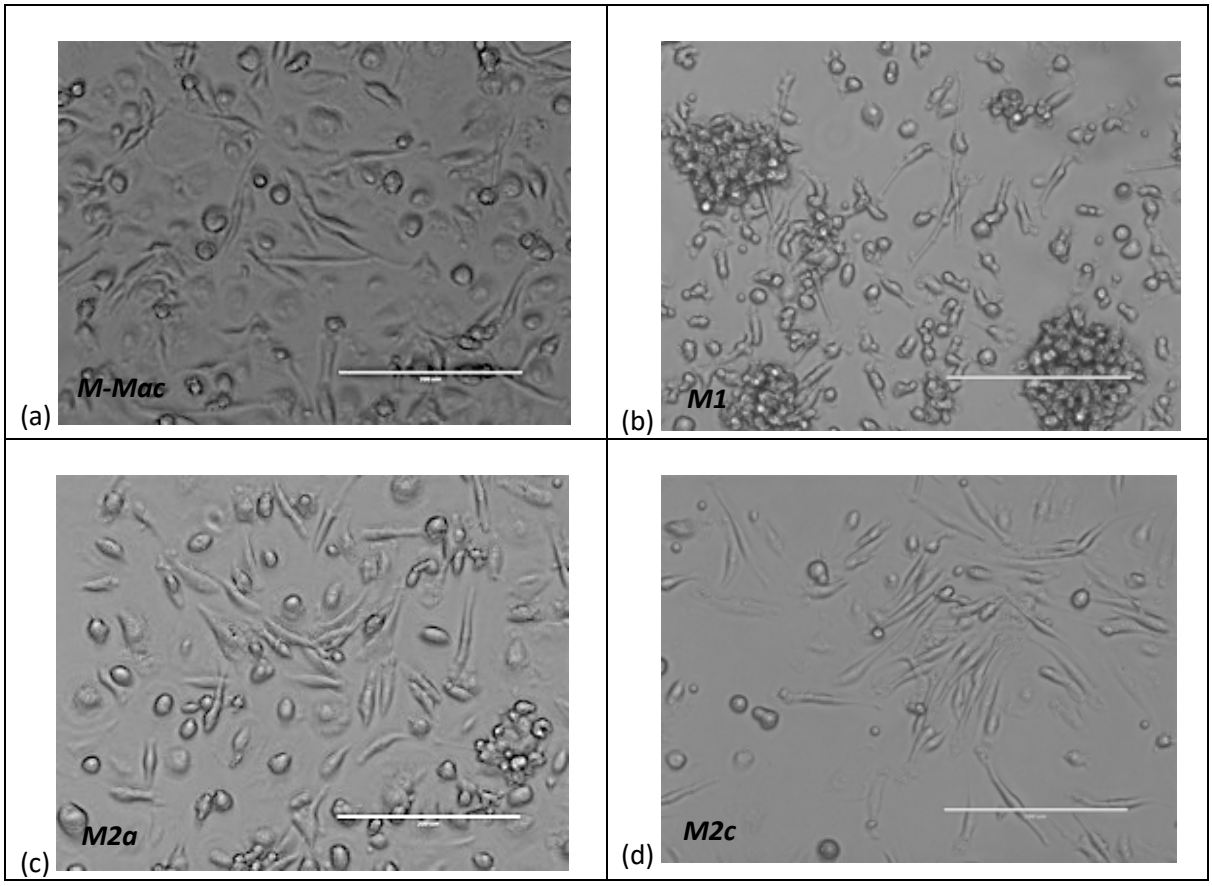

Figure 3.4.2 Effect of M1 and M2 polarisation on the morphology of M-CSF matured human macrophages

Representative phase contrast microscopy images of seven-day M-CSF (40ng/ml) matured human macrophages (M-Mac) (a) without polarisation, or polarisation with either (b) LPS (100 ng/ml) and IFNγ (20ng/ml) to generate M1 macrophages, (c) IL-4 (20ng/ml) to generate M2a macrophages, or (d) IL-10 (20ng/ml) to generate M2c macrophages, for two days. Scale bars represent 200 μm.

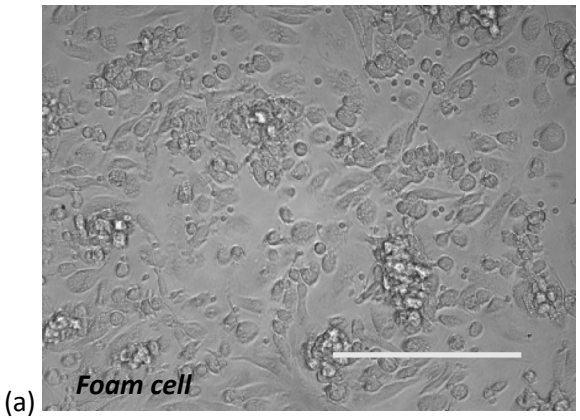

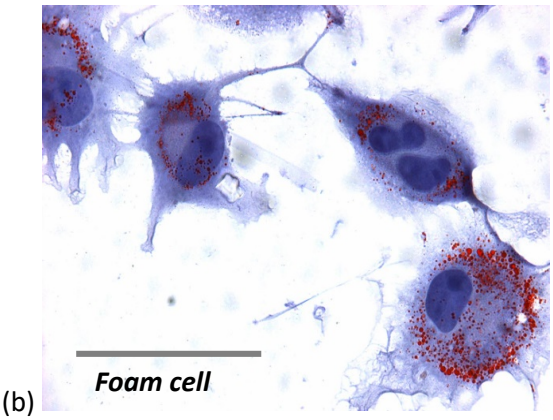

Figure 3.4.3 Photomicrograph of foam cells in culture.

(a) Phase contrast microscopy of oxLDL-activated M-CSF macrophages (foam cells). Scale bar represents 200 μm. (b) Oil red O staining of foam cells. Lipid stained red/orange while nucleus-stained dark purple, and the cytoplasm stained light purple. Scale bar represents 100 μm.

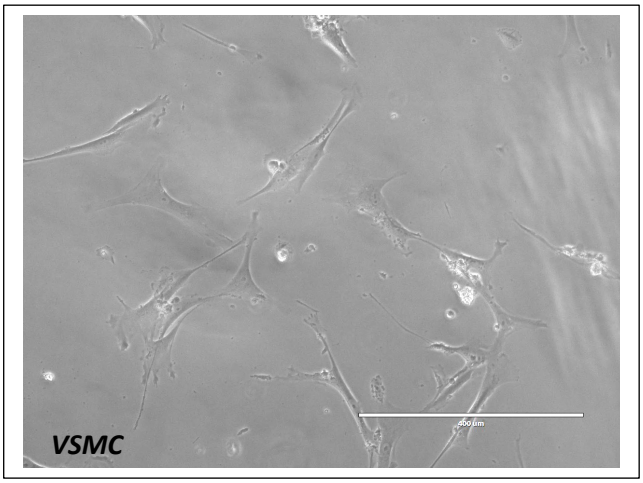

Figure 3.4.4 Photomicrograph of primary arterial vascular smooth muscle culture in DMEM full media.

Scale bar represent 400 μm.

3.4.2 GM-CSF-directed macrophage maturation is associated with increased expression of VSMC-associated markers in comparison to M-CSF matured macrophages

Considering the marked differences in morphology observed between M-CSF and GM-CSF matured human macrophages, the expression profile of a selection of VSMC-associated markers were analysed after seven-days maturation between the two phenotypes. Intriguingly, both M-CSF and GM-CSF seven-day differentiated macrophages expressed all the VSMC-related markers examined, at both the mRNA and protein level (Figure 3.4.5 - Figure 3.4.10). Interestingly, when compared to M-CSF matured macrophages (M-Mac), the protein expression of α-SM-actin, caldesmon, calmodulin, myosin heavy chain-11, smoothelin and vimentin were all significantly up-regulated in GM-CSF differentiated human monocyte-derived macrophages (Figure 3.4.5 - Figure 3.4.10). Although, at the mRNA level, reciprocal changes in caldesmon (Figure 3.4.6) and myosin heavy chain-11 (Figure 3.4.8) were not observed. Notably, other VSMC-specific markers assessed, including calponin, desmin and transgelin were not expressed (at the level of detection) within either M-CSF or GM-CSF matured macrophages (data not shown).

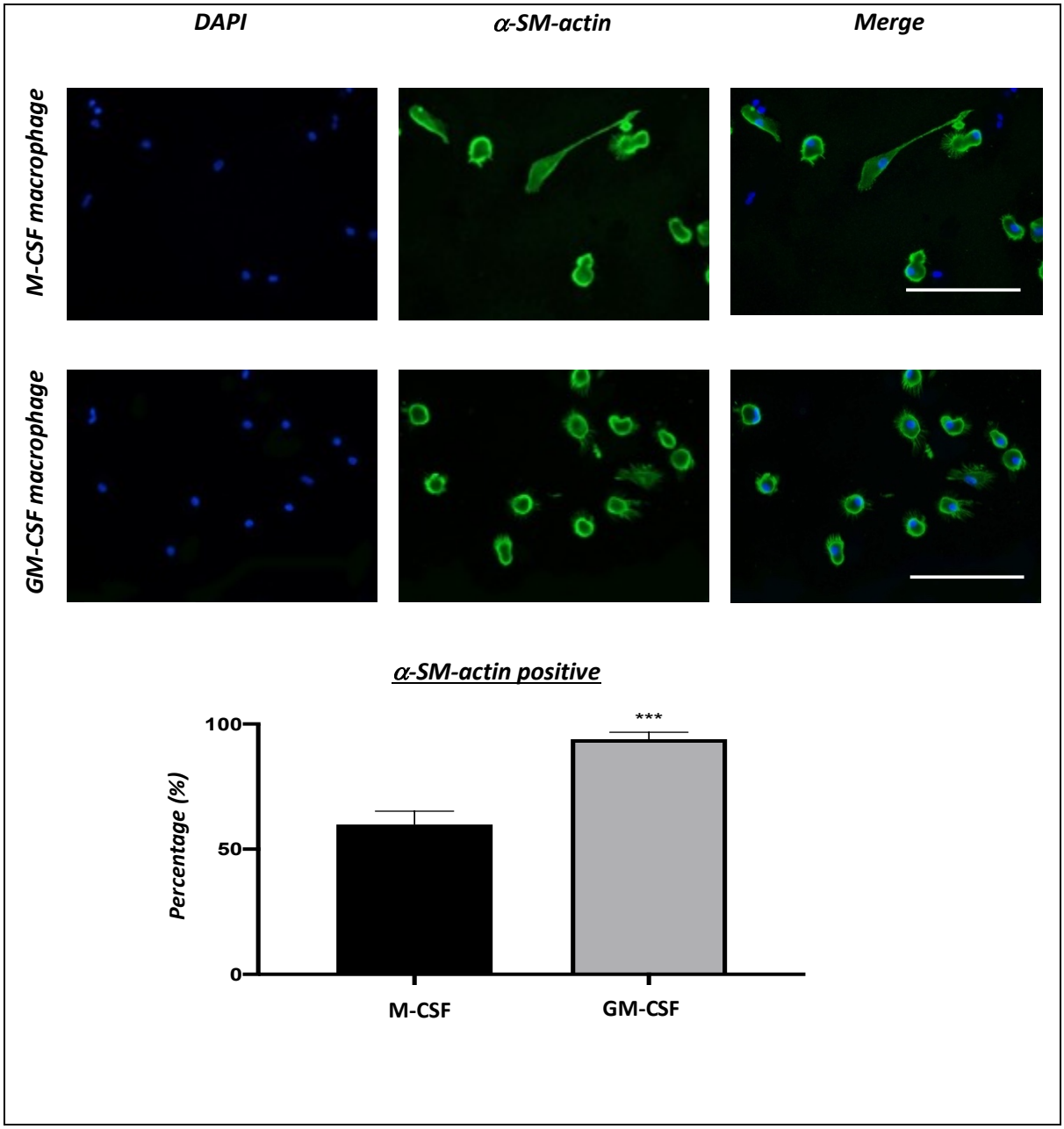

Figure 3.4.5 GM-CSF maturation increases human macrophage α-SM-actin protein expression compared to M-CSF matured macrophages.

*Representative images and quantification of immunofluorescent labelling for α-SM-actin expression in seven-day M-CSF or GM-CSF differentiated human macrophages. Green colour indicates α-SM-actin immunopositivity, and blue indicates nuclei (DAPI counterstain). Scale bars represent 100 μM. Data are expressed as percentage of α-SM-actin immuno-positive cells against M-CSF matured control macrophages, (mean ±SEM; n=6; ***P < 0.001 denotes significant difference compared to M-CSF macrophages; paired t-test).*

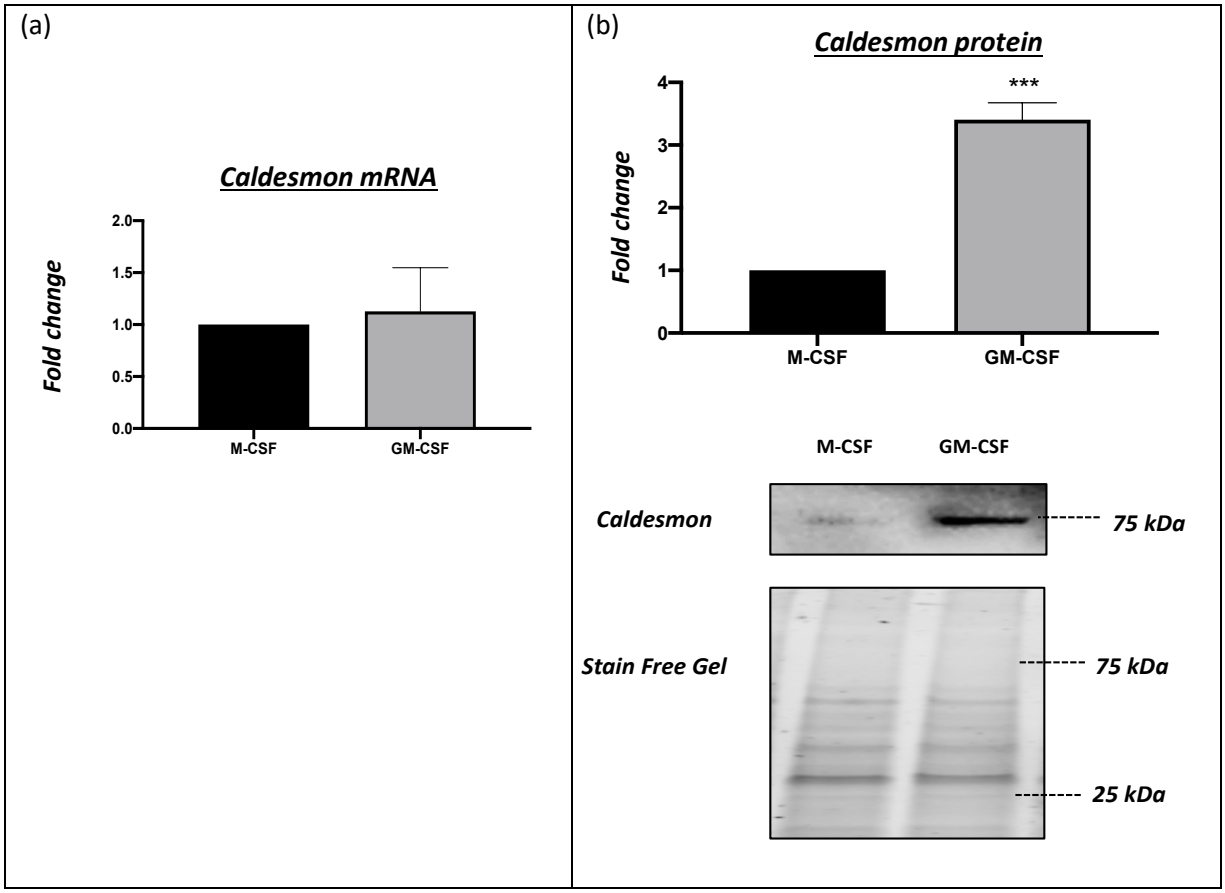

Figure 3.4.6 Caldesmon mRNA and protein expression in macrophage baseline cultures.

(a) Caldesmon mRNA levels in GM-CSF macrophages relative to M-CSF directed control macrophages, (mean±SEM; n=6; paired t-test).

*(b) Quantification and representative western blots for caldesmon protein expression in GM-CSF macrophage relative to M-CSF directed control macrophages. Stain free gel is shown as loading control. Data are expressed as fold change against M-CSF-directed control macrophages, (mean±SEM; n=6; ***P < 0.001 denotes significant difference compared to M-CSF macrophages; paired t-test).*

Refer to appendix A; (8.1.2) for CT values and (8.1.3) full blot image.

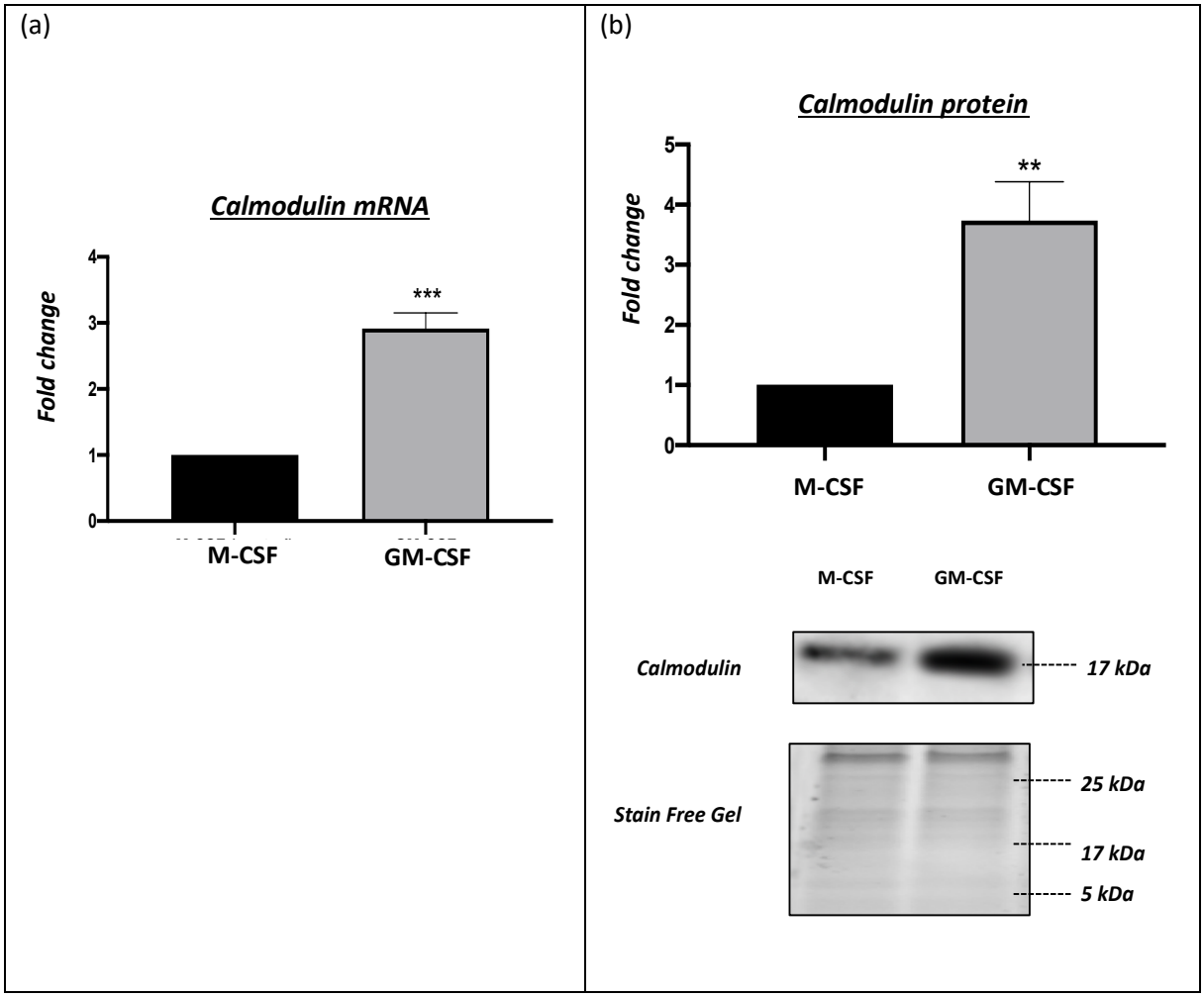

Figure 3.4.7 GM-CSF maturation increases human macrophage calmodulin mRNA and protein expression compared to M-CSF matured macrophages.

*(a) Calmodulin mRNA levels in GM-CSF macrophages relative to M-CSF directed control macrophages, (mean±SEM; n=6; ***P < 0.001 denotes significant difference compared to M-CSF directed control macrophages; paired t-test).*

*(b) Quantification and representative western blots for calmodulin protein expression in GM-CSF macrophages relative to M-CSF directed control macrophages. Stain free gel is shown as loading control. Data are expressed as fold change against M-CSF-directed control macrophages, (mean±SEM; n=6; **P < 0.01 denotes significant difference compared to M-CSF macrophages; paired t-test).*

Refer to appendix A; (8.1.4) for CT values and (8.1.5) full blot image.

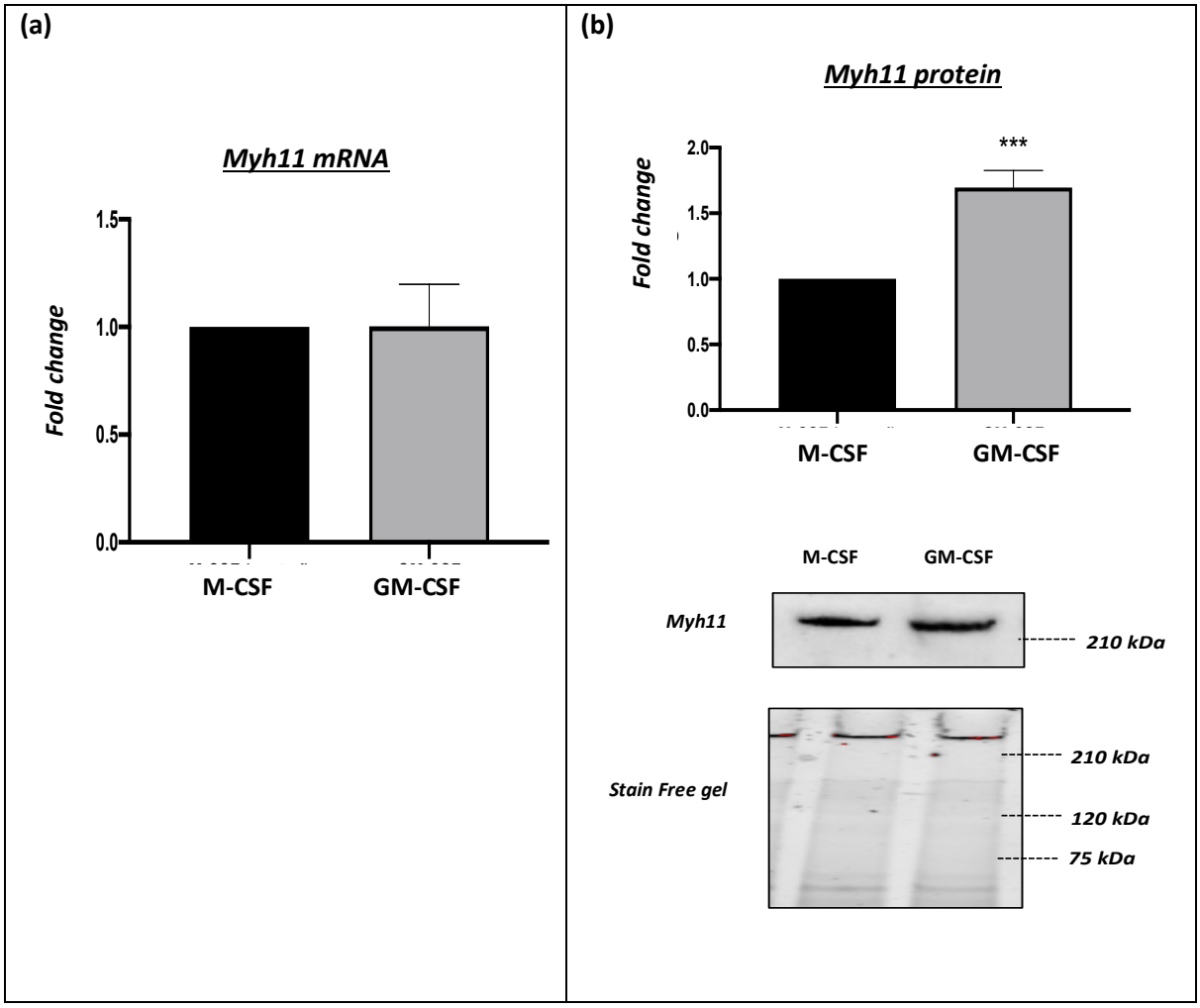

Figure 3.4.8 Myh11 mRNA and protein expression in macrophage baseline cultures.

(a) Myh11 mRNA levels in GM-CSF macrophages relative to M-CSF directed control macrophages, (mean±SEM; n=6; paired t-test).

*(b) Quantification and representative western blots for Myh11 protein expression in GM-CSF macrophages relative to M-CSF directed control macrophage. Stain free gel is shown as loading control. Data are expressed as fold change against M-CSF-directed control macrophages, (mean±SEM; n=6; ***P < 0.001 denotes significant difference compared to M-CSF macrophages; paired t-test).*

Refer to appendix A; (8.1.6) CT values and (8.1.7) for full blot image.

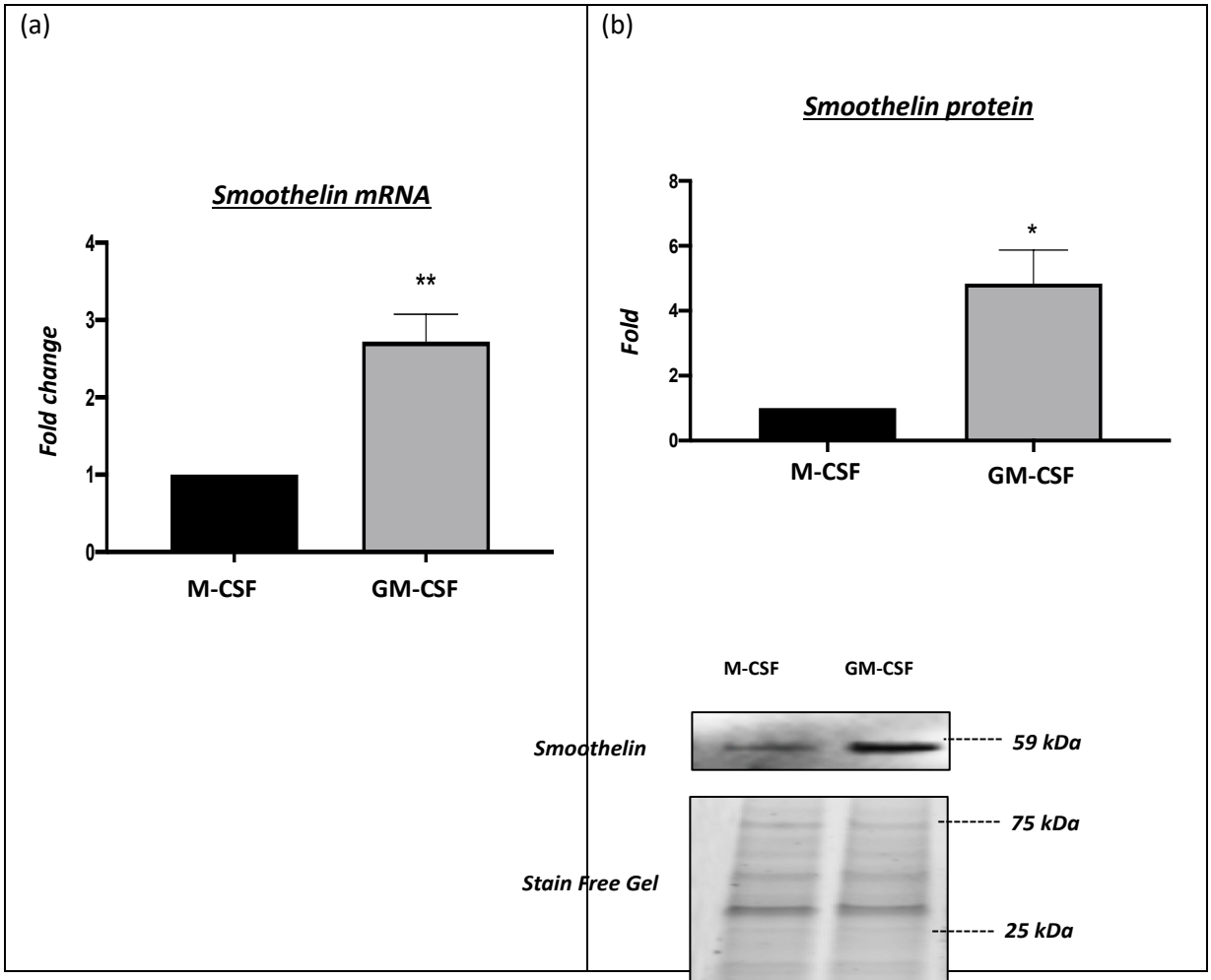

Figure 3.4.9 GM-CSF maturation increases human macrophage smoothelin mRNA and protein expression compared to M-CSF matured macrophages.

*(a) Smoothelin mRNA levels in GM-CSF macrophages relative to M-CSF directed control macrophages, (mean±SEM; n=6; **P < 0.01 denotes significant difference compared to M-CSF directed control macrophages; paired t-test).*

*(b) Quantification and representative western blots for smoothelin protein expression in GM-CSF macrophages relative to M-CSF directed control macrophages. Stain free gel is shown as loading control. Data are expressed as fold change against M-CSF-directed control macrophages, (mean±SEM; n=6; *P < 0.05 denotes significant difference compared to M-CSF macrophages; paired t-test).*

Refer to appendix A; (8.1.8) CT values and (8.1.9) for full blot image.

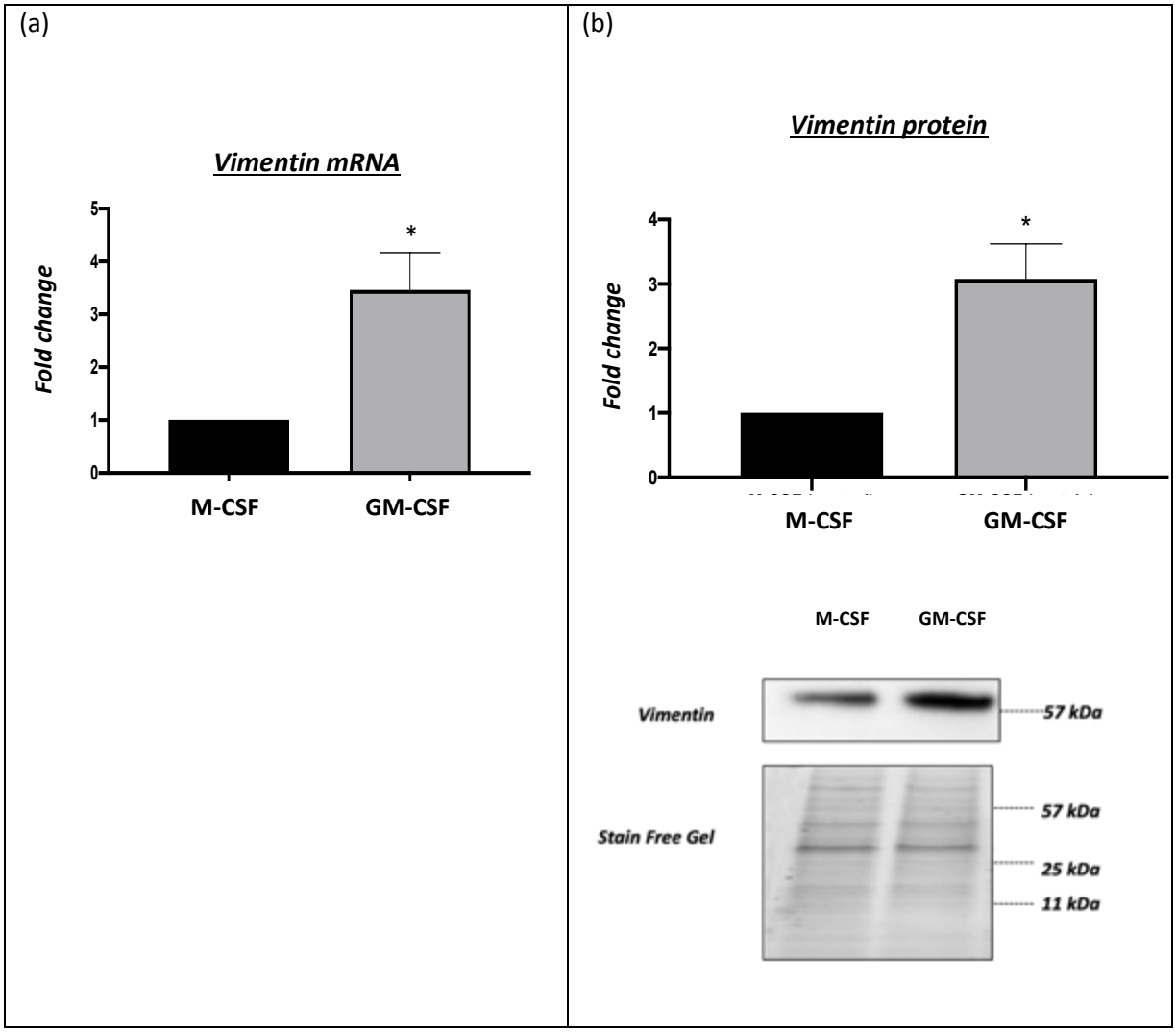

Figure 3.4.10 GM-CSF maturation increases human macrophage vimentin mRNA and protein expression compared to M-CSF matured macrophages.

*(a) Vimentin mRNA levels in GM-CSF macrophages relative to M-CSF directed control macrophages, (mean±SEM; n=6; *P < 0.05 denotes significant difference compared to M-CSF directed control macrophages; paired t-test).*

*(b) Quantification and representative western blots for vimentin protein expression in GM-CSF macrophages relative to M-CSF directed control macrophages. Stain free gel is shown as loading control. Data are expressed as fold change against M-CSF-directed control macrophages, (mean±SEM; n=6; *P < 0.05 denotes significant difference compared to M-CSF macrophages; paired t-test).*

Refer to appendix A; (8.1.10) CT values and (8.1.11) for full blot image.

3.4.3 PDGF-BB and TGFβ1 co-stimulation divergently affects VSMC-associated marker expression between M-CSF and GM-CSF-matured macrophages

Previous evidence has shown a combination of PDGF-BB and TGFβ1 can differentiate human stem cells towards a VSMC-like lineage (Gerecht-Nir *et al.,* 2003; Vo *et al.,* 2010; Wanjare *et al.,* 2013), while both growth factors are well characterised modulators of VSMC behaviour, including phenotypic modulation. Accordingly, the effects of PDGF-BB and TGFβ1 co-stimulation (for 3 days) on VSMC-associated marker expression was evaluated in seven-day M-CSF or GM-CSF matured human macrophages. The results are organised into two sections, reporting the effects of PDGF-BB and TGFβ1 co-incubation on M-CSF directed macrophages and GM-CSF directed macrophages within sections 3.4.3.1 and 3.4.3.2, respectively.

Surprisingly, PDGF-BB/TGFβ1 co-stimulation significantly upregulated protein expression of calmodulin (2.6-fold change; $P<0.05$; n=6; Figure 3.4.11 b), Myh11 (1.6-fold change; $P<0.05$; n=6; Figure 3.4.12 b) smoothelin (1.8-fold change; $P<0.05$; n=6; Figure 3.4.13 b) and vimentin (1.7-fold change; $P<0.05$; n=6; Figure 3.4.14 b). However, only a reciprocal increase in vimentin mRNA expression was detected (1.8-fold change; $P<0.05$ n=6; Figure 3.4.14 a), with no change in calmodulin, Myh11, or smoothelin mRNA expression identified (Figure 3.4.11 - Figure 3.4.13). No effect of PDGF-BB/TGFβ1 co-stimulation on caldesmon or α-SM-actin mRNA and protein levels were observed (data not shown).

With regard to GM-CSF matured macrophages, an opposing pattern was observed. PDGF-BB/TGFβ1 co-stimulation significantly decreased protein expression of caldesmon (39%; $P<0.01$; n=6; Figure 3.4.15 b), calmodulin (30% change; $P<0.05$; n=6; Figure 3.4.16 b), and vimentin (33%; $P<0.05$; n=6; Figure 3.4.17 b), although no corresponding differences in mRNA levels were seen (Figure 3.4.15 a - Figure 3.4.17 a). No effect of PDGF-BB/TGFβ1 co-stimulation on smoothelin, Myh11, or α-SM-actin mRNA and protein levels were observed (data not shown). Of note, high molecular weight caldesmon (120 kDa) was not detected by Western blotting in either M-CSF or GM-CSF matured

macrophages, but readily observed in primary VSMCs (see Appendix A (8.1.3) for a representative image).

3.4.3.1 PDGF-BB and TGFβ1 co-stimulation increases the expression of specific VSMC-associated markers in M-CSF matured human macrophages

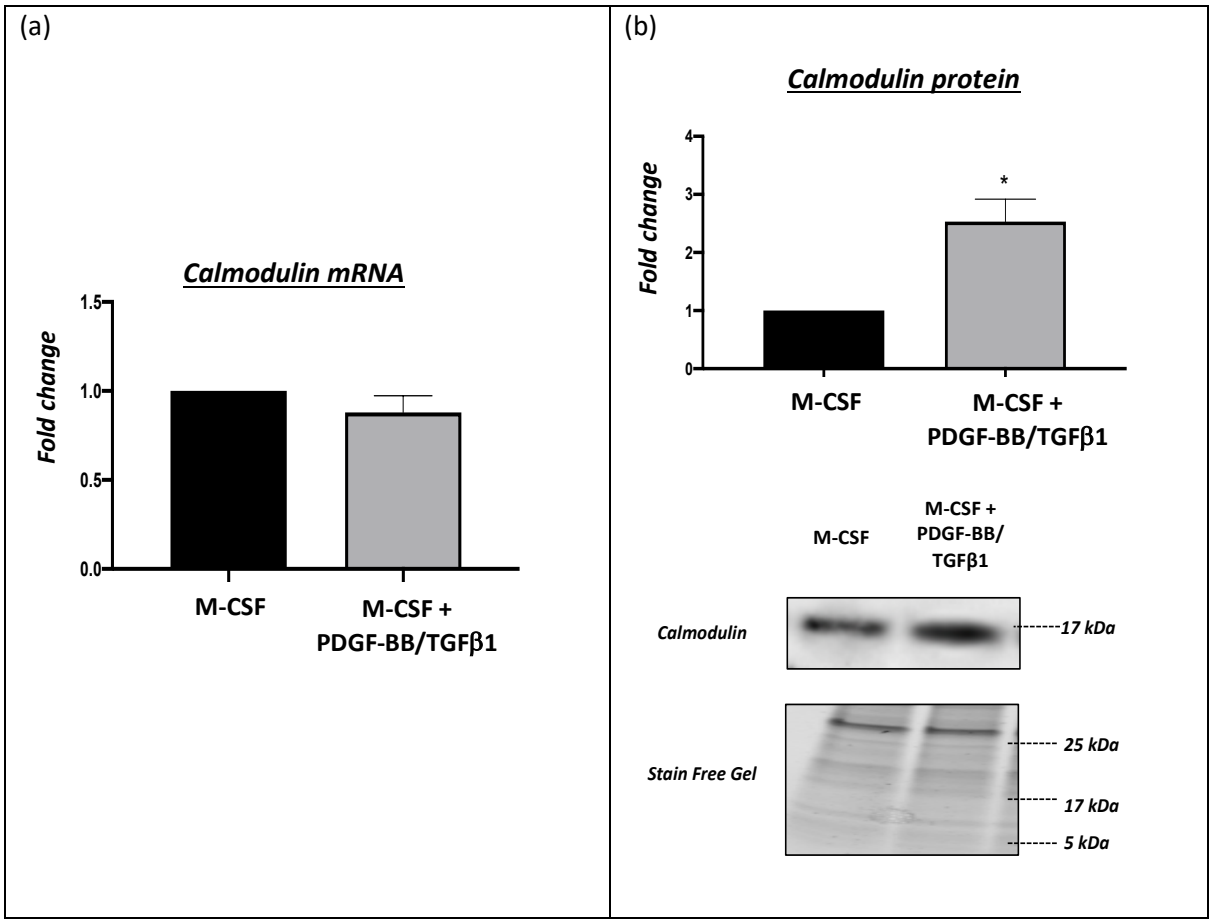

Figure 3.4.11 The effects of PDGF-BB and TGFβ1 co-stimulation on calmodulin mRNA and protein expression in M-CSF polarised macrophages.

(a) Calmodulin mRNA levels in PDGF-BB and TGFβ1 treated M-CSF macrophages relative to untreated M-CSF directed control macrophages, (mean±SEM; n=6; paired t-test).

*(b) Quantification and representative western blots for calmodulin protein expression in PDGF-BB and TGFβ1 treated M-CSF macrophages relative to untreated M-CSF directed control macrophages. Stain free gel is shown as loading control. Data are expressed as fold change against untreated M-CSF-directed control macrophages, (mean±SEM; n=6; *P < 0.05 denotes significant difference compared to M-CSF macrophages; paired t-test).*

Refer to appendix A; (8.1.4) CT values and (8.1.5) for full blot image.

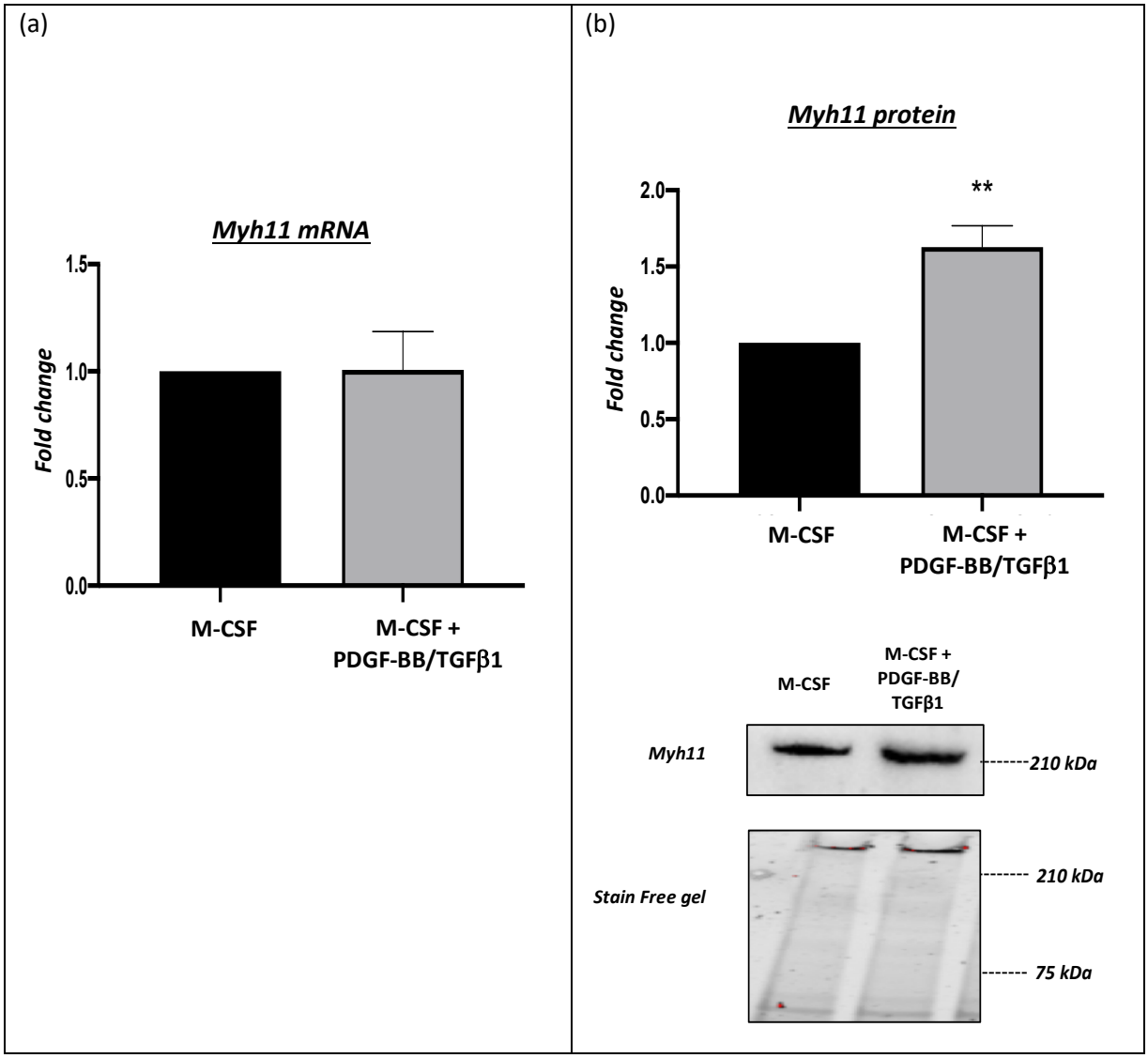

Figure 3.4.12 The effects of PDGF-BB and TGFβ1 co-stimulation on Myh11 mRNA and protein expression in M-CSF polarised macrophages.

(a) Myh11 mRNA levels in PDGF-BB and TGFβ1 treated M-CSF macrophages relative to untreated M-CSF directed control macrophages, (mean±SEM; n=6; paired t-test).

*(b) Quantification and representative western blots for Myh11 protein expression in PDGF-BB and TGFβ1 treated M-CSF macrophages relative to untreated M-CSF directed control macrophages. Stain free gel is shown as loading control. Data are expressed as fold change against untreated M-CSF-directed control macrophages, (mean±SEM; n=6; **P < 0.01 denotes significant difference compared to M-CSF macrophages; paired t-test).*

Refer to appendix A; (8.1.6) CT values and (8.1.7) full blot image.

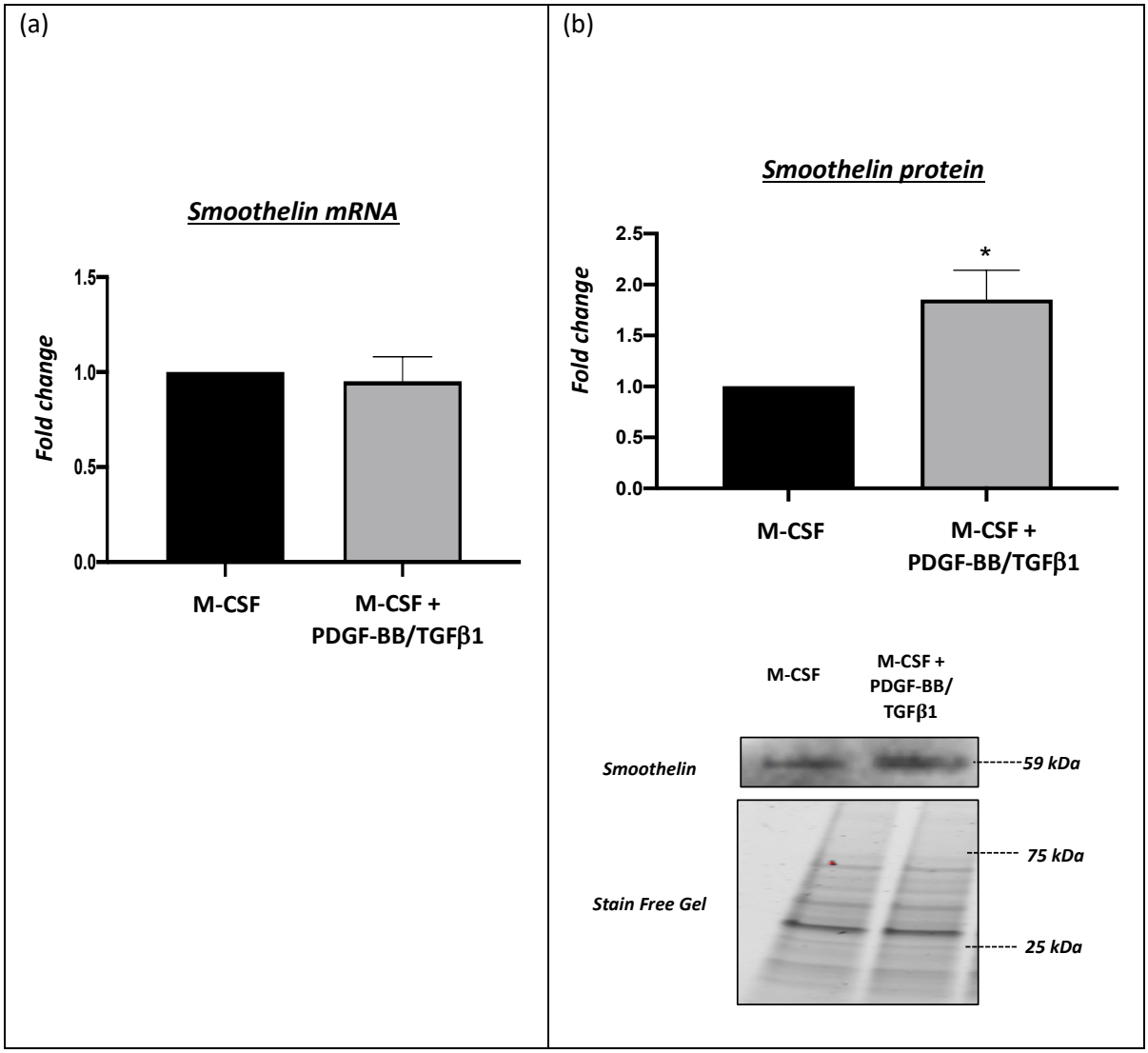

Figure 3.4.13 The effects of PDGF-BB and TGFβ1 co-stimulation on smoothelin mRNA and protein expression in M-CSF polarised macrophages.

(a) Smoothelin mRNA levels in PDGF-BB and TGFβ1 treated M-CSF macrophages relative to untreated M-CSF directed control macrophages, (mean±SEM; n=6; paired t-test).

*(b) Quantification and representative western blots for smoothelin protein expression in PDGF-BB and TGFβ1 treated M-CSF macrophages relative to untreated M-CSF directed control macrophages. Stain free gel is shown as loading control. Data are expressed as fold change against untreated M-CSF-directed control macrophages, (mean±SEM; n=6; **P < 0.01 denotes significant difference compared to M-CSF macrophages; paired t-test).*

Refer to appendix A; (8.1.8) CT values and (8.1.9) for full blot image.

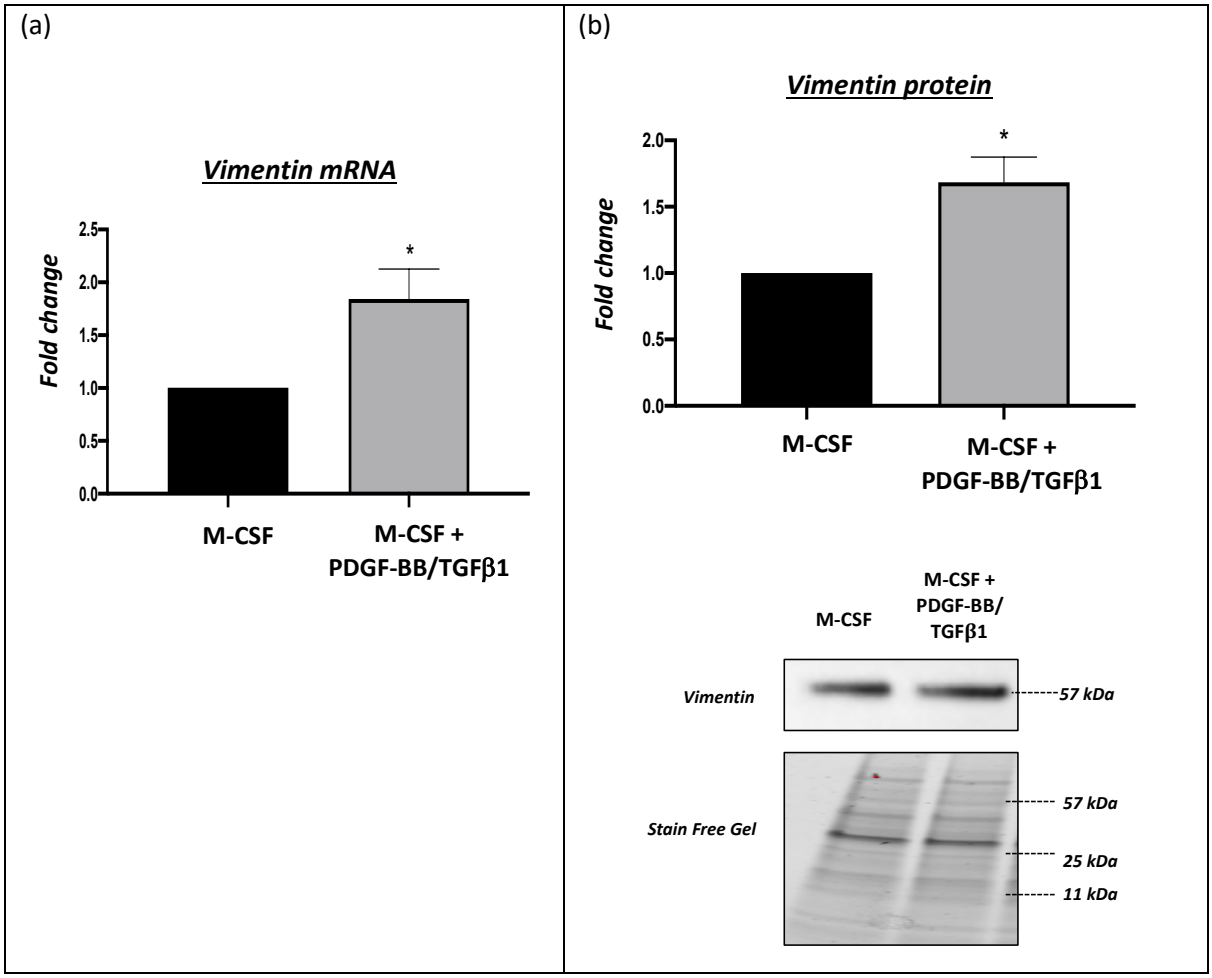

Figure 3.4.14 PDGF-BB and TGFβ1 increases human M-CSF polarised macrophage vimentin mRNA and protein expression.

*(a) Vimentin mRNA levels in PDGF-BB and TGFβ1 treated M-CSF macrophages relative to untreated M-CSF directed control macrophages, (mean±SEM; n=6; *P < 0.05 denotes significant difference compared to M-CSF macrophages; paired t-test).*

*(b) Quantification and representative western blots for vimentin protein expression in PDGF-BB and TGFβ1 treated M-CSF macrophages relative to untreated M-CSF directed control macrophages. Stain free gel is shown as loading control. Data are expressed as fold change against untreated M-CSF-directed control macrophages, (mean±SEM; n=6; *P < 0.05 denotes significant difference compared to M-CSF macrophages; paired t-test).*

Refer to appendix A; (8.1.10) CT values and (8.1.11) for full blot image.

3.4.3.2 PDGF-BB and TGFβ1 co-stimulation decreases protein expression of specific VSMC-associated markers in GM-CSF matured human macrophages

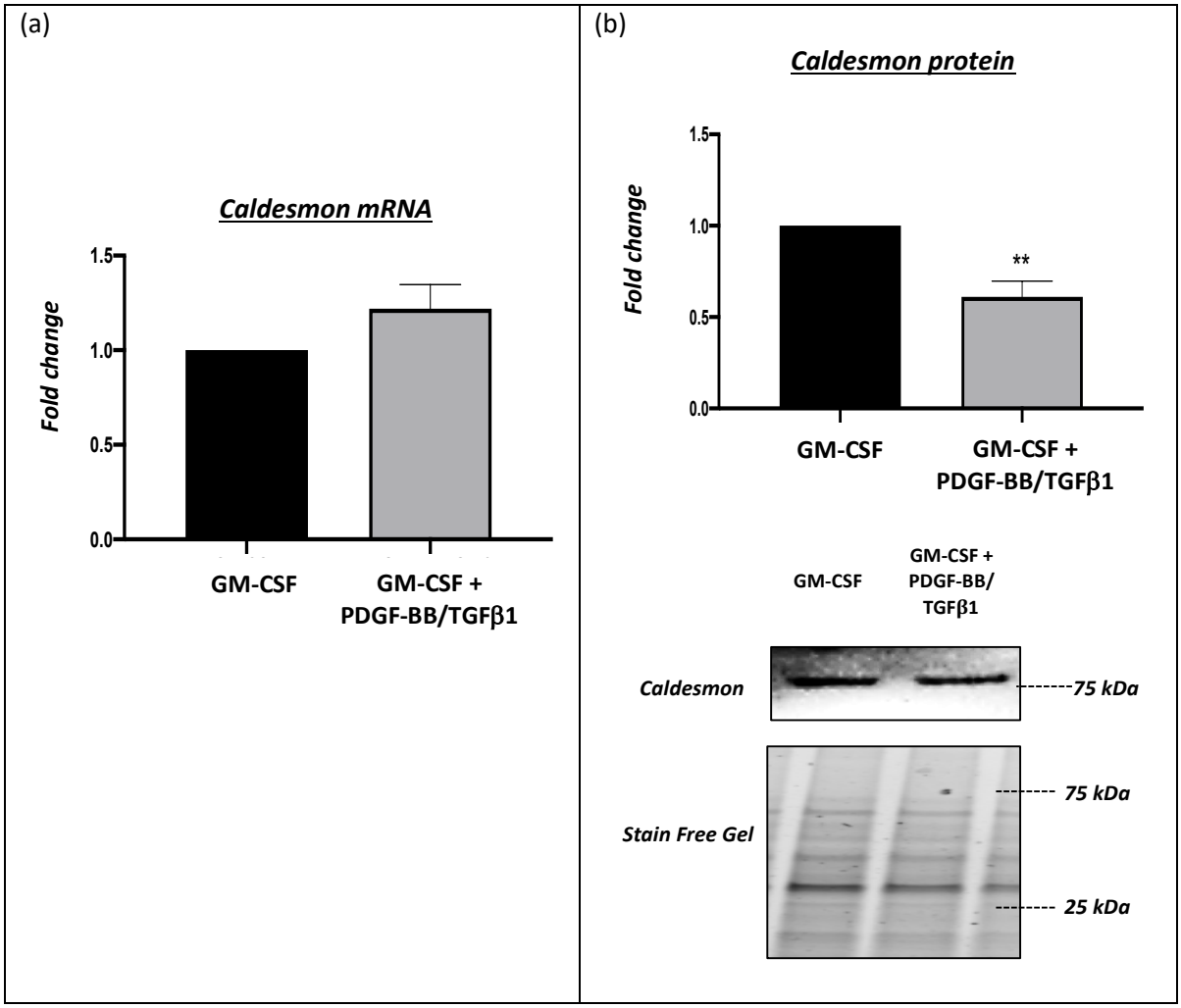

Figure 3.4.15 The effect of PDGF-BB and TGFβ1 co-stimulation on caldesmon mRNA and protein expression in GM-CSF polarised macrophages.

(a) Caldesmon mRNA levels in PDGF-BB and TGFβ1 treated GM-CSF macrophages relative to untreated GM-CSF directed control macrophages, (mean±SEM; n=6; paired t-test).

*(b) Quantification and representative western blots for caldesmon protein expression in PDGF-BB and TGFβ1 treated GM-CSF macrophages relative to untreated GM-CSF directed control macrophages. Stain free gel is shown as loading control. Data are expressed as fold change against untreated GM-CSF-directed control macrophages, (mean±SEM; n=6; **P < 0.01 denotes significant difference compared to GM-CSF macrophages; paired t-test).*

Refer to appendix A; (8.1.2) CT values and (8.1.3) for full blot image.

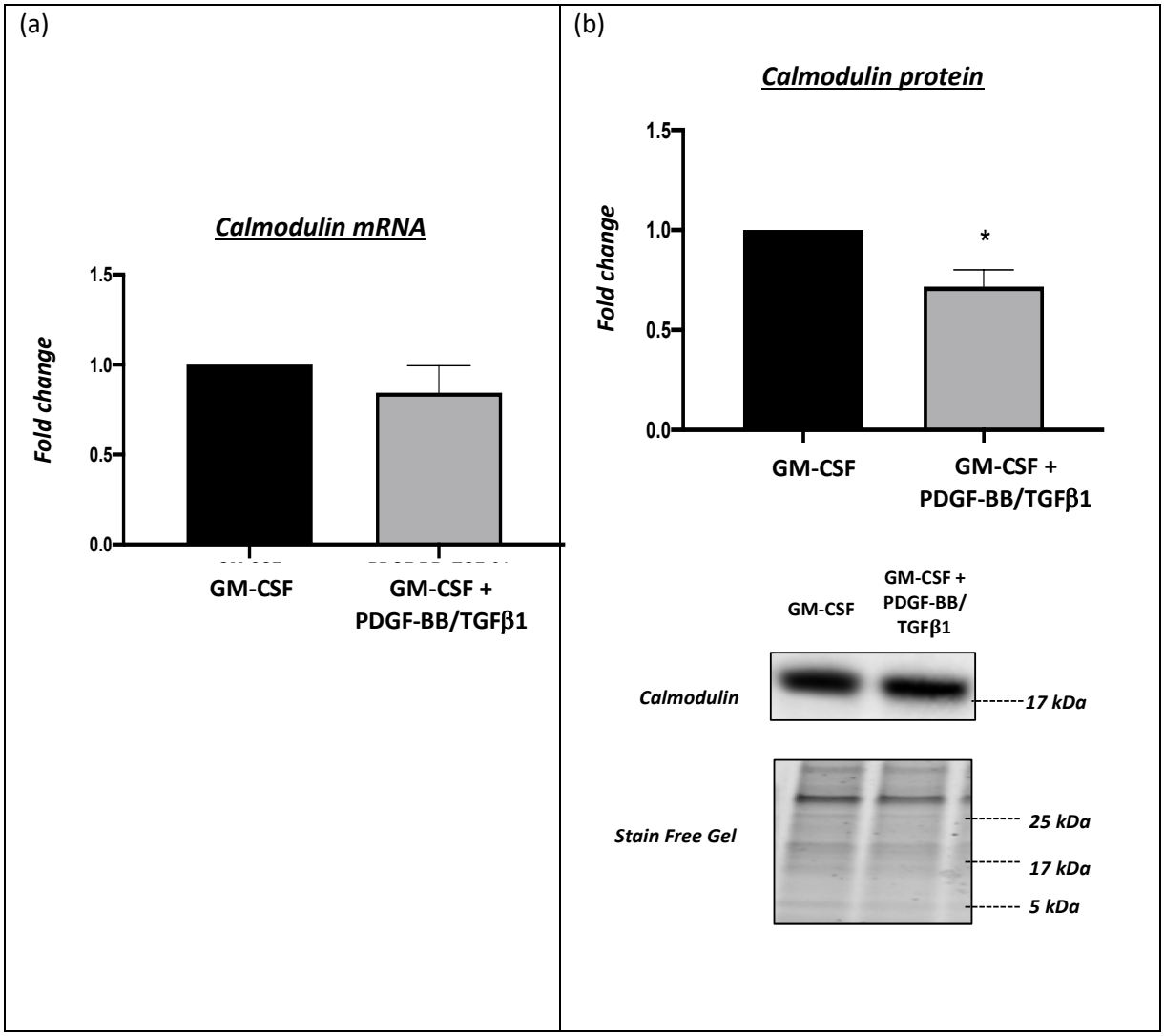

Figure 3.4.16 The effects of PDGF-BB and TGFβ1 co-stimulation on calmodulin mRNA and protein expression in GM-CSF polarised macrophages.

(a) Calmodulin mRNA levels in PDGF-BB and TGFβ1 treated GM-CSF macrophages relative to untreated GM-CSF directed control macrophages, (mean±SEM; n=6; paired t-test).

*(b) Quantification and representative western blots for calmodulin protein expression in PDGF-BB and TGFβ1 treated GM-CSF macrophages relative to untreated GM-CSF directed control macrophages. Stain free gel is shown as loading control. Data are expressed as fold change against untreated GM-CSF-directed control macrophages, (mean±SEM; n=6; **P < 0.01 denotes significant difference compared to GM-CSF macrophages; paired t-test).*

Refer to appendix A; (8.1.4) CT values and (8.1.5) for full blot image.

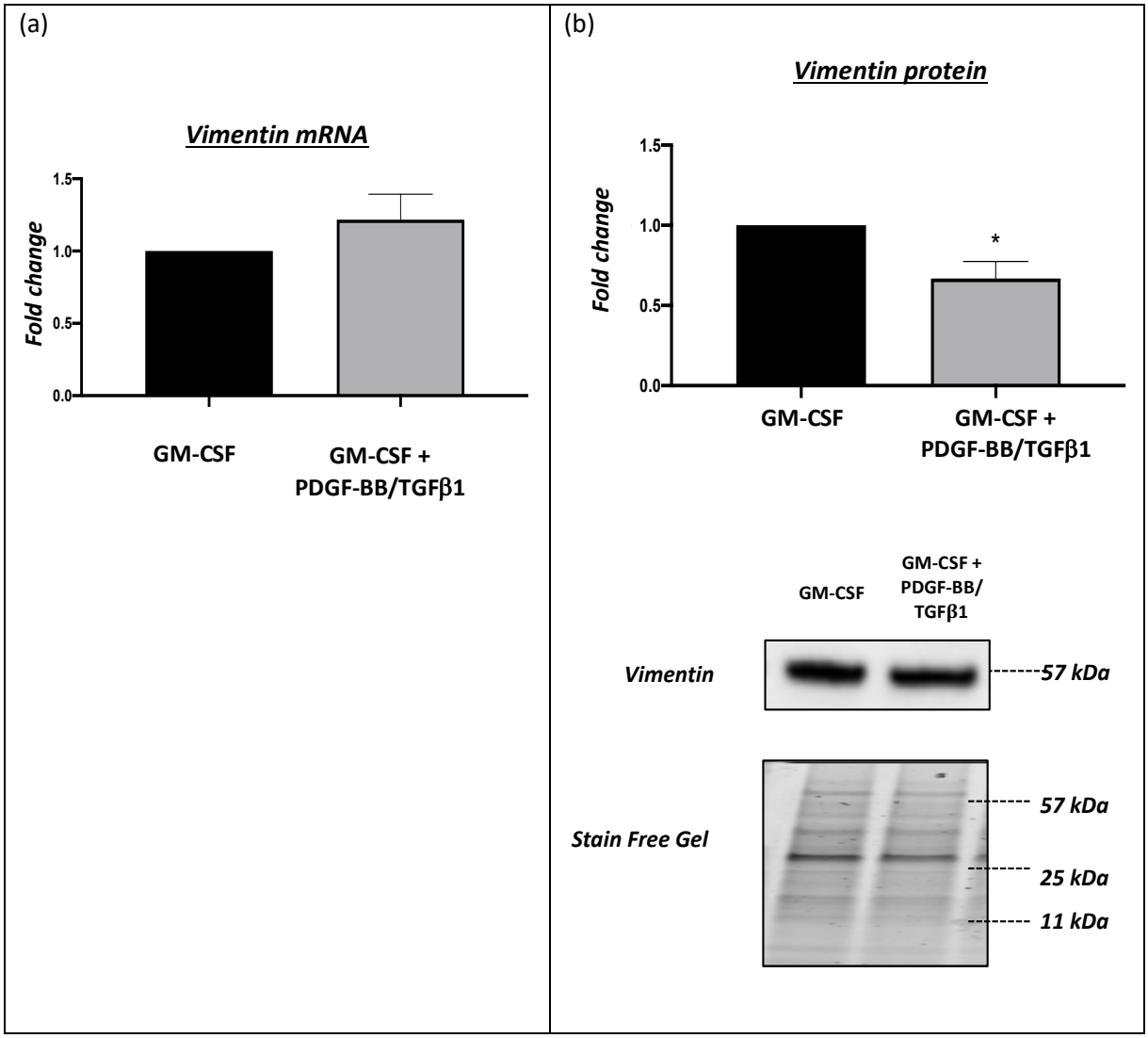

Figure 3.4.17 The effects of PDGF-BB and TGFβ1 co-stimulation on vimentin mRNA and protein expression in GM-CSF polarised macrophages.

(a) Vimentin mRNA levels in PDGF-BB and TGFβ1 treated GM-CSF macrophages relative to untreated GM-CSF directed control macrophages, (mean±SEM; n=6; paired t-test).

*(b) Quantification and representative western blots for vimentin protein expression in PDGF-BB and TGFβ1 treated GM-CSF macrophages relative to untreated GM-CSF directed control macrophages. Stain free gel is shown as loading control. Data are expressed as fold change against untreated GM-CSF-directed control macrophages, (mean±SEM; n=6; **P < 0.01 denotes significant difference compared to GM-CSF macrophages; paired t-test).*

Refer to appendix A; (8.1.10) CT values and (8.1.11) for full blot image.

3.4.4 Differing human macrophage phenotypes display distinct changes in their expression of VSMC-associated markers

The expression of markers considered specific for VSMCs were also evaluated in multiple differing macrophage phenotypes *in vitro*. Seven-day M-CSF matured human macrophages (sometimes referred to as M0) were activated with different inducers for three days to generate different macrophage phenotypes before stimulation with PDGF-BB and TGFβ1. The inducers used are described in detail under section 3.3.3, and include IFNγ and LPS for M1 macrophage polarisation (Martinez *et al.,* 2006), IL-4 for M2a macrophage polarisation (Stein *et al.,* 1992), IL-10 for M2c macrophage polarisation (Lang *et al.,* 2002), PF4 (CXCL4) for M4 macrophage polarisation (Gleissner *et al.,* 2010), oxPAPC for Mox macrophage polarisation (Kadl *et al.,* 2010), and oxLDL for foam cell macrophage formation (Kruth *et al.,* 2002). See summary Figure 3.4.35 detailing the results in this section.

Collectively, the expression of VSMC-associated marker genes/proteins showed variable responses amongst the differing macrophage phenotypes, when compared to control M-CSF directed macrophages (please see summary Figure 3.4.35). M1 polarisation with IFNγ and LPS co-stimulation significantly down-regulated protein expression of caldesmon (41% change; $P<0.01$; n=6; Figure 3.4.18 b), calmodulin (37% change; $P<0.05$; n=6; Figure 3.4.19 b), smoothelin, (45% change; $P<0.05$; n=6; Figure 3.4.20 b), and vimentin (41% change; $P<0.05$; n=6; Figure 3.4.21 b). Conversely, increased mRNA expression of calmodulin (3.0-fold change; $P<0.05$; n=6; Figure 3.4.19 a) and vimentin (1.6-fold change; $P<0.05$; n=6; Figure 3.4.21 a) was detected, with no change in caldesmon or smoothelin mRNA expression identified (Figure 3.4.18 and Figure 3.4.20). No effect of IFNγ and LPS co-stimulation on Myh11 mRNA and protein levels were observed (data not shown).

With regard to IL-4 stimulated macrophages to induce M2a polarisation, the mRNA and protein expression of Myh11, smoothelin, and vimentin were unchanged when compared to unstimulated control M-CSF macrophages (see summary Figure 3.4.35). However, both the mRNA and protein

levels of caldesmon were decreased (35% and 39% change; P<0.05; n=6; Figure 3.4.22 b), while calmodulin protein expression was increased (1.8-fold change; P<0.05; n=6; Figure 3.4.23 b). Similarly, no effect of M2c macrophage polarisation with IL-10 was detected for caldesmon, Myh11 and vimentin mRNA and protein expression (see summary Figure 3.4.35). Although, a reduction in the protein expression of calmodulin (55% change; P<0.01; n=6; Figure 3.4.24 b) and smoothelin was detected (35% change; P<0.05; n=6; Figure 3.4.25 b), but with no effect at the mRNA level observed. Comparably, M4 macrophage polarisation through stimulation with PF4 had no effect on mRNA and protein expression of caldesmon, calmodulin, Myh11 or smoothelin (see summary Figure 3.4.35), relative to unstimulated control M-CSF macrophages, with only an increase in vimentin protein expression observed (1.7-fold change; P<0.05; n=6; Figure 3.4.26 b).

The stimulation of human macrophages with oxPAPC to induce Mox polarisation significantly increased protein expression of Myh11 (1.7-fold change; P<0.05; n=6; Figure 3.4.27) and vimentin (1.8-fold change; P<0.05; n=6; Figure 3.4.28) although no corresponding differences in mRNA levels were seen (Figure 3.4.27 - Figure 3.4.28). Conversely, smoothelin mRNA and protein expression were decreased (36% change and 52% change; P<0.05; n=6; Figure 3.4.29), when compared to control M-CSF macrophages. The induction of macrophage foam cell formation through the addition of oxLDL to human macrophages affected all VSMC-related markers, with significant elevations in the protein expression of caldesmon (1.6-fold change; P<0.05; n=6; Figure 3.4.30 b), calmodulin (1.8-fold change; P<0.05; n=6; Figure 3.4.31 b), Myh11 (1.8-fold change; P<0.05; n=6; Figure 3.4.32 b) and vimentin (3.5-fold change; P<0.05; n=6; Figure 3.4.33 b) detected in comparison to control unstimulated M-CSF macrophages. However, no changes were seen at the mRNA level for any of the markers (see summary Figure 3.4.35). In opposition oxLDL-induced foam cell formation was associated with a decreased mRNA and protein expression of smoothelin (34.7% and 52.8%; P<0.05; n=6; Figure 3.4.34).

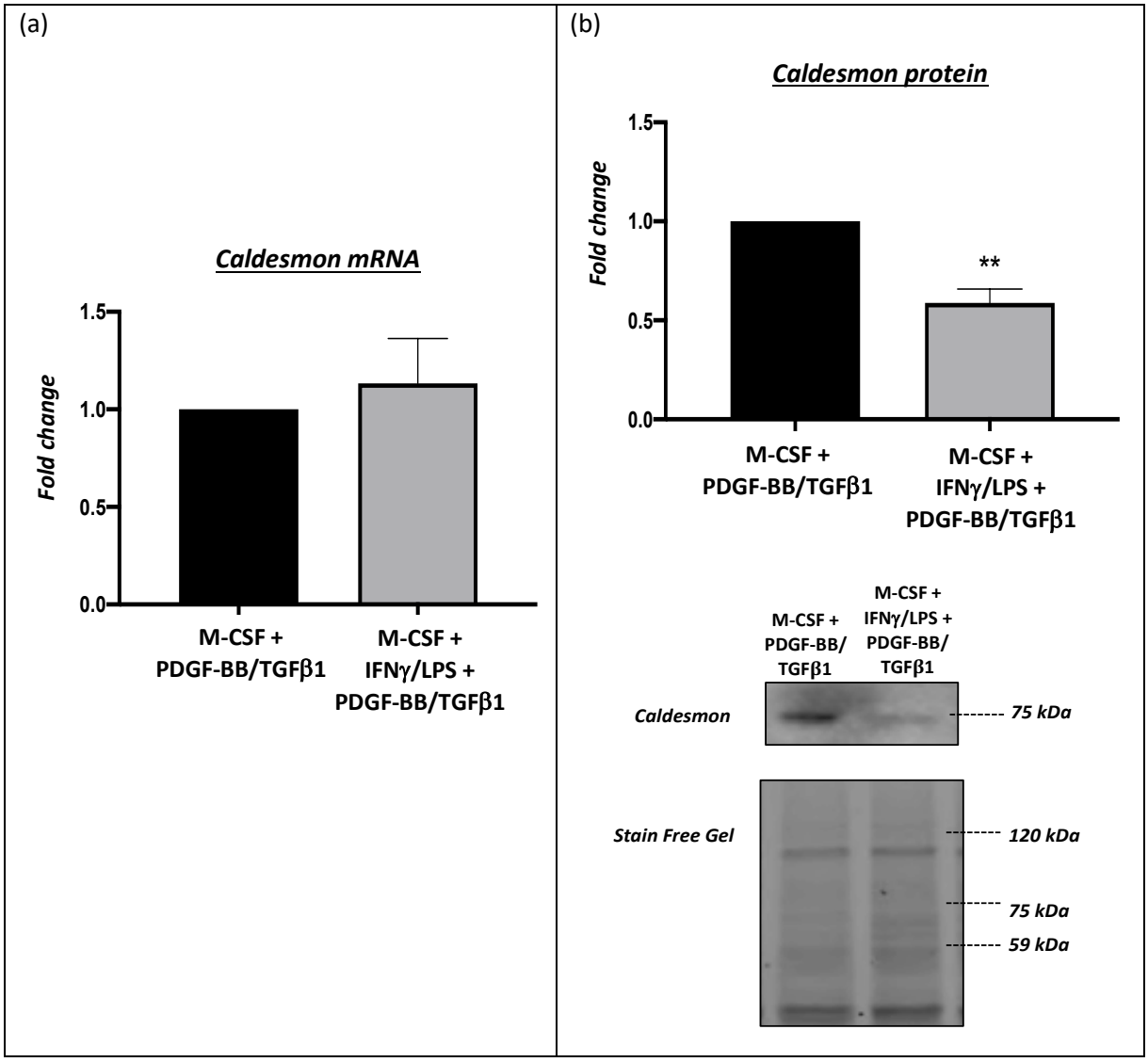

Figure 3.4.18 The effects of PDGF-BB and TGFβ1 co-stimulation on caldesmon mRNA and protein expression in M-CSF/IFNγ/LPS polarised macrophages.

(a) Caldesmon mRNA levels in M-CSF/IFNγ/LPS macrophages relative to M-CSF directed macrophages, (mean±SEM; n=6; paired t-test).

*(b) Quantification and representative western blots for caldesmon protein expression in M-CSF/IFNγ/LPS macrophages relative to M-CSF directed macrophages. Stain free gel is shown as loading control. Data are expressed as fold change against untreated M-CSF-directed macrophages, (mean±SEM; n=6; **P < 0.01 denotes significant difference compared to M-CSF macrophages; paired t-test).*

Refer appendix A; (8.2.3) CT values and (8.2.4) full blot image.

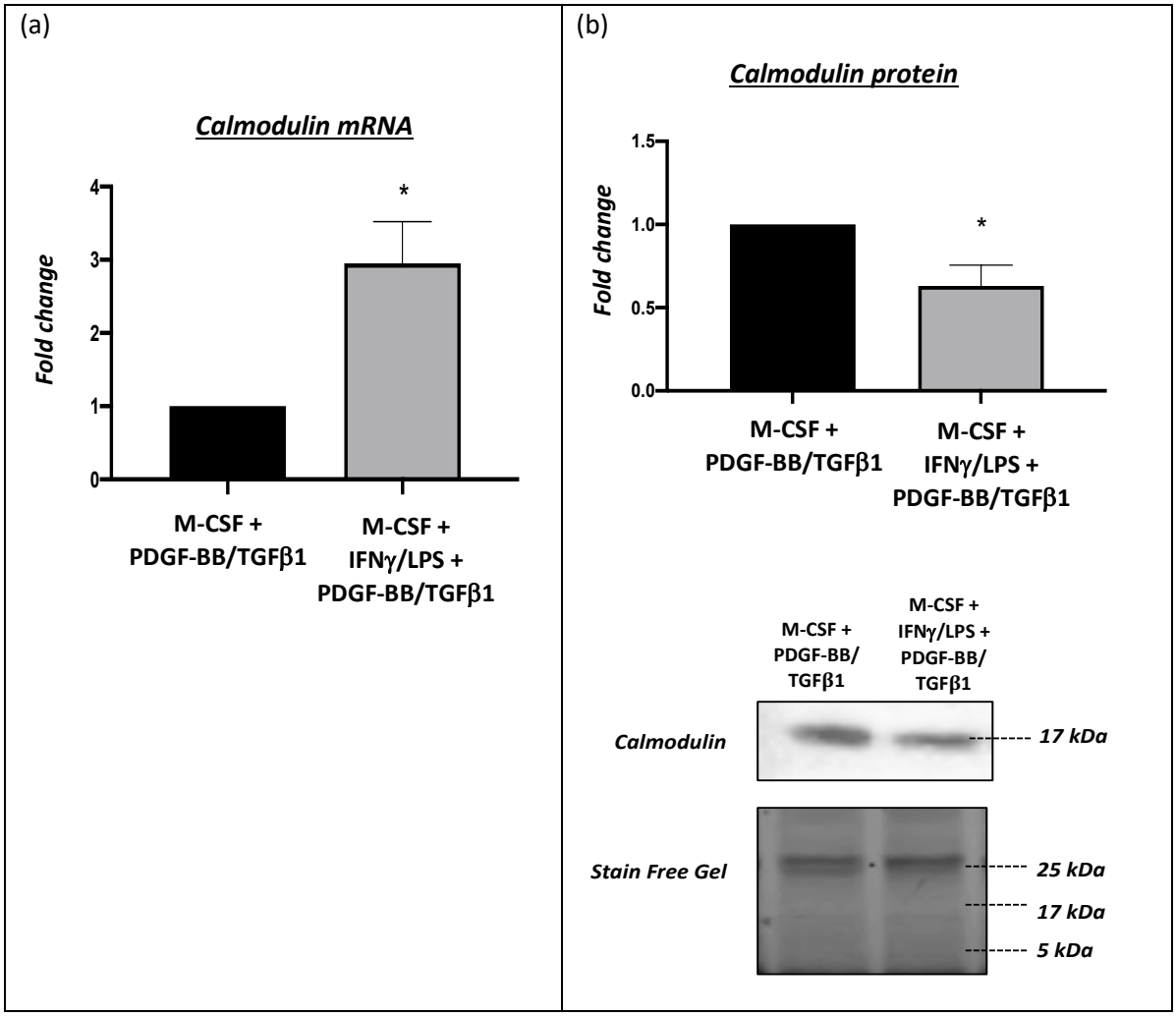

Figure 3.4.19 The effects of PDGF-BB and TGFβ1 co-stimulation on calmodulin mRNA and protein expression in M-CSF/IFNγ/LPS polarised macrophages.

*(a) Calmodulin mRNA levels in M-CSF/IFNγ/LPS macrophages relative to M-CSF directed macrophages, (mean±SEM; n=6; *P < 0.05 denotes significant difference compared to M-CSF macrophages; paired t-test).*

*(b) Quantification and representative western blots for calmodulin protein expression in M-CSF/IFNγ/LPS macrophages relative to M-CSF directed macrophages. Stain free gel is shown as loading control. Data are expressed as fold change against untreated M-CSF-directed macrophages, (mean±SEM; n=6; *P < 0.05 denotes significant difference compared to M-CSF macrophages; paired t-test).*

Refer appendix A; (8.2.5) CT values and (8.2.6) full blot image.

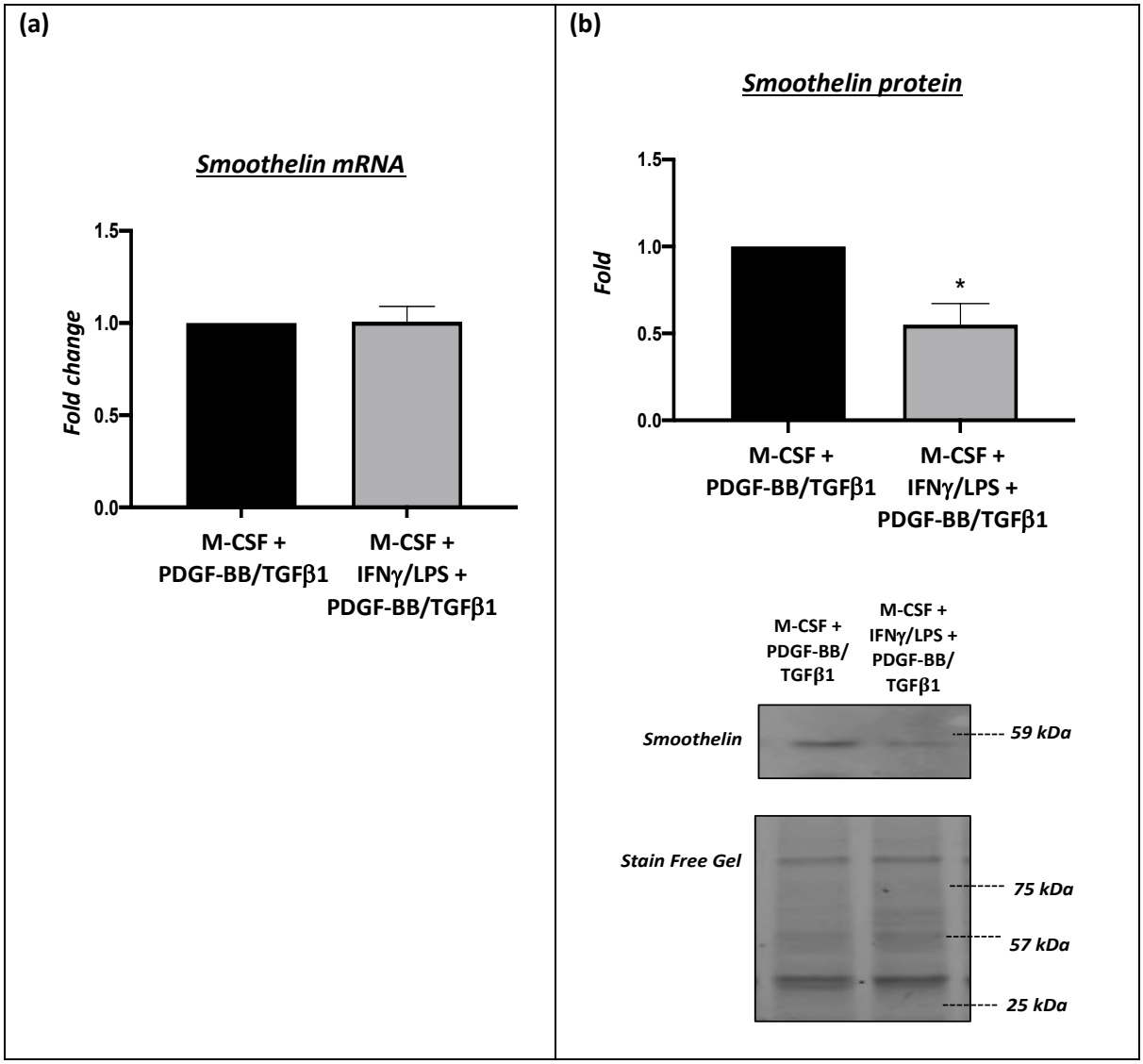

Figure 3.4.20 The effects of PDGF-BB and TGFβ1 co-stimulation on smoothelin mRNA and protein expression in M-CSF/IFNγ/LPS polarised macrophages.

(a) Smoothelin mRNA levels in M-CSF/IFNγ/LPS macrophages relative to M-CSF directed macrophages, (mean±SEM; n=6; paired t-test).

*(b) Quantification and representative western blots for smoothelin protein expression in M-CSF/IFNγ/LPS macrophages relative to M-CSF directed macrophages. Stain free gel is shown as loading control. Data are expressed as fold change against untreated M-CSF-directed macrophages, (mean±SEM; n=6; *P < 0.05 denotes significant difference compared to M-CSF macrophages; paired t-test).*

Refer appendix A; (8.2.7) CT values and (8.2.8) full blot image.

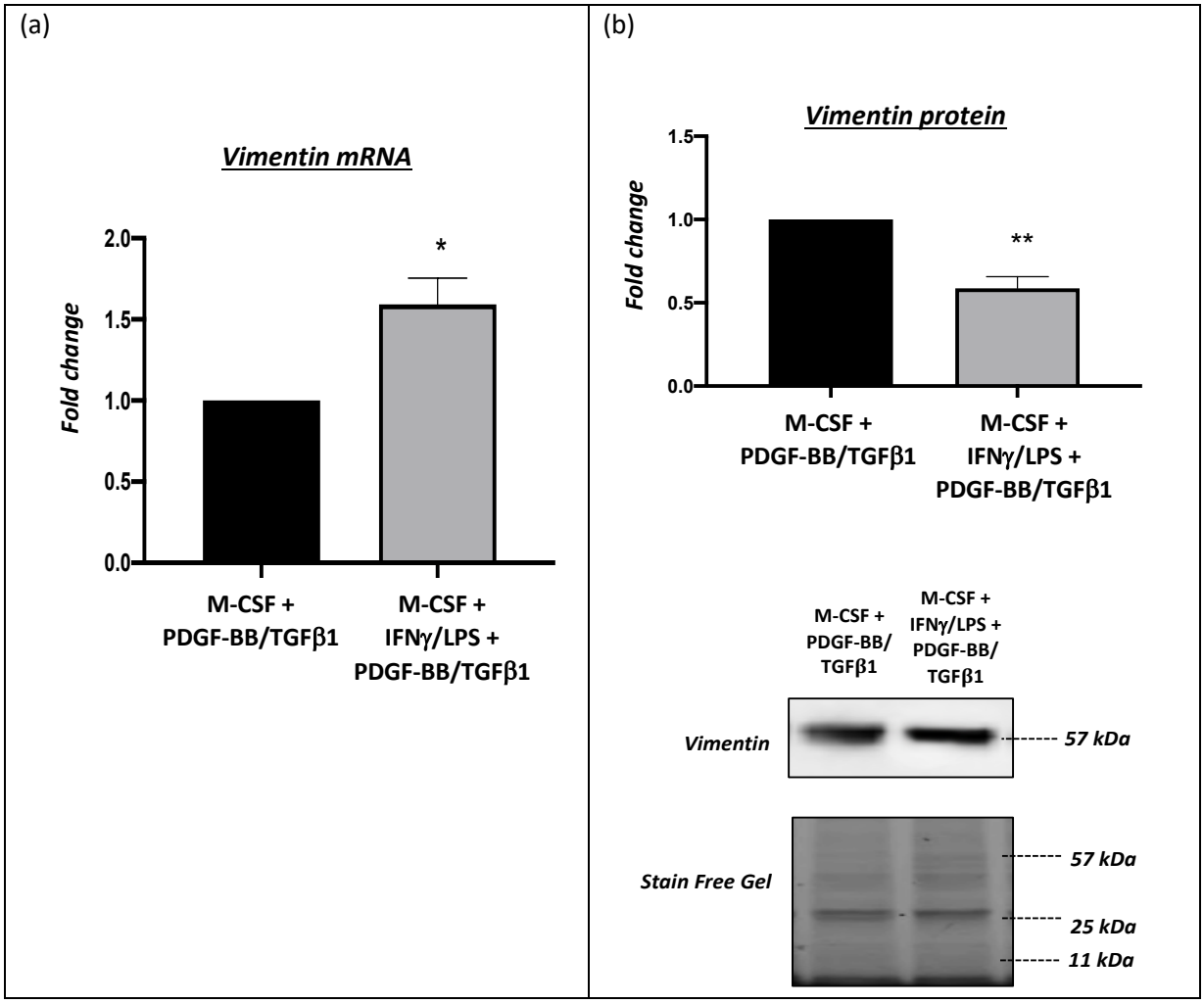

Figure 3.4.21 The effects of PDGF-BB and TGFβ1 co-stimulation on vimentin mRNA and protein expression in M-CSF/IFNγ/LPS polarised macrophages.

*(a) Vimentin mRNA levels in M-CSF/IFNγ/LPS macrophages relative to M-CSF directed macrophages, (mean±SEM; n=6; *P < 0.05 denotes significant difference compared to M-CSF macrophages; paired t-test).*

*(b) Quantification and representative western blots for vimentin protein expression in M-CSF/IFNγ/LPS macrophages relative to M-CSF directed macrophages. Stain free gel is shown as loading control. Data are expressed as fold change against untreated M-CSF-directed macrophages, (mean±SEM; n=6; **P < 0.01 denotes significant difference compared to M-CSF macrophages; paired t-test).*

Refer appendix A; (8.2.9) CT values and (8.2.10) full blot image.

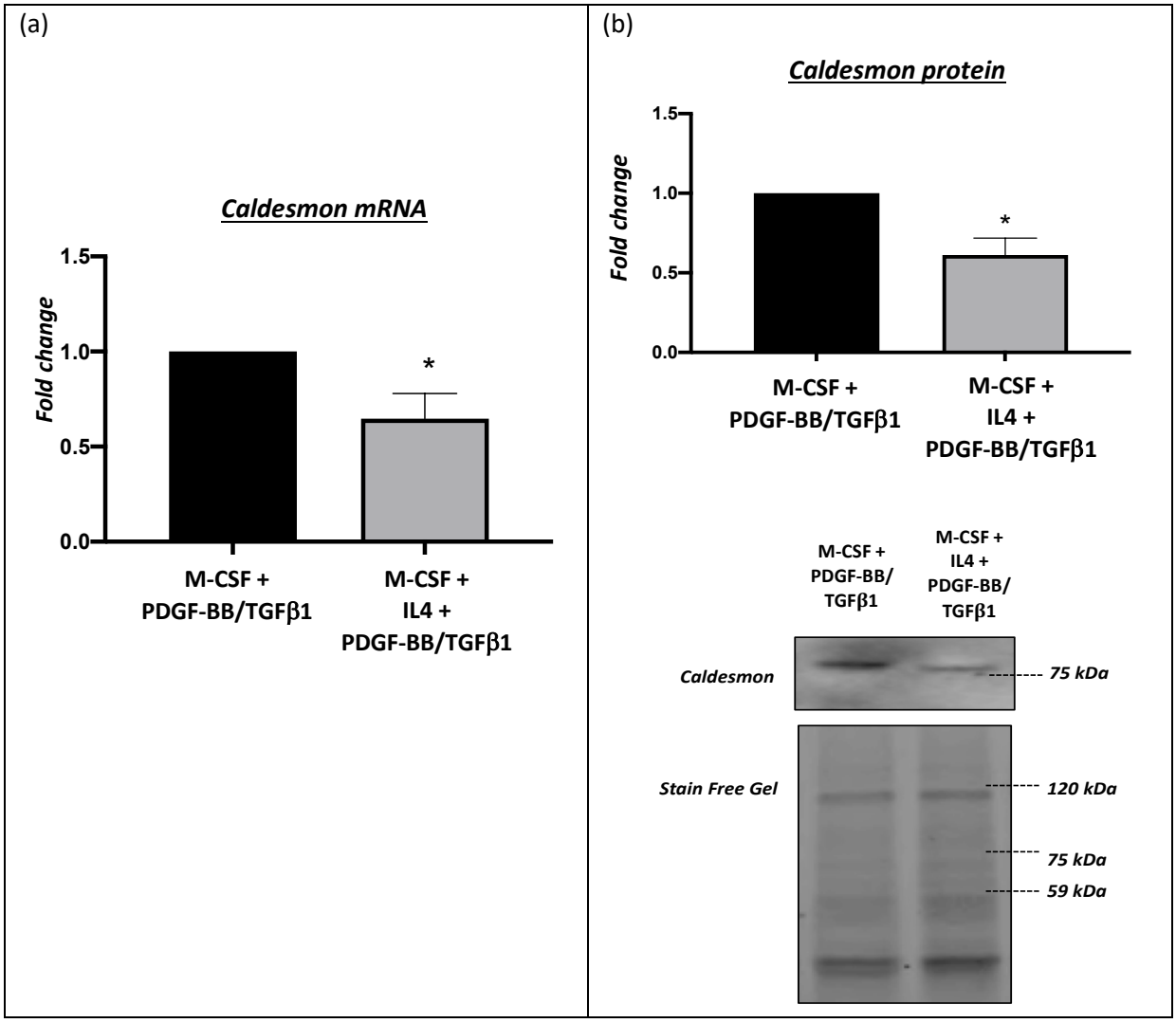

Figure 3.4.22 The effects of PDGF-BB and TGFβ1 co-stimulation on caldesmon mRNA and protein expression in M-CSF/IL4 polarised macrophages.

*(a) Caldesmon mRNA levels in M-CSF/IL4 macrophages relative to M-CSF directed macrophages, (mean±SEM; n=6; *P < 0.05 denotes significant difference compared to M-CSF macrophages; paired t-test).*

*(b) Quantification and representative western blots for cladesmon protein expression in M-CSF/IL4 macrophages relative to M-CSF directed macrophages. Stain free gel is shown as loading control. Data are expressed as fold change against untreated M-CSF-directed macrophages, (mean±SEM; n=6; **P < 0.01 denotes significant difference compared to M-CSF macrophages; paired t-test).*

Refer appendix A; (8.2.3) CT values and (8.2.4) full blot image.

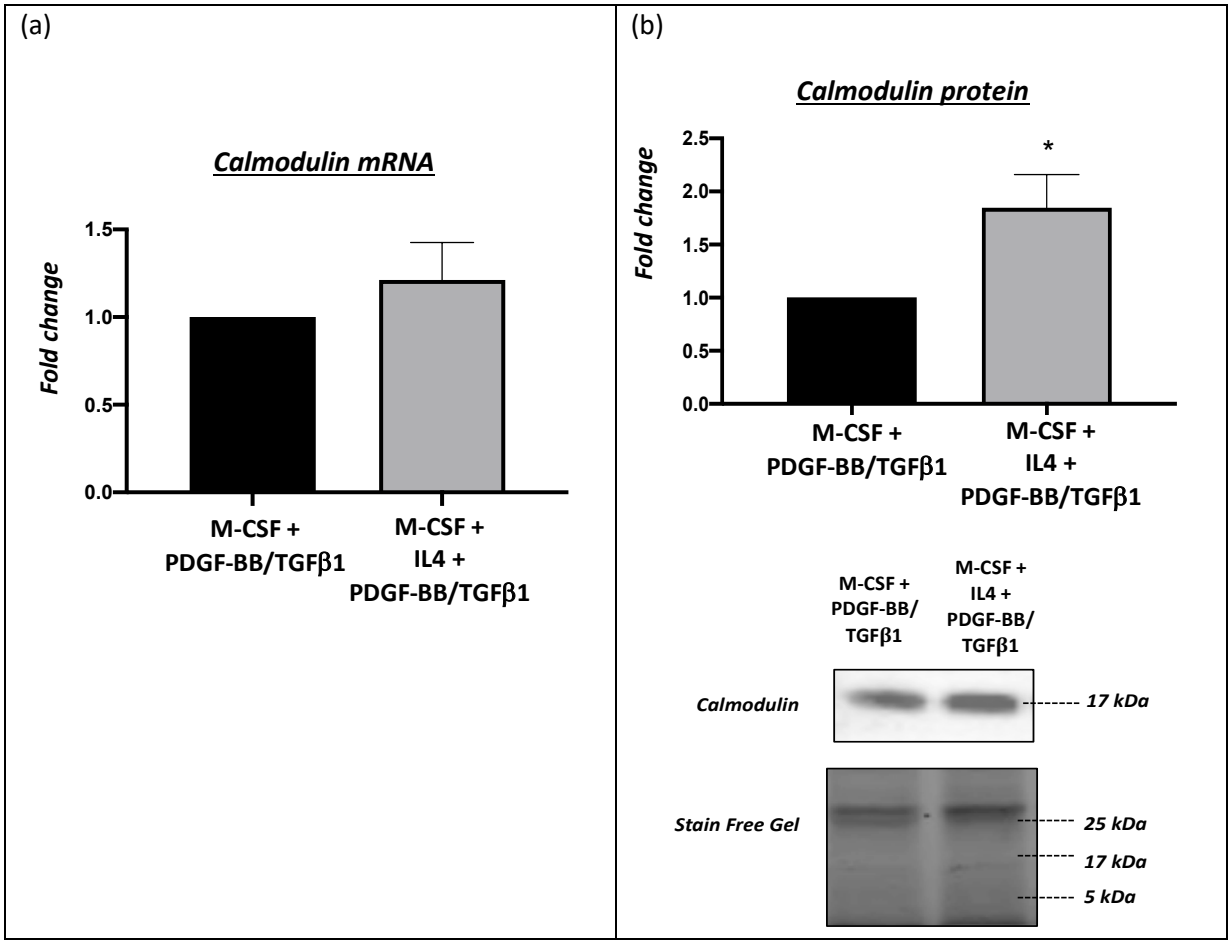

Figure 3.4.23 The effects of PDGF-BB and TGFβ1 co-stimulation on calmodulin mRNA and protein expression in M-CSF/IL4 polarised macrophages.

(a) Calmodulin mRNA levels in M-CSF/IL4 macrophages relative to M-CSF directed macrophages, (mean±SEM; n=6; paired t-test).

*(b) Quantification and representative western blots for calmodulin protein expression in M-CSF/IL4 macrophages relative to M-CSF directed macrophages. Stain free gel is shown as loading control. Data are expressed as fold change against untreated M-CSF-directed macrophages, (mean±SEM; n=6; *P < 0.05 denotes significant difference compared to M-CSF macrophages; paired t-test).*

Refer appendix A; (8.2.5) CT values and (8.2.6) full blot image.

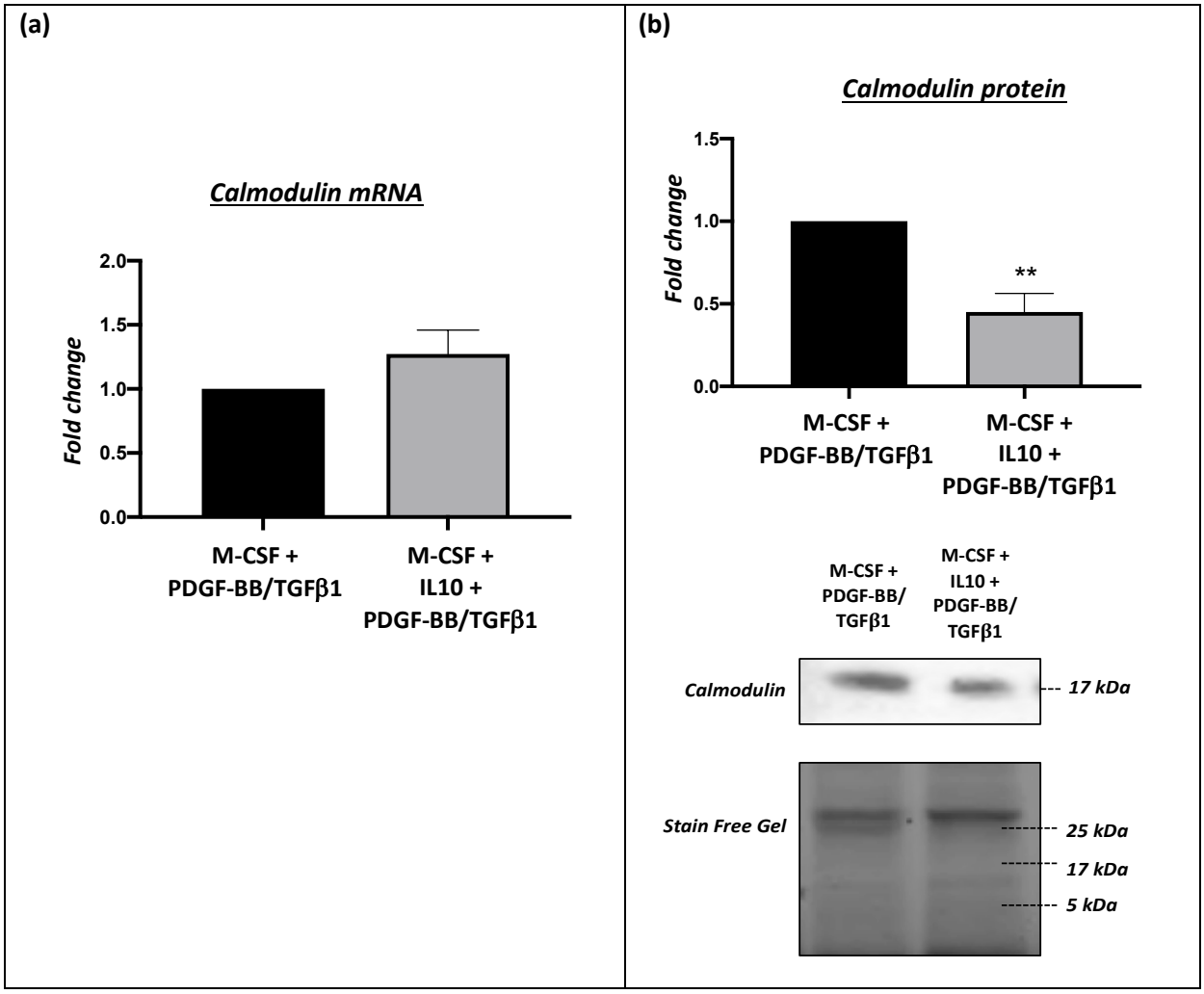

Figure 3.4.24 The effects of PDGF-BB and TGFβ1 co-stimulation on calmodulin mRNA and protein expression in M-CSF/IL10 polarised macrophages.

(a) Calmodulin mRNA levels in M-CSF/IL10 macrophages relative to M-CSF directed macrophages, (mean±SEM; n=6; paired t-test).

*(b) Quantification and representative western blots for calmodulin protein expression in M-CSF/IL10 macrophages relative to M-CSF directed macrophages. Stain free gel is shown as loading control. Data are expressed as fold change against untreated M-CSF-directed macrophages, (mean±SEM; n=6; **P < 0.01 denotes significant difference compared to M-CSF macrophages; paired t-test).*

Refer appendix A; (8.2.5) CT values and (8.2.6) full blot image.

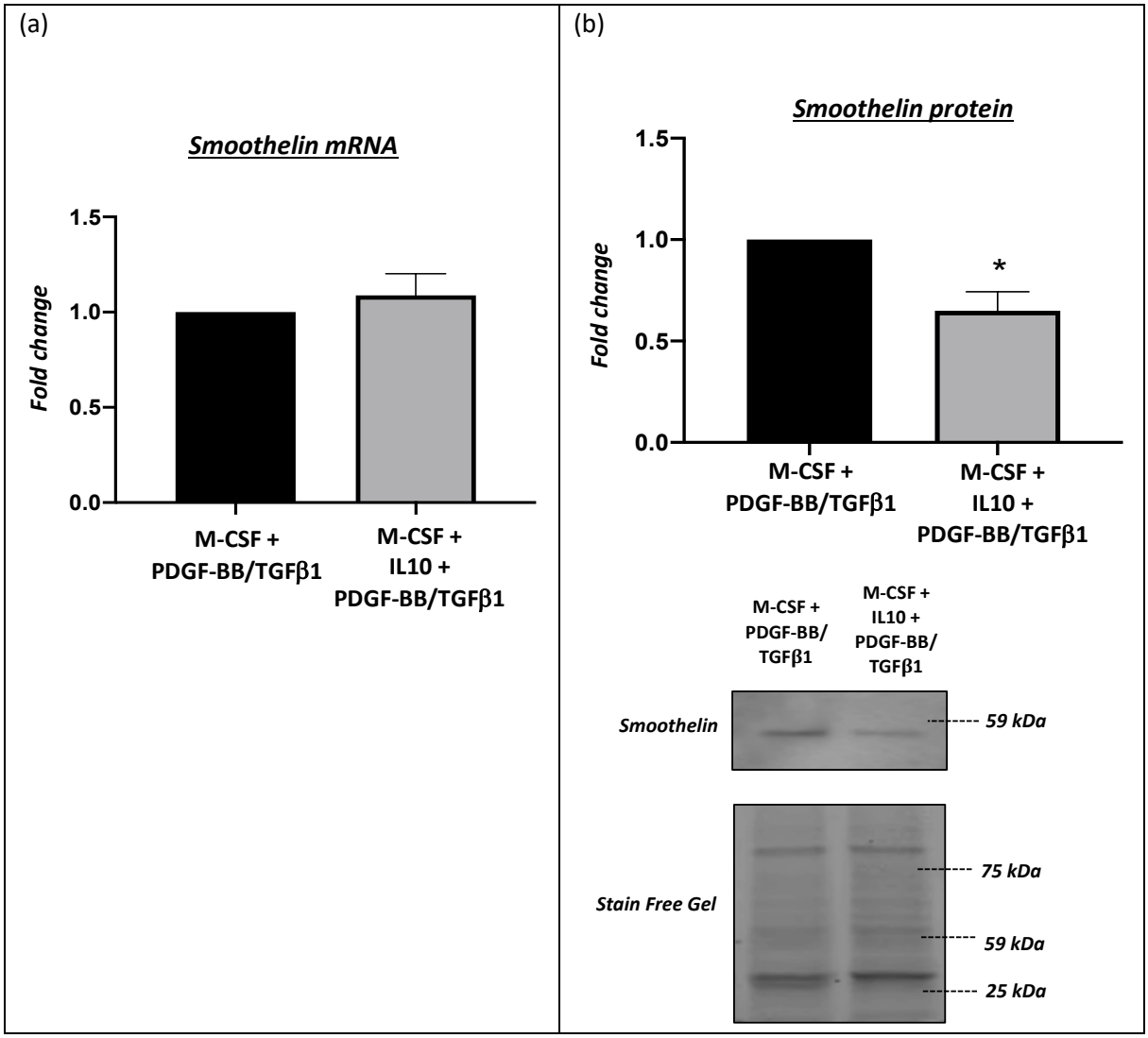

Figure 3.4.25 The effects of PDGF-BB and TGFβ1 co-stimulation on smoothelin mRNA and protein expression in M-CSF/IL10 polarised macrophages.

(a) Smoothelin mRNA levels in M-CSF/IL10 macrophages relative to M-CSF directed macrophages, (mean±SEM; n=6; paired t-test).

*(b) Quantification and representative western blots for smoothelin protein expression in M-CSF/IL10 macrophages relative to M-CSF directed macrophages. Stain free gel is shown as loading control. Data are expressed as fold change against untreated M-CSF-directed macrophages, (mean±SEM; n=6; *P < 0.05 denotes significant difference compared to M-CSF macrophages; paired t-test).*

Refer appendix A; (8.2.7) CT values and (8.2.8) full blot image.

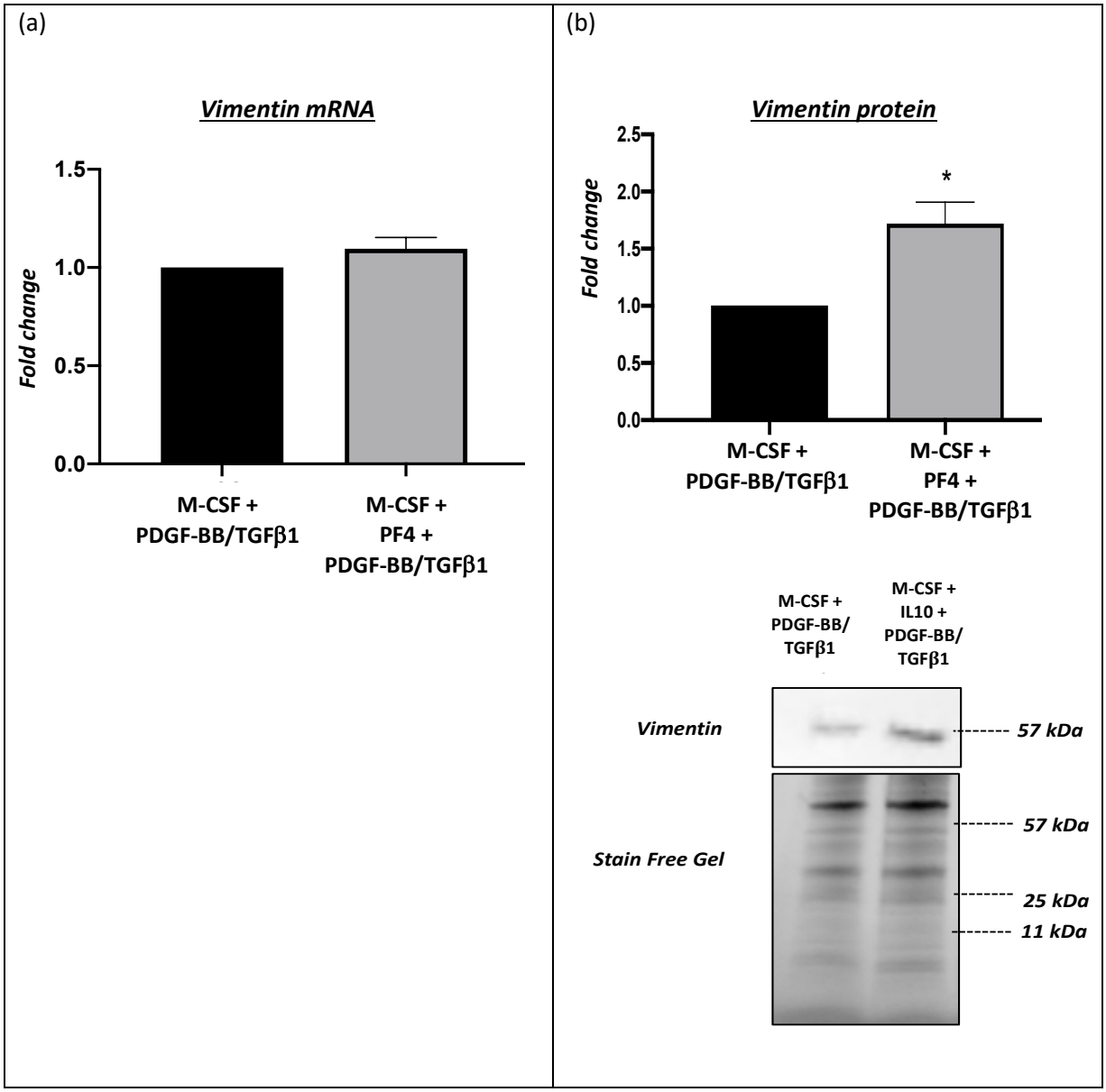

Figure 3.4.26 The effects of PDGF-BB and TGFβ1 co-stimulation on vimentin mRNA and protein expression in M-CSF/PF4 polarised macrophages.

(a) Vimentin mRNA levels in M-CSF/PF4 macrophages relative to M-CSF directed macrophages, (mean±SEM; n=6; paired t-test).

*(b) Quantification and representative western blots for vimentin protein expression in M-CSF/PF4 macrophages relative to M-CSF directed macrophages. Stain free gel is shown as loading control. Data are expressed as fold change against untreated M-CSF-directed macrophages, (mean±SEM; n=6; *P < 0.05 denotes significant difference compared to M-CSF macrophages; paired t-test).*

Refer appendix A; (8.2.9) CT values and (8.2.11) full blot image.

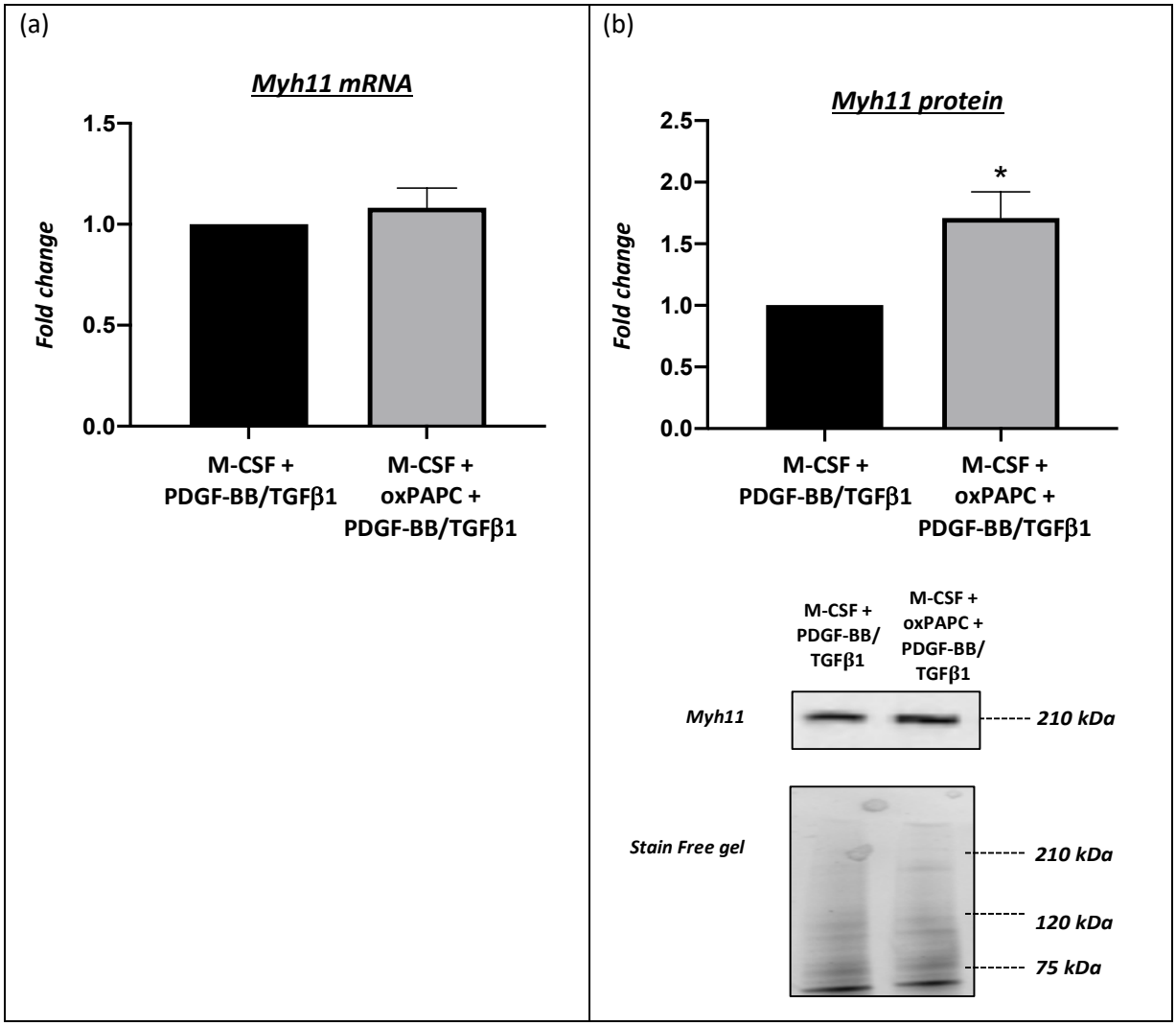

Figure 3.4.27 The effects of PDGF-BB and TGFβ1 co-stimulation on Myh11 mRNA and protein expression in M-CSF/oxPAPC polarised macrophages.

(a) Myh11 mRNA levels in M-CSF/oxPAPC macrophages relative to M-CSF directed macrophages, (mean±SEM; n=6; paired t-test).

*(b) Quantification and representative western blots for Myh11 protein expression in M-CSF/oxPAPC macrophages relative to M-CSF directed macrophages. Stain free gel is shown as loading control. Data are expressed as fold change against untreated M-CSF-directed macrophages, (mean±SEM; n=6; *P < 0.05 denotes significant difference compared to M-CSF macrophages; paired t-test).*

Refer appendix A; (8.2.12) CT values and (8.2.13) full blot image.

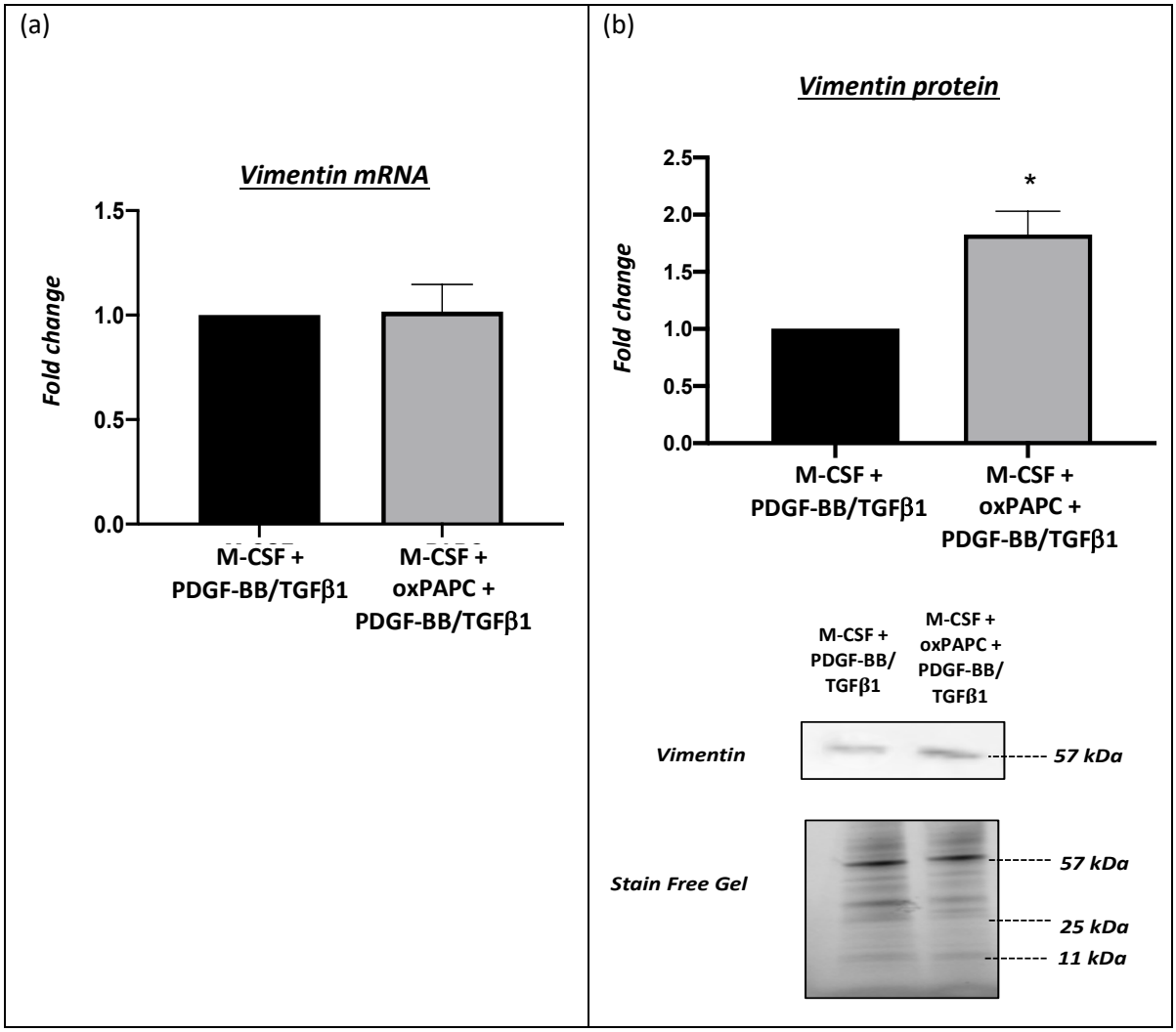

Figure 3.4.28 The effects of PDGF-BB and TGFβ1 co-stimulation on vimentin mRNA and protein expression in M-CSF/oxPAPC polarised macrophages.

(a) Vimentin mRNA levels in M-CSF/oxPAPC macrophages relative to M-CSF directed macrophages, (mean±SEM; n=6; paired t-test).

*(b) Quantification and representative western blots for vimentin protein expression in M-CSF/oxPAPC macrophages relative to M-CSF directed macrophages. Stain free gel is shown as loading control. Data are expressed as fold change against untreated M-CSF-directed macrophages, (mean±SEM; n=6; *P < 0.05 denotes significant difference compared to M-CSF macrophages; paired t-test).*

Refer appendix A; (8.2.9) CT values and (8.2.11) full blot image.

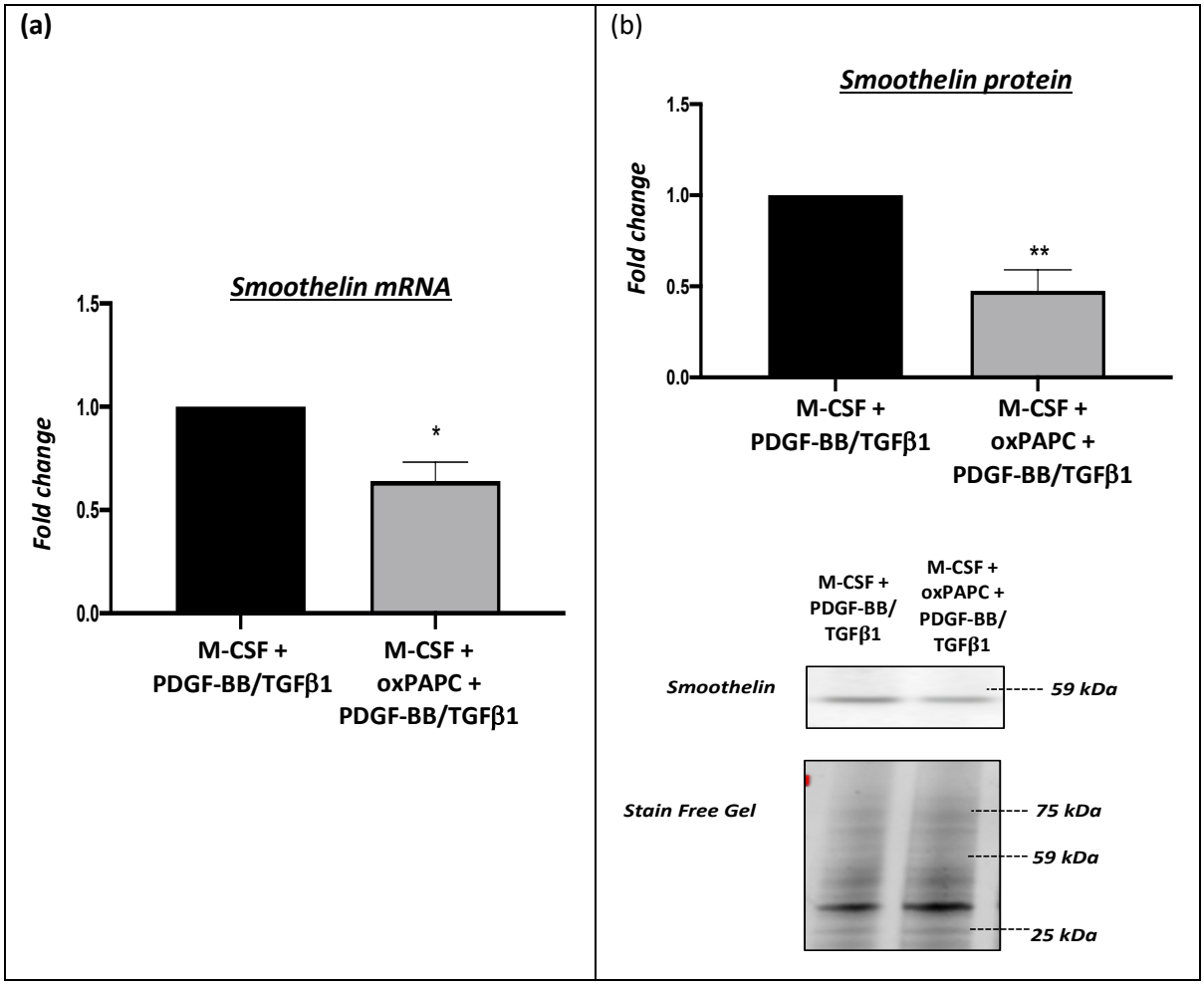

Figure 3.4.29 The effects of PDGF-BB and TGFβ1 co-stimulation on smoothelin mRNA and protein expression in M-CSF/oxPAPC polarised macrophages.

*(a) Smoothelin mRNA levels in M-CSF/oxPAPC macrophages relative to M-CSF directed macrophages, (mean±SEM; n=6; *P < 0.05 denotes significant difference compared to M-CSF macrophages; paired t-test).*

*(b) Quantification and representative western blots for smoothelin protein expression in M-CSF/oxPAPC macrophages relative to M-CSF directed macrophages. Stain free gel is shown as loading control. Data are expressed as fold change against untreated M-CSF-directed macrophages, (mean±SEM; n=6; **P < 0.01 denotes significant difference compared to M-CSF macrophages; paired t-test).*

Refer appendix A; (8.2.7) CT values and (8.2.14) full blot image.

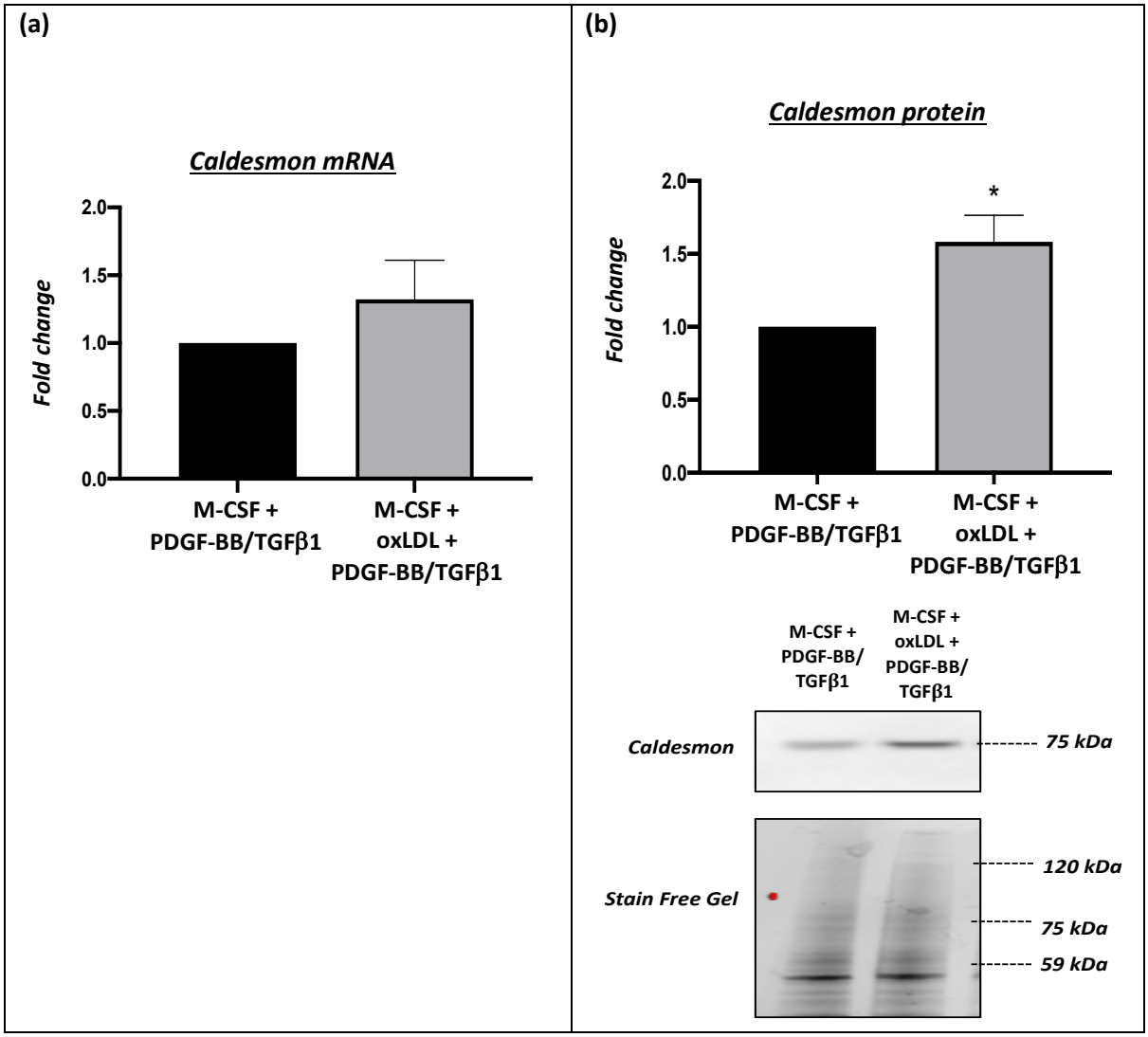

Figure 3.4.30 The effects of PDGF-BB and TGFβ1 co-stimulation on caldesmon mRNA and protein expression in M-CSF/oxLDL polarised macrophages.

(a) Caldesmon mRNA levels in M-CSF/oxLDL macrophages relative to M-CSF directed macrophages, (mean±SEM; n=6; paired t-test).

*(b) Quantification and representative western blots for caldesmon protein expression in M-CSF/oxLDL macrophages relative to M-CSF directed macrophages. Stain free gel is shown as loading control. Data are expressed as fold change against untreated M-CSF-directed macrophages, (mean±SEM; n=6; *P < 0.05 denotes significant difference compared to M-CSF macrophages; paired t-test).*

Refer appendix A; (8.2.3) CT values and (8.2.15) full blot image.

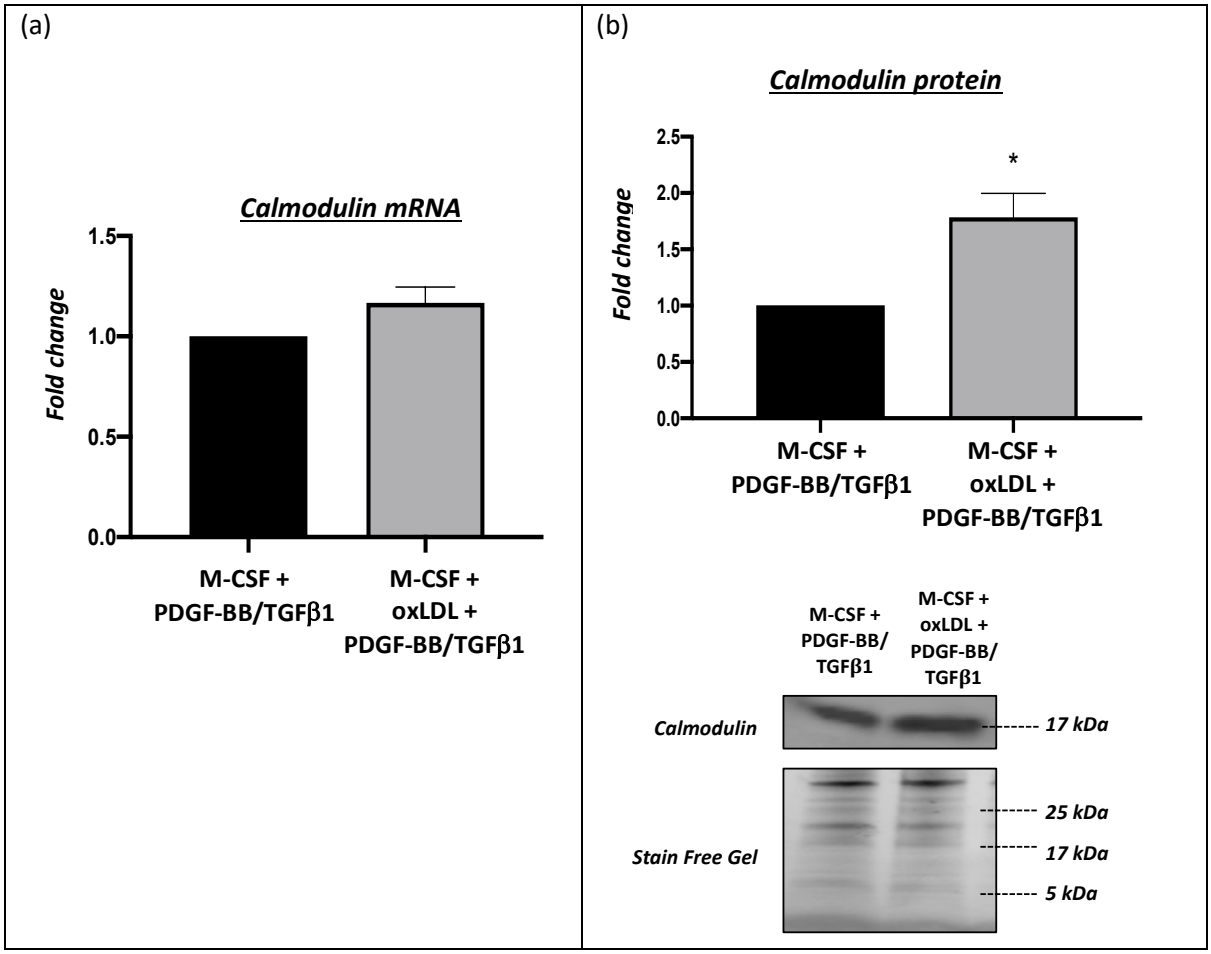

Figure 3.4.31 The effects of PDGF-BB and TGFβ1 co-stimulation on calmodulin mRNA and protein expression in M-CSF/oxLDL polarised macrophages.

(a) Calmodulin mRNA levels in M-CSF/oxLDL macrophages relative to M-CSF directed macrophages, (mean±SEM; n=6; paired t-test).

*(b) Quantification and representative western blots for calmodulin protein expression in M-CSF/oxLDL macrophages relative to M-CSF directed macrophages. Stain free gel is shown as loading control. Data are expressed as fold change against untreated M-CSF-directed macrophages, (mean±SEM; n=6; *P < 0.05 denotes significant difference compared to M-CSF macrophages; paired t-test).*

Refer appendix A; (8.2.5) CT values and (8.2.16) full blot image.

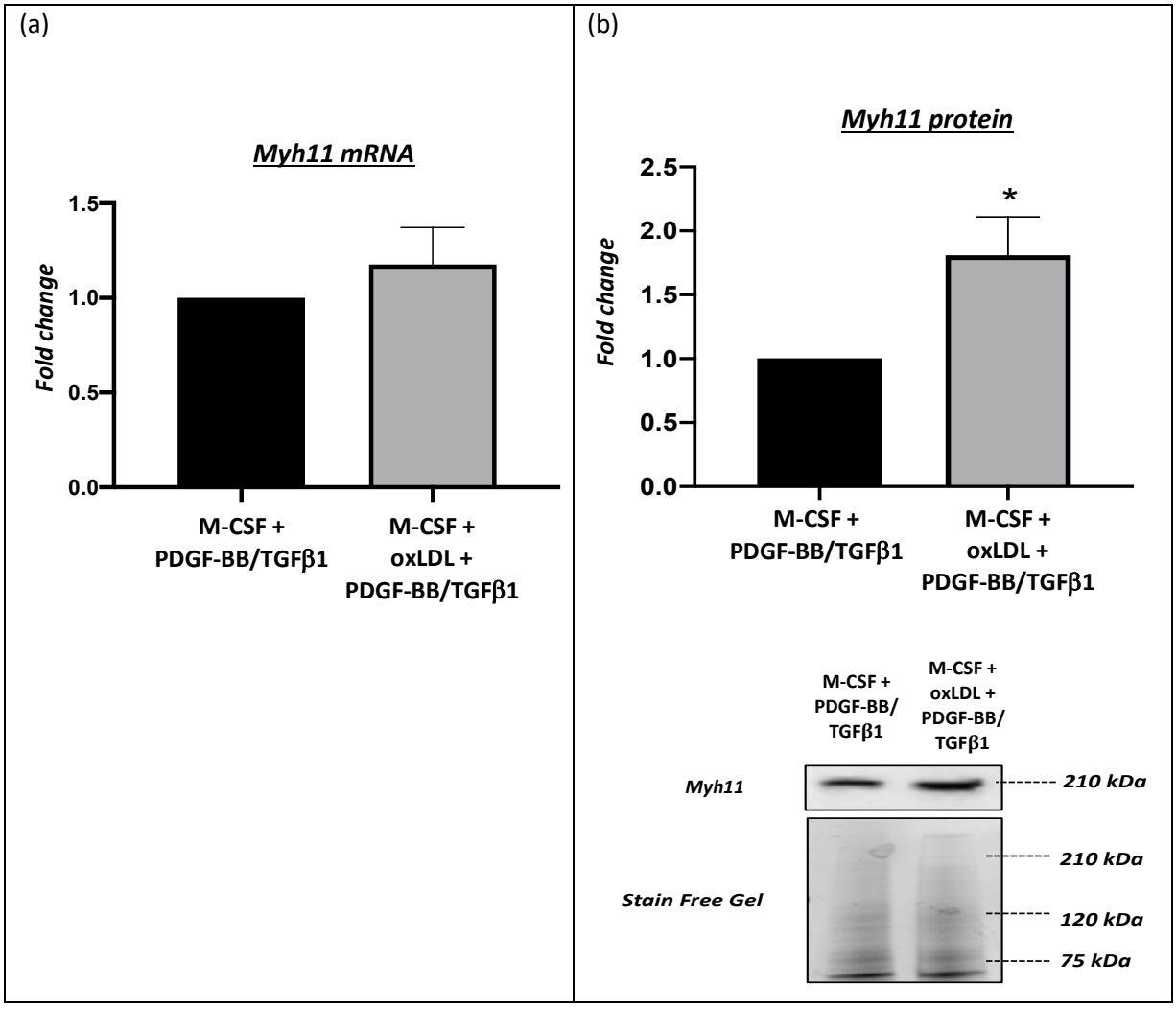

Figure 3.4.32 The effects of PDGF-BB and TGFβ1 co-stimulation on Myh11 mRNA and protein expression in M-CSF/oxLDL polarised macrophages.

(a) Myh11 mRNA levels in M-CSF/oxLDL macrophages relative to M-CSF directed macrophages, (mean±SEM; n=6; paired t-test).

*(b) Quantification and representative western blots for Myh11 protein expression in M-CSF/oxLDL macrophages relative to M-CSF directed macrophages. Stain free gel is shown as loading control. Data are expressed as fold change against untreated M-CSF-directed macrophages, (mean±SEM; n=6; *P < 0.05 denotes significant difference compared to M-CSF macrophages; paired t-test).*

Refer appendix A; (8.2.12) CT values and (8.2.13) full blot image.

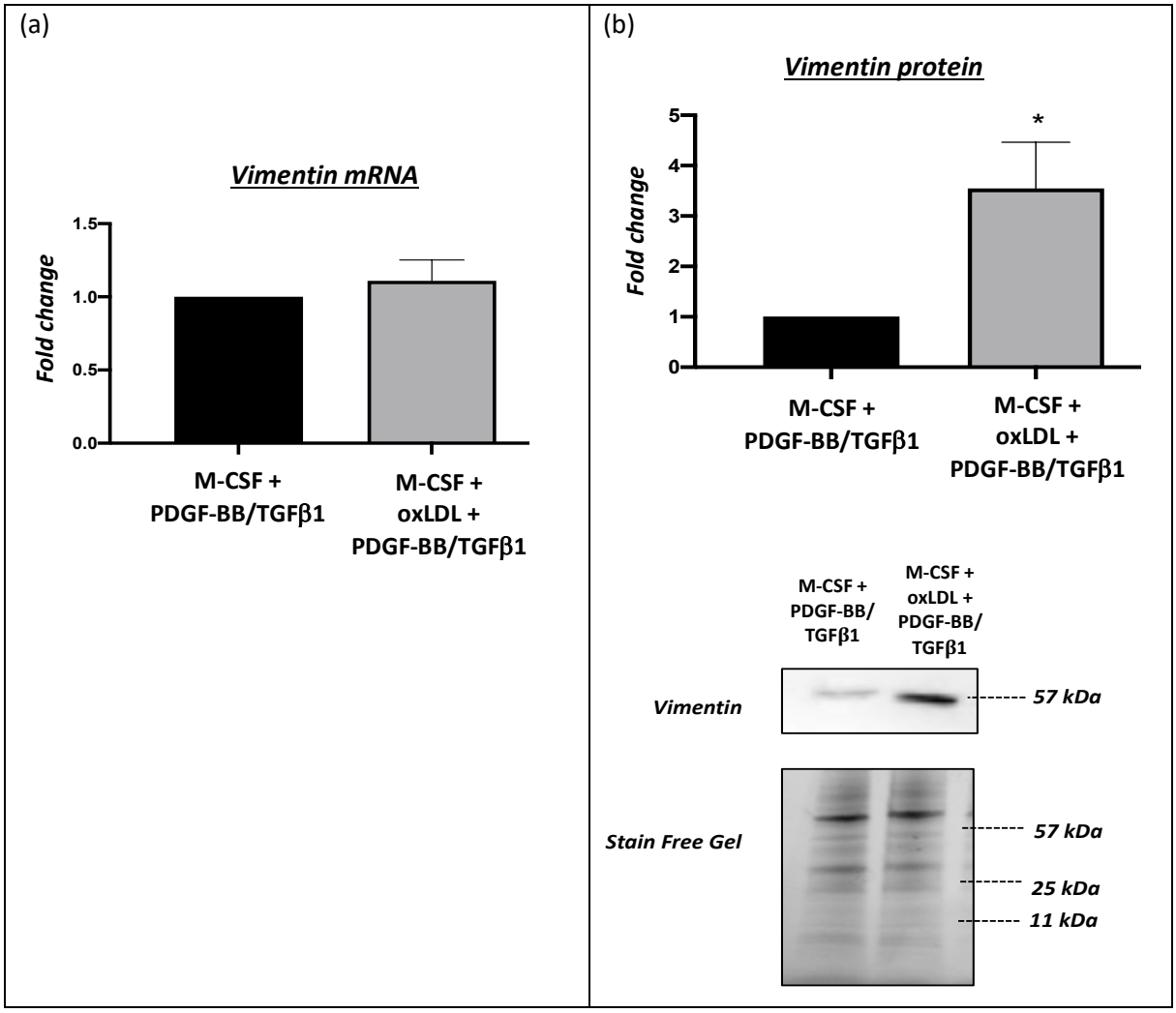

Figure 3.4.33 The effects of PDGF-BB and TGFβ1 co-stimulation on vimentin mRNA and protein expression in M-CSF/oxLDL polarised macrophages.

(a) Vimentin mRNA levels in M-CSF/oxLDL macrophages relative to M-CSF directed macrophages, (mean±SEM; n=6; paired t-test).

(b) Quantification and representative western blots for vimentin *protein expression in M-CSF/oxLDL macrophages relative to M-CSF directed macrophages. Stain free gel is shown as loading control. Data are expressed as fold change against untreated M-CSF-directed macrophages, (mean±SEM; n=6; *P < 0.05 denotes significant difference compared to M-CSF macrophages; paired t-test).*

Refer appendix A; (8.2.9) CT values and (8.2.11) full blot image.

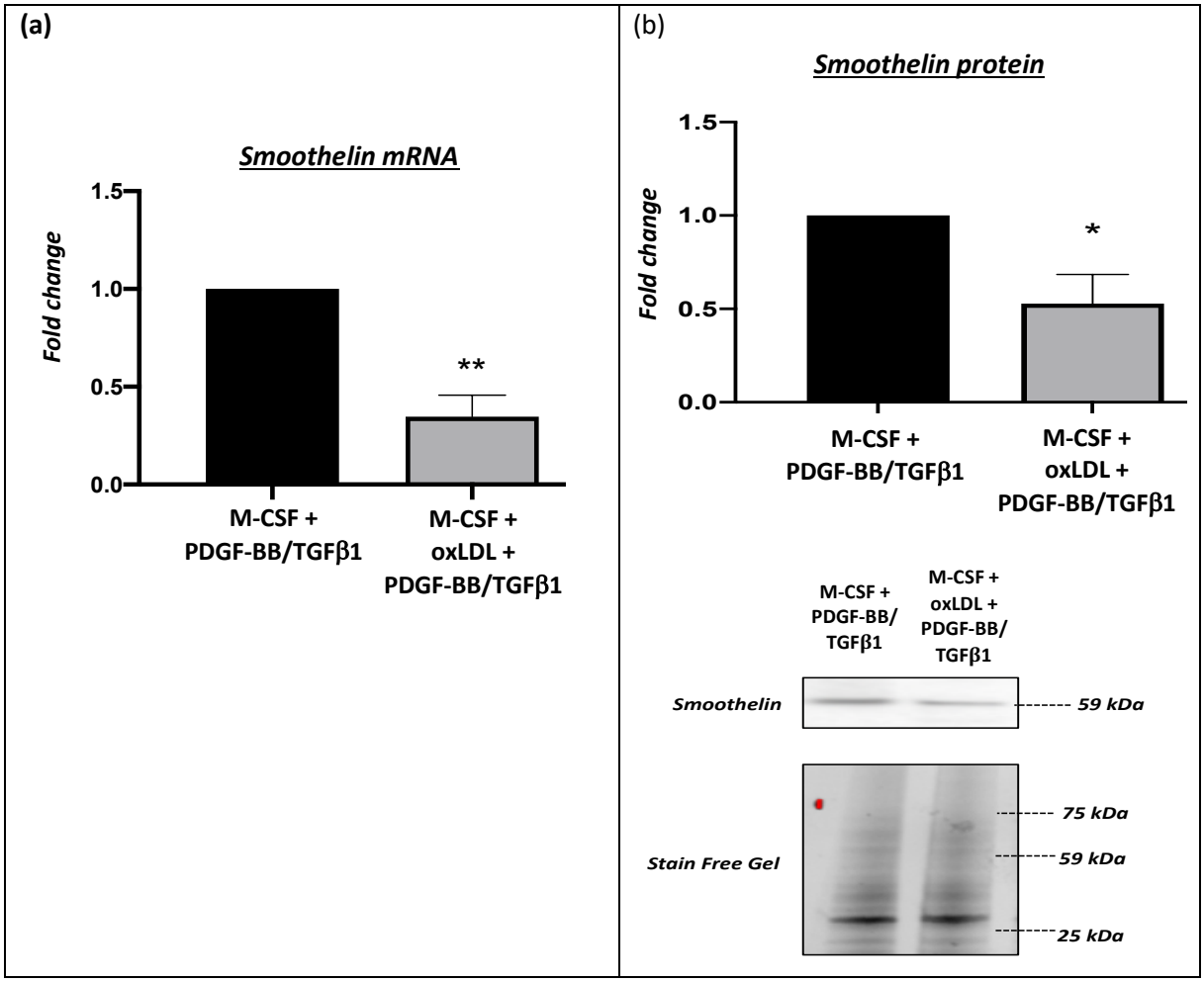

Figure 3.4.34 The effects of PDGF-BB and TGFβ1 co-stimulation on smoothelin mRNA and protein expression in M-CSF/oxLDL polarised macrophages.

*(a) Smoothelin mRNA levels in M-CSF/oxLDL macrophages relative to M-CSF directed macrophages, (mean±SEM; n=6; **P < 0.01 denotes significant difference compared to M-CSF macrophages; paired t-test).*

*(b) Quantification and representative western blots for smoothelin protein expression in M-CSF/oxLDL macrophages relative to M-CSF directed macrophages. Stain free gel is shown as loading control. Data are expressed as fold change against untreated M-CSF-directed macrophages, (mean±SEM; n=6; *P < 0.05 denotes significant difference compared to M-CSF macrophages; paired t-test).*

Refer appendix A; (8.2.7) CT values and (8.2.14) full blot image.

Polarisation factor(s)	Caldesmon		Calmodulin		Myh11		Smoothelin		Vimentin	
	mRNA	*protein*	*mRNA*	*protein*	*mRNA*	*protein*	*mRNA*	*protein*	*mRNA*	*protein*
IFNγ + LPS	1.1	0.6	2.9	0.6	1.0	1.1	1.0	0.6	1.6	0.6
IL-4	0.6	0.6	1.2	1.8	1.0	1.2	1.1	1.1	1.1	1.1
IL-10	1.0	1.0	1.1	0.4	1.2	1.1	1.1	0.6	1.1	1.2
PF4	1.2	1.1	1.1	1.1	1.0	1.1	1.1	1.1	1.1	1.7
oxPAPC	1.1	1.0	1.2	1.1	1.1	1.7	0.6	0.5	1.0	1.8
oxLDL	1.3	1.6	1.2	1.8	1.2	1.8	0.3	0.5	1.1	3.5

Figure 3.4.35 Summary result for polarised M-CSF macrophages with PDGF-BB + TGFβ1 co-stimulation

Fold change in mRNA and protein expression of VSMC-associated markers compared to PDGF-BB/TGFβ1 treated M-CSF matured human macrophages without administration of polarisation factors. Green boxes indicate significantly reduced expression, whereas red boxes indicate significantly increased levels.

3.4.5 The expression of VSMC-related markers in M-CSF and GM-CSF matured macrophages relative to human coronary artery VSMCs

Although all VSMC-associated markers were present within human macrophages, and expression patterns varied between M-CSF or GM-CSF-matured cells with and without stimulation with PDGF-BB/TGFβ1, it was deemed important to relate expression levels to those observed in primary VSMCs, as an indicator of macrophages truly shifting towards a VSMC-like phenotype. Accordingly, the expression of VSMC-related markers was compared between human macrophage baseline cultures (M-Mac and GM-Mac) and human primary coronary artery VSMC cultures. Although M-CSF matured macrophages expressed all the markers evaluated, protein levels for all were significantly lower than those detected by Western blotting in coronary artery VSMCs; caldesmon (40% change; $P<0.01$; n=6; Figure 3.4.36 b), calmodulin (69% change; $P<0.05$; n=6; Figure 3.4.37 b), Myh11 (38% change; $P<0.01$; n=6; Figure 3.4.38 b), smoothelin (65% change; $P<0.0001$; n=6; Figure 3.4.39 b) and vimentin (67% change; $P<0.001$; n=6; Figure 3.4.40 b). Reciprocal changes at the mRNA level were also observed, with the exception of Myh11 where no difference was seen (see summary Figure 3.4.41). A distinctly different pattern was observed in GM-CSF matured macrophages, which displayed comparable protein levels for calmodulin, Myh11 and smoothelin as those detected in human coronary artery VSMCS (see summary Figure 3.4.41). Moreover, caldesmon protein expression was significantly increased within GM-CSF matured macrophages (1.9-fold change; $P<0.05$; n=6; Figure 3.4.36 b) in relation to VSMCs, although mRNA levels were seen to decrease (99.95% change; $P<0.0001$; n=6; Figure 3.4.36 a). Mirroring the pattern in M-CSF matured macrophages, vimentin mRNA and protein expression was significantly decreased in GM-CSF differentiated macrophages compared to VSMCs (18% and 49% change; $P<0.05$; n=6; Figure 3.4.40). It should be noted that for caldesmon, a high molecular weight isoform (120 kDa) was detected in primary VSMC cultures which was not apparent in either macrophage population (please see appendix A (8.1.3) for full western blot image).

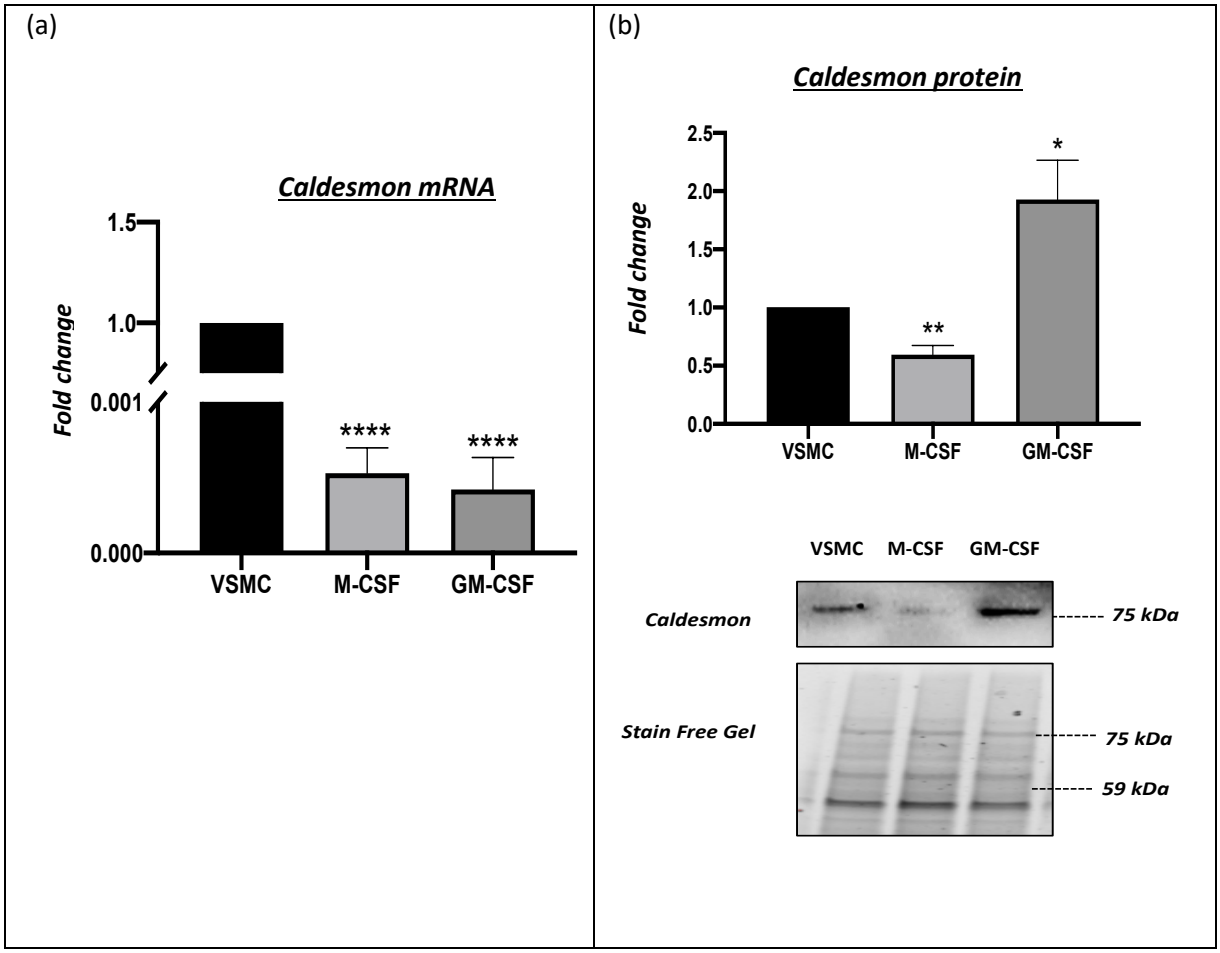

Figure 3.4.36 Caldesmon mRNA and protein expression in M-CSF or GM-CSF polarised macrophages relative to human coronary artery VSMC.

*(a) Caldesmon mRNA levels in M-CSF and GM-CSF macrophages relative to human coronary artery VSMC, (mean±SEM; n=6; ****P < 0.0001 denotes significant difference compared to VSMC, ANOVA Tukey-Kramer multiple comparison test).*

*(b) Quantification and representative western blots for caldesmon protein expression in M-CSF and GM-CSF macrophages relative to human coronary artery VSMC. Stain free gel is shown as loading control. Data are expressed as fold change against human coronary artery VSMC, (mean±SEM; n=6; **P<0.01 denotes significant difference compared to VSMC, ANOVA Tukey-Kramer multiple comparison test).*

Refer appendix A; (8.1.2) CT values and (8.1.3) full blot image.

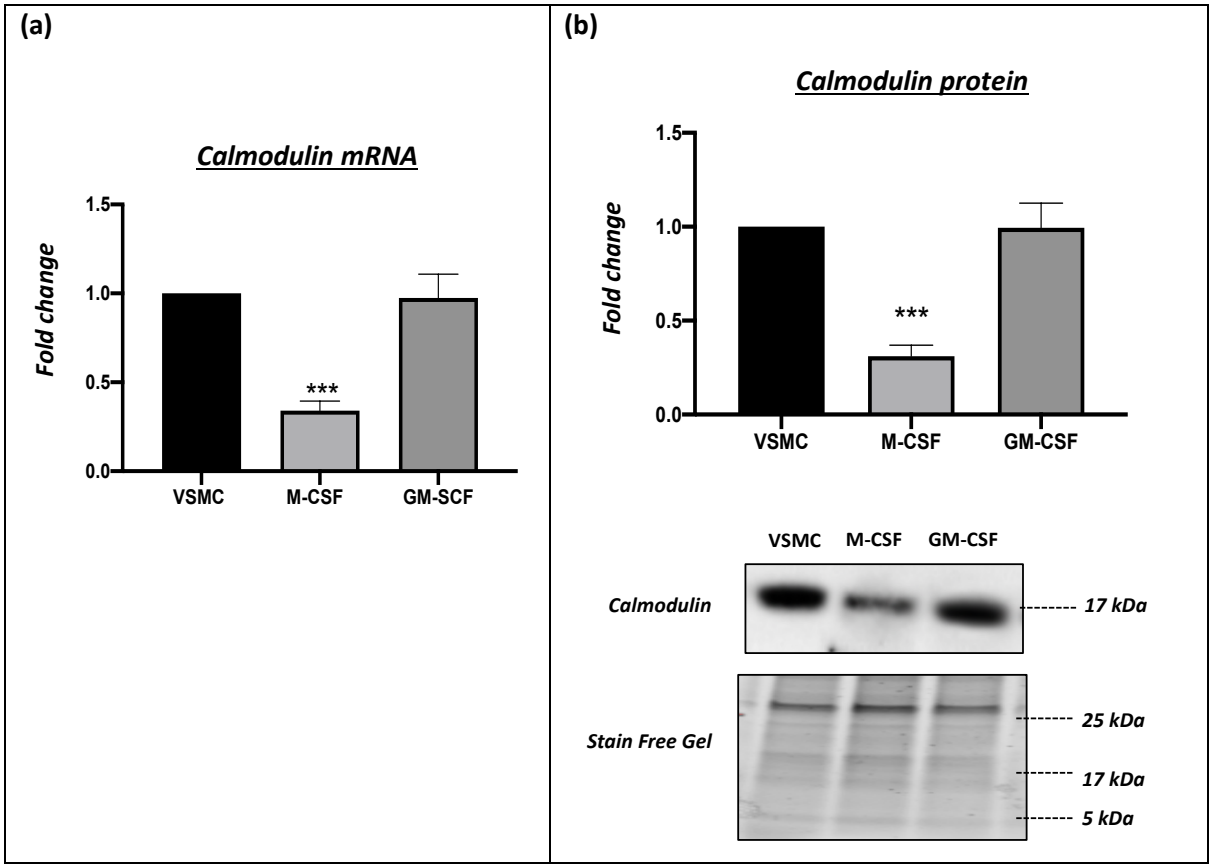

Figure 3.4.37 Calmodulin mRNA and protein expression in M-CSF or GM-CSF polarised macrophages relative to human coronary artery VSMCs.

*(a) Calmodulin mRNA levels in M-CSF and GM-CSF macrophages relative to human coronary artery VSMC, (mean±SEM; n=6; ***P < 0.001 denotes significant difference compared to VSMC, ANOVA Tukey-Kramer multiple comparison test).*

*(b) Quantification and representative western blots for calmodulin protein expression in M-CSF and GM-CSF macrophages relative to human coronary artery VSMC. Stain free gel is shown as loading control. Data are expressed as fold change against human coronary artery VSMC, (mean±SEM; n=6; **P<0.01 denotes significant difference compared to VSMC, ANOVA Tukey-Kramer multiple comparison test).*

Refer appendix A; (8.1.4) CT values and (8.1.5) full blot image.

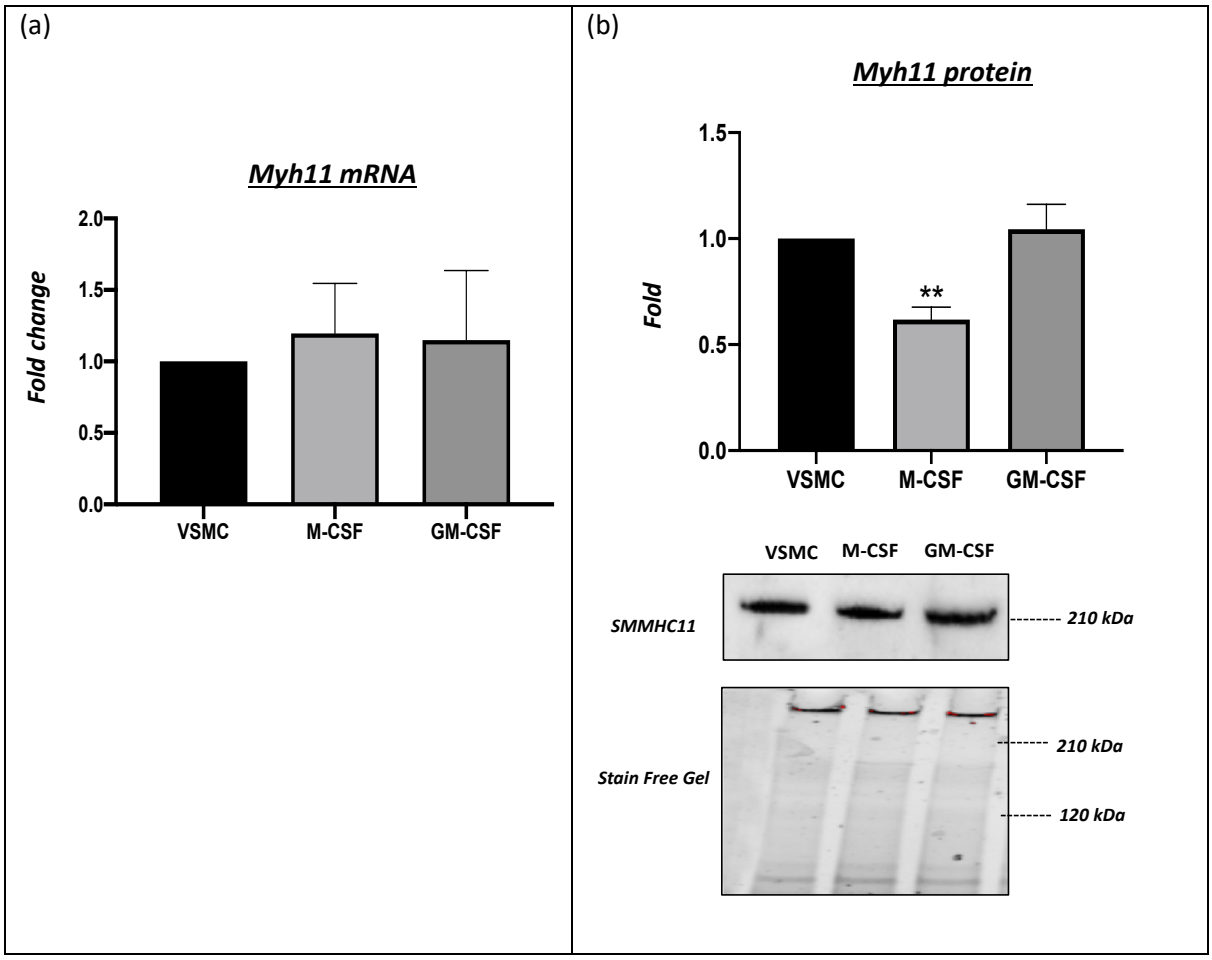

Figure 3.4.38 Myh11 mRNA and protein expression in M-CSF or GM-CSF polarised macrophages relative to human coronary artery VSMCs.

(a) Myh11 mRNA levels in M-CSF and GM-CSF macrophages relative to human coronary artery VSMC, (mean±SEM; n=6; ANOVA Tukey-Kramer multiple comparison test).

*(b) Quantification and representative western blots for Myh11 protein expression in M-CSF and GM-CSF macrophages relative to human coronary artery VSMC. Stain free gel is shown as loading control. Data are expressed as fold change against human coronary artery VSMC, (mean±SEM; n=6; **P<0.01 denotes significant difference compared to VSMC, ANOVA Tukey-Kramer multiple comparison test).*

Refer appendix A; (8.1.6) CT values and (8.1.7) full blot image.

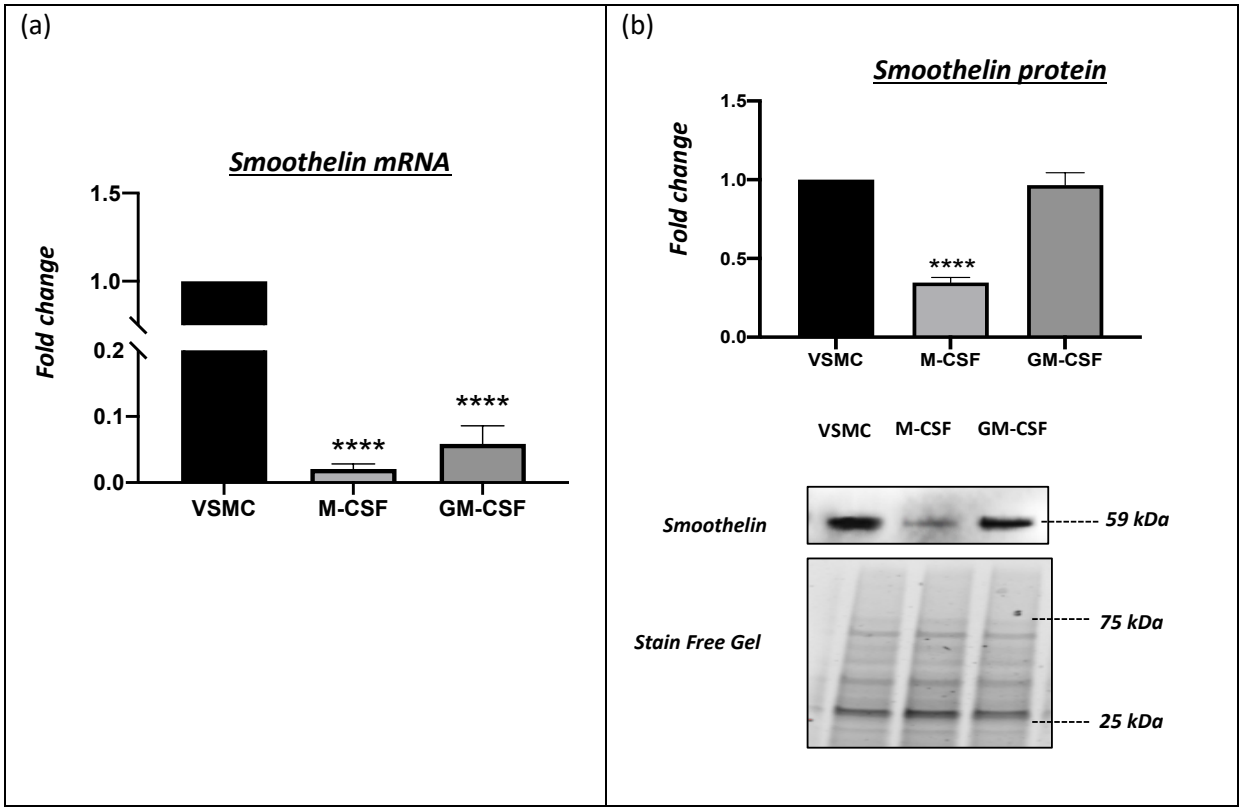

Figure 3.4.39 Smoothelin mRNA and protein expression in M-CSF or GM-CSF polarised macrophages relative to human coronary artery VSMCs.

*(a) Smoothelin mRNA levels in MCSF and GM-CSF macrophages relative to human coronary artery VSMC, (mean±SEM; n=6; ****P < 0.0001 denotes significant difference compared to VSMC, ANOVA Tukey-Kramer multiple comparison test).*

*(b) Quantification and representative western blots for smoothelin protein expression in M-CSF and GM-CSF macrophages relative to human coronary artery VSMC. Stain free gel is shown as loading control. Data are expressed as fold change against human coronary artery VSMC, (mean±SEM; n=6; ****P<0.0001 denotes significant difference compared to VSMC, ANOVA Tukey-Kramer multiple comparison test).*

Refer appendix A; (8.1.8) CT values and (8.1.9) full blot image.

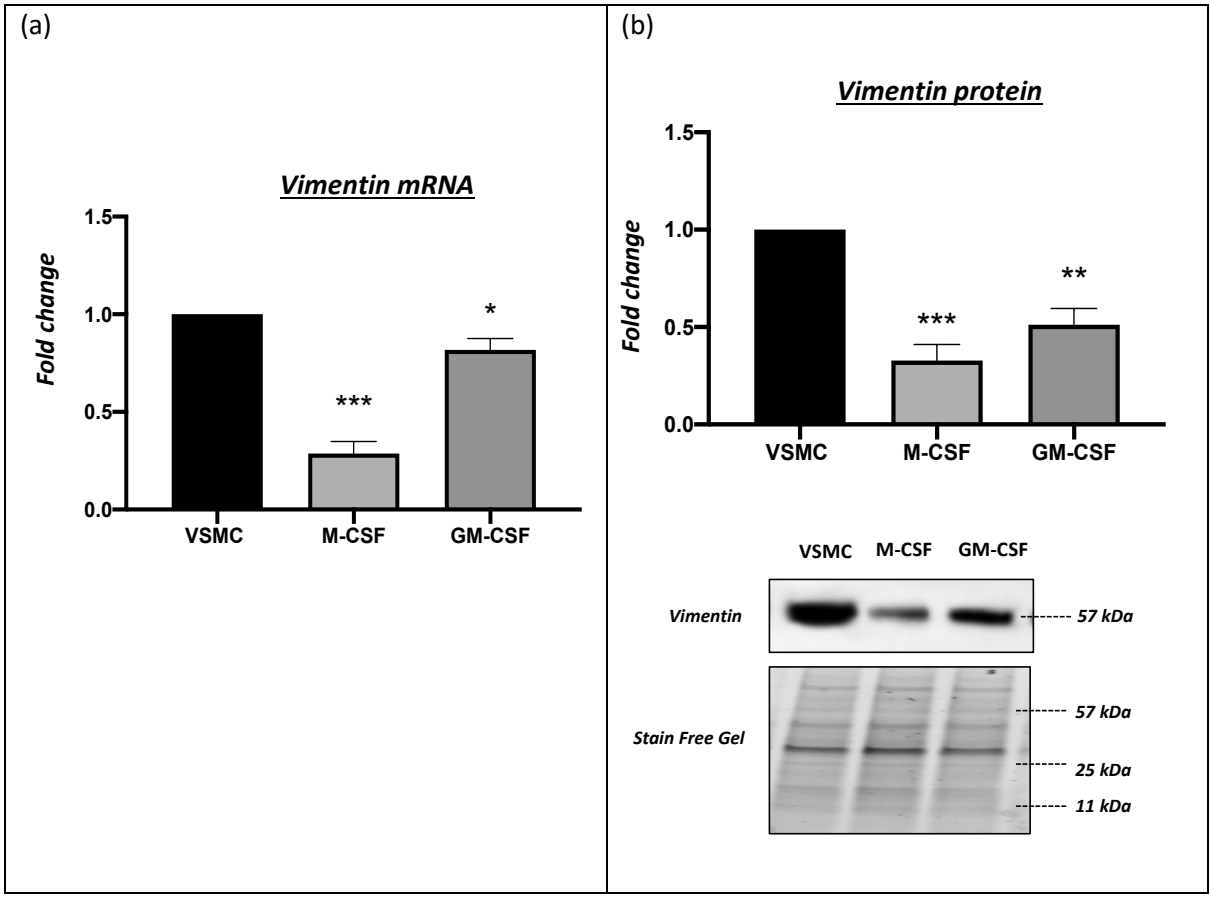

Figure 3.4.40 Vimentin mRNA and protein expression in M-CSF or GM-CSF polarised macrophages relative to human coronary artery VSMCs.

*(a) Vimentin mRNA levels in MCSF and GM-CSF macrophages relative to human coronary artery VSMC, (mean±SEM; n=6; ***P < 0.001 and *P<0.05 denotes significant difference compared to VSMC, ANOVA Tukey-Kramer multiple comparison test).*

*(b) Quantification and representative western blots for vimentin protein expression in M-CSF and GM-CSF macrophages relative to human coronary artery VSMC. Stain free gel is shown as loading control. Data are expressed as fold change against human coronary artery VSMC, (mean±SEM; n=6; ***P < 0.001 and **P<0.01 denotes significant difference compared to VSMC, ANOVA Tukey-Kramer multiple comparison test).*

Refer appendix A; (8.1.10) CT values and (8.1.11) full blot image.

	Caldesmon		Calmodulin		Myh11		Smoothelin		Vimentin	
Cell type	*mRNA*	*protein*	*mRNA*	*protein*	*mRNA*	*protein*	*mRNA*	*protein*	*mRNA*	*protein*
VSMC	1.0	1.0	1.0	1.0	1.0	1.0	1.0	1.0	1.0	1.0
M-CSF	0.0†	0.6	0.3	0.3	1.2	0.6	0.0†	0.3	0.3	0.3
GM-CSF	0.0‡	1.9	1.0	1.0	1.1	1.0	0.1	1.0	0.8	0.5

Figure 3.4.41 Summary result for VSMC and macrophage

Fold change in mRNA and protein expression of VSMC-associated markers in baseline M-CSF or GM-CSF polarised macrophages compared to human coronary artery VSMCs. Green boxes indicate significantly reduced expression, whereas red boxes indicate significantly increased levels.

†M-CSF caldesmon mRNA = 0.00052-fold change; smoothelin mRNA = 0.02063-fold change.

‡GM-CSF caldesmon mRNA = 0.00042-fold change.

3.4.6 *In vitro* macrophages retain macrophage marker expression after co-stimulation with PDGF-BB and TGFβ1

The above evidence demonstrates that human macrophages matured with either M-CSF or GM-CSF, express an array of VSMC-associated markers which can be further modulated through co-stimulation with the VSMC-related growth factors PDGF-BB and TGFβ1. Considering the expression of VSMC-associated markers suggest a subsequent shift towards a VSMC-like phenotype, macrophages may deviate from their macrophage lineage. Accordingly, the expression of a macrophage marker, Mac-2 (Galectin-3), was evaluated in macrophage cultures by immunofluorescence staining to assess if expression was affected upon culture and stimulation with PDGF-BB and TGFβ1 (Figure 3.4.42). As can be observed within Figure 3.4.43, greater than 90% of M-CSF and GM-CSF matured macrophages displayed positive immunolabelling for Mac-2 (galectin-3). Subsequent co-incubation with PDGF-BB and TGFβ1 did not affect macrophage Mac-2 expression in either subset (Figure 3.4.43).

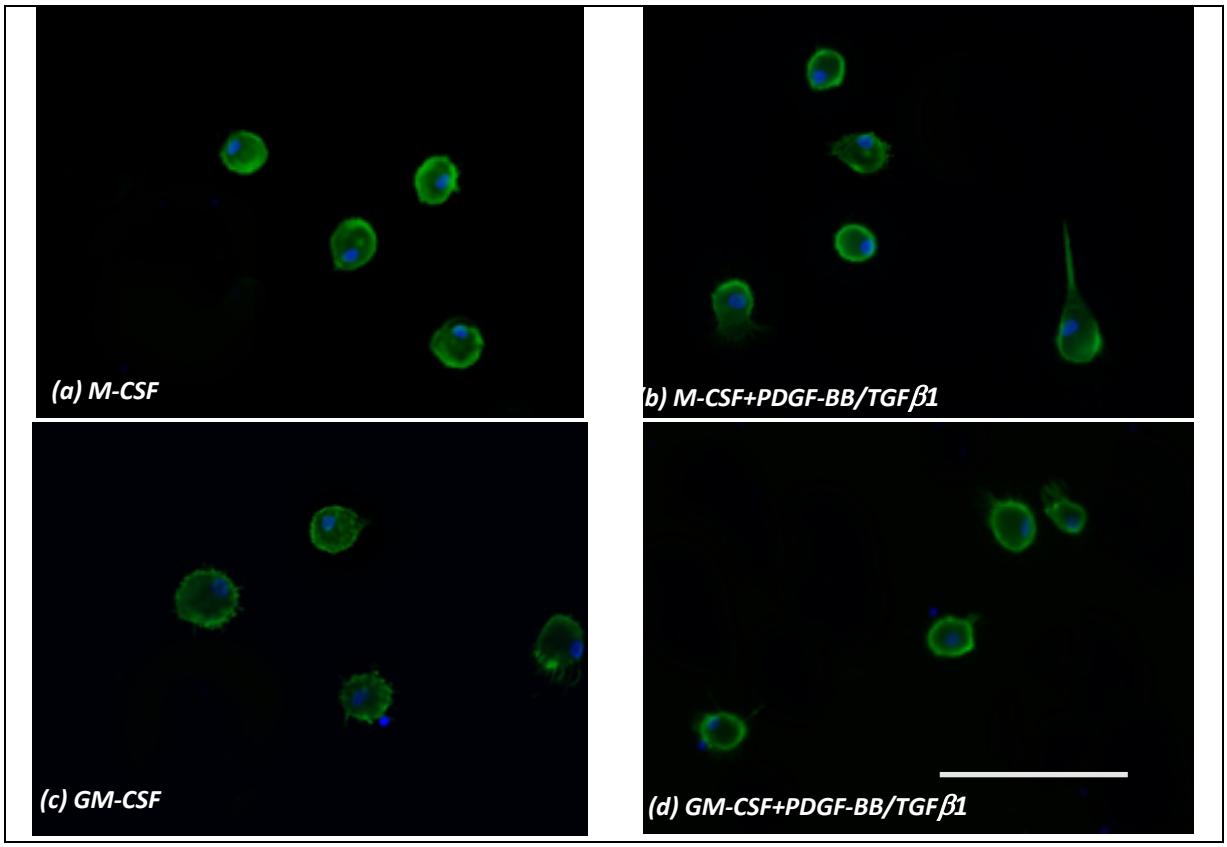

Figure 3.4.42 Fluorescent immunocytochemistry for Mac-2 (galectin-3) protein expression in human macrophage subsets with and without PDGF-BB and TGFβ1 co-stimulation.

Representative images of in vitro human monocyte-derived macrophages matured with either M-CSF or GM-CSF for seven, followed with or without co-stimulation with PDGF-BB and TGFβ1 for three days, then subjected to immunocytochemistry for Mac-2 (green) and counterstained with DAPI (blue; nuclei). Scale bar in panel D represents 100 μM and is applicable to all panels.

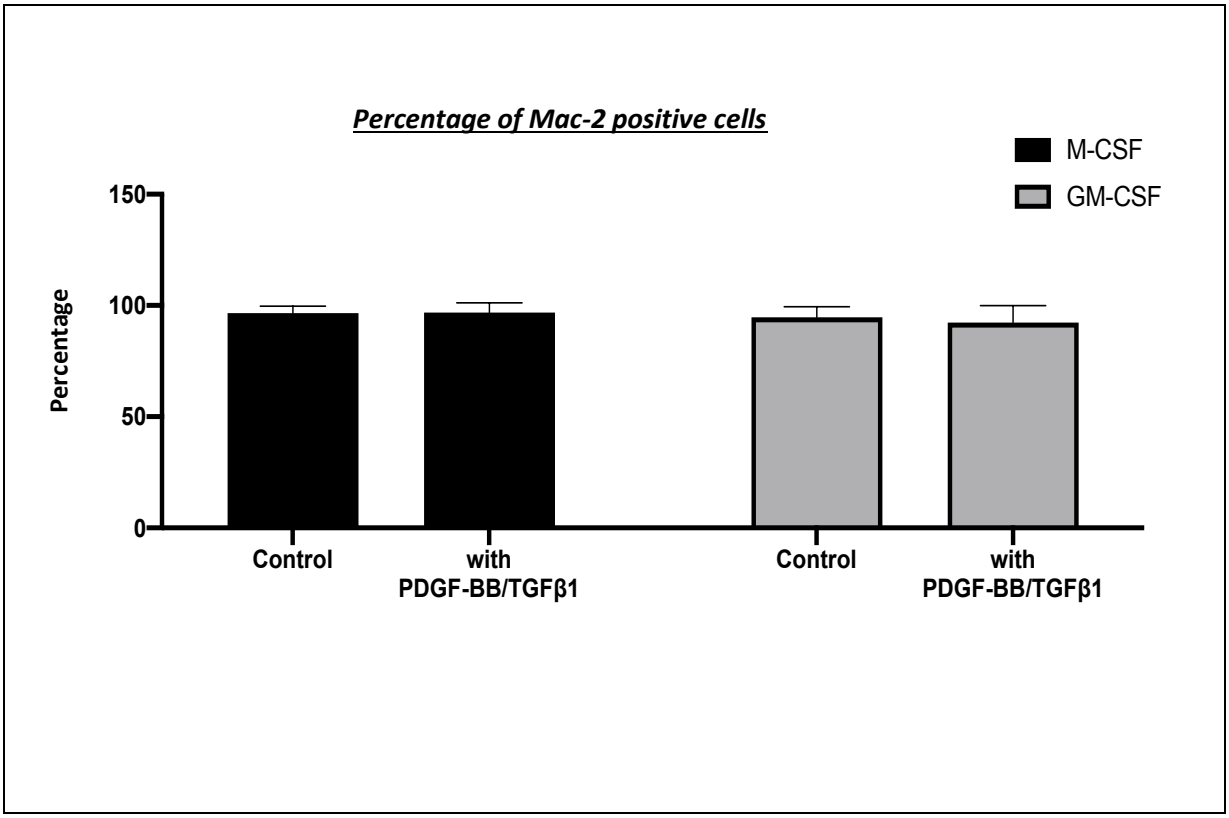

Figure 3.4.43 Effect of M-CSF or GM-CSF macrophage maturation and subsequent co-incubation with PDGF-BB and TGFβ1 on Mac-2 expression.

Quantification of in vitro human monocyte-derived macrophages matured with either M-CSF or GM-CSF for seven days, followed with or without co-stimulation with PDGF-BB and TGFβ1 for three days, and then subjected to immunocytochemistry for Mac-2 (green) and counterstained with DAPI (blue; nuclei). Data are expressed as fold change in percentage of Mac-2 positive cells against control M-CSF matured macrophages (Mean ±SEM; n=6).

3.5 Discussion

Macrophages have been described as terminally differentiated mononuclear phagocytes which exist as heterogeneous populations (Takahashi *et al.,* 1989). Terminally differentiated macrophages are considered to principally participate in immune regulation responses and can display characteristics of end stage killer cells through their ability to produce NO. Macrophages can then die from autocrine NO production and further propagate inflammatory responses through the need for their replacement by newly recruited cells, mainly derived from bone marrow (Italiani and Boraschi, 2014). However, the understanding on the heterogenous concept of macrophages has recently changed. It is now well accepted that macrophages can exhibit plasticity depending on the stimulus they encounter, enabling them to adapt to changing microenvironments through exposure to pro-inflammatory or anti-inflammatory cytokines and growth factors (Stout and Suttles, 2004). Macrophages can be converted into a state whereby they resume cell division (during early development i.e., embryogenesis and haematopoiesis) and also revert back to a non-proliferative form (Ruhnke *et al.,* 2005a). Therefore, macrophages can potentially serve as a source for the generation of non-haematopoietic cells by modulating their behaviour through creating a specific microenvironment which they are capable of reacting to.

Cell-type transformation, macrophage conversion to a VSMC-like cell for instance, will involve changes in the organisation of the cell microstructure, such as the organisation of the cytoskeleton, morphology, motility, adhesion-dependent cell growth, contact inhibition and change in cellular adhesiveness. These processes may involve disruption of actin filaments and changes in focal adhesions, following cell transformation induced by various stimuli (Pawlak and Helfman, 2001).

Within this chapter, two distinct *in vitro* macrophage phenotypes have been assessed, which show different cellular morphology under the influence of M-CSF or GM-CSF signalling cues (described in detail in section 3.4.1), which is in agreement with previous reports (Waldo *et al.,* 2008). Similarly, during polarisation towards classically or alternatively activated phenotypes, *in vitro* macrophages

were observed to undergo cytoskeletal adaptation, with the changes described in detail above (under the section 3.4.1), which are in line with published findings demonstrating specific cytoskeletal organisational changes such as changes in cell shape and size (McWhorter *et al.,* 2013). Indeed, macrophage polarisation to an alternatively activated phenotype (M2) is associated with cell elongation, whereas classically activated macrophages (M1) display reduced cell length (McWhorter *et al.,* 2013). Generally, the shape of alternatively activated macrophages (either with IL-4, IL-10, PF4 or oxPAPC) have been described to acquire a mixture of rounded and stretched cell morphology (Young *et al.,* 1990) similar to conventional inactivated macrophages (control M-CSF polarised macrophages, sometimes referred to as M0 macrophages) (Gleissner *et al.,* 2010). In addition, PF4-polarised macrophages are associated with marked pseudopodia formation (Scheuerer *et al.,* 2000). Interestingly, PDGF-BB and TGFβ1 co-stimulation did not alter cellular morphology of *in vitro* macrophages, through phase contrast observation.

Reportedly, *in vitro* cultured VSMCs assume a synthetic phenotype (Wanjare *et al.,* 2013) with a more epithelioid morphology as opposed to the spindle/elongated shape attributed to the contractile phenotype (Hao *et al.,* 2003). Early passage *in vitro* primary VSMCs are characterised by their high density of myofilaments and expression of contractile genes/proteins such as α-SM-actin alongside low proliferative capacity. However, after several days in tissue culture conditions they attain a synthetic phenotype with a high proliferative capacity and reduced expression of α-SM-actin, which is a typical VSMC phenotype commonly found during vascular development and regeneration (Metz *et al.,* 2012). It has been postulated that during culture, VSMCs may enter a senescence stage and lose their proliferative capacity, especially arterial derived VSMCs. Indeed, this was observed during this study, with late passage VSMC cultures displaying reduced confluency when compared to early passage cultures. In addition, late passage primary VSMCs may transform into a state where they lose their replicative capability, even though already transformed into a synthetic phenotype, due to a process termed senescence (Metz *et al.,* 2012).

The main findings within this chapter demonstrate that *in vitro* macrophages express genes and proteins commonly associated and used as markers of VSMCs. This is in line with previous findings where (embryonic) Myh11, α-SM-actin and calponin were shown to be expressed by rat peritoneal macrophages *in vitro* (Ninomiya *et al.,* 2006). In our study, however, calponin was not expressed by macrophage cultures, but other genes/proteins commonly associated with VSMCs were expressed by *in vitro* macrophages, including α-SM-actin, caldesmon, calmodulin, Myh11, smoothelin, and vimentin. There is some support for these novel observations from recent single-cell transcriptomic analyses of mouse atherosclerotic aortas, where intraplaque macrophage populations display significant enrichment for vimentin and calmodulin-1 (Cochain *et al.,* 2018), alongside α-SM-actin and transgelin (Kim *et al.,* 2018). Moreover, inflammatory activation of human and mouse macrophages was shown to induce expression of α-SM-actin *in vitro* and was confirmed *in vivo* using a mouse MI-model (Haider *et al.,* 2019). Similarly, exposure of macrophages to foreign bodies and their subsequent engulfment was associated with elevated α-SM-actin expression (Mesure *et al.,* 2010).

The above suggests that inflammatory stimulation appears to drive macrophages towards a smooth muscle cell-like phenotype. Interestingly and in relation to the findings within this chapter, GM-CSF is associated with inducing a pro-inflammatory macrophage phenotype, whereas M-CSF is described as an anti-inflammatory inducer (Di Gregoli *et al.,* 2017; Johnson *et al.,* 2014; Johnson *et al.,* 2008). Indeed, based upon the expression changes in the VSMC-related markers, GM-CSF directed macrophages demonstrated a greater transition towards a VSMC-like phenotype through higher expression of a suite of VSMC-related genes and proteins compared to M-CSF directed macrophages. Thus, under baseline tissue culture conditions, GM-CSF directed macrophages can be considered to already display divergent polarisation towards a VSMC-like phenotype.

Contrastingly, the addition of PDGF-BB and TGFβ1, growth factors which support phenotypic modulation of VSMCs (Guo and Chen, 2012; Heldin and Westermark, 1999), endows M-CSF directed

macrophages with VSMC-like characteristics but downregulates the expression of the same suite of VSMC-associated markers in GM-CSF directed macrophage. The upregulation of VSMC-markers in M-CSF polarised macrophages is possibly due to an anti-inflammatory environment created by addition of PDGF-BB and TGFβ1. As described previously, cytokines and growth factors found within the inflammatory milieu, such as TGFβ1, can promote expression of numerous VSMC-related markers in cultured macrophages, and TGFβ1 can exert ant-inflammatory actions in addition to promoting fibrosis (Ninomiya *et al.,* 2006).

What is additionally interesting is the observation that the changes in marker expression are largely restricted to the protein level, suggesting post-translational regulatory mechanisms independently or through a network, modulate VSMC-related protein levels. MicroRNA regulation of protein expression represents such a mechanism, which while beyond the scope of the present study, warrants further examination. Indeed, previous findings have demonstrated divergent expression profiles of microRNAs between M-CSF and GM-CSF polarised macrophages and subsequent effects on macrophage function and behaviour (Di Gregoli *et al.,* 2014; Di Gregoli *et al.,* 2017). On the other hand, a possible explanation for the downregulation of VSMC-associated markers in GM-CSF macrophages by PDGF-BB and TGFβ1 could be through a negative feedback regulatory mechanism, where gene and protein expression in immune cells such as monocytes and macrophages are tightly controlled at both transcriptional and post-transcriptional levels (Schott *et al.,* 2014). Indeed, recent work from my supervisor's lab demonstrated that the pro-inflammatory behaviour of GM-CSF-polarised macrophages is negatively regulated by TGFβ signalling (Di Gregoli *et al.,* 2020). This area in relation to VSMC-like-transformation would be interesting to explore in future studies.

Similarly, variations in the expression of VSMC-connected markers were observed between the other macrophage subsets assessed. Relative to M-CSF-polarised macrophages co-stimulated with PDGF-BB and TGFβ1, pro-inflammatory macrophages induced with IFNγ and LPS (M1 subset) appear to shift away from a VSMC-like phenotype, while IL-4 (M2a), IL-10 (M2c), or PF4 (M4) polarised

macrophages (which can be considered anti-inflammatory) showed minimal changes in VSMC marker expression.

Previous studies have implied that macrophage lipid accumulation may be associated with a pro-fibrotic response (Thomas *et al.,* 2015a), similar to that observed when synthetic VSMCs predominate during wound healing and vascular injury (Thomas *et al.,* 2015b). In line with this proposition, oxLDL-induced macrophage foam cell formation was the only macrophage phenotype that showed consistent upregulation of VSMC-related markers at the protein level (refer to 3.4.4), suggesting lipid accumulation within macrophages induces their transformation towards a VSMC-like phenotype which can participate in pro-fibrotic responses. Foam cell macrophages are considered the hallmark of atherosclerotic plaque development, alongside VSMC-driven formation of the protective fibrous cap (George and Lyon, 2010). As described above, foam cells are commonly thought to originate from lipid accumulation within monocyte-derived macrophages (Johnson and Newby, 2009). However, recent findings have challenged this dogma and propose that VSMCs may significantly contribute to intraplaque foam cell numbers (Huff and Pickering, 2015; Rong *et al.,* 2003). However, the data within this chapter demonstrating foam cell macrophages express VSMC-associated proteins (which are commonly used to identify VSMCs within plaque tissues), implies that VSMC-derived foam cells within plaques may actually be of macrophage origin. Although beyond the scope of this thesis, this interesting proposition requires further investigation and may provide a new understanding of the mechanisms underlying early atherosclerotic plaque formation, such as the transition from adaptive to pathological intimal thickenings.

There is suggestive evidence to support the plasticity and transformation capacity of monocyte/macrophages, especially towards a VSMC-like phenotype. CD34 is considered a marker for hematopoietic stem/progenitor cells but has also recently been shown to be expressed by monocytes (D'Aveni *et al.,* 2015), inferring that isolation of circulating stem/progenitor cells based upon CD34 expression may inadvertently also include monocytes. Analysis of a human peripheral

blood $CD34^+$-enriched cell population transplanted into the left ventricle of mice with surgically-induced MI suggested CD34+ cells *trans*-differentiated towards cardiomyocytes, endothelial cells and VSMCs (Yeh *et al.,* 2003). However, this finding (Yeh *et al.,* 2003) emphasised the necessity of contact between CD34+ cells and resident cells through cell fusion or cell-to-cell contact to permit tissue regeneration post-injury (MI). In another report, *in vitro trans*-differentiation of macrophages towards a VSMC-like phenotype was proposed due to the observed increased expression of the VSMC-associated markers α-SM-actin, calponin and Myh11 after stimulation of rat peritoneal exudate macrophages with TGFβ1 (Ninomiya *et al.,* 2006). Interestingly, a concomitant decreased expression of the commonly used macrophage marker CD11b was reported, potentially underlying the aforementioned mis-identification of intraplaque foam cells as of VSMC-origin.

A further indication that macrophages acquire the ability to shift their phenotype towards other cell-like types is hinted through their ability to regain proliferative capacity when matured from monocytes with M-CSF and interleukin-3 (IL-3) (Ruhnke *et al.,* 2005b), as resumption of proliferation is a characteristic of pluripotent progenitor cells (Busch *et al.,* 2015; Grinenko *et al.,* 2018). Indeed, Ruhnke and colleagues demonstrated that M-CSF and IL-3 matured monocyte-derived macrophages exposed to specific biochemical cues, could be programmed into another cell lineages, including hepatocyte-like cells (with FGF4) and pancreatic islet-like cells (with insulin and C-peptide), which was associated with down-regulation of transcriptional repressor genes regulating cell-cycle and DNA synthesis (Ruhnke *et al.,* 2005b). Interestingly, cell cycle regulators such as cyclin dependant kinases (CDK) and their inhibitors has been implicated not only in immune cell expansion (Laphanuwat and Jirawatnotai, 2019), but also activation of innate immune responses through type I interferon production (Cingöz and Goff, 2018).

Collectively, these studies alongside the findings within this chapter imply that the polarisation of specific macrophage subsets modulates their ability to convert towards a programmable cell, capable of transforming into other cell-types/lineages when stimulated with the appropriate factor.

However, the reversion of macrophages to a programmable phenotype is probably transient and not fully towards a haematopoietic pluripotent stem cell type, as some monocyte/macrophage markers are retained (Ruhnke *et al.,* 2005b), whereas established haemopoietic stem cell markers are poorly expressed, suggesting such programmable macrophage subsets are similar in nature to common monocytic/granulocytic progenitor cells (Friedman, 2002). Such reprogramming of a cell lineage without inducing full reversion to haematopoietic stem cells is known as *trans*-differentiation (Graf and Enver, 2009). Lineage conversion/switching of terminally differentiated cells or mature somatic cells, such as macrophages, through *trans*-differentiation involves forcing the cell to change lineage without reversion to a primitive multi- or pluri-potent state (induced pluripotency), followed by re-differentiation into another tissue lineage (Graf and Enver, 2009). Cell fusion is another mechanism of cell programming which permits a committed cell lineage to change without the necessity to revert back to pluripotency (Verfaillie, 2002). It is plausible to reason that monocyte/macrophages harbour the ability to *trans*-differentiate to other cell types to aid recovery after injury, and therefore provide temporary protection, before replacement by resident cells. Indeed, marked recruitment of monocyte/macrophages is observed acutely after injury and persists during the healing process, potentially providing a reservoir of cells capable of masquerading as resident cells to bestow protection before healing is concluded. An example could be at sites of vascular injury, where recruited monocyte/macrophages *trans*-differentiate towards an endothelial cell-like phenotype to provide temporary barrier function before re-growth of resident endothelial cells. Indeed, blood outgrowth endothelial cells (which are a derivative of endothelial progenitor cells (Yoder *et al.,* 2007)) are proposed to play a similar role (Dauwe *et al.,* 2016), and interestingly are derived from PBMCs using the same protocol as for monocyte isolation, raising the possibility that blood outgrowth endothelial cells may indeed be monocytes. Although conjecture, these possibilities would be worthwhile of future investigation with ramifications for regenerative medicine therapies.

3.6 Conclusion

The findings within this chapter demonstrate that *in vitro* human monocyte-derived macrophages express genes and proteins which are commonly associated with VSMCs, supporting the proposition that primary macrophages harbour the potential to *trans*-differentiate towards a VSMC-like phenotype. Additionally, macrophage polarisation towards pro-inflammatory, anti-inflammatory, and lipid-laden phenotypes differentially modulates expression of VSMC-associated markers, with GM-CSF-directed maturation and foam cell formation favouring *trans*-differentiation towards a VSMC-like phenotype. Nevertheless, *in vitro* macrophages maintain their original cellular lineage as evidenced by maintained expression of macrophage markers, suggesting *trans*-differentiation is a temporary response. As such, macrophages can be considered a distinct population of haematopoietic cells that are capable of interim *trans*-differentiation towards another cell lineage during a response to injury, while maintaining their macrophage lineage.

4 *In vitro* macrophages display divergent polarisation towards endothelial cell-like phenotypes by pro-angiogenic growth factor

4.1 Introduction

4.1.1 Endothelial cell phenotypes

The vascular endothelium is comprised of a confluent monolayer of endothelial cells and serves as a protective anatomical barrier between circulating blood and underlying tissues. Microscopically, endothelial cells are characterised by a flattened shape with a single central nucleus. Besides its role as a protective barrier, the endothelium is also regarded as a metabolically dynamic organ that maintains vascular homeostasis through the release of regulatory bioactive substances, for instance nitric oxide (NO), endothelin and thrombomodulin. These bioactive substances are released by endothelial cells in response to various stimuli, such as through physical forces (or shear stress) applied by blood flow, blood-viscosity, as well as cell-cell interactions (Deanfield *et al.,* 2007; Gori *et al.,* 2007). Bioactive substances released by endothelial cells may act on the endothelial cells themselves (autocrine) and also to surrounding vascular cells (paracrine) such as VSMCs, connective tissue cells within the vessel wall (i.e. fibroblasts), and circulating cells within the lumen (i.e. platelets and monocytes) (Gori *et al.,* 2007). Briefly, the general function of endothelial derived bioactive substances is to ensure uninterrupted blood flows over the endothelial-luminal surface by creating a non-sticky surface to circulating blood (hence preventing the formation of blood clot), as well as controlling the tone of the vessel wall for non-resistance and effective blood flow.

Endothelial cells display heterogeneity based upon their function and location, for example, tight junctions are numerous in arterial-endothelial cells compared to venous-endothelial cells (Simionescu *et al.,* 1976). Moreover, the long and narrow features of endothelial cells within arteries accommodate its high pressure and pulsatile characteristics whereas venous endothelial cells are wider and shorter owing to low luminal pressure. In view of health and disease, endothelial cells are

further classified into quiescent or activated phenotypes. Generally, in healthy vessels, endothelial cells are in a state of quiescence to serve their physiological role as a protective barrier regulating molecular transport across the endothelial layer (Zecchin *et al.,* 2017). Quiescent endothelial cells are non-adhesive, and display anti-coagulant and vasodilatory properties to accommodate smooth blood flow over the luminal surface of the vessels, while at the same time in a state capable of responding to changing environmental cues (homeostasis) (Aird, 2008). On the other hand, activated endothelial cells (sometimes termed pro-inflammatory) are at the other end of the spectrum and characterised by acquiring adhesive (to circulating leukocytes and platelet), pro-coagulant, and enhanced permeability properties, while also promoting vasoconstriction (Aird, 2008). As inferred above, the generation of an activated endothelial cell phenotype can involve adaptive responses to physiological changes (to maintain homeostasis), or through non-adaptive responses due to exaggerated stimuli (pathological changes). On a different note, endothelial dysfunction during atherogenesis is regarded as a maladaptive response of activated endothelial cells, and is described as an abnormally hyper-adhesive endothelial cell phenotype due to increased expression of adhesion molecules (such as E-selectin and VCAM-1) which enhance monocyte adherence to the vascular wall, and is therefore classified as in a pro-inflammatory state (Aird, 2008).

Intriguingly, endothelial cells respond to the pattern of blood flow upon its surface. For example, in a straight part of an artery where blood flows is in a steady laminar state, the endothelial cells align in an elongated morphology in line with the direction of flow, whereas endothelial cells in areas of arterial branching and curvatures, where the blood flow becomes multi-directional and disturbed, the shape of endothelial cells is rounded (Nigro *et al.,* 2011). *In vitro* experiments showed that static confluent endothelial cells also exhibit a rounded or polygonal morphology compared to exposure to laminar flow. As described above (in section 1.1), the straight segment of an artery is associated with steady high laminar flow and is associated with the vessels being protected from atherosclerosis,

whereas in the arterial branches where the flow is disturbed, endothelial cell dysfunction is prevalent and related to the development of atherosclerosis.

4.1.2 Modulators of endothelial cell behaviour and function

Vascular endothelial growth factor A (VEGF-A) and fibroblast growth factor 2 (FGF2) are among the widely described growth factors that support the differentiation of endothelial cells and play a significant role in angiogenesis (Cross and Claesson-Welsh, 2001). Reportedly, human adipose-derived stem cells exhibit endothelial cell-like characteristics when cultured with VEGF-A and FGF2, determined through their expression of several key markers deemed to identify endothelial cells such as Platelet Endothelial Cell Adhesion Molecule-1 (PECAM-1), vWF, VE-cadherin and eNOS (Khan *et al.,* 2017). In a similar study, recombinant VEGF-A addition to swine bone marrow-derived mesenchymal stem cells induced their expression of multiple endothelial cell markers, particularly PECAM-1, VE-cadherin and vWF (Ikhapoh *et al.,* 2015). Additionally, the population of positive cells (for endothelial cell markers) significantly increased upon co-stimulation with angiotensin II and the cells organised into vessel networks when assessed within an *in vitro* angiogenesis assay (Ikhapoh *et al.,* 2015). In another study, VEGF-A promoted proliferation and differentiation of human amniotic fluid derived-mesenchymal stem cells into endothelial cells (Tancharoen *et al.,* 2017). In addition, human bone marrow-derived mesenchymal stem cells differentiated into cells positive for vWF with tube like formation within a Matrigel angiogenesis assay when stimulated with VEGF-A (Oswald *et al.,* 2004).

Other key regulators of endothelial cell growth include hepatocyte growth factor (HGF), insulin-like growth factors (IGF), and angiopoietin-like 5 (ANGPTL5). A study using human aorta derived-mesenchymal stem cells showed upregulation in the expression of endothelial cell markers such as vWF, CD31, and KDR (or also known as VEGFR2) by flow cytometry analysis and the cells organised into tube-like structures when stimulated with hepatocyte growth factor (HGF) (Valente *et al.,* 2016). Reportedly, ANGPTL5 is associated with the expansion of cultured human cord blood $CD34^+$ and

$CD133^+$ cells (Zhang *et al.,* 2008). On a different note, IGF-1 is associated with the migration of endothelial cells, enhances tube formation, and promotes their survival through preventing apoptosis (Bach, 2015). In addition, with regards to angiogenesis, IGF-1 may prevent vessel regression from newly developed vessels (Jacobo and Kazlauskas, 2015).

4.1.3 Gene and protein expression markers commonly associated with an endothelial cell

The cell membrane of endothelial cells display a unique molecular organisation called junctional complexes which play a vital role in maintaining the integrity of vessels. These structures upon the endothelial cell membrane form bridging connections with partners on neighbouring endothelial cells within the inter-endothelial cleft. These connections are anchored to the endothelial cell cytoskeleton and therefore forms a solid binding mechanism between adjacent endothelial cells, and are commonly described as adhesion molecules. In addition to its important role in maintaining the integrity of the endothelium, these adhesion molecules can also be a useful tool to identify endothelial cells in a laboratory setting. Among the commonly use adhesion molecules as endothelial cell specific markers include VE-cadherin and PECAM-1, and their expression by disparate macrophage phenotypes are explored within this chapter.

Vascular endothelial cadherin (VE-cadherin) is the main adhesion molecule that modulates endothelial cell permeability (Vestweber, 2008). It is comprised of calcium dependent adhesion molecules (cadherin) within the extracellular domain which serves to mediate adhesion with a complimentary motif upon neighbouring endothelial cells. VE-cadherin is a central molecule that regulates barrier function and endothelial permeability, in part through binding to VEGFR2 to block VEGF-VEGFR2 complex endocytosis and inhibiting subsequent VEGF signalling (Takahashi *et al.,* 2001). Activation of the VEGFR2 signalling pathway is associated with angiogenesis (Bates, 2010), whereby VE-cadherin molecules disengage to permit cell proliferation and migration to take place (Lamalice *et al.,* 2007). During angiogenesis, VE-cadherin is responsible for mediating cell-cell binding

to form tube structures succeeding cell proliferation and migration (Wallez *et al.,* 2006). PECAM-1 (also known as cluster of differentiation 31; CD31) mediates endothelial cell interaction with circulating immune cells such as platelets and leukocytes (Dejana, 2004), but reportedly, may also mediate endothelial cell-cell junctions to maintain vascular integrity (Lertkiatmongkol *et al.,* 2016).

4.2 Aim of this chapter

The aim of this chapter was to evaluate the expression of genes and proteins commonly associated with endothelial cells, in distinct human *in vitro* macrophage subsets, namely M-CSF directed, and GM-CSF directed macrophages in day-7, -11 and -14 polarisation *in vitro*.

Subsequently, the dose dependent effects of VEGF-A, FGF2, IGF-1, HGF, and ANGPTL5 on endothelial cell-associated mRNA expression was determined in 7-day *in vitro* human macrophages. Next, EC-related mRNA and protein expression were analysed following 4-day stimulation with EC-related growth factors. Lastly, a comparison of the expression patterns between primary macrophages and primary endothelial cells *in vitro* was conducted.

4.3 Materials and Methods

4.3.1 Macrophage culture

Human monocyte-derived macrophages were isolated and generated as outlined in the methods sections 2.1 and 2.2. M-CSF and GM-CSF directed macrophages were maintained in culture for 7-, 11- and 14-days according to the experimental protocol described in the methods section 2.3. In addition, magnetic-bead cell sorting and purification for pan monocytes were also performed to obtain pure CD14+ and CD16+ monocyte populations according to the later-mentioned protocol.

Materials: 0.5% bovine serum albumin (BSA) in PBS, Pan Monocyte Isolation Kit (MACS Miltenyi Biotec; cat number : 130-096-537) [contains FcR Blocking Reagent (human Ig), Pan Monocyte Biotin-Antibody Cocktail (biotin-conjugated monoclonal antibodies against antigens that are not expressed

on human monocytes), Anti-Biotin MicroBeads (MicroBeads conjugated to monoclonal anti-biotin antibodies)], autoMACS rinsing solution and MS Columns and MACS magnetic separators.

Magnetic-bead cell sorting was performed according to the manufacturers protocol. The procedure was performed using pre-chilled solutions while keeping the cells cool throughout the procedure. Cell number was determined prior to cell sorting for a working total number of 1 x 10^7 total cells. After a final HBSS wash (as in section 2.1.2), the cell pellet was resuspended in 40 μl of buffer before the addition of 10 μl of FcR blocking reagent and 10 μl of biotin-antibody cocktail. The preparation was mixed well and incubated for 5 minutes at 2-8^{o}C. Next, 30 μl buffer was added followed by 20 μl of anti-biotin microbeads. After mixing well, the preparation was incubated for 10 minutes at 2-8^{o}C.

Magnetic separation was performed after the final incubation using MS columns inserted within the magnetic field of a MACS separator. The columns were activated by rinsing with 500 μl buffer before the cell suspensions were added to the columns. The flow-through (which contains pan-monocytes) were collected and the column washed with buffer for three times. This isolation technique yields enrichment of pure monocytes which consist of classical ($CD14^{++}CD16^{-}$), non-classical ($CD14^{+}CD16^{++}$) and intermediate ($CD14^{++}CD16^{+}$) monocyte populations.

4.3.2 Stimulation of human macrophages with endothelial cell-associated growth factors

Following seven days differentiation and maturation in culture, M-CSF polarised and GM-CSF directed macrophages were stimulated for 24 hours with either VEGF-A, FGF2, IGF-1, HGF or ANGPTL5 to assess their capacity to differentiate towards an endothelial cell (EC)-like phenotype. In the first instance, concentrations of 1 ng/ml, 10 ng/ml and 100 ng/ml were assessed for dose-dependent effects (Table 4.3.1) to determine the optimal dose for the subsequent experiments

Stimulation with growth factors was undertaken for four days, with the media and growth factors changed one day before cell collection.

Table 4.3.1 Endothelial cell-associated growth factors used for macrophage stimulation
(VEGF-A = vascular endothelial growth factor A, FGF2 = fibroblast growth factor 2, IGF-1 = Insulin-like growth factor 1, HGF = Hepatocyte growth factor and ANPTL5 = Angiopoietin-like 5; Hm = human)

Factors	Stock concentration	Working concentration (ng/ml)	Brand/Company	Catalogue No.
Hm VEGFA (165) IS	100 µg/ml	1, 10 and 100	MACS/Miltenyi Biotec	130-109-383
Hm FGF2	100 µg/ml	1, 10 and 100	R&D System/Bio-techne	130-093-838
Hm IGF-1	50 µg/ml	1, 10 and 100	MACS/Miltenyi Biotec	130-093-885
Hm HGF	10 µg/ml	1, 10 and 100	Gibco®/Life Technologies	PHG0254
Hm ANGPTL5	5 µg/ml	1, 10 and 100	MACS/Miltenyi Biotec	130-086-125

4.3.3 Culture of human umbilical vein endothelial cells

Human umbilical vein endothelial cells (HUVECs) were used as a positive control for this study. HUVECs were maintained under culture conditions within Dulbecco's modified Eagle's Medium (DMEM) (Sigma-Aldrich; PAA, E15-005) supplemented with endothelial cell growth media (Promo cell; C-22010), Penicillin/Streptomycin (100 U/ml Penicillin; 100 µg/ml streptomycin) (Invitrogen), 10% Fetal Bovine/ Calf Serum (Gibco), 200 mM L-Glutamine and 10 mg/ml Gentamicin (PAA). All supplements were added using a syringe filter to prevent infection, mixed well, and stored at 4°C. HUVECs were cultured for three days (with a media and growth factor change after day two) prior to collection for mRNA and QPCR analysis, or protein isolation and western blotting analysis.

4.4 Results

4.4.1 GM-CSF-directed macrophage maturation is associated with increased expression of EC-associated markers in comparison to M-CSF matured macrophages

The mRNA and protein expression of the endothelial cell (EC) related markers PECAM-1 and VE-cadherin were analysed in M-CSF and GM-CSF directed macrophages after 7-day, 11-day, and 14-day polarisation.

M-CSF directed macrophage polarisation was associated with a significant upregulation in PECAM1 mRNA levels at day 14 (3.6-fold change; $P<0.05$; n=6; Figure 4.4.1 a) compared to day-7 and -11, with no difference observed between day-7 and day-11 M-CSF polarised macrophages. Conversely, GM-CSF polarised macrophages showed downregulation of PECAM1 mRNA levels at day-11 (23.2%; $P<0.05$; n=6; Figure 4.4.1 a) compared to their day-7 and day-14 counterparts (Figure 4.4.1 a). Comparisons between the two subsets revealed 7-day GM-CSF polarised macrophages expressed significantly higher PECAM1 mRNA levels relative to 7-day M-CSF directed macrophages (3.5-fold change; $P<0.05$; n=6; Figure 4.4.1 a), however, no changes at day-11 and day-14 between the two macrophage phenotypes were detected (Figure 4.4.1 a).

Western blot analysis demonstrated that GM-CSF directed macrophages displayed markedly higher PECAM-1 protein expression compared to M-CSF polarised macrophages at all three time points; day-7 (3.5-fold change; $P<0.05$; n=6; Figure 4.4.1 b), day-11 (5.6-fold change; $P<0.05$; n=6; Figure 4.4.1 b), and day-14 (4.0 fold change; $P<0.05$; n=6; Figure 4.4.1 b). However, PECAM-1 protein expression remained constant across all time points within each macrophage phenotype (Figure 4.4.1 b).

Immunocytochemistry on 7-day differentiated macrophages showed a higher percentage of GM-CSF macrophages were positive for PECAM-1 expression (43.1% PECAM-1 positive) compared to M-CSF macrophages (31.4% PECAM-1 positives; $P<0.05$; n=6; Figure 4.4.2).

The results are summarised in Figure 4.4.23 at the end of this section.

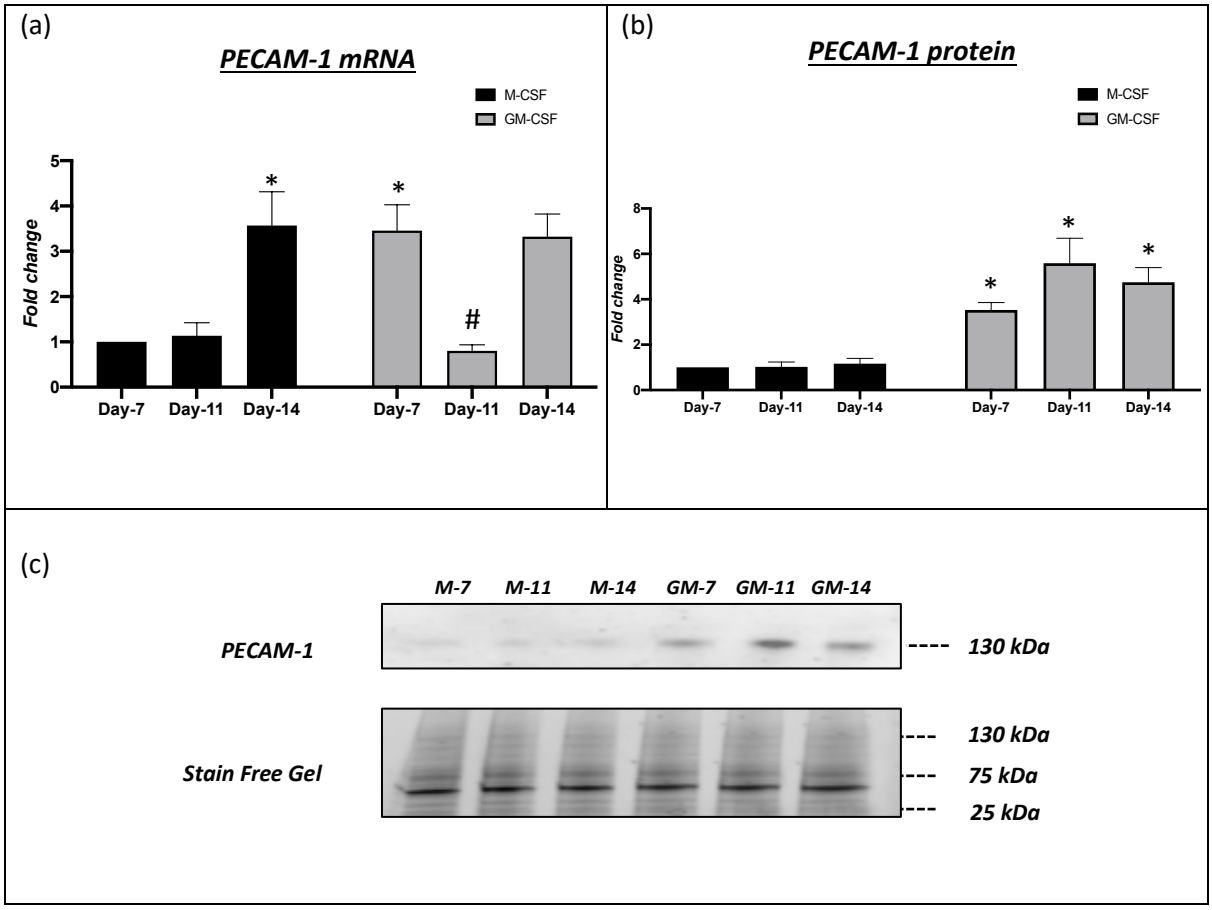

Figure 4.4.1 PECAM-1 mRNA and protein expression in macrophage baseline cultures.

*(a) PECAM1 mRNA levels in M-CSF and GM-CSF macrophages expressed as fold change relative to 7-day M-CSF directed control macrophages, (mean±SEM; n=6; * P < 0.05 denotes significant difference compared to day-7 and -11 M-CSF directed macrophages; # P < 0.05 denotes significant difference compared to day-7 and -14 GM-CSF directed macrophages; one-way ANOVA Tukey's multiple comparison test).*

*(b) Quantification and (c) representative western blots for PECAM-1 protein expression relative to the fold change of 7-day M-CSF directed control macrophages, (mean±SEM; n=6; * P < 0.05 denotes significant difference compared to day-7, -11, and -14 M-CSF directed macrophages; one-way ANOVA Tukey's multiple comparison test). Stain free gel is shown as a loading control. (M-7, M-11, and M-14 = M-CSF directed macrophages at day-7, -11, and -14 respectively; GM-7, GM-11, and GM-14 = GM-CSF directed macrophages at day-7, -11, and -14 respectively).*

Refer to appendix B; (9.1.1) for CT values and (9.1.2) for full blot image.

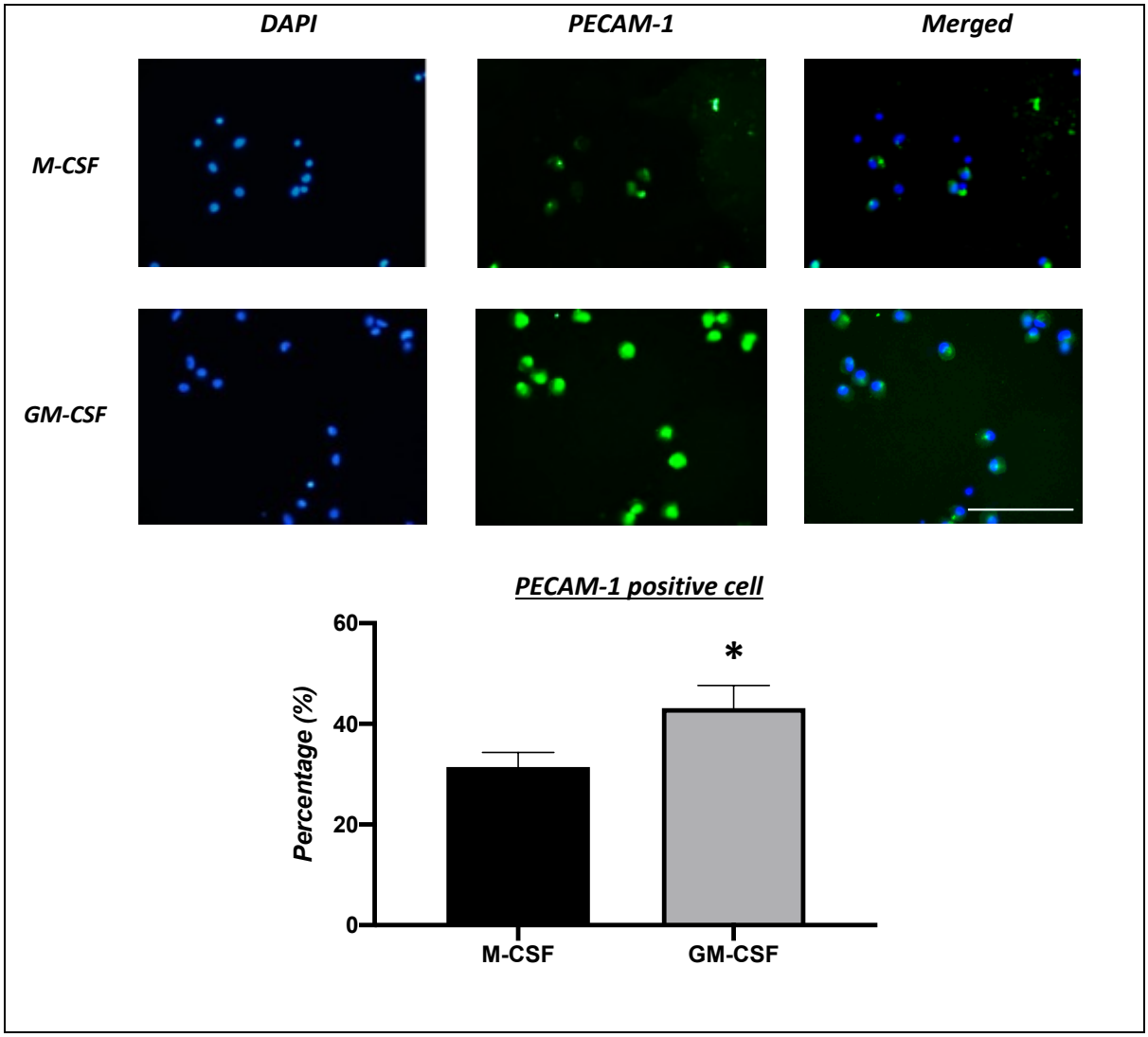

Figure 4.4.2 GM-CSF maturation increases human macrophage PECAM-1 protein expression compared to M-CSF matured macrophages.

*Representative images and quantification of immunofluorescent labelling for PECAM-1 expression in seven-day M-CSF or GM-CSF differentiated human macrophages. Green colour indicates PECAM-1 immunopositivity, and blue indicates nuclei (DAPI counterstain). Scale bar represents 100 μM and is applicable to all panels. Data are expressed as percentage of PECAM-1 immuno-positive cells (mean±SEM; n=6; *P < 0.05 denotes significant difference compared to M-CSF macrophages; paired t-test).*

VE-cadherin (CDH5) mRNA expression was significantly upregulated in M-CSF macrophage with increasing time in culture, with elevated expression at day-11 (21.0-fold change; P<0.01; n=6 Figure 4.4.3 a) and day-14 (35.4-fold change; P<0.01; n=6 Figure 4.4.3 a), when compared to 7-day-M-CSF matured macrophages. As such, CDH5 mRNA levels in 14-day M-CSF matured macrophages were significantly increased compared to their day-11 counterparts (1.7-fold-change; P<0.05; n=6 Figure 4.4.3 a).

In contrast to the pattern observed within the M-CSF macrophage phenotype, GM-CSF matured macrophages exhibited comparable CDH5 mRNA levels at day-7 and day-11, but were significantly upregulated at day-14 (2.0-fold-change; P<0.05; n=6 Figure 4.4.3 a). Mirroring the expression of PECAM-1, 7-day matured GM-CSF macrophages expressed significantly higher CDH5 mRNA levels (15.4-fold change; P<0.01; n=6 Figure 4.4.3 a) than their 7-day M-CSF macrophage comparators. however, similar levels were observed at day-11 and day-14 between the two macrophage phenotypes (Figure 4.4.3 a).

Similar to PECAM-1 protein expression, GM-CSF matured macrophages exhibited higher VE-cadherin protein expression compared to M-CSF macrophages at all time points; day-7 (3.0-fold change; P <0.01; n=6; Figure 4.4.3 b), day-11 (2.3-fold change; P <0.05; n=6; Figure 4.4.3 b), and day-14 (2.3-fold change; P <0.05; n=6; Figure 4.4.3 b). However, no differences in VE-cadherin protein expression were detected across time points within each macrophage phenotype (Figure 4.4.3 b).

Immunocytochemistry on 7-day differentiated macrophages showed a higher percentage of GM-CSF macrophages were positive for VE-cadherin expression (49.2% VE-cadherin positive) compared to M-CSF macrophage (35.7% VE-cadherin positive, P<0.01; n=6; Figure 4.4.4).

The results are summarised in Figure 4.4.23 at the end of this section.

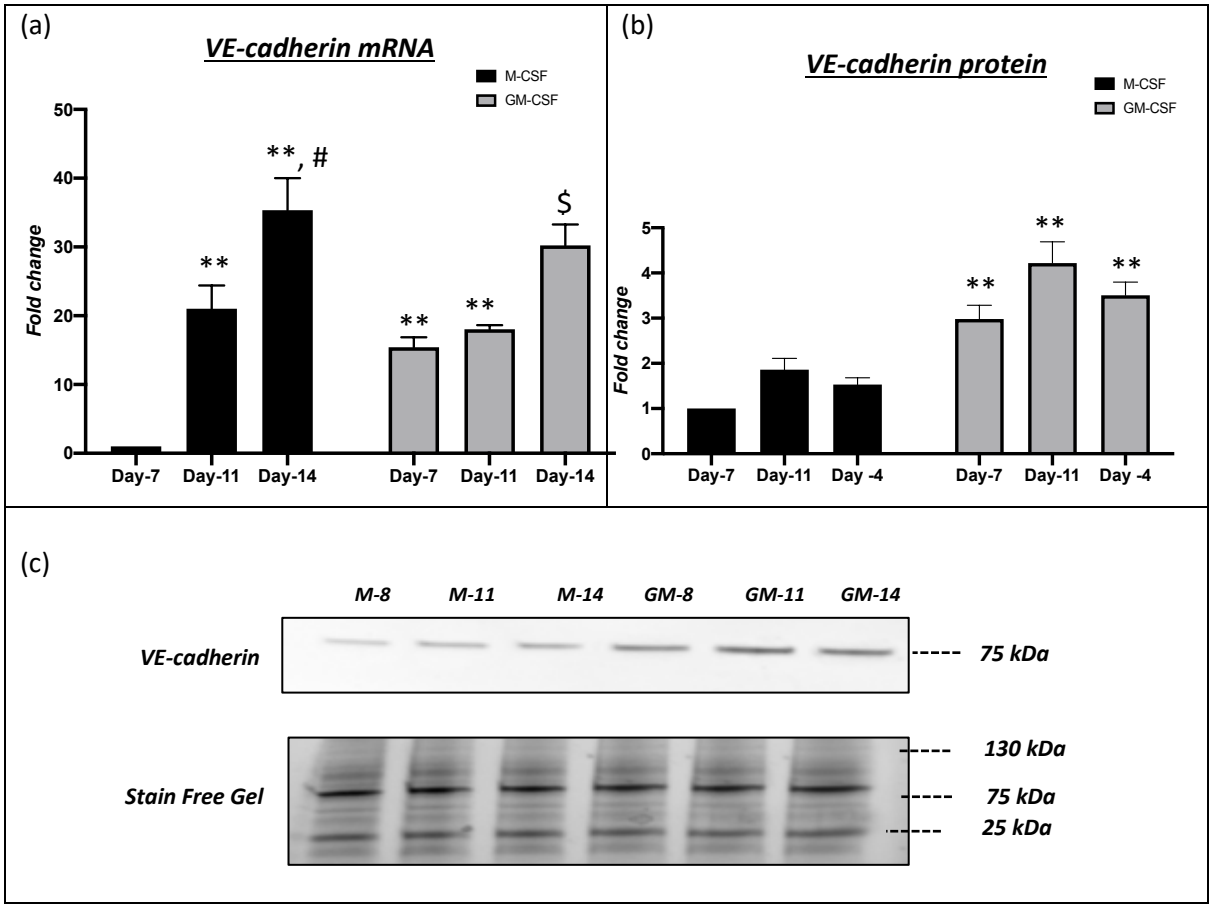

Figure 4.4.3 VE-cadherin mRNA and protein expression in macrophage baseline cultures

*(a) CDH5 mRNA levels in M-CSF and GM-CSF macrophages expressed as fold change relative to 7-day M-CSF directed control macrophages, (mean±SEM; n=6; ** P <0.01 denotes significant difference compared to day-7 M-CSF directed macrophages; # P < 0.05 denotes significant difference compared to day-11 M-CSF directed macrophages; $ P < 0.05 denotes significant difference compared to day-7 and -11 GM-CSF directed macrophages; one-way ANOVA Tukey's multiple comparison test).*

*(b) Quantification and (c) representative western blots for VE-cadherin protein expression relative to the fold change of 7-day M-CSF directed control macrophages, (mean±SEM; n=6; ** P < 0.01 denotes significant difference compared to day-7, -11, and -14 M-CSF directed macrophages; one-way ANOVA Tukey's multiple comparison test). Stain free gel is shown as a loading control. (M-7, M-11, and M-14 = M-CSF directed macrophages at day-7, -11, and -14 respectively; GM-7, GM-11, and GM-14 = GM-CSF directed macrophages at day-7, -11, and -14 respectively).*

Refer to appendix B; (9.1.3) for CT values and (9.1.4) for full blot image.

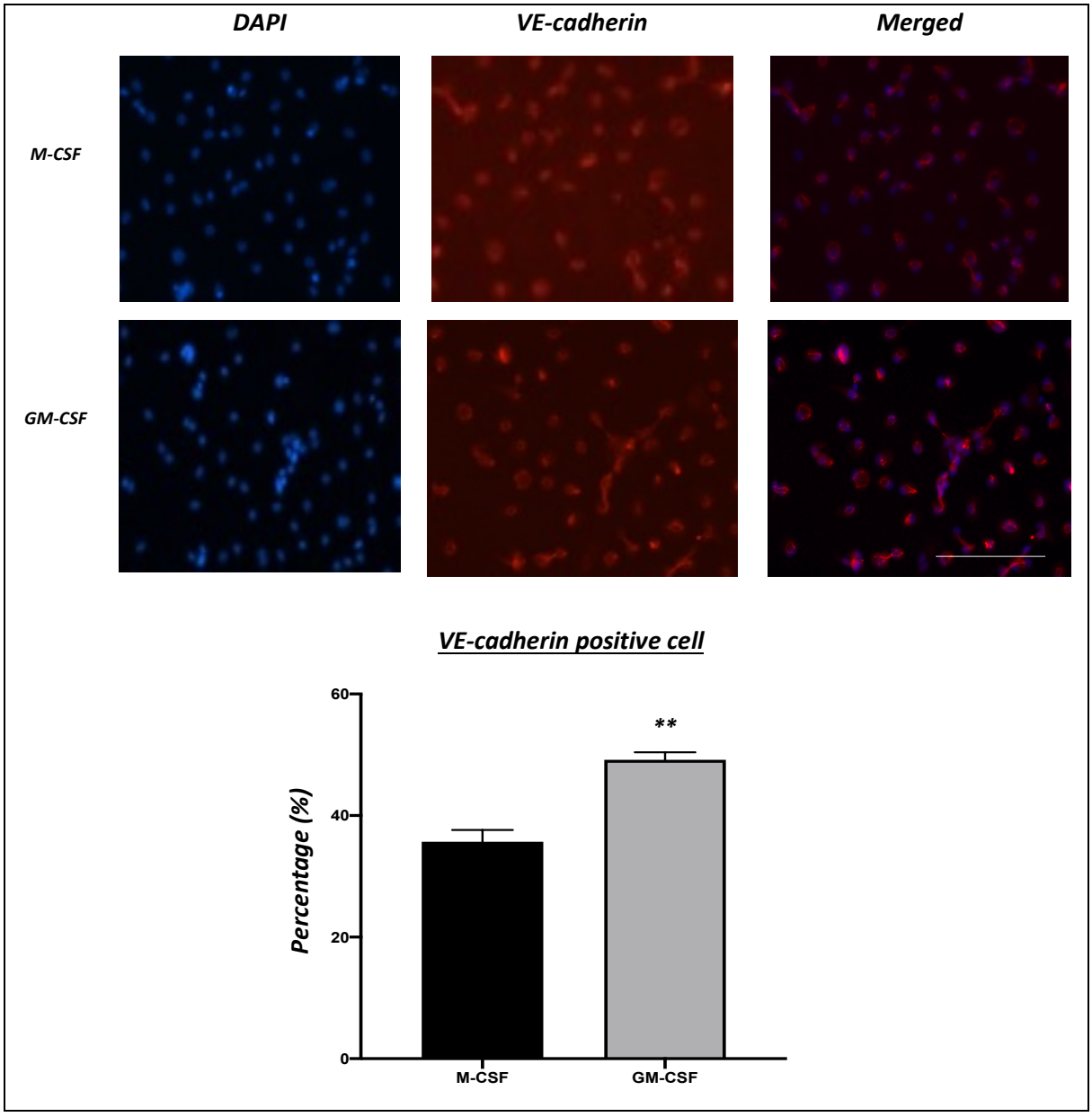

Figure 4.4.4 GM-CSF maturation increases human macrophage VE-cadherin protein expression compared to M-CSF matured macrophages

*Representative images and quantification of immunofluorescent labelling for VE-cadherin expression in seven-day M-CSF or GM-CSF differentiated human macrophages. Red colour indicates VE-cadherin immunopositivity, and blue indicates nuclei (DAPI counterstain). Scale bars represent 200 μM. Data are expressed as percentage of VE-cadherin immuno-positive macrophages (mean±SEM; n=6; **P < 0.01 denotes significant difference compared to M-CSF macrophages; paired t-test).*

4.4.2 The effect of endothelial cell-associated growth factors on macrophage subset expression of endothelial cell-related genes

The mRNA expression of PECAM1 and CDH5 (VE-cadherin) were analysed 24 hours after stimulation with endothelial-cell related growth factors, namely VEGF-A, FGF2, IGF-1, HGF and ANGPTL5 at 1 ng/ml, 10 ng/ml and 100 ng/ml concentrations, in seven-day differentiated M-CSF and GM-CSF macrophage subsets. The aim of this sub-study was to determine the optimal dose of the associated growth factors to be used for subsequent experiments.

Both VEGF-A and FGF2 stimulation increased M-CSF macrophage PECAM1 and CDH5 mRNA expression in a dose-dependent manner (Figure 4.4.5 a, and Figure 4.4.6 a; see a summary of results in Figure 4.4.7). Specifically, 1 ng/ml, 10 ng/ml, and 100ng/ml of VEGF-A upregulated PECAM-1 mRNA levels in M-CSF macrophages (1.9-fold change; $P<0.05$, 2.7-fold change; $P<0.01$ and 3.7-fold change; $P<0.05$, respectively; n=6; Figure 4.4.5 a). Between doses, PECAM-1 mRNA levels were significantly higher in 10 ng/ml (1.5-fold change; $P<0.05$; n=6; Figure 4.4.5 a) and 100 ng/ml (1.9-fold change; $P<0.05$; n=6; Figure 4.4.5 a). VEGF-A treated M-CSF macrophages compared to cells stimulated with 1 ng/ml VEGF-A, with no significant difference between the 10 ng/ml and 100 ng/ml doses of VEGF-A (Figure 4.4.5 a).

Similarly, 1 ng/ml, 10 ng/ml and 100 ng/ml concentrations of FGF2 consistently up-regulated PECAM-1 mRNA expression in M-CSF macrophages (2.2-fold change, $P<0.01$; 2.8-fold change; $P<0.01$ and 3.8-fold change; $P<0.05$, respectively; n=6; Figure 4.4.5 a), although no differences were detected between the different FGF2 concentrations.

With regard to CDH5 (VE-cadherin) mRNA expression, concentrations of 1 ng/ml, 10 ng/ml and 100 ng/ml of VEGF-A comparably upregulated VE-cadherin mRNA expression in M-CSF polarised macrophages (2.6-fold change; $P<0.05$, 2.5-fold change; $P<0.05$ and 2.9-fold change; $P<0.01$, respectively; n=6; Figure 4.4.6 a). Similarly, 1 ng/ml, 10 ng/ml and 100 ng/ml concentrations of FGF2 upregulated CDH5 mRNA levels in M-CSF macrophages (2.4-fold change, $P<0.05$; 3.0-fold change;

P<0.05 and 3.6-fold change; P<0.01, respectively; n=6; Figure 4.4.6 a), although the greatest increase in CDH5 mRNA expression was detected with 100 ng/ml FGF2 (1.5-fold change; P<0.05; n=6; Figure 4.4.6 a) when compared to the 1 ng/ml concentration.

The other growth factors tested, IGF-1, HGF and ANGPTL5, did not statistically affect either PECAM1 or CDH5 mRNA expression in M-CSF macrophage macrophages when compared to unstimulated control cells (Figure 4.4.5 a, and Figure 4.4.6 a).

As opposed to M-CSF polarised macrophages, the mRNA expression of PECAM1 and CDH5 was not affected in GM-CSF directed macrophages by the addition of any of the endothelial cell-related growth factors (Figure 4.4.5 b and Figure 4.4.6 b).

Based upon the above findings alongside evidence from previous studies (Table 4.4.1), the concentration for all growth factors to exert optimal effects *in vitro* was deemed to be as 50 ng/ml, and was therefore used in all subsequent associated experiments.

Table 4.4.1 References for endothelial cell-related growth factors concentrations used *in vitro*

(VEGF-A = vascular endothelial growth factor A, FGF2 = fibroblast growth factor 2, IGF-1 = Insulin-like growth factor 1, HGF = Hepatocyte growth factor and ANPTL5 = Angiopoietin-like 5)

Factors	Concentration (ng/ml)	References
Human VEGF-A (165)	2, 25, 50	(Ikhapoh *et al.,* 2015)
Human FGF2	10	(Khan *et al*. 2017)
HGF	2.5, 5, 10, and 70	(Valente *et al*. 2016)
Human IGF-1	100	(Huat *et al.,* 2014; Supeno *et al.,* 2013)
ANGPTL5	100	(Zhang *et al.,* 2008)

The effects of VEGF-A and FGF2 summarised in Figure 4.4.7.

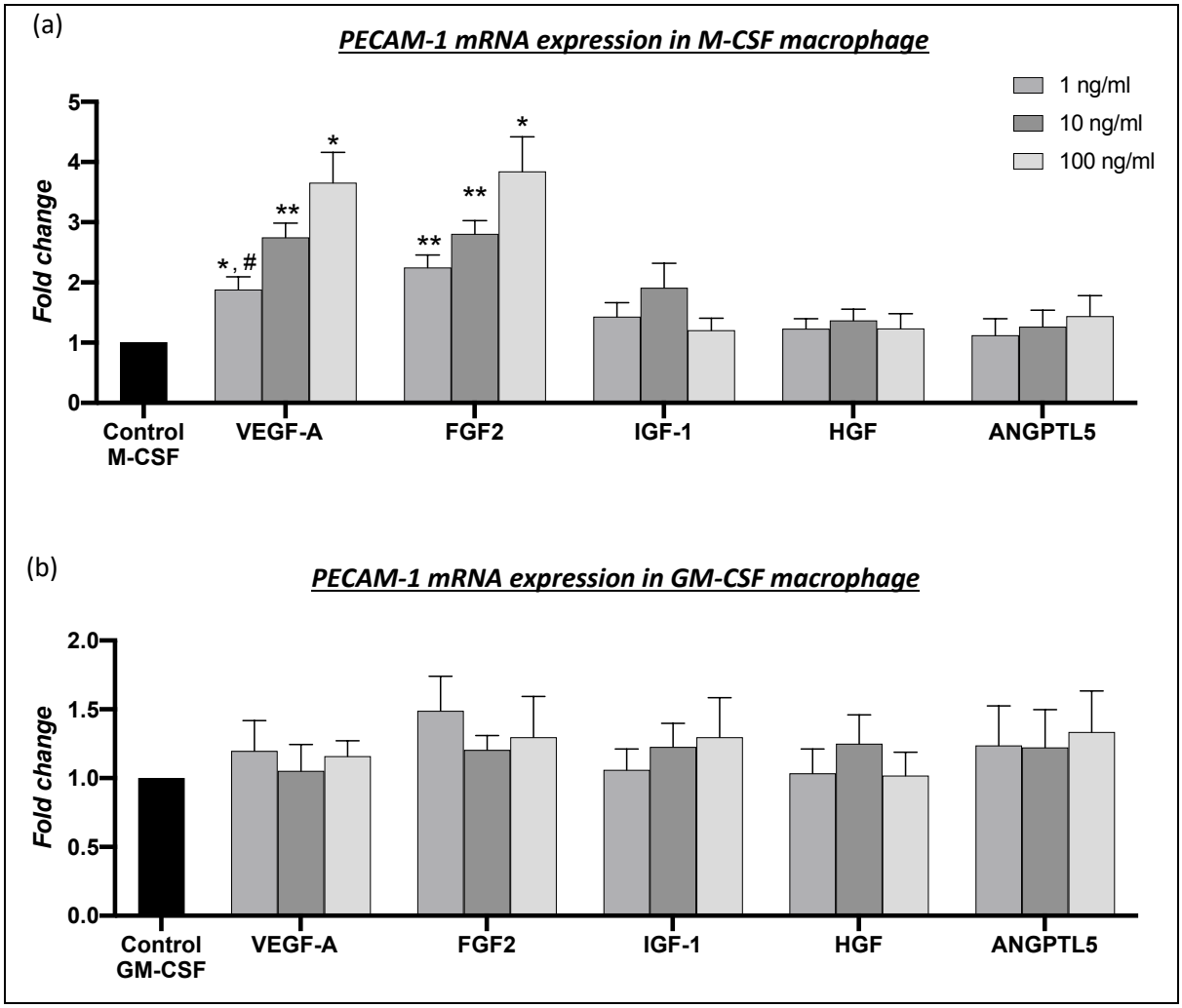

Figure 4.4.5 PECAM-1 mRNA expression in human macrophages stimulated with endothelial cell related growth factors for 24 hours.

*PECAM-1 mRNA expression in seven-day differentiated (a) M-CSF macrophages and (b) GM-CSF macrophages after 24 hours stimulation with 1 ng/ml, 10 ng/ml and 100 ng/ml of VEGF-A, FGF2, IGF-1, HGF or ANGPTL5 expressed as fold change relative to unstimulated control M-CSF directed and GM-CSF-polarised macrophages, respectively, (*P < 0.05 and ** P <0.01 denotes significant difference compared to control M-CSF macrophages, # P <0.05 denotes significant difference compared to VEGF-A 10 ng/ml and 100 ng/ml; one-way ANOVA post-hoc Tukey's multiple comparison test; mean ±SEM; n=6).*

Refer to appendix B (9.1.5) for CT values.

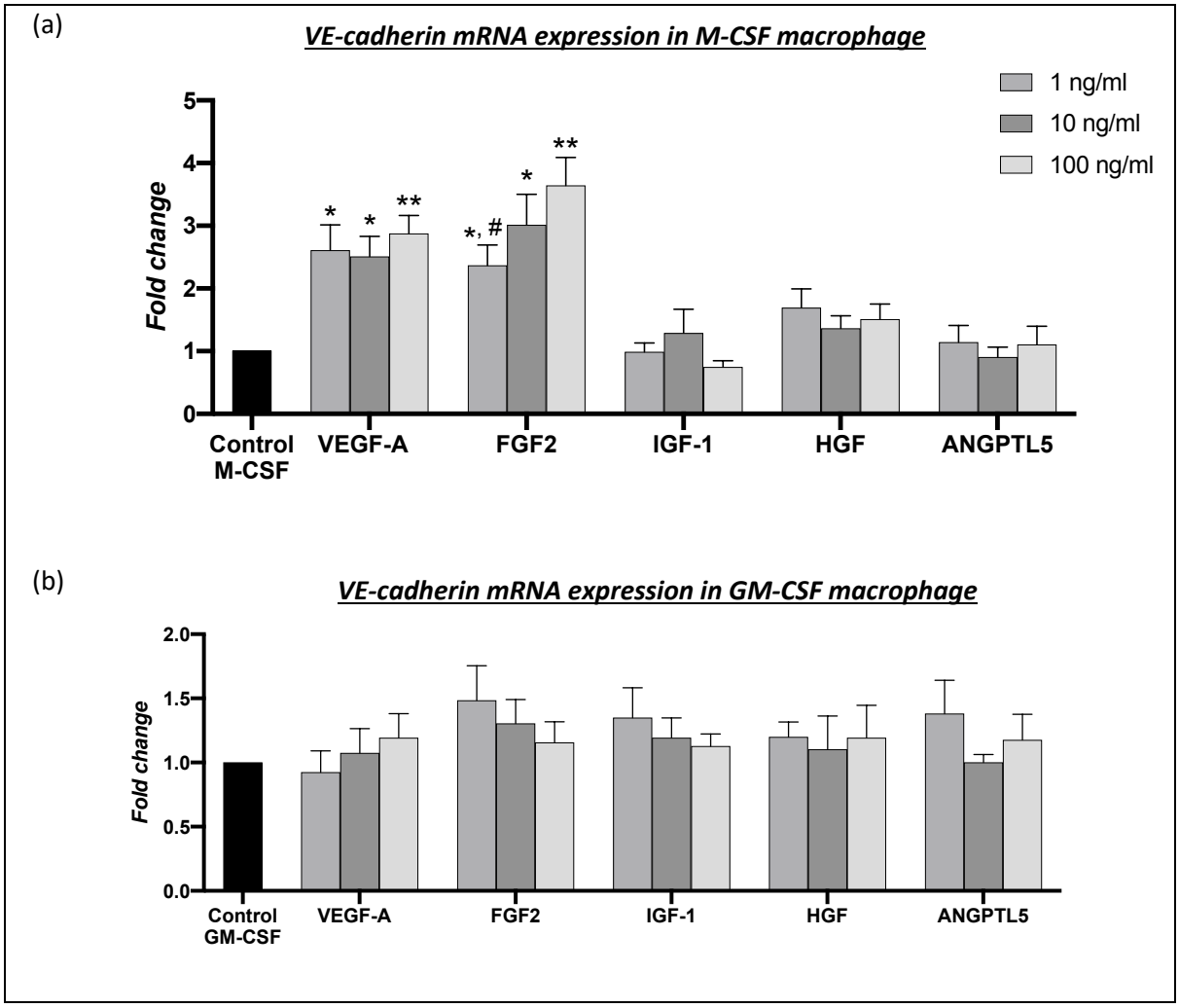

Figure 4.4.6 VE-cadherin mRNA expression in human macrophages stimulated with endothelial cell related growth factors for 24 hours.

*VE-cadherin mRNA expression in seven-day differentiated (a) M-CSF macrophages and (b) GM-CSF macrophages after 24 hours stimulation with 1 ng/ml, 10 ng/ml and 100 ng/ml of VEGF-A, FGF2, IGF-1, HGF or ANGPTL5 expressed as fold change relative to unstimulated control M-CSF directed and GM-CSF-polarised macrophages, respectively, (*P < 0.05 and ** P <0.01 denotes significant difference compared to control M-CSF macrophages, # P < 0.05 denotes significant difference compared to 100 ng/ml FGF2; one-way ANOVA post-hoc Tukey's multiple comparison test; mean ±SEM; n=6).*

Refer to appendix B (9.1.6) for CT values.

		PECAM-1 mRNA	*VE-cadherin mRNA*
M-CSF	Baseline	1.0	1.0
	VEGF-A 1 ng/ml	1.9	2.6
	VEGF-A 10 ng/ml	2.7	2.5
	VEGF-A 100 ng/ml	3.7	2.9
	FGF2 1 ng/ml	2.2	2.4
	FGF2 10 ng/ml	2.8	3.0
	FGF2 100 ng/ml	3.8	3.6
GM-CSF	Baseline	1.0	1.0
	VEGF-A 1 ng/ml	1.2	0.9
	VEGF-A 10 ng/ml	1.1	1.1
	VEGF-A 100 ng/ml	1.2	1.2
	FGF2 1 ng/ml	1.5	1.5
	FGF2 10 ng/ml	1.2	1.3
	FGF2 100 ng/ml	1.3	1.2

Figure 4.4.7 Summary of results for the effect of 24 hour stimulation with VEGF-A or FGF2 on the mRNA expression of PECAM1 and CDH5 (VE-cadherin) in 7-day differentiated macrophages

Fold change in mRNA expression of endothelial cell-associated markers (PECAM1 and CDH5) in seven-day M-CSF or GM-CSF differentiated macrophages after 24 hours stimulation with three different doses of either VEGF-A or FGF2, relative to unstimulated control macrophages (baseline).

4.4.3 Upregulation of PECAM-1 and VE-cadherin upon 4-days stimulation with VEGF-A and FGF2 in M-CSF macrophage

Next, the effect of four day stimulation with 50 ng/ml of VEGF-A, FGF2, HGF, IGF-1, or ANGPTL5 on PECAM1 and CDH5 (VE-cadherin) mRNA and protein expression were determined in seven-day M-CSF and GM-CSF differentiated macrophages. Consistent with the previous findings after four day stimulation, VEGF-A and FGF2 upregulated PECAM-1 mRNA and protein expression in M-CSF macrophages, but was unaffected by stimulation with IGF-1, HGF and ANGPTL5 (Figure 4.4.8 a).

Individually, PECAM1 mRNA expression was significantly upregulated by 1.7-fold in both VEGF-A ($P<0.01$; n=6; Figure 4.4.8 a) and FGF2 ($P<0.05$; n=6; Figure 4.4.8 a) in M-CSF macrophage, when compared to unstimulated control cells. At the protein level, Western blotting revealed PECAM-1 expression was increased in M-CSF macrophages 4.1-fold and 7.0-fold-with VEGF-A and FGF2, respectively ($P<0.05$; n=6; Figure 4.4.8 b and c).

Similarly, immunocytochemistry demonstrated that VEGF-A or FGF2 stimulation resulted in a greater percentage of macrophages positive for PECAM-1 (49.6% and 42.2%, respectively) compared to unstimulated control M-CSF macrophages (33.5%; Figure 4.4.9 and Figure 4.4.10).

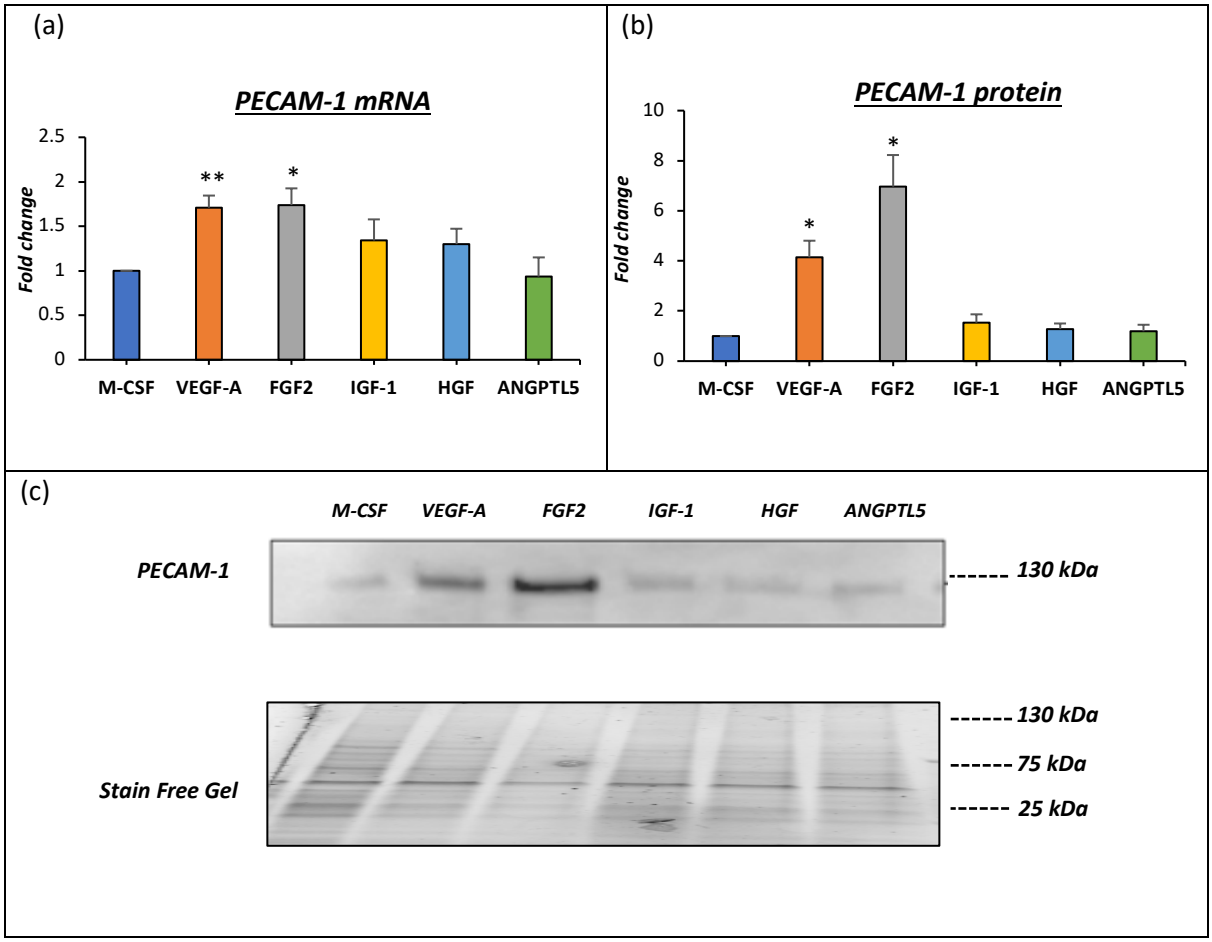

Figure 4.4.8 PECAM-1 mRNA and protein expression in M-CSF macrophages stimulated with endothelial cell related growth factors for four-days.

*(a) PECAM1 mRNA levels in mature M-CSF macrophages following four-day stimulation with 50 ng/ml VEGF-A, FGF2, IGF-1, HGF and ANGPTL5 in seven-day M-CSF differentiated human macrophages, expressed as fold change relative to unstimulated 11-day M-CSF control macrophages, (mean±SEM; n=6; * P < 0.05 and ** P <0.01 denotes significant difference compared to unstimulated 11-day-M-CSF directed macrophages; one-way ANOVA Tukey's multiple comparison test).*

*(b) Quantification and (c) representative western blots for PECAM-1 protein expression, expressed as fold change relative to unstimulated 11-day M-CSF directed control macrophages, (mean±SEM; n=6; * P < 0.05 and ** P <0.01 denotes significant difference compared to unstimulated 11-day-M-CSF directed macrophages; one-way ANOVA Tukey's multiple comparison test). Stain free gel is shown as a loading control.*

Refer to appendix B; (9.1.7) for CT values and (9.2.1) for full blot image.

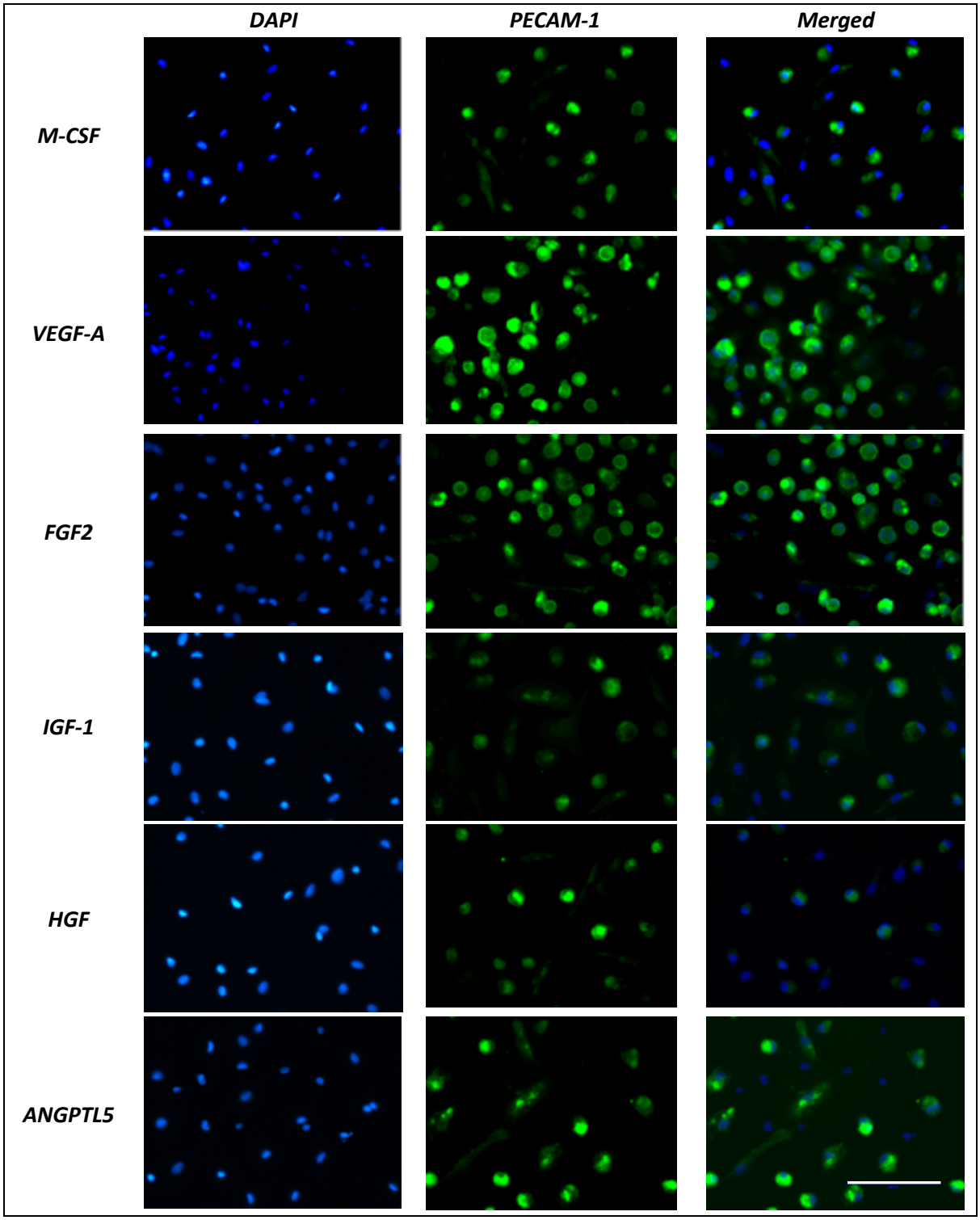

Figure 4.4.9 Immunofluorescence localisation of PECAM-1 in M-CSF macrophages stimulated with endothelial cell-related growth factors for four-day.

Representative images of immunofluorescent labelling for PECAM-1 expression following four-day stimulation with 50 ng/ml VEGF-A, FGF2, IGF-1, HGF and ANGPTL5 in seven-day M-CSF differentiated human macrophages. Green colour indicates PECAM-1 immunopositivity, and blue indicates nuclei (DAPI counterstain). Scale bar in lower right panel represents 100 μM and applicable to all panels. Refer to Figure 4.4.10 for associated quantification.

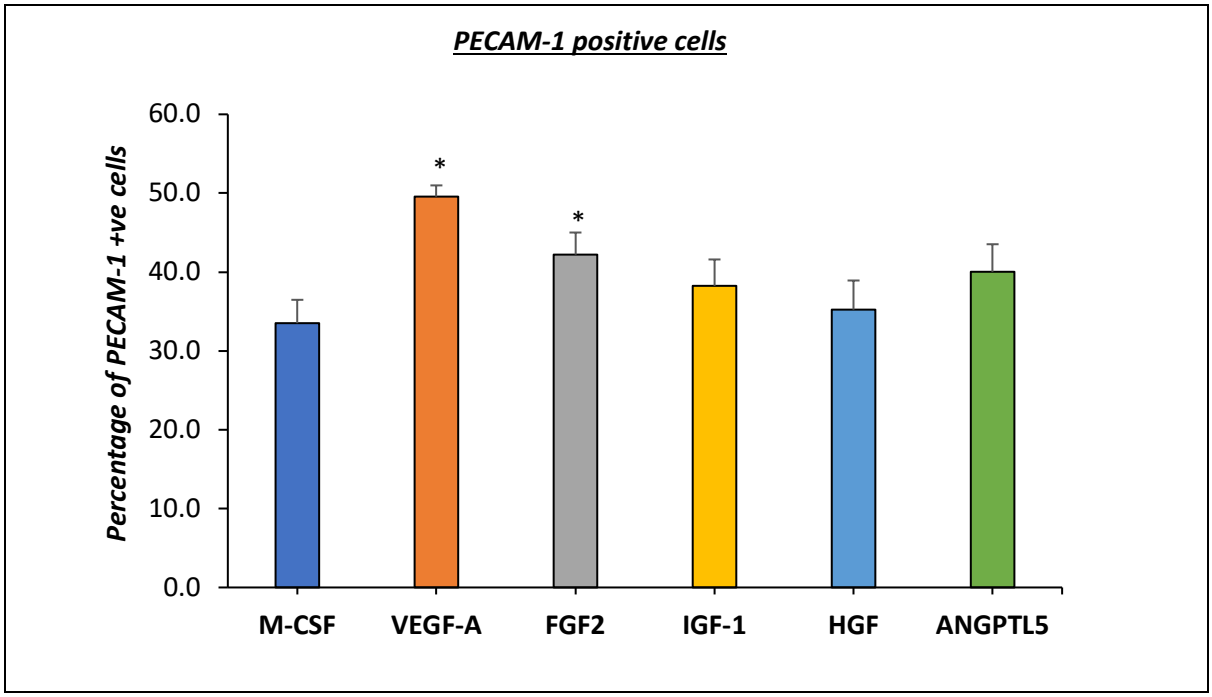

Figure 4.4.10 Quantification of immunofluorescence cell positivity of PECAM-1 in M-CSF macrophages stimulated with endothelial-cell related growth factors for four-days.

*Quantification of immunofluorescent labelling for PECAM-1 expression following four-day stimulation with 50 ng/ml VEGF-A, FGF2, IGF-1, HGF or ANGPTL5 in seven-day M-CSF differentiated human macrophages. Data are expressed as percentage of PECAM-1 immuno-positive macrophages, (mean ±SEM; n=6; *P < 0.05 denotes significant difference compared to unstimulated M-CSF macrophages; one-way ANOVA Tukey's multiple comparison test). Refer to Figure 4.4.9 for associated representative images.*

In regard to VE-cadherin expression, stimulation of M-CSF matured macrophages with individual endothelial cell-related growth factors for four-days significantly upregulated VE-cadherin protein expression (4.2, 7.3, 3.9, 3.9 and 3.8-fold increase for VEGF-A, FGF2, IGF-1, HGF and ANGPTL5 respectively; $P < 0.05$ except for FGF2 $P < 0.01$; n=6; Figure 4.4.11 b and c), as assessed through Western blotting. Mirroring these findings, immunocytochemistry for VE-cadherin demonstrated all endothelial cell-related growth factors increased the percentage of M-CSF matured macrophages expressing VE-cadherin (ranging between 40.4% to 47.4%; $P<0.05$, n=6; Figure 4.4.12 and Figure 4.4.13), when compared to unstimulated control M-CSF macrophages (32.6% positive; Figure 4.4.12 and Figure 4.4.13).

However, CDH5 mRNA levels were not affected by any of the factors with the exception of FGF2 which in opposition to the protein levels, downregulated CDH5 (VE-cadherin) mRNA expression (45%; $P<0.01$; n=6; Figure 4.4.11 a).

On the other hand, qPCR, Western blotting and immunocytochemical analyses revealed that the mRNA and protein expression of PECAM-1 and VE-cadherin were unaffected in GM-CSF matured macrophages, upon subsequent four-day stimulation with any of the endothelial cell-related growth factors (Figure 4.4.14 - Figure 4.4.19). All of the above results are summarised in Figure 4.4.20.

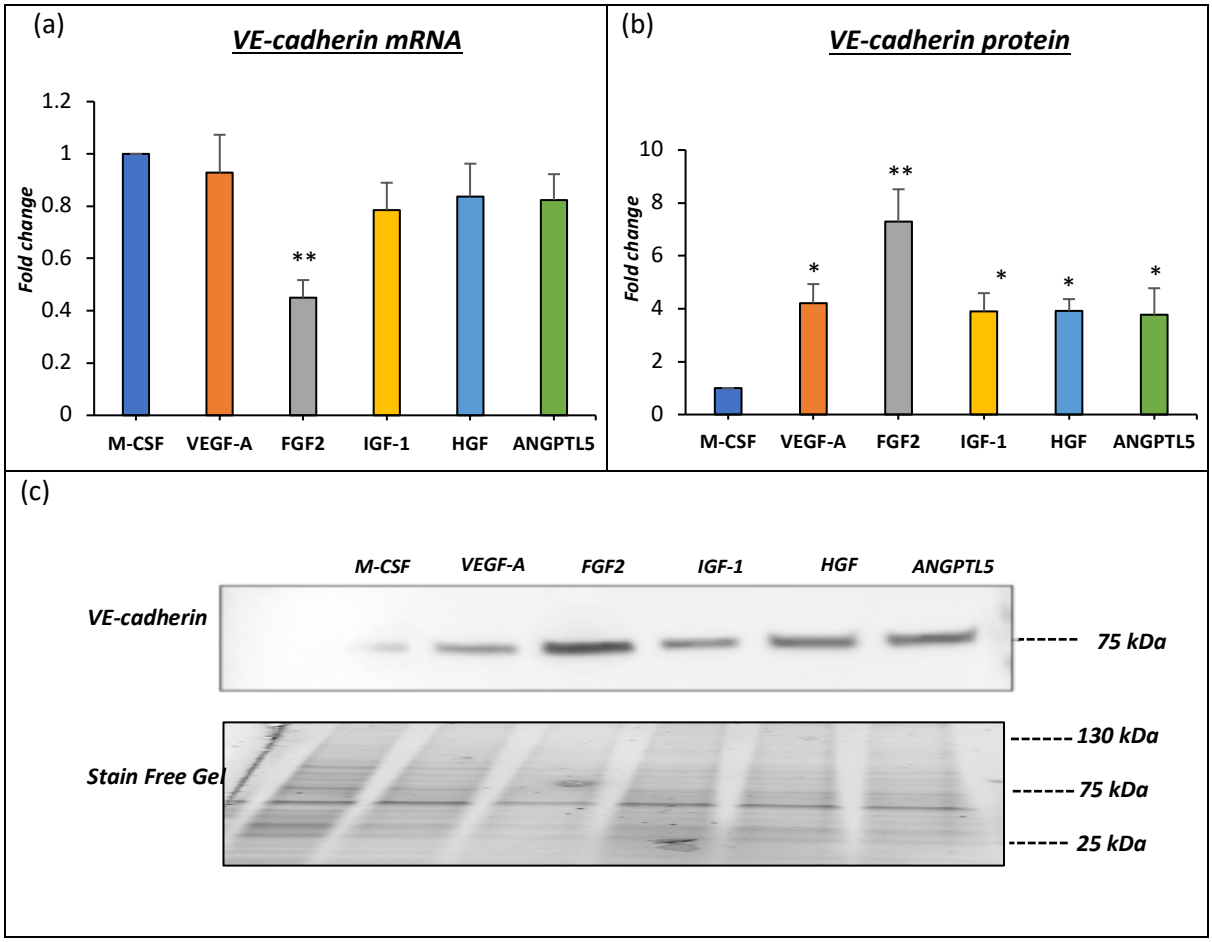

Figure 4.4.11 VE-cadherin mRNA and protein expression in M-CSF macrophages stimulated with endothelial cell-related growth factors for four-days.

*(a) CDH5 (VE-cadherin) mRNA expression in mature M-CSF macrophages following four-day stimulation with 50 ng/ml VEGF-A, FGF2, IGF-1, HGF and ANGPTL5 in seven-day M-CSF differentiated human macrophages, expressed as fold change relative to unstimulated 11-day M-CSF control macrophages, (mean±SEM; n=6; ** P <0.01 denotes significant difference compared to unstimulated 11-day-M-CSF directed macrophages; one-way ANOVA Tukey's multiple comparison test).*

*(b) Quantification and (c) representative western blots for VE-cadherin protein expression, expressed as fold change relative to unstimulated 11-day M-CSF directed control macrophages, (mean±SEM; n=6; * P < 0.05 and ** P <0.01 denotes significant difference compared to unstimulated 11-day-M-CSF directed macrophages; one-way ANOVA Tukey's multiple comparison test). Stain free gel is shown as a loading control.*

Refer to appendix B; (9.2.2) for CT values and (9.2.3) for full blot image.

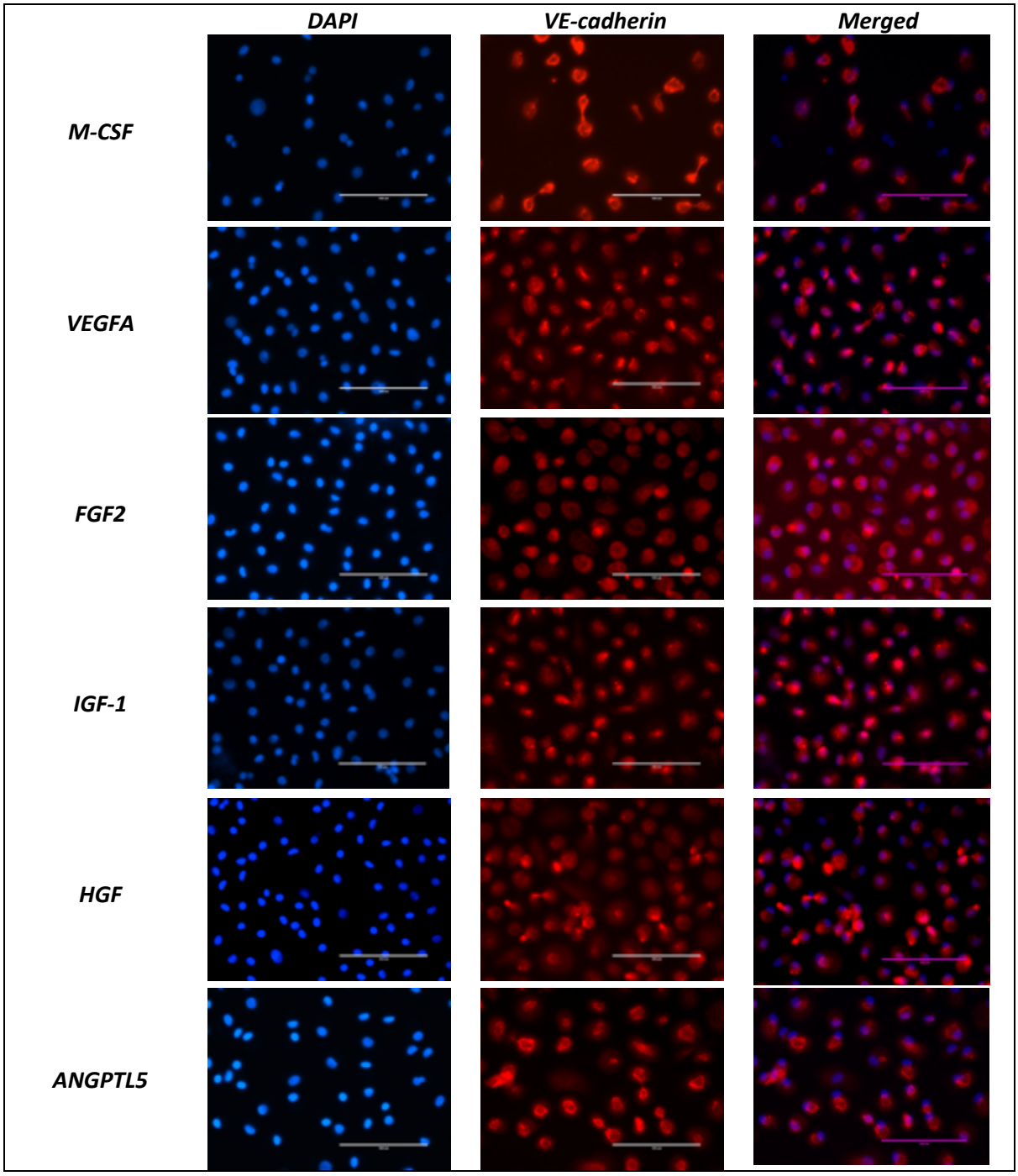

Figure 4.4.12 Immunofluorescence localisation of VE-cadherin in M-CSF macrophages stimulated with endothelial cell-related growth factors for four-days.

Representative images of immunofluorescent labelling for VE-cadherin expression following four-day stimulation with 50 ng/ml VEGF-A, FGF2, IGF-1, HGF and ANGPTL5 in seven-day M-CSF differentiated human macrophages. Red colour indicates VE-cadherin immunopositivity, and blue indicates nuclei (DAPI counterstain). Scale bars represent 100 μM. Refer to Figure 4.4.13 for associated quantification.

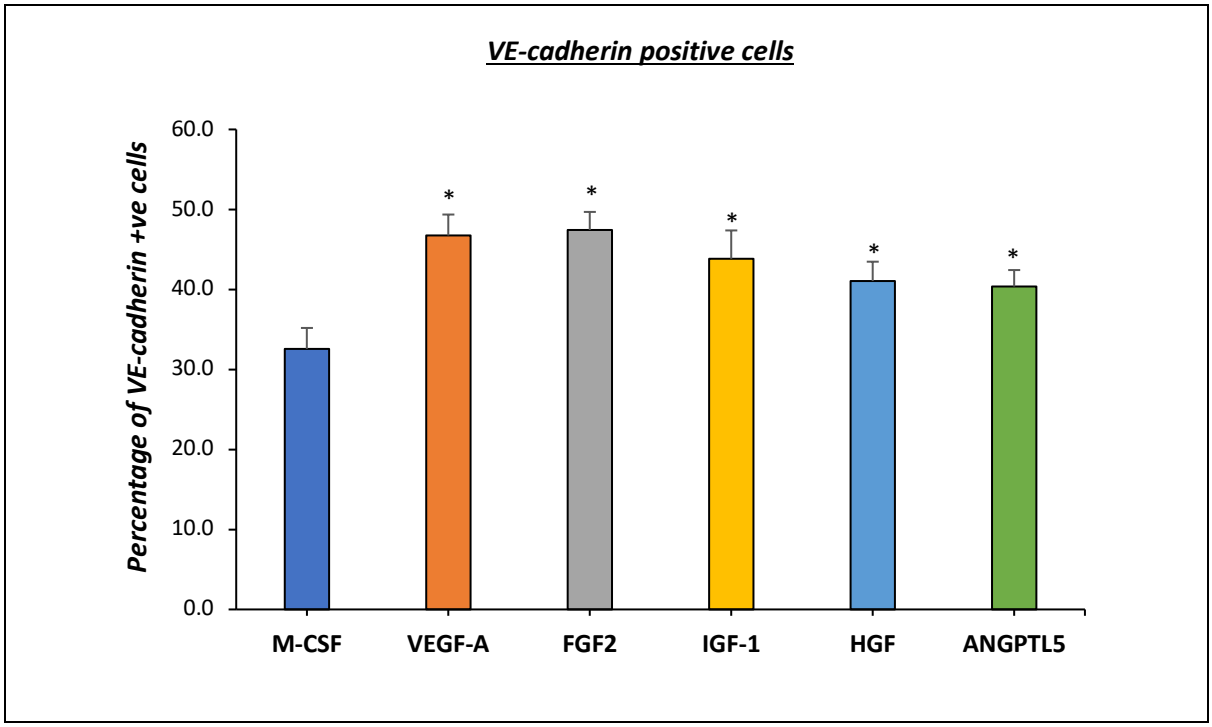

Figure 4.4.13 Quantification of immunofluorescence cell positivity of VE-cadherin in M-CSF macrophages stimulated with endothelial cell-related growth factors for four-days.

*Quantification of immunofluorescent labelling for VE-cadherin expression following four-day stimulation with 50 ng/ml VEGF-A, FGF2, IGF-1, HGF and ANGPTL5 in seven-day M-CSF differentiated human macrophages. Data are expressed as percentage of VE-cadherin immuno-positive, (mean ±SEM; n=6). * P < 0.05 denotes significant difference compared to M-CSF macrophages; one-way ANOVA Tukey's multiple comparison test). Refer Figure 4.4.12 for representative images.*

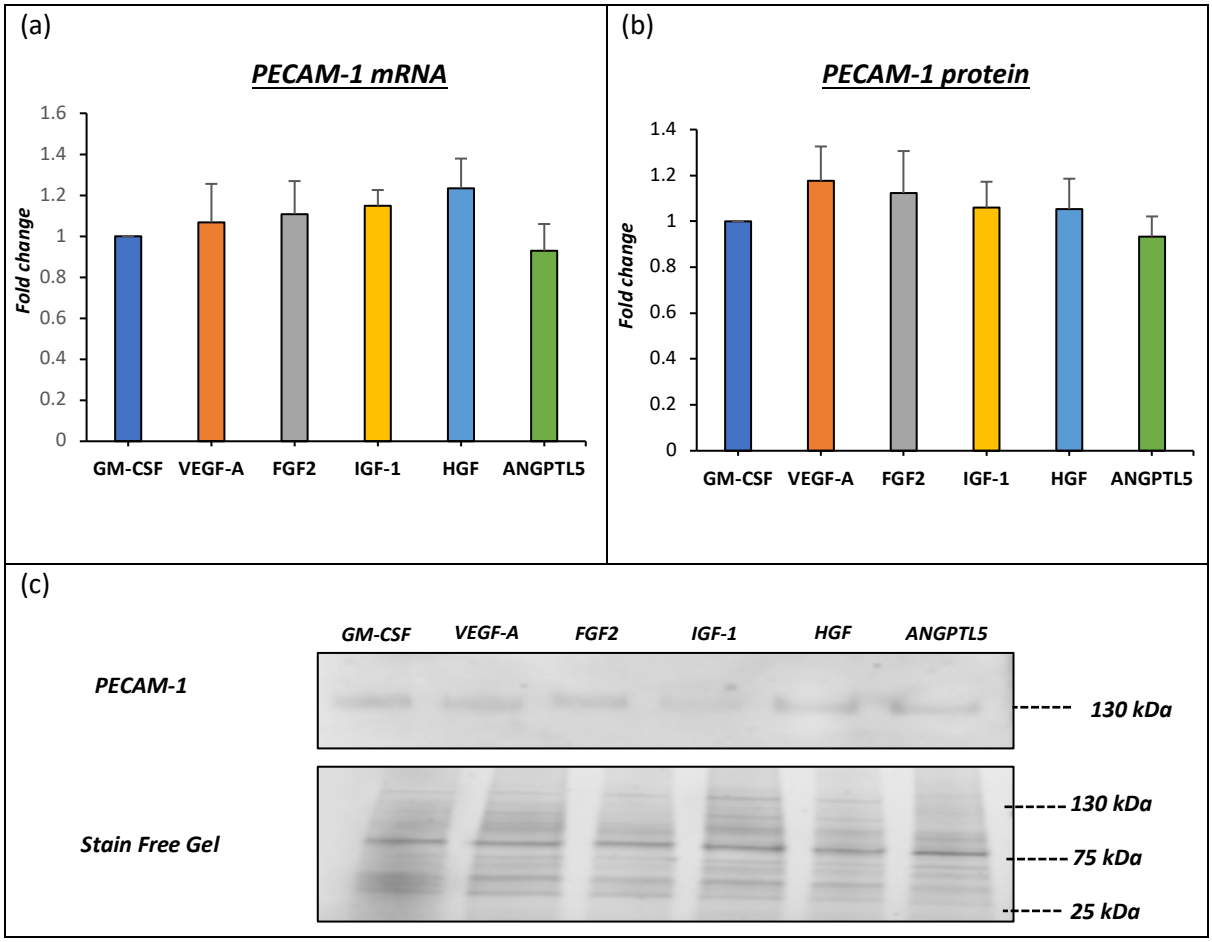

Figure 4.4.14 PECAM-1 mRNA and protein expression in GM-CSF macrophages stimulated with endothelial cell-related growth factors for four-days.

(a) PECAM1 mRNA expression in mature GM-CSF macrophages following four-day stimulation with 50 ng/ml VEGF-A, FGF2, IGF-1, HGF and ANGPTL5 in seven-day GM-CSF differentiated human macrophages, expressed as fold change relative to unstimulated 11-day GM-CSF control macrophages, (mean±SEM; n=6).

(b) Quantification and (c) representative western blots for PECAM-1 protein expression, expressed as fold change relative to unstimulated 11-day GM-CSF directed control macrophages, (mean±SEM; n=6). Stain free gel is shown as a loading control.

Refer to appendix B; (9.2.4) for CT values and (9.3.1) for full blot image.

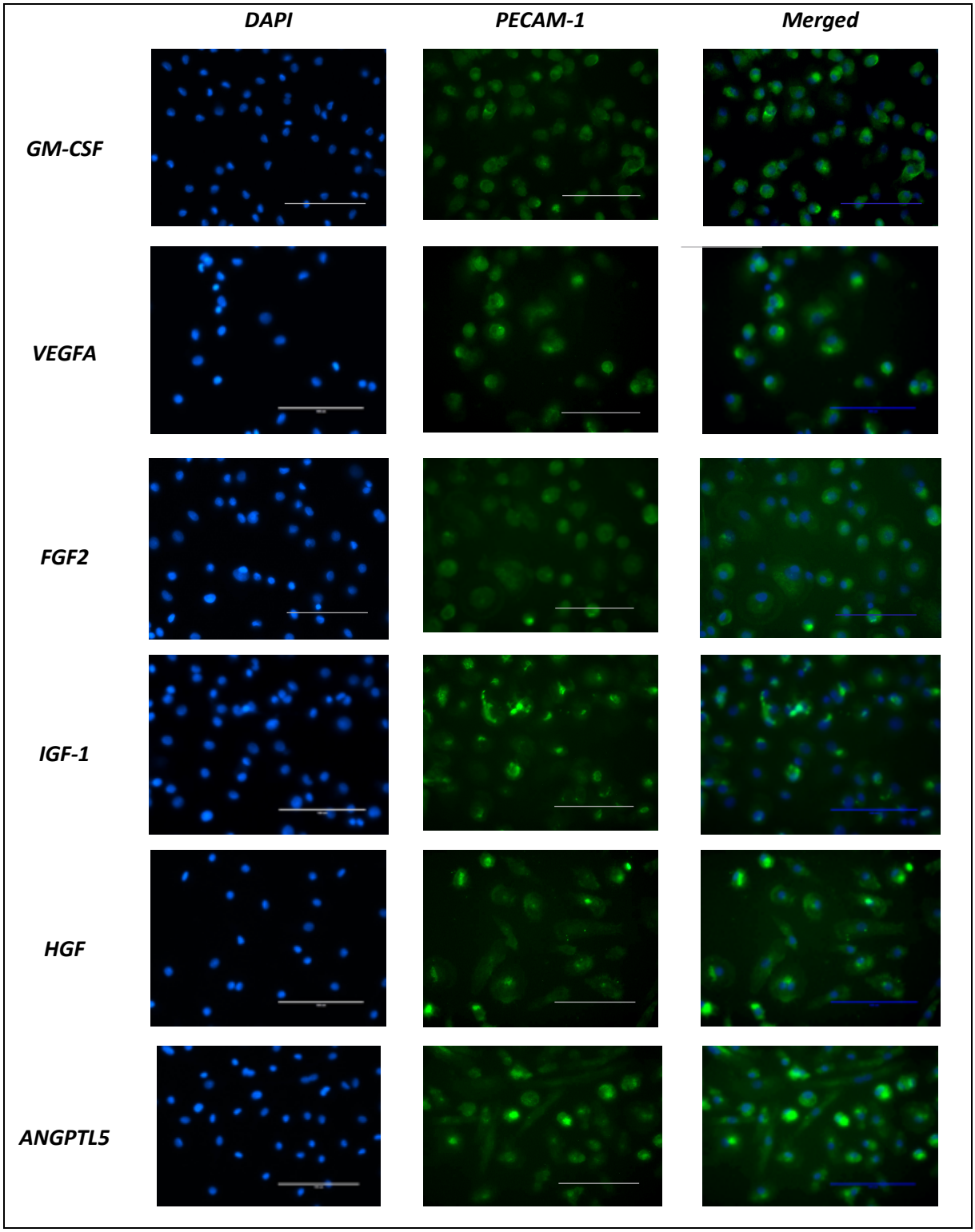

Figure 4.4.15 Immunofluorescence localisation of PECAM-1 in GM-CSF macrophages stimulated with endothelial cell-related growth factors for four-days.

Representative images of immunofluorescent labelling for PECAM-1 expression following four-day stimulation with 50 ng/ml VEGF-A, FGF2, IGF-1, HGF and ANGPTL5 in seven-day GM-CSF differentiated human macrophages. Green colour indicates PECAM-1 immunopositivity, and blue indicates nuclei (DAPI counterstain). Scale bars represent 100 μM. Refer to Figure 4.4.16 for associated quantification.

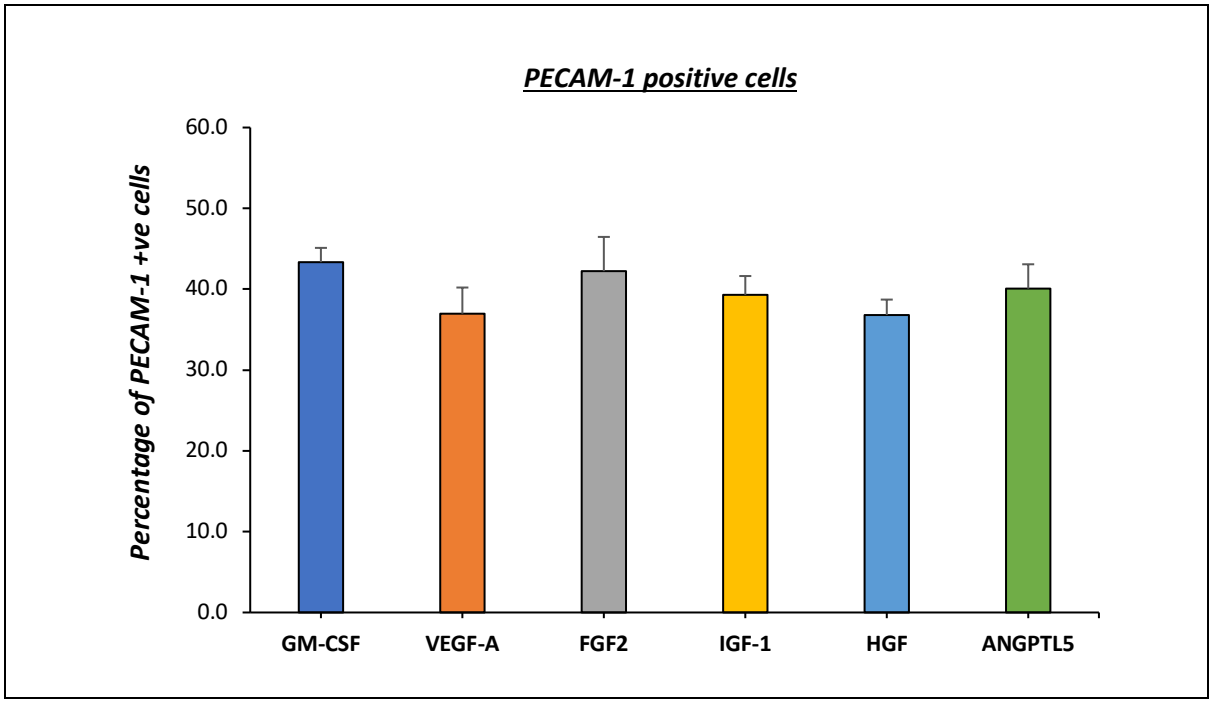

Figure 4.4.16 Quantification of immunofluorescence cell positivity of PECAM-1 in GM-CSF macrophages stimulated with endothelial cell-related growth factors for four-days.

Quantification of immunofluorescent labelling for PECAM-1 expression following four-day stimulation with 50 ng/ml VEGF-A, FGF2, IGF-1, HGF and ANGPTL5 in seven-day GM-CSF differentiated human macrophages. Data are expressed as percentage of PECAM-1 immuno-positive macrophages (mean ±SEM; n=6). Refer to Figure 3.4.15 for associated representative images.

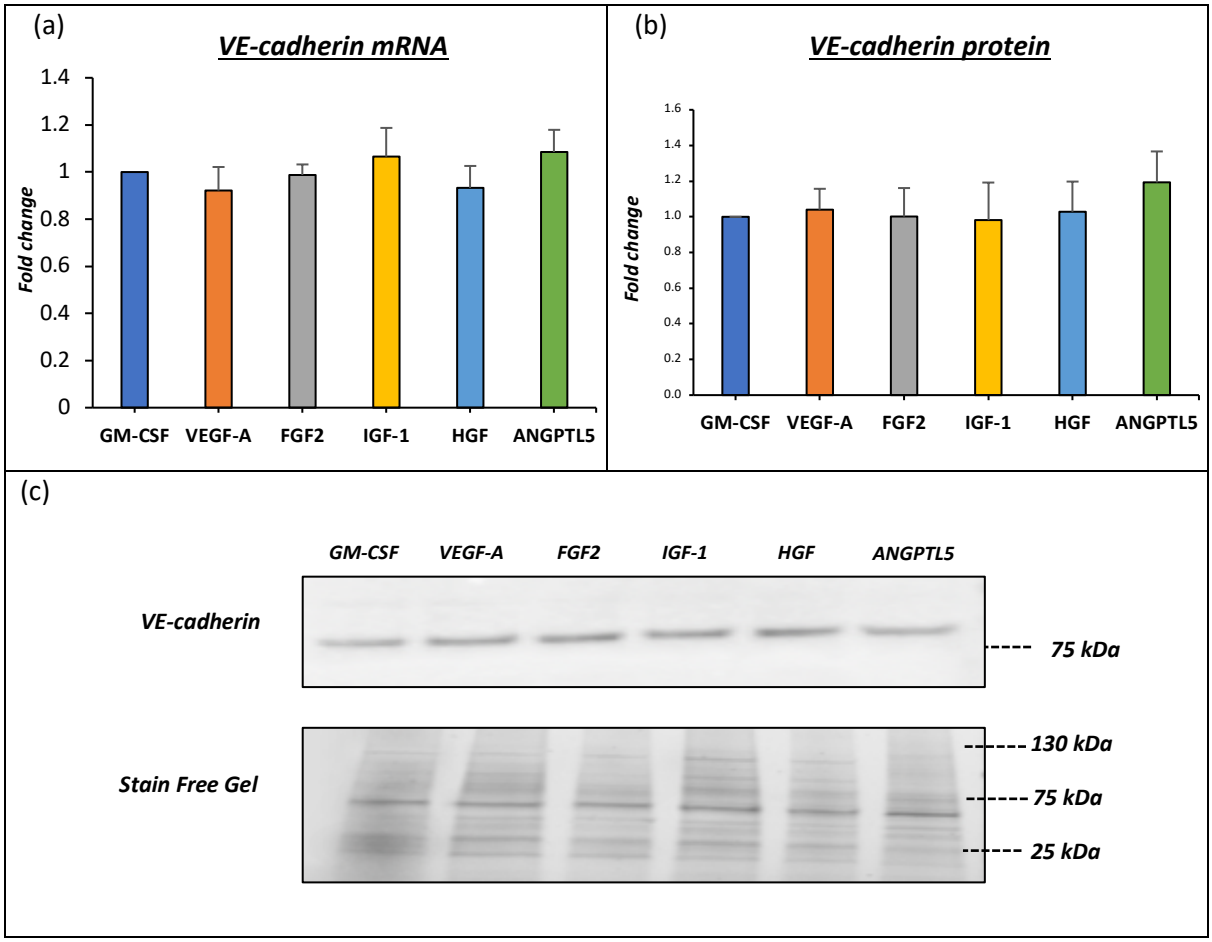

Figure 4.4.17 CDH5 (VE-cadherin) mRNA and protein expression in GM-CSF macrophages stimulated with endothelial cell-related growth factors for four-days.

(a) CDH5 (VE-cadherin) mRNA expression in mature GM-CSF macrophages following four-day stimulation with 50 ng/ml VEGF-A, FGF2, IGF-1, HGF and ANGPTL5 in seven-day GM-CSF differentiated human macrophages, expressed as fold change relative to unstimulated 11-day GM-CSF control macrophages, (mean±SEM; n=6).

(b) Quantification and (c) representative western blots for VE-cadherin protein expression, expressed as fold change relative to unstimulated 11-day GM-CSF directed control macrophages, (mean±SEM; n=6). Stain free gel is shown as a loading control.

Refer to appendix B; (9.3.2) for CT values and (9.3.3) for full blot image.

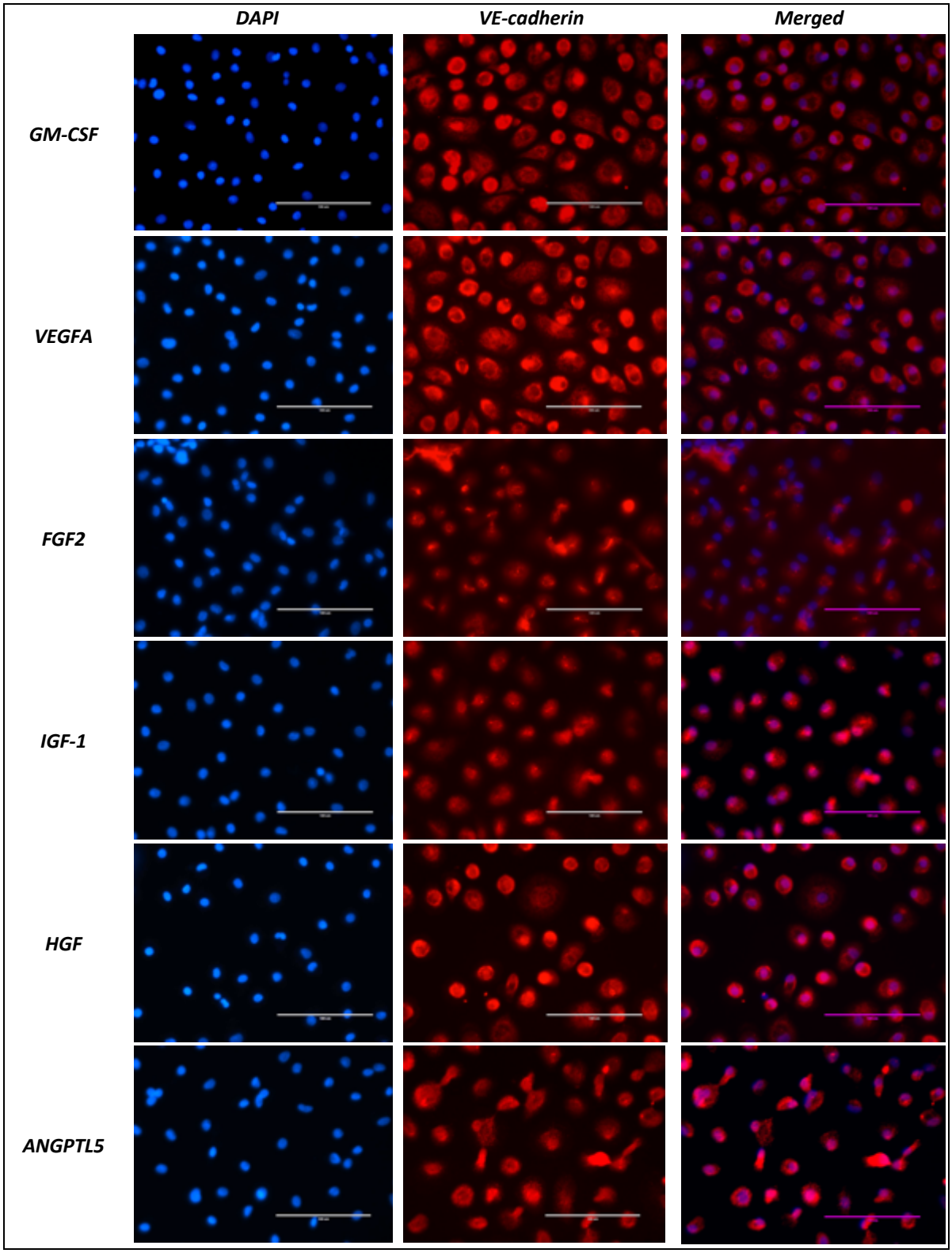

Figure 4.4.18 Immunofluorescence localisation of VE-cadherin in GM-CSF macrophages stimulated with endothelial cell-related growth factors for four-days.

Representative images of immunofluorescent labelling for VE-cadherin expression following four-day stimulation with 50 ng/ml VEGF-A, FGF2, IGF-1, HGF and ANGPTL5 in seven-day GM-CSF differentiated human macrophages. Red colour indicates VE-cadherin immunopositivity, and blue indicates nuclei (DAPI counterstain). Scale bars represent 100 μM. Refer to Figure 4.4.19 for associated quantification.

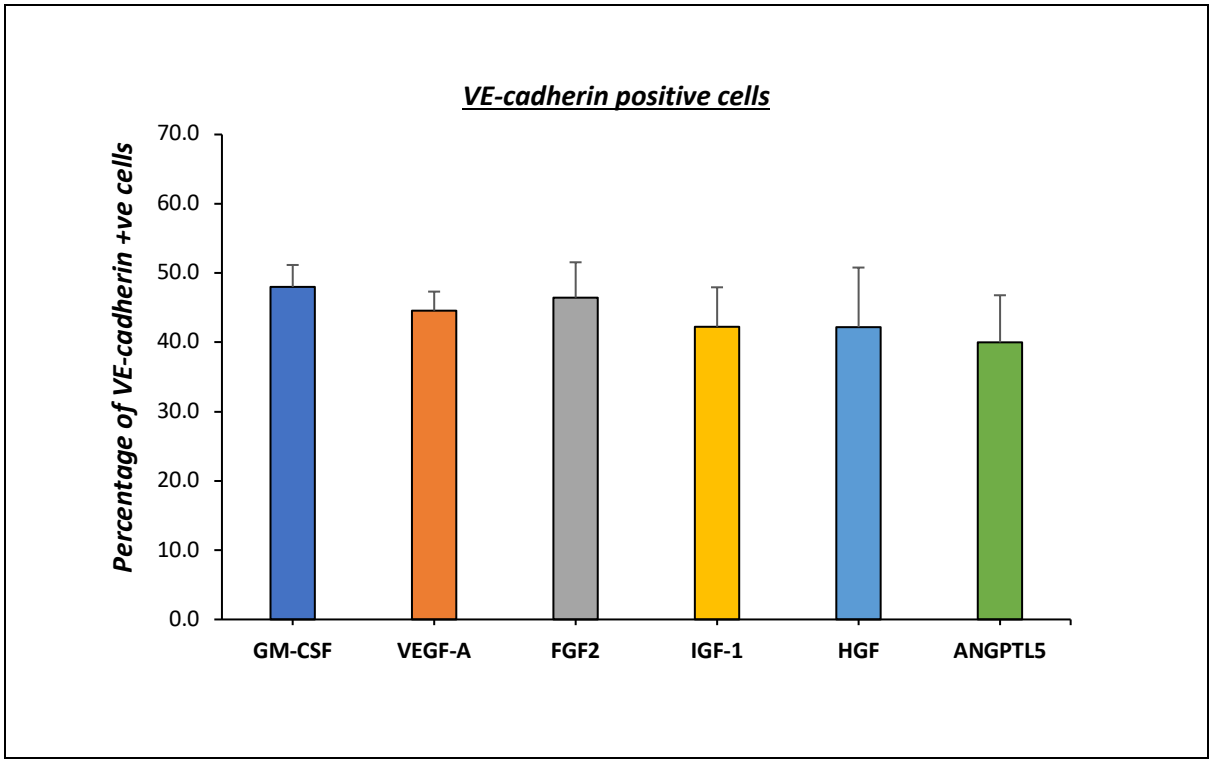

Figure 4.4.19 Quantification of immunofluorescence cell positivity of VE-cadherin in GM-CSF macrophages stimulated with endothelial cell-related growth factors for four-days.

Quantification of immunofluorescent labelling for VE-cadherin expression following four-day stimulation with 50 ng/ml VEGF-A, FGF2, IGF-1, HGF and ANGPTL5 in seven-day GM-CSF differentiated human macrophages. Data are expressed as percentage of VE-cadherin immuno-positive macrophages (mean ±SEM; n=6). Refer to Figure 4.4.18 for associated representative image.

	PECAM-1			VE-cadherin		
	mRNA	*Protein (WB)*	*Protein (IF)*	*mRNA*	*Protein (WB)*	*Protein (IF)*
M-CSF	1.0	1.0	33.5%	1.0	1.0	32.6%
VEGF-A	1.7	4.1	49.6%	0.9	4.2	46.7%
FGF2	1.7	7.0	42.2%	0.5	7.3	47.4%
IGF-1	1.3	1.5	38.3%	0.8	3.9	43.8%
HGF	1.3	1.3	35.2%	0.8	3.9	41.4%
ANGPTL5	0.9	1.2	40.0%	0.8	3.8	40.4%
GM-CSF	1.0	1.0	43.3%	1.0	1.0	48.0%
VEGF-A	1.1	1.2	37.0%	0.9	1.0	44.6%
FGF2	1.1	1.1	42.2%	1.0	1.0	46.4%
IGF-1	1.1	1.1	39.3%	1.1	0.9	42.2%
HGF	1.2	1.1	36.8%	0.9	1.0	42.1%
ANGPTL5	0.9	0.9	40.1%	1.1	1.2	40.0%

Figure 4.4.20 Summary of results for the effects of 4-day stimulation with endothelial cell-related growth factors on the mRNA and protein expression of PECAM-1 and CDH5 (VE-cadherin) in 7-day differentiated macrophages.

Fold change in mRNA and protein expression of endothelial cell-associated markers in seven-day M-CSF or GM-CSF differentiated macrophages following 4-day stimulation with individual endothelial cell-related growth factors, relative to respective M-CSF or GM-CSF unstimulated macrophages (baseline). Percentage of PECAM-1 and VE-cadherin immuno-positive macrophages are also included. (WB = western blot, IF = immunofluorescence).

4.4.4 The expression of endothelial cell-related markers in M-CSF and GM-CSF matured macrophages relative to human umbilical vascular endothelial cell levels

The expression of PECAM-1 and CDH5 (VE-cadherin) in human macrophage subsets were compared to levels within human primary endothelial cells (human umbilical vein endothelial cells, HUVEC). Although baseline macrophage cultures expressed detectable levels of PECAM-1 and VE-cadherin, the mRNA levels were significantly lower compared to HUVECs (Figure 4.4.21 a, and Figure 4.4.22 a). Specifically, PECAM-1 mRNA expression in HUVECs was 130-fold greater compared to both macrophage subsets, irrespective of time in culture ($P<0.0001$, n=6, Figure 4.4.21 a). VE-cadherin mRNA expression in HUVECs was even more dramatically increased (55000-fold higher) compared to both macrophage subsets at all time points ($P<0.0001$, n=6, Figure 4.4.22 a).

At the protein level, HUVEC expression of PECAM-1 and VE-cadherin were 15.0-fold and 17.7-fold higher compared to both macrophage subsets at all time points ($P<0.0001$, n=6, Figure 4.4.21 b, and Figure 4.4.22 b). These results are summarised within Figure 4.4.23.

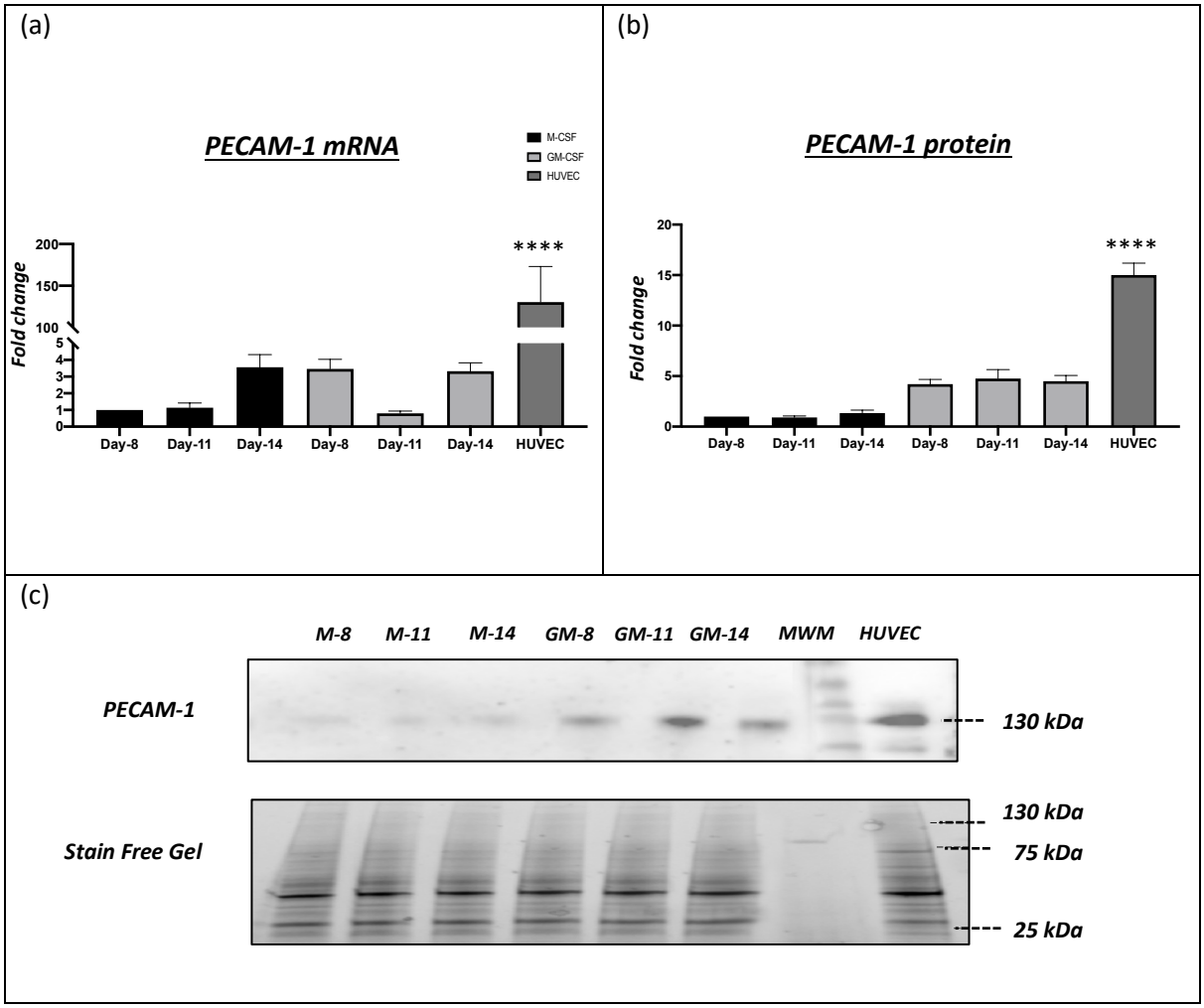

Figure 4.4.21 PECAM-1 mRNA and protein expression in human macrophage subsets and human umbilical vein endothelial cells.

*(a) PECAM-1 mRNA expression in M-CSF and GM-CSF macrophage subsets and HUVECs after 8-, 11-, and 14-days in culture, expressed as fold change relative to 8-day M-CSF macrophages. (****P < 0.0001 denotes significant difference compared to macrophages under all conditions; ANOVA Tukey's multiple comparison test).*

*(b) Quantification and (c) representative western blots for PECAM-1 protein expression, expressed as fold change relative to 8-day M-CSF macrophages, (****P < 0.0001 denotes significant difference compared to macrophages under all conditions; ANOVA Tukey's multiple comparison test). Stain free gel is shown as a loading control (HUVEC = human umbilical vein endothelial cell, MWM = molecular weight marker).*

Refer to appendix B; (9.1.1) for CT values and (9.1.2) for full blot image.

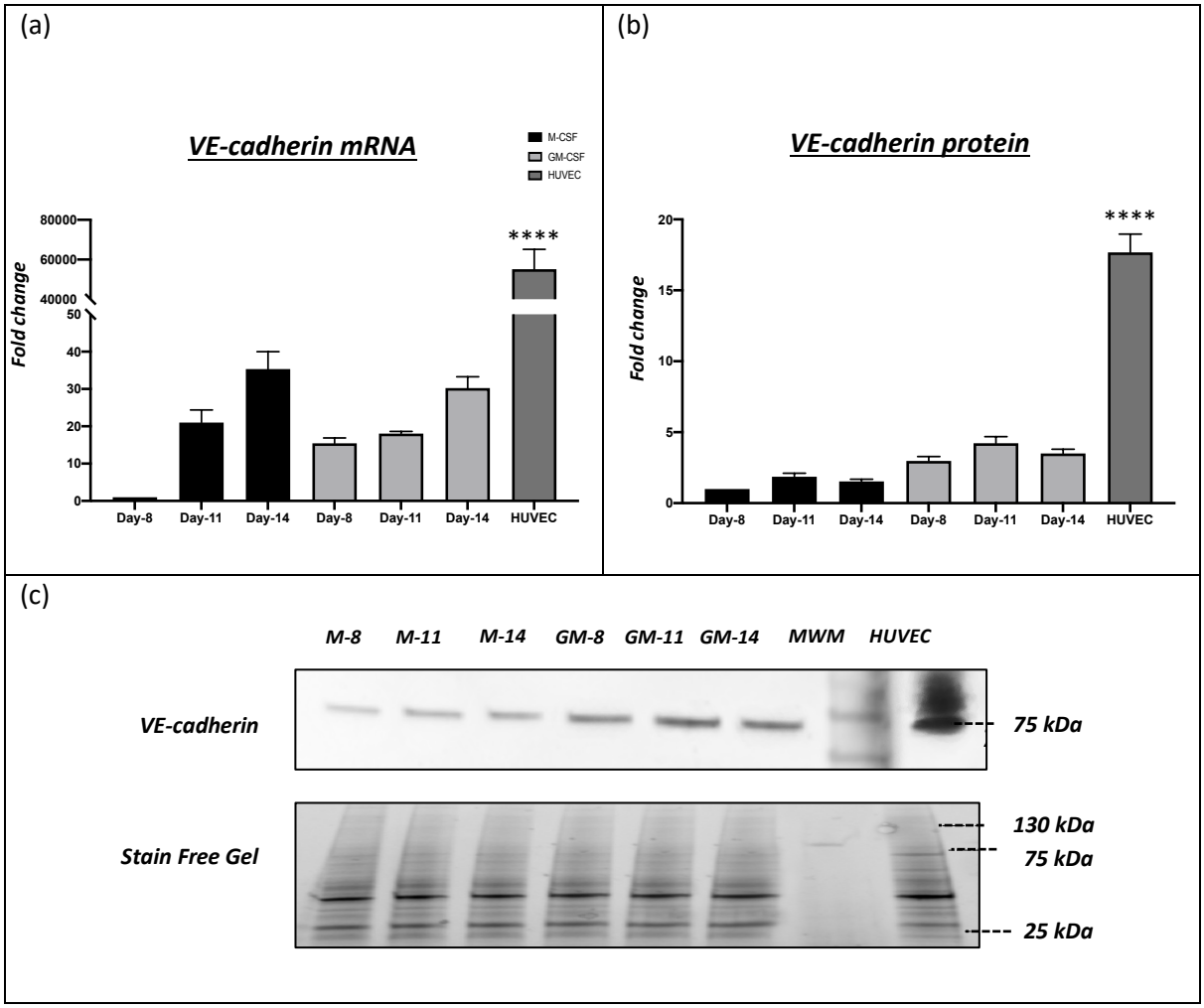

Figure 4.4.22 CDH5 (VE-cadherin) mRNA and protein expression in human macrophages and human umbilical vein endothelial cells.

*(a) CDH5 (VE-cadherin) mRNA levels in M-CSF and GM-CSF macrophage subsets and HUVECs after 8-, 11-, and 14-days in culture, expressed as fold change relative to 8-day M-CSF macrophages, (****P < 0.0001 denotes significant difference compared to macrophages under all conditions; ANOVA Tukey's multiple comparison test).*

*(b) Quantification (c) representative western blots for VE-cadherin protein expression, expressed as fold change relative to 8-day M-CSF macrophages, (****P < 0.0001 denotes significant difference compared to macrophages under all conditions; ANOVA Tukey's multiple comparison test). Stain free gel is shown as loading control (HUVEC = human umbilical vein endothelial cell, MWM = molecular weight marker).*

Refer to appendix B; (9.1.3) for CT values and (9.1.4) for full blot image.

		PECAM-1			VE-cadherin		
		mRNA	*Protein (WB)*	*Protein (IF)*	*mRNA*	*Protein (WB)*	*Protein (IF)*
M-CSF	Day-7	1.0	1.0	31.4%	1.0	1.0	35.7%
	Day-11	1.1	1.0	NA	21.0	1.9	NA
	Day-14	3.6	1.2	NA	35.4	1.5	NA
GM-CSF	Day-7	3.5	3.5	43.1%	15.4	3.0	49.2%
	Day-11	0.8	5.6	NA	18.0	4.2	NA
	Day-14	3.3	4.8	NA	30.2	3.5	NA
HUVEC		130.3	15.0	NA	$5.5X10^4$	17.7	NA

Figure 4.4.23 Summary of results for the relative mRNA and protein expression of PECAM-1 and VE-cadherin in baseline macrophage subsets and HUVECs.

Fold change in mRNA and protein expression (by western blotting) of endothelial cell-associated markers in baseline macrophage subsets after seven-, eleven- and fourteen-day differentiation and seven-day HUVECs. All data expressed as fold change relative to 7-day M-CSF directed macrophages, with red highlighting indicating significantly increased expression and green highlighting indicating significantly decreased levels. Percentage of immuno-positive cells for PECAM-1 and VE-cadherin after seven-day differentiation are also included, (WB = western blot, IF = immunofluorescence; NA = not available).

4.5 Discussion

In this study, it is demonstrated that *in vitro* human PBMC-derived macrophages under culture conditions express detectable levels of proteins commonly used as markers for endothelial cells (Goncharov *et al.,* 2017), namely PECAM-1 and VE-cadherin. Echoing the findings in the previous results chapter which assessed VSMC-related markers, baseline GM-CSF directed macrophages (GM-Mac) showed higher expression of the endothelial cell-related markers compared to M-CSF directed macrophage (M-Mac). In addition to these two markers, vWF was also expressed by macrophage cultures in this study (results were not shown).

Supporting the observations within this chapter, macrophages derived from human peripheral blood ($CD34^-$ $CD14^+$) monocytes and stimulated for four weeks with VEGF-A, FGF2 or IGF-1 were shown to express the endothelial cell markers vWF, VE-cadherin and nitric oxide synthase (NOS) through FACS analysis and RT-PCR, without losing expression of hematopoietic lineage markers such as CD45 and CD68 (Schmeisser *et al.,* 2001). Interestingly, it was demonstrated that these cells not only assemble clusters or colonies *in vitro* (as observed in this thesis, previous chapter 3.4.1), but they also formed tube-like structures upon Matrigel, a common approach to analyse angiogenesis formation (Schmeisser *et al.,* 2001). It is essential to highlight that these cells were not deemed as circulating mesenchymal stem cells (CD34 positive cells), with previous reports demonstrating that cord-blood and peripheral blood derived $CD34^+$ cells express VE-cadherin (Peichev *et al.,* 2000). Circulating mesenchymal stem cells are found within the peripheral blood of healthy individuals at a low level, but can increase in number under certain pathological conditions such as bone sarcoma (Bian *et al.,* 2009) and following corneal injury (Lan *et al.,* 2012). Additionally, circulating stem cells may also contribute to the formation of osteoblast-like cells, and are associated with vascular calcification in atherosclerosis (Leszczynska and Murphy, 2018). Besides CD34, other cell-surface markers that can be used to distinguish circulating stem cells from the monocyte/macrophage lineage include CD90, CD105 and CD73, among others (Dominici *et al.,* 2006).

In a different study, macrophages from transgenic CX3CR1$^{GFP/GFP}$ mice were shown to express PECAM-1 (CD31) by immunofluorescence staining and harbour the capacity to form vascular networks within a subcutaneous angiogenesis assay (Barnett *et al.,* 2016). Similarly deploying a subcutaneous angiogenesis assay, macrophages formed a network of interconnected PECAM-1 positive cells within wild type C57BL/6J mice. In addition, supplementation with pro-angiogenic growth factors (such as VEGF) and pro-inflammatory cytokines (such as IFNγ and GM-CSF) induced macrophages to develop similar angiogenic-like networks (Barnett *et al.,* 2016). Taken together, the findings above alongside those presented within this chapter support the notion that macrophages can express endothelial-related cell markers under certain conditions, and highlight GM-CSF as a potential modulator of this ability.

Nevertheless, in this chapter it is shown that the expression of PECAM-1 and VE-cadherin by both *in vitro* macrophage subsets (M-Mac and GM-Mac) were low compared to primary endothelial cells (HUVEC) suggesting that the PECAM-1 and VE-cadherin-expressing macrophages are non-identical to endothelial cells-lineage but ostensibly of leukocyte-lineage with the ability to display endothelial cell-like characteristics. This further affirms monocyte/macrophage's heterogeneity and plasticity concepts, and that they can potentially be considered as a form of progenitor cell.

The peripheral blood used in this study to isolate monocytes was obtained from healthy donors, suggesting that very low numbers of circulating mesenchymal stem cells or mature endothelial cells would be present, which is important as these cell types are commonly associated with atherosclerosis (Boos *et al.,* 2007). Circulating endothelial cells are identified as a population of mature cells that have detached from the vessel wall following vessel damage, with their endothelial cell population identified through expression of CD146 (Goon *et al.,* 2006). Reportedly, higher numbers of circulating endothelial cells (CD146 positive) are present within the whole blood of coronary artery disease patients (such as those displaying unstable angina or myocardial infarction) compared to healthy subjects (Boos *et al.,* 2007). In addition, the frequency of circulating endothelial

cell are increased within patients with severe atherosclerotic disease, thus their quantification can potentially be used as a bio-marker and therefore predict risk of future cardiovascular events (Boos *et al.,* 2007). Therefore, the possibility that circulating endothelial cells contributed and/or were responsible for the marked PECAM-1 and VE-cadherin levels observed within the *in vitro* macrophages studies included within this chapter is highly unlikely, as the monocytes were isolated from healthy volunteers. Moreover, the culture media used in this study supports the differentiation and maintenance of monocyte/macrophage populations and is not recommended for endothelial cells, therefore, theoretically any possible circulating (mature) endothelial cells or stem/progenitor cells should have a reduced chance of survival under the culture conditions deployed in this study.

Furthermore, the isolation of blood-derived monocytes was also performed through deployment of an indirect magnetic-bead cell-sorting technique which yields highly pure unlabelled monocytes ($CD14^+$) before further adherence separation. Pertinently, $CD14^+$ monocytes obtained from healthy individuals and chronic myeloid leukaemia patients potently supressed the growth of *in vitro* haematopoietic progenitor cells (i.e $CD34^+$) (Heissig *et al.,* 2000). In another study, it was demonstrated that endothelial cell colonies do not survive in the presence of monocyte/macrophage colonies (Lindner *et al.,* 1997). Therefore, these two lines of evidence strongly suggest that it is likely the cells isolated and assessed within the studies described in this chapter are of a monocyte/macrophage lineage and not from any contaminating circulating endothelial cells or their progenitors.

In line with the previous results chapter, *in vitro* GM-CSF matured/polarised human monocyte-derived macrophages (GM-Mac) displayed higher expression levels of the assessed endothelial cell-related markers than their M-CSF differentiated (M-Mac) counterparts. As emphasised before, GM-CSF is associated with inducing a pro-inflammatory macrophage phenotype and taken together, the results in this chapter and its predecessor strongly suggest that GM-CSF induces macrophages to display not only a VSMC-like phenotype but also an endothelial cell-like phenotype, as determined

by their expression of specific genes/proteins. This implies that *in vitro* peripheral blood-derived macrophages following polarisation with colony stimulating factors, mainly GM-CSF, exhibit progenitor potential and have the capacity to *trans*-differentiate towards other vascular cell types such as VSMCs and ECs. This raises question whether M-Mac and GM-Mac subsets can behave like vascular wall-chameleon cells, differentiating into any cell type. As such, it will be interesting to further assess the potential of *in vitro* macrophages under the direction of M-CSF or GM-CSF to acquire properties of other resident vascular cells such as fibroblasts, which is a common cell type located within the connective tissue surrounding the vascular wall and perivascular adipocytes which play an important regulatory role during vascular inflammation (Britton and Fox, 2011; Stenmark *et al.,* 2013).

Interestingly, GM-CSF has also been shown to promote the development and function of endothelial progenitor cells (EPCs) (Cho *et al.,* 2003; Qiu *et al.,* 2014; Wang *et al.,* 2009). In particular, GM-CSF was demonstrated to promote the re-endothelialisation of injured arteries within a rabbit balloon-injury model, assessed through cellular expression of CD31 (PECAM-1) (Cho *et al.,* 2003). This beneficial effect was attributed to the enhanced mobilisation and growth of EPCs at the site of vascular injury. However, the validative *in vitro* aspects of the study relied upon the use of PBMCs and did not assess if the EPCs (CD31+ cells) were of a monocytic lineage. Indeed, two further studies (Qiu *et al.,* 2014; Wang *et al.,* 2009) utilised mouse bone marrow-derived cells and PBMCs, respectively, to generate EPCs through culture in 'endothelial cell culture media' supplemented with GM-CSF. In both studies the EPCs were characterised and validated through their expression of CD31, ability to form colonies, and capacity to uptake modified lipoproteins (acetylated-LDL), which are all properties characteristic of macrophages, including CD31 expression in GM-CSF matured macrophages as shown in this chapter. Again, the possibility that the 'EPCs' were not of monocyte origin was not determined. Consequently, given the findings within this chapter it can be speculated that monocyte differentiation in the presence of GM-CSF promotes their differentiation towards an

endothelial cell-like phenotype that can play a protective barrier function role during vascular injury, and may have been previously mis-identified as endothelial progenitor cells. Although not assessed within this chapter, it would be pertinent to evaluate if indeed GM-CSF polarised macrophages acquire endothelial cell properties, in addition to simply elevating their expression of PECAM-1 (CD31) and VE-cadherin.

Surprisingly, stimulation with VEGF-A or FGF2, which both support phenotypic modulation of endothelial cells (Cross and Claesson-Welsh, 2001) endows M-CSF directed macrophages with endothelial cell-like characteristics as inferred by the up-regulation of PECAM-1 and VE-cadherin. However, neither growth factor altered the expression levels of the endothelial cell-related genes/proteins in GM-CSF directed macrophages. Indeed, it was interesting to note that the increased PECAM-1 and VE-cadherin expression induced in M-CSF macrophages through stimulation with VEGF-A or FGF2 brought the expression to comparable levels as those detected in unstimulated GM-CSF matured macrophages. These findings infer that GM-CSF polarised macrophages may behave as a well-differentiated (or stable) phenotype compared to M-CSF directed macrophages, and that the M-CSF-directed macrophage population can be further modulated into EC-like cells or a proangiogenic phenotype through stimulation with the angiogenesis-associated growth factors VEGF-A or FGF2. Furthermore, both VEGF-A and FGF2 are considered as pro-inflammatory cytokines (Andrés *et al.,* 2009; Reinders *et al.,* 2003), thus in the presence of these growth factors M-CSF macrophages may potentially shift from an anti-inflammatory subset (Di Gregoli *et al.,* 2017; Johnson *et al.,* 2014; Johnson *et al.,* 2008), towards a more pro-inflammatory phenotype, behaving more closely to their GM-CSF counterparts.

Another exciting finding within this chapter is the inverse relationship between the mRNA and protein expression of VE-cadherin in M-CSF directed macrophages, particularly under stimulation with FGF2. This novel observation suggests FGF2 induces a post-translational mechanism in M-CSF macrophages to regulate VE-cadherin protein levels, raising the possible role of a microRNA-

dependent process, and warrants further investigation. Indeed, the post-transcriptional regulation of VE-cadherin forms the main body of work within the next chapter.

4.6 Conclusion

The findings within this chapter demonstrate that *in vitro* human monocyte-derived macrophages express genes and proteins which are commonly associated with endothelial cells, supporting the proposition that primary macrophages harbour the potential to *trans*-differentiate towards an endothelial cell-like phenotype. Additionally, macrophage polarisation towards pro-inflammatory and anti-inflammatory phenotypes modulates expression of endothelial cell-associated markers, with GM-CSF-directed maturation favouring *trans*-differentiation towards an endothelial cell-like phenotype. Nevertheless, the *trans*-differentiation of macrophages into an endothelial cell-like phenotype is probably not permanent, as the levels of the endothelial markers PECAM-1 an VE-cadherin are markedly lower when compared to their expression in HUVECs, suggesting the macrophages maintain their original and distinct haematopoietic cell lineage and the transformation towards an endothelial cell-like phenotype is transient. In summary, based upon the findings within this chapter and the previous results chapter, we can conclude that macrophages *in vitro* harbour the potential to serve as vascular progenitor cells.

5 Regulation of VE-cadherin expression in macrophage by miR-27a-FGFR1-STAT3 pathway

5.1 Introduction

5.1.1 The role of macrophage in angiogenesis

Angiogenesis is the formation of new blood vessels that occurs throughout life. It is an essential step in the development of an organ during embryogenesis, and subsequent body growth and maturation. Numerous biological process such as wound healing and menstruation also require angiogenesis to be in place. Angiogenesis is also implicated in the pathogenesis of various vascular conditions including tumorigenesis and atherosclerosis (Carmeliet, 2003). Essentially, the balance between pro-angiogenic mediators (such as VEGF, MMP9 and hypoxia) and anti-angiogenic factors (such as thrombospondin-1 and interferon β) regulates angiogenesis through controlling the angiogenic switch of endothelial cells (Ribatti *et al.,* 2007).

In addition to endothelial cells, macrophage have also been shown to play an active and central role in angiogenesis. Reportedly, an *in vivo* study using mice with deficiency in PU.1, a regulator of macrophage differentiation, showed reduced vascular network formation within the hindbrain vessels of 11.5-day post-coital mice, and the retina of post-natal mice, attributed to the failure of macrophages to mature (Fantin *et al.,* 2010). One of the essential roles ascribed to macrophages during angiogenesis is to link endothelial tip cells, as proven by laser confocal observation in a zebrafish angiogenesis model (Fantin *et al.,* 2010).

Macrophages also secrete several cytokines/growth factors which can support angiogenesis such as VEGF, TNF-α and TGFβ1 (Corliss *et al.,* 2016). These factors act through paracrine stimulation to promote the sprouting of endothelial tip cells. In addition, during vessel pruning and remodeling, macrophages can secrete molecules capable of retarding angiogenesis such as thrombospondin 1 and 2, in order to stabilise newly formed vessels (Lawler and Lawler, 2012).

Another important role macrophages play in angiogenesis is the modulation of extracellular matrix breakdown through the release of matrix metalloproteinases (i.e MMP-9). MMPs degrade extracellular matrix proteins in order to facilitate endothelial cell migration while also contributing to vascular permeability by degradation of endothelial cell basement membrane proteins (van Hinsbergh and Koolwijk, 2008).

A recent study using a novel live imaging technique showed macrophages mediate vascular repair within the zebrafish brain by adherence to damage-induced gaps between endothelial cells with subsequent mechanical traction to seal the gap (Figure 5.1.1) (Liu *et al.,* 2016). The study proposed that ATP release is required from the injured endothelial cells to recruit macrophages to the site of damage. This finding suggests that macrophages can temporarily acquire endothelial-like properties to provide transient barrier function while also facilitating the repair of damaged blood vessels.

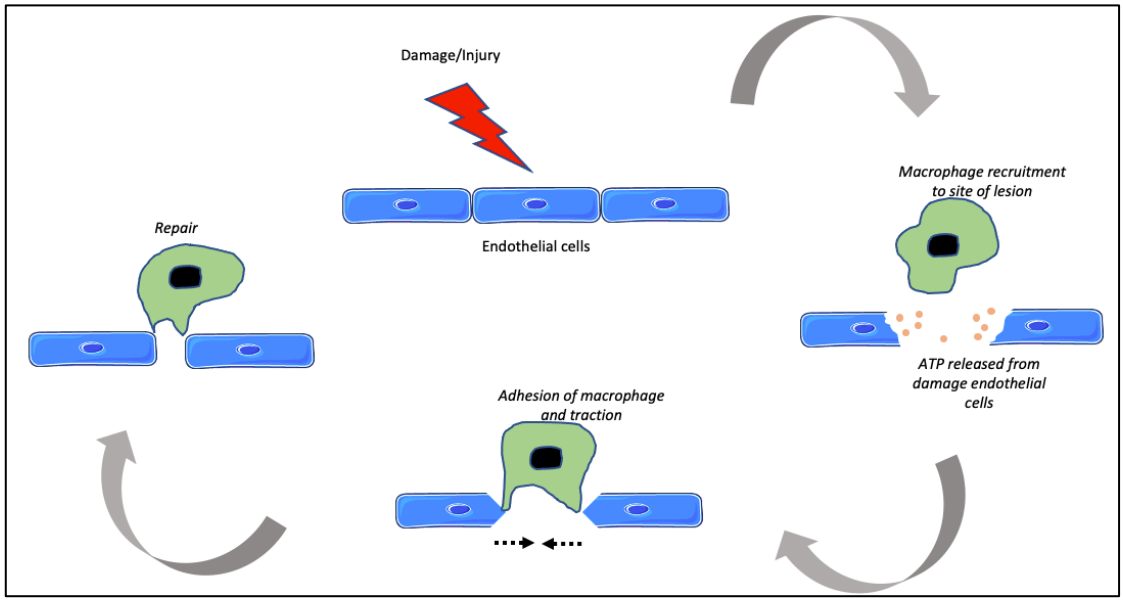

Figure 5.1.1 Macrophage role in brain endothelium repair
Upon blood vessel rupture, ATP released from injured endothelial cells serves as a chemoattractant for macrophage migration towards the site of injury. Subsequently, macrophages directly adhere to breaking points employing adhesion molecules such as CDH5 (VE-cadherin) and PECAM-1 to close the gap (Liu et al. 2016). Next, the macrophage may exert tensional forces to bring the two endothelial cells together. Image adapted from original source (Liu et al. 2016) and made using elements retrieved from https://smart.servier.com.

5.1.2 Non-endothelial vasculature

The formation of a vascular network from non-endothelial cells occurs during placenta development, whereby epithelial cells *trans*-differentiate into endothelial-like cells (Zhou *et al.,* 1997a). This is evidenced through the upregulation of adhesion molecules such as VE-cadherin, PECAM-1 and α4-integrin by *in vitro* human cytotrophoblasts (foetal placental cells) (Zhou *et al.,* 1997a). This finding is supported by the analysis of tissue-sections from pre-eclampsia affected human placentas, which demonstrated that foetal placental cells are deficient for αV-family-integrins, VCAM-1 and VE-cadherin, suggesting that during pre-eclampsia there is a defect in normal placenta vasculature, which is now known as endovascular invasion, a commonly described pathology in pre-eclampsia placenta (Zhou *et al.,* 1997b).

Another term commonly used for a non-endothelial vessel is vascular mimicry. It is described as the formation of functional vascular channels by cancer cells (Fernández-Cortés *et al.,* 2019). One of the earliest documented accounts of vascular mimicry was through the histological analysis of solid melanoma tumours, which showed tube structures filled with erythrocytes (Maniotis *et al.,* 1999). Subsequent immunohistochemical analysis of the cells of the melanoma vasculature showed lack of markers such as CD31, CD34, and VEGFR2 (KDR/Flk-1), which implies the presence of non-endothelial derived vessels (Maniotis *et al.,* 1999). This finding was further supported by *in vitro* observations which demonstrated that aggressive forms of melanoma developed tube structures with perfusion characteristics on matrigel/type I collagen assay that were not endothelial cell-derived (Maniotis *et al.,* 1999). Similarly, the vasculature within glioblastoma tumours are comprised of a mixture of neoplastic cells and endothelial cells (Ricci-Vitiani *et al.,* 2010). Furthermore, a significant reduction in tumour growth was associated with reduced vessel network when glioblastomas were treated with intra-peritoneal ganciclovir, which is known to target neoplastic cells rather than endothelial cells (Ricci-Vitiani *et al.,* 2010). In addition, vascular mimicry has been documented by *in vitro* and *in vivo* studies using various human-derived tumour cells such as breast

cancer (Shirakawa *et al.,* 2002), colon cancer (Baeten *et al.,* 2009), ovarian cancer (Qi *et al.,* 2014) and lung cancer (Yao *et al.,* 2014).

Intriguingly, a recent report showed vascular mimicry derived from macrophages as indicated by positive CD163 immunohistochemical staining of the vasculature of solid tumours of melanoma, schwannoma, cerebellar haemangioma, meningioma and glioblastoma (Barnett *et al.,* 2016). This finding was supported by *in vivo* angiogenesis studies, whereby F4/80 and CX3CR1^{GFP} macrophages formed networks of interconnected cells with cord and filopodial extensions. Interestingly, these proposed macrophage-derived cells also expressed the endothelial cell marker CD31 (Barnett *et al.,* 2016). The authors also revealed that hypoxia inducible factor (HIF-1α) played an important role in the formation of vascular mimicry, as HIF-1α knockout mice presented reduced network formation and tumour growth (Barnett *et al.,* 2016).

5.1.3 MicroRNA and angiogenesis

MicroRNAs (miR) are small non-coding single stranded RNA molecules comprised of between 19-25 nucleotides (O'Brien *et al.,* 2018). Unlike messenger RNA (mRNA), microRNA are not translated into proteins, but regulate translation of target mRNA into protein through a post-transcriptional mechanism, therefore the more abundant a microRNA, the lower the protein level of its targeted mRNA. Although contradictory with the majority of the published literature, it has been claimed that microRNA may potentially activate and upregulate protein translation (Vasudevan, 2012), for example miR-466l expressed in mouse embryonic cells is associated with upregulation of IL-10 (Ma *et al.,* 2010), although there is limited evidence in human cells demonstrating microRNA expression is associated with the upregulation of protein translation.

Within the nucleus, microRNA are transcribed from their respective DNA sequence (genome) as a primary transcript (pri-microRNA) by the RNA polymerase II enzyme, the same enzyme which transcribes mRNA from DNA sequences. Pri-microRNA consists of around 60-70 nucleotides in the form of hairpin stem loop structure. Subsequently, pri-microRNA are cleaved by an enzyme which

belongs to the ribonuclease III family called Drosha, which results in the generation of a shorter nucleotide called a precursor microRNA (pre-microRNA) hairpin.

The Drosha enzyme requires the nuclear protein known as DiGeorge Syndrome Critical Region 8 (DGCR8) as a co-factor, in order to recognise and bind pri-microRNA. Both Drosha and DGCR8 form a multi-processor complex whereby in the absence of DGCR8, pri-microRNA may not be cleaved into pre-microRNA (Gregory *et al.,* 2004). Nuclear pre-microRNA are then transported into the cytoplasm by nuclear transport factor exportin 5 before being processed by cytoplasmic a RNAse III enzyme called Dicer to generate a microRNA duplex which is comprised of two substrings called the 5' strand and 3' strand. Eventually, only one strand will be incorporated into the silencing complex of mature microRNA (called the guide strand) which can be either of the 5' or 3' strands (Karathanasis *et al.,* 2015). The unloaded strand is called the passenger strand (abbreviated as microRNA*), and may undergo degradation. The description of microRNA processing described above is a canonical pathway for microRNA biogenesis, although reportedly, some microRNA biogenesis may skip either the Drosha or Dicer cleavage steps (O'Brien *et al.,* 2018). The microRNA-silencing complex consists of the microRNA guide strand and a protein called argonaute (AGO). AGO is increasingly recognised as an important factor for the proper function of microRNA as a protein silencing mechanism.

The silencing of protein translation is achieved by base-pairing of the microRNA with the target 3' or 5' untranslated region (UTR) of messenger mRNA (mRNA) to result in mRNA destabilisation and degradation (when complete alignment occurs – such as in plants) or by inhibition of protein translation when partial alignment takes place, as is the case in mammalian cells. Reportedly, besides 3' and/or 5' UTR mRNA, microRNA may also form silencing complexes with coding sequences or gene promoters (O'Brien *et al.,* 2018). The interaction of microRNA and their target mRNA depends on several factors, including microRNA availability within the cytoplasm, the abundance of the microRNA and the target mRNA, and the interaction affinity (O'Brien *et al.,* 2018). Interestingly, microRNA may also be released from cells by means of vesicular particles or binding

proteins to regulate protein expression in other cells. For instance, an *in vitro* study demonstrated that tumour-associated macrophages release exosomes enriched in microRNA-223 which can enter and regulate the invasiveness of breast cancer cells through targeting of myocyte enhancer factor (MEF2C) (Yang *et al.,* 2011), thus released microRNA can also be regarded as a form of paracrine intercellular messenger (Chen *et al.,* 2012).

Recent updates have now documented more than 1900 precursors and more than 2500 mature microRNA sequences from the human genome (Kozomara *et al.,* 2019). Each single microRNA may have a dual role for example, it modulates cell proliferation in one cell type but inhibit cell growth in others (Shen *et al.,* 2019). Nevertheless, the biological function of most microRNAs remains to be discovered. Another unique feature of microRNAs is the diversity of their targets, which affects an enormous number of genes, in other words it is not limited to a single target, with most individual microRNAs having >500 predicted mRNA targets (Shen *et al.,* 2019).

There is a growing body of evidence which supports the role of microRNAs in physiology as well as diseases (O'Connell *et al.,* 2010). This includes the regulation of immune cells including the early development of haematopoietic cells, myeloid cell development, as well as regulation of adaptive immune cell (T and B cells) development (O'Connell *et al.,* 2010). Of interest, the expression of a cluster of microRNAs (miR-17-5p, miR-20a and miR-106a), which can all target and therefore repress Runt-related transcription factor 1 (RUNX1) expression, are all decreased during the differentiation and maturation of monocytes from their haematopoietic progenitors. Mechanistically, the RUNX1 transcription factor withdrives the expression of the M-CSF receptor to promote the differentiation and maturation of monocytes (O'Connell *et al.,* 2010). Studies have identified microRNAs which are elevated in macrophages during inflammation, miR-155 (O'Connell *et al.,* 2007) and miR-9 (Bazzoni *et al.,* 2009). In contrast, some microRNA, for instance, miR-146a, can repress inflammation through the targeting of mRNA which participate in the NFκB pro-inflammatory pathway, such as IL-1R-associated kinase1 (IRAK1) and TNFR-associated factor 6 (TRAF6) (Gao *et al.,* 2015).

MicroRNAs have also been documented to play a contributory role in angiogenesis, whereby deletion of the Dicer enzyme (resulting in global microRNA reduction) lead to defective angiogenesis both *in vitro* (Shilo *et al.,* 2008; Suárez *et al.,* 2007) and *in vivo* (Suárez *et al.,* 2008). Specific microRNAs proposed to regulate angiogenesis include miR-126, miR-221/222, miR-23/27, and the miR-17-92 cluster (Caporali and Emanueli, 2011; Wang and Olson, 2009). For example, miR-126 knockdown mice are embryogenically lethal due to generalised oedema and vascular abnormalities from failed angiogenesis (Wang *et al.,* 2008). Target mRNA of miR-126 include Sprouty-related EVH domain-containing protein (Spred-1) (Wang *et al.,* 2008), phosphoinositol-3 kinase (PI3K) regulatory subunit 2 (Fish *et al.,* 2008) and VCAM-1 (Harris *et al.,* 2008). Accordingly, Spred-1 and PI3K regulatory subunit 2 repression are associated with anti-angiogenic signalling through regulation of the VEGF pathway (Fish *et al.,* 2008). In addition, miR-126 shares close gene location with epidermal growth factor-like domain 7 (Egfl7), which is responsible for bridging endothelial cells during angiogenesis (Nikolic *et al.,* 2010), thus, both miR-126 and Efgl7 may work in concert to promote angiogenesis, although Efgl7 is not a target gene for miR-126, but may be up-regulated simultaneously.

The miR-221/222 cluster are further microRNAs associated with angiogenesis , as they exert anti-proliferative, anti-migratory and pro-apoptotic effects in endothelial cells to serve as angiogenesis inhibitors (Celic *et al.,* 2017). In addition, miR-221/222 are implicated in VSMC proliferation and neointimal hyperplasia (Liu *et al.,* 2009), through opposing effects to that in endothelial cells. The proposed target mRNAs for the miR221/222 cluster are stem cell factor/c-kit (Poliseno *et al.,* 2006) and signal transducer and activator of transcription 5A (STAT5A) (Dentelli *et al.,* 2010).

MicroRNA-210 is one of the most widely investigated microRNAs. Besides its association with hypoxia and VEGF induced angiogenesis (Wang and Olson, 2009), it is also implicated in various biological process such as erythropoiesis (Kosaka *et al.,* 2008), neurogenesis (Zeng *et al.,* 2014), spermatogenesis (Duan *et al.,* 2016) and bone cell differentiation (Mizuno *et al.,* 2009). In addition,

miR-210 is associated with the progression of various tumours including lung cancer (Puisségur *et al.,* 2011), renal cell carcinoma (Samaan *et al.,* 2015), colorectal carcinoma (Tagscherer *et al.,* 2016) and liver cancer (Ji *et al.,* 2018). Thus miR-210 has many proposed effector target mRNAs such as NFκB (Yu *et al.,* 2009), activin A receptor type 1B (Mizuno *et al.,* 2009), electron transport chain (Puisségur *et al.,* 2011), and CXC chemokine receptor 4 (Feng *et al.,* 2018). Reportedly, the miR-17-92 cluster is associated with human adenocarcinoma angiogenesis through targeting thrombospondin-1 and connective tissue growth factor (CTGF, also known as CCN2), both are anti-angiogenesis factors (Dews *et al.,* 2006).

In addition, multiple microRNA are proposed to be involved in macrophage polarisation, for example miR-155, miR-127 and miR-125b. Reportedly, miR-155 targets the IL-13/STAT6A pathway to prevent M2 phenotype polarisation, while blocking miR-155 is associated with reduced M1 polarisation (Cai *et al.,* 2012). In addition, an *in vivo* study showed miR-155 knockdown was associated with reduced M1 and increased M2 macrophage infiltration within the remodelling heart with elevation of IL-1 and IL-14 alongside reduced IFNγ expression (Zhang *et al.,* 2016). M1 polarisation is associated with increased expression of miR-127, and is suppressed by IL-4, TGFβ and IL-10 (Ying *et al.,* 2015). In addition, an *in vivo* study showed that forced expression of miR-127 resulted in upregulation of pro-inflammatory cytokines upon LPS stimulation in alveolar macrophages (Ying *et al.,* 2015). On a different note, microRNAs which are associated with M2 polarised macrophages include miR-146a (Li *et al.,* 2016), miR-511-3p (Squadrito *et al.,* 2012), miR-223 (Zhuang *et al.,* 2012), and let-7c (Zhang *et al.,* 2015).

5.2 Aim of this chapter

The inverse relationship between VE-cadherin mRNA and protein expression in M-CSF directed macrophages observed within the previous results chapter warrants further investigation, particularly the potential involvement of microRNA regulation. This is in line with previous reports

whereby divergent miR-24 and miR-181b levels between M-CSF and GM-CSF directed macrophages was observed (Di Gregoli *et al.,* 2014; Di Gregoli *et al.,* 2017).

Based on these findings, this chapter aims to investigate the potential microRNA-mediated regulation of VE-cadherin protein expression in *in vitro* macrophages. This chapter also aims to investigate the role of the FGF2 receptor and its downstream signalling pathway, signal transducer and activator of transcription-3 (STAT3), on microRNA-mediated VE-cadherin expression, and finally to investigate *in vitro* angiogenesis potential of macrophage subsets.

5.3 Materials and Methods

5.3.1 Macrophage culture and stimulation with FGF2 growth factor

Human monocyte-derived macrophages were isolated and generated as outlined in methods section 2.1. M-CSF directed macrophages (M-Mac) were maintained in culture for seven-days followed by stimulation with 50 ng/ml human recombinant FGF2 for four-days. In addition, magnetic-bead cell sorting and purification for purified pan-monocyte populations were also performed to obtain pure CD14+ and CD16+ monocytes according to the protocol described in section 4.3.1.

5.3.2 Quantitative-PCR for microRNAs

Through utilising the microRNA online database (www.targetscan.org), three mature microRNAs were identified that are predicted to target human VE-cadherin, which are microRNA-27a, microRNA-101 and microRNA-125. Accordingly, the expression of both the 3p and 5p strands for each microRNA were analysed in the seven-day differentiated macrophages, with and without subsequent four-day stimulation with FGF2. At the end of the experiments, microRNA from samples were collected according to the method as described in section 2.4. Quantitative-PCR (Q-PCR) reaction as described in section 2.8 was performed using the Qiagen primer assay (Table 5.3.1). Detection of each microRNA was performed with 10X universal primer (Qiagen Cat. No. 218300) according to the reaction in Table 5.3.2, 10X miScript primer assay was prepared by adding 550 ml TE, pH 9.0 and vortexed prior to aliquoting in DNAse free tubes.

Table 5.3.1 Primer assay used for QPCR

Qiagen miScript primers contain a mix of lyophilized primer for a specific microRNA. Each assay is derived from mature human microRNA sequences in the miRbase database (https://microrna.sanger.ac.uk).

Assay name	Gene symbol	Cat. No.	Sequence
Hs_miR-27a-3p	MIR27A	MS00003241	UUCACAGUGGCUAAGUUCCGC
Hs_miR-27a-5p	MIR27A	MS00009240	AGGGCUUAGCUGCUUGUGAGCA
Hs_miR-101-3p	MIR101-1	MS00008379	CAGUUAUCACAGUGCUGAUGCU
Hs_miR-101-5p	MIR101-1	MS00008372	UACAGUACUGUGAUAACUGAA
Hs_miR-125b-3p	MIR125B1	MS00008561	UCCCUGAGACCCUAACUUGUGA
Hs_miR-125b-5p	MIR125B1	MS00008693	UCCCUGAGACCCUAACUUGUGA

Table 5.3.2 Master reaction mixture LightCycler® 480 SYBR Green I Master for microRNA Q-PCR

Reagent/components	Volume (µl)
Water, PCR grade	3
10X miScript Primer Assay	0.5
10X miScript universal primer	0.5
SYBR Green I Master	5
Total volume/reaction	9

The Q-PCR reaction was performed in a similar method as described in section 2.8, by which 1µl of the sample (cDNA at the same concentration) were added to the reaction mix (Table 5.3.2) for a total volume of 10µl QPCR reaction. Similar reaction protocol as described in the section 2.8 was applied, however the annealing temperature was set at 55^{o}C according to the manufacturer instructions.

5.3.3 Transfection experiment

Following analysis of microRNAs in section 5.3.2, microRNA-27a-3p was found to show a regulatory association with VE-cadherin expression. In order to evaluate the effects of microRNA-27a-3p on VE-cadherin expression in human macrophage cultures, transfection experiments through incubation with either a microRNA-mimic or -inhibitor (Table 5.3.3) were performed in the seven-day differentiated human macrophages. A chimeric peptide derived from rabies virus glycoprotein nona-D-arginine, RVG-9dR, was used as a vehicle to deliver the microRNA-mimic or -inhibitor into the cell using serum free (reduced) antibiotics media (Opti-MEM, Thermo Fisher Cat. No. 31985062) over a four-hour incubation period at 37^{o}C. Firstly, the RVG-9dR complex with either the microRNA-mimic or -inhibitor were incubated at room temperature for 10 min to allow the formation of transfection complexes before addition to the cells. A previous report demonstrated the efficacy of using RVG-9dR as a tool to increase RNA complex uptake by macrophages and ensuing induction of gene silencing in macrophages and microglia (Kim *et al.,* 2010). Negative controls were also deployed which consist of a scrambled equal length of RNA (Table 5.3.3). After a four-hour incubation, the

media was replaced with 10% FCS/RPMI (full) media with subsequent four-day stimulation with FGF2.

Table 5.3.3 Reagents used in transfection experiment
(RVG-9dR = Chimeric Rabies Virus Glycoprotein Fragment)

Reagent	Supplier/Cat No.	Stock concentration	Working concentration
Syn-hsa-miR-27a-3p miScript miRNA Mimic	Qiagen/ MSY0000084	20 μM	5 nM
Anti-hsa-miR-27a-3p miScript miRNA Inhibitor	Qiagen/ MIN0000084	20 μM	5 nM
RVG-9dR	GenScript/ SC1208	1 mM	1 μM
All Stars Negative Control siRNA	Qiagen/ SI03650318	20 μM	5 nM

5.3.4 Neutralising FGFR1-antibody experiment

To assess the association of FGF-receptor 1 (FGFR1)-mediated signalling to VE-cadherin expression by FGF2 in M-CSF-matured macrophages (M-Mac), a neutralising antibody (NAb) experiment using a monoclonal immunoglobulin G (IgG) antibody raised against human FGFR1 was performed. The antibody was a human FGF R1 (IIIb) monoclonal mouse IgG1 antibody (Cat. number: MAB765; R&D systems), and was used at a concentration of 1 μg/ml. The antibody was added to 7-day differentiated M-Macs alongside recombinant FGF2 for 4 days. Mouse IgG1 at the same IgG concentration was used as a control.

5.3.5 STAT3 inhibitor experiment

In order to evaluate the regulatory role of the STAT3 transcription factor to FGF2-induced VE-cadherin protein expression in M-CSF directed macrophages, niclosamide, a known STAT3 inhibitor and widely used as an antihelminth drug (Chen *et al.,* 2018), was assessed in M-CSF directed macrophages. A dose dependent effect was evaluated with 1, 5 and 10 μM concentrations of niclosamide. Reportedly, niclosamide showed a dose-dependent inhibition of STAT3 phosphorylation in a human prostate cancer cell line (Ren *et al.,* 2010). In brief, seven-day differentiated M-CSF directed macrophages were stimulated with FGF2 (50ng/ml) alongside niclosamide at

concentrations of 1, 5 and 10 μM. Niclosamide (50mg) (cat. number 4079/50; Bio-techne Ltd) was diluted in dimethyl sulfoxide (DMSO), accordingly, a DMSO (vehicle) control was also used.

5.3.6 Matrigel angiogenesis assay

To investigate the angiogenic potential of macrophage subsets, the formation of tube/network-like structures was assessed using a Matrigel angiogenesis assay. In brief, M-CSF and GM-CSF matured macrophages were seeded at $1x10^4$ on Matrigel (Growth factor-reduced Matrigel; Scientific Lab Supplies, cat. no.354230; stored at −20 °C) within the wells of a 48-well plastic tissue culture plate. The effects of recombinant human FGF2 (50ng/ml) was assessed, and live cell images captured at 10x magnification after 24 hours seeding. The effect of STAT3 inhibition with niclosamide on tube formation in M-CSF directed macrophages was also assessed. In brief, M-CSF matured macrophages were seeded at $1x10^4$ on Matrigel within the wells of a 48-well plastic tissue culture plate with and without niclosamide or with the relevant concentration of DMSO as a control. Live cell images were captured at 4x magnification after 24 hours seeding. In all experiments, images from four random fields were examined, and the number of tube-like structures were determined and plotted against control/baseline.

5.4 Results

In the previous results chapter (Figure 4.4.11), an inverse relationship between VE-cadherin mRNA and protein expression was detected in M-CSF macrophages, suggesting the role of a post-translational mechanism such as microRNA regulation of VE-cadherin protein levels. Stimulation with FGF2 markedly suppressed VE-cadherin mRNA levels while protein expression was significantly upregulated in M-CSF matured macrophages (Figure 4.4.11; Chapter 4). Furthermore, the observation that VE-cadherin mRNA expression remained unchanged by stimulation with other endothelial cell-related growth factors but concomitantly upregulated of VE-cadherin protein expression, further supports the post-translation regulation of VE-cadherin in macrophages (Figure 4.4.11; Chapter 4). Interestingly, such a divergent regulation of VE-cadherin mRNA and protein levels was not observed in GM-CSF matured macrophages. Based upon this finding, the expression of three microRNAs predicted to target VE-cadherin (miR-27a, miR-101, and miR-125) were analysed.

5.4.1 FGF2 stimulation downregulates microRNA-27a-3p expression in M-CSF directed macrophages

Assessment of the candidate microRNAs in human PBMC-derived macrophages matured with M-CSF or GM-CSF, showed detectable expression levels of miR-27a and miR-101, whereas miR-125 was not expressed in macrophages under any of the conditions (below the level of detection). Although miR-101-3p and miR-101-5p levels were readily detected, no significant differences in their expression were observed between macrophage phenotypes or after stimulation with individual EC-related growth factors (refer to appendix C, 10.1.1 and 10.1.2 for CT values). On the other hand, the expression of miR-27a-3p and miR-27a-5p were downregulated in GM-CSF directed macrophages (84%; $P<0.0001$; n=6; Figure 5.4.1 and 55%; $P<0.01$; n=6; Figure 5.4.2, respectively) compared to M-CSF directed macrophages. None of the endothelial cell-related growth factors affected miR-27a-3p or -5p levels in either subset with the exception of FGF2 stimulation, which significantly reduced miR-27a-3p expression in M-CSF matured macrophages (42%; $P<0.05$; n=6; Figure 5.4.1), without changing miR-27a-5p levels (Figure 5.4.2).

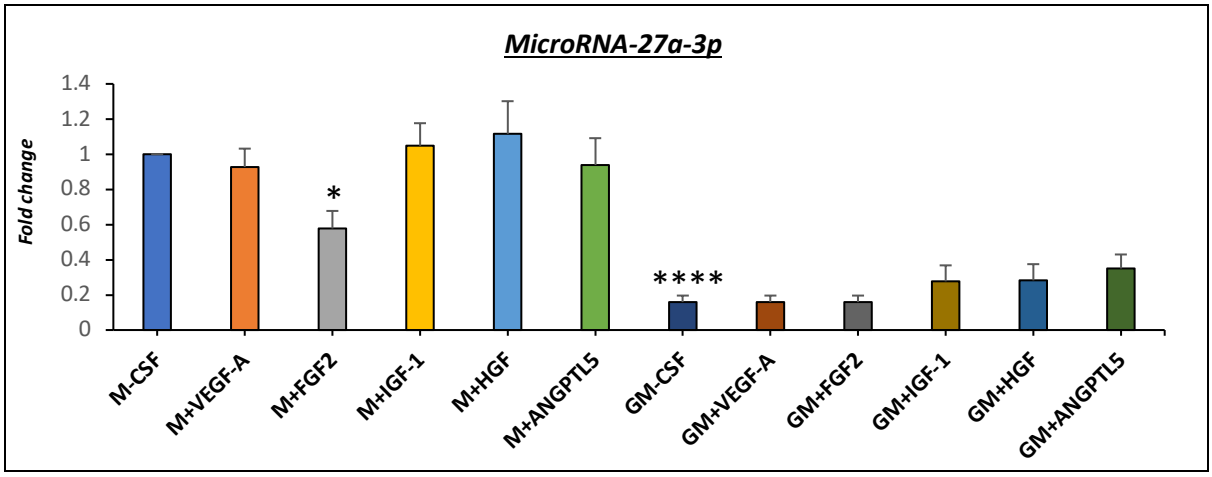

Figure 5.4.1 Expression of miR-27a-3p in human macrophage subsets.

QPCR analysis for miR-27a-3p levels in M-CSF and GM-CSF matured macrophages with subsequent four-day stimulation with 50 ng/ml VEGF-A, FGF2, IGF-1, HGF, or ANGPTL5, expressed as fold change compared to unstimulated M-CSF matured macrophages. (P < 0.05 and **** P < 0.0001 denotes significant difference compared to unstimulated M-CSF macrophages; one-way ANOVA Tukey's multiple comparison test; n=6). Refer appendix C (10.1.3) for CT-values. (M = M-CSF macrophage, GM = GM-CSF macrophage).*

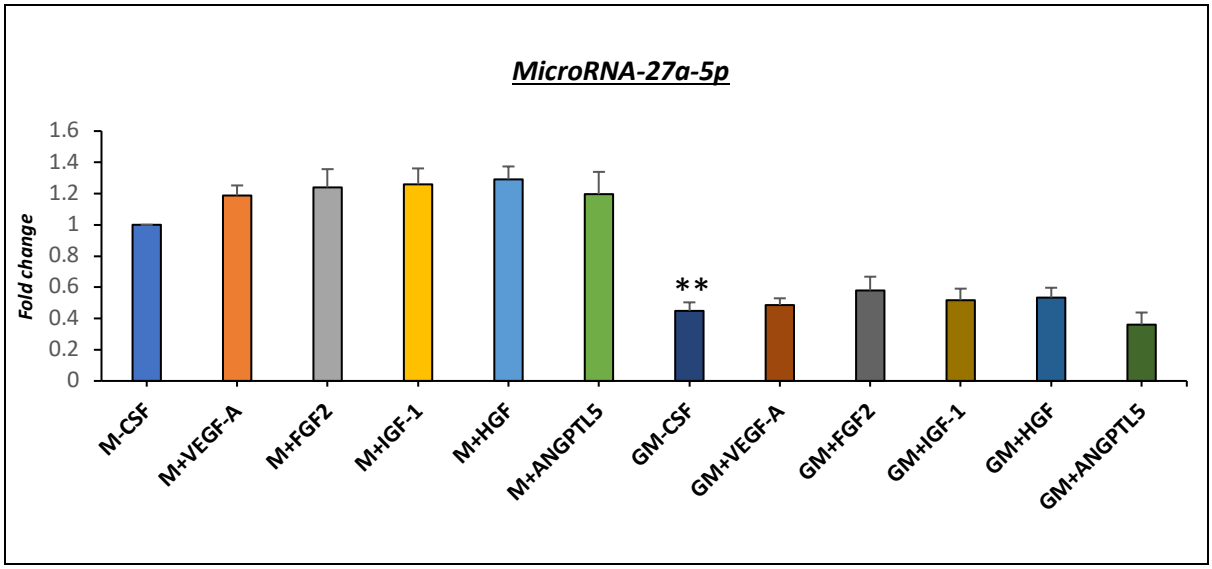

Figure 5.4.2 Expression of miR-27a-5p in human macrophage subsets

*QPCR analysis for miR-27a-5p levels in M-CSF and GM-CSF matured macrophages with subsequent four-day stimulation with 50 ng/ml VEGF-A, FGF2, IGF-1, HGF, or ANGPTL5, expressed as fold change compared to unstimulated M-CSF matured macrophages (** P < 0.01 denotes significant difference compared to unstimulated M-CSF macrophages; one-way ANOVA Tukey's multiple comparison test; n=6). Refer appendix C (10.1.4) for CT-values. (M = M-CSF macrophage, GM = GM-CSF macrophage).*

	M-Mac			GM-Mac		
	VE-cadherin mRNA	VE-cadherin protein	microRNA-27a-3p	VE-cadherin mRNA	VE-cadherin protein	microRNA-27a-3p
Control	1.0	1.0	1.0	1.0	2.3	0.1
FGF2	0.4	7.3	0.6	1.0	1.0	1.0

Figure 5.4.3 Summary of results for the relative VE-cadherin mRNA and protein expression alongside miR-27a-3p levels in M-CSF and GM-CSF matured macrophage subsets with and without FGF2 stimulation

Fold change in mRNA and protein expression (by Western blotting) of VE-cadherin and miR-27a-3p levels in seven-day matured M-CSF and GM-CSF human macrophages with and without subsequent four-day stimulation with FGF2. All data expressed as fold change relative to 11-day M-CSF directed macrophages without FGF2 stimulation, with red highlighting indicating significantly increased expression and green highlighting indicating significantly decreased levels.

For VE-cadherin mRNA and protein expression in; (i) M-CSF directed macrophages refer to Figure 4.4.11; (ii) GM-CSF directed macrophage refer to Figure 4.4.3 (comparison with 11-day M-CSF macrophages) and (iii) FGF2 effects on GM-CSF directed macrophages (refer to Figure 4.4.17). (M-Mac = M-CSF directed macrophage, GM-Mac = GM-CSF directed macrophage).

The results within the previous chapter showed higher protein expression of VE-cadherin in GM-CSF directed macrophages (2.3-fold-change; P <0.05; n=6; Figure 4.4.3 b) but equivalent mRNA levels in comparison to M-CSF directed macrophages (Figure 4.4.3 a). This pattern of elevated VE-cadherin protein expression in GM-CSF macrophages is associated with their reduced levels of miR-27a-3p (84%; P <0.0001; n=6; Figure 5.4.1). Interestingly, the addition of FGF2 to M-CSF directed macrophages upregulated VE-cadherin protein expression (7.3-fold-change; P<0.01; n=6; Figure 4.4.11) to match that observed in GM-CSF macrophages, without a complimentary increase in mRNA levels (Figure 4.4.11). The elevated VE-cadherin protein expression afforded through FGF2 stimulation was associated with reduced expression of miR-27a-3p in M-CSF directed macrophages (42%; P<0.05; Figure 5.4.1). However, the expression of VE-cadherin mRNA and protein expression as well as miR-27a-3p levels were unchanged by FGF2 addition to GM-CSF directed macrophages (refer to Figure 4.4.17 and Figure 5.4.1).

Taken together the effects of FGF2 on VE-cadherin mRNA and protein expression, and microRNA-27a-3p, are summarised in Figure 5.4.3. The divergent effects of VE-cadherin mRNA and protein

levels by FGF2 in M-CSF macrophage strongly related to the converse changes in miR-27a-3p levels, implying a regulatory role for this microRNA in regulating M-CSF macrophage VE-cadherin expression upon FGF2 stimulation.

5.4.2 Regulation of VE-cadherin protein expression by miR-27a-3p in M-CSF directed macrophages

In order to determine whether VE-cadherin protein expression regulation involves miR-27a-3p, M-CSF matured macrophages were transfected with either a miR-27a-3p mimic or inhibitor. A condition similar to overexpression of microRNA-27a-3p was created through addition of the mimic, whereas the inhibitor resulted in the disintegration of microRNA-27a-3p, thus similar to knockdown or downregulation of microRNA-27a-3p. Subsequently, the VE-cadherin protein expression was analysed in the presence of FGF2 (50ng/ml). This experiment was designed to validate the association of microRNA-27a-3p with VE-cadherin protein expression by FGF2 stimulation.

The results are shown in Figure 5.4.4 - Figure 5.4.8. Firstly, the All Stars Negative Control siRNA which was used to control for RVG-9dR-mediated transfection, showed comparable VE-cadherin protein expression in unstimulated (baseline) M-CSF matured macrophages. Similarly, VE-cadherin levels were equally up-regulated through FGF2 stimulation in control transfected (2.8-fold change; $P<0.05$; n-6; Figure 5.4.4) and non-transfected M-CSF macrophages (2.5-fold change; $P<0.05$; n-6; Figure 5.4.4). It was therefore concluded that RVG-9dR-mediatied transfection did not affect VE-cadherin regulation in M-CSF macrophage, validating this approach for the subsequent experiments involving miR-27a-3p modulation. Assessment of Western blotting revealed that the addition of a miR-27a-3p-mimic significantly downregulated (32%; $P<0.05$; n=6; Figure 5.4.5 a) VE-cadherin protein expression in M-CSF matured macrophages, while a miR-27a-3p-inhibitor markedly up-regulated VE-cadherin protein levels (2.6-fold change; $P<0.05$; n=6; Figure 5.4.5 b) , when compared to negative control macrophages. Additionally, FGF2-induced upregulation of VE-cadherin in M-CSF matured macrophages was significantly blunted through co-incubation with a miR-27a-3p-mimic (49%; $P<0.05$; n=6; Figure 5.4.5 c).

VE-cadherin protein expression was also evaluated by immunocytochemistry and showed similar results as those reported for Western blotting (Figure 5.4.6 and Figure 5.4.7). Baseline M-CSF

directed macrophages and negative control-transfected cells showed a comparable increase in the percentage of VE-cadherin positive macrophages, either unstimulated (69.9% and 71.7%, respectively; $P<0.05$; n=6; Figure 5.4.7a and b), or in response to FGF2 stimulation (79.3% and 85.0%, respectively; $P<0.05$; n=6; Figure 5.4.7a and b). As expected from the Western blotting results, the percentage of VE-cadherin positive macrophages was significantly increased with addition of a miR-27a-3p-inhibitor (84.3%) compared to the negative control cells (71.7%; $P<0.05$; n=6; Figure 5.4.7d). However, the miR-27a-3p-mimic increased VE-cadherin positive M-CSF macrophages (79.8%) compared to negative control (71.7%; $P<0.01$; n=6; Figure 5.4.7c) opposing the results obtained by western blot analysis. Nonetheless, under FGF2 stimulation, the percentage of VE-cadherin positive macrophages (63.4%) was markedly reduced in the presence of the miR-27a-3p-mimic, compared to negative control macrophages with FGF2 stimulation (85.5%; $P<0.01$; n=6; Figure 5.4.7 e).

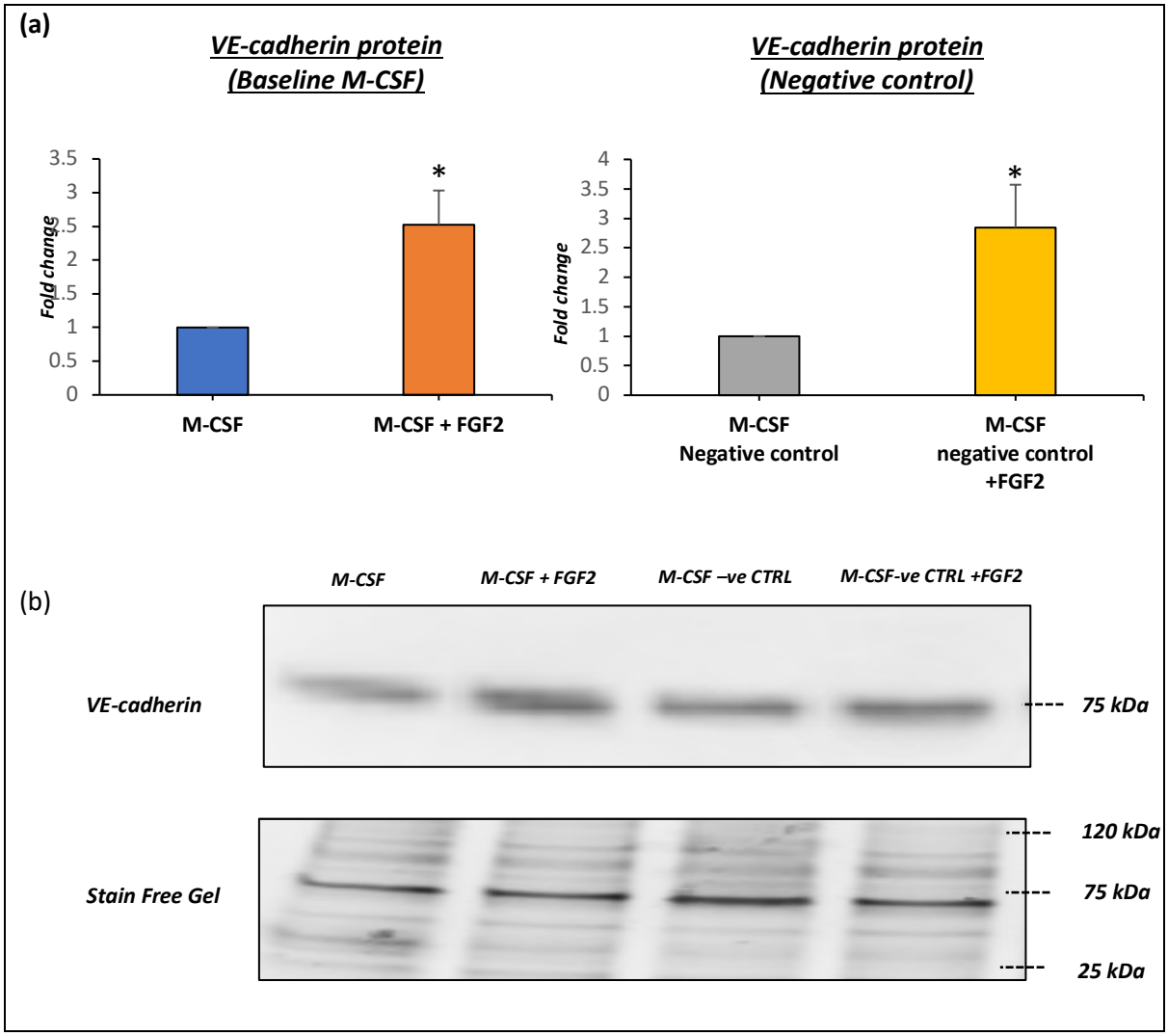

Figure 5.4.4 Validation of RVG-9dr-mediated transfection.

*(a) Quantification and (b) representative Western blotting of VE-cadherin protein expression in seven-day (baseline) M-CSF matured macrophages with and without FGF2 stimulation (50ng/ml), and with or without RVG-9dr-mediated transfection with a negative control scrambled RNA (negative control). Data are expressed as fold change against each control, (*P < 0.05 denotes significant difference compared to respective controls; paired t-test; n=6) (Stain free gel is shown as a loading control).*

Refer to appendix C (10.1.5) for full blot image.

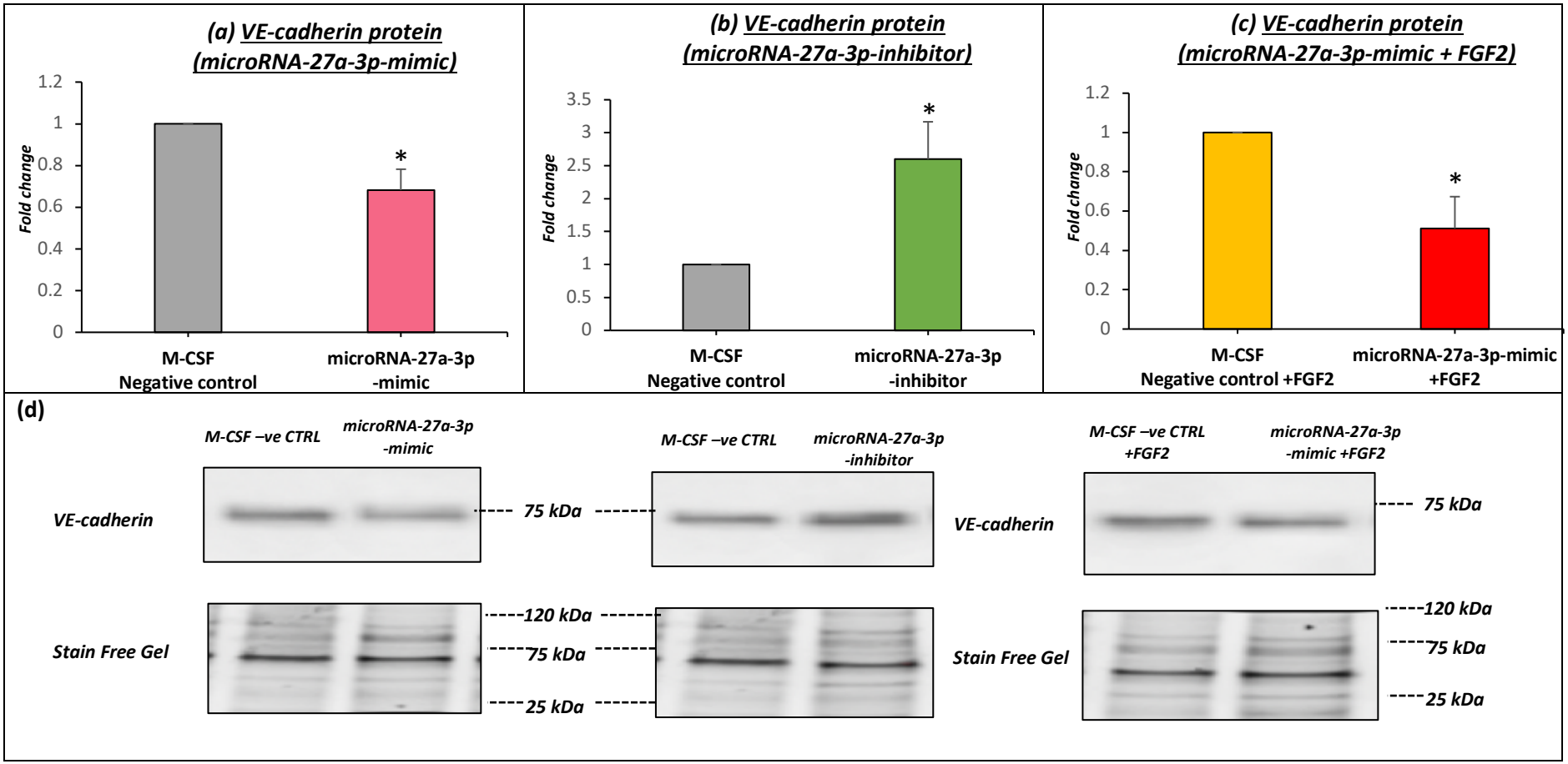

Figure 5.4.5 VE-cadherin protein expression in M-CSF directed macrophages with or without a miR-27a-3p-mimic or inhibitor.

*Quantification (a-c) and representative Western blots (d) of VE-cadherin protein expression in M-CSF matured macrophages with or without FGF2 stimulation (50ng/ml) and RVG-9dr-mediated transfection with a miR-27a-3p mimic, a miR-27a-3p inhibitor, or negative control scrambled RNA. Data are expressed as fold change against each control, (*P < 0.05 denotes significant difference compared to relative negative control (for a and b), and with negative control + FGF2 (for c); paired t-test; n=6) Stain free gel is shown as a loading control.*

Refer to appendix C (10.1.5) for full blot image.

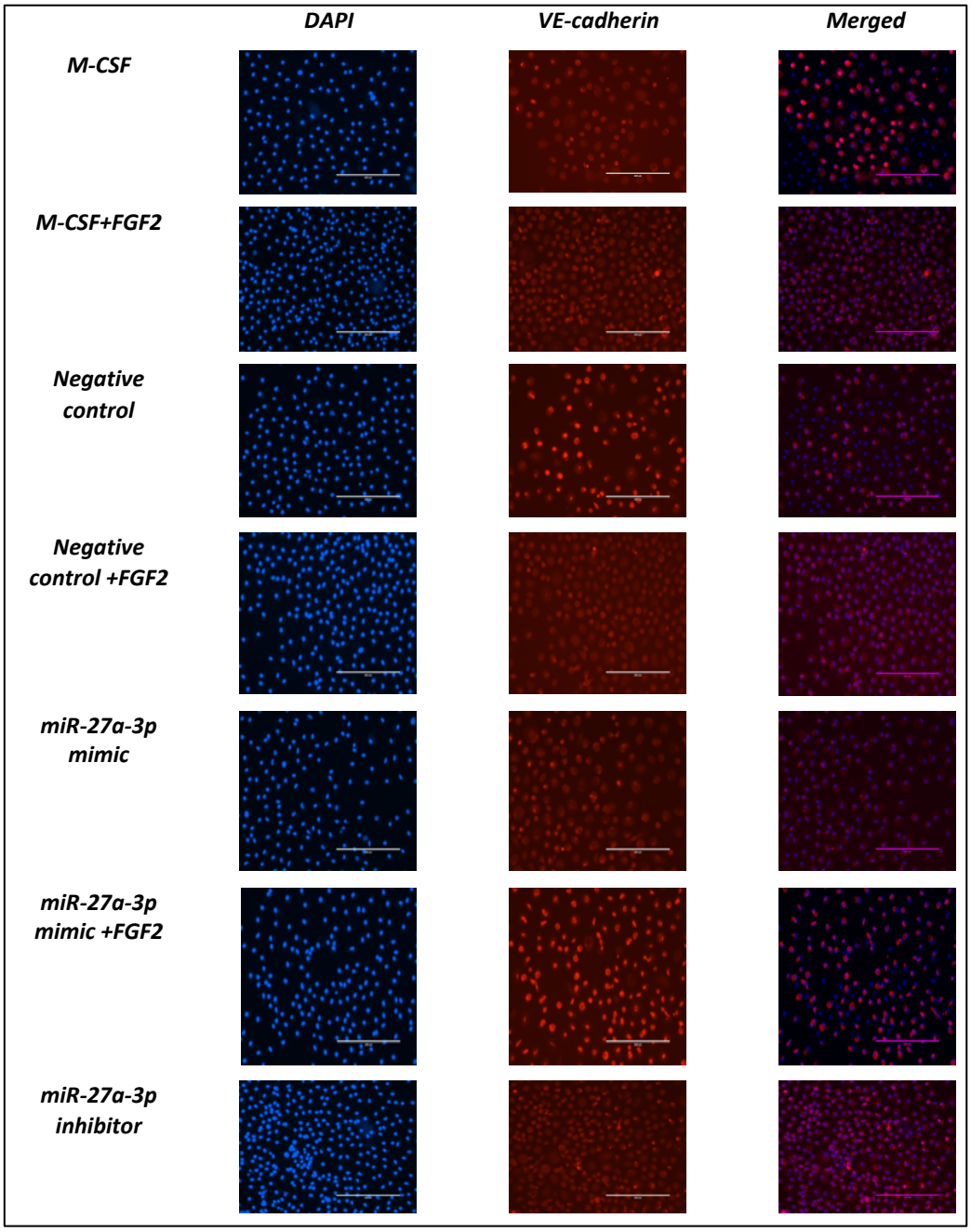

Figure 5.4.6 Immunofluorescence labelling for VE-cadherin in M-CSF directed macrophages with or without a miR-27a-3p-mimic or inhibitor.

Representative images of immunofluorescent labelling for VE-cadherin expression in M-CSF differentiated human macrophages treated with either a miR-27a-3p mimic or inhibitor and with or without subsequent stimulation with FGF2 (50ng/ml). Red colour indicates VE-cadherin immuno-positive macrophages, and blue indicates nuclei (DAPI counterstain). Scale bars represent 200 μM.

For quantification refer to Figure 5.4.7.

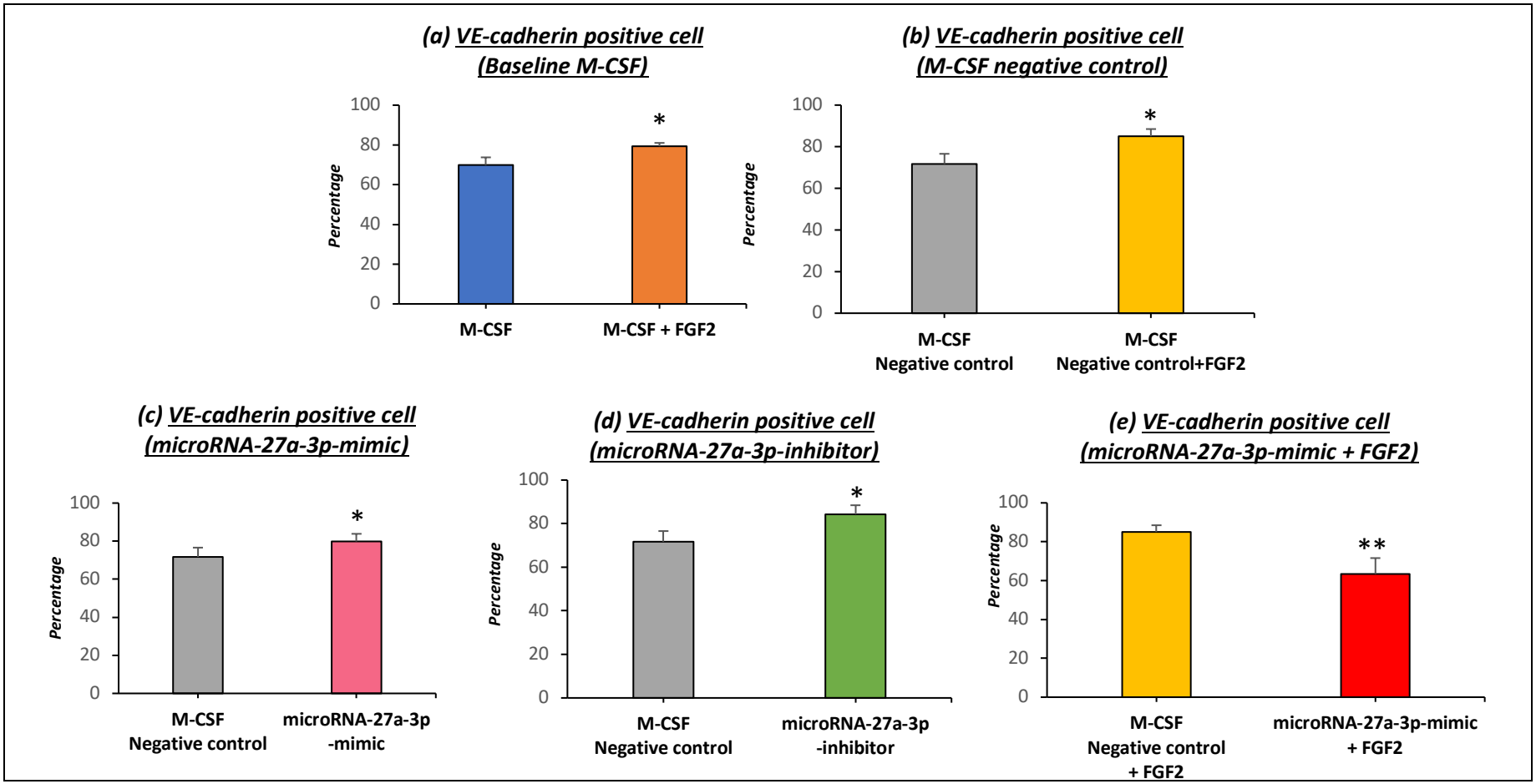

Figure 5.4.7 Quantification of immunofluorescence cell positivity of VE-cadherin in M-CSF macrophages with or without a miR-27a-3p-mimic or inhibitor.

*Quantification of immunofluorescent labelling for VE-cadherin protein levels in M-CSF matured macrophages at (a) baseline (±FGF2), (b) negative control (±FGF2), (c) miR-27a-3p-mimic treated, (d) miR-27a-3p-inhibitor treated, or (e) FGF2 ±miR-27a-3p-mimic treated. Data are expressed as percentage of VE-cadherin immuno-positive cells (*P< 0.05 and **P<0.01 denotes significant difference compared to relative control group; paired t-test; mean ±SEM; n=6). For immunofluorescence images refer to Figure 5.4.6.*

These findings support the hypothesis that miR-27a-3p regulates VE-cadherin protein levels within M-CSF matured macrophages (M-Mac). Modulation of miR-27a-3p in GM-CSF differentiated macrophages showed no changes (results not shown), in line with no discrepancies between the mRNA and protein expression of in VE-cadherin in GM-CSF matured macrophages. To ensure the observed changes in VE-cadherin protein levels afforded from miR-27a-3p modulation were not due to reciprocal alterations at the mRNA level, QPCR analysis was evaluated and showed that RVG-9dR-mediated transfection of either the miR-27a-3p-mimic or -inhibitor did not adversely affect VE-cadherin (CDH5) mRNA levels (Figure 5.4.8). Indeed, in agreement with the findings in chapter 4, CDH5 mRNA levels were down-regulated by FGF2 stimulation (52%; $P<0.01$; n=6; Figure 5.4.8a), an effect unperturbed by RVG-9dr-mediated transfection (44%; $P<0.01$; n=6; Figure 5.4.8b).

These findings consistently suggest that when VE-cadherin protein elevation is observed, it is mirrored by an inverse reduction at the mRNA level, potentially through increased translation as microRNA expression is diminished. In support, the mRNA expression of CDH5 (VE-cadherin) in M-CSF matured macrophages was not decreased through addition of a miR-27a-3p-mimic (Figure 5.4.8c). However, in the presence of a miR-27a-3p-inhibitor which increases VE-cadherin protein levels, CDH5 mRNA expression was reduced (47%; $P<0.01$; n=6; Figure 5.4.8d), indicating restored translation of mRNA into VE-cadherin protein, as shown earlier (Figure 5.4.5b and Figure 5.4.7d). This inverse pattern of mRNA and protein expression of VE-cadherin afforded with a miR-27a-3p inhibitor, mirrors the changes observed with FGF2 stimulation, which was shown to reduce miR-27a-3p levels (Figure 5.4.1). Consequently, the addition of a miR-27a-3p mimic to FGF-stimulated M-CSF macrophages significantly upregulated CDH5 (VE-cadherin) levels (1.7-fold change; $P<0.05$; n=6; Figure 5.4.8e), again suggestive of mRNA accumulation as a result of reduced protein translation Figure 5.4.5c and Figure 5.4.7e).

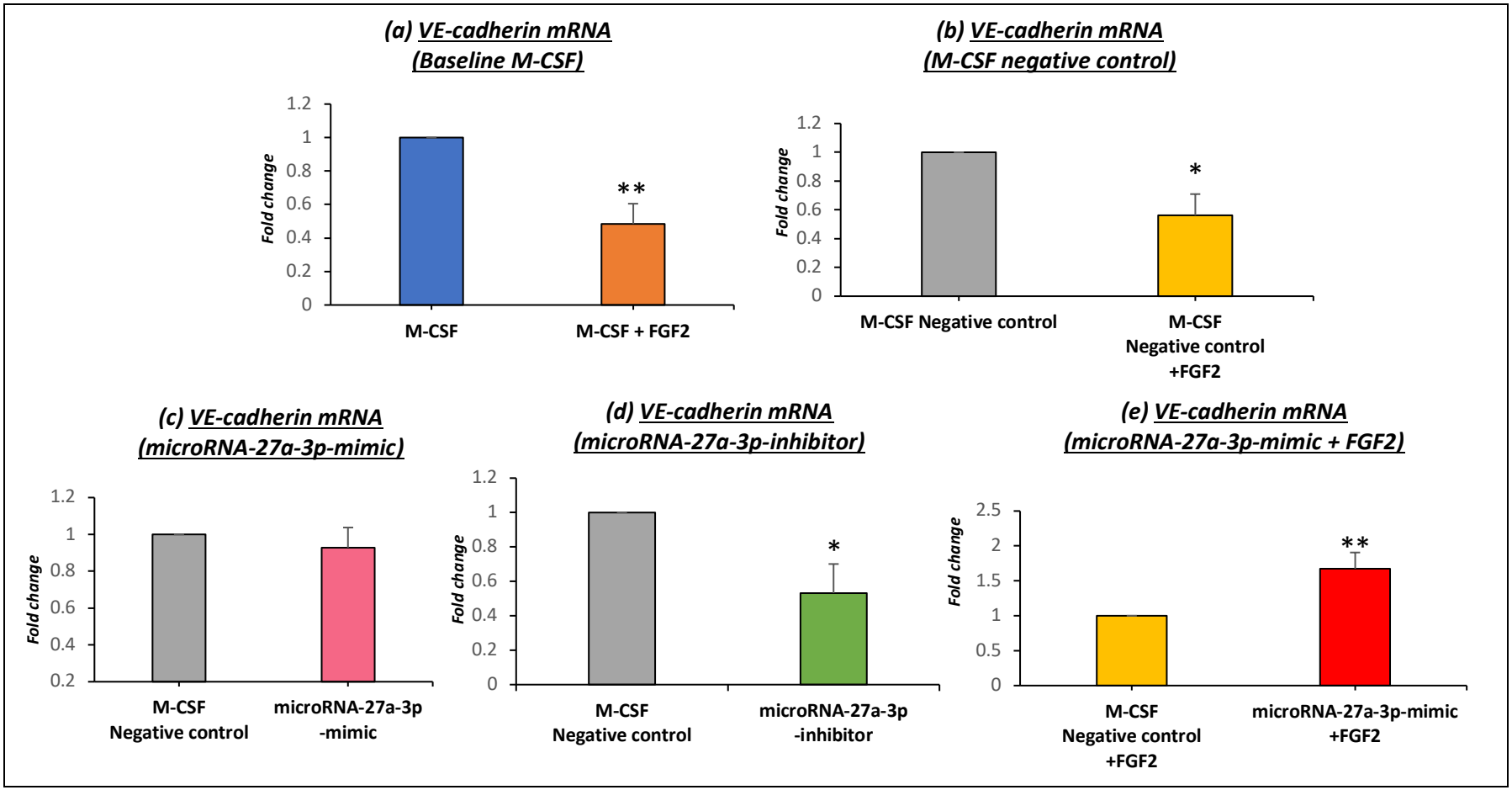

Figure 5.4.8 CDH5 (VE-cadherin) mRNA expression in M-CSF directed macrophage with or without a miR-27a-3p-mimic and -inhibitor.

*Quantification of QPCR for CDH5 (VE-cadherin) mRNA levels in M-CSF matured macrophages at (a) baseline (± FGF2), (b) negative control (±FGF2), (c) miR-27a-3p-mimic treated, (d) miR-27a-3p-inhibitor treated, or (e) FGF2 ± miR-27a-3p-mimic treated. Data are expressed as fold change against the relative control group (*P< 0.05 and **P<0.01 denotes significant difference compared to relative control group; paired t-test; mean ± SEM; n=6).*

Refer to appendix C (10.1.610.1.3) for CT-values.

Next, the effect of RVG-9dr-mediated delivery of the miR-27a-3p -mimic and -inhibitor on miR-27a-3p expression was assessed. FGF2 stimulation decreased miR-27a-3p levels in the presence of RVG-9dr-mediated delivery of a scrambled RNA (38%; $P<0.05$; n=6; Figure 5.4.9a), reproducing the similar decrease observed in baseline M-CSF directed macrophages (refer to Figure 5.4.1). No changes in miR-27a-3p expression were detected with the addition of the mimic (Figure 5.4.9b) compared to negative control cells, consistent with no change in CDH5 (VE-cadherin) mRNA levels (Figure 5.4.8c) and low protein levels (Figure 5.4.5a) Therefore, it could be postulated that the basal endogenous levels of miR-27a-3p are so abundant that addition of the mimic does not translate to an increase in total miR-27a-3p levels.

On the other hand, the addition of a miR-27a-3p inhibitor to M-CSF matured macrophages was associated with a significant reduction in miR-27a-3p levels (29%; $P<0.05$; n=6; Figure 5.4.9c), consistent with elevated VE-cadherin protein expression (Figure 5.4.5b and Figure 5.4.7d) and reduced CDH5 (VE-cadherin) mRNA levels (Figure 5.4.8d). Conversely, microRNA-27a-3p expression was significantly upregulated in FGF2-stimulated M-CSF macrophages treated with the miR-27a-3p mimic (1.8-fold change; $P<0.01$; n=6; Figure 5.4.9e), in line with higher CDH5 (VE-cadherin) mRNA levels (Figure 5.4.8 e) and reduced protein expression (Figure 5.4.5c and Figure 5.4.7e).

A summary of the above results are provided within Figure 5.4.10.

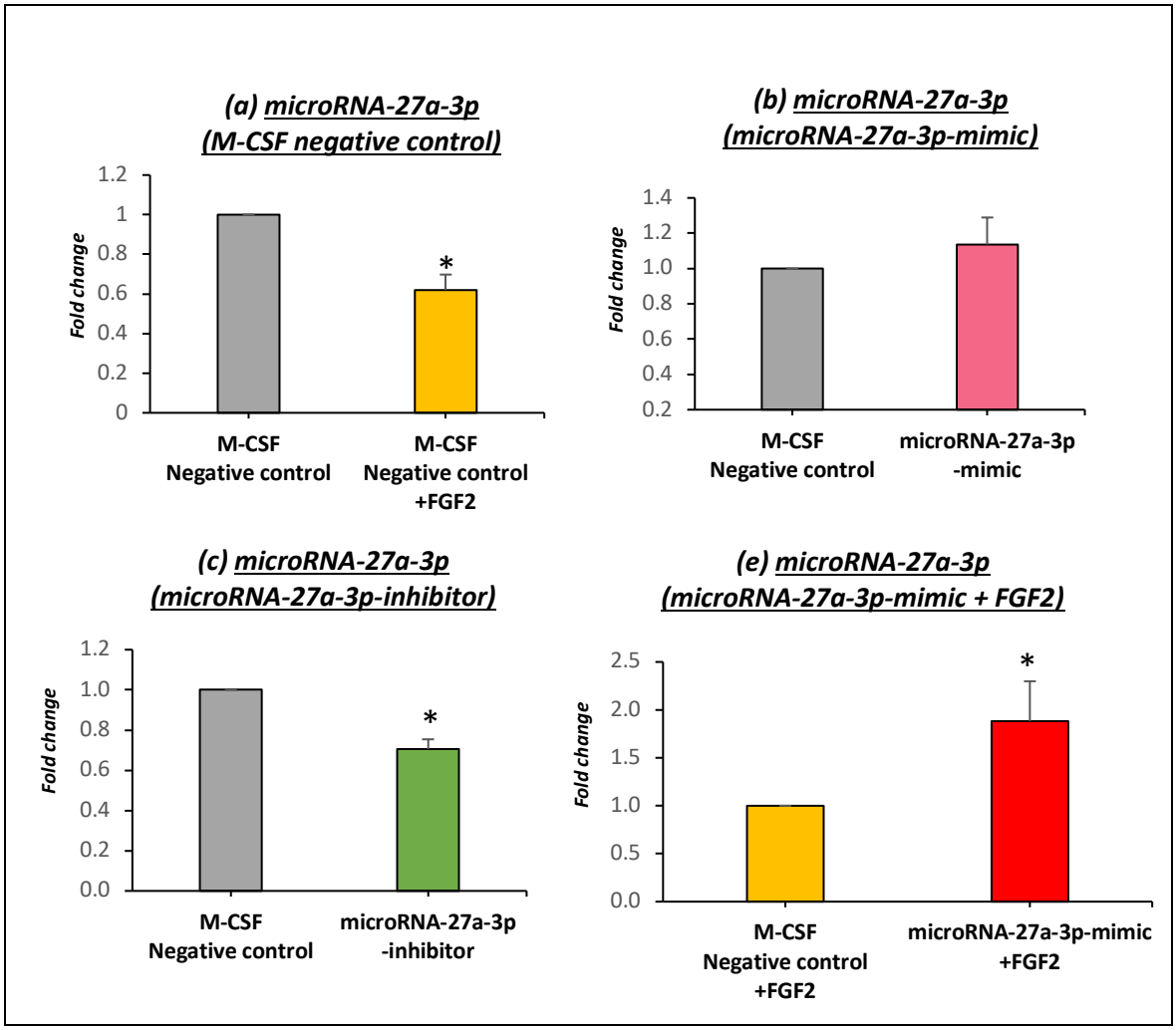

Figure 5.4.9 Effect of miR-27a-3p mimic or inhibitor treatment on M-CSF matured macrophage miR-27a-3p levels.

*Quantification of QPCR for miR-27a-3p levels in M-CSF matured macrophages treated with (a) scrambled negative control RNA (negative control) ± FGF2; (b) negative control ± miR-27a-3p mimic; (c) negative control ± miR-27a-3p-inhibitor; or (d) negative control + FGF2 ± miR-27a-3p-mimic treated. Data are expressed as fold change against the relative control group (*P< 0.05 denotes.*

Refer appendix C (10.1.7) for CT-values.

	Baseline				Negative control				MicroRNA-27a-3p-mimic				MicroRNA-27a-3p-inhibitor			
	VE-cadherin			miR27a-3p	VE-cadherin			miR27a-3p	VE-cadherin			miR27a-3p	VE-cadherin			miR27a-3p
	mRNA	WB	IF		mRNA	WB	IF		mRNA	WB	IF		mRNA	WB	IF	
M-CSF	1.0	1.0	69.9%	1.0	1.0	1.0	71.7%	1.0	0.9	0.7	79.8%	1.1	0.5	2.6	84.3%	0.7
+FGF2	0.5	2.5	79.3%	0.6	0.6	2.8	85.0%	0.6	1.7	0.5	63.4%	1.8				

Figure 5.4.10 Summary of results assessing the effect of a miR-27a-3p mimic or inhibitor on mRNA and protein expression of VE-cadherin alongside miR-27a-3p levels in M-CSF directed macrophages with and without FGF2 stimulation.

Fold change in expression of VE-cadherin mRNA, protein and microRNA-27a-3p, and percentage of immuno-positive VE-cadherin macrophages without treatment (baseline), or treatment with a scrambled RNA negative control, a microRNA-27a-3p -mimic, or a miR-27a-3p inhibitor. All cells were either stimulated with or without FGF2. For baseline and negative control groups, data are expressed as fold change compared to M-CSF non-FGF2 stimulated. For microRNA-27a-3p-mimic and -inhibitor treated groups, data are expressed as fold change compared to non-FGF2-stimulated negative control. For microRNA-27a-3p-mimic group with FGF2 stimulation, data are expressed as fold change compared to FGF2 stimulated macrophages treated with negative control. Red highlighting indicating significantly increased expression and green highlighting indicating significantly decreased levels.

5.4.3 FGF2 signalling through FGFR1 regulates M-CSF matured macrophage VE-cadherin expression FGF2/FGFR1 regulates VE-cadherin expression

Next, the FGF2 signalling pathway was interrogated to determine the manner in which FGF2 induced VE-cadherin expression through downregulation of microRNA-27a-3p. Firstly, the expression of the FGF-receptor 1 (FGFR1) was evaluated in human M-CSF matured macrophages, with or without FGF2 stimulation, and in the presence or absence of a miR-27a-3p mimic or inhibitor. QPCR analysis revealed the mRNA expression of FGFR1 was not affected by FGF2 stimulation, and/or with addition of a miR-27a-mimic or -inhibitor (Figure 5.4.11).

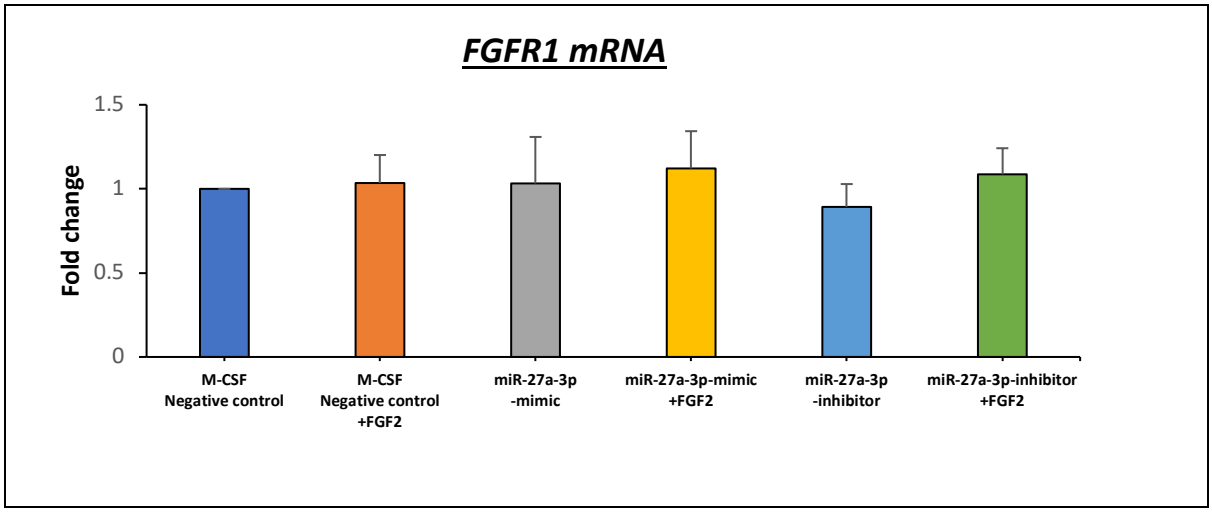

Figure 5.4.11 FGFR1 mRNA expression in M-CSF matured macrophages.
Quantification of QPCR for FGF-receptor-1 (FGFR1) mRNA levels in M-CSF matured macrophages treated with a scrambled negative control RNA ± FGF2, a miR-27a-3p mimic ± FGF2, or a miR-27a-3p-inhibitor ± FGF2. Data are expressed as fold change compared to the scrambled RNA negative control group (mean ± SEM; n=6).

Refer to appendix C (10.1.8) for CT-values.

To investigate whether FGF2-induced upregulation of VE-cadherin requires the FGF-receptor 1 (FGFR1), a FGFR1 neutralising antibody was deployed, and the results are shown in Figure 5.4.12. By blocking FGFR1 with a specific neutralising antibody, the FGF2-induced downregulation of CDH-5 (VE-cadherin) mRNA expression was inhibited, resulting in similar levels as that observed in unstimulated M-CSF macrophages and a IgG negative control (Figure 5.4.12a). Accordingly, the

increased VE-cadherin protein levels afforded through FGF2 stimulation were blunted by the FGFR1 neutralising antibody, reducing expression comparable to that detected in control M-CSF macrophages without FGF2-stimulation (Figure 5.4.12b). These findings support the hypothesis that FGF signals through FGFR1 to modulate VE-cadherin protein levels in a microRNA-dependent manner. Strengthening the proposition that miR-27a-3p plays such a role down-stream of FGF2, miR-27a-3p levels were restored to those detected in unstimulated control M-CSF macrophages upon co-incubation with the FGFR1 neutralising antibody in the presence of FGF2 (Figure 5.4.13), consolidating the previous findings indicating that microRNA-27a-3p regulates M-CSF macrophage VE-cadherin protein expression.

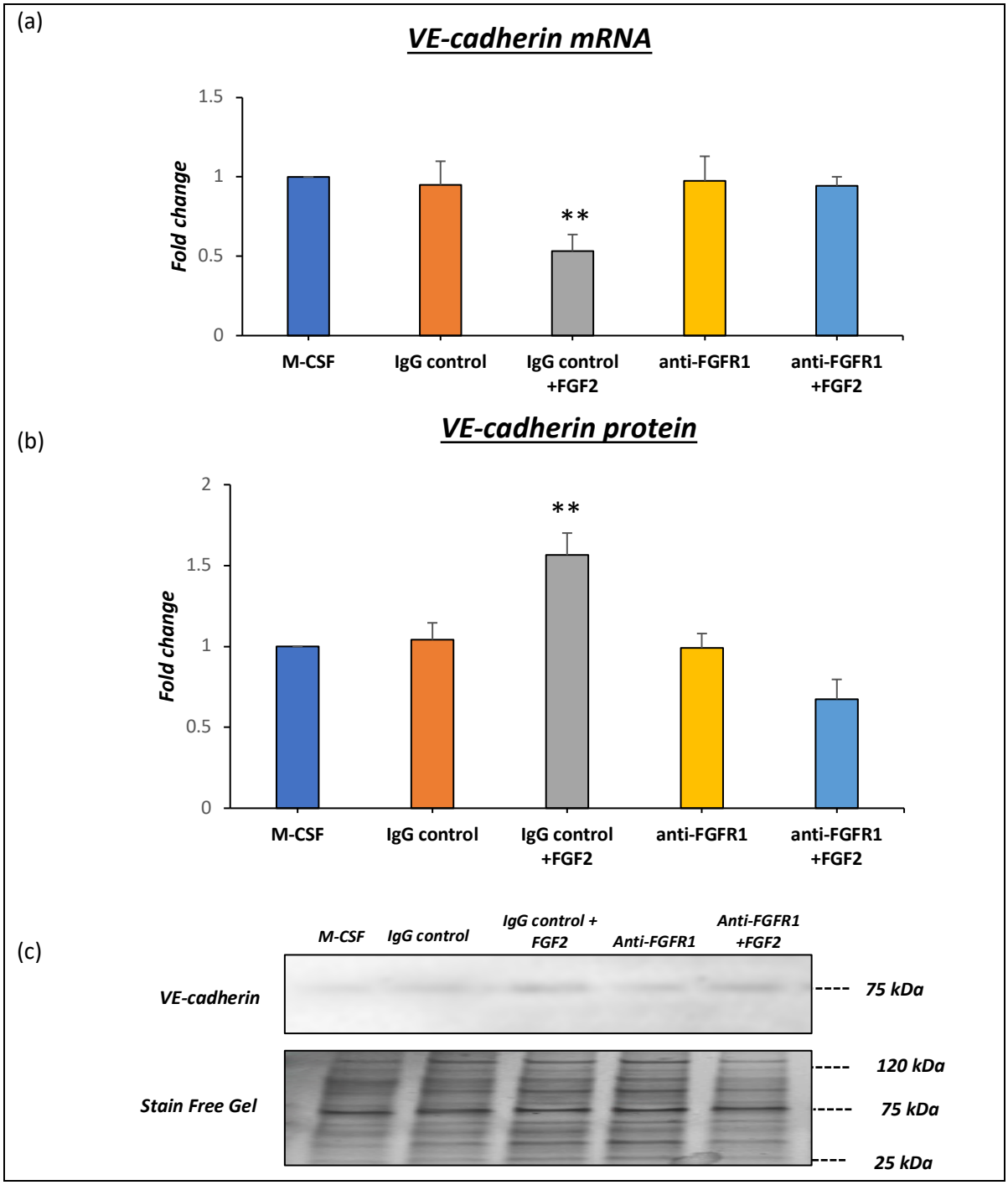

Figure 5.4.12 Addition of a FGFR1 neutralising antibody prevents FGF2-induced regulation of VE-cadherin mRNA and protein expression in M-CSF matured macrophages.

*Quantification of QPCR analysis (a), alongside quantification and representative Western blots (b and c) for mRNA and protein expression of VE-cadherin in M-CSF matured macrophages treated with an anti-FGFR1 neutralising antibody with and without FGF2 (50ng/ml), alongside unstimulated and relevant IgG controls. Data are expressed as fold change compared to unstimulated control M-CSF macrophages, (** P < 0.01 denotes significant difference from all other groups; one-way ANOVA Tukey's multiple comparison test; mean±SEM; n=6).*

Refer to appendix C; (10.1.9) for CT values and (10.1.10) for full blot image.

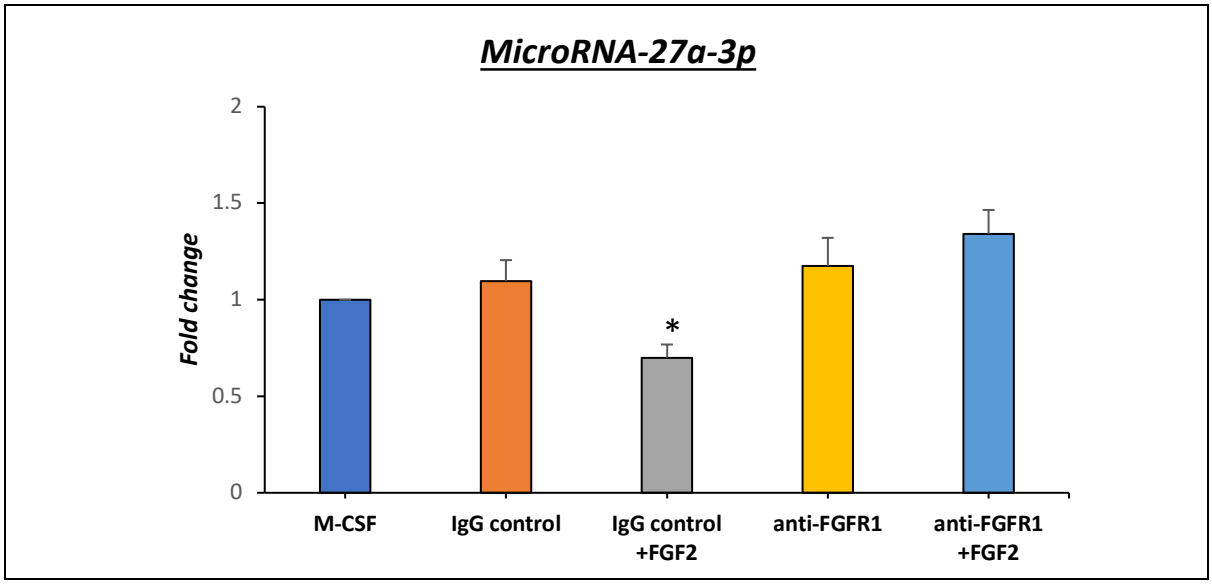

Figure 5.4.13 Addition of a FGFR1 neutralising antibody prevents FGF2-induced regulation of miR-27a-3p expression in M-CSF matured macrophages.

Quantification of QPCR for miR-27a-3p levels in M-CSF matured macrophages treated with an anti-FGFR1 neutralising antibody with and without FGF2 (50ng/ml), alongside unstimulated and relevant IgG controls. Data are expressed as fold change compared to unstimulated control M-CSF macrophages, (P < 0.05 denotes significant difference from all other groups; one-way ANOVA Tukey's multiple comparison test; mean±SEM; n=6).*

Refer to appendix C; (10.1.11) for CT values.

Next, it was assessed if blocking the function of FGFR1 altered its expression, indirectly underlying the subsequent regulation of miR-27a-3p levels. However, both the mRNA and protein expression of FGFR1 were unaffected in M-CSF macrophages through addition of either a FGFR1 neutralising antibody (anti-FGFR1) or with FGF2 stimulation (Figure 5.4.14). The above results are also summarised within Figure 5.4.20.

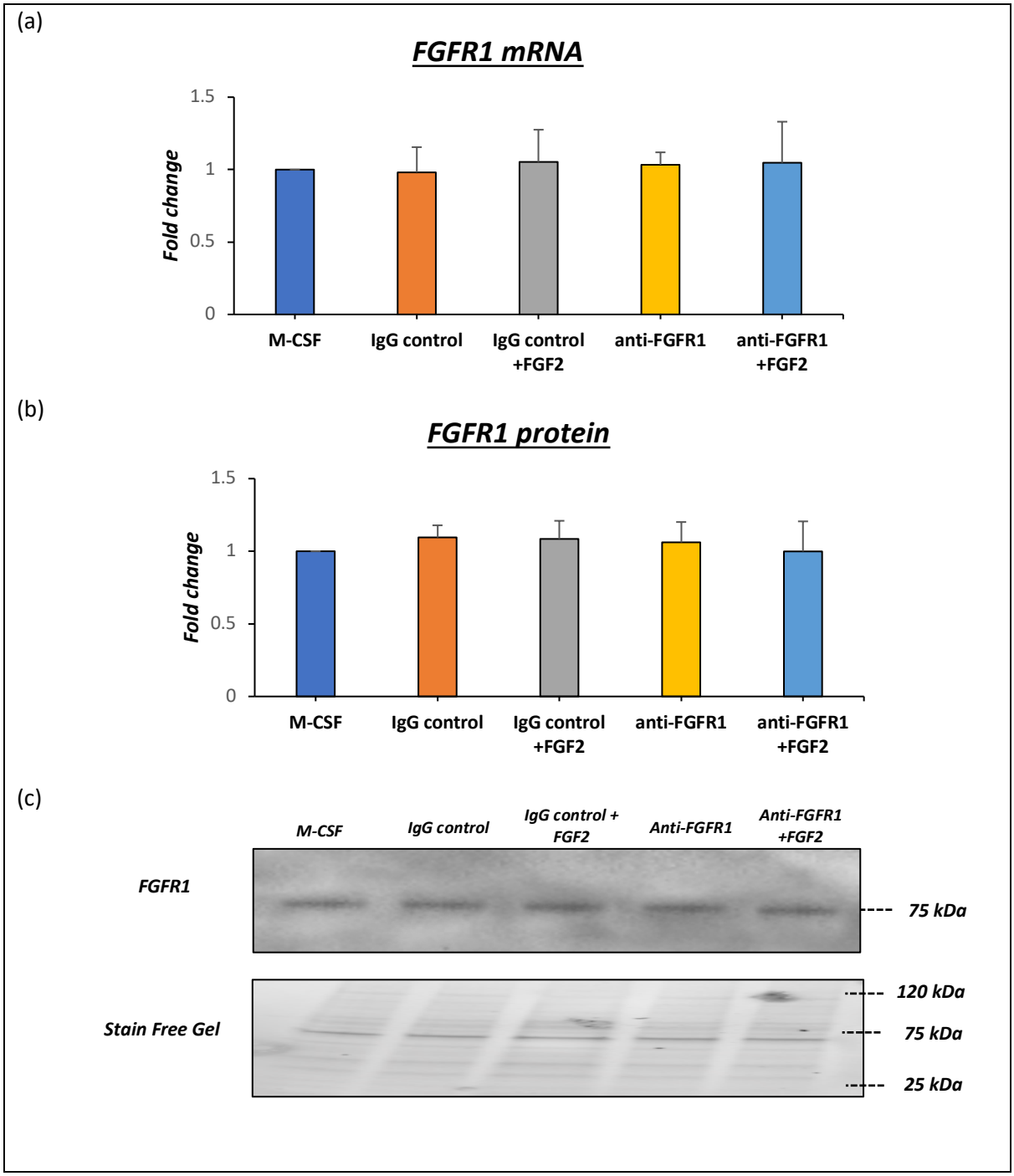

Figure 5.4.14 FGFR1 mRNA and protein expression were unaffected by addition of a FGFR1 neutralising antibody in M-CSF matured macrophages.

Quantification of QPCR analysis (a), alongside quantification and representative Western blots (b and c) for mRNA and protein expression of FGFR1 in M-CSF matured macrophages treated with an anti-FGFR1 neutralising antibody with and without FGF2 (50ng/ml), alongside unstimulated and relevant IgG controls. Data are expressed as fold change compared to unstimulated control M-CSF macrophages, (mean±SEM; n=6).

Refer to appendix C; (10.1.12) for CT values and (10.1.13) for full blot.

5.4.4 The STAT3 transcription factor regulates VE-cadherin expression in M-CSF matured macrophages

FGF2 ligation of FGFR1 is known to induce downstream signalling through activation (phosphorylation) of the STAT3 transcription factor and may therefore represent a mechanism through which FGF2 controls M-CSF macrophage levels of miR-27a-3p, and subsequent VE-cadherin protein expression. Firstly, M-CSF macrophages stimulated with FGF2 demonstrated a significant increase in STAT3 phosphorylation (1.6-fold change; $P<0.05$; $n=6$; Figure 5.4.15), which was prevented in the presence of a FGFR1 neutralising antibody (Figure 5.4.15). This finding illustrates that FGF2 stimulation induces STAT3 phosphorylation in human M-CSF matured macrophages.

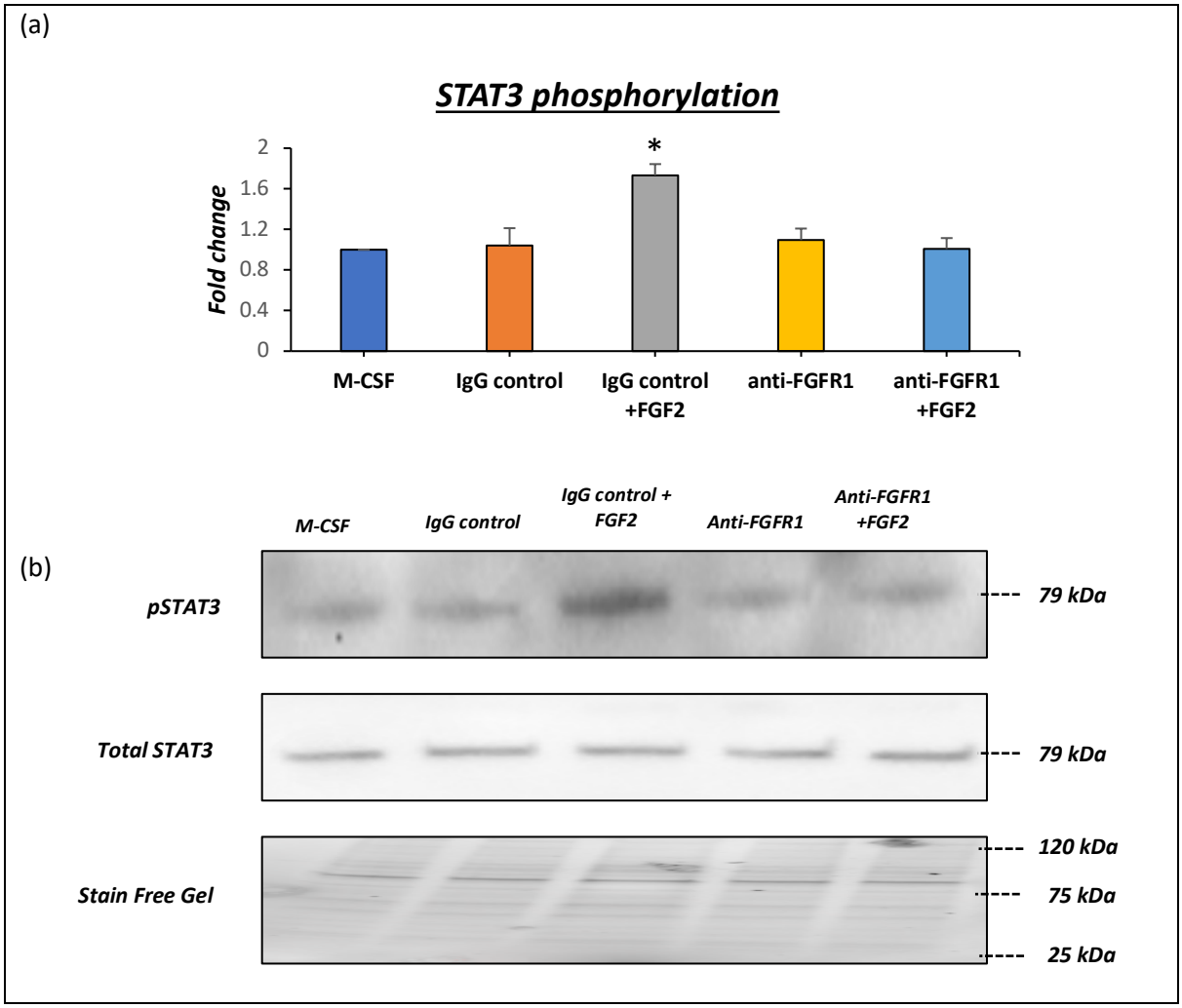

Figure 5.4.15 FGF2 stimulation increases STAT3 phosphorylation in M-CSF matured macrophages and is dependent on FGFR1.

(a) Quantification and (b) representative western blots for STAT3 phosphorylation (pSTAT3) and total STAT3 expression in M-CSF matured macrophages treated with an anti-FGFR1 neutralising antibody with and without FGF2 (50ng/ml) stimulation, alongside unstimulated and relevant IgG controls. Data are expressed as fold change compared to unstimulated control M-CSF macrophages, (P < 0.05 denotes significant difference from all other groups; one-way ANOVA Tukey's multiple comparison test; mean±SEM; n=6) Stain free gel is shown as a loading control.*

Refer to appendix C; (10.1.14) for full blot.

To validate a role for STAT3 activation (phosphorylation) in the regulation of FGF2-induced VE-cadherin expression in M-CSF matured macrophages, niclosamide was deployed as a STAT3 inhibitor. Indeed, FGF-2 stimulated upregulation of VE-cadherin protein expression was significantly reduced by co-incubation with niclosamide in a dose-related fashion (Figure 5.4.16). Specifically, VE-cadherin levels were reduced by 54% (P<0.01), 84% (P<0.01) and 85% (P<0.01) with 1 µM, 5 µM, and

10 μM niclosamide, respectively, compared to DMSO control (P<0.01; n=6; Figure 5.4.16). Consistent with the observed reduction in VE-cadherin levels reliant on STAT3 activation, niclosamide treatment also markedly reduced STAT3 phosphorylation levels and STAT3 expression by 41% (P<0.05), 66% (P<0.05) and 76% (P<0.01), with 1 μM, 5 μM and 10 μM niclosamide, respectively when compared to DMSO controls, while total STAT3 levels were unaffected (n=6; Figure 5.4.16).

In addition, fluorescence immunocytochemistry for VE-cadherin and STAT3 phosphorylation showed similar results as those observed by Western blotting analysis (Figure 5.4.17). Addition of 1 μM, 5 μM, or 10 μM niclosamide to FGF2-stimulated M-CSF matured macrophages resulted in a 15% (P<0.05), 20% (P<0.05) and 34% (P<0.01) reduction in the percentage of VE-cadherin positive cells, respectively, (n=6; Figure 5.4.18a). Supportingly, the percentage of macrophages displaying STAT3 phosphorylation was significantly lower with addition of 1 μM (14%; P<0.05), 5 μM (19%; P<0.05), or 10 μM (32%; P<0.01) niclosamide, compared to DMSO controls (n=6; Figure 5.4.18b).

In accordance with the above observations, FGF2 stimulated M-CSF macrophage CDH5 (VE-cadherin) mRNA expression was upregulated in the presence of 1 μM (1.4-fold change; P<0.05), 5 μM (1.5-fold change; P<0.01), or 10 μM (1.7-fold change; P<0.05) niclosamide compared to control cells (n=6; Figure 5.4.19a). The decreased protein expression alongside elevated mRNA levels of VE-cadherin is consistent with miR-27a-3p regulation, the expression of which was expectedly increased in the presence of 1 μM (1.3-fold change; P<0.01), 5 μM (1.4-fold change; P<0.01), or 10 μM (1.5-fold change; P<0.05) niclosamide, relative to control macrophages, (n=6; Figure 5.4.19b). The findings within this section are summarised within Figure 5.4.21, and collectively demonstrate that FGF2 stimulation of M-CSF matured macrophages increases VE-cadherin protein expression, which is in part reliant on STAT3-dependent suppression of miR-27a-3p levels.

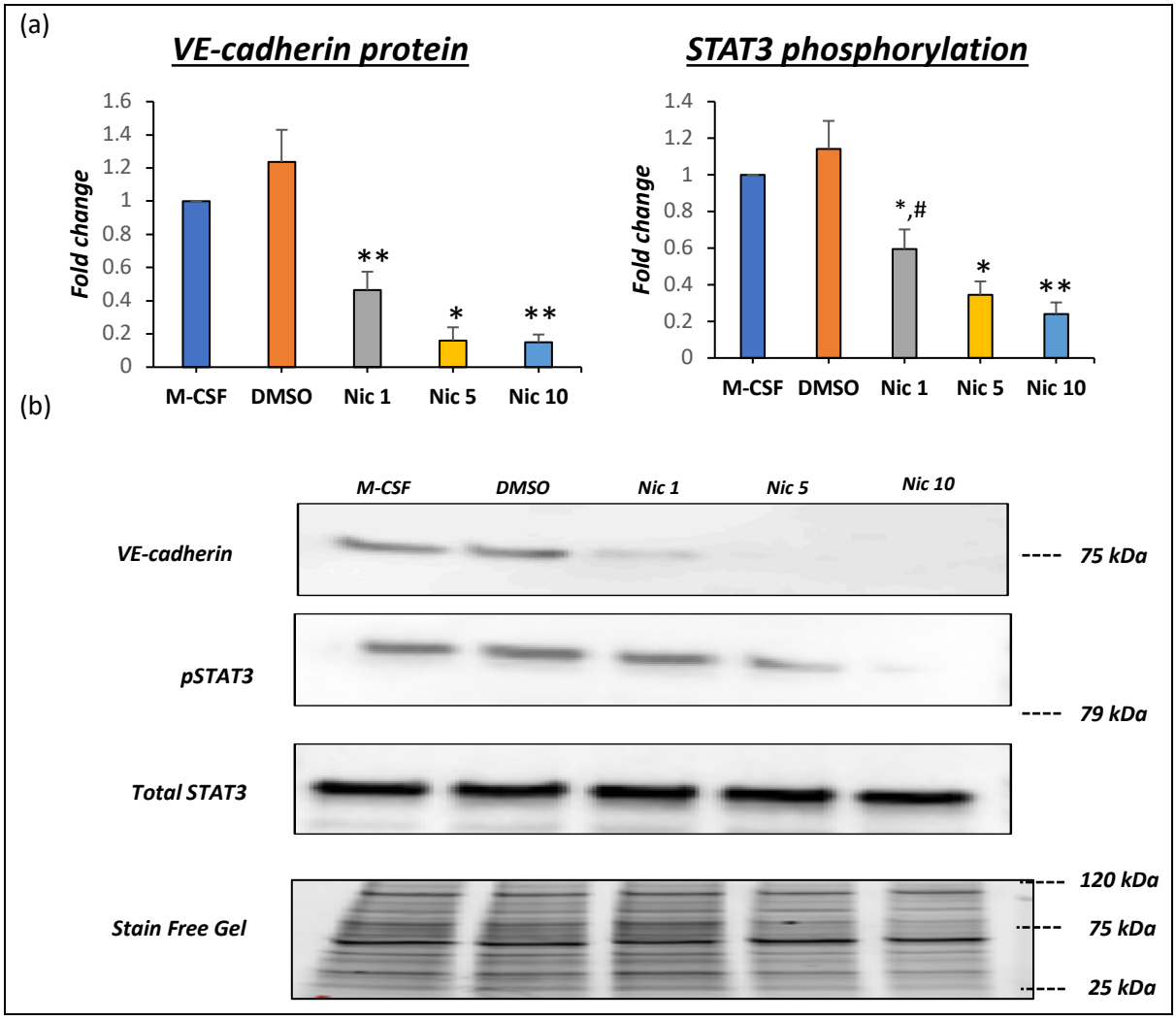

Figure 5.4.16 Niclosamide (STAT3 inhibitor) decreases VE-cadherin protein expression and STAT3 phosphorylation in FGF2 stimulated M-CSF macrophages.

*(a) Quantification and (b) representative Western blot images of VE-cadherin, STAT3 phosphorylation (pSTAT3), and total STAT3 expression in M-CSF matured macrophages stimulated with FGF2 (50ng/ml) and treated with niclosamide (STAT3 inhibitor) or DMSO as a vehicle control. Data are expressed as fold change compared to unstimulated control M-CSF macrophages, (*P <0.05 and **P <0.01 denotes significant differences compared to DMSO control; #P <0.05 denotes significant differences compared to 10 µM niclosamide; one-way ANOVA Tukey's multiple comparison test; n=6; mean ±SEM).*

Refer to appendix C; (10.1.15) for full blot.

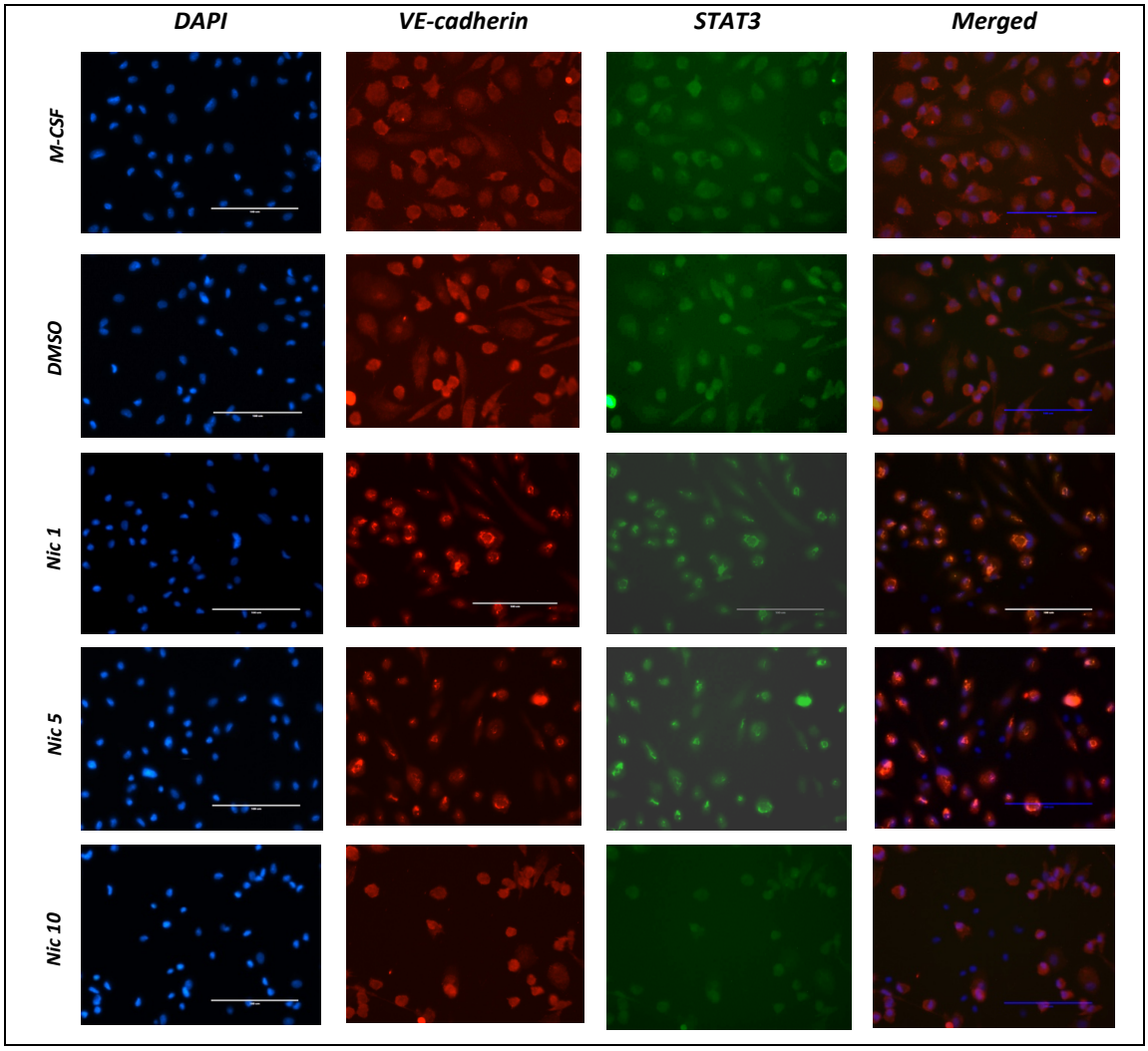

Figure 5.4.17 Niclosamide decreases VE-cadherin expression and STAT3 phosphorylation in FGF2 stimulated M-CSF macrophages.

Representative images of immunofluorescent labelling for VE-cadherin and phosphorylated STAT3 (pSTAT3) in FGF2-stimulated M-CSF differentiated human macrophages treated with niclosamide (1, 5, or 10 μM). Red colour indicates VE-cadherin immuno-positive macrophages, green colour indicates STAT3 phosphorylation, and blue indicates nuclei (DAPI counterstain). Scale bars represent 100 μM. For quantification refer to Figure 5.4.18. (DMSO = vehicle control for niclosamide; Nic = niclosamide).

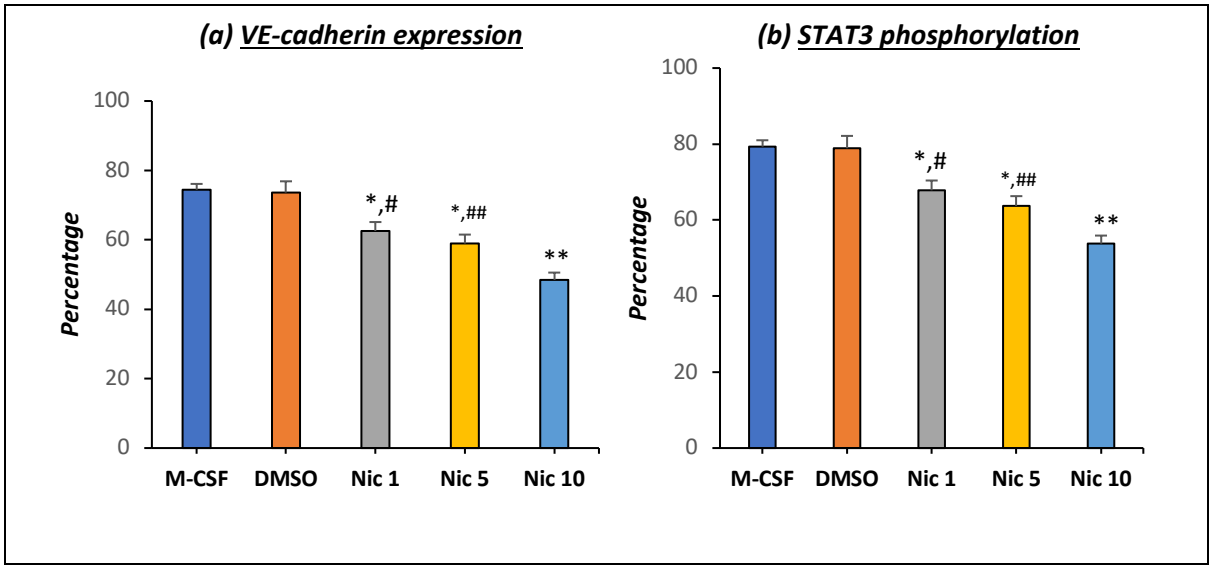

Figure 5.4.18 Niclosamide (STAT3 inhibitor) reduces VE-cadherin protein expression and STAT3 phosphorylation in FGF2 stimulated M-CSF macrophages.

*Quantification of immunofluorescent labelling for (a) VE-cadherin and (b) phosphorylated STAT3 (pSTAT3) in FGF2-stimulated M-CSF matured macrophages treated with the STAT3 inhibitor niclosamide (1, 5 or 10 μM). Data are expressed as percentage of (a) VE-cadherin positive and (b) phosphorylated STAT3 expressing macrophages, (*P< 0.05, ** P <0.01 denotes significant difference compared to DMSO control cells; # P <0.05 and ## P<0.01 denotes significant difference compared to Nic 10 μM (one-way ANOVA Tukey's multiple comparison test; mean ± SEM; n=6). For immunofluorescence images refer to Figure 5.4.17. (DMSO = vehicle control for niclosamide; Nic 1, 5 and 10 = niclosamide 1, 5 and 10 μM, respectively).*

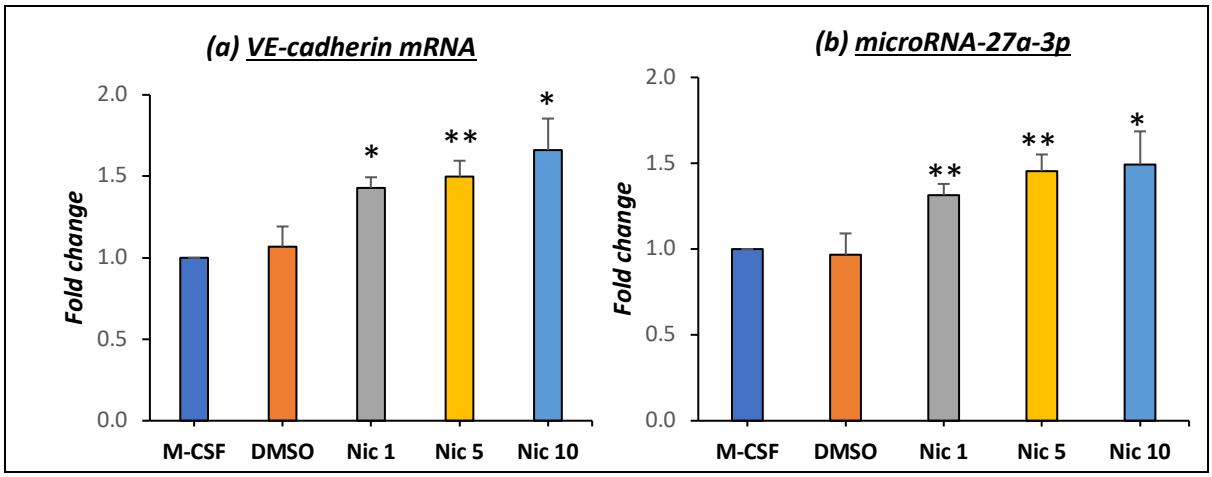

Figure 5.4.19 Niclosamide (STAT3 inhibitor) increases CDH5 (VE-cadherin) mRNA expression and microRNA-27a-3p levels in FGF2 stimulated M-CSF macrophages.

Quantification of QPCR for (a) CDH5 (VE-cadherin) mRNA expression and (b) miR-27a-3p levels in FGF2-stimulated M-CSF matured macrophages treated with the STAT3 inhibitor niclosamide (1, 5 or 10 μM). Data are expressed as fold change compared to unstimulated control M-CSF macrophages,(P < 0.05 and ** P < 0.01 denotes significant differences compared to DMSO control macrophages (one-way ANOVA Tukey's multiple comparison test; mean ±SEM; n=6). Refer to appendix C; (10.1.16) for CT values.*

	VE-cadherin		MicroRNA-27a-3p	FGFR1		STAT3
	mRNA	protein		mRNA	protein	
M-CSF	1.0	1.0	1.0	1.0	1.0	1.0
IgG	1.0	1.0	1.1	1.0	1.1	1.0
IgG+FGF2	0.5	1.6	0.7	1.1	1.1	1.7
Anti-FGFR1	1.0	1.0	1.2	1.0	1.0	1.1
Anti-FGFR1+FGF2	0.9	0.7	1.3	1.1	1.0	1.0

Figure 5.4.20 Summary of results assessing the effect of a FGFR1 neutralising antibody on M-CSF directed macrophages.

Fold change in expression of VE-cadherin mRNA and protein, microRNA-27a-3p, FGFR1 mRNA and protein, and STAT3 phosphorylation in human M-CSF matured macrophages treated with an anti-FGFR1 neutralising antibody with and without FGF2 (50ng/ml), alongside unstimulated and relevant IgG controls. Data are expressed as fold change compared to unstimulated control M-CSF macrophages. Red highlighting indicates significantly increased expression and green highlighting indicates significantly decreased levels.

	VE-cadherin			STAT3		microRNA-27a-3p
	WB	ICC	mRNA	WB	ICC	
M-CSF	1.0	74.4%	1.0	1.0	79.3%	1.0
DMSO	1.2	73.6%	1.1	1.1	78.9%	1.0
Nic 1	0.5	62.6%	1.4	0.6	67.8%	1.3
Nic 5	0.2	59.0%	1.5	0.3	63.7%	1.4
Nic 10	0.2	48.4%	1.7	0.2	53.8%	1.5

Figure 5.4.21 Summary of results assessing the effect of STAT3 inhibition on FGF2-stimulated M-CSF directed macrophages.

Fold change in expression of VE-cadherin mRNA and protein alongside percentage of immuno-positive VE-cadherin macrophages, STAT3 phosphorylation by Western blotting (WB) and immunocytochemistry (ICC), and miR-27a-3p levels, in FGF2-stimulated M-CSF matured macrophages treated with the STAT3 inhibitor niclosamide (1, 5 or 10 μM). Data are expressed as fold change compared to unstimulated control M-CSF macrophages for mRNA and WB analysis, or is expressed as percentage of VE-cadherin positive or phosphorylated STAT3 expressing macrophages, for the ICC. Red highlighting indicates significantly increased expression and green highlighting indicates significantly decreased levels.

5.4.5 FGF2 stimulation of M-CSF matured macrophages increases *in vitro* angiogenesis

The *in vitro* Matrigel angiogenesis assay involves culturing cells upon Matrigel for 24-hours, then assessing the formation of tube-like structures and the number of branches from the structures, representing the development of immature angiogenic networks. The previous data presented within this chapter and chapter 4 would suggest that GM-CSF matured macrophages are more pro-angiogenic than their M-CSF directed counterparts. Indeed, while M-CSF matured macrophages developed some tube-like structures, significantly reduced branching formation (5-8 branches) was observed in comparison to GM-CSF directed macrophages (12-17 branches; $P < 0.001$; n=6; Figure 5.4.22). However, the stimulation of M-CSF matured macrophages with FGF2 (50ng/ml) increased the formation of tube-like structures, as shown through a 2.3-fold increase in the number of branches compared to unstimulated M-CSF macrophages ($P < 0.001$; n=6; Figure 5.4.22), which is equivalent to that observed in unstimulated and FGF2 stimulated GM-CSF directed macrophages.

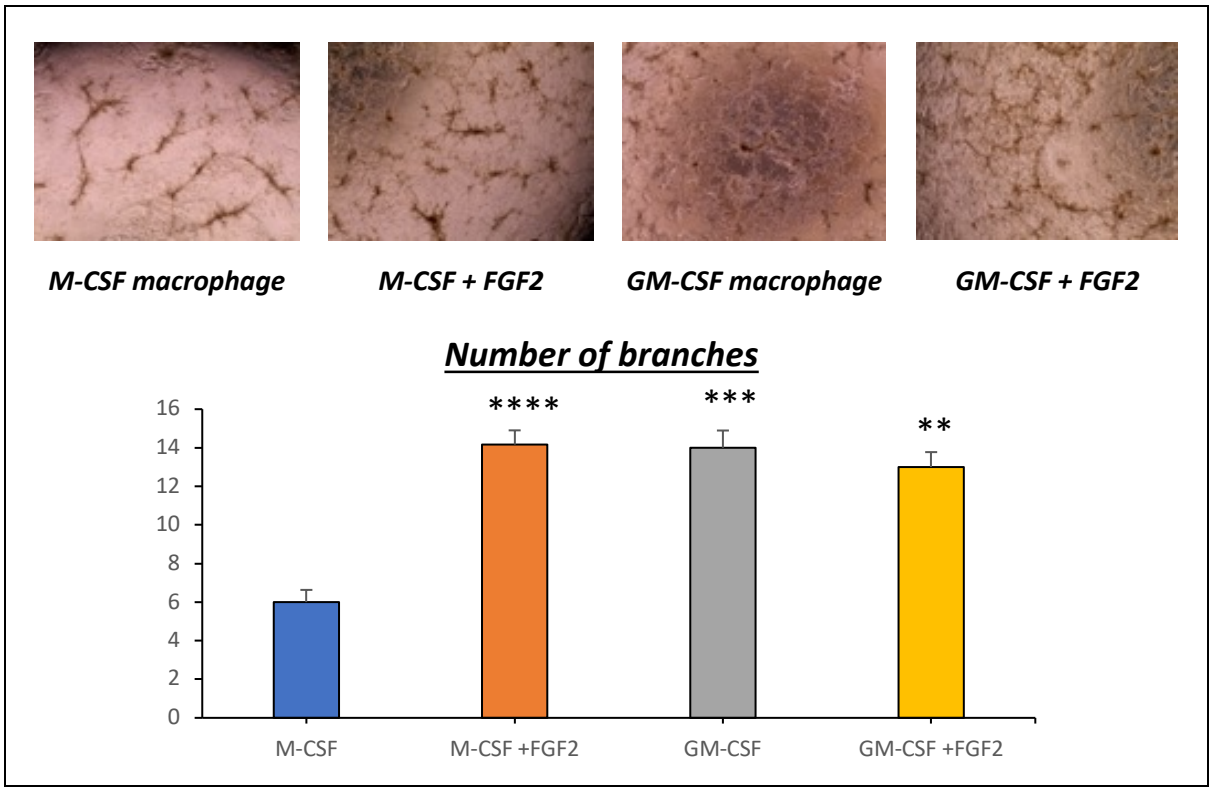

Figure 5.4.22 FGF2 stimulation of M-CSF matured macrophages increases *in vitro* angiogenesis.

*Representative images and quantification of tube-like formation in M-CSF and GM-CSF matured human macrophages with and without FGF2 stimulation (50ng/ml). Data are expressed as average number of branches per x10 magnification field, (****P < 0.0001, *** P<0.001 and **P<0.01 denotes significant differences compared to unstimulated M-CSF macrophages; one-way ANOVA Tukey's multiple comparison test; mean ± SEM; n=6).*

Next, the effects of the STAT3 inhibitor niclosamide on tube-like formation in FGF2 stimulated M-CSF macrophages was investigated. In the presence of niclosamide, tube-like formation (assessed through the number of branches) was almost completely abolished (91%; P<0.0001; n=6; Figure 5.4.23), compared to control macrophages. This suggests FGF2 induction of angiogenesis is STAT3 dependent.

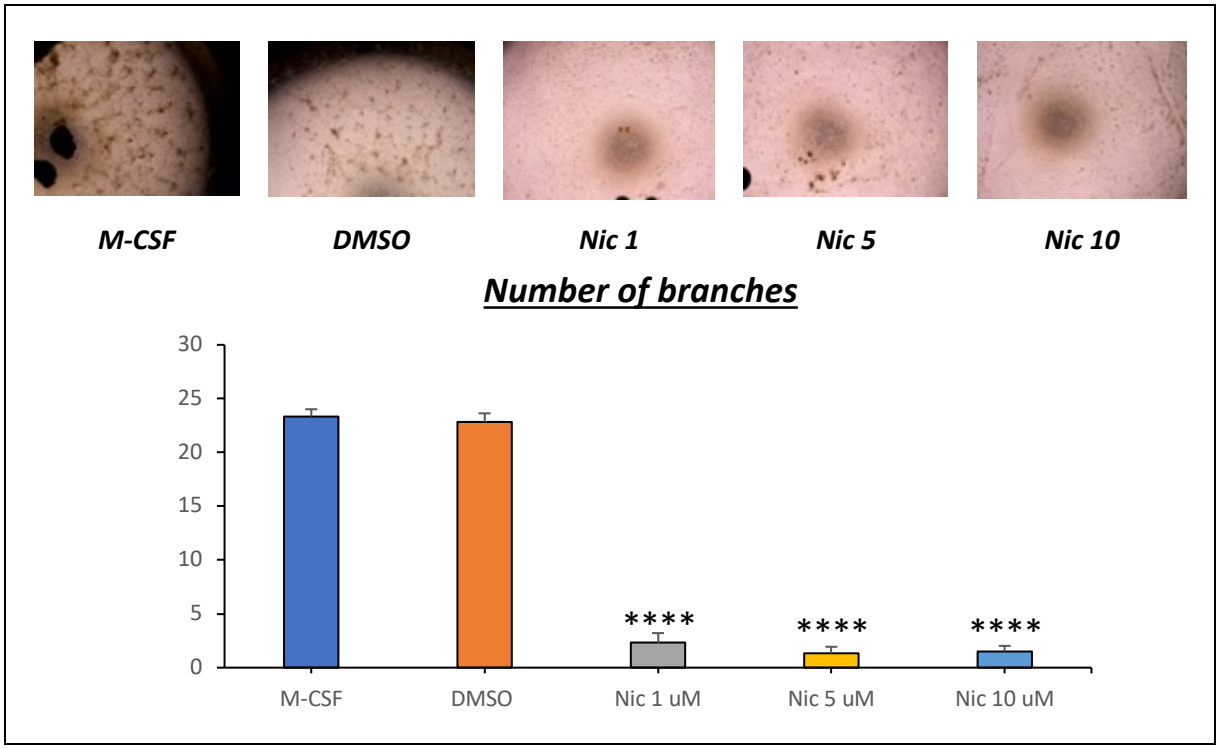

Figure 5.4.23 Niclosamide (STAT3 inhibitor) reduces *in vitro* angiogenesis in FGF2-stimulated M-CSF matured macrophages.

*Representative images and quantification of tube-like formation in FGF2 stimulated M-CSF matured human macrophages in FGF2-stimulated (50ng/ml) M-CSF matured macrophages treated with the STAT3 inhibitor niclosamide (1, 5 or 10 μM), or DMSO as a vehicle control. Data are expressed as average number of branches per x4 magnification field, (****P < 0.0001 denotes significant difference compared to DMSO control macrophages; one-way ANOVA Tukey's multiple comparison test; mean ±SEM; n=6).*

5.5 Discussion

The findings within this study demonstrate that low levels of VE-cadherin protein expression are consistent with elevated expression of microRNA-27a-3p in M-CSF matured macrophages (M-Mac - an anti-inflammatory macrophage phenotype), effects which are reversed with FGF2 stimulation. These novel observations suggest that VE-cadherin protein levels are under the regulatory control of miR-27a-3p within M-CSF macrophages. This association was validated by utilising a miR-27a-3p-mimic and inhibitor to modulate miR-27a-3p levels within macrophages. Increasing miR-27a-3p levels with the mimic attenuated FGF2-induced VE-cadherin protein expression in M-Mac, while retarding miR-27a-3p function with the inhibitor augmented VE-cadherin protein levels upon FGF2 stimulation. Considering the above mechanism, it is not therefore surprising that the elevated VE-cadherin protein expression observed in GM-CSF directed macrophages (GM-Mac - a pro-inflammatory phenotype), was associated with low levels of microRNA-27a-3p, and was unaffected by FGF2 stimulation. Indeed, the VE-cadherin protein and reciprocal miR-27a-3p levels were comparable between FGF2 stimulated M-Mac and unstimulated GM-Mac, suggesting that FGF2 drives M-Mac towards a GM-Mac phenotype in regard to displaying endothelial cell-like properties.

The canonical signalling pathways for FGF2 involves its receptor (FGFR1) and tyrosine kinase down-stream signalling molecules including STAT3, PI3K, and MAPK. The evidence provided within this chapter demonstrates that FGF2 modulation of miR-27a-3p levels and ensuing VE-cadherin protein expression in M-Mac, is in part dependent on FGFR1 and subsequent activation (phosphorylation) of STAT3. Translating these findings into functional effects, M-CSF matured macrophages stimulated with FGF2 displayed an increased propensity to form tube-like structures during an angiogenesis assay, suggesting the augmented VE-cadherin protein levels affords M-Macs to acquire functions normally attributed solely to endothelial cells and their progenitors. Moreover, inhibition of STAT3 activation with niclosamide retarded FGF2-induced the *in vitro* angiogenic response of M-CSF macrophages, supporting a FGF2-FGFR1-STAT3 axis in regulating the endothelial cell-like transition

of macrophage subsets. Interestingly, GM-CSF matured macrophages showed angiogenic potential without FGF2 stimulation, in line with their low levels of miR-27a-3p and heightened protein expression of VE-cadherin. This implies that FGF2 stimulation of M-CSF macrophages shifts their phenotype towards that closely linked to GM-CSF macrophages, particularly in regard to acquiring endothelial cell-like expression patterns and angiogenic properties. In addition, these observations further confirm the specific features of macrophage subsets in response to different microenvironment cues.

MicroRNA-27a has been identified among one of the microRNAs involved in endothelial cell angiogenesis (Zhou *et al.,* 2011). It is highly expressed in the endothelial cells of highly vascularised tissues such as lung and heart (Zhou *et al.,* 2011), and forms a cluster with miR-23a and miR-24-2 within MIR23AHG (the miR-23a/27a/24-2 cluster host gene), which has been proposed to regulate biological processes in various cancers including leukaemia, breast cancer and colorectal cancer (Chhabra *et al.,* 2010). In particular, miR-27a is associated with VEGF-mediated endothelial cell proliferation, migration and matrigel tube-like formation, attributed to its targeting of Sprouty2 and SEMA6A proteins (Zhou *et al.,* 2011). These proteins are associated with anti-angiogenic effects by interfering with the VEGF-induced MAPK pathway (Urbich *et al.,* 2012; Wietecha *et al.,* 2011). In another study, miR-27a levels were reported to be downregulated in response to angiogenesis stimulatory molecules such as VEGF (Young *et al.,* 2013). In support of the findings within this chapter pertaining to pro-angiogenic macrophage subsets, heightened miR-27a expression is associated with reduced angiogenesis through targeting of VE-cadherin in HUVECs and mouse capillaries (Young *et al.,* 2013). Additionally, elevated miR-27a levels were associated with the inhibition of vascular leaks induced by thrombin and ischaemia (Young *et al.,* 2013).

Additionally, miR-27a has been implicated in indirectly promoting macrophage polarisation towards a pro-inflammatory phenotype through suppressing expression of the anti-inflammatory mediator IL-10 (Xie *et al.,* 2014). In addition, miR27a may work in unison with its cluster-related microRNAs

miR-23a and miR-24, to promote a pro-inflammatory macrophage phenotype with enhanced expression of pro-inflammatory cytokines such as IL-1β, IL-6, and TNFα (Ma *et al.,* 2016). Thus, based on these reports, elevated miR-27a expression can be regarded as a feature of pro-inflammatory macrophages. However, this is in contrast to the findings within this chapter, whereby the pro-inflammatory GM-Mac subset expressed lower levels of miRNA-27a-3p (as well as its passenger strand miR-27a-5p), compared to their anti-inflammatory M-Mac counterparts.

However, the inverse correlation of miR-27a-3p and VE-cadherin protein levels and angiogenic potential demonstrated within this chapter are in line with another report, although in different cell type. Reportedly, miR-27a downregulation is associated with *in vitro* endothelial cell angiogenesis and *in vivo* new vessel formation (Young *et al.,* 2013). Elevated expression of miR-27a was associated with reduced VE-cadherin expression and related diminished capillary tube formation (Young *et al.,* 2013). Moreover, addition of a miR-27a-inhibitor reduced VEGF-induced vascular permeability, with vascular leakage due to increased permeability serving as a common observation in angiogenesis, thus highlighting miR-27a-inhibition as a potential pro-angiogenic agent resulting in a lessened oedematous effect (Young *et al.,* 2013). It would be interesting to investigate the regulatory effect of FGF2-induced miR-27a suppression on macrophage-derived tube formation with regard to perfusion characteristics and vascular permeability aspects. On a different note, and as described in the previous chapter, under FGF2 stimulation M-Mac shift towards an endothelial cell-like phenotype which could be regarded as a pro-inflammatory phenotype. Collectively, these original findings suggest that the pro-inflammatory and pro-angiogenic phenotype of FGF2-induced M-Mac is in part regulated by diminished miR-27a-3p expression which in turn permits VE-cadherin translation and an ensuing increase in protein levels.

Another important finding in this study is the identification of a key regulatory role for STAT3 signalling in FGF2-induced VE-cadherin protein expression by M-Mac. To induce down-stream target gene transcription, STAT3 requires activation through phosphorylation of tyrosine residue 705 and

subsequent translocation into the nucleus, enhancing the expression of various genes regulating cell growth and apoptosis, among others (Yuan *et al.,* 2004). STAT3 activation and upregulation of its target genes have been implicated in early mouse development (Takeda *et al.,* 1997), cell growth (Hirano *et al.,* 2000), and angiogenesis (Chen and Han, 2008). Consequently, STAT3 has been ascribed a significant role in the development of heart disease (Kurdi *et al.,* 2018) and various tumours (Yu *et al.,* 2009). In addition, STAT3 has been implicated in VEGF-induced endothelial cell migration and capillary tube formation (Yahata *et al.,* 2003). In another study, FGF2-induced endothelial cell proliferation was shown to be mediated by co-activation of platelet activating factor and STAT3 (Deo *et al.,* 2002). A recent study deploying an *ex vivo* model of choroidal endothelial sprouting demonstrated that FGF2-induced angiogenesis is associated with enhanced STAT3 signalling (Dong *et al.,* 2019). The findings in this chapter reveal a similar mechanism exists within human macrophages under *in vitro* conditions, whereby FGF2-induced tube formation in M-Mac was prevented by inhibiting STAT3 signalling. This intimates FGF2 engenders specific macrophage subsets (M-Mac) with the capacity to acquire an endothelial cell-like phenotype. Relatedly, it was recently shown that FGF2 modulates the phenotypic programming of tumour-associated macrophages to increase tumour growth, which was associated with increased angiogenesis (Im *et al.,* 2020). Unfortunately, this study did not explore the possibility that the angiogenesis formed within the tumours was in part macrophage-derived, alongside development from resident endothelial cells.

Under inflammatory conditions, STAT3 is activated by IL-6 to induce a pro-inflammatory macrophage phenotype (Tugal *et al.,* 2013). This report supports the observation in this chapter showing that FGF2-induced VE-cadherin expression is regulated via STAT3 in M-Mac, which attains a pro-inflammatory macrophage phenotype, based on upon VE-cadherin protein upregulation and miR-27a-3p downregulation. However, a contradictory study suggests STAT3 promotes the generation of an anti-inflammatory macrophage phenotype, through upregulation of IL-10 (Hutchins *et al.,* 2013).

Again, these conflicting finding are not surprising given that macrophage phenotype behaviour can be altered by different biochemical cues and is usually transient.

Focussing on endothelial cell function, IL-6-induced vascular permeability and subsequent loss of barrier function was dependent on STAT3 activation and altered ensuing expression patterns of ZO1 and VE-cadherin, key cell junctional proteins (Alsaffar *et al.,* 2018). A further study similarly demonstrated that STAT3 signalling was associated with increased vascular permeability through adverse regulation of VE-cadherin expression patterns and its down-stream transcription factor β-catenin (Hox *et al.,* 2016). These reports are in opposition to the negative relationship shown in this chapter, albeit in macrophages, STAT3 activation is associated with macrophage-derived tube formation through upregulation of VE-cadherin in FGF2-stimulated M-Mac. A possible explanation for the differential expression and function of STAT3 and VE-cadherin may be attributed to cell-specific mechanisms, with M-CSF matured macrophages utilising a disparate regulation of VE-cadherin through STAT3 activation than that which takes place in endothelial cells, particularly in response to FGF2. Nevertheless, other studies have shown that STAT3 activation supports angiogenesis through upregulation of VE-cadherin (Chen and Han, 2008; Osugi *et al.,* 2002), which supports the findings in M-Mac.

A potential limitation of the findings presented within this chapter is the expression of VE-cadherin and STAT3 were only assessed for their regulation at the mRNA and protein levels. The cellular characterisation of VE-cadherin and STAT3 were not evaluated with a cytoplasmic shift of VE-cadherin and associated proteins and nuclear translocation of β-catenin alongside nuclear accumulation of phosphorylated STAT3 a commonly observed finding in activated HUVECs (Noria *et al.,* 1999). Additional confocal microscopy analysis and quantification of cell localisation of VE-cadherin, and STAT3 phosphorylation would be informative, and indeed demonstrate if the altered expression patterns seen in endothelial cells also occur in M-Mac. However, niclosamide addition demonstrated that the increased VE-cadherin protein levels were largely STAT3-dependent.

Nonetheless, it remains plausible that STAT3 and VE-cadherin regulation and interaction in macrophages may differ compared to primary endothelial cells.

The finding that GM-CSF polarised macrophages develop tube-like structures within the Matrigel angiogenesis assay and is mirrored by M-CSF matured macrophages with FGF stimulation is in accordance with previous observations reporting macrophages can form tube like structures on Matrigel (Barnett *et al.,* 2016; Schmeisser *et al.,* 2001). However, the novel aspect presented within this chapter is that the angiogenic potential differs between macrophage subsets at baseline, with the pro-inflammatory GM-Mac readily forming tube-like structures, whereas M-Mac require FGF2 stimulation to display a comparable angiogenic response, in a STAT3-dependent manner.

5.6 Conclusions

In this chapter, a novel pro-angiogenic regulatory axis is reported involving FGF2/FGFR1/STAT3/miR-27a-3p regulation of VE-cadherin protein levels in *in vitro* M-CSF matured human macrophages. As such, in response to vascular injury, when FGF2 production is increased, anti-inflammatory macrophage subsets (under M-CSF cues) may be responsible to provide an endothelial cell-like phenotype to provide temporary protection and facilitate healing. This beneficial role involves the downregulation of miR-27a-3p levels to drive VE-cadherin protein expression via STAT3-dependent signalling. On the other hand, baseline GM-Mac are readily pro-angiogenic which is not reliant on FGF2 signalling and may therefore provide a more acute response during vascular injury, such as providing barrier function before resident endothelial cells can recover. However, in advanced atherosclerotic plaques where neovascularisation is associated with plaque instability and subsequent adverse clinical outcomes, intra-plaque macrophages acquiring an endothelial cell-like phenotype may represent a deleterious response.

6 General Discussion, conclusion, limitations and future directions

6.1 General Discussion

The intricate process of tissue repair and remodelling after injury includes angiogenesis which involves the adaptation of vascular cells, such as VSMCs and endothelial cells. These two cell types are the predominant cells which constitute the vascular wall, together with extracellular matrix components serving as a scaffold such as basement membrane proteins alongside collagens and elastin (Davis and Senger, 2005). In addition, various connective tissue cells such as fibroblasts and perivascular adipocytes found within the adventitial region of blood vessels, may also play an active role in ensuring proper function of vascular networks. For instance, fibroblast-derived factors support neovessel sprouting and lumen formation (Newman *et al.,* 2011), whereas perivascular adipocytes may change phenotype during inflammation to support VSMC proliferation and migration (Horimatsu *et al.,* 2017; Verhagen and Visseren, 2011). Together with recruited monocyte/macrophage populations and resident adventitial macrophages, these divergent cell types work in concert to establish a new vascular network (angiogenesis) to provide effective and fast delivery of oxygenation and nutrients to the ischaemic or injured site, while also ensuring the competent removal of toxic products and apoptotic bodies.

Therefore, under physiological conditions, angiogenesis can be considered as an advantageous tissue response to ensure normal function is kept in check. Besides its role in perfusion physiology, angiogenesis can also be regarded as a deleterious mechanism in response to chronic pathological remodelling such as neovascularisation of atherosclerotic plaques and malignant cancerous tissue. The common dogma is that the angiogenesis/neovascularisation that develops within advanced atherosclerotic plaques, cancers, wound sites, and around areas of ischaemia (such as a myocardial infarct) are derived from resident VSMCs and endothelial cells. (Furuya *et al.,* 2005; Moreno *et al.,* 2006). However, given that immune cells, especially monocyte/macrophages, are rapidly recruited

and accumulate within the locus of injury and ischaemia, and the process of angiogenesis occurs before the complete resolution of inflammation (such as in chronic inflammation), it is plausible monocyte/macrophages directly contribute to new vessel formation. Indeed, challenging the concept that VSMCs and endothelial cells exclusively form angiogenic vessels, perhaps monocyte/macrophages harbour the ability to *trans*-differentiate towards a VSMC-like and/or endothelial cell-like phenotype, and subsequently actively participate in new vessel formation during inflammation-associated injury.

Although the role attributed to monocyte/macrophages are mainly with regard to the resolution of inflammation through the clearance of apoptotic bodies and foreign material (Gregory and Devitt, 2004), the concept that macrophages can adapt to different environmental cues which can reprogramme their phenotype, strengthen the idea of their direct role in the establishment of early neovessel networks through a progenitor capacity to give rise to vascular-like cells. Another interesting aspect to consider whether monocyte/macrophages act similar to the mechanism involved in developmental angiogenesis whereby circulating stem cells and existing resident progenitor cells within the site of injury/inflammation can differentiate into vascular cells.

Accordingly, the work within this study was designed to investigate the potential progenitor capacity of macrophages to *trans*-differentiate towards vascular-like cells, namely VSMCs and endothelial cells. The growth and differentiation of human monocyte-derived macrophages is controlled by the biochemical signals within the surrounding microenvironment. To investigate the possibility that human macrophages may serve as a potential source of VSMC-like and endothelial-like cells during angiogenesis, it is essential to understand how *in vitro* biochemical signals regulate macrophage *trans*-differentiation towards a phenotype similar to VSMCs or endothelial cells. Within this thesis two distinct macrophage populations were produced from human blood-derived monocytes, utilising the colony stimulating factors M-CSF and GM-CSF to generate well-characterised anti-inflammatory and pro-inflammatory phenotypes. Then, VSMC-associated markers were

characterised in both populations. Additional macrophage phenotypes were also investigated at the beginning, but in the later part of the thesis the focus is solely on the M-Mac and GM-Mac subsets.

Similarly, endothelial cell-like characteristics in the M-Mac and GM-Mac phenotypes were evaluated *in vitro*. Initial studies assessed the expression patterns of the candidate markers over different time periods (refer to section 4.4.1), with prolonged exposure to growth factors providing similar results as those observed in seven-day macrophages. Accordingly, subsequent studies were conducted in seven-day differentiated human macrophages followed by four-day growth factor stimulation, accepting that seven-day macrophage maturation is common duration for *in vitro* macrophage studies (Jin and Kruth, 2016).

A major finding of this study was the divergent effect of FGF2 stimulation on M-Mac VE-cadherin mRNA and protein expression. As such, focus was given to identifying the potential mechanism underlying the unique post-transcriptional regulation of VE-cadherin expression in macrophages. Collectively, the findings identified a novel signalling axis within M-CSF matured macrophages whereby FGF2/FGFR1-mediated signalling induces STAT3 activation (phosphorylation) and subsequent down-regulation of miR-27a-3p levels, which in turn permits increased VE-cadherin protein expression. To confirm this regulatory axis stimulated M-Macs to acquire a functional endothelial cell-like phenotype afforded through the increase in VE-cadherin protein expression, *in vitro* angiogenesis was assessed and indeed demonstrated increased tube-like formation by FGF2-induced M-Macs that was dependent upon STAT3 activation. However, if STAT3 directly or indirectly down-regulated miR-27a-3p levels was not explored due to time constraints. Nonetheless, previous evidence has demonstrated that STAT3 can act as both a transcriptional activator and suppressor and is therefore capable of directly up- and down-regulating target gene expression (Lu *et al.,* 2018). Indeed, analysis of the upstream sequence of miR-27a-3p using the JASPAR database identified two highly-conserved predicted STAT3 binding sites, with supporting findings in a tumour cell line demonstrating that miR-27a-3p down-regulation may be mediated by STAT3 (Wang *et al.,*

2018). Therefore, it can be speculated that FGF2-induced STAT3 activation down-regulates miR-27a-3p in M-Macs, leading to the elevated VE-cadherin protein levels and their associated endothelial-like function.

Macrophages are key effector cells of the innate immune system and play central inflammatory and remodelling functions during the development and progression of atherosclerosis (refer to section 1.4 and 1.5), despite their purported beneficial role in modulating angiogenesis (refer to section 5.1.1). The findings within this thesis support the proposition that macrophages can play a potential progenitor cell role in the formation of non-resident endothelial cell vascular network formation (refer to section 5.1.2). Accordingly, within specific microenvironments with the correct cues/stimuli, macrophages can directly form nascent tube-like structures reminiscent of capillaries, for instance during tumorigenesis, before the establishment of a mature vasculature by resident 'true' endothelial cells, or possibly the direct *trans*-differentiation of macrophages. Indeed, the functional perfusion of macrophage-derived vascular networks has been previously demonstrated (Barnett *et al.,* 2016). The premise that macrophages harbour the ability to *trans*-differentiate into endothelial cells is not a recent one. Previous research has postulated this idea based upon the observation that macrophages form branched cell columns when cultured upon synthetic extracellular matrix proteins (Anghelina *et al.,* 2004). Further studies have suggested that macrophages can *trans*-differentiate into endothelial-like cells (Kumar *et al.,* 2013; Schmeisser *et al.,* 2001) and VSMC-like cells (Kumar *et al.,* 2010). Similar observations are reported within this thesis, but excitingly, demonstrate that the progenitor potential of macrophages to *trans*-differentiate into VSMC- and endothelial-like cells is dictated by their polarisation/phenotype, while also identifying the possible novel signalling pathways involved.

Progenitor cells are more or less similar to stem cells whereby they are defined through their ability to differentiate into a specific cell type. However, in opposed to undifferentiated stem cells which have purported indefinite proliferative capacity, as descendants of stem cells progenitor cells have

restricted proliferative potential, and are therefore considered a differentiated cell with the capability to be induced into other target cell types (Seaberg and van der Kooy, 2003). Thus, macrophages with phagocytotic activity as their main feature, can be described as a differentiated type of haematopoietic population of cells with progenitor potential.

The expression of certain VSMC and endothelial cell-associated markers support the unique observation and proposition that macrophages can serve as progenitor cells. However, it is possible that the monocyte/macrophages used in the studies within this thesis contain a population of stem/progenitor cell. Yet, the protocol deployed for the isolation of monocytes is a well-established and characterised procedure which relies upon the subsequent use of macrophage-specific colony stimulating factors for their maturation. In addition, monocyte isolation using magnetic-bead separation yields similar findings as those that rely upon adherence isolation and are consistent with the practices for isolating and obtaining macrophage-pure cultures. As such, the observation that features of *trans*-differentiation persist (acquired VSMC and endothelial cell marker expression) under these conditions provide confidence that the cells are macrophage populations and not from circulating stem cells. Indeed, this proposition is further strengthened by the observation that the expression of a macrophage-specific marker is maintained. It could equally be proposed that VSMCs and/or endothelial cells were present within the collected blood and gave rise to the observed increases in gene and protein expression of VSMC and endothelial cell-related markers. However, the expression pattern of these markers in the macrophage subsets were markedly different from primary human VSMCs and endothelial cells, as indicated at the end of chapter 3 and 4 respectively (refer section 3.4.5 and 4.4.4). Therefore, these further observations lend support to the concept that macrophages harbour progenitor potential and plasticity, in regard to their expression of vascular cell-like features under certain conditions.

A further prominent finding in this thesis is the recognition that macrophage subsets have a disparate capacity to display vascular cell-related markers and functions. Macrophages matured with

GM-CSF (GM-Mac) are considered a pro-inflammatory phenotype (Di Gregoli and Johnson, 2012), and upon maturation readily expressed select VSMC- and endothelial cell-related markers compared to their M-CSF matured counterparts (M-Mac), which are classed as an anti-inflammatory phenotype (Di Gregoli and Johnson, 2012). Moreover, GM-Macs freely formed capillary tube-like structures upon Matrigel without the need of exogenous stimuli. However, upon stimulation with FGF2, M-Macs showed comparable VE-cadherin protein levels and capillary tube-like formation as that observed in unstimulated GM-Macs. Similarly, M-Macs displayed diminished expression of multiple VSMC-associated markers relative to pro-inflammatory GM-Macs, which could be increased to comparable levels through stimulation with PDGF-BB/TGFβ1. Although, whether the acquired expression of VSMC-related markers afforded the macrophage subsets with VSMC functions was not explored.

Nonetheless, the findings reported here imply a relationship between M-Macs acquiring a more pro-inflammatory phenotype and displaying progenitor potential when exposed to specific stimuli, rendering them similar to their GM-Mac equivalent. It would therefore be interesting and informative to examine the inflammatory expression profile of PDGF-BB/TGFβ1 and FGF2 stimulated M-Mac, to determine if they do indeed become more pro-inflammatory. Relatedly, the inflammatory cytokines released by macrophages during angiogenesis include IL-1β, IL-6 and TNF-α, which are important to ensure the persistent infiltration of immune cells (Fahey and Doyle, 2019; Fajardo *et al.,* 1992; Heidemann *et al.,* 2003). Reportedly, alternatively activated (anti-inflammatory) macrophages (IL-4 polarised macrophage) are associated with reduced TIMP-1 expression and associated high MMP-9 activity, which favours a pro-angiogenic environment (Zajac *et al.,* 2013). In addition, systemic depletion of macrophages through deficiency of M-CSF in osteopetrotic (op/op) mice supresses angiogenesis (Kubota *et al.,* 2009) whereas *in vivo* addition of macrophages supports angiogenesis in the mouse hind limb ischaemia model (Hirose *et al.,* 2008) and embryonic zebrafish (Britto *et al.,* 2018). Furthermore, different macrophage phenotypes have been linked to different

stages of the angiogenic response, with pro-inflammatory M1-polarised macrophages purported to support angiogenesis but their pro-longed accumulation to cause vessel regression, whereas various anti-inflammatory M2-phenotypes are associated with modulation of pericytes and endothelial cells during angiogenic vessel maturation (Graney *et al.,* 2020). These findings demonstrate that macrophages play a pivotal role in angiogenesis, but their direct contribution to vessel formation through their transformation into endothelial-like cells was never considered or examined.

This study has added new knowledge to the potential mechanisms by which macrophage -derived neo-vasculature may occur. Colony stimulating factors are essential cues for the differentiation and maturation of monocytes into macrophages, with the capacity to give rise to different macrophage phenotypes, with divergent innate capacity to exhibit vascular cell-like progenitor potential. The ensuing interaction of macrophages (under the control of M-CSF) with further stimuli including PDGF-BB, TGFβ1, VEGF and FGF2, can shift macrophages towards vascular-like cells. Consequently, the participation of macrophages to the formation of capillary tube-like structures during the early phase of angiogenesis is not merely a response to vascular injury and to assist the growth of new vessels, but they may also participate directly to the formation of angiogenic vessels through their conversion to endothelial-like cells. With the associated identification of a possible regulatory pathway, it potentially permits the discovery of novel therapeutic targets for preventing early pathological angiogenesis. Such strategies could include localised or systemic delivery of; a FGFR1-blocker, a STAT3-inhibitor to restore miR-27a-3p levels, or a miR-27a-3p mimic in order to suppress VE-cadherin protein levels to disrupt macrophage derived neo-vasculature formation during the early stages of tumour growth, or to limit neovascularisation in advanced atherosclerotic plaques. Reassuringly, FGFR1-neutralisation and inhibition of STAT-3 are therapeutic approaches under assessment in clinical trials for a variety of different diseases, including several cancers. In addition, multiple microRNA-based therapeutics have advanced to evaluation in clinical trials (Rupaimoole and Slack, 2017). Nevertheless, further work is required within *in vitro* and *in vivo* studies, to validate

whether such therapeutic approaches modulate the direct contribution of macrophages to angiogenesis/neovascularisation and ensuing adverse disease progression.

6.2 Concluding remarks

GM-CSF matured macrophages (GM-Mac) are pro-inflammatory and can be considered to intrinsically display VSMC-like and endothelial cell-like properties and function based upon their expression of associated markers, alongside their capacity to form capillary tube-like structures *in vitro*. Conversely, the M-CSF matured macrophages (M-Mac) are anti-inflammatory and require PDGF-BB/TGFβ1 co-stimulation or FGF2 signalling in order to display comparable VSMC-like and endothelial cell-like features, respectively. In addition, lipid-laden foam cell macrophages induces a VSMC-like transition. Collectively, it can be speculated that M-Mac and GM-Mac (*in vitro*) represent two ends of macrophage phenotypic spectrum and should be used as baseline references for experimental studies. These findings add new attributes to *in vitro* M-CSF and GM-CSF directed macrophages as described in section 1.6 above, in regard to their progenitor potential that warrant further *in vivo* investigation and validation. The salient findings from this thesis are summarised in the following figure: -

M-Mac

- Macrophage colony stimulating factor
- Anti-inflammatory
- Less VSMC-like and EC-like characteristics
- ↑ miR-27a-3p, ↓ VE-cadherin protein/ ↓ STAT3 activation
- Less tube formation (less angiogenic)

PDGF-BB+TGFβ1

- Shift towards 'pro-inflammatory'
- ↑ VSMC-like characteristics

Foam cell

- Shift towards 'pro-inflammatory'
- ↑ VSMC-like characteristics

FGF2

- Shift towards 'pro-inflammatory'
- ↑ EC-like characteristics
- ↓ miR-27a-3p, ↑ VE-cadherin protein
- ↑ tube formation/STAT3 activation

GM-Mac

- Granulocyte Macrophage-colony stimulating factor
- Pro-inflammatory
- More VSMC-like and EC-like cells characteristics
- ↓ miR-27a-3p, ↑ VE-cadherin protein/ ↑ STAT3 activation
- ↑ tube formation (pro-angiogenic)

PDGF-BB+TGFβ1

- ↓ VSMC-like characteristics
- Less/not affected by the growth factors

FGF2

- Maintain EC-like characteristics
- Not affected by growth factors

6.3 Limitations of the study

One of the limitations in this study is the use of monocyte-derived macrophages from random healthy donors without prior investigation and specification of the monocyte subset percentages (based on cell-surface expression of CD14 and CD16) for each individual. This was not included in this study, even though as described in chapter 5, we used pan-monocyte isolation (isolation of all CD14+ and CD16+ monocytes) for subsequent differentiation and maturation into macrophages. The use of different monocyte subsets (as described in Table 1.2.1), may have provided insight into the differential capacity of the monocytes subsets (inflammatory, patrolling, and phagocytotic subsets), to differentiate into M-Mac and GM-Mac, and subsequent expression of VSMC and endothelial cell-related-markers. Additionally, CD16+ monocytes are increased in individuals with cardiovascular disease and are therefore considered pro-inflammatory and drive plaque instability. Although our donors appear healthy, certain individuals may have subclinical atherosclerosis with an associated increased number of circulating CD16+ monocytes, which may have altered progenitor capacity. However, the small variance and normal distribution of our data from n=6 donors suggest this was not the case. Nonetheless, it would be interesting to determine if monocytes (particularly the CD16+ population) from cardiovascular disease patients are more pro-inflammatory and display augmented progenitor potential towards VSMC and endothelial-like cells, compared to age/gender-matched healthy controls.

On a different note, different *in vitro* culture durations may also lead to conflicting results and thus confound the consistency of the presented results, as briefly mentioned in chapter 5. It is plausible that shorter or longer culture periods may differentially affect the macrophage phenotypes, with the expression patterns of the assessed markers varying depending on time in culture. Indeed, macrophages may undergo distinct phenotype modulation such as changes in pro-inflammatory cytokine expression in response to prolonged culture (Chamberlain *et al.,* 2015). Additionally, LPS

and IFNγ (or M1)-activated macrophages show differential responses to angiogenesis at earlier time points compared to the later stages of angiogenesis (Graney *et al.,* 2020).

The expression of the VSMC and endothelial cell-associated markers by macrophages in this study are reliant on the robustness and validity of the primary antibodies used. Nonetheless, Western blotting for all proteins was validated in primary human VSMCs or HUVECs to ensure that the detected bands were of the correct predicted weight. On some occasions there were slight discrepancies which requires the findings to be interpreted carefully. For example, many antibodies raised against VE-cadherin for use in Western blotting detect bands at a molecular weight between 120-130 kDa alongside a band around 75 kDa. Although bands at both molecular weights were observed in HUVECs, the 75 kDa band was the most intense (refer to figure in section 9.1.4), while it was the only band detected in human macrophage lysates under any condtions. Furthermore, the immunofluorescence staining in this study also used the same antibody as for western blotting, thus the analysis of VE-cadherin expression in this study is consistent. Possible reasons for the detection of different molecular weight bands detected between macrophages and HUVECs maybe due to the different prevalence of splice variants, degree of glycosylation, or multimers of the proteins, which would require further investigation.

6.4 Future directions

The studies within this thesis have raised additional new questions which would require further attention and experimental work to address. In the first result chapter, divergent effects of PDGF-BB/TGFβ1 on selected VSMC-markers was observed, whereby down-regulation of protein levels were detected while mRNA expression was largely unaffected in GM-Mac. This differential pattern suggests the contribution of a post-transcriptional regulatory mechanism, highlighting possible microRNA involvement and/or a negative feedback process. The higher expression of VSMC-markers afforded by PDGF-BB/TGFβ1 co-stimulation -in GM-Mac may involve a negative feedback mechanism as baseline GM-Mac already displayed high expression of VSMC-markers. This observation may also suggest that GM-Mac are a differentiated macrophage phenotype with innate VSMC-like features. In contrast, M-Mac require further modulation (PDGF-BB/TGFβ1 co-stimulation) in order to *trans*-differentiate towards a VSMC-like phenotype. Future studies could also examine if the observed marked expression of the VSMC-associated proteins in macrophages resulted in them acquiring functions normally attributed to VSMCs. For example, the contractile ability of macrophages could be investigated. Additional biochemical stimuli alongside mechanical force/cyclic strain could be applied to the macrophage subsets to further characterise their capability to function as VSMC-like cells.

Another experiment worthy of further investigation is the *in vivo* angiogenic capacity of macrophages to form neo-vessels. This could be achieved either by a subcutaneous matrigel angiogenesis assay or choroidal angiogenesis in transgenic mice where the monocyte/macrophages are fluorescently labelled, such as CD68-GFP-Tg mice. In addition, wound healing angiogenesis may also be feasibly investigated. Such *in vivo* angiogenesis experiments would validate the *in vitro* findings reported within this thesis. Additionally, the perfusion function and permeability of macrophage derived neo-vessel formation can also be assessed, for example laser confocal microscopy analysis would permit the analysis of capillary tube-like formation as well as perfusion

function (Fantin *et al.,* 2010). Additionally, it would be interesting to investigate the contribution of hypoxia macrophage derived neovessel formation, as hypoxia is a known main inducer of angiogenesis and inflammatory cell recruitment (Krock *et al.,* 2011).

Finally, monocyte/macrophages have been implicated as a potential source of osteoblast-like cells, therefore potentially capable of contributing to vascular calcification in advanced atherosclerosis (Burgmaier *et al.,* 2018). Therefore, the progenitor potential of macrophages to *trans*-differentiate into bone-like cells in regard to atherosclerotic plaques could be investigated. In addition, the potential of macrophages to *trans*-differentiate into cardiomyocyte-like cells is further potential area for future examination, particularly given myocardial infarction induces marked accumulation of monocyte/macrophages ripe for potential reprogramming. Furthermore, the regeneration of cardiomyocytes following heart failure requires progenitor cell recruitment (Mekala *et al.,* 2018), thus a similar study could be undertaken to evaluate if macrophages can serve as potential progenitor cells able to *trans*-differentiate into cardiomyocyte-like cells and protect from future heart failure.

7 References

Aikawa, M., Sivam, P. N., Kuro-o, M., Kimura, K., Nakahara, K., Takewaki, S., Periasamy, M. (1993). Human smooth muscle myosin heavy chain isoforms as molecular markers for vascular development and atherosclerosis. *Circ Res*, *73*(6), 1000-1012.

Aird, W. C. (2008). Endothelium in health and disease. *Pharmacol Rep*, *60*(1), 139-143.

Akagawa, K. S. (2002). Functional heterogeneity of colony-stimulating factor-induced human monocyte-derived macrophages. *Int. J. Hematol, 76*(1), 27-34. https://doi.org/10.1007/bf02982715

Alsaffar, H., Martino, N., Garrett, J. P., & Adam, A. P. (2018). Interleukin-6 promotes a sustained loss of endothelial barrier function via Janus kinase-mediated STAT3 phosphorylation and de novo protein synthesis. *Am J Physiol Cell Physiol*, *314*(5), C589-C602. https://doi.org/10.1152/ajpcell.00235.2017

Ancuta, P., Rao, R., Moses, A., Mehle, A., Shaw, S. K., Luscinskas, F. W., & Gabuzda, D. (2003). Fractalkine preferentially mediates arrest and migration of CD16+ monocytes. *J Exp Med*, *197*(12), 1701-1707. https://doi.org/10.1084/jem.20022156

Andrés, G., Leali, D., Mitola, S., Coltrini, D., Camozzi, M., Corsini, M., Presta, M. (2009). A pro-inflammatory signature mediates FGF2-induced angiogenesis. *J Cell Mol Med*, *13*(8B), 2083-2108. https://doi.org/10.1111/j.1582-4934.2008.00415.x

Anghelina, M., Krishnan, P., Moldovan, L., & Moldovan, N. I. (2004). Monocytes and macrophages form branched cell columns in matrigel: implications for a role in neovascularization. *Stem Cells Dev*, *13*(6), 665-676. https://doi.org/10.1089/scd.2004.13.665

Araujo, J. A., Zhang, M., & Yin, F. (2012). Heme oxygenase-1, oxidation, inflammation, and atherosclerosis. *Front Pharmacol*, *3*, 119. https://doi.org/10.3389/fphar.2012.00119

Arbab-Zadeh, A., & Fuster, V. (2015). The myth of the "vulnerable plaque": transitioning from a focus on individual lesions to atherosclerotic disease burden for coronary artery disease risk assessment. *J Am Coll Cardiol*, *65*(8), 846-855. https://doi.org/10.1016/j.jacc.2014.11.041

Arciniegas, E., Sutton, A. B., Allen, T. D., & Schor, A. M. (1992). Transforming growth factor beta 1 promotes the differentiation of endothelial cells into smooth muscle-like cells *in vitro*. *J Cell Sci*, *103 (Pt 2)*, 521-529.

Arsenault, B. J., Boekholdt, S. M., & Kastelein, J. J. (2011). Lipid parameters for measuring risk of cardiovascular disease. *Nat Rev Cardiol*, *8*(4), 197-206. https://doi.org/10.1038/nrcardio.2010.223

Auffray, C., Sieweke, M. H., & Geissmann, F. (2009). Blood monocytes: development, heterogeneity, and relationship with dendritic cells. *Annu Rev Immunol*, *27*, 669-692. https://doi.org/10.1146/annurev.immunol.021908.132557

Bach, L. A. (2015). Endothelial cells and the IGF system. *J Mol Endocrinol*, *54*(1), R1-13. https://doi.org/10.1530/JME-14-0215

Baeten, C. I., Hillen, F., Pauwels, P., de Bruine, A. P., & Baeten, C. G. (2009). Prognostic role of vasculogenic mimicry in colorectal cancer. *Dis Colon Rectum*, *52*(12), 2028-2035. https://doi.org/10.1007/DCR.0b013e3181beb4ff

Ball, S. G., Shuttleworth, C. A., & Kielty, C. M. (2010). Platelet-derived growth factor receptors regulate mesenchymal stem cell fate: implications for neovascularization. *Expert Opin Biol Ther*, *10*(1), 57-71. https://doi.org/10.1517/14712590903379510

Barnett, F. H., Rosenfeld, M., Wood, M., Kiosses, W. B., Usui, Y., Marchetti, V., Friedlander, M. (2016). Macrophages form functional vascular mimicry channels *in vivo*. *Sci Rep*, *6*, 36659. https://doi.org/10.1038/srep36659

Barreda, D. R., Hanington, P. C., & Belosevic, M. (2004). Regulation of myeloid development and function by colony stimulating factors. *Dev Comp Immunol*, *28*(5), 509-554. https://doi.org/10.1016/j.dci.2003.09.010

Barstow, C., Rice, M., & McDivitt, J. D. (2017). Acute Coronary Syndrome: Diagnostic Evaluation. *Am Fam Physician*, *95*(3), 170-177.

Bates, D. O. (2010). Vascular endothelial growth factors and vascular permeability. *Cardiovasc Res*, *87*(2), 262-271. https://doi.org/10.1093/cvr/cvq105

Bazzoni, F., Rossato, M., Fabbri, M., Gaudiosi, D., Mirolo, M., Mori, L., Locati, M. (2009). Induction and regulatory function of miR-9 in human monocytes and neutrophils exposed to proinflammatory signals. *Proc Natl Acad Sci U S A*, *106*(13), 5282-5287. https://doi.org/10.1073/pnas.0810909106

Beamish, J. A., He, P., Kottke-Marchant, K., & Marchant, R. E. (2010). Molecular regulation of contractile smooth muscle cell phenotype: implications for vascular tissue engineering. *Tissue Eng Part B Rev*, *16*(5), 467-491. https://doi.org/10.1089/ten.TEB.2009.0630

Beneš, P., Macečková, V., Zdráhal, Z., Konečná, H., Zahradníčková, E., Mužík, J., & Šmarda, J. (2006). Role of vimentin in regulation of monocyte/macrophage differentiation. *Differentiation*, *74*(6), 265-276. https://doi.org/http://dx.doi.org/10.1111/j.1432-0436.2006.00077.x

Bennett, M. R. (1999). Apoptosis of vascular smooth muscle cells in vascular remodelling and atherosclerotic plaque rupture. *Cardiovasc Res*, *41*(2), 361-368. https://doi.org/10.1016/s0008-6363(98)00212-0

Bian, Z. Y., Li, G., Gan, Y. K., Hao, Y. Q., Xu, W. T., & Tang, T. T. (2009). Increased number of mesenchymal stem cell-like cells in peripheral blood of patients with bone sarcomas. *Arch Med Res*, *40*(3), 163-168. https://doi.org/10.1016/j.arcmed.2009.01.002

Blankenberg, S., Barbaux, S., & Tiret, L. (2003). Adhesion molecules and atherosclerosis. *Atherosclerosis*, *170*(2), 191-203.

Blobe, G. C., Schiemann, W. P., & Lodish, H. F. (2000). Role of transforming growth factor beta in human disease. *N Engl J Med*, *342*(18), 1350-1358. https://doi.org/10.1056/nejm200005043421807

Bonetti, P. O., Lerman, L. O., & Lerman, A. (2003). Endothelial dysfunction: a marker of atherosclerotic risk. *Arterioscler Thromb Vasc Biol*, *23*(2), 168-175.

Boos, C. J., Soor, S. K., Kang, D., & Lip, G. Y. (2007). Relationship between circulating endothelial cells and the predicted risk of cardiovascular events in acute coronary syndromes. *Eur Heart J*, *28*(9), 1092-1101. https://doi.org/10.1093/eurheartj/ehm070

Borén, J., & Williams, K. J. (2016). The central role of arterial retention of cholesterol-rich apolipoprotein-B-containing lipoproteins in the pathogenesis of atherosclerosis: a triumph of simplicity. *Curr Opin Lipidol*, *27*(5), 473-483. https://doi.org/10.1097/MOL.0000000000000330

Bowen-Pope, D. F., & Raines, E. W. (2011). History of discovery: platelet-derived growth factor. *Arterioscler Thromb Vasc Biol*, *31*(11), 2397-2401. https://doi.org/10.1161/atvbaha.108.179556

Britto, D. D., Wyroba, B., Chen, W., Lockwood, R. A., Tran, K. B., Shepherd, P. R., . . . Astin, J. W. (2018). Macrophages enhance Vegfa-driven angiogenesis in an embryonic zebrafish tumour xenograft model. *Dis Model Mech*, *11*(12). https://doi.org/10.1242/dmm.035998

Britton, K. A., & Fox, C. S. (2011). Perivascular adipose tissue and vascular disease. *Clin Lipidol*, *6*(1), 79-91. https://doi.org/10.2217/clp.10.89

Brånén, L., Hovgaard, L., Nitulescu, M., Bengtsson, E., Nilsson, J., & Jovinge, S. (2004). Inhibition of tumor necrosis factor-alpha reduces atherosclerosis in apolipoprotein E knockout mice. *Arterioscler Thromb Vasc Biol*, *24*(11), 2137-2142. https://doi.org/10.1161/01.ATV.0000143933.20616.1b

Burgmaier, M., Milzi, A., Dettori, R., Burgmaier, K., Marx, N., & Reith, S. (2018). Co-localization of plaque macrophages with calcification is associated with a more vulnerable plaque phenotype and a greater calcification burden in coronary target segments as determined by OCT. *PLoS One*, *13*(10), e0205984. https://doi.org/10.1371/journal.pone.0205984

Burke, A. P., Kolodgie, F. D., Farb, A., Weber, D. K., Malcom, G. T., Smialek, J., & Virmani, R. (2001). Healed plaque ruptures and sudden coronary death: evidence that subclinical rupture has a role in plaque progression. *Circulation*, *103*(7), 934-940. https://doi.org/10.1161/01.cir.103.7.934

Busch, K., Klapproth, K., Barile, M., Flossdorf, M., Holland-Letz, T., Schlenner, S. M., . . . Rodewald, H. R. (2015). Fundamental properties of unperturbed haematopoiesis from stem cells *in vivo*. *Nature*, *518*(7540), 542-546. https://doi.org/10.1038/nature14242

Cai, X., Yin, Y., Li, N., Zhu, D., Zhang, J., Zhang, C. Y., & Zen, K. (2012). Re-polarization of tumor-associated macrophages to pro-inflammatory M1 macrophages by microRNA-155. *J Mol Cell Biol*, *4*(5), 341-343. https://doi.org/10.1093/jmcb/mjs044

Caporali, A., & Emanueli, C. (2011). MicroRNA regulation in angiogenesis. *Vascul Pharmacol*, *55*(4), 79-86. https://doi.org/10.1016/j.vph.2011.06.006

Carmeliet, P. (2003). Angiogenesis in health and disease. *Nat Med*, *9*(6), 653-660. https://doi.org/10.1038/nm0603-653

Carr, S. S., Hooper, A. J., Sullivan, D. R., & Burnett, J. R. (2019). Non-HDL-cholesterol and apolipoprotein B compared with LDL-cholesterol in atherosclerotic cardiovascular disease risk assessment. *Pathology*, *51*(2), 148-154. https://doi.org/10.1016/j.pathol.2018.11.006

Casagrande, V., Menghini, R., Menini, S., Marino, A., Marchetti, V., Cavalera, M., Federici, M. (2012). Overexpression of tissue inhibitor of metalloproteinase 3 in macrophages reduces atherosclerosis in low-density lipoprotein receptor knockout mice. *Arterioscler Thromb Vasc Biol*, *32*(1), 74-81. https://doi.org/10.1161/ATVBAHA.111.238402

Casscells, W. (1991). Smooth muscle cell growth factors. *Prog Growth Factor Res*, *3*(3), 177-206.

Cathcart, M. K., Morel, D. W., & Chisolm, G. M. (1985). Monocytes and neutrophils oxidize low density lipoprotein making it cytotoxic. *J Leukoc Biol*, *38*(2), 341-350. https://doi.org/10.1002/jlb.38.2.341

Celic, T., Metzinger-Le Meuth, V., Six, I., Massy, Z. A., & Metzinger, L. (2017). The mir-221/222 Cluster is a Key Player in Vascular Biology via the Fine-Tuning of Endothelial

Cell Physiology. *Curr Vasc Pharmacol*, *15*(1), 40-46. https://doi.org/10.2174/1570161114666160914175149
Chamberlain, L. M., Holt-Casper, D., Gonzalez-Juarrero, M., & Grainger, D. W. (2015). Extended culture of macrophages from different sources and maturation results in a common M2 phenotype. *J Biomed Mater Res A*, *103*(9), 2864-2874. https://doi.org/10.1002/jbm.a.35415
Chen, D., Xia, M., Hayford, C., Tham, e.-L., Semik, V., Hurst, S., Dorling, A. (2015). Expression of human tissue factor pathway inhibitor on vascular smooth muscle cells inhibits secretion of macrophage migration inhibitory factor and attenuates atherosclerosis in ApoE-/- mice. *Circulation*, *131*(15), 1350-1360. https://doi.org/10.1161/CIRCULATIONAHA.114.013423
Chen, L., DeWispelaere, A., Dastvan, F., Osborne, W. R., Blechner, C., Windhorst, S., & Daum, G. (2016). Smooth Muscle-Alpha Actin Inhibits Vascular Smooth Muscle Cell Proliferation and Migration by Inhibiting Rac1 Activity. *PLoS One*, *11*(5), e0155726. https://doi.org/10.1371/journal.pone.0155726
Chen, W., Mook, R. A., Premont, R. T., & Wang, J. (2018). Niclosamide: Beyond an antihelminthic drug. *Cell Signal*, *41*, 89-96. https://doi.org/10.1016/j.cellsig.2017.04.001
Chen, X., Liang, H., Zhang, J., Zen, K., & Zhang, C. Y. (2012). Secreted microRNAs: a new form of intercellular communication. *Trends Cell Biol*, *22*(3), 125-132. https://doi.org/10.1016/j.tcb.2011.12.001
Chen, Z., & Han, Z. C. (2008). STAT3: a critical transcription activator in angiogenesis. *Med Res Rev*, *28*(2), 185-200. https://doi.org/10.1002/med.20101
Chhabra, R., Dubey, R., & Saini, N. (2010). Cooperative and individualistic functions of the microRNAs in the miR-23a~27a~24-2 cluster and its implication in human diseases. *Mol Cancer*, *9*, 232. https://doi.org/10.1186/1476-4598-9-232
Chien, S. (2003). Molecular and mechanical bases of focal lipid accumulation in arterial wall. *Prog Biophys Mol Biol*, *83*(2), 131-151.
Chinetti-Gbaguidi, G., Baron, M., Bouhlel, M. A., Vanhoutte, J., Copin, C., Sebti, Y., Staels, B. (2011). Human atherosclerotic plaque alternative macrophages display low cholesterol handling but high phagocytosis because of distinct activities of the PPARγ and LXRα pathways. *Circ Res*, *108*(8), 985-995. https://doi.org/10.1161/circresaha.110.233775
Chistiakov, D. A., Orekhov, A. N., & Bobryshev, Y. V. (2015). Vascular smooth muscle cell in atherosclerosis. *Acta Physiol (Oxf)*, *214*(1), 33-50. https://doi.org/10.1111/apha.12466
Chiu, J. J., & Chien, S. (2011). Effects of disturbed flow on vascular endothelium: pathophysiological basis and clinical perspectives. *Physiol Rev*, *91*(1), 327-387. https://doi.org/10.1152/physrev.00047.2009
Chiu, J. J., Wang, D. L., Chien, S., Skalak, R., & Usami, S. (1998). Effects of disturbed flow on endothelial cells. *J Biomech Eng*, *120*(1), 2-8. https://doi.org/10.1115/1.2834303
Cho, H. J., Kim, H. S., Lee, M. M., Kim, D. H., Yang, H. J., Hur, J., Park, Y. B. (2003). Mobilized endothelial progenitor cells by granulocyte-macrophage colony-stimulating factor accelerate reendothelialization and reduce vascular inflammation after intravascular radiation. *Circulation*, *108*(23), 2918-2925. https://doi.org/10.1161/01.CIR.0000097001.79750.78

Cho, K. Y., Miyoshi, H., Kuroda, S., Yasuda, H., Kamiyama, K., Nakagawara, J., Atsumi, T. (2013). The phenotype of infiltrating macrophages influences arteriosclerotic plaque vulnerability in the carotid artery. *J Stroke Cerebrovasc Dis*, *22*(7), 910-918. https://doi.org/10.1016/j.jstrokecerebrovasdis.2012.11.020

Cines, D. B., Pollak, E. S., Buck, C. A., Loscalzo, J., Zimmerman, G. A., McEver, R. P., Stern, D. M. (1998). Endothelial cells in physiology and in the pathophysiology of vascular disorders. *Blood*, *91*(10), 3527-3561.

Cingöz, O., & Goff, S. P. (2018). Cyclin-dependent kinase activity is required for type I interferon production. *Proc Natl Acad Sci U S A*, *115*(13), E2950-E2959. https://doi.org/10.1073/pnas.1720431115

Cochain, C., Vafadarnejad, E., Arampatzi, P., Pelisek, J., Winkels, H., Ley, K., Zernecke, A. (2018). Single-Cell RNA-Seq Reveals the Transcriptional Landscape and Heterogeneity of Aortic Macrophages in Murine Atherosclerosis. *Circ Res*, *122*(12), 1661-1674. https://doi.org/10.1161/CIRCRESAHA.117.312509

Colin, S., Chinetti-Gbaguidi, G., & Staels, B. (2014). Macrophage phenotypes in atherosclerosis. *Immunol Rev*, *262*(1), 153-166. https://doi.org/10.1111/imr.12218

Corliss, B. A., Azimi, M. S., Munson, J. M., Peirce, S. M., & Murfee, W. L. (2016). Macrophages: An Inflammatory Link Between Angiogenesis and Lymphangiogenesis. *Microcirculation*, *23*(2), 95-121. https://doi.org/10.1111/micc.12259

Cross, M. J., & Claesson-Welsh, L. (2001). FGF and VEGF function in angiogenesis: signalling pathways, biological responses and therapeutic inhibition. *Trends Pharmacol Sci*, *22*(4), 201-207. https://doi.org/10.1016/s0165-6147(00)01676-x

D'Aveni, M., Rossignol, J., Coman, T., Sivakumaran, S., Henderson, S., Manzo, T., Rubio, M. T. (2015). G-CSF mobilizes CD34+ regulatory monocytes that inhibit graft-versus-host disease. *Sci Transl Med*, *7*(281), 281ra242. https://doi.org/10.1126/scitranslmed.3010435

Dauwe, D., Pelacho, B., Wibowo, A., Walravens, A. S., Verdonck, K., Gillijns, H., Janssens, S. (2016). Neovascularization Potential of Blood Outgrowth Endothelial Cells From Patients With Stable Ischemic Heart Failure Is Preserved. *J Am Heart Assoc*, *5*(4), e002288. https://doi.org/10.1161/JAHA.115.002288

Davis, G. E., & Senger, D. R. (2005). Endothelial extracellular matrix: biosynthesis, remodeling, and functions during vascular morphogenesis and neovessel stabilization. *Circ Res*, *97*(11), 1093-1107. https://doi.org/10.1161/01.RES.0000191547.64391.e3

Deanfield, J. E., Halcox, J. P., & Rabelink, T. J. (2007). Endothelial function and dysfunction: testing and clinical relevance. *Circulation*, *115*(10), 1285-1295. https://doi.org/10.1161/CIRCULATIONAHA.106.652859

Dejana, E. (2004). Endothelial cell-cell junctions: happy together. *Nat Rev Mol Cell Biol*, *5*(4), 261-270. https://doi.org/10.1038/nrm1357

Dentelli, P., Rosso, A., Orso, F., Olgasi, C., Taverna, D., & Brizzi, M. F. (2010). microRNA-222 controls neovascularization by regulating signal transducer and activator of transcription 5A expression. *Arterioscler Thromb Vasc Biol*, *30*(8), 1562-1568. https://doi.org/10.1161/ATVBAHA.110.206201

Deo, D. D., Axelrad, T. W., Robert, E. G., Marcheselli, V., Bazan, N. G., & Hunt, J. D. (2002). Phosphorylation of STAT-3 in response to basic fibroblast growth factor occurs through a mechanism involving platelet-activating factor, JAK-2, and Src in human

umbilical vein endothelial cells. Evidence for a dual kinase mechanism. *J Biol Chem*, *277*(24), 21237-21245. https://doi.org/10.1074/jbc.M110955200

Derynck, R., Gelbart, W. M., Harland, R. M., Heldin, C. H., Kern, S. E., Massagué, J., Wang, X. F. (1996). Nomenclature: vertebrate mediators of TGFbeta family signals. *Cell*, *87*(2), 173. https://doi.org/10.1016/s0092-8674(00)81335-5

Deuel, T. F., Senior, R. M., Huang, J. S., & Griffin, G. L. (1982). Chemotaxis of monocytes and neutrophils to platelet-derived growth factor. *J Clin Invest*, *69*(4), 1046-1049.

Dewberry, R., Holden, H., Crossman, D., & Francis, S. (2000). Interleukin-1 receptor antagonist expression in human endothelial cells and atherosclerosis. *Arterioscler Thromb Vasc Biol*, *20*(11), 2394-2400. https://doi.org/10.1161/01.atv.20.11.2394

Dews, M., Homayouni, A., Yu, D., Murphy, D., Sevignani, C., Wentzel, E., Thomas-Tikhonenko, A. (2006). Augmentation of tumor angiogenesis by a Myc-activated microRNA cluster. *Nat Genet*, *38*(9), 1060-1065. https://doi.org/10.1038/ng1855

Di Gregoli, K., Jenkins, N., Salter, R., White, S., Newby, A. C., & Johnson, J. L. (2014). MicroRNA-24 regulates macrophage behavior and retards atherosclerosis. *Arterioscler Thromb Vasc Biol*, *34*(9), 1990-2000. https://doi.org/10.1161/ATVBAHA.114.304088

Di Gregoli, K., & Johnson, J. L. (2012). Role of colony-stimulating factors in atherosclerosis. *Curr Opin Lipidol*, *23*(5), 412-421. https://doi.org/10.1097/MOL.0b013e328357ca6e

Di Gregoli, K., Mohamad Anuar, N. N., Bianco, R., White, S. J., Newby, A. C., George, S. J., & Johnson, J. L. (2017). MicroRNA-181b Controls Atherosclerosis and Aneurysms Through Regulation of TIMP-3 and Elastin. *Circ Res*, *120*(1), 49-65. https://doi.org/10.1161/CIRCRESAHA.116.309321

Di Gregoli, K., Somerville, M., Bianco, R., Thomas, A. C., Frankow, A., Newby, A. C., Johnson, J. L. (2020). Galectin-3 Identifies a Subset of Macrophages With a Potential Beneficial Role in Atherosclerosis. *Arterioscler Thromb Vasc Biol*, *40*(6), 1491-1509. https://doi.org/10.1161/atvbaha.120.314252

Dickson, M. C., Martin, J. S., Cousins, F. M., Kulkarni, A. B., Karlsson, S., & Akhurst, R. J. (1995). Defective haematopoiesis and vasculogenesis in transforming growth factor-beta 1 knock out mice. *Development*, *121*(6), 1845-1854.

Dobnikar, L., Taylor, A. L., Chappell, J., Oldach, P., Harman, J. L., Oerton, E., Jørgensen, H. F. (2018). Disease-relevant transcriptional signatures identified in individual smooth muscle cells from healthy mouse vessels. *Nat Commun*, *9*(1), 4567. https://doi.org/10.1038/s41467-018-06891-x

Dominici, M., Le Blanc, K., Mueller, I., Slaper-Cortenbach, I., Marini, F., Krause, D., Horwitz, E. (2006). Minimal criteria for defining multipotent mesenchymal stromal cells. The International Society for Cellular Therapy position statement. *Cytotherapy*, *8*(4), 315-317. https://doi.org/10.1080/14653240600855905

Domschke, G., & Gleissner, C. A. (2019). CXCL4-induced macrophages in human atherosclerosis. *Cytokine*, *122*, 154141. https://doi.org/10.1016/j.cyto.2017.08.021

Dong, Z., Santeford, A., Ban, N., Lee, T. J., Smith, C., Ornitz, D. M., & Apte, R. S. (2019). FGF2-induced STAT3 activation regulates pathologic neovascularization. *Exp Eye Res*, *187*, 107775. https://doi.org/10.1016/j.exer.2019.107775

Duan, Z., Huang, H., & Sun, F. (2016). The functional and predictive roles of miR-210 in cryptorchidism. *Sci Rep*, *6*, 32265. https://doi.org/10.1038/srep32265

Duewell, P., Kono, H., Rayner, K. J., Sirois, C. M., Vladimer, G., Bauernfeind, F. G., Latz, E. (2010). NLRP3 inflammasomes are required for atherogenesis and activated by

cholesterol crystals. *Nature*, *464*(7293), 1357-1361. https://doi.org/10.1038/nature08938
Fahey, E., & Doyle, S. L. (2019). IL-1 Family Cytokine Regulation of Vascular Permeability and Angiogenesis. *Front Immunol*, *10*, 1426. https://doi.org/10.3389/fimmu.2019.01426
Fajardo, L. F., Kwan, H. H., Kowalski, J., Prionas, S. D., & Allison, A. C. (1992). Dual role of tumor necrosis factor-alpha in angiogenesis. *Am J Pathol*, *140*(3), 539-544.
Fan, Y., Zhang, J., Chen, C. Y., Xiao, Y. B., Asico, L. D., Jose, P. A., Zeng, C. Y. (2017). Macrophage migration inhibitory factor triggers vascular smooth muscle cell dedifferentiation by a p68-serum response factor axis. *Cardiovasc Res*, *113*(5), 519-530. https://doi.org/10.1093/cvr/cvx025
Fantin, A., Vieira, J. M., Gestri, G., Denti, L., Schwarz, Q., Prykhozhij, S., Ruhrberg, C. (2010). Tissue macrophages act as cellular chaperones for vascular anastomosis downstream of VEGF-mediated endothelial tip cell induction. *Blood*, *116*(5), 829-840. https://doi.org/10.1182/blood-2009-12-257832
Farias-Itao, D. S., Pasqualucci, C. A., Nishizawa, A., da Silva, L. F. F., Campos, F. M., Bittencourt, M. S., Suemoto, C. K. (2019). B Lymphocytes and Macrophages in the Perivascular Adipose Tissue Are Associated With Coronary Atherosclerosis: An Autopsy Study. *J Am Heart Assoc*, *8*(24), e013793. https://doi.org/10.1161/JAHA.119.013793
Feingold, K. R., & Grunfeld, C. (2018). Introduction to Lipids and Lipoproteins. In *Introduction to Lipids and Lipoproteins.* MDText.com, Inc.
Feng, M., Li, Z., Wang, D., Wang, F., Wang, C., & Ding, F. (2018). MicroRNA-210 aggravates hypoxia-induced injury in cardiomyocyte H9c2 cells by targeting CXCR4. *Biomed Pharmacother*, *102*, 981-987. https://doi.org/10.1016/j.biopha.2018.03.151
Fernandez Pujol, B., Lucibello, F. C., Gehling, U. M., Lindemann, K., Weidner, N., Zuzarte, M. L., Havemann, K. (2000). Endothelial-like cells derived from human CD14 positive monocytes. *Differentiation*, *65*(5), 287-300.
Ferns, G. A., Raines, E. W., Sprugel, K. H., Motani, A. S., Reidy, M. A., & Ross, R. (1991). Inhibition of neointimal smooth muscle accumulation after angioplasty by an antibody to PDGF. *Science*, *253*(5024), 1129-1132. https://doi.org/10.1126/science.1653454
Fernández-Cortés, M., Delgado-Bellido, D., & Oliver, F. J. (2019). Vasculogenic Mimicry: Become an Endothelial Cell "But Not So Much". *Front Oncol*, *9*, 803. https://doi.org/10.3389/fonc.2019.00803
Finn, A. V., & Jain, R. K. (2010). Coronary plaque neovascularization and hemorrhage: a potential target for plaque stabilization? *JACC Cardiovasc Imaging*, *3*(1), 41-44. https://doi.org/10.1016/j.jcmg.2009.11.001
Fish, J. E., Santoro, M. M., Morton, S. U., Yu, S., Yeh, R. F., Wythe, J. D., Srivastava, D. (2008). miR-126 regulates angiogenic signaling and vascular integrity. *Dev Cell*, *15*(2), 272-284. https://doi.org/10.1016/j.devcel.2008.07.008
Fitzgerald, T. N., Shepherd, B. R., Asada, H., Teso, D., Muto, A., Fancher, T., Dardik, A. (2008). Laminar shear stress stimulates vascular smooth muscle cell apoptosis via the Akt pathway. *J Cell Physiol*, *216*(2), 389-395. https://doi.org/10.1002/jcp.21404
Fledderus, J. O., Boon, R. A., Volger, O. L., Hurttila, H., Ylä-Herttuala, S., Pannekoek, H., Horrevoets, A. J. (2008). KLF2 primes the antioxidant transcription factor Nrf2 for activation in endothelial cells. *Arterioscler Thromb Vasc Biol*, *28*(7), 1339-1346. https://doi.org/10.1161/ATVBAHA.108.165811

Fledderus, J. O., van Thienen, J. V., Boon, R. A., Dekker, R. J., Rohlena, J., Volger, O. L., Horrevoets, A. J. (2007). Prolonged shear stress and KLF2 suppress constitutive proinflammatory transcription through inhibition of ATF2. *Blood*, *109*(10), 4249-4257. https://doi.org/10.1182/blood-2006-07-036020

Fleetwood, A. J., Dinh, H., Cook, A. D., Hertzog, P. J., & Hamilton, J. A. (2009). GM-CSF- and M-CSF-dependent macrophage phenotypes display differential dependence on type I interferon signaling. *J Leukoc Biol*, *86*(2), 411-421. https://doi.org/10.1189/jlb.1108702

Friedman, A. D. (2002). Transcriptional regulation of granulocyte and monocyte development. *Oncogene*, *21*(21), 3377-3390. https://doi.org/10.1038/sj.onc.1205324

Furuya, M., Nishiyama, M., Kasuya, Y., Kimura, S., & Ishikura, H. (2005). Pathophysiology of tumor neovascularization. *Vasc Health Risk Manag*, *1*(4), 277-290. https://doi.org/10.2147/vhrm.2005.1.4.277

Förstermann, U. (2010). Nitric oxide and oxidative stress in vascular disease. *Pflugers Arch*, *459*(6), 923-939. https://doi.org/10.1007/s00424-010-0808-2

Gan, Q., Yoshida, T., Li, J., & Owens, G. K. (2007). Smooth muscle cells and myofibroblasts use distinct transcriptional mechanisms for smooth muscle alpha-actin expression. *Circ Res*, *101*(9), 883-892. https://doi.org/10.1161/circresaha.107.154831

Gao, M., Wang, X., Zhang, X., Ha, T., Ma, H., Liu, L., Li, C. (2015). Attenuation of Cardiac Dysfunction in Polymicrobial Sepsis by MicroRNA-146a Is Mediated via Targeting of IRAK1 and TRAF6 Expression. *J Immunol*, *195*(2), 672-682. https://doi.org/10.4049/jimmunol.1403155

Garanich, J. S., Pahakis, M., & Tarbell, J. M. (2005). Shear stress inhibits smooth muscle cell migration via nitric oxide-mediated downregulation of matrix metalloproteinase-2 activity. *Am J Physiol Heart Circ Physiol*, *288*(5), H2244-2252. https://doi.org/10.1152/ajpheart.00428.2003

Genest, J., McNamara, J. R., Ordovas, J. M., Jenner, J. L., Silberman, S. R., Anderson, K. M., Schaefer, E. J. (1992). Lipoprotein cholesterol, apolipoprotein A-I and B and lipoprotein (a) abnormalities in men with premature coronary artery disease. *J Am Coll Cardiol*, *19*(4), 792-802.

George, S. J., & Lyon, C. (2010). Pathogenesis of Atherosclerosis. In *Atherosclerosis : Molecular and Cellular Mechanisms* (pp. 1-20). Wiley-VCH Verlag GmbH & Co. KGaA. https://doi.org/doi.org/10.1002/9783527629589.ch1

Gerecht-Nir, S., Ziskind, A., Cohen, S., & Itskovitz-Eldor, J. (2003). Human embryonic stem cells as an *in vitro* model for human vascular development and the induction of vascular differentiation. *Lab Invest*, *83*(12), 1811-1820.

Gimbrone, M. A., & García-Cardeña, G. (2016). Endothelial Cell Dysfunction and the Pathobiology of Atherosclerosis. *Circ Res*, *118*(4), 620-636. https://doi.org/10.1161/CIRCRESAHA.115.306301

Glass, C. K., & Witztum, J. L. (2001). Atherosclerosis. the road ahead. *Cell*, *104*(4), 503-516.

Gleissner, C. A., Shaked, I., Little, K. M., & Ley, K. (2010). CXC chemokine ligand 4 induces a unique transcriptome in monocyte-derived macrophages. *J Immunol*, *184*(9), 4810-4818. https://doi.org/10.4049/jimmunol.0901368

Goncharov, N. V., Nadeev, A. D., Jenkins, R. O., & Avdonin, P. V. (2017). Markers and Biomarkers of Endothelium: When Something Is Rotten in the State. *Oxid Med Cell Longev*, *2017*, 9759735. https://doi.org/10.1155/2017/9759735

Gong, D., Shi, W., Yi, S.-j., Chen, H., Groffen, J., & Heisterkamp, N. (2012). TGFβ signaling plays a critical role in promoting alternative macrophage activation [journal article]. *BMC Immunology*, *13*(1), 31. https://doi.org/10.1186/1471-2172-13-31

Goon, P. K., Lip, G. Y., Boos, C. J., Stonelake, P. S., & Blann, A. D. (2006). Circulating endothelial cells, endothelial progenitor cells, and endothelial microparticles in cancer. *Neoplasia*, *8*(2), 79-88. https://doi.org/10.1593/neo.05592

Gordon, S., & Plüddemann, A. (2019). The Mononuclear Phagocytic System. Generation of Diversity. *Front Immunol*, *10*, 1893. https://doi.org/10.3389/fimmu.2019.01893

Gori, T., Dragoni, S., Di Stolfo, G., & Forconi, S. (2007). Endothelium and haemorheology. *Ann Ist Super Sanita*, *43*(2), 124-129.

Gotsman, I., & Lichtman, A. H. (2007). Targeting interferon-gamma to treat atherosclerosis. *Circ Res*, *101*(4), 333-334. https://doi.org/10.1161/CIRCRESAHA.107.155838

Graf, T., & Enver, T. (2009). Forcing cells to change lineages. *Nature*, *462*(7273), 587-594. https://doi.org/10.1038/nature08533

Graney, P. L., Ben-Shaul, S., Landau, S., Bajpai, A., Singh, B., Eager, J., Spiller, K. L. (2020). Macrophages of diverse phenotypes drive vascularization of engineered tissues. *Sci Adv*, *6*(18), eaay6391. https://doi.org/10.1126/sciadv.aay6391

Greenow, K., Pearce, N. J., & Ramji, D. P. (2005). The key role of apolipoprotein E in atherosclerosis. *J Mol Med (Berl)*, *83*(5), 329-342. https://doi.org/10.1007/s00109-004-0631-3

Gregory, C. D., & Devitt, A. (2004). The macrophage and the apoptotic cell: an innate immune interaction viewed simplistically? *Immunology*, *113*(1), 1-14. https://doi.org/10.1111/j.1365-2567.2004.01959.x

Gregory, R. I., Yan, K. P., Amuthan, G., Chendrimada, T., Doratotaj, B., Cooch, N., & Shiekhattar, R. (2004). The Microprocessor complex mediates the genesis of microRNAs. *Nature*, *432*(7014), 235-240. https://doi.org/10.1038/nature03120

Grinenko, T., Eugster, A., Thielecke, L., Ramasz, B., Krüger, A., Dietz, S., Wielockx, B. (2018). Hematopoietic stem cells can differentiate into restricted myeloid progenitors before cell division in mice. *Nat Commun*, *9*(1), 1898. https://doi.org/10.1038/s41467-018-04188-7

Guo, L., Akahori, H., Harari, E., Smith, S. L., Polavarapu, R., Karmali, V., Finn, A. V. (2018). CD163+ macrophages promote angiogenesis and vascular permeability accompanied by inflammation in atherosclerosis. *J Clin Invest*, *128*(3), 1106-1124. https://doi.org/10.1172/JCI93025

Guo, X., & Chen, S. Y. (2012). Transforming growth factor-β and smooth muscle differentiation. *World J Biol Chem*, *3*(3), 41-52. https://doi.org/10.4331/wjbc.v3.i3.41

Gupte, A. A., Lyon, C. J., & Hsueh, W. A. (2013). Nuclear factor (erythroid-derived 2)-like-2 factor (Nrf2), a key regulator of the antioxidant response to protect against atherosclerosis and nonalcoholic steatohepatitis. *Curr Diab Rep*, *13*(3), 362-371. https://doi.org/10.1007/s11892-013-0372-1

Haider, N., Boscá, L., Zandbergen, H. R., Kovacic, J. C., Narula, N., González-Ramos, S., Narula, J. (2019). Transition of Macrophages to Fibroblast-Like Cells in Healing Myocardial Infarction. *J Am Coll Cardiol*, *74*(25), 3124-3135. https://doi.org/10.1016/j.jacc.2019.10.036

Han, X., & Boisvert, W. A. (2015). Interleukin-10 protects against atherosclerosis by modulating multiple atherogenic macrophage function. *Thromb Haemost*, *113*(3), 505-512. https://doi.org/10.1160/TH14-06-0509

Hansson, G. K. (2009). Inflammatory mechanisms in atherosclerosis. *J Thromb Haemost*, *7 Suppl 1*, 328-331. https://doi.org/10.1111/j.1538-7836.2009.03416.x
Hao, H., Gabbiani, G., & Bochaton-Piallat, M. L. (2003). Arterial smooth muscle cell heterogeneity: implications for atherosclerosis and restenosis development. *Arterioscler Thromb Vasc Biol*, *23*(9), 1510-1520. https://doi.org/10.1161/01.ATV.0000090130.85752.ED
Harats, D., Shaish, A., George, J., Mulkins, M., Kurihara, H., Levkovitz, H., & Sigal, E. (2000). Overexpression of 15-lipoxygenase in vascular endothelium accelerates early atherosclerosis in LDL receptor-deficient mice. *Arterioscler Thromb Vasc Biol*, *20*(9), 2100-2105. https://doi.org/10.1161/01.atv.20.9.2100
Harraz, M., Jiao, C., Hanlon, H. D., Hartley, R. S., & Schatteman, G. C. (2001). CD34- blood-derived human endothelial cell progenitors. *Stem Cells*, *19*(4), 304-312. https://doi.org/10.1634/stemcells.19-4-304
Harris, T. A., Yamakuchi, M., Ferlito, M., Mendell, J. T., & Lowenstein, C. J. (2008). MicroRNA-126 regulates endothelial expression of vascular cell adhesion molecule 1. *Proc Natl Acad Sci U S A*, *105*(5), 1516-1521. https://doi.org/10.1073/pnas.0707493105
Haskó, G., & Pacher, P. (2012). Regulation of macrophage function by adenosine. *Arterioscler Thromb Vasc Biol*, *32*(4), 865-869. https://doi.org/10.1161/ATVBAHA.111.226852
Heidemann, J., Ogawa, H., Dwinell, M. B., Rafiee, P., Maaser, C., Gockel, H. R., Binion, D. G. (2003). Angiogenic effects of interleukin 8 (CXCL8) in human intestinal microvascular endothelial cells are mediated by CXCR2. *J Biol Chem*, *278*(10), 8508-8515. https://doi.org/10.1074/jbc.M208231200
Heinecke, J. W. (2006). Lipoprotein oxidation in cardiovascular disease: chief culprit or innocent bystander? *J Exp Med*, *203*(4), 813-816. https://doi.org/10.1084/jem.20060218
Heissig, B., Pasternak, G., Hörner, S., Schwerdtfeger, R., Rossol, S., & Hehlmann, R. (2000). CD14+ peripheral blood mononuclear cells from chronic myeloid leukemia and normal donors are inhibitory to short- and long-term cultured colony-forming cells. *Leuk Res*, *24*(3), 217-231. https://doi.org/10.1016/s0145-2126(99)00171-x
Heldin, C.-H., & Westermark, B. (1999). Mechanism of action and *in vivo* role of platelet-derived growth factor. *Physiol. Rev.*, *79*(4), 1283-1316.
Hemn, H. O., Noordin, M. M., Rahman, H. S., Hazilawati, H., Zuki, A., & Chartrand, M. S. (2015). Antihypercholesterolemic and antioxidant efficacies of zerumbone on the formation, development, and establishment of atherosclerosis in cholesterol-fed rabbits. *Drug Des Devel Ther*, *9*, 4173-4208. https://doi.org/10.2147/DDDT.S76225
Hirano, T., Ishihara, K., & Hibi, M. (2000). Roles of STAT3 in mediating the cell growth, differentiation and survival signals relayed through the IL-6 family of cytokine receptors. *Oncogene*, *19*(21), 2548-2556. https://doi.org/10.1038/sj.onc.1203551
Hirose, K., Iwabuchi, K., Shimada, K., Kiyanagi, T., Iwahara, C., Nakayama, H., & Daida, H. (2011). Different responses to oxidized low-density lipoproteins in human polarized macrophages. *Lipids Health Dis*, *10*, 1. https://doi.org/10.1186/1476-511x-10-1
Hirose, N., Maeda, H., Yamamoto, M., Hayashi, Y., Lee, G. H., Chen, L., Sasaguri, S. (2008). The local injection of peritoneal macrophages induces neovascularization in rat ischemic hind limb muscles. *Cell Transplant*, *17*(1-2), 211-222. https://doi.org/10.3727/000000008783906919

Hong, L., Du, X., Li, W., Mao, Y., Sun, L., & Li, X. (2018). EndMT: A promising and controversial field. *Eur J Cell Biol*, *97*(7), 493-500. https://doi.org/10.1016/j.ejcb.2018.07.005

Horimatsu, T., Kim, H. W., & Weintraub, N. L. (2017). The Role of Perivascular Adipose Tissue in Non-atherosclerotic Vascular Disease. *Front Physiol*, *8*, 969. https://doi.org/10.3389/fphys.2017.00969

Hox, V., O'Connell, M. P., Lyons, J. J., Sackstein, P., Dimaggio, T., Jones, N., Milner, J. D. (2016). Diminution of signal transducer and activator of transcription 3 signaling inhibits vascular permeability and anaphylaxis. *J Allergy Clin Immunol*, *138*(1), 187-199. https://doi.org/10.1016/j.jaci.2015.11.024

Hsieh, C. C., Yen, M. H., Yen, C. H., & Lau, Y. T. (2001). Oxidized low density lipoprotein induces apoptosis via generation of reactive oxygen species in vascular smooth muscle cells. *Cardiovasc Res*, *49*(1), 135-145. https://doi.org/10.1016/s0008-6363(00)00218-2

Huat, T. J., Khan, A. A., Pati, S., Mustafa, Z., Abdullah, & J. M., Jaafar H. (2014). IGF-1 enhances cell proliferation and survival during early differentiation of mesenchymal stem cells to neural progenitor-like cells. *BMC Neurosci*. 15, 91. doi: 10.1186/1471-2202-15-91.

Huff, M. W., & Pickering, J. G. (2015). Can a vascular smooth muscle-derived foam-cell really change its spots? *Arterioscler Thromb Vasc Biol*, *35*(3), 492-495. https://doi.org/10.1161/ATVBAHA.115.305225

Huo, Y., Zhao, L., Hyman, M. C., Shashkin, P., Harry, B. L., Burcin, T., Ley, K. (2004). Critical role of macrophage 12/15-lipoxygenase for atherosclerosis in apolipoprotein E-deficient mice. *Circulation*, *110*(14), 2024-2031. https://doi.org/10.1161/01.CIR.0000143628.37680.F6

Hutchins, A. P., Diez, D., & Miranda-Saavedra, D. (2013). The IL-10/STAT3-mediated anti-inflammatory response: recent developments and future challenges. *Brief Funct Genomics*, *12*(6), 489-498. https://doi.org/10.1093/bfgp/elt028

Hwang, B., Song, J. H., Park, S. L., Kim, J. T., Kim, W. J., & Moon, S. K. (2020). Carnosine impedes PDGF-stimulated proliferation and migration of vascular smooth muscle cells *in vitro* and sprout outgrowth *ex vivo*. *Nutrients*, *12*(9). https://doi.org/10.3390/nu12092697

Idzkowska, E., Eljaszewicz, A., Miklasz, P., Musial, W. J., Tycinska, A. M., & Moniuszko, M. (2015). The Role of Different Monocyte Subsets in the Pathogenesis of Atherosclerosis and Acute Coronary Syndromes. *Scand J Immunol*, *82*(3), 163-173. https://doi.org/10.1111/sji.12314

Ikhapoh, I. A., Pelham, C. J., & Agrawal, D. K. (2015). Synergistic effect of angiotensin II on vascular endothelial growth factor-A-mediated differentiation of bone marrow-derived mesenchymal stem cells into endothelial cells. *Stem Cell Res Ther*, *6*, 4. https://doi.org/10.1186/scrt538

Im, J. H., Buzzelli, J. N., Jones, K., Franchini, F., Gordon-Weeks, A., Markelc, B., Muschel, R. J. (2020). FGF2 alters macrophage polarization, tumour immunity and growth and can be targeted during radiotherapy. *Nat Commun*, *11*(1), 4064. https://doi.org/10.1038/s41467-020-17914-x

Inaba, T., Shimano, H., Gotoda, T., Harada, K., Shimada, M., Ohsuga, J., et al. (1993). Expression of platelet-derived growth factor beta receptor on human monocyte-

derived macrophages and effects of platelet-derived growth factor BB dimer on the cellular function. *J Biol Chem*, *268*(32), 24353-24360.
Insull, W. (2009). The pathology of atherosclerosis: plaque development and plaque responses to medical treatment. *Am J Med*, *122*(1 Suppl), S3-S14. https://doi.org/10.1016/j.amjmed.2008.10.013
Italiani, P., & Boraschi, D. (2014). From Monocytes to M1/M2 Macrophages: Phenotypical vs. Functional Differentiation. *Front Immunol*, *5*, 514. https://doi.org/10.3389/fimmu.2014.00514
Ivanova, E. A., Myasoedova, V. A., Melnichenko, A. A., Grechko, A. V., & Orekhov, A. N. (2017). Small Dense Low-Density Lipoprotein as Biomarker for Atherosclerotic Diseases. *Oxid Med Cell Longev*, *2017*, 1273042. https://doi.org/10.1155/2017/1273042
Jacobo, S. M., & Kazlauskas, A. (2015). Insulin-like growth factor 1 (IGF-1) stabilizes nascent blood vessels. *J Biol Chem*, *290*(10), 6349-6360. https://doi.org/10.1074/jbc.M114.634154
Jawien, A., Bowen-Pope, D. F., Lindner, V., Schwartz, S. M., & Clowes, A. W. (1992). Platelet-derived growth factor promotes smooth muscle migration and intimal thickening in a rat model of balloon angioplasty. *J Clin Invest*, *89*(2), 507-511. https://doi.org/10.1172/JCI115613
Jha, P., & Das, H. (2017). KLF2 in Regulation of NF-κB-Mediated Immune Cell Function and Inflammation. *Int J Mol Sci*, *18*(11). https://doi.org/10.3390/ijms18112383
Ji, J., Rong, Y., Luo, C. L., Li, S., Jiang, X., Weng, H., Wang, F. B. (2018). Up-Regulation of hsa-miR-210 Promotes Venous Metastasis and Predicts Poor Prognosis in Hepatocellular Carcinoma. *Front Oncol*, *8*, 569. https://doi.org/10.3389/fonc.2018.00569
Jimi, S., Sakata, N., & Takebayashi, S. (1994). Oxidized LDL induces an increase in the relative collagen synthesis of rabbit aortic smooth muscle cells. *J Atheroscler Thromb*, *1*(1), 53-59. https://doi.org/10.5551/jat1994.1.53
Jimi, S., Saku, K., Uesugi, N., Sakata, N., & Takebayashi, S. (1995). Oxidized low density lipoprotein stimulates collagen production in cultured arterial smooth muscle cells. *Atherosclerosis*, *116*(1), 15-26. https://doi.org/10.1016/0021-9150(95)05515-x
Jin, X., & Kruth, H. S. (2016). Culture of Macrophage Colony-stimulating Factor Differentiated Human Monocyte-derived Macrophages. *J Vis Exp*(112). https://doi.org/10.3791/54244
Jneid, H., Addison, D., Bhatt, D. L., Fonarow, G. C., Gokak, S., Grady, K. L., Pancholy, S. (2017). 2017 AHA/ACC Clinical Performance and Quality Measures for Adults With ST-Elevation and Non-ST-Elevation Myocardial Infarction: A Report of the American College of Cardiology/American Heart Association Task Force on Performance Measures. *J Am Coll Cardiol*, *70*(16), 2048-2090. https://doi.org/10.1016/j.jacc.2017.06.032
Johnson, J. L. (2017). Metalloproteinases in atherosclerosis. *Eur J Pharmacol*, *816*, 93-106. https://doi.org/10.1016/j.ejphar.2017.09.007
Johnson, J. L., Jenkins, N. P., Huang, W. C., Di Gregoli, K., Sala-Newby, G. B., Scholtes, V. P., Newby, A. C. (2014). Relationship of MMP-14 and TIMP-3 expression with macrophage activation and human atherosclerotic plaque vulnerability. *Mediators Inflamm*, *2014*, 276457. https://doi.org/10.1155/2014/276457
Johnson, J. L., & Newby, A. C. (2009). Macrophage heterogeneity in atherosclerotic plaques. *Curr Opin Lipidol*, *20*(5), 370-378. https://doi.org/10.1097/MOL.0b013e3283309848

Johnson, J. L., Sala-Newby, G. B., Ismail, Y., Aguilera, C. M., & Newby, A. C. (2008). Low tissue inhibitor of metalloproteinases 3 and high matrix metalloproteinase 14 levels defines a subpopulation of highly invasive foam-cell macrophages. *Arterioscler Thromb Vasc Biol*, *28*(9), 1647-1653. https://doi.org/10.1161/ATVBAHA.108.170548

Kadl, A., Meher, A. K., Sharma, P. R., Lee, M. Y., Doran, A. C., Johnstone, S. R., Leitinger, N. (2010). Identification of a novel macrophage phenotype that develops in response to atherogenic phospholipids via Nrf2. *Circ Res*, *107*(6), 737-746. https://doi.org/10.1161/circresaha.109.215715

Karathanasis, N., Tsamardinos, I., & Poirazi, P. (2015). MiRduplexSVM: A High-Performing MiRNA-Duplex Prediction and Evaluation Methodology. *PLoS One*, *10*(5), e0126151. https://doi.org/10.1371/journal.pone.0126151

Katsumoto, T., Mitsushima, A., & Kurimura, T. (1990). The role of the vimentin intermediate filaments in rat 3Y1 cells elucidated by immunoelectron microscopy and computer-graphic reconstruction. *Biol Cell*, *68*(2), 139-146.

Khalil, M. F., Wagner, W. D., & Goldberg, I. J. (2004). Molecular interactions leading to lipoprotein retention and the initiation of atherosclerosis. *Arterioscler Thromb Vasc Biol*, *24*(12), 2211-2218. https://doi.org/10.1161/01.ATV.0000147163.54024.70

Khan, S., Villalobos, M. A., Choron, R. L., Chang, S., Brown, S. A., Carpenter, J. P., Zhang, P. (2017). Fibroblast growth factor and vascular endothelial growth factor play a critical role in endotheliogenesis from human adipose-derived stem cells. *J Vasc Surg*, *65*(5), 1483-1492. https://doi.org/10.1016/j.jvs.2016.04.034

Kim, H. R., Gallant, C., Leavis, P. C., Gunst, S. J., & Morgan, K. G. (2008). Cytoskeletal remodeling in differentiated vascular smooth muscle is actin isoform dependent and stimulus dependent. *Am J Physiol Cell Physiol*, *295*(3), C768-778. https://doi.org/10.1152/ajpcell.00174.2008

Kim, K., Shim, D., Lee, J. S., Zaitsev, K., Williams, J. W., Kim, K. W., Choi, J. H. (2018). Transcriptome Analysis Reveals Nonfoamy Rather Than Foamy Plaque Macrophages Are Proinflammatory in Atherosclerotic Murine Models. *Circ Res*, *123*(10), 1127-1142. https://doi.org/10.1161/CIRCRESAHA.118.312804

Kim, S. S., Ye, C., Kumar, P., Chiu, I., Subramanya, S., Wu, H., Manjunath, N. (2010). Targeted delivery of siRNA to macrophages for anti-inflammatory treatment. *Mol Ther*, *18*(5), 993-1001. https://doi.org/10.1038/mt.2010.27

King, N. M., & Perrin, J. (2014). Ethical issues in stem cell research and therapy. *Stem Cell Res Ther*, *5*(4), 85. https://doi.org/10.1186/scrt474

Kita, T., Nagano, Y., Yokode, M., Ishii, K., Kume, N., Ooshima, A., Kawai, C. (1987). Probucol prevents the progression of atherosclerosis in Watanabe heritable hyperlipidemic rabbit, an animal model for familial hypercholesterolemia. *Proc Natl Acad Sci U S A*, *84*(16), 5928-5931. https://doi.org/10.1073/pnas.84.16.5928

Kodama, H., Inoue, T., Watanabe, R., Yasuoka, H., Kawakami, Y., Ogawa, S., Kuwana, M. (2005). Cardiomyogenic potential of mesenchymal progenitors derived from human circulating CD14+ monocytes. *Stem Cells Dev*, *14*(6), 676-686. https://doi.org/10.1089/scd.2005.14.676

Kodama, H., Inoue, T., Watanabe, R., Yasutomi, D., Kawakami, Y., Ogawa, S., Kuwana, M. (2006). Neurogenic potential of progenitors derived from human circulating CD14+ monocytes. *Immunol Cell Biol*, *84*(2), 209-217. https://doi.org/10.1111/j.1440-1711.2006.01424.x

Kolodgie, F. D., Burke, A. P., Nakazawa, G., & Virmani, R. (2007). Is pathologic intimal thickening the key to understanding early plaque progression in human atherosclerotic disease? *Arterioscler Thromb Vasc Biol*, *27*(5), 986-989. https://doi.org/10.1161/ATVBAHA.0000258865.44774.41

Kolodgie, F. D., Gold, H. K., Burke, A. P., Fowler, D. R., Kruth, H. S., Weber, D. K., Virmani, R. (2003). Intraplaque hemorrhage and progression of coronary atheroma. *N Engl J Med*, *349*(24), 2316-2325. https://doi.org/10.1056/NEJMoa035655

Kosaka, N., Sugiura, K., Yamamoto, Y., Yoshioka, Y., Miyazaki, H., Komatsu, N., Kato, T. (2008). Identification of erythropoietin-induced microRNAs in haematopoietic cells during erythroid differentiation. *Br J Haematol*, *142*(2), 293-300. https://doi.org/10.1111/j.1365-2141.2008.07151.x

Kozaki, K., Kaminski, W. E., Tang, J., Hollenbach, S., Lindahl, P., Sullivan, C., Raines, E. W. (2002). Blockade of platelet-derived growth factor or its receptors transiently delays but does not prevent fibrous cap formation in ApoE null mice. *Am J Pathol*, *161*(4), 1395-1407. https://doi.org/10.1016/s0002-9440(10)64415-x

Kozomara, A., Birgaoanu, M., & Griffiths-Jones, S. (2019). miRBase: from microRNA sequences to function. *Nucleic Acids Res*, *47*(D1), D155-D162. https://doi.org/10.1093/nar/gky1141

Krock, B. L., Skuli, N., & Simon, M. C. (2011). Hypoxia-induced angiogenesis: good and evil. *Genes Cancer*, *2*(12), 1117-1133. https://doi.org/10.1177/1947601911423654

Kruth, H. S., Huang, W., Ishii, I., & Zhang, W.-Y. (2002). Macrophage Foam Cell Formation with Native Low Density Lipoprotein. *J. Biol. Chem*, *277*(37), 34573-34580. https://doi.org/10.1074/jbc.M205059200

Krämer, J., Quensel, C., Meding, J., Cardoso, M. C., & Leonhardt, H. (2001). Identification and characterization of novel smoothelin isoforms in vascular smooth muscle. *J Vasc Res*, *38*(2), 120-132. https://doi.org/51039

Kubota, Y., Takubo, K., Shimizu, T., Ohno, H., Kishi, K., Shibuya, M., Suda, T. (2009). M-CSF inhibition selectively targets pathological angiogenesis and lymphangiogenesis. *J Exp Med*, *206*(5), 1089-1102. https://doi.org/10.1084/jem.20081605

Kumar, A., & Cannon, C. P. (2009). Acute coronary syndromes: diagnosis and management, part I. *Mayo Clin Proc*, *84*(10), 917-938. https://doi.org/10.1016/S0025-6196(11)60509-0

Kumar, A. H., Martin, K., Turner, E. C., Buneker, C. K., Dorgham, K., Deterre, P., & Caplice, N. M. (2013). Role of CX3CR1 receptor in monocyte/macrophage driven neovascularization. *PLoS One*, *8*(2), e57230. https://doi.org/10.1371/journal.pone.0057230

Kumar, A. H., Metharom, P., Schmeckpeper, J., Weiss, S., Martin, K., & Caplice, N. M. (2010). Bone marrow-derived CX3CR1 progenitors contribute to neointimal smooth muscle cells via fractalkine CX3CR1 interaction. *FASEB J*, *24*(1), 81-92. https://doi.org/10.1096/fj.09-132225

Kunjathoor, V. V., Febbraio, M., Podrez, E. A., Moore, K. J., Andersson, L., Koehn, S., Freeman, M. W. (2002). Scavenger receptors class A-I/II and CD36 are the principal receptors responsible for the uptake of modified low density lipoprotein leading to lipid loading in macrophages. *J Biol Chem*, *277*(51), 49982-49988. https://doi.org/10.1074/jbc.M209649200

Kurdi, M., Zgheib, C., & Booz, G. W. (2018). Recent Developments on the Crosstalk Between STAT3 and Inflammation in Heart Function and Disease. *Front Immunol*, *9*, 3029. https://doi.org/10.3389/fimmu.2018.03029

Kuwana, M., Okazaki, Y., Kodama, H., Izumi, K., Yasuoka, H., Ogawa, Y., Ikeda, Y. (2003). Human circulating CD14+ monocytes as a source of progenitors that exhibit mesenchymal cell differentiation. *J Leukoc Biol*, *74*(5), 833-845. https://doi.org/10.1189/jlb.0403170

Kuwana, M., Okazaki, Y., Kodama, H., Satoh, T., Kawakami, Y., & Ikeda, Y. (2006). Endothelial differentiation potential of human monocyte-derived multipotential cells. *Stem Cells*, *24*(12), 2733-2743. https://doi.org/10.1634/stemcells.2006-0026

Lachmann, H. J., Kone-Paut, I., Kuemmerle-Deschner, J. B., Leslie, K. S., Hachulla, E., Quartier, P., . . . Group, C. i. C. S. (2009). Use of canakinumab in the cryopyrin-associated periodic syndrome. *N Engl J Med*, *360*(23), 2416-2425. https://doi.org/10.1056/NEJMoa0810787

Lamalice, L., Le Boeuf, F., & Huot, J. (2007). Endothelial cell migration during angiogenesis. *Circ Res*, *100*(6), 782-794. https://doi.org/10.1161/01.RES.0000259593.07661.1e

Lamarche, B., Tchernof, A., Moorjani, S., Cantin, B., Dagenais, G. R., Lupien, P. J., & Després, J. P. (1997). Small, dense low-density lipoprotein particles as a predictor of the risk of ischemic heart disease in men. Prospective results from the Québec Cardiovascular Study. *Circulation*, *95*(1), 69-75. https://doi.org/10.1161/01.cir.95.1.69

Lan, Y., Kodati, S., Lee, H. S., Omoto, M., Jin, Y., & Chauhan, S. K. (2012). Kinetics and function of mesenchymal stem cells in corneal injury. *Invest Ophthalmol Vis Sci*, *53*(7), 3638-3644. https://doi.org/10.1167/iovs.11-9311

Lang, R., Patel, D., Morris, J. J., Rutschman, R. L., & Murray, P. J. (2002). Shaping Gene Expression in Activated and Resting Primary Macrophages by IL-10. *J. Immunol*, *169*(5), 2253-2263. https://doi.org/10.4049/jimmunol.169.5.2253

Laphanuwat, P., & Jirawatnotai, S. (2019). Immunomodulatory Roles of Cell Cycle Regulators. *Front Cell Dev Biol*, *7*, 23. https://doi.org/10.3389/fcell.2019.00023

Lawler, P. R., & Lawler, J. (2012). Molecular basis for the regulation of angiogenesis by thrombospondin-1 and -2. *Cold Spring Harb Perspect Med*, *2*(5), a006627. https://doi.org/10.1101/cshperspect.a006627

Leal, A., Endele, S., Stengel, C., Huehne, K., Loetterle, J., Barrantes, R., Rautenstrauss, B. (2003). A novel myosin heavy chain gene in human chromosome 19q13.3. *Gene*, *312*, 165-171.

Lee, C. W., Hwang, I., Park, C. S., Lee, H., Park, D. W., Kang, S. J., Park, S. J. (2013). Macrophage heterogeneity of culprit coronary plaques in patients with acute myocardial infarction or stable angina. *Am J Clin Pathol*, *139*(3), 317-322. https://doi.org/10.1309/ajcp7keygn3obgqx

Lertkiatmongkol, P., Liao, D., Mei, H., Hu, Y., & Newman, P. J. (2016). Endothelial functions of platelet/endothelial cell adhesion molecule-1 (CD31). *Curr Opin Hematol*, *23*(3), 253-259. https://doi.org/10.1097/MOH.0000000000000239

Leszczynska, A., & Murphy, J. M. (2018). Vascular Calcification: Is it rather a Stem/Progenitor Cells Driven Phenomenon? *Front Bioeng Biotechnol*, *6*, 10. https://doi.org/10.3389/fbioe.2018.00010

Li, D., Duan, M., Feng, Y., Geng, L., Li, X., & Zhang, W. (2016). MiR-146a modulates macrophage polarization in systemic juvenile idiopathic arthritis by targeting INHBA. *Mol Immunol*, *77*, 205-212. https://doi.org/10.1016/j.molimm.2016.08.007

Li, P. F., Dietz, R., & von Harsdorf, R. (1997). Reactive oxygen species induce apoptosis of vascular smooth muscle cell. *FEBS Lett*, *404*(2-3), 249-252. https://doi.org/10.1016/s0014-5793(97)00093-8

Libby, P., & Theroux, P. (2005). Pathophysiology of coronary artery disease. *Circulation*, *111*(25), 3481-3488. https://doi.org/10.1161/CIRCULATIONAHA.105.537878

Lindner, H., Holler, E., Ertl, B., Multhoff, G., Schreglmann, M., Klauke, I., Eissner, G. (1997). Peripheral blood mononuclear cells induce programmed cell death in human endothelial cells and may prevent repair: role of cytokines. *Blood*, *89*(6), 1931-1938.

Lindner, V., Lappi, D. A., Baird, A., Majack, R. A., & Reidy, M. A. (1991). Role of basic fibroblast growth factor in vascular lesion formation. *Circ Res*, *68*(1), 106-113. https://doi.org/10.1161/01.res.68.1.106

Linton, M., PG Yancey, Sean S Davies, W. Gray Jerome, Edward F Linton , Wenliang L Song , Amanda C Doran, Kasey C Vickers ,. (2019). *Role of Lipids and Lipoproteins in Atherosclerosis*. MDText.com, Inc.

Liu, C., Wu, C., Yang, Q., Gao, J., Li, L., Yang, D., & Luo, L. (2016). Macrophages Mediate the Repair of Brain Vascular Rupture through Direct Physical Adhesion and Mechanical Traction. *Immunity*, *44*(5), 1162-1176. https://doi.org/10.1016/j.immuni.2016.03.008

Liu, J., Ren, Y., Kang, L., & Zhang, L. (2014). Oxidized low-density lipoprotein increases the proliferation and migration of human coronary artery smooth muscle cells through the upregulation of osteopontin. *Int J Mol Med*, *33*(5), 1341-1347. https://doi.org/10.3892/ijmm.2014.1681

Liu, X., Cheng, Y., Zhang, S., Lin, Y., Yang, J., & Zhang, C. (2009). A necessary role of miR-221 and miR-222 in vascular smooth muscle cell proliferation and neointimal hyperplasia. *Circ Res*, *104*(4), 476-487. https://doi.org/10.1161/CIRCRESAHA.108.185363

Lu, L., Zhu, F., Zhang, M., Li, Y., Drennan, A. C., Kimpara, S., Rui, L. (2018). Gene regulation and suppression of type I interferon signaling by STAT3 in diffuse large B cell lymphoma. *Proc Natl Acad Sci U S A*, *115*(3), E498-E505. https://doi.org/10.1073/pnas.1715118115

Ludewig, B., & Laman, J. D. (2004). The in and out of monocytes in atherosclerotic plaques: Balancing inflammation through migration. *Proc Natl Acad Sci U S A*, *101*(32), 11529-11530. https://doi.org/10.1073/pnas.0404612101

Ludin, A., Itkin, T., Gur-Cohen, S., Mildner, A., Shezen, E., Golan, K., Lapidot, T. (2012). Monocytes-macrophages that express α-smooth muscle actin preserve primitive hematopoietic cells in the bone marrow. *Nat Immunol*, *13*(11), 1072-1082. https://doi.org/10.1038/ni.2408

Lusis, A. J. (2000). Atherosclerosis. *Nature*, *407*(6801), 233-241. https://doi.org/10.1038/35025203

Lynch, D. T., Hall, J., & Foucar, K. (2018). How I investigate monocytosis. *Int J Lab Hematol*, *40*(2), 107-114. https://doi.org/10.1111/ijlh.12776

Ma, F., Liu, X., Li, D., Wang, P., Li, N., Lu, L., & Cao, X. (2010). MicroRNA-466l upregulates IL-10 expression in TLR-triggered macrophages by antagonizing RNA-binding protein tristetraprolin-mediated IL-10 mRNA degradation. *J Immunol*, *184*(11), 6053-6059. https://doi.org/10.4049/jimmunol.0902308

Ma, S., Liu, M., Xu, Z., Li, Y., Guo, H., Ge, Y., Shi, J. (2016). A double feedback loop mediated by microRNA-23a/27a/24-2 regulates M1 versus M2 macrophage polarization and

thus regulates cancer progression. *Oncotarget*, *7*(12), 13502-13519. https://doi.org/10.18632/oncotarget.6284

Madan, M., Bishayi, B., Hoge, M., & Amar, S. (2008). Atheroprotective role of interleukin-6 in diet- and/or pathogen-associated atherosclerosis using an ApoE heterozygote murine model. *Atherosclerosis*, *197*(2), 504-514. https://doi.org/10.1016/j.atherosclerosis.2007.02.023

Maiolino, G., Rossitto, G., Caielli, P., Bisogni, V., Rossi, G. P., & Calò, L. A. (2013). The role of oxidized low-density lipoproteins in atherosclerosis: the myths and the facts. *Mediators Inflamm*, *2013*, 714653. https://doi.org/10.1155/2013/714653

Maniotis, A. J., Folberg, R., Hess, A., Seftor, E. A., Gardner, L. M., Pe'er, J., Hendrix, M. J. (1999). Vascular channel formation by human melanoma cells *in vivo* and *in vitro*: vasculogenic mimicry. *Am J Pathol*, *155*(3), 739-752. https://doi.org/10.1016/S0002-9440(10)65173-5

Mann, J., & Davies, M. J. (1999). Mechanisms of progression in native coronary artery disease: role of healed plaque disruption. *Heart*, *82*(3), 265-268. https://doi.org/10.1136/hrt.82.3.265

Martin, S. S., Qasim, A. N., Mehta, N. N., Wolfe, M., Terembula, K., Schwartz, S., Reilly, M. P. (2009). Apolipoprotein B but not LDL cholesterol is associated with coronary artery calcification in type 2 diabetic whites. *Diabetes*, *58*(8), 1887-1892. https://doi.org/10.2337/db08-1794

Martinez, F. O., Gordon, S., Locati, M., & Mantovani, A. (2006). Transcriptional Profiling of the Human Monocyte-to-Macrophage Differentiation and Polarization: New Molecules and Patterns of Gene Expression. *J. Immunol*, *177*(10), 7303-7311. https://doi.org/10.4049/jimmunol.177.10.7303

McWhorter, F. Y., Wang, T., Nguyen, P., Chung, T., & Liu, W. F. (2013). Modulation of macrophage phenotype by cell shape. *Proc Natl Acad Sci U S A*, *110*(43), 17253-17258. https://doi.org/10.1073/pnas.1308887110

Mekala, S. R., Wörsdörfer, P., Bauer, J., Stoll, O., Wagner, N., Reeh, L., Ergün, S. (2018). Generation of Cardiomyocytes From Vascular Adventitia-Resident Stem Cells. *Circ Res*, *123*(6), 686-699. https://doi.org/10.1161/CIRCRESAHA.117.312526

Mesure, L., De Visscher, G., Vranken, I., Lebacq, A., & Flameng, W. (2010). Gene expression study of monocytes/macrophages during early foreign body reaction and identification of potential precursors of myofibroblasts. *PLoS One*, *5*(9), e12949. https://doi.org/10.1371/journal.pone.0012949

Metcalf, D. (2008). Hematopoietic cytokines. *Blood*, *111*(2), 485-491. https://doi.org/10.1182/blood-2007-03-079681

Metz, R. P., Patterson, J. L., & Wilson, E. (2012). Vascular smooth muscle cells: isolation, culture, and characterization. *Methods Mol Biol*, *843*, 169-176. https://doi.org/10.1007/978-1-61779-523-7_16

Michel, J. B., Virmani, R., Arbustini, E., & Pasterkamp, G. (2011). Intraplaque haemorrhages as the trigger of plaque vulnerability. *Eur Heart J*, *32*(16), 1977-1985, 1985a, 1985b, 1985c. https://doi.org/10.1093/eurheartj/ehr054

Mizuno, Y., Tokuzawa, Y., Ninomiya, Y., Yagi, K., Yatsuka-Kanesaki, Y., Suda, T., Okazaki, Y. (2009). miR-210 promotes osteoblastic differentiation through inhibition of AcvR1b. *FEBS Lett*, *583*(13), 2263-2268. https://doi.org/10.1016/j.febslet.2009.06.006

Moreno, P. R., Purushothaman, K. R., Zias, E., Sanz, J., & Fuster, V. (2006). Neovascularization in human atherosclerosis. *Curr Mol Med*, *6*(5), 457-477. https://doi.org/10.2174/156652406778018635

Mosser, D. M. (2003). The many faces of macrophage activation. *J Leukoc Biol*, *73*(2), 209-212.

Mosser, D. M., & Edwards, J. P. (2008). Exploring the full spectrum of macrophage activation. *Nat Rev Immunol*, *8*(12), 958-969. https://doi.org/10.1038/nri2448

Mudd, J. O., Borlaug, B. A., Johnston, P. V., Kral, B. G., Rouf, R., Blumenthal, R. S., & Kwiterovich, P. O. (2007). Beyond low-density lipoprotein cholesterol: defining the role of low-density lipoprotein heterogeneity in coronary artery disease. *J Am Coll Cardiol*, *50*(18), 1735-1741. https://doi.org/10.1016/j.jacc.2007.07.045

Nagel, T., Resnick, N., Dewey, C. F., & Gimbrone, M. A. (1999). Vascular endothelial cells respond to spatial gradients in fluid shear stress by enhanced activation of transcription factors. *Arterioscler Thromb Vasc Biol*, *19*(8), 1825-1834.

Nakano, T., Nakajima, K., Niimi, M., Fujita, M. Q., Nakajima, Y., Takeichi, S., Tanaka, A. (2008). Detection of apolipoproteins B-48 and B-100 carrying particles in lipoprotein fractions extracted from human aortic atherosclerotic plaques in sudden cardiac death cases. *Clin Chim Acta*, *390*(1-2), 38-43. https://doi.org/10.1016/j.cca.2007.12.012

Nakashima, Y., Chen, Y. X., Kinukawa, N., & Sueishi, K. (2002). Distributions of diffuse intimal thickening in human arteries: preferential expression in atherosclerosis-prone arteries from an early age. *Virchows Arch*, *441*(3), 279-288. https://doi.org/10.1007/s00428-002-0605-1

Nakashima, Y., Fujii, H., Sumiyoshi, S., Wight, T. N., & Sueishi, K. (2007). Early human atherosclerosis: accumulation of lipid and proteoglycans in intimal thickenings followed by macrophage infiltration. *Arterioscler Thromb Vasc Biol*, *27*(5), 1159-1165. https://doi.org/10.1161/ATVBAHA.106.134080

National Clinical Guidelines Centre, United Kingdom. (2011). Stable Angina: Methods, Evidence & Guidance. London: Royal College of Physicians (UK).

Nayak, L., Lin, Z., & Jain, M. K. (2011). "Go with the flow": how Krüppel-like factor 2 regulates the vasoprotective effects of shear stress. *Antioxid Redox Signal*, *15*(5), 1449-1461. https://doi.org/10.1089/ars.2010.3647

Newby, A. C. (2005). Dual role of matrix metalloproteinases (matrixins) in intimal thickening and atherosclerotic plaque rupture. *Physiol Rev*, *85*(1), 1-31. https://doi.org/10.1152/physrev.00048.2003

Newby, A. C. (2007). Metalloproteinases and vulnerable atherosclerotic plaques. *Trends Cardiovasc Med*, *17*(8), 253-258. https://doi.org/10.1016/j.tcm.2007.09.001

Newman, A. C., Nakatsu, M. N., Chou, W., Gershon, P. D., & Hughes, C. C. (2011). The requirement for fibroblasts in angiogenesis: fibroblast-derived matrix proteins are essential for endothelial cell lumen formation. *Mol Biol Cell*, *22*(20), 3791-3800. https://doi.org/10.1091/mbc.E11-05-0393

Niessen, P., Rensen, S., Gijbels, M., De Laet, A., De Man, J., van Deursen, J., van Eys, G. Impaired smooth muscle contractility in smoothelin deficient mice results in lethality. *Cardiovasc Pathol*, *13*(3), 38. https://doi.org/10.1016/j.carpath.2004.03.106

Niessen, P., Rensen, S., van Deursen, J., De Man, J., De Laet, A., Vanderwinden, J. M., van Eys, G. (2005). Smoothelin-a is essential for functional intestinal smooth muscle

contractility in mice. *Gastroenterology*, *129*(5), 1592-1601. https://doi.org/10.1053/j.gastro.2005.08.018
Nigro, P., Abe, J., & Berk, B. C. (2011). Flow shear stress and atherosclerosis: a matter of site specificity. *Antioxid Redox Signal*, *15*(5), 1405-1414. https://doi.org/10.1089/ars.2010.3679
Nikolic, I., Plate, K. H., & Schmidt, M. H. H. (2010). EGFL7 meets miRNA-126: an angiogenesis alliance. *J Angiogenes Res*, *2*(1), 9. https://doi.org/10.1186/2040-2384-2-9
Ninomiya, K., Takahashi, A., Fujioka, Y., Ishikawa, Y., & Yokoyama, M. (2006). Transforming growth factor-beta signaling enhances transdifferentiation of macrophages into smooth muscle-like cells. *Hypertens Res*, *29*(4), 269-276. https://doi.org/10.1291/hypres.29.269
Niu, C., Wang, X., Zhao, M., Cai, T., Liu, P., Li, J., . . . Zheng, L. (2016). Macrophage Foam Cell-Derived Extracellular Vesicles Promote Vascular Smooth Muscle Cell Migration and Adhesion. *J Am Heart Assoc*, *5*(10). https://doi.org/10.1161/JAHA.116.004099
Noria, S., Cowan, D. B., Gotlieb, A. I., & Langille, B. L. (1999). Transient and steady-state effects of shear stress on endothelial cell adherens junctions. *Circ Res*, *85*(6), 504-514. https://doi.org/10.1161/01.res.85.6.504
O'Brien, J., Hayder, H., Zayed, Y., & Peng, C. (2018). Overview of MicroRNA Biogenesis, Mechanisms of Actions, and Circulation. *Front Endocrinol (Lausanne)*, *9*, 402. https://doi.org/10.3389/fendo.2018.00402
O'Connell, R. M., Rao, D. S., Chaudhuri, A. A., & Baltimore, D. (2010). Physiological and pathological roles for microRNAs in the immune system. *Nat Rev Immunol*, *10*(2), 111-122. https://doi.org/10.1038/nri2708
O'Connell, R. M., Taganov, K. D., Boldin, M. P., Cheng, G., & Baltimore, D. (2007). MicroRNA-155 is induced during the macrophage inflammatory response. *Proc Natl Acad Sci U S A*, *104*(5), 1604-1609. https://doi.org/10.1073/pnas.0610731104
Odronitz, F., & Kollmar, M. (2007). Drawing the tree of eukaryotic life based on the analysis of 2,269 manually annotated myosins from 328 species. *Genome Biol*, *8*(9), R196. https://doi.org/10.1186/gb-2007-8-9-r196
Osugi, T., Oshima, Y., Fujio, Y., Funamoto, M., Yamashita, A., Negoro, S., Kishimoto, T. (2002). Cardiac-specific activation of signal transducer and activator of transcription 3 promotes vascular formation in the heart. *J Biol Chem*, *277*(8), 6676-6681. https://doi.org/10.1074/jbc.M108246200
Oswald, J., Boxberger, S., Jørgensen, B., Feldmann, S., Ehninger, G., Bornhäuser, M., & Werner, C. (2004). Mesenchymal stem cells can be differentiated into endothelial cells *in vitro*. *Stem Cells*, *22*(3), 377-384. https://doi.org/10.1634/stemcells.22-3-377
Owens, G. K., Kumar, M. S., & Wamhoff, B. R. (2004). Molecular regulation of vascular smooth muscle cell differentiation in development and disease. *Physiol Rev*, *84*(3), 767-801. https://doi.org/10.1152/physrev.00041.2003
Pal, S., Semorine, K., Watts, G. F., & Mamo, J. (2003). Identification of lipoproteins of intestinal origin in human atherosclerotic plaque. *Clin Chem Lab Med*, *41*(6), 792-795. https://doi.org/10.1515/CCLM.2003.120
Palumbo, R., Gaetano, C., Antonini, A., Pompilio, G., Bracco, E., Rönnstrand, L., Capogrossi, M. C. (2002). Different effects of high and low shear stress on platelet-derived growth factor isoform release by endothelial cells: consequences for smooth muscle cell migration. *Arterioscler Thromb Vasc Biol*, *22*(3), 405-411. https://doi.org/10.1161/hq0302.104528

Park, Y. M. (2014). CD36, a scavenger receptor implicated in atherosclerosis. *Exp Mol Med*, *46*, e99. https://doi.org/10.1038/emm.2014.38

Pawlak, G., & Helfman, D. M. (2001). Cytoskeletal changes in cell transformation and tumorigenesis. *Curr Opin Genet Dev*, *11*(1), 41-47.

Peichev, M., Naiyer, A. J., Pereira, D., Zhu, Z., Lane, W. J., Williams, M., Rafii, S. (2000). Expression of VEGFR-2 and AC133 by circulating human CD34(+) cells identifies a population of functional endothelial precursors. *Blood*, *95*(3), 952-958.

Pierce, G. F., Mustoe, T. A., Lingelbach, J., Masakowski, V. R., Griffin, G. L., Senior, R. M., & Deuel, T. F. (1989). Platelet-derived growth factor and transforming growth factor-beta enhance tissue repair activities by unique mechanisms. *J Cell Biol*, *109*(1), 429-440.

Poliseno, L., Tuccoli, A., Mariani, L., Evangelista, M., Citti, L., Woods, K., Rainaldi, G. (2006). MicroRNAs modulate the angiogenic properties of HUVECs. *Blood*, *108*(9), 3068-3071. https://doi.org/10.1182/blood-2006-01-012369

Pufe, T., Petersen, W., Fändrich, F., Varoga, D., Wruck, C. J., Mentlein, R., Ruhnke, M. (2008). Programmable cells of monocytic origin (PCMO): a source of peripheral blood stem cells that generate collagen type II-producing chondrocytes. *J Orthop Res*, *26*(3), 304-313. https://doi.org/10.1002/jor.20516

Puisségur, M. P., Mazure, N. M., Bertero, T., Pradelli, L., Grosso, S., Robbe-Sermesant, K., Mari, B. (2011). miR-210 is overexpressed in late stages of lung cancer and mediates mitochondrial alterations associated with modulation of HIF-1 activity. *Cell Death Differ*, *18*(3), 465-478. https://doi.org/10.1038/cdd.2010.119

Pukac, L., Huangpu, J., & Karnovsky, M. J. (1998). Platelet-derived growth factor-BB, insulin-like growth factor-I, and phorbol ester activate different signaling pathways for stimulation of vascular smooth muscle cell migration. *Exp Cell Res*, *242*(2), 548-560. https://doi.org/10.1006/excr.1998.4138

Qi, H., Sun, B., Zhao, X., Du, J., Gu, Q., Liu, Y., Dong, X. (2014). Wnt5a promotes vasculogenic mimicry and epithelial-mesenchymal transition via protein kinase Cα in epithelial ovarian cancer. *Oncol Rep*, *32*(2), 771-779. https://doi.org/10.3892/or.2014.3229

Qiu, C., Xie, Q., Zhang, D., Chen, Q., Hu, J., & Xu, L. (2014). GM-CSF induces cyclin D1 expression and proliferation of endothelial progenitor cells via PI3K and MAPK signaling. *Cell Physiol Biochem*, *33*(3), 784-795. https://doi.org/10.1159/000358652

Que, X., Hung, M. Y., Yeang, C., Gonen, A., Prohaska, T. A., Sun, X., Witztum, J. L. (2018). Oxidized phospholipids are proinflammatory and proatherogenic in hypercholesterolaemic mice. *Nature*, *558*(7709), 301-306. https://doi.org/10.1038/s41586-018-0198-8

Quintar, A., McArdle, S., Wolf, D., Marki, A., Ehinger, E., Vassallo, M., Buscher, K. (2017). Endothelial Protective Monocyte Patrolling in Large Arteries Intensified by Western Diet and Atherosclerosis. *Circ Res*, *120*(11), 1789-1799. https://doi.org/10.1161/CIRCRESAHA.117.310739

Raffai, R. L., Loeb, S. M., & Weisgraber, K. H. (2005). Apolipoprotein E promotes the regression of atherosclerosis independently of lowering plasma cholesterol levels. *Arterioscler Thromb Vasc Biol*, *25*(2), 436-441. https://doi.org/10.1161/01.ATV.0000152613.83243.12

Raffort, J., Lareyre, F., Clément, M., Hassen-Khodja, R., Chinetti, G., & Mallat, Z. (2017). Monocytes and macrophages in abdominal aortic aneurysm. *Nat Rev Cardiol*. https://doi.org/10.1038/nrcardio.2017.52

Rapp, J. H. (1989). Lipoproteins and the artery wall. *J. Vasc. Surg. Cases*, *9*(2), 383–384.
Reinders, M. E., Sho, M., Izawa, A., Wang, P., Mukhopadhyay, D., Koss, K. E., Briscoe, D. M. (2003). Proinflammatory functions of vascular endothelial growth factor in alloimmunity. *J Clin Invest*, *112*(11), 1655-1665. https://doi.org/10.1172/JCI17712
Ren, X., Duan, L., He, Q., Zhang, Z., Zhou, Y., Wu, D., Ding, K. (2010). Identification of Niclosamide as a New Small-Molecule Inhibitor of the STAT3 Signaling Pathway. *ACS Med Chem Lett*, *1*(9), 454-459. https://doi.org/10.1021/ml100146z
Rensen, S. S., Niessen, P. M., van Deursen, J. M., Janssen, B. J., Heijman, E., Hermeling, E., van Eys, G. J. (2008). Smoothelin-B deficiency results in reduced arterial contractility, hypertension, and cardiac hypertrophy in mice. *Circulation*, *118*(8), 828-836. https://doi.org/10.1161/circulationaha.107.743690
Ribatti, D., Nico, B., Crivellato, E., Roccaro, A. M., & Vacca, A. (2007). The history of the angiogenic switch concept. *Leukemia*, *21*(1), 44-52. https://doi.org/10.1038/sj.leu.2404402
Ricci-Vitiani, L., Pallini, R., Biffoni, M., Todaro, M., Invernici, G., Cenci, T., De Maria, R. (2010). Tumour vascularization via endothelial differentiation of glioblastoma stem-like cells. *Nature*, *468*(7325), 824-828. https://doi.org/10.1038/nature09557
Ridker, P. M., Everett, B. M., Thuren, T., MacFadyen, J. G., Chang, W. H., Ballantyne, C., Group, C. T. (2017). Antiinflammatory Therapy with Canakinumab for Atherosclerotic Disease. *N Engl J Med*, *377*(12), 1119-1131. https://doi.org/10.1056/NEJMoa1707914
Romagnani, P., Annunziato, F., Liotta, F., Lazzeri, E., Mazzinghi, B., Frosali, F., Romagnani, S. (2005). CD14+CD34low cells with stem cell phenotypic and functional features are the major source of circulating endothelial progenitors. *Circ Res*, *97*(4), 314-322. https://doi.org/10.1161/01.RES.0000177670.72216.9b
Rong, J. X., Shapiro, M., Trogan, E., & Fisher, E. A. (2003). Transdifferentiation of mouse aortic smooth muscle cells to a macrophage-like state after cholesterol loading. *Proc Natl Acad Sci U S A*, *100*(23), 13531-13536. https://doi.org/10.1073/pnas.1735526100
Ross, R., Glomset, J., Kariya, B., & Harker, L. (1974). A platelet-dependent serum factor that stimulates the proliferation of arterial smooth muscle cells *in vitro*. *Proc Natl Acad Sci U S A*, *71*(4), 1207-1210.
Ruhnke, M., Nussler, A. K., Ungefroren, H., Hengstler, J. G., Kremer, B., Hoeckh, W., Fandrich, F. (2005a). Human monocyte-derived neohepatocytes: a promising alternative to primary human hepatocytes for autologous cell therapy. *Transplantation*, 79(9), 1097-1103.
Ruhnke, M., Ungefroren, H., Nussler, A., Martin, F., Brulport, M., Schormann, W., Fändrich, F. (2005b). Differentiation of *in vitro*-modified human peripheral blood monocytes into hepatocyte-like and pancreatic islet-like cells. *Gastro*, *128*(7), 1774-1786.
Rupaimoole, R., & Slack, F. J. (2017). MicroRNA therapeutics: towards a new era for the management of cancer and other diseases. *Nat Rev Drug Discov*, *16*(3), 203-222. https://doi.org/10.1038/nrd.2016.246
Ruperto, N., Brunner, H. I., Quartier, P., Constantin, T., Wulffraat, N., Horneff, G., PRCSG. (2012). Two randomized trials of canakinumab in systemic juvenile idiopathic arthritis. *N Engl J Med*, *367*(25), 2396-2406. https://doi.org/10.1056/NEJMoa1205099

Rutherford, C., Martin, W., Salame, M., Carrier, M., Anggård, E., & Ferns, G. (1997). Substantial inhibition of neo-intimal response to balloon injury in the rat carotid artery using a combination of antibodies to platelet-derived growth factor-BB and basic fibroblast growth factor. *Atherosclerosis*, *130*(1-2), 45-51. https://doi.org/10.1016/s0021-9150(96)06042-x

Rye, K. A., Bursill, C. A., Lambert, G., Tabet, F., & Barter, P. J. (2009). The metabolism and anti-atherogenic properties of HDL. *J Lipid Res*, *50 Suppl*, S195-200. https://doi.org/10.1194/jlr.R800034-JLR200

Saederup, N., Chan, L., Lira, S. A., & Charo, I. F. (2008). Fractalkine deficiency markedly reduces macrophage accumulation and atherosclerotic lesion formation in CCR2-/- mice: evidence for independent chemokine functions in atherogenesis. *Circulation*, *117*(13), 1642-1648. https://doi.org/10.1161/circulationaha.107.743872

Samaan, S., Khella, H. W., Girgis, A., Scorilas, A., Lianidou, E., Gabril, M., Yousef, G. M. (2015). miR-210 is a prognostic marker in clear cell renal cell carcinoma. *J Mol Diagn*, *17*(2), 136-144. https://doi.org/10.1016/j.jmoldx.2014.10.005

Sanchis-Gomar, F., Perez-Quilis, C., Leischik, R., & Lucia, A. (2016). Epidemiology of coronary heart disease and acute coronary syndrome. *Ann Transl Med*, *4*(13), 256. https://doi.org/10.21037/atm.2016.06.33

Sanda, G. M., Deleanu, M., Toma, L., Stancu, C. S., Simionescu, M., & Sima, A. V. (2017). Oxidized LDL-Exposed Human Macrophages Display Increased MMP-9 Expression and Secretion Mediated by Endoplasmic Reticulum Stress. *J Cell Biochem*, *118*(4), 661-669. https://doi.org/10.1002/jcb.25637

Sarwar, N., Butterworth, A. S., Freitag, D. F., Gregson, J., Willeit, P., Gorman, D. N., Collaboration, I. R. G. C. E. R. F. (2012). Interleukin-6 receptor pathways in coronary heart disease: a collaborative meta-analysis of 82 studies. *Lancet*, *379*(9822), 1205-1213. https://doi.org/10.1016/S0140-6736(11)61931-4

Satelli, A., & Li, S. (2011). Vimentin in cancer and its potential as a molecular target for cancer therapy. *Cell Mol Life Sci*, *68*(18), 3033-3046. https://doi.org/10.1007/s00018-011-0735-1

Sato, Y., Hatakeyama, K., Yamashita, A., Marutsuka, K., Sumiyoshi, A., & Asada, Y. (2005). Proportion of fibrin and platelets differs in thrombi on ruptured and eroded coronary atherosclerotic plaques in humans. *Heart*, *91*(4), 526-530. https://doi.org/10.1136/hrt.2004.034058

Scheuerer, B., Ernst, M., Dürrbaum-Landmann, I., Fleischer, J., Grage-Griebenow, E., Brandt, E., . . . Petersen, F. (2000). The CXC-chemokine platelet factor 4 promotes monocyte survival and induces monocyte differentiation into macrophages. *Blood*, *95*(4), 1158-1166.

Schieffer, B., Selle, T., Hilfiker, A., Hilfiker-Kleiner, D., Grote, K., Tietge, U. J., Drexler, H. (2004). Impact of interleukin-6 on plaque development and morphology in experimental atherosclerosis. *Circulation*, *110*(22), 3493-3500. https://doi.org/10.1161/01.CIR.0000148135.08582.97

Schildmeyer, L. A., Braun, R., Taffet, G., Debiasi, M., Burns, A. E., Bradley, A., & Schwartz, R. J. (2000). Impaired vascular contractility and blood pressure homeostasis in the smooth muscle alpha-actin null mouse. *FASEB J*, *14*(14), 2213-2220. https://doi.org/10.1096/fj.99-0927com

Schmeisser, A., Garlichs, C. D., Zhang, H., Eskafi, S., Graffy, C., Ludwig, J., Daniel, W. G. (2001). Monocytes coexpress endothelial and macrophagocytic lineage markers and

form cord-like structures in Matrigel under angiogenic conditions. *Cardiovasc Res*, *49*(3), 671-680.
Schoenhagen, P., Ziada, K. M., Vince, D. G., Nissen, S. E., & Tuzcu, E. M. (2001). Arterial remodeling and coronary artery disease: the concept of "dilated" versus "obstructive" coronary atherosclerosis. *J Am Coll Cardiol*, *38*(2), 297-306. https://doi.org/10.1016/s0735-1097(01)01374-2
Schott, J., Reitter, S., Philipp, J., Haneke, K., Schäfer, H., & Stoecklin, G. (2014). Translational regulation of specific mRNAs controls feedback inhibition and survival during macrophage activation. *PLoS Genet*, *10*(6), e1004368. https://doi.org/10.1371/journal.pgen.1004368
Schrans-Stassen, B. H., Lue, H., Sonnemans, D. G., Bernhagen, J., & Post, M. J. (2005). Stimulation of vascular smooth muscle cell migration by macrophage migration inhibitory factor. *Antioxid Redox Signal*, *7*(9-10), 1211-1216. https://doi.org/10.1089/ars.2005.7.1211
Schwenke, D. C., & Carew, T. E. (1989). Initiation of atherosclerotic lesions in cholesterol-fed rabbits. II. Selective retention of LDL vs. selective increases in LDL permeability in susceptible sites of arteries. *Arteriosclerosis*, *9*(6), 908-918.
Seaberg, R. M., & van der Kooy, D. (2003). Stem and progenitor cells: the premature desertion of rigorous definitions. *Trends Neurosci*, *26*(3), 125-131. https://doi.org/10.1016/S0166-2236(03)00031-6
SenBanerjee, S., Lin, Z., Atkins, G. B., Greif, D. M., Rao, R. M., Kumar, A., Jain, M. K. (2004). KLF2 Is a novel transcriptional regulator of endothelial proinflammatory activation. *J Exp Med*, *199*(10), 1305-1315. https://doi.org/10.1084/jem.20031132
Seta, N., & Kuwana, M. (2007). Human circulating monocytes as multipotential progenitors. *Keio J Med*, *56*(2), 41-47.
Seta, N., & Kuwana, M. (2010). Derivation of multipotent progenitors from human circulating CD14+ monocytes. *Exp Hematol*, *38*(7), 557-563. https://doi.org/10.1016/j.exphem.2010.03.015
Shapiro, M. D., & Fazio, S. (2017). Apolipoprotein B-containing lipoproteins and atherosclerotic cardiovascular disease. *F1000Res*, *6*, 134. https://doi.org/10.12688/f1000research.9845.1
Shen, K., Cao, Z., Zhu, R., You, L., & Zhang, T. (2019). The dual functional role of MicroRNA-18a (miR-18a) in cancer development. *Clin Transl Med*, *8*(1), 32. https://doi.org/10.1186/s40169-019-0250-9
Shilo, S., Roy, S., Khanna, S., & Sen, C. K. (2008). Evidence for the involvement of miRNA in redox regulated angiogenic response of human microvascular endothelial cells. *Arterioscler Thromb Vasc Biol*, *28*(3), 471-477. https://doi.org/10.1161/ATVBAHA.107.160655
Shirakawa, K., Kobayashi, H., Heike, Y., Kawamoto, S., Brechbiel, M. W., Kasumi, F., Wakasugi, H. (2002). Hemodynamics in vasculogenic mimicry and angiogenesis of inflammatory breast cancer xenograft. *Cancer Res*, *62*(2), 560-566.
Simionescu, M., Simionescu, N., & Palade, G. E. (1976). Segmental differentiations of cell junctions in the vascular endothelium. Arteries and veins. *J Cell Biol*, *68*(3), 705-723. https://doi.org/10.1083/jcb.68.3.705
Singh, U., & Jialal, I. (2006). Oxidative stress and atherosclerosis. *Pathophysiology*, *13*(3), 129-142. https://doi.org/10.1016/j.pathophys.2006.05.002

Sinha, S., Hoofnagle, M. H., Kingston, P. A., McCanna, M. E., & Owens, G. K. (2004). Transforming growth factor-beta1 signaling contributes to development of smooth muscle cells from embryonic stem cells. *Am J Physiol Cell Physiol*, *287*(6), C1560-1568. https://doi.org/10.1152/ajpcell.00221.2004

Skjøt-Arkil, H., Barascuk, N., Register, T., & Karsdal, M. A. (2010). Macrophage-mediated proteolytic remodeling of the extracellular matrix in atherosclerosis results in neoepitopes: a potential new class of biochemical markers. *Assay Drug Dev Technol*, *8*(5), 542-552. https://doi.org/10.1089/adt.2009.0258

Smallwood, H. S., Shi, L., & Squier, T. C. (2006). Increases in calmodulin abundance and stabilization of activated inducible nitric oxide synthase mediate bacterial killing in RAW 264.7 macrophages. *Biochemistry*, *45*(32), 9717-9726. https://doi.org/10.1021/bi060485p

Smith, E. B., & Staples, E. M. (1982). Plasma protein concentrations in interstitial fluid from human aortas. *Proc R Soc Lond B Biol Sci*, *217*(1206), 59-75. https://doi.org/10.1098/rspb.1982.0094

Somara, S., Gilmont, R., & Bitar, K. N. (2009). Role of thin-filament regulatory proteins in relaxation of colonic smooth muscle contraction. *Am J Physiol Gastrointest Liver Physiol*, *297*(5), G958-966.

Squadrito, M. L., Pucci, F., Magri, L., Moi, D., Gilfillan, G. D., Ranghetti, A., De Palma, M. (2012). miR-511-3p modulates genetic programs of tumor-associated macrophages. *Cell Rep*, *1*(2), 141-154. https://doi.org/10.1016/j.celrep.2011.12.005

Stansfield, B. K., & Ingram, D. A. (2015). Clinical significance of monocyte heterogeneity. *Clin Transl Med*, *4*, 5. https://doi.org/10.1186/s40169-014-0040-3

Stary, H. C. (2000). Natural history and histological classification of atherosclerotic lesions: an update. *Arterioscler Thromb Vasc Biol*, *20*(5), 1177-1178.

Stein, M., Keshav, S., Harris, N., & Gordon, S. (1992). Interleukin 4 potently enhances murine macrophage mannose receptor activity: a marker of alternative immunologic macrophage activation. *J Exp Med*, *176*(1), 287-292. https://doi.org/10.1084/jem.176.1.287

Stenmark, K. R., Yeager, M. E., El Kasmi, K. C., Nozik-Grayck, E., Gerasimovskaya, E. V., Li, M., Frid, M. G. (2013). The adventitia: essential regulator of vascular wall structure and function. *Annu Rev Physiol*, *75*, 23-47. https://doi.org/10.1146/annurev-physiol-030212-183802

Stiko-Rahm, A., Hultgårdh-Nilsson, A., Regnström, J., Hamsten, A., & Nilsson, J. (1992). Native and oxidized LDL enhances production of PDGF AA and the surface expression of PDGF receptors in cultured human smooth muscle cells. *Arterioscler Thromb*, *12*(9), 1099-1109. https://doi.org/10.1161/01.atv.12.9.1099

Stout, R. D., & Suttles, J. (2004). Functional plasticity of macrophages: reversible adaptation to changing microenvironments. *J Leukoc Biol*, *76*(3), 509-513. https://doi.org/10.1189/jlb.0504272

Stöger, J. L., Gijbels, M. J., van der Velden, S., Manca, M., van der Loos, C. M., Biessen, E. A., de Winther, M. P. (2012). Distribution of macrophage polarization markers in human atherosclerosis. *Atherosclerosis*, *225*(2), 461-468. https://doi.org/10.1016/j.atherosclerosis.2012.09.013

Sundell, C. L., Somers, P. K., Meng, C. Q., Hoong, L. K., Suen, K. L., Hill, R. R., Saxena, U. (2003). AGI-1067: a multifunctional phenolic antioxidant, lipid modulator, anti-

inflammatory and antiatherosclerotic agent. *J Pharmacol Exp Ther*, *305*(3), 1116-1123. https://doi.org/10.1124/jpet.102.048132

Supeno, N. E., Pati, S., Hadi, R. A., Ghani, A. R., Mustafa, Z., Abdullah, J. M., Idris, F. M., Han, X., & Jaafar, H. (2013). IGF-1 acts as controlling switch for long-term proliferation and maintenance of EGF/FGF-responsive striatal neural stem cells. International journal of medical sciences, 10(5), 522–531. https://doi.org/10.7150/ijms.5325

Suárez, Y., Fernández-Hernando, C., Pober, J. S., & Sessa, W. C. (2007). Dicer dependent microRNAs regulate gene expression and functions in human endothelial cells. *Circ Res*, *100*(8), 1164-1173. https://doi.org/10.1161/01.RES.0000265065.26744.17

Suárez, Y., Fernández-Hernando, C., Yu, J., Gerber, S. A., Harrison, K. D., Pober, J. S., Sessa, W. C. (2008). Dicer-dependent endothelial microRNAs are necessary for postnatal angiogenesis. *Proc Natl Acad Sci U S A*, *105*(37), 14082-14087. https://doi.org/10.1073/pnas.0804597105

Swerdlow, D. I., Holmes, M. V., Kuchenbaecker, K. B., Engmann, J. E., Shah, T., Sofat, R., Consortium, I.-R. M. R. A. I. R. M. (2012). The interleukin-6 receptor as a target for prevention of coronary heart disease: a mendelian randomisation analysis. *Lancet*, *379*(9822), 1214-1224. https://doi.org/10.1016/S0140-6736(12)60110-X

Tacke, F., Alvarez, D., Kaplan, T. J., Jakubzick, C., Spanbroek, R., Llodra, J., Randolph, G. J. (2007). Monocyte subsets differentially employ CCR2, CCR5, and CX3CR1 to accumulate within atherosclerotic plaques. *J Clin Invest*, *117*(1), 185-194. https://doi.org/10.1172/JCI28549

Tagscherer, K. E., Fassl, A., Sinkovic, T., Richter, J., Schecher, S., Macher-Goeppinger, S., & Roth, W. (2016). MicroRNA-210 induces apoptosis in colorectal cancer via induction of reactive oxygen. *Cancer Cell Int*, *16*, 42. https://doi.org/10.1186/s12935-016-0321-6

Takahashi, K., Yamamura, F., & Naito, M. (1989). Differentiation, maturation, and proliferation of macrophages in the mouse yolk sac: a light-microscopic, enzyme-cytochemical, immunohistochemical, and ultrastructural study. *J Leukoc Biol*, *45*(2), 87-96.

Takahashi, T., Yamaguchi, S., Chida, K., & Shibuya, M. (2001). A single autophosphorylation site on KDR/Flk-1 is essential for VEGF-A-dependent activation of PLC-gamma and DNA synthesis in vascular endothelial cells. *EMBO J*, *20*(11), 2768-2778. https://doi.org/10.1093/emboj/20.11.2768

Takeda, K., Noguchi, K., Shi, W., Tanaka, T., Matsumoto, M., Yoshida, N., Akira, S. (1997). Targeted disruption of the mouse Stat3 gene leads to early embryonic lethality. *Proc Natl Acad Sci U S A*, *94*(8), 3801-3804. https://doi.org/10.1073/pnas.94.8.3801

Tall, A. R., Yvan-Charvet, L., Terasaka, N., Pagler, T., & Wang, N. (2008). HDL, ABC transporters, and cholesterol efflux: implications for the treatment of atherosclerosis. *Cell Metab*, *7*(5), 365-375. https://doi.org/10.1016/j.cmet.2008.03.001

Tancharoen, W., Aungsuchawan, S., Pothacharoen, P., Markmee, R., Narakornsak, S., Kieodee, J., Tasuya, W. (2017). Differentiation of mesenchymal stem cells from human amniotic fluid to vascular endothelial cells. *Acta Histochem*, *119*(2), 113-121. https://doi.org/10.1016/j.acthis.2016.11.009

Tang, J., Kozaki, K., Farr, A. G., Martin, P. J., Lindahl, P., Betsholtz, C., & Raines, E. W. (2005). The absence of platelet-derived growth factor-B in circulating cells promotes

immune and inflammatory responses in atherosclerosis-prone ApoE-/- mice. *Am J Pathol*, *167*(3), 901-912. https://doi.org/10.1016/s0002-9440(10)62061-5

Tang, Y., Yang, X., Friesel, R. E., Vary, C. P., & Liaw, L. (2011). Mechanisms of TGF-β-induced differentiation in human vascular smooth muscle cells. *J Vasc Res*, *48*(6), 485-494. https://doi.org/10.1159/000327776

Tardif, J. C., Grégoire, J., L'Allier, P. L., Ibrahim, R., Anderson, T. J., Reeves, F., Investigators, C.-. (2008a). Effects of the antioxidant succinobucol (AGI-1067) on human atherosclerosis in a randomized clinical trial. *Atherosclerosis*, *197*(1), 480-486. https://doi.org/10.1016/j.atherosclerosis.2006.11.039

Tardif, J. C., McMurray, J. J., Klug, E., Small, R., Schumi, J., Choi, J., Investigators, A. R. o. I. S. E. A. T. (2008b). Effects of succinobucol (AGI-1067) after an acute coronary syndrome: a randomised, double-blind, placebo-controlled trial. *Lancet*, *371*(9626), 1761-1768. https://doi.org/10.1016/S0140-6736(08)60763-1

Thomas, A. C., Eijgelaar, W. J., Daemen, M. J., & Newby, A. C. (2015a). Foam cell formation *in vivo* converts macrophages to a pro-fibrotic phenotype. *PLoS One*, *10*(7), e0128163. https://doi.org/10.1371/journal.pone.0128163

Thomas, A. C., Eijgelaar, W. J., Daemen, M. J., & Newby, A. C. (2015b). The pro-fibrotic and anti-inflammatory foam cell macrophage paradox. *Genom*, *6*, 136-138. https://doi.org/10.1016/j.gdata.2015.08.027

Thorin, E., Hamilton, C. A., Dominiczak, M. H., & Reid, J. L. (1994). Chronic exposure of cultured bovine endothelial cells to oxidized LDL abolishes prostacyclin release. *Arterioscler Thromb*, *14*(3), 453-459. https://doi.org/10.1161/01.atv.14.3.453

Toma, I., & McCaffrey, T. A. (2012). Transforming growth factor-β and atherosclerosis: interwoven atherogenic and atheroprotective aspects. *Cell Tissue Res*, *347*(1), 155-175. https://doi.org/10.1007/s00441-011-1189-3

Tran-Lundmark, K., Tran, P. K., Paulsson-Berne, G., Fridén, V., Soininen, R., Tryggvason, K., Hedin, U. (2008). Heparan sulfate in perlecan promotes mouse atherosclerosis: roles in lipid permeability, lipid retention, and smooth muscle cell proliferation. *Circ Res*, *103*(1), 43-52. https://doi.org/10.1161/CIRCRESAHA.108.172833

Tugal, D., Liao, X., & Jain, M. K. (2013). Transcriptional control of macrophage polarization. *Arterioscler Thromb Vasc Biol*, *33*(6), 1135-1144. https://doi.org/10.1161/ATVBAHA.113.301453

Ueba, H., Kawakami, M., & Yaginuma, T. (1997). Shear stress as an inhibitor of vascular smooth muscle cell proliferation. Role of transforming growth factor-beta 1 and tissue-type plasminogen activator. *Arterioscler Thromb Vasc Biol*, *17*(8), 1512-1516. https://doi.org/10.1161/01.atv.17.8.1512

Ungefroren, H., & Fändrich, F. (2010). The programmable cell of monocytic origin (PCMO): a potential adult stem/progenitor cell source for the generation of islet cells. *Adv Exp Med Biol*, *654*, 667-682. https://doi.org/10.1007/978-90-481-3271-3_29

Ungefroren, H., Groth, S., Hyder, A., Thomsen, N., Hinz, H., Reiling, N., . . . Fändrich, F. (2010). The generation of programmable cells of monocytic origin involves partial repression of monocyte/macrophage markers and reactivation of pluripotency genes. *Stem Cells Dev*, *19*(11), 1769-1780. https://doi.org/10.1089/scd.2009.0351

Urbich, C., Kaluza, D., Frömel, T., Knau, A., Bennewitz, K., Boon, R. A., Dimmeler, S. (2012). MicroRNA-27a/b controls endothelial cell repulsion and angiogenesis by targeting semaphorin 6A. *Blood*, *119*(6), 1607-1616. https://doi.org/10.1182/blood-2011-08-373886

Valente, S., Ciavarella, C., Pasanisi, E., Ricci, F., Stella, A., & Pasquinelli, G. (2016). Hepatocyte Growth Factor Effects on Mesenchymal Stem Cells Derived from Human Arteries: A Novel Strategy to Accelerate Vascular Ulcer Wound Healing. *Stem Cells Int*, *2016*, 3232859. https://doi.org/10.1155/2016/3232859

van der Loop, F. T., Gabbiani, G., Kohnen, G., Ramaekers, F. C., & van Eys, G. J. (1997). Differentiation of smooth muscle cells in human blood vessels as defined by smoothelin, a novel marker for the contractile phenotype. *Arterioscler Thromb Vasc Biol*, *17*(4), 665-671.

van der Loop, F. T., Schaart, G., Timmer, E. D., Ramaekers, F. C., & van Eys, G. J. (1996). Smoothelin, a novel cytoskeletal protein specific for smooth muscle cells. *J Cell Biol*, *134*(2), 401-411.

van der Vorst, E. P., Döring, Y., & Weber, C. (2015). MIF and CXCL12 in Cardiovascular Diseases: Functional Differences and Similarities. *Front Immunol*, *6*, 373. https://doi.org/10.3389/fimmu.2015.00373

van Engeland, N. C. A., Suarez Rodriguez, F., Rivero-Müller, A., Ristori, T., Duran, C. L., Stassen, O. M. J. A., Sahlgren, C. M. (2019). Vimentin regulates Notch signaling strength and arterial remodeling in response to hemodynamic stress. *Sci Rep*, *9*(1), 12415. https://doi.org/10.1038/s41598-019-48218-w

van Eys, G. J., Niessen, P. M., & Rensen, S. S. (2007). Smoothelin in vascular smooth muscle cells. *Trends Cardiovasc Med*, *17*(1), 26-30. https://doi.org/10.1016/j.tcm.2006.11.001

van Hinsbergh, V. W., & Koolwijk, P. (2008). Endothelial sprouting and angiogenesis: matrix metalloproteinases in the lead. *Cardiovasc Res*, *78*(2), 203-212. https://doi.org/10.1093/cvr/cvm102

van Tits, L. J., Stienstra, R., van Lent, P. L., Netea, M. G., Joosten, L. A., & Stalenhoef, A. F. (2011). Oxidized LDL enhances pro-inflammatory responses of alternatively activated M2 macrophages: a crucial role for Krüppel-like factor 2. *Atherosclerosis*, *214*(2), 345-349. https://doi.org/10.1016/j.atherosclerosis.2010.11.018

Vasudevan, S. (2012). Posttranscriptional upregulation by microRNAs. *Wiley Interdiscip Rev RNA*, *3*(3), 311-330. https://doi.org/10.1002/wrna.121

Verfaillie, C. M. (2002). Adult stem cells: assessing the case for pluripotency. *Trends Cell Biol*, *12*(11), 502-508.

Verhagen, S. N., & Visseren, F. L. (2011). Perivascular adipose tissue as a cause of atherosclerosis. *Atherosclerosis*, *214*(1), 3-10. https://doi.org/10.1016/j.atherosclerosis.2010.05.034

Vestweber, D. (2008). VE-cadherin: the major endothelial adhesion molecule controlling cellular junctions and blood vessel formation. *Arterioscler Thromb Vasc Biol*, *28*(2), 223-232. https://doi.org/10.1161/ATVBAHA.107.158014

Virmani, R., Kolodgie, F. D., Burke, A. P., Farb, A., & Schwartz, S. M. (2000). Lessons from sudden coronary death: a comprehensive morphological classification scheme for atherosclerotic lesions. *Arterioscler Thromb Vasc Biol*, *20*(5), 1262-1275. https://doi.org/10.1161/01.atv.20.5.1262

Vo, E., Hanjaya-Putra, D., Zha, Y., Kusuma, S., & Gerecht, S. (2010). Smooth-muscle-like cells derived from human embryonic stem cells support and augment cord-like structures *in vitro*. *Stem Cell Rev*, *6*(2), 237-247. https://doi.org/10.1007/s12015-010-9144-3

Waldo, S. W., Li, Y., Buono, C., Zhao, B., Billings, E. M., Chang, J., & Kruth, H. S. (2008). Heterogeneity of human macrophages in culture and in atherosclerotic plaques. *Am J Pathol*, *172*(4), 1112-1126. https://doi.org/10.2353/ajpath.2008.070513

Wallez, Y., Vilgrain, I., & Huber, P. (2006). Angiogenesis: the VE-cadherin switch. *Trends Cardiovasc Med*, *16*(2), 55-59. https://doi.org/10.1016/j.tcm.2005.11.008

Walsh, M. P. (1994). Calmodulin and the regulation of smooth muscle contraction. *Mol Cell Biochem*, *135*(1), 21-41.

Wang, M., Sun, J., Xu, B., Chrusciel, M., Gao, J., Bazert, M., Li, X. (2018). Functional Characterization of MicroRNA-27a-3p Expression in Human Polycystic Ovary Syndrome. *Endocrinology*, *159*(1), 297-309. https://doi.org/10.1210/en.2017-00219

Wang, Q. R., Wang, F., Zhu, W. B., Lei, J., Huang, Y. H., Wang, B. H., & Yan, Q. (2009). GM-CSF accelerates proliferation of endothelial progenitor cells from murine bone marrow mononuclear cells *in vitro*. *Cytokine*, *45*(3), 174-178. https://doi.org/10.1016/j.cyto.2008.12.002

Wang, R., Li, Q., & Tang, D. D. (2006). Role of vimentin in smooth muscle force development. *Am J Physiol Cell Physiol*, *291*(3), C483-489. https://doi.org/10.1152/ajpcell.00097.2006

Wang, S., Aurora, A. B., Johnson, B. A., Qi, X., McAnally, J., Hill, J. A., Olson, E. N. (2008). The endothelial-specific microRNA miR-126 governs vascular integrity and angiogenesis. *Dev Cell*, *15*(2), 261-271. https://doi.org/10.1016/j.devcel.2008.07.002

Wang, S., & Olson, E. N. (2009). AngiomiRs--key regulators of angiogenesis. *Curr Opin Genet Dev*, *19*(3), 205-211. https://doi.org/10.1016/j.gde.2009.04.002

Wanjare, M., Kuo, F., & Gerecht, S. (2013). Derivation and maturation of synthetic and contractile vascular smooth muscle cells from human pluripotent stem cells. *Cardiovasc. Res*, *97*(2), 321-330. https://doi.org/10.1093/cvr/cvs315

Weber, T. J., Smallwood, H. S., Kathmann, L. E., Markillie, L. M., Squier, T. C., & Thrall, B. D. (2006). Functional link between TNF biosynthesis and CaM-dependent activation of inducible nitric oxide synthase in RAW 264.7 macrophages. *Am J Physiol Cell Physiol*, *290*(6), C1512-1520. https://doi.org/10.1152/ajpcell.00527.2005

Weiner, L. M., Li, W., Holmes, M., Catalano, R. B., Dovnarsky, M., Padavic, K., & Alpaugh, R. K. (1994). Phase I trial of recombinant macrophage colony-stimulating factor and recombinant gamma-interferon: toxicity, monocytosis, and clinical effects. *Cancer Res*, *54*(15), 4084-4090.

White, S. J., Newby, A. C., & Johnson, T. W. (2016). Endothelial erosion of plaques as a substrate for coronary thrombosis. *Thromb Haemost*, *115*(3), 509-519. https://doi.org/10.1160/TH15-09-0765

Wietecha, M. S., Chen, L., Ranzer, M. J., Anderson, K., Ying, C., Patel, T. B., & DiPietro, L. A. (2011). Sprouty2 downregulates angiogenesis during mouse skin wound healing. *Am J Physiol Heart Circ Physiol*, *300*(2), H459-467. https://doi.org/10.1152/ajpheart.00244.2010

Williams, K. J., & Wu, X. (2016). Imbalanced insulin action in chronic over nutrition: Clinical harm, molecular mechanisms, and a way forward. *Atherosclerosis*, *247*, 225-282. https://doi.org/10.1016/j.atherosclerosis.2016.02.004

Wong, K. L., Tai, J. J., Wong, W. C., Han, H., Sem, X., Yeap, W. H., Wong, S. C. (2011). Gene expression profiling reveals the defining features of the classical, intermediate, and nonclassical human monocyte subsets. *Blood*, *118*(5), e16-31. https://doi.org/10.1182/blood-2010-12-326355

World Health Organisation. (2014). Global status report on noncommunicable diseases.
Wraith, K. S., Magwenzi, S., Aburima, A., Wen, Y., Leake, D., & Naseem, K. M. (2013). Oxidized low-density lipoproteins induce rapid platelet activation and shape change through tyrosine kinase and Rho kinase-signaling pathways. *Blood*, *122*(4), 580-589. https://doi.org/10.1182/blood-2013-04-491688
Wågsäter, D., Zhu, C., Björck, H. M., & Eriksson, P. (2009). Effects of PDGF-C and PDGF-D on monocyte migration and MMP-2 and MMP-9 expression. *Atherosclerosis*, *202*(2), 415-423. https://doi.org/10.1016/j.atherosclerosis.2008.04.050
Xie, N., Cui, H., Banerjee, S., Tan, Z., Salomao, R., Fu, M., . . . Liu, G. (2014). miR-27a regulates inflammatory response of macrophages by targeting IL-10. *J Immunol*, *193*(1), 327-334. https://doi.org/10.4049/jimmunol.1400203
Xu, S., Ogura, S., Chen, J., Little, P. J., Moss, J., & Liu, P. (2013). LOX-1 in atherosclerosis: biological functions and pharmacological modifiers. *Cell Mol Life Sci*, *70*(16), 2859-2872. https://doi.org/10.1007/s00018-012-1194-z
Yahata, Y., Shirakata, Y., Tokumaru, S., Yamasaki, K., Sayama, K., Hanakawa, Y., Hashimoto, K. (2003). Nuclear translocation of phosphorylated STAT3 is essential for vascular endothelial growth factor-induced human dermal microvascular endothelial cell migration and tube formation. *J Biol Chem*, *278*(41), 40026-40031. https://doi.org/10.1074/jbc.M301866200
Yamada, H., Yoshida, M., Nakano, Y., Suganami, T., Satoh, N., Mita, T., Ogawa, Y. (2008). *In vivo* and *in vitro* inhibition of monocyte adhesion to endothelial cells and endothelial adhesion molecules by eicosapentaenoic acid. *Arterioscler Thromb Vasc Biol*, *28*(12), 2173-2179. https://doi.org/10.1161/ATVBAHA.108.171736
Yamaguchi, H., Igarashi, M., Hirata, A., Tsuchiya, H., Susa, S., Tominaga, M., Kato, T. (2001). Characterization of platelet-derived growth factor-induced p38 mitogen-activated protein kinase activation in vascular smooth muscle cells. *Eur J Clin Invest*, *31*(8), 672-680. https://doi.org/10.1046/j.1365-2362.2001.00865.x
Yang, J., Zhang, L., Yu, C., Yang, X. F., & Wang, H. (2014). Monocyte and macrophage differentiation: circulation inflammatory monocyte as biomarker for inflammatory diseases. *Biomark Res*, *2*(1), 1. https://doi.org/10.1186/2050-7771-2-1
Yang, M., Chen, J., Su, F., Yu, B., Lin, L., Liu, Y., Song, E. (2011). Microvesicles secreted by macrophages shuttle invasion-potentiating microRNAs into breast cancer cells. *Mol Cancer*, *10*, 117. https://doi.org/10.1186/1476-4598-10-117
Yao, L., Sun, B., Zhao, X., Gu, Q., Dong, X., Zheng, Y., An, J. (2014). Overexpression of Wnt5a promotes angiogenesis in NSCLC. *Biomed Res Int*, *2014*, 832562. https://doi.org/10.1155/2014/832562
Yeh, E. T., Zhang, S., Wu, H. D., Körbling, M., Willerson, J. T., & Estrov, Z. (2003). Transdifferentiation of human peripheral blood CD34+-enriched cell population into cardiomyocytes, endothelial cells, and smooth muscle cells *in vivo*. *Circulation*, *108*(17), 2070-2073. https://doi.org/10.1161/01.cir.0000099501.52718.70
Ying, H., Kang, Y., Zhang, H., Zhao, D., Xia, J., Lu, Z., Shi, L. (2015). MiR-127 modulates macrophage polarization and promotes lung inflammation and injury by activating the JNK pathway. *J Immunol*, *194*(3), 1239-1251. https://doi.org/10.4049/jimmunol.1402088
Ylitalo, R., Oksala, O., Ylä-Herttuala, S., & Ylitalo, P. (1994). Effects of clodronate (dichloromethylene bisphosphonate) on the development of experimental atherosclerosis in rabbits. *J Lab Clin Med*, *123*(5), 769-776.

Yoder, M. C., Mead, L. E., Prater, D., Krier, T. R., Mroueh, K. N., Li, F., Ingram, D. A. (2007). Redefining endothelial progenitor cells via clonal analysis and hematopoietic stem/progenitor cell principals. *Blood*, *109*(5), 1801-1809. https://doi.org/10.1182/blood-2006-08-043471

Young, D. A., Lowe, L. D., & Clark, S. C. (1990). Comparison of the effects of IL-3, granulocyte-macrophage colony-stimulating factor, and macrophage colony-stimulating factor in supporting monocyte differentiation in culture. Analysis of macrophage antibody-dependent cellular cytotoxicity. *J Immunol*, *145*(2), 607-615.

Young, J. A., Ting, K. K., Li, J., Moller, T., Dunn, L., Lu, Y., Gamble, J. R. (2013). Regulation of vascular leak and recovery from ischemic injury by general and VE-cadherin-restricted miRNA antagonists of miR-27. *Blood*, *122*(16), 2911-2919. https://doi.org/10.1182/blood-2012-12-473017

Yu, H., Pardoll, D., & Jove, R. (2009). STATs in cancer inflammation and immunity: a leading role for STAT3. *Nat Rev Cancer*, *9*(11), 798-809. https://doi.org/10.1038/nrc2734

Yu, Y., Wan, Y., & Huang, C. (2009). The biological functions of NF-kappaB1 (p50) and its potential as an anti-cancer target. *Curr Cancer Drug Targets*, *9*(4), 566-571. https://doi.org/10.2174/156800909788486759

Yuan, Z. L., Guan, Y. J., Wang, L., Wei, W., Kane, A. B., & Chin, Y. E. (2004). Central role of the threonine residue within the p+1 loop of receptor tyrosine kinase in STAT3 constitutive phosphorylation in metastatic cancer cells. *Mol Cell Biol*, *24*(21), 9390-9400. https://doi.org/10.1128/MCB.24.21.9390-9400.2004

Zajac, E., Schweighofer, B., Kupriyanova, T. A., Juncker-Jensen, A., Minder, P., Quigley, J. P., & Deryugina, E. I. (2013). Angiogenic capacity of M1- and M2-polarized macrophages is determined by the levels of TIMP-1 complexed with their secreted proMMP-9. *Blood*, *122*(25), 4054-4067. https://doi.org/10.1182/blood-2013-05-501494

Zecchin, A., Kalucka, J., Dubois, C., & Carmeliet, P. (2017). How Endothelial Cells Adapt Their Metabolism to Form Vessels in Tumors. *Front Immunol*, *8*, 1750. https://doi.org/10.3389/fimmu.2017.01750

Zeng, L., He, X., Wang, Y., Tang, Y., Zheng, C., Cai, H., Yang, G. Y. (2014). MicroRNA-210 overexpression induces angiogenesis and neurogenesis in the normal adult mouse brain. *Gene Ther*, *21*(1), 37-43. https://doi.org/10.1038/gt.2013.55

Zernecke, A., & Weber, C. (2014). Chemokines in atherosclerosis: proceedings resumed. *Arterioscler Thromb Vasc Biol*, *34*(4), 742-750. https://doi.org/10.1161/ATVBAHA.113.301655

Zhang, C. C., Kaba, M., Iizuka, S., Huynh, H., & Lodish, H. F. (2008). Angiopoietin-like 5 and IGFBP2 stimulate ex vivo expansion of human cord blood hematopoietic stem cells as assayed by NOD/SCID transplantation. *Blood*, *111*(7), 3415-3423. https://doi.org/10.1182/blood-2007-11-122119

Zhang, W., Liu, H., Liu, W., Liu, Y., & Xu, J. (2015). Polycomb-mediated loss of microRNA let-7c determines inflammatory macrophage polarization via PAK1-dependent NF-κB pathway. *Cell Death Differ*, *22*(2), 287-297. https://doi.org/10.1038/cdd.2014.142

Zhang, X., Sessa, W. C., & Fernández-Hernando, C. (2018). Endothelial Transcytosis of Lipoproteins in Atherosclerosis. *Front Cardiovasc Med*, *5*, 130. https://doi.org/10.3389/fcvm.2018.00130

Zhang, Y., Zhang, M., Li, X., Tang, Z., Wang, X., Zhong, M., Lv, K. (2016). Silencing MicroRNA-155 Attenuates Cardiac Injury and Dysfunction in Viral Myocarditis via Promotion of

M2 Phenotype Polarization of Macrophages. *Sci Rep*, *6*, 22613. https://doi.org/10.1038/srep22613

Zhao, Y., Biswas, S. K., McNulty, P. H., Kozak, M., Jun, J. Y., & Segar, L. (2011). PDGF-induced vascular smooth muscle cell proliferation is associated with dysregulation of insulin receptor substrates. *Am J Physiol Cell Physiol*, *300*(6), C1375-1385. https://doi.org/10.1152/ajpcell.00670.2008

Zhao, Y., Glesne, D., & Huberman, E. (2003). A human peripheral blood monocyte-derived subset acts as pluripotent stem cells. *Proc Natl Acad Sci U S A*, *100*(5), 2426-2431. https://doi.org/10.1073/pnas.0536882100

Zhou, J., Tang, Z., Gao, S., Li, C., Feng, Y., & Zhou, X. (2020). Tumor-Associated Macrophages: Recent Insights and Therapies. *Front Oncol*, *10*, 188. https://doi.org/10.3389/fonc.2020.00188

Zhou, Q., Gallagher, R., Ufret-Vincenty, R., Li, X., Olson, E. N., & Wang, S. (2011). Regulation of angiogenesis and choroidal neovascularization by members of microRNA-23~27~24 clusters. *Proc Natl Acad Sci U S A*, *108*(20), 8287-8292. https://doi.org/10.1073/pnas.1105254108

Zhou, Y., Damsky, C. H., & Fisher, S. J. (1997a). Preeclampsia is associated with failure of human cytotrophoblasts to mimic a vascular adhesion phenotype. One cause of defective endovascular invasion in this syndrome? *J Clin Invest*, *99*(9), 2152-2164. https://doi.org/10.1172/JCI119388

Zhou, Y., Fisher, S. J., Janatpour, M., Genbacev, O., Dejana, E., Wheelock, M., & Damsky, C. H. (1997b). Human cytotrophoblasts adopt a vascular phenotype as they differentiate. A strategy for successful endovascular invasion? *J Clin Invest*, *99*(9), 2139-2151. https://doi.org/10.1172/JCI119387

Zhuang, G., Meng, C., Guo, X., Cheruku, P. S., Shi, L., Xu, H., Zhou, B. (2012). A novel regulator of macrophage activation: miR-223 in obesity-associated adipose tissue inflammation. *Circulation*, *125*(23), 2892-2903. https://doi.org/10.1161/CIRCULATIONAHA.111.087817

8 Appendix A – (Result, Chapter 3)

8.1 Expression of VSMC-related markers in baseline M-CSF and GM-CSF macrophage and the effects of PDGF-BB and TGFβ1

(for section 3.4.2 and 3.4.3)

8.1.1 Representative image for Stain Free Gel for baseline macrophage

Figure 24 (b) – Figure 35 (b)

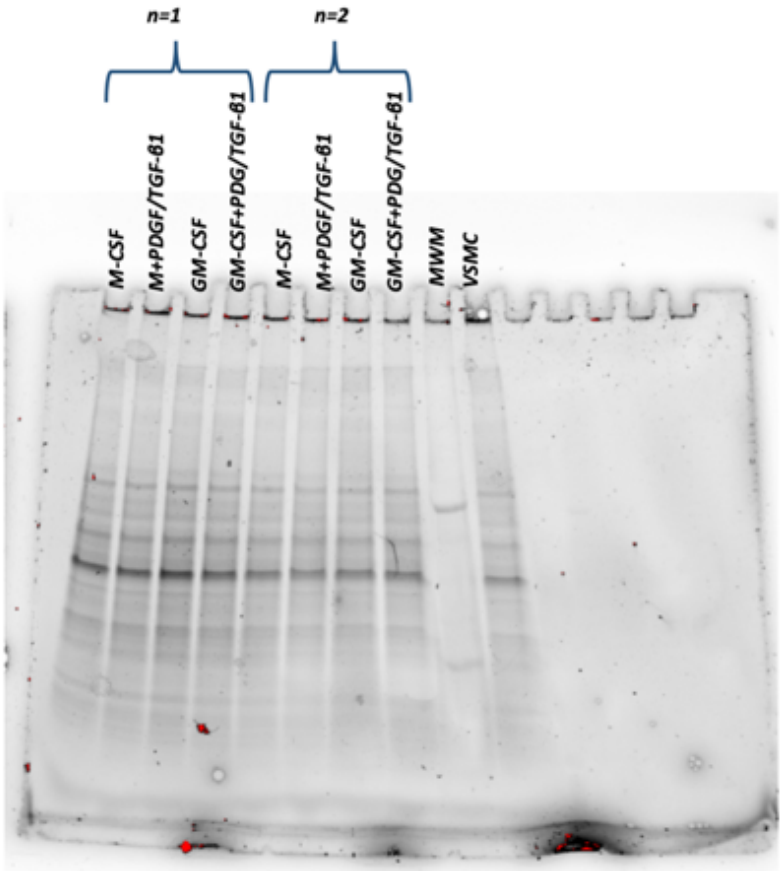

8.1.2 CT values - caldesmon

Figure 3.4.6 (a), Figure 3.4.15 (a) and Figure 3.4.36 (a)

Caldesmon mRNA	CT Min	CT Max	CT average
M-CSF	32.7	35.6	33.9
M-CSF + PDGF-BB/TGFβ1	33.1	36.1	34.7
GM-CSF	33.0	35.9	34.5
GM-CSF + PDGF-BB/TGFβ1	33.1	35.6	34.2
VSMC	21.7	23.9	22.5

8.1.3 Full blot image - caldesmon

Figure 3.4.6 (b), Figure 3.4.15 (b) and Figure 3.4.36 (b)

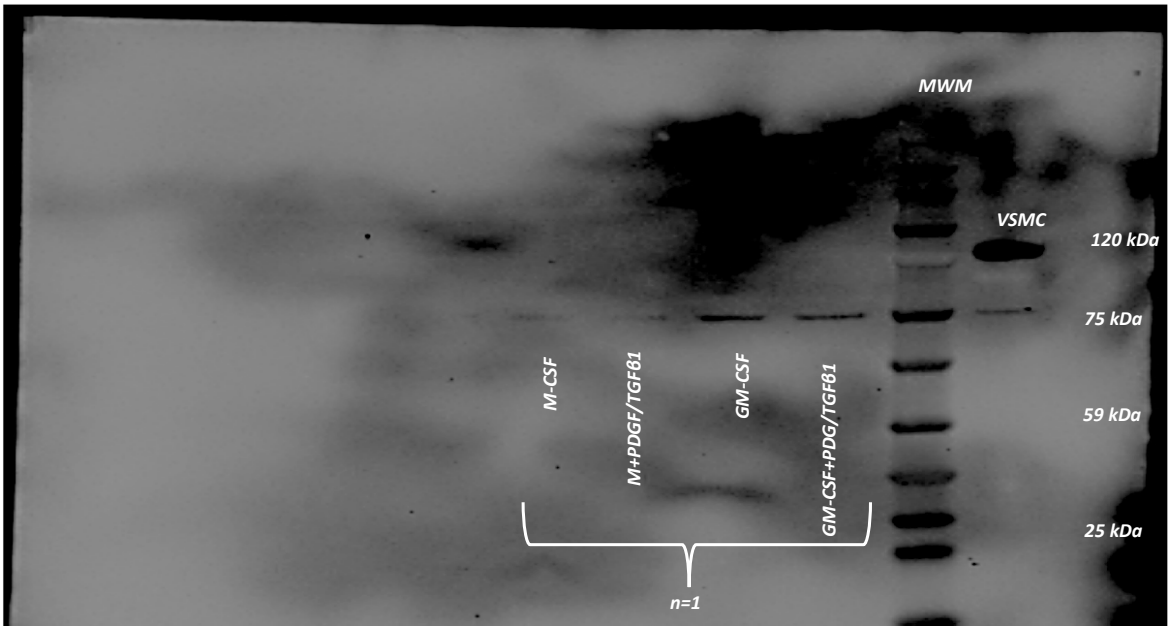

8.1.4 CT values - calmodulin

Figure 3.4.7 (a), Figure 3.4.11 (a), Figure 3.4.16 (a) and Figure 3.4.37 (a)

Calmodulin mRNA	CT Min	CT Max	CT average
M-CSF	25.0	26.5	25.8
M-CSF + PDGF-BB/TGFβ1	25.7	26.7	26.1
GM-CSF	23.5	25.0	24.3
GM-CSF + PDGF-BB/TGFβ1	23.9	25.8	24.8
VSMC	23.7	24.7	24.2

8.1.5 Full blot image - calmodulin

Figure 3.4.7 (b), Figure 3.4.11 (b), Figure 3.4.16 (b) and Figure 3.4.37 (b)

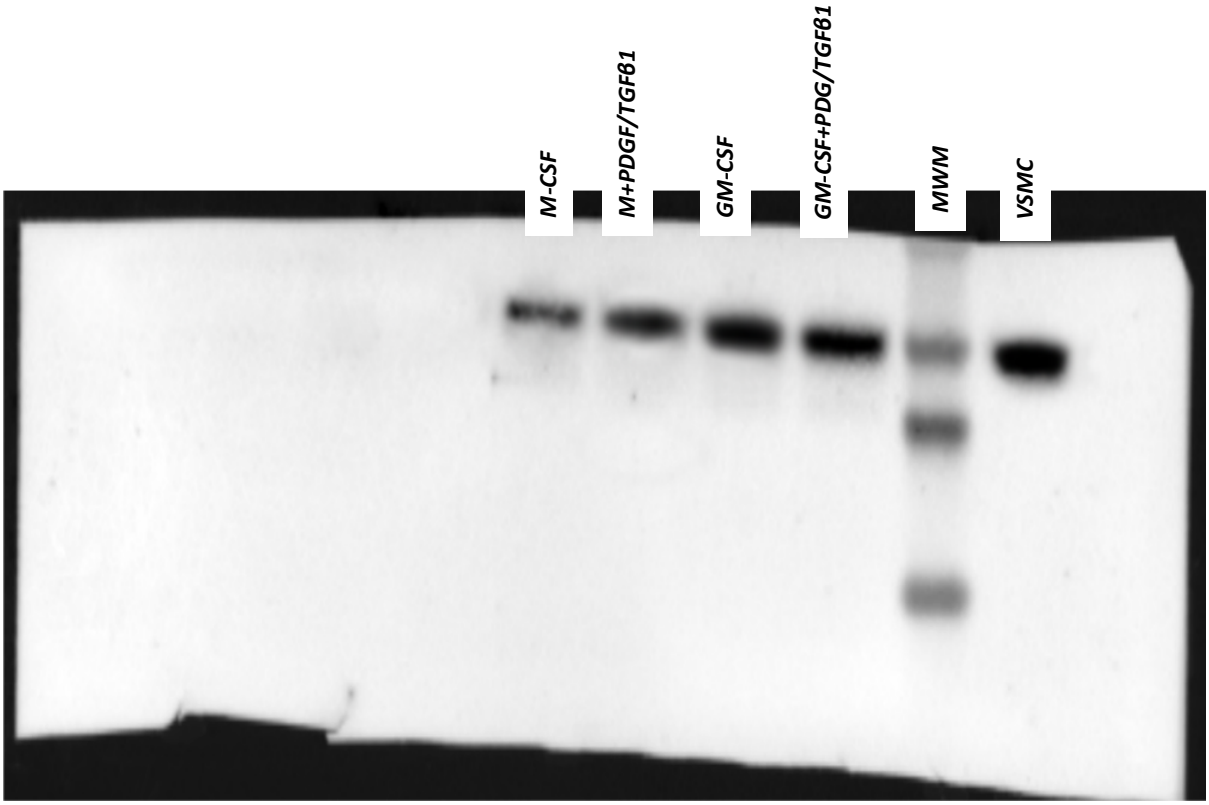

8.1.6 CT values - Myh11

Figure 3.4.8 (a), Figure 3.4.12 (a) and Figure 3.4.38 (a)

Myh11 mRNA	CT Min	CT Max	CT average
M-CSF	29.5	33.1	31.4
M-CSF + PDGF-BB/TGFβ1	29.9	34.0	31.5
GM-CSF	29.5	32.9	31.5
GM-CSF + PDGF-BB/TGFβ1	30.0	33.2	31.3
VSMC	34.5	37.8	36.1

8.1.7 Full blot image - Myh11

Figure 3.4.8 (b), Figure 3.4.12 (b) and Figure 3.4.38 (b)

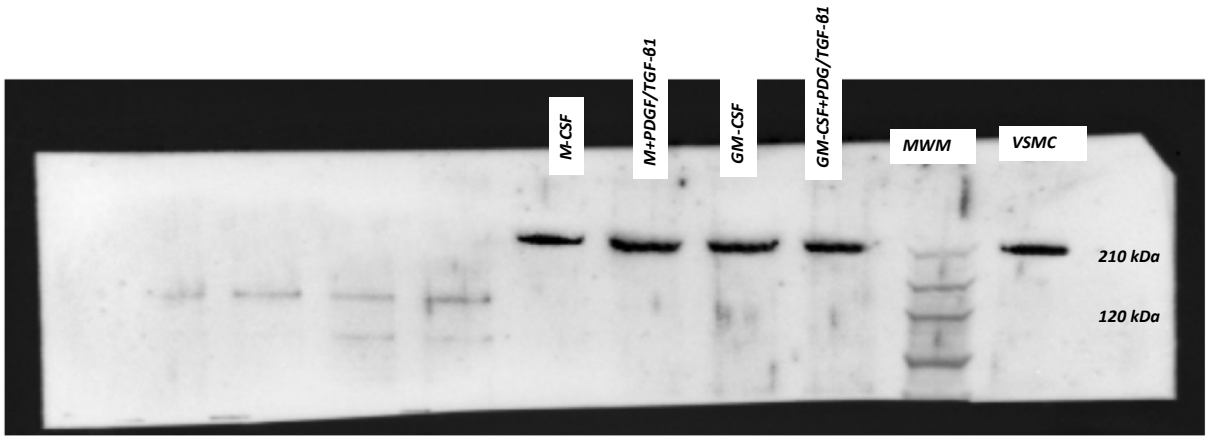

8.1.8 CT values - smoothelin

Figure 3.4.9 (a), Figure 3.4.13 (a) and Figure 3.4.39 (a)

Smoothelin mRNA	CT Min	CT Max	CT average
M-CSF	32.4	33.2	32.8
M-CSF + PDGF-BB/TGFβ1	32.0	34.2	32.9
GM-CSF	31.0	31.8	31.4
GM-CSF + PDGF-BB/TGFβ1	31.0	32.0	31.5
VSMC	25.7	28.6	26.8

8.1.9 Full blot image - smoothelin

Figure 3.4.9 (b), Figure 3.4.13 (b) and Figure 3.4.39 (b)

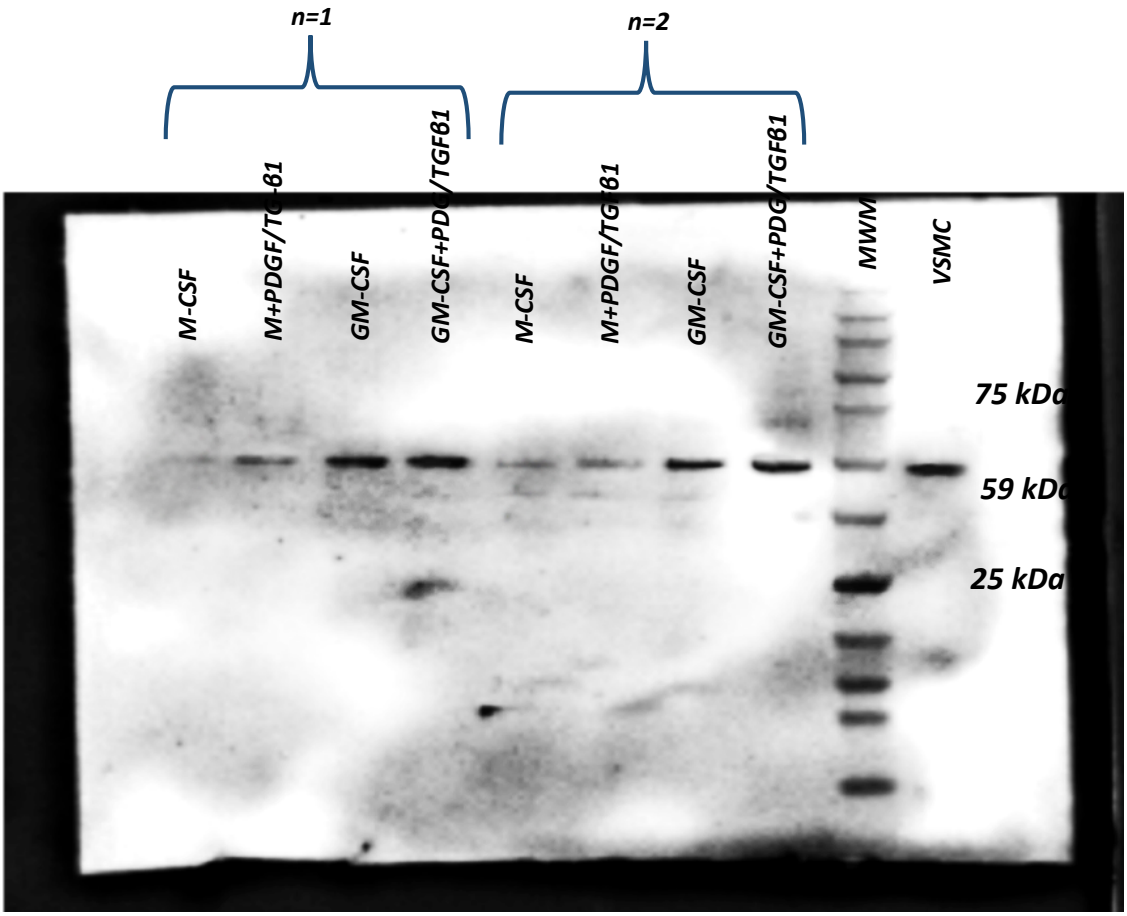

8.1.10 CT values - vimentin

Figure 3.4.10 (a), Figure 3.4.14 (a), Figure 3.4.17 (a), Figure 3.4.40 (a)

Vimentin mRNA	CT Min	CT Max	CT average
M-CSF	21.5	22.9	22.0
M-CSF + PDGF-BB/TGFβ1	20.6	21.5	21.2
GM-CSF	19.3	21.6	20.4
GM-CSF + PDGF-BB/TGFβ1	19.1	21.3	20.2
VSMC	19.2	21.3	20.0

8.1.11 Full blot image - vimentin

Figure 3.4.10 (b), Figure 3.4.14 (b), Figure 3.4.17 (b), Figure 3.4.40 (b)

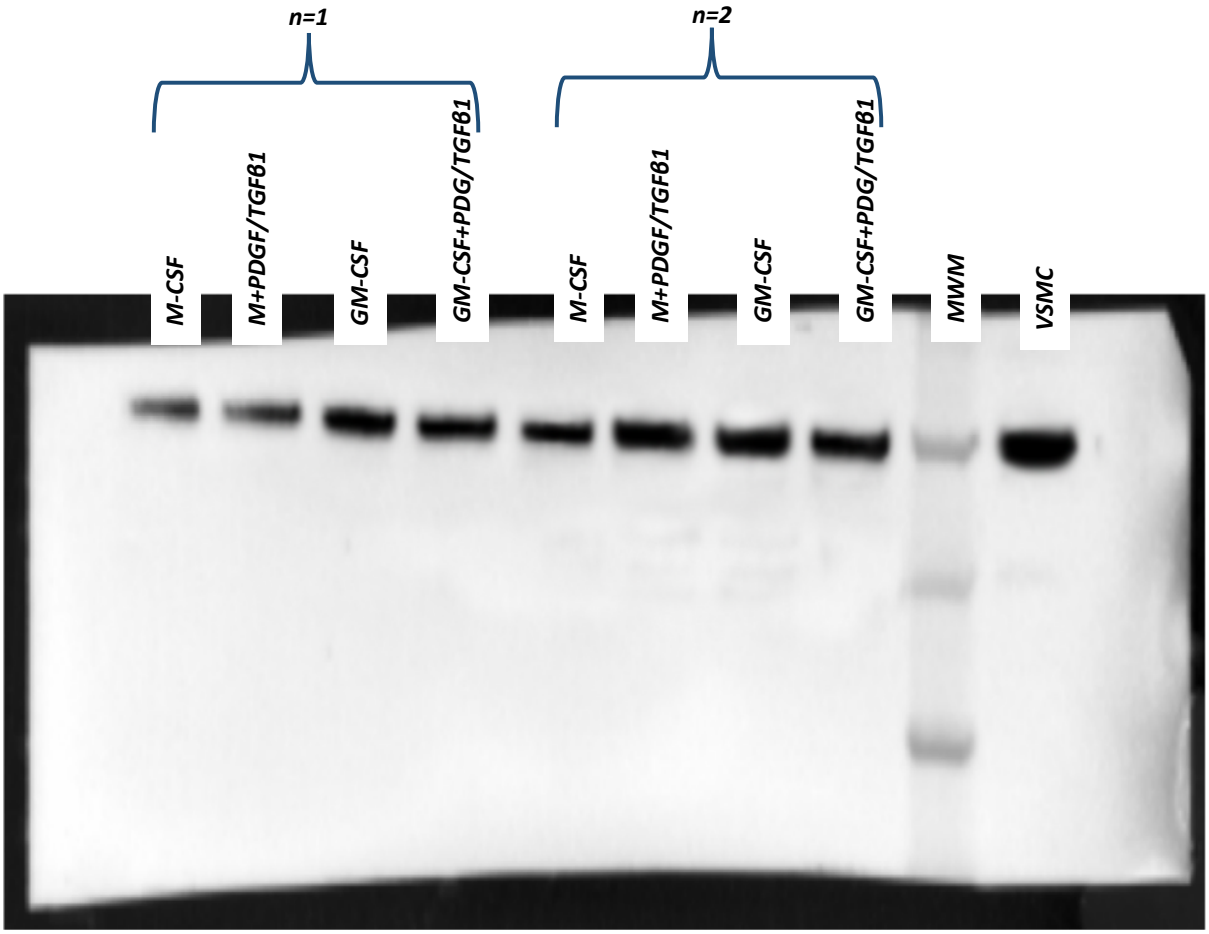

8.2 Differing human macrophage phenotypes display distinct changes in their expression of VSMC-associated markers

8.2.1 Representative image for Stain Free Gel for M-CSF macrophage, IFNγ /LPS, IL-4 and IL-10, co-stimulation with PBGF-BB and TGFβ1

Figure 36 (b) – Figure 43 (b)

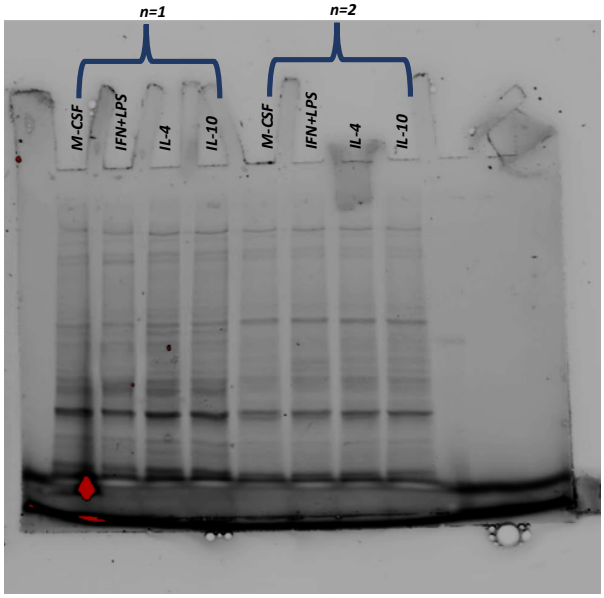

8.2.2 Representative image for Stain Free Gel for M-CSF, OxPAPC, PF4 and OxLDL

Figure 44(b) – Figure 52 (b)

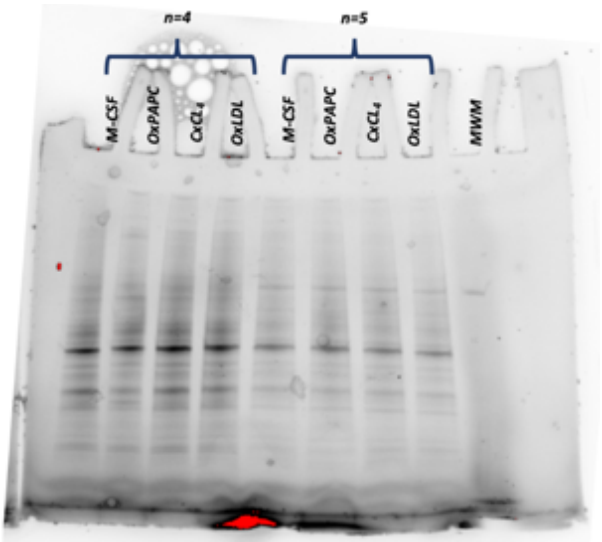

8.2.3 CT values - caldesmon

Figure 3.4.18 (a), Figure 3.4.22 (a), Figure 3.4.30 (a)

Caldesmon mRNA	CT Min	CT Max	CT average
M-CSF	32.1	35.2	34.1
IFNγ/LPS	31.9	35.0	34.0
IL-4	32.2	36.8	35.0
IL-10	32.2	35.7	34.2
PF4	31.8	36.2	34.0
oxPAPC	31.7	35.1	34.0
oxLDL	32.6	35.2	33.9

8.2.4 Full blot image – caldesmon

Figure 3.4.18 (b), Figure 3.4.22 (b)

All groups showed reduced expression compared to M-CSF macrophage (control)

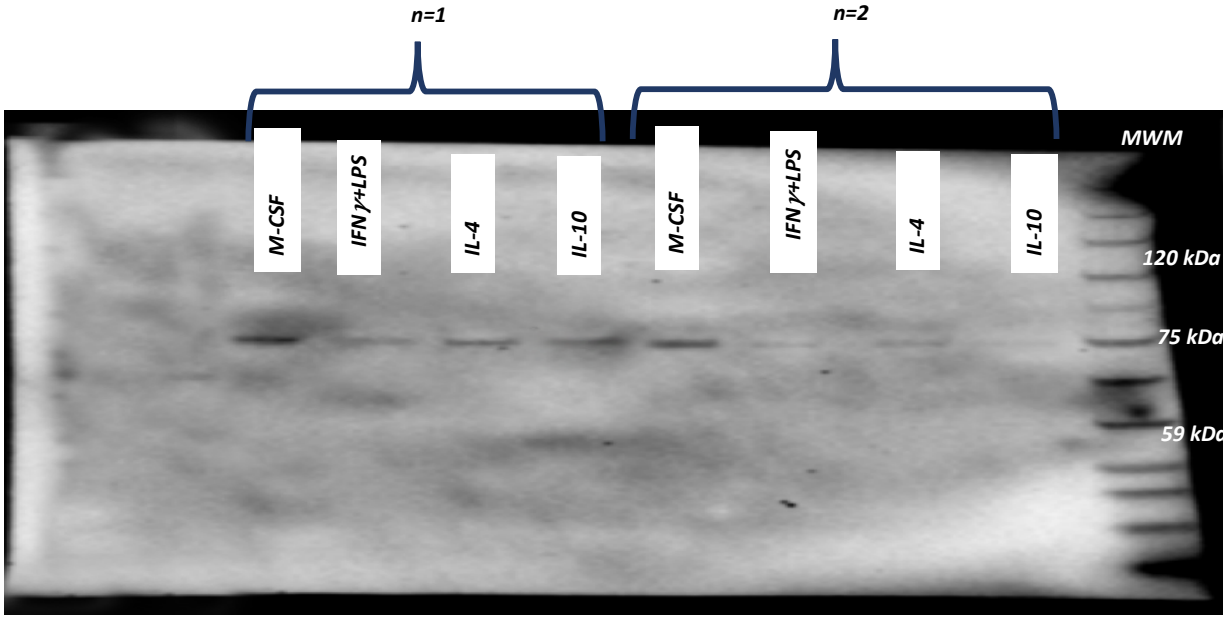

8.2.5 CT values – calmodulin

Figure 3.4.19 (a), Figure 3.4.23 (a), Figure 3.4.24 (a) and Figure 3.4.31 (a)

Calmodulin mRNA	CT Min	CT Max	CT average
M-CSF	25.0	27.2	26.4
IFNγ/LPS	23.6	26.3	25.0
IL-4	24.4	27.6	26.2
IL-10	24.0	27.3	26.2
PF4	24.9	27.4	26.4
oxPAPC	25.0	27.0	26.2
oxLDL	24.7	27.3	26.2

8.2.6 Full blot image – calmodulin

Figure 3.4.19 (b), Figure 3.4.23 (b), Figure 3.4.24 (b)

IFNγ /LPS and IL-10 groups showed reduced expression, whereas IL-4 group showed upregulation

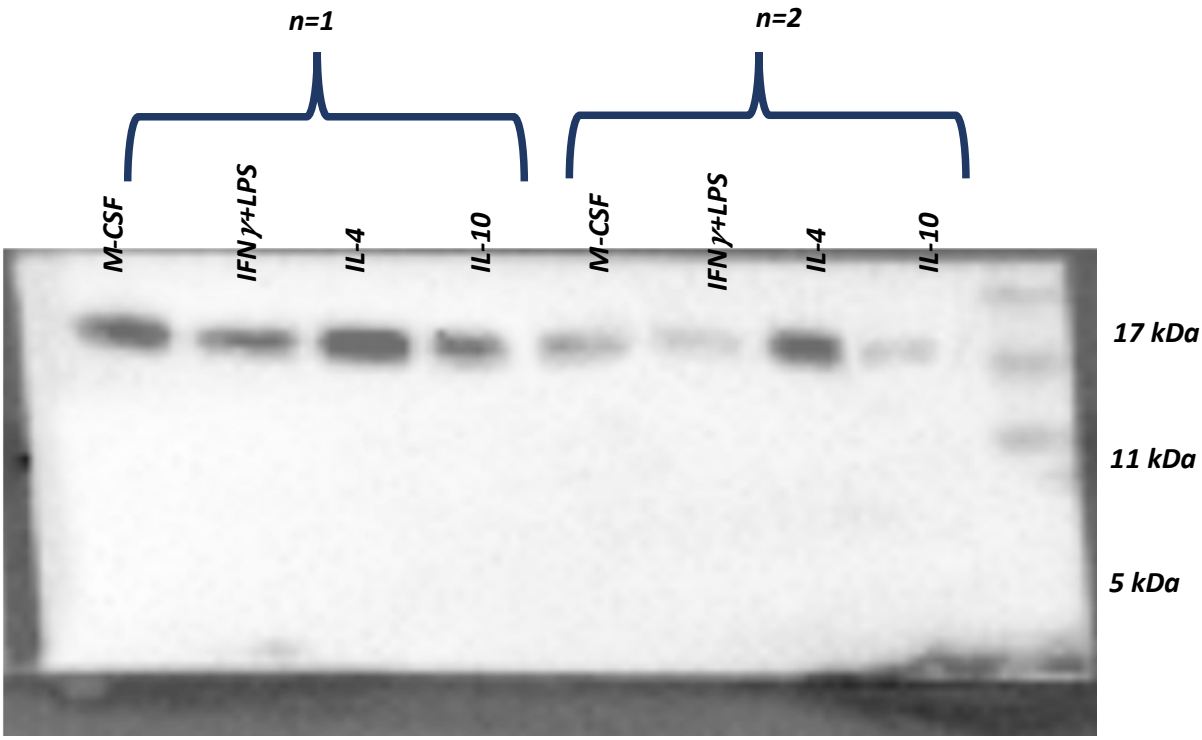

8.2.7 CT value – smoothelin

Figure 3.4.20 (a), Figure 3.4.25 (a), Figure 3.4.29 (a), Figure 3.4.34 (a)

*downregulation in oxPAPC and oxLDL group

Smoothelin mRNA	CT Min	CT Max	CT average
M-CSF	32.6	35.2	33.6
IFNγ/LPS	32.8	35.6	33.6
IL-4	33.2	34.3	33.6
IL-10	32.5	34.9	33.5
PF4	32.8	35.3	33.5
oxPAPC	33.0	36.7	34.3
oxLDL	33.0	38.4	35.5

8.2.8 Full blot image – smoothelin

Figure 3.4.20 (b) and Figure 3.4.25 (b)

IFNγ/LPS group and IL-10 showed downregulation, with unchanged expression in IL-4 group

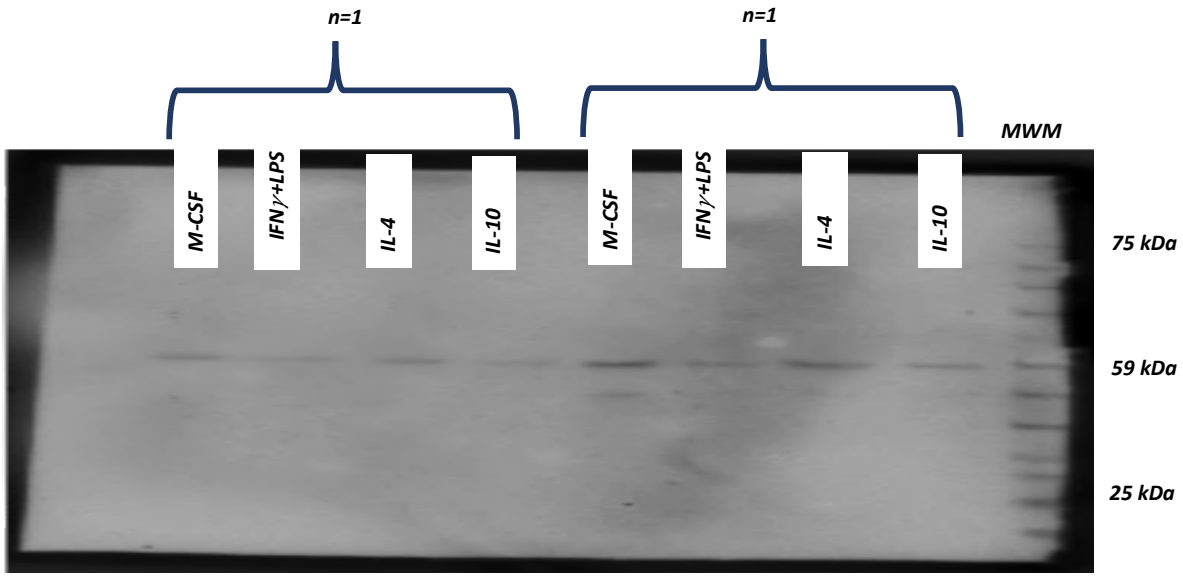

8.2.9 CT value - vimentin

Figure 3.4.21 (a), Figure 3.4.26 (a), Figure 3.4.28 (a), Figure 3.4.33 (a)

*no changes except for IFNγ/LPS

Vimentin mRNA	CT Min	CT Max	CT average
M-CSF	21.3	23.0	22.2
IFNγ/LPS	20.6	22.8	21.6
IL-4	21.5	22.9	22.2
IL-10	21.5	23.1	22.2
PF4	21.3	22.7	22.1
oxPAPC	21.4	22.8	22.3
oxLDL	21.3	23.5	22.2

8.2.10 Full blot image – vimentin

Figure 3.4.21 (b)

*only IFNγ /LPS group showed significant changes

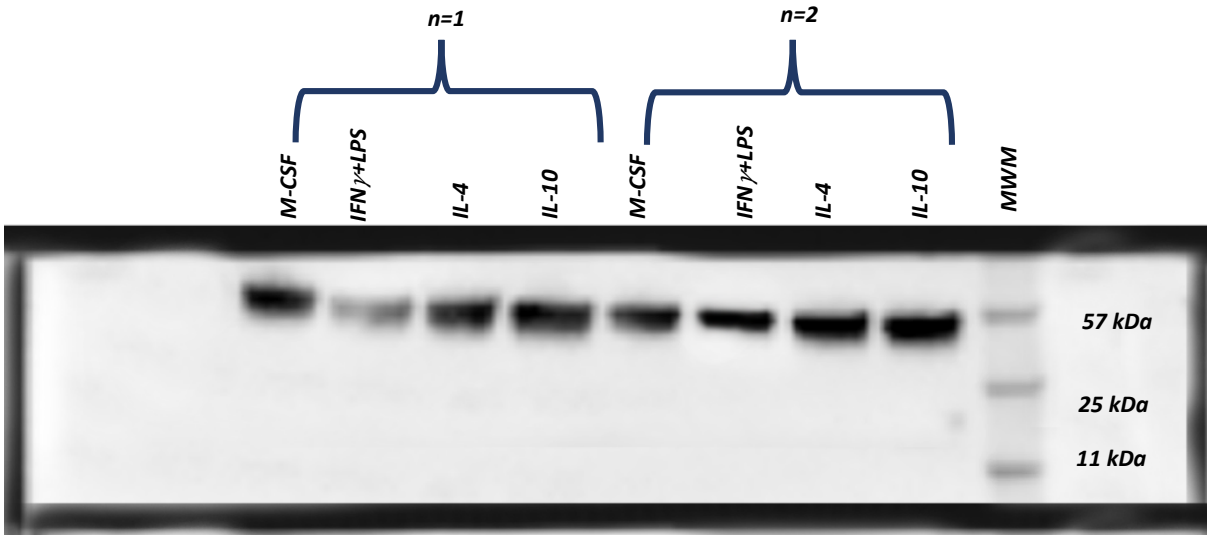

8.2.11 Full blot image - vimentin

Figure 3.4.26 (b), Figure 3.4.28 (b), and Figure 3.4.33 (b)

vimentin in all groups significantly upregulated compared to control (M-CSF)

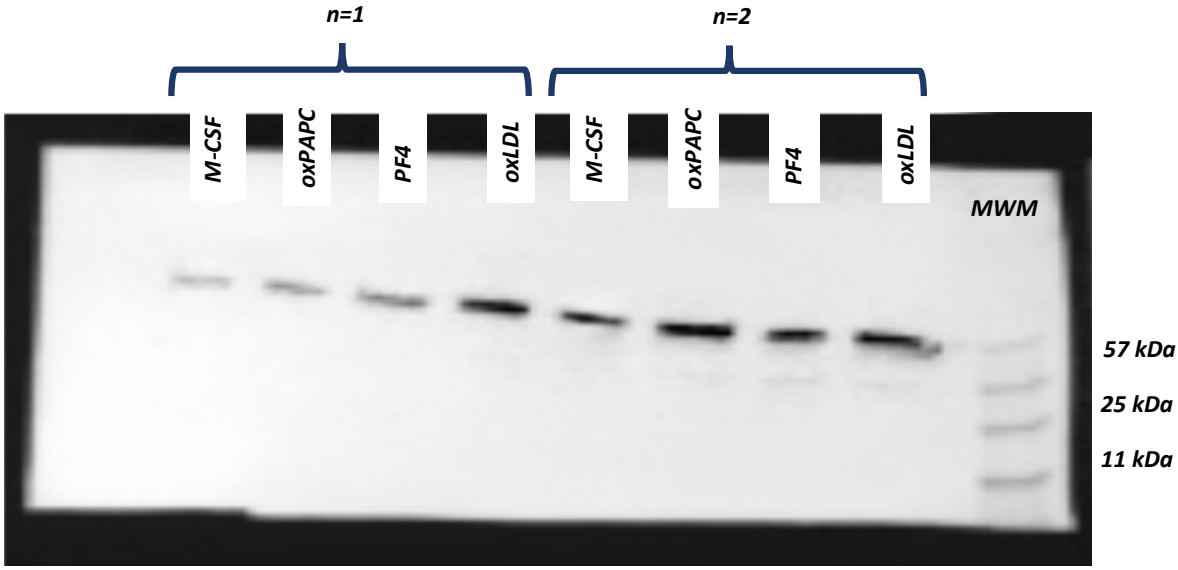

8.2.12 CT value – Myh11

Figure 3.4.27 (a), Figure 3.4.32 (a)

*all macrophage phenotypes showed no changes

Myh11 mRNA	CT Min	CT Max	CT average
M-CSF	29.4	31.6	30.4
IFNγ/LPS	29.2	31.6	30.4
IL-4	29.6	31.9	30.6
IL-10	29.5	31.0	30.2
PF4	29.7	31.4	30.5
oxPAPC	29.2	31.3	30.4
oxLDL	29.4	31.2	30.3

8.2.13 Full blot image – Myh11

Figure 3.4.27 (b), Figure 3.4.32 (b)

oxPAPC and oxLDL group showed higher expression compared to M-CSF macrophage (control)

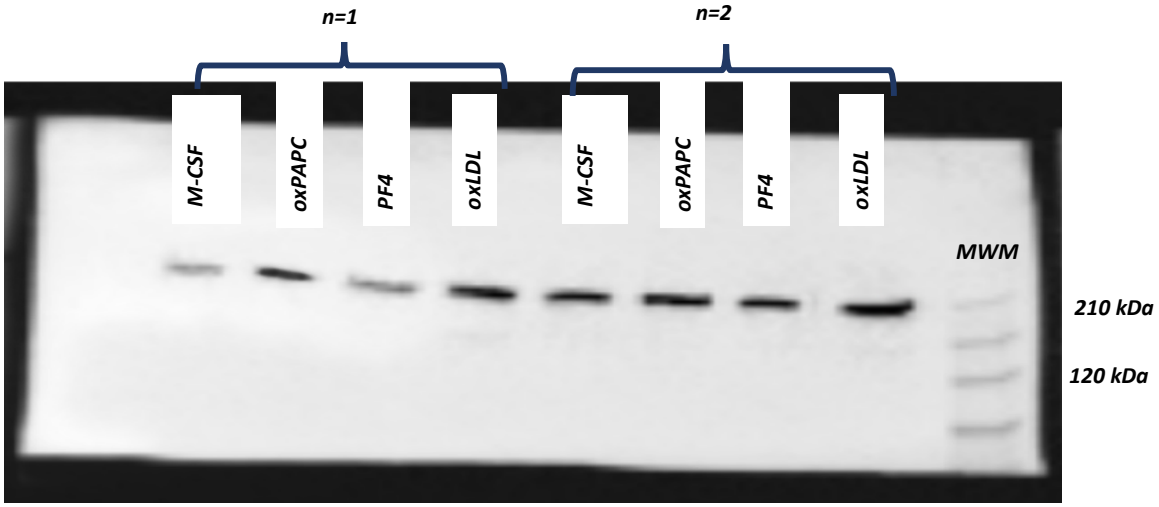

8.2.14 Full blot image - smoothelin

Figure 3.4.29 (b), and Figure 3.4.34 (b)

*oxPAPC and oxLDL groups showed downregulation, with unchanged expression in PF4 group

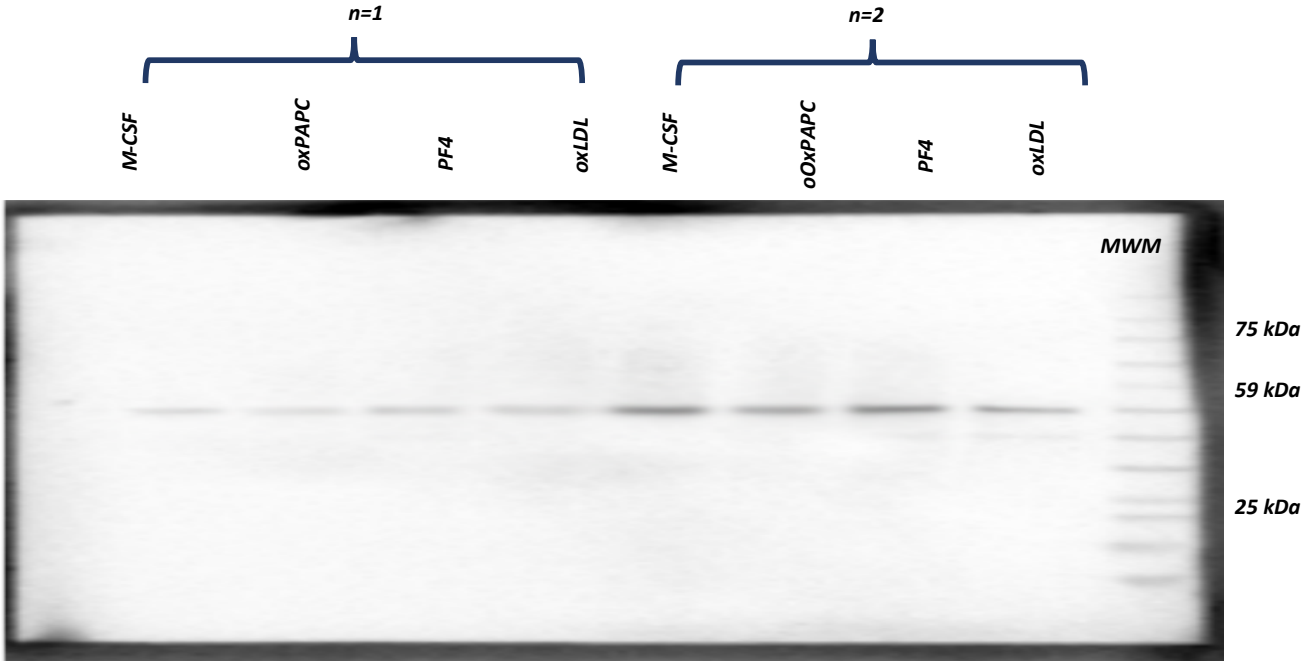

8.2.15 Full blot image - caldesmon

Figure 3.4.30 (b)

*Only OxLDL group showed higher expression compared to M-CSF macrophage (control)

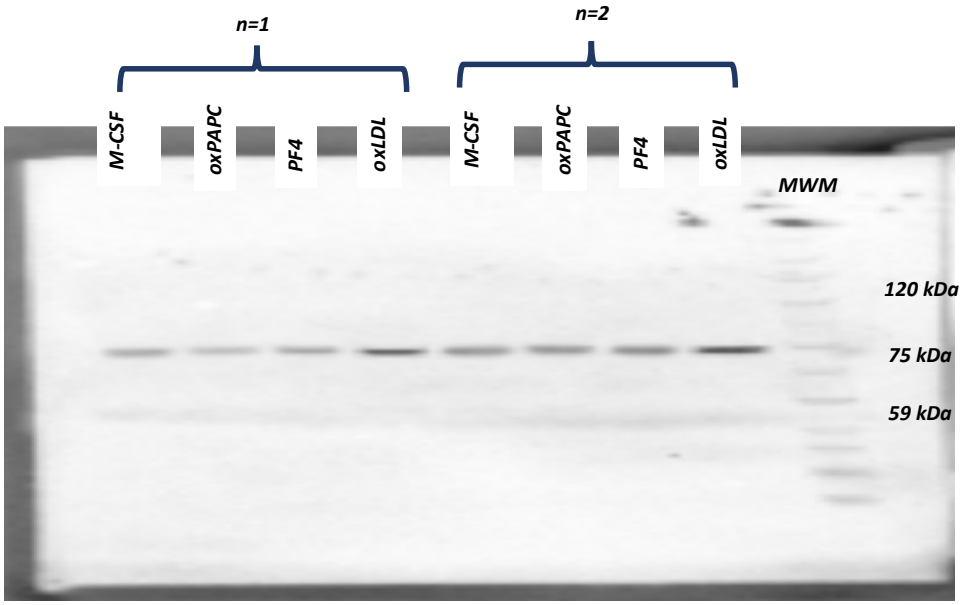

8.2.16 Full blot image - calmodulin

Figure 3.4.31 (b)

Only OxLDL groups showed upregulated expression

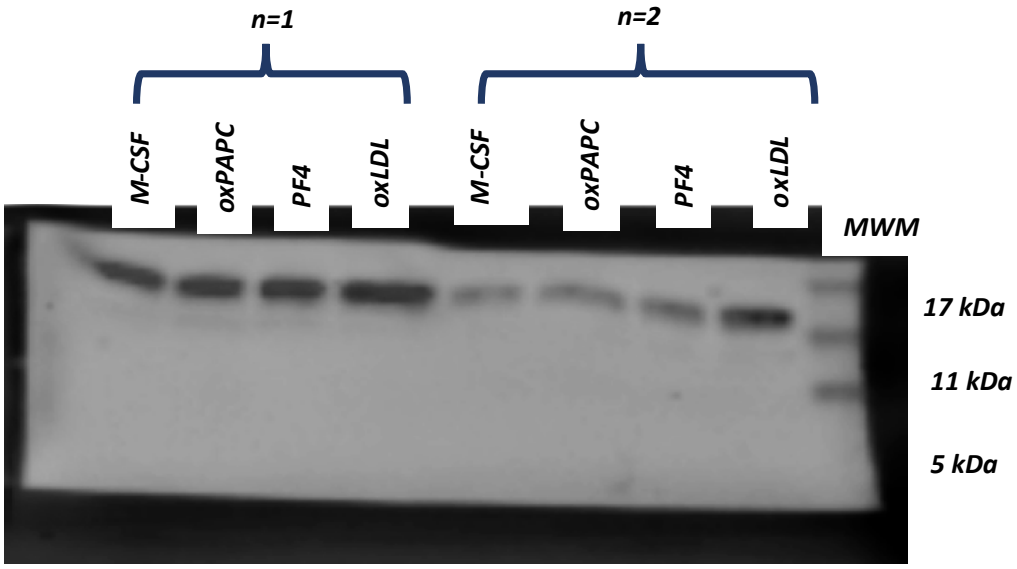

9 Appendix B (Result, Chapter 4)

9.1 Representative image for Stain Free Gel for baseline macrophage M-CSF & GM-CSF day-8, day-11 and day-14

Figure 4.4.1 and Figure 71

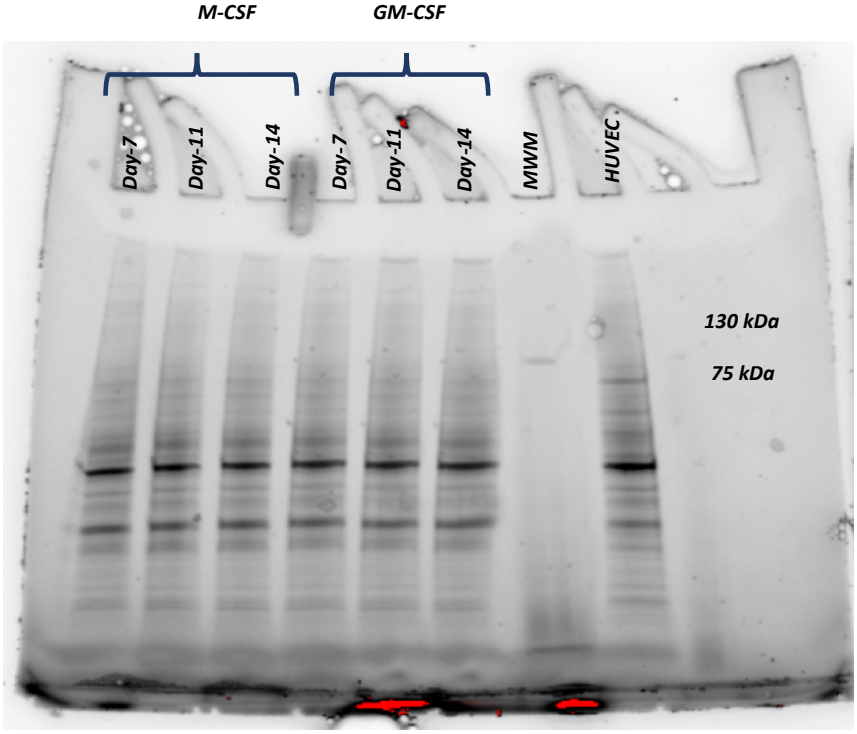

9.1.1 CT values - PECAM-1

Figure 4.4.1 (a) and Figure 4.4.21 (a)

PECAM-1 mRNA	*CT Min*	*CT Max*	*CT average*
M-CSF day-7	25.2	27.9	26.8
M-CSF day-11	26.2	27.2	26.9
M-CSF day-14	24.5	26.0	25.1
GM-CSF day-7	24.0	25.9	25.1
GM-CSF day-11	25.9	28.3	27.2
GM-CSF day-14	24.0	25.9	25.1
HUVEC	20.8	21.1	20.4

9.1.2 Full blot image – Stain free gel and PECAM-1

Figure 4.4.1 (b) and Figure 4.4.21 (c)

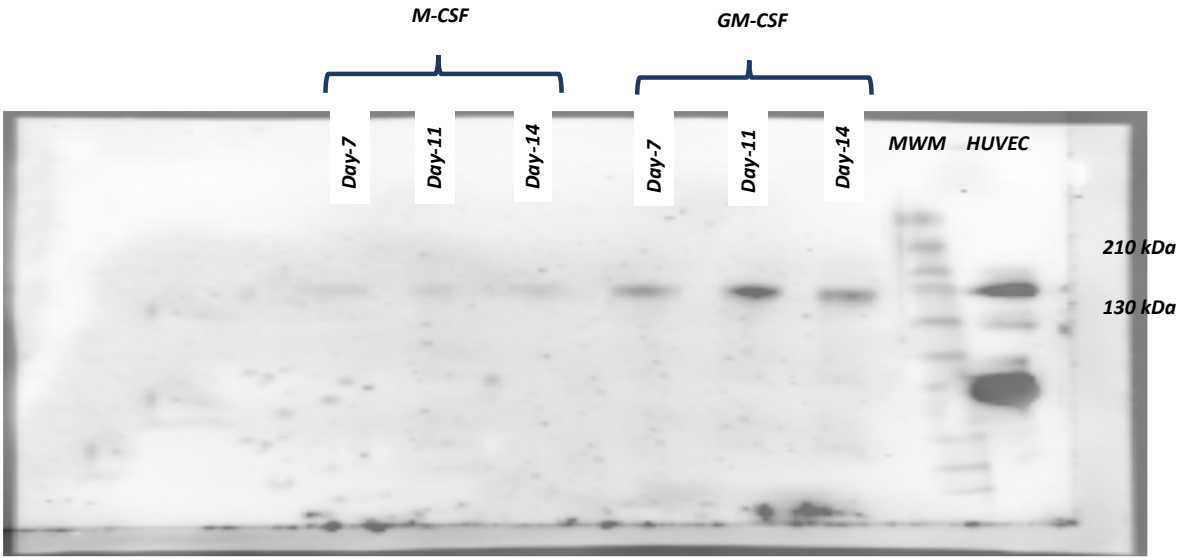

9.1.3 CT values - VE-cadherin

Figure 4.4.3 (a) and Figure 4.4.22 (a)

VE-cadherin mRNA	*CT Min*	*CT Max*	*CT average*
M-CSF day-7	36.3	37.3	36.8
M-CSF day-11	31.9	33.2	32.5
M-CSF day-14	31.0	32.8	31.8
GM-CSF day-7	32.1	33.5	32.9
GM-CSF day-11	32.3	33.2	32.7
GM-CSF day-14	31.4	32.5	32.0
HUVEC	20.1	21.9	21.2

9.1.4 Full blot image – VE-cadherin

Figure 4.4.3 (b) and Figure 4.4.22 (b)

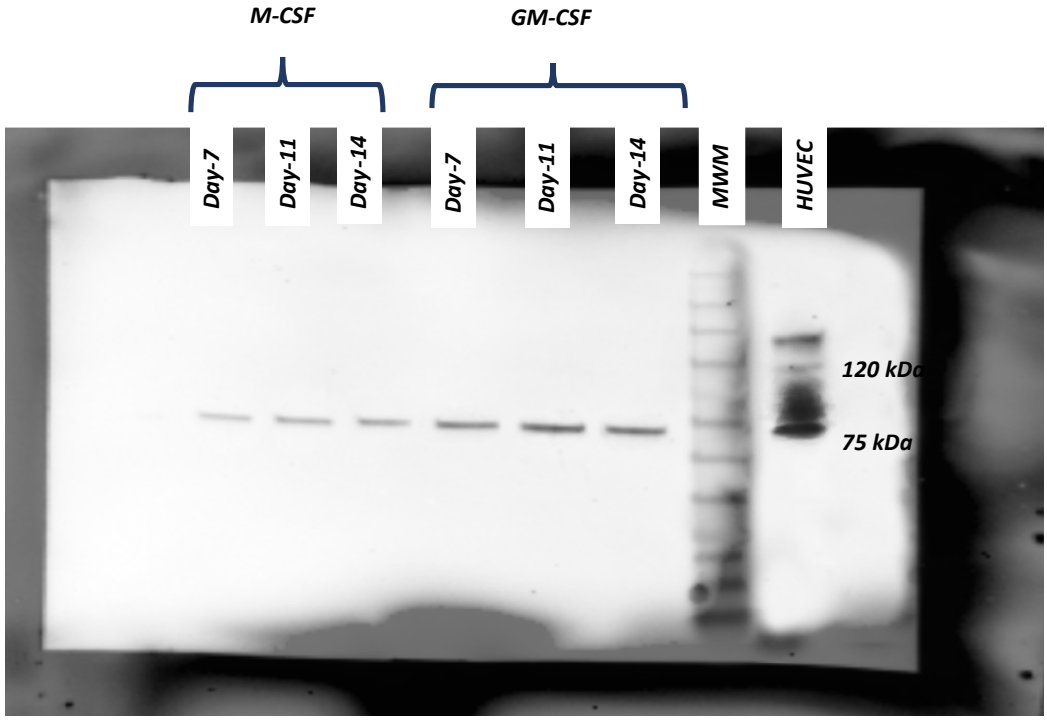

9.1.5 CT values - PECAM-1

Figure 4.4.5 (a)

PECAM-1 mRNA	CT Min	CT Max	CT average
M-CSF	27.2	27.8	27.5
VEGF-A 1 ng/ml	24.3	27.2	26.0
VEGF-A 10 ng/ml	23.5	26.5	25.5
VEGF-A 100 ng/ml	23.3	26.2	25.1
FGF2 1 ng/ml	24.3	26.9	25.8
FGF2 10 ng/ml	24.0	26.4	25.4
FGF2 100 ng/ml	24.2	25.8	25.2
IGF-1 1 ng/ml	25.4	27.5	26.5
IGF-1 10 ng/ml	24.8	27.2	26.1
IGF-1 100 ng/ml	26.0	27.4	26.7
HGF 1 ng/ml	25.6	27.8	26.7
HGF 10 ng/ml	25.3	27.7	26.5
HGF 100 ng/ml	25.8	27.8	26.7
ANGPTL5 1 ng/ml	25.9	27.7	26.9
ANGPTL5 10ng/ml	26.1	27.9	26.8
ANGPTL5 100 ng/ml	25.7	27.9	26.6

Figure 4.4.5 (b)

PECAM-1 mRNA	CT min	CT Max	CT Average
GM-CSF	24.6	26.3	25.8
VEGF-A 1 ng/ml	23.9	26.6	25.7
VEGF-A 10 ng/ml	25.0	27.0	25.9
VEGF-A 100 ng/ml	24.7	26.5	25.6
FGF2 1 ng/ml	24.2	26.9	25.4
FGF2 10 ng/ml	24.7	26.2	25.6
FGF2 100 ng/ml	24.6	27.1	25.6
IGF-1 1 ng/ml	25.2	26.7	25.8
IGF-1 10 ng/ml	24.6	26.3	25.6
IGF-1 100 ng/ml	24.1	26.7	25.6
HGF 1 ng/ml	25.4	26.8	25.9
HGF 10 ng/ml	24.0	27.0	25.6
HGF 100 ng/ml	25.5	26.4	25.9
ANGPTL5 1 ng/ml	24.3	26.9	25.7
ANGPTL5 10ng/ml	24.1	27.2	25.7
ANGPTL5 100 ng/ml	24.9	27.0	25.6

9.1.6 CT values – VE-cadherin

Figure 4.4.6 (a)

VE-cadherin mRNA	CT Min	CT Max	CT average
M-CSF	36.0	40.0	38.3
VEGF-A 1 ng/ml	34.0	38.9	34.0
VEGF-A 10 ng/ml	35.3	38.7	35.3
VEGF-A 100 ng/ml	35.2	38.5	35.2
FGF2 1 ng/ml	34.3	39.4	34.3
FGF2 10 ng/ml	33.7	38.7	33.7
FGF2 100 ng/ml	33.6	38.2	33.6
IGF-1 1 ng/ml	35.4	40.0	35.4
IGF-1 10 ng/ml	35.9	40.0	35.9
IGF-1 100 ng/ml	36.2	40.0	36.2
HGF 1 ng/ml	34.7	39.1	34.7
HGF 10 ng/ml	35.3	39.5	35.3
HGF 100 ng/ml	36.2	40.0	36.2
ANGPTL5 1 ng/ml	37.0	38.4	37.0
ANGPTL5 10ng/ml	37.0	40.0	37.0
ANGPTL5 100 ng/ml	37.1	39.1	37.1

Figure 4.4.6 (b)

VE-cadherin mRNA	CT Min	CT Max	CT average
GM-CSF	33.1	34.9	33.8
VEGF-A 1 ng/ml	33.2	35.3	34.1
VEGF-A 10 ng/ml	33.1	34.8	33.8
VEGF-A 100 ng/ml	32.7	34.8	33.7
FGF2 1 ng/ml	33.0	33.9	33.4
FGF2 10 ng/ml	32.7	34.8	33.5
FGF2 100 ng/ml	32.5	34.7	33.7
IGF-1 1 ng/ml	32.1	35.1	33.5
IGF-1 10 ng/ml	32.6	34.8	33.6
IGF-1 100 ng/ml	33.0	34.8	33.7
HGF 1 ng/ml	32.8	35.0	33.6
HGF 10 ng/ml	32.5	35.0	33.9
HGF 100 ng/ml	32.0	35.0	33.7
ANGPTL5 1 ng/ml	32.1	34.9	33.5
ANGPTL5 10ng/ml	32.9	35.1	33.8
ANGPTL5 100 ng/ml	32.2	34.9	33.7

9.1.7 CT values – PECAM1

Figure 4.4.8 a

PECAM-1 mRNA	CT Min	CT Max	CT average
M-CSF	26.8	27.8	27.3
VEGF-A	25.8	27.0	26.5
FGF2	25.7	26.8	26.5
IGF-1	26.1	27.6	26.9
HGF	26.4	27.6	26.9
ANGPTL5	26.7	28.7	27.5

9.2 Representative image for Stain Free Gel for baseline macrophage M-CSF stimulated with 50 ng/ml endothelial growth factor for four-day

Figure 4.4.8 c and Figure 78 c

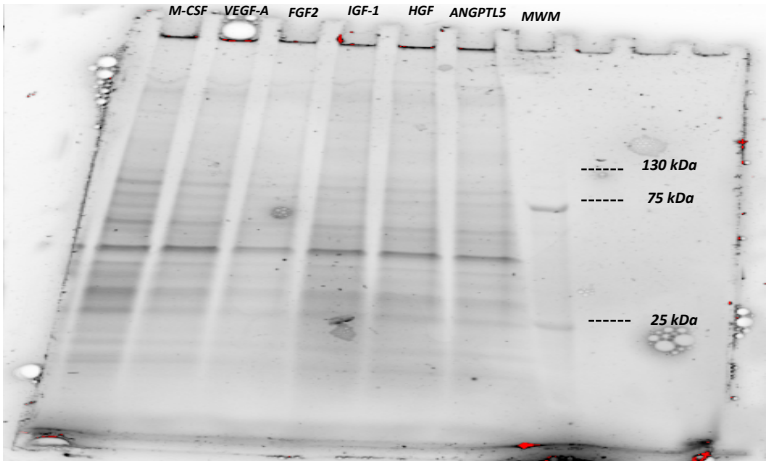

9.2.1 Full blot image – PECAM-1

Figure 4.4.8 c

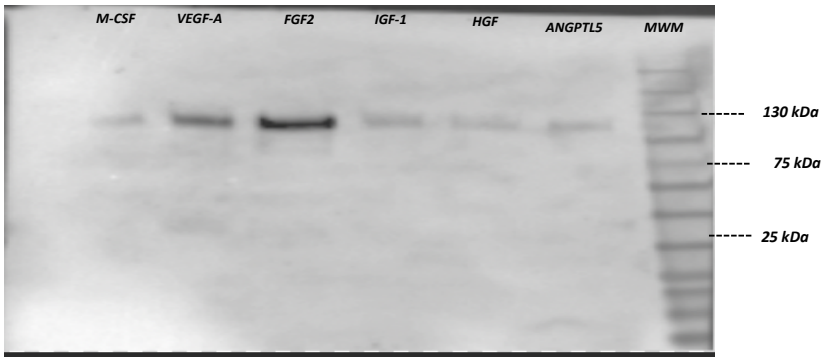

9.2.2 CT values – VE-cadherin

Figure 4.4.11 a

VE-cadherin mRNA	CT Min	CT Max	CT average
M-CSF	31.7	33.1	32.5
VEGF-A	32.0	33.2	32.6
FGF2	33.0	34.8	33.7
IGF-1	32.2	33.9	32.8
HGF	31.7	33.8	32.8
ANGPTL5	32.1	33.7	32.8

9.2.3 Full blot image – VE-cadherin

Figure 4.4.11 c

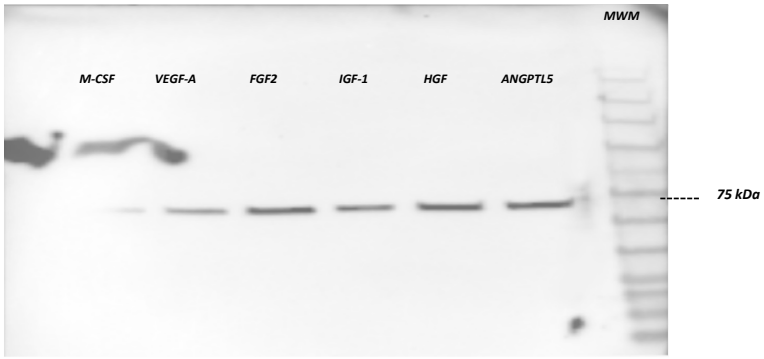

9.2.4 CT values – PECAM1

Figure 81 a

PECAM-1 mRNA	CT Min	CT Max	CT average
GM-CSF	26.1	28.3	27.3
VEGF-A	26.4	28.4	27.3
FGF2	26.5	28.1	27.2
IGF-1	26.0	28.0	27.1
HGF	26.5	27.9	27.1
ANGPTL5	25.9	28.1	27.5

9.3 Representative image for Stain Free Gel for baseline macrophage GM-CSF stimulated with 50 ng/ml endothelial growth factor for four-day

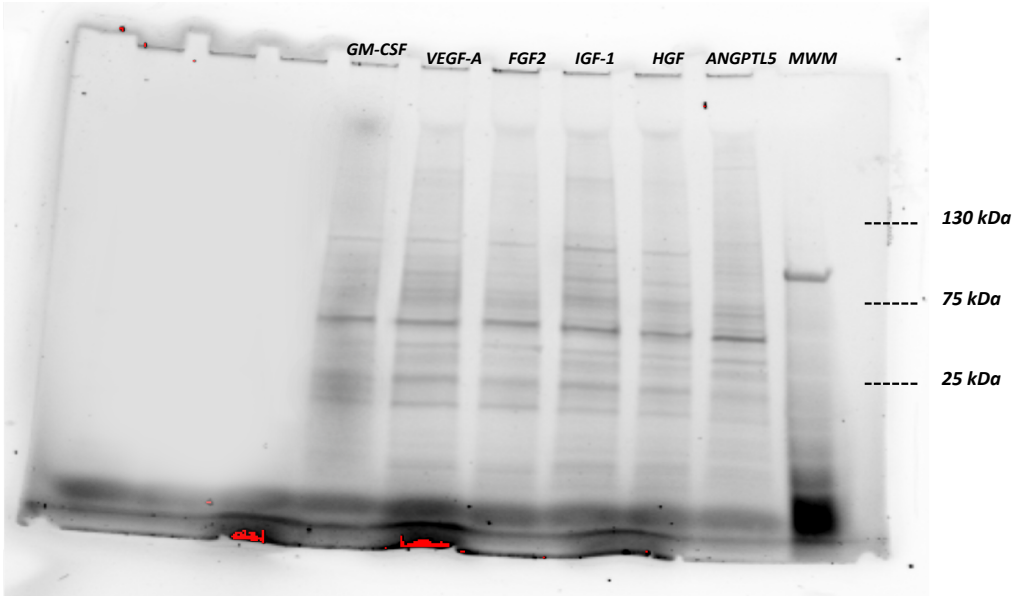

9.3.1 Full blot image – PECAM-1

(GM-CSF after 4-day stimulation with EC-GF)

Figure 4.4.14 c

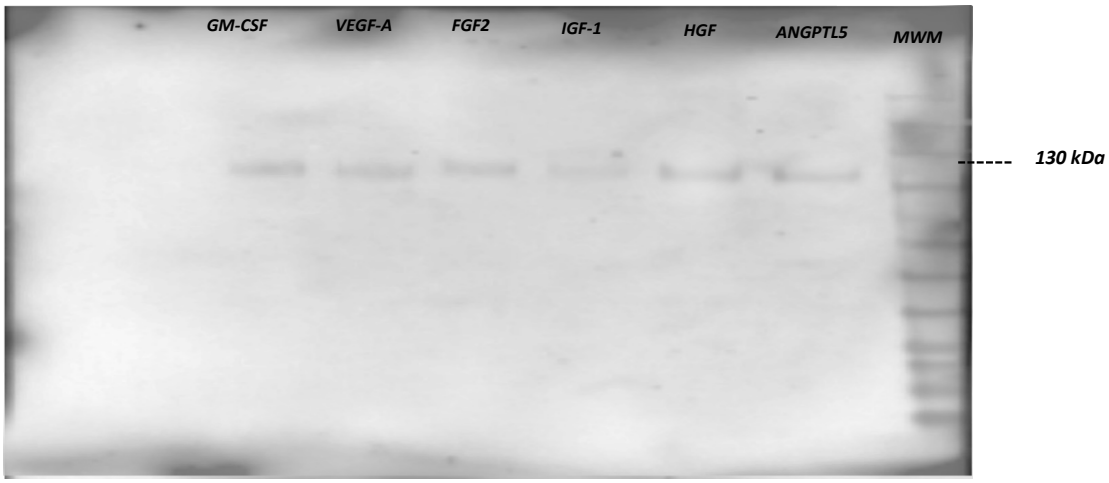

9.3.2 CT values – VE-cadherin

Figure 4.4.17 c

VE-cadherin mRNA	CT Min	CT Max	CT average
GM-CSF	31.9	33.3	32.6
VEGF-A	31.9	33.6	32.8
FGF2	31.8	33.5	32.7
IGF-1	31.8	33.4	32.6
HGF	31.8	33.8	32.8
ANGPTL5	31.5	33.4	32.5

9.3.3 Full blot image – VE-cadherin

Figure 4.4.17 c

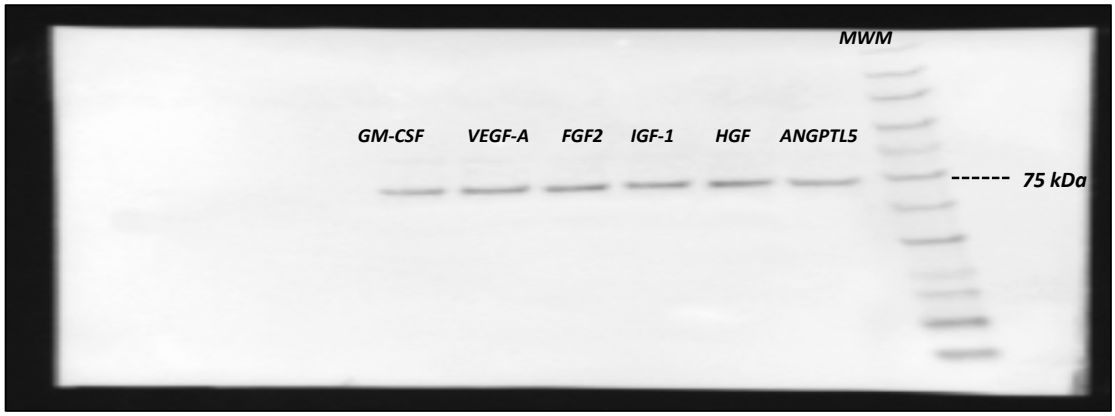

10 Appendix C (Result, Chapter 5)

10.1 CT values for microRNA

10.1.1 CT values for microRNA-101-3p

microRNA-101-3p	CT Min	CT Max	CT average
M-CSF	35.1	36.5	35.6
M+VEGFA	34.5	35.6	35.0
M+FGF2	34.6	36.9	35.7
M+IGF-1	35.9	36.3	35.9
M+HGF	34.4	36.2	35.9
M+ANGPTL5	34.1	36.9	35.2
GM-CSF	34.1	36.1	35.2
GM+VEGFA	35.9	36.0	35.7
GM+FGF2	33.2	35.5	34.3
GM+IGF-1	33.2	35.4	34.7
GM+HGF	34.7	36.5	35.5
GM+ANGPTL5	34.0	35.5	35.3

10.1.2 CT values for microRNA-101-5p

microRNA-101-5p	CT Min	CT Max	CT average
M-CSF	37.1	38.9	38.5
M+VEGFA	36.9	38.1	37.8
M+FGF2	37.1	38.3	37.6
M+IGF-1	37.0	38.3	37.4
M+HGF	36.1	38.3	37.6
M+ANGPTL5	36.7	38.4	37.9
GM-CSF	37.4	38.7	38.1
GM+VEGFA	36.6	37.9	37.2
GM+FGF2	36.5	37.4	36.9
GM+IGF-1	36.6	37.5	37.0
GM+HGF	36.9	37.6	37.3
GM+ANGPTL5	36.9	37.8	37.6

10.1.3 CT values for microRNA-27a-3p

Figure 5.4.1

microRNA-27a-3p	CT Min	CT Max	CT average
M-CSF	36.4	38.0	37.2
M+VEGFA	36.3	38.0	37.4
M+FGF2	36.9	38.7	37.8
M+IGF-1	36.0	38.0	37.2
M+HGF	36.0	37.8	37.1
M+ANGPTL5	36.5	38.5	37.4
GM-CSF	40.0	40.0	40.0
GM+VEGFA	40.0	40.0	40.0
GM+FGF2	40.0	40.0	40.0
GM+IGF-1	37.6	40.0	39.4
GM+HGF	38.0	40.0	39.3
GM+ANGPTL5	37.9	40.0	38.9

10.1.4 CT values for microRNA-27a-5p

Figure 5.4.2

microRNA-27a-5p	CT Min	CT Max	CT average
M-CSF	29.9	31.1	30.4
M+VEGFA	30.0	31.1	30.5
M+FGF2	29.3	31.7	30.4
M+IGF-1	29.7	31.4	30.3
M+HGF	29.6	30.6	30.0
M+ANGPTL5	29.7	32.1	30.5
GM-CSF	30.9	32.0	31.6
GM+VEGFA	30.1	32.6	31.5
GM+FGF2	30.3	31.9	31.2
GM+IGF-1	30.4	32.7	31.8
GM+HGF	30.6	32.4	31.4
GM+ANGPTL5	30.9	31.7	31.1

10.1.5 Full blot image for transfection experiment

Figure 5.4.4 and Figure 5.4.5

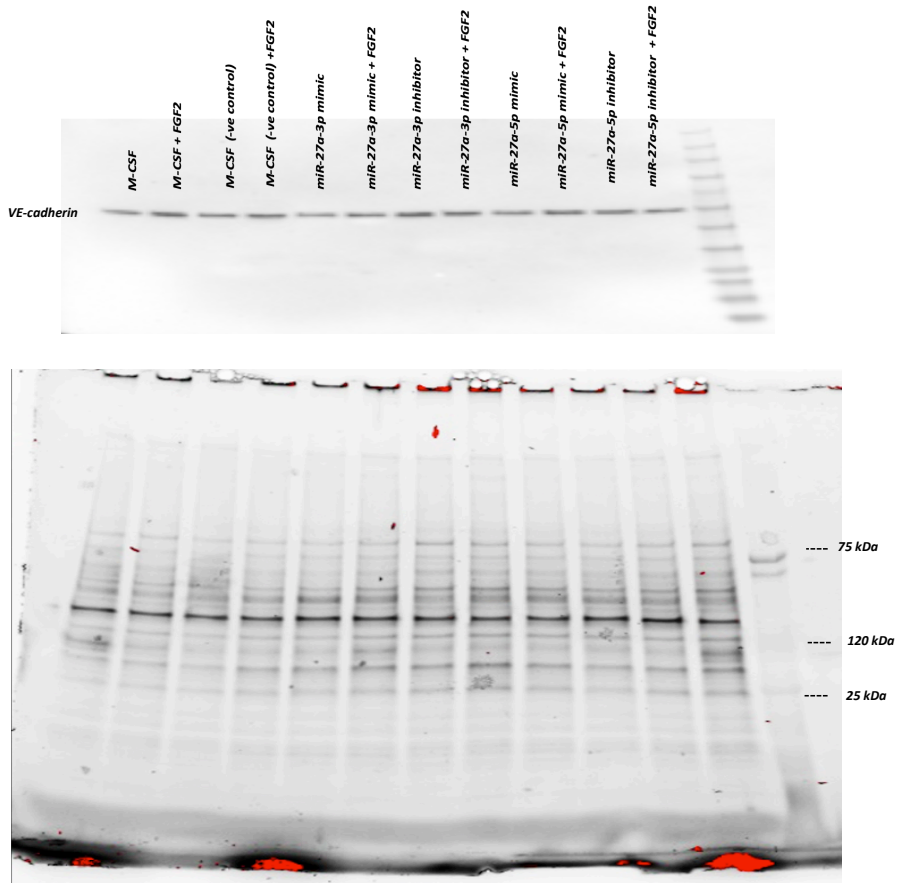

10.1.6CT values VE-cadherin mRNA (transfection experiment)

Figure 5.4.8

VE-cadherin mRNA	CT Min	CT Max	CT average
M-CSF	31.7	33.1	32.5
M+FGF2	32.8	35.0	33.7
NEG CTRL	30.2	33.3	31.9
NEG CTRL +FGF2	30.4	35.0	32.9
microRNA-27a-3p-mimic	30.1	33.2	32.1
microRNA -27a-3p-mimic +FGF2	30.0	34.1	32.2
microRNA -27a-3p-inhibitor	30.4	35.3	33.2
microRNA -27a-3p-inhibitor +FGF2	31.7	33.1	32.5

10.1.7 CT values microRNA-27a-3p (transfection experiment)

Figure 5.4.9

microRNA-27a-3p	CT Min	CT Max	CT average
NEG CTRL	36.1	38.2	37.3
NEG CTRL +FGF2	37.0	39.0	38.1
microRNA-27a-3p-mimic	36.4	38.5	37.2
microRNA -27a-3p-mimic +FGF2	36.0	38.2	37.2
microRNA -27a-3p-inhibitor	36.5	38.5	37.9
microRNA -27a-3p-inhibitor +FGF2	37.5	38.6	38.0

10.1.8 CT values FGFR1 mRNA (transfection experiment)

Figure 5.4.11

FGFR1 mRNA	CT Min	CT Max	CT average
NEG CTRL	28.1	29.2	28.7
NEG CTRL +FGF2	27.4	29.4	28.7
microRNA-27a-3p-mimic	27.2	30.1	28.9
microRNA -27a-3p-mimic +FGF2	27.6	29.7	28.8
microRNA -27a-3p-inhibitor	28.0	30.0	29.0
microRNA -27a-3p-inhibitor +FGF2	27.8	29.6	28.5

10.1.9 CT values VE-cadherin mRNA (FGFR1 neutralising antibody experiment)

Figure 5.4.12 a

VE-cadherin mRNA	CT Min	CT Max	CT average
M-CSF	30.20	33.07	31.87
IgG control	30.39	33.60	32.01
IgG control +FGF2	31.72	33.94	32.88
anti-FGFR1	31.18	33.16	31.99
anti-FGFR1 +FGF2	30.48	33.17	31.97

10.1.10 Full blot (FGFR1 neutralising antibody experiment)

Figure 5.4.12 b

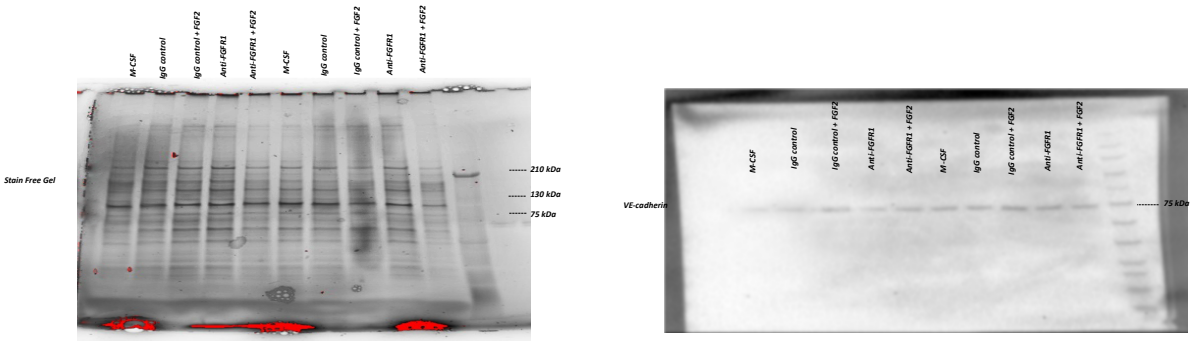

10.1.11 CT values microRNA-27a-3p (FGFR1 neutralising antibody experiment)

Figure 5.4.13

microRNA-27a-3p	CT Min	CT Max	CT average
M-CSF	36.13	37.94	36.91
IgG control	36.28	37.53	36.81
IgG control +FGF2	36.74	38.27	37.46
anti-FGFR1	36.09	37.95	36.72
anti-FGFR1 +FGF2	35.70	37.58	36.51

10.1.12 CT values FGFR1 mRNA (neutralising antibody experiment)

Figure 5.4.14

microRNA-27a-3p	CT Min	CT Max	CT average
M-CSF	36.13	37.94	36.91
IgG control	36.28	37.53	36.81
IgG control +FGF2	36.74	38.27	37.46
anti-FGFR1	36.09	37.95	36.72
anti-FGFR1 +FGF2	35.70	37.58	36.51

10.1.13 Full blot (FGFR1 neutralising antibody experiment)

Stain Free Gel for Figure 5.4.14

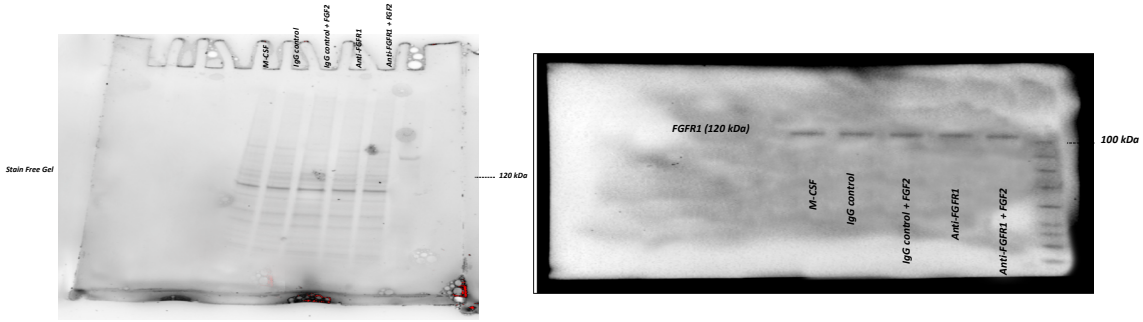

10.1.14 Full blot STAT3 (neutralising antibody experiment)

Figure 5.4.15

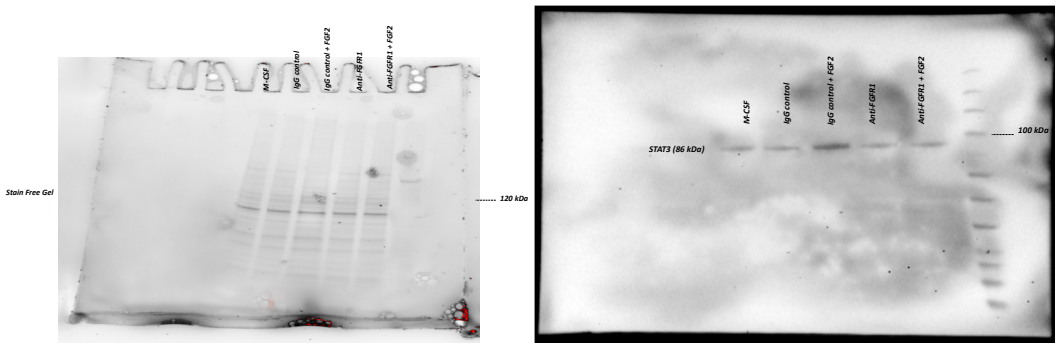

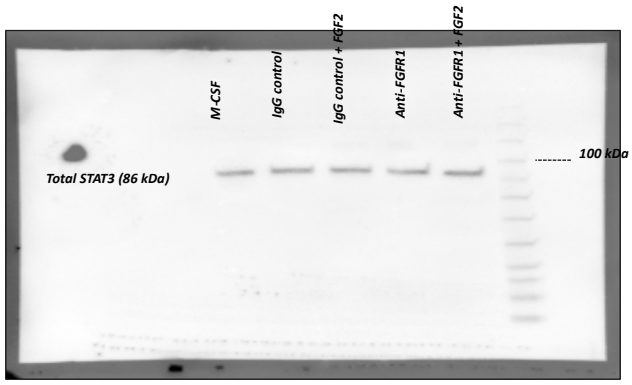

10.1.15 Full blot VE-cadherin and STAT3 (niclosamide experiment)

Figure 5.4.16

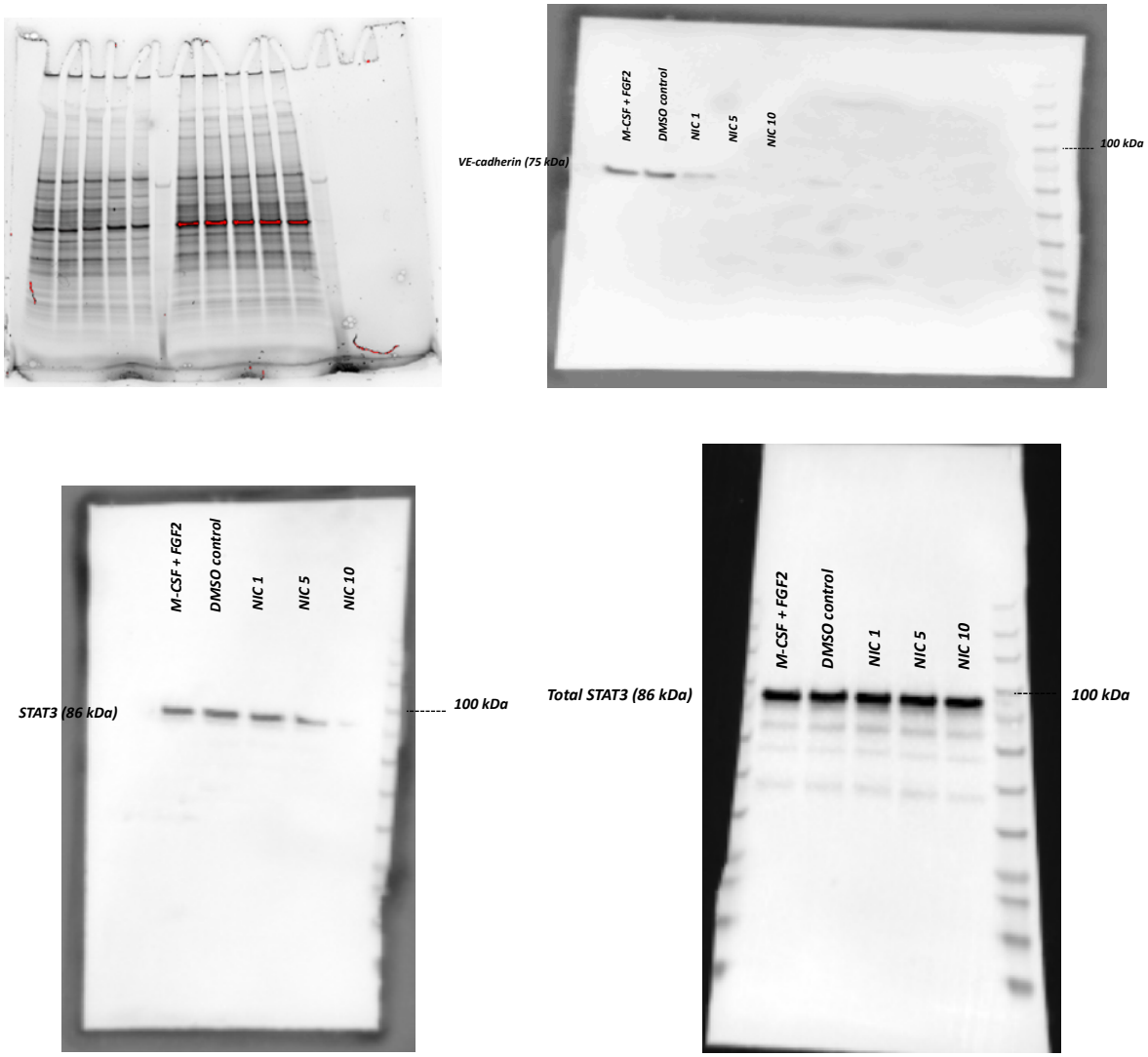

10.1.16 CT values VE-cadherin mRNA (niclosamide experiment)

Figure 5.4.19

VE-cadherin mRNA	CT Min	CT Max	CT average
M-CSF + FGF2	32.50	34.05	33.30
DMSO	32.90	34.20	33.24
Nic 1	31.94	33.61	32.79
Nic 5	32.08	33.73	32.73
Nic 10	32.03	33.51	32.60

microRNA-27a-3p mRNA	CT Min	CT Max	CT average
M-CSF + FGF2	36.55	37.79	37.06
DMSO	36.43	37.83	37.13
Nic 1	36.22	37.18	36.67
Nic 5	35.91	37.05	36.54
Nic 10	35.90	37.06	36.50